The University Of Sheffield.

A bioarchaeological examination of the impact of early-life stress on later-life outcomes using a Procrustean assessment of dental fluctuating asymmetry

Ben Robert Wigley

Submitted for the degree of Doctor of Philosophy

Department of Archaeology & School of Mathematics and Statistics

The University of Sheffield

January 2023

Acknowledgements

Many people have made this PhD research project possible and deserve recognition. Firstly, I would like to thank my supervisors. When I began this project in 2019, I did not appreciate the scale or complexities of the task I was undertaking and would undoubtedly have become unstuck without the guidance of Dr Lizzy Craig-Atkins and Dr Eleanor Stillman. The advice and insights of Dr Sophie Newman in the early stages of project design were also incredibly valuable. This research was supported by the Arts & Humanities Research Council (179466810 AH/R012733/1) through the White Rose College of the Arts & Humanities.

I would like to acknowledge the contributions of the Department of Archaeology. In addition to the difficulties associated with the pandemic, the past two years have been incredibly testing for the department. Despite this, the archaeological community has remained generous and friendly. Yvette Marks deserves special mention for organising the opening of the laboratories for research during lockdown as does Dr Guglielmo Strapazzon who supervised the stores and helped transfer materials to and from the laboratory – without them data collection would have been impossible. The PhD community within the department has also been the source of much friendship and entertainment which has made the project not only academically engaging but also an enjoyable experience.

Special thanks go to my family, especially my father, Bernard, who has provided a great deal of support as well as my brother, James, and his partner, Alba, who were kind enough to put up with me when I wanted a holiday. More than anyone else, however, I would like to thank my mother, Janet, who passed away during the course of the PhD but whose unwavering help and encouragement I have always relied upon.

Abstract

Early life is a time of heightened vulnerability to stress which, due to the high phenotypic plasticity which characterises the period, shapes life-course trajectories. For dependent offspring, mothers play a crucial role in mediating stress (e.g., by contributing to immunity and nutritional provisioning *in utero* and in later breastfeeding) and the effects of their influences during development impact later-life outcomes. Investigating early-life stress and the mother-child nexus bioarchaeologically has proven challenging. However, as first permanent molars (M1s) form during early life without remodelling, stress-induced deviations to symmetry, known as fluctuating asymmetry (FA), can be evaluated to explore this critical time.

In this thesis, FA was quantified through geometric morphometric (GM) techniques so that early-life experience could be investigated and relationships with later-life outcomes identified. It was found that skeletally immature remains were associated with significantly higher FA than mature individuals, and within the immature cohort there was a significant positive correlation between FA and age-at-death. Higher FA was linked to markers of active and systemic infection and a proinflammatory physiology, while childhood stress was associated with growth deficits. Thus, stress experience at different periods was connected to specific outcomes. Elevated early-life stress appears to have increased frailty and decreased resilience, contributing to mortality risk and delayed somatic development, but may also have been associated with phenotypic programming that promoted short-term survival, supporting the Thrifty Phenotype Hypothesis. Despite significant between-site differences in childhood and later-life stress, site-based differences in FA were largely insignificant, suggesting that

mothers successfully mediated contextual stressors for offspring in early life and that within-group differences reflect variance in maternal health.

These findings are the first to demonstrate the viability of GM assessed M1 FA as a proxy for early-life stress and successfully reveal connections between formative experiences, maternal influences and life-course trade-offs in past lives.

Abbreviations

A/M – active/mixed

ANOVA – Analysis of Variance

BG – Black Gate

BL – buccolingual

CI – confidence interval

CO – cribra orbitalia

CPR – crude prevalence rate

DZ – dizygotic

FA – fluctuating asymmetry

GM – geometric morphometric

GPA – Generalised Procrustes Analysis

HOA – hypertrophic osteoarthropathy

ICC – intra-class correlation coefficient

LEH – linear enamel hypoplasia

M1 – first permanent molar

M^1 – maxillary first permanent molar

M_1 – mandibular first permanent molar

MD – mesiodistal

MZ – monozygotic

No. – number

PAR – Predictive Adaptive Response

PCA – principal components analysis

PCM – patterning cascade model

PD – periodontal disease

PHV – peak height velocity

PNBF – periosteal new bone formation

RRPP – residual randomisation permutation procedure

SH – South Shields

SK – skeleton

Std dev – standard deviation

TB – tuberculosis

TPR – true prevalence rate

WS – Warwick

YB – York Barbican

Table of Contents

List of Figures

List Of Tables

Chapter 1: Introduction

1.1 The Role of Bioarchaeology

Bioarchaeology can be defined as the study of remains from archaeological contexts to investigate the interaction of biological and cultural factors in the past (Agarwal 2021; Cheverko *et al.* 2021; Buikstra 1977). Although bioarchaeology may encompass the study of any archaeologically-recovered biological materials, it has almost become synonymous with the study of the human skeleton (Appendix 1) to reconstruct past lifeways and frequently incorporates social theory as well as contextual and historical data (Agarwal 2021; Cheverko *et al.* 2021; Larsen 1997). As skeletal tissues have the capacity to reflect and preserve the influences of both biological and cultural factors, they offer an unparalleled opportunity to investigate forces that shaped both individual lives and societies more broadly (Cheverko *et al.* 2021; Agarwal 2016). Moreover, while a great deal is lost due to the vicissitudes of archaeological survival, skeletal remains endure in the majority of temporal and geographical contexts and in many cases constitute the only artefacts through which most people are represented (Cheverko *et* al. 2021; Larsen 1997: 2-3). The recovery, recording and description of human remains followed by bioarchaeological investigation therefore has the capacity to play a key role in understanding and informing human experience.

1.2 The Importance of Early Life

Life-course outcomes in growth and development as well as morbidity and mortality are impacted by prior stress experience (Gowland 2015; Barker 2012). Stress is a term that describes any exogenous stimuli that places a demand upon the body to readjust itself to maintain homeostasis, thereby causing a reduction in the efficient deployment of physiological resources. Stress is therefore non-specific and the nature of a stress-inducing stimulus is in some ways immaterial (Escós *et al.* 2000: 331; Selye 1973).

Clinical research has shown that the first 1000 days of life are especially stress-sensitive as well as important in defining life-course trajectories. Mothers are critical to offspring survival and developmental homeostasis during this period. For instance, through transplacental transmission and breastfeeding, mothers provide nutritional support, transfer immune factors (thereby protecting immunologically naive foetuses/infants), and facilitate colonisation of the offspring's intestinal microbiome (e.g., through foetal ingestion of amniotic fluid) (Kapourchali and Cresci 2020: 387; Chong *et al.* 2018: 3; Pannaraj *et al.* 2017; Simon *et al.* 2015). Due to the demands placed upon mothers and the dependence of offspring, the mother-child dyad is exceptionally vulnerable to environmental stress with the late-foetal and early-postnatal periods being particularly sensitive (Barker 2012). For example, among famine survivors it has been found that those exposed to severe deprivation in late-gestation had higher mortality rates up to 50 years of age than foetuses exposed earlier in gestation or conceived after the famine (Roseboom *et al.* 2001: 95). As can be surmised, maternally-mediated stress plays a disproportionately significant role in influencing life-course trajectories and later-life outcomes.

Developmental stage can be determined from skeletal remains, facilitating the discussion of the life-course and the impact of stressors across it. The following definitions were employed (Table 1.1). Broadly speaking, skeletons were divided into *immature* and *mature* groups. In this instance, maturity references skeletal development and mature skeletons are those with both fully formed and erupted dentition and among whom long bone epiphyses are fused and further skeletal growth is not possible. More specific terms are also used to describe the immature cohort which, broadly speaking, includes the remains of individuals whose somatic development and growth was incomplete at time-of-death. Firstly, the term *early-life* is employed to describe the period of late-foetal to early-postnatal development (approximately until the end of the first year of life). Earlier stages of foetal development are omitted as the skeletal structure only begins to ossify after the second to third months *in utero* and therefore archaeological remains do not survive prior to this point (Lewis 2017: 113; Schaefer *et al.* 2009; Scheuer and Black 2000). When discussing *maternal dependence*, reference is being made to the period encompassed by foetal growth and breastfeeding (i.e., when offspring are physiologically dependent on their mothers). The time between the end of the first year and twelfth is termed *childhood*, while *adolescence* describes the time between the end of childhood and the attainment of skeletal maturity. Although some of the vocabulary is specific to this thesis and reflects the intended scope of the project as well as parameters associated with the methods employed, the thresholds are consistent with and comparable to past research (e.g., Newman 2016: 15; Raynor *et al.* 2011: 27; Lewis 2007).

Terminology	Definition
early life	late-foetal – <1 year
childhood	>1 year – <12 years
adolescence	>12 years – skeletal maturity
skeletally mature	Skeletal growth is complete and epiphyses fused.

Table 1.1 Periods of the life-course. While a plethora of terms has been used in previous research, these categorisations are made to facilitate the discussion of themes relevant to this thesis. Chronological ages are approximate to reflect the accuracy of available methods for determining skeletal age-at-death.

1.3 The Bioarchaeology of Early-life Stress

It is not possible to measure stress in skeletal remains directly, but proxies can be employed. A variety of stress markers persist in skeletal remains which reflect the impact of environmental perturbations to normal physiological processes and the ability of the skeletal system to mitigate change, make adaptations and endure despite environmental instability (Escós *et al.* 2000: 331; Graham *et al.* 1998: 2; Selye 1973; Waddington 1957). Importantly for a life-course approach, for some markers (examples below) the timing of stress experience can be estimated approximately.

Skeletal remains can provide a great deal of information pertaining to stress experienced during childhood, for instance (Figure 1.1). Defects in the imbricational enamel of the permanent dentition and porosity in the orbits, known as linear enamel hypoplasia (LEH) and cribra orbitalia (CO) respectively, form during development in response to stress. While bone remodelling can obscure CO, LEH are a remarkably durable record of childhood stress events (Brickley 2018: 899; Primeau *et al.* 2015). Moreover, as pubertal development and the final stages of skeletal growth are affected by influences experienced during adolescence, long bone lengths and pubertal tempo can be assessed to infer the impact of stress during later development (Lewis *et al.* 2016; Gowland 2015). In contrast, the presence of bone growth upon the outer cortical surface, referred to as periosteal new bone formation (PNBF), evidences either a localised or systemic stress response; as these deposits can remodel and become lost over time, they provide information about morbidity closer to time-of-death (Weston 2008). Moreover, pathologies such as periodontal disease (PD) can be employed to track irreversible degenerative changes in mature skeletons (Ogden 2008).

The assessment of stressors affecting early life in most archaeologically-recovered skeletons is difficult, however. For example, aside from the challenges associated with assessing fragile bones that are often poorly preserved and highly fragmented, difficulties can be encountered when trying to distinguish between normal growth and abnormal changes which, due to the higher rate of modelling in foetal/infant bones, may be quickly obscured or lost (Hodson and Gowland 2020: 54; Lewis 2017: 115). As such, the identification of skeletal pathologies is exceptionally difficult in foetal and infant remains. Furthermore, although the deciduous dentition forms before most permanent teeth, extending the period over which stress-related perturbations can be explored to include the early stages of *in utero* development, as deciduous teeth only remain in a small number of "non-survivors" (i.e., individuals with short lives) their evaluation is limited to an unrepresentative subset of the population under study (DeWitte and Stojanowski 2015: 416-418; Wood *et al.* 1992: 349).

Figure 1.1 A graphic illustrating the approximate association between stress indicators and specific periods of the life-course. Note that LEH specifically refers to those occurring in the permanent dentition. Growth (i.e., of skeletal elements) and PNBF are linked here to childhood stress and later as foetal remains survive poorly in the archaeological record and periosteal reactions are difficult to differentiate from normal bone deposition in foetal/infant bones (Hodson and Gowland 2020: 54; Lewis 2017: 115).

Given the importance of the early-life period, bioarchaeologists have been encouraged to both refine and go beyond the traditional suite of stress markers to explore early-life stress more fully in past populations (Agarwal 2016; Gowland 2015; Klaus 2014). One potential opportunity is the analysis of stress-induced deviations from symmetry in bilateral structures, known as fluctuating asymmetry (FA), which form during the critical early-life period (Klingenberg 2015; Graham *et al.* 2010; Van Valen 1962). As first permanent molar (M1) occlusal morphology (Figure 1.2) is determined during early life and M1s endure in the remains of survivors and non-survivors (Lynnerup and Klaus 2019: 52; Antoine and Hillson 2016; Harris 2016: 145; Jernvall and Jung 2000), it is hypothesised that M1 FA provides a means to evaluate stress experience during early life and the influence it has on later-life outcomes in skeletal samples.

Figure 1.2 A maxillary M1. Symmetric development between left and right sides is sensitive to stress and can therefore be explored to measure stress. Moreover, as M1s develop during foetal and early-postnatal growth and are morphologically complex, morphometric assessments of M1 FA should act as a proxy for early-life stress.

1.4 Research Questions, Aims and Objectives

To guide the investigation and the discussion of its findings, a set of questions was formulated. To facilitate answering those questions, three research aims and a series of objectives were also developed.

1.4.1 Research Questions

1. Is dental fluctuating asymmetry a sensitive indicator of early-life physiological stress?
2. In past populations, to what extent did early-life stress determine life-course trajectories in growth, development, morbidity and mortality?
3. Is it possible to infer which factors and dynamics created disparities in stress experience?

1.4.2 Research Aims

1. Develop a statistically-valid and precise method of quantifying M1 FA in the dentition of archaeological human remains.
2. Use the data generated under aim 1 to examine exposure to stress during early-life.
3. Explore the impact of early-life stressors on life-course trajectories and later-life outcomes.

1.4.3 Research Objectives

1. Review past research so fluctuating asymmetry and its relation to developmental stress can be better appreciated and utilised to inform subsequent investigation and discussion.
2. With a preliminary sample of teeth 1) develop a methodology for data collection, 2) refine the process to ensure its viability for a larger scale project and 3) explore methodological reliability and quantify the contribution of error to overall variance.
3. Define the statistical techniques necessary to analyse M1 FA and compute an individual index of fluctuating asymmetry which can be compared to osteological markers of later-life stress experience and outcomes.
4. Establish the osteological markers which enable the reconstruction of stress experience over the life-course in skeletal remains.
5. Collect dental and skeletal data from the Black Gate, South Shields, Warwick and York Barbican osteological collections so that the impact of contextual factors on stress experience can be assessed.
6. Using descriptive and inferential statistics, identify differences between groups in stress experience and the connections between different stages of the life-course and use this data to construct models illustrating the relationships between 1) developmental stress, 2) contextual and biological influences (e.g., environment and sex) and 3) later-life outcomes (e.g., morbidity and mortality risk).
7. To critically evaluate the methods employed and their potential future application, explore the pathways through which stress is embodied skeletally and how this affects assessments of stress in cross-sectional archaeological samples.

1.5 Thesis Outline

To deliver research aims and objectives as well as answer the questions posed here, this thesis is organised according to the layout described below.

Chapter 2: A Life-Course Approach to Development

This chapter begins by discussing environmental and genetic explanations of health and development to establish the knowledge gap this thesis fills. Following this, life-course theory is introduced and the means through which a life-course approach can be applied in an archaeological sample is reviewed along with potential complications. Next, the Developmental Origins of Health and Disease (DOHaD) Hypothesis is discussed to illustrate that the engagement of life-course theory in clinical and bioarchaeological research has led to more nuanced understandings of health in past and present populations (Gowland 2015; Barker 2012). Finally, evolutionary perspectives on early-life plasticity are discussed.

Chapter 3: Dental Development and Morphology

Firstly, a general introduction to the descriptive conventions employed by dental anthropologists as well as a discussion of the timing of dental growth is provided. This develops into more specific descriptions of M1 morphology and the stages of dental development. Next, the Patterning Cascade Model (Salazar-Ciudad and Jernvall 2002; Jernvall and Jung 2000), which it is theorised explains stress-induced variations in dental development, is reviewed. Finally, amelogenesis is described in order to illustrate how early-life dental morphological variation is preserved. The aim of the chapter is to establish that M1 morphological variation reflects, and can act as a proxy for, stress experienced during early life.

Chapter 4: Evaluating Dental Morphology

Initially, the non-metric method of assessing dental morphology is critiqued. Following this, geometric morphometric (GM) methods are reviewed with examples given of how different techniques (such as Eigenshape and Fourier analysis) have been applied to dental materials. From this, it is proposed that Procrustean methods are best suited to quantify dental morphology. Next, different types of asymmetries are introduced with focus placed on the significance of fluctuating asymmetry. Finally, the methods through which FA has been assessed in past research are summarised. This encompasses bioarchaeological projects which have utilised linear measurements of teeth, but ends by providing examples (drawn largely from ecology) that have employed GM methods. The overall purpose is to demonstrate 1) that asymmetries can be detected in human teeth, 2) the utility of GM methods, 3) and that more work needs to be done to link FA with other markers of health.

Chapter 5: Materials

The Black Gate, South Shields, Warwick and York Barbican skeletal assemblages are introduced and contextualised in this chapter. This includes reviews of historical, archaeological and osteological data. Thus, practical problems (e.g., fragmentation and preservation) and observations from whole-assemblage analyses are introduced alongside data pertaining to sociocultural and environmental setting which can be employed to explain patterns identified in the Results.

Chapter 6: Methods – Osteological

This chapter begins by describing the methods used to estimate sex and age. Next proxies employed to explore childhood and adolescent stress experience are detailed (e.g., linear enamel hypoplasia, cribra orbitalia and long bone lengths). The recording criteria

for lesions associated with a later-life proinflammatory physiology (PNBF and PD) are provided. Finally, a description of the diagnostic process for specific conditions is given.

Chapter 7: Methods – Geometric Morphometric

Initially, GM data acquisition is described (i.e., imaging and digitisation of morphological features and outlines). This is followed by a review of the process through which coordinate configurations are handled to isolate differences in M1 shape (i.e, by sliding semi-landmarks and subjecting configurations to a Generalised Procrustes Analysis). Next the results of a pilot study are presented to justify decisions taken regarding the number of replicate measures and outline points employed as well as to demonstrate that methodological error is low. Details of how fluctuating asymmetric variance is identified in the sample through a Procrustes ANOVA and individual measures of FA are computed are also provided. Finally, the statistical methods used to compare M1 FA between-groups and evaluate to what extent M1 FA (as a proxy for early-life stress) can predict later-life outcomes are detailed.

Chapter 8: Results

The results are divided into three sections. The first describes patterns in the osteological data (e.g., the demographic composition of the sample and overall patterns in stress marker prevalence). The second section focuses on M1 FA, its contribution to overall M1 morphometric variation and the effects of size on asymmetry. Differences between groups (e.g., site and sex) are also contrasted. The last section evaluates M1 FA scores as predictors of later-life outcomes to imply the extent to which early-life stress is responsible for shaping the life-course.

Chapter 9: Discussion

Several themes for discussion emerge from the Results, including 1) the factors that define life-course trajectories, especially the role mothers played in mediating environmental stressors, 2) the impact stressors experienced during critical periods have on specific life-course outcomes and their potential adaptive significance, 3) the developmental mechanisms through which early-life stress is embodied and 4) the limitations in the method developed for this project and potential means through which it could be improved.

Chapter 10: Conclusion

The research objectives and questions are revisited here to summarise the important points raised throughout the thesis and suggestions are given for future research.

Chapter 2: A Life-Course Approach to Development

2.1 Introduction

Growth and development, as well as morbidity and mortality, can be considered functions of genetic predisposition and environmental pressures. However, a more nuanced appreciation of the complex variation observed between individuals and groups has been achieved through the adoption of a life-course approach which posits that outcomes are also influenced by the accumulation and coalescence of stress experiences at critical times (Cheverko 2021; Gowland 2018; Hendricks 2012). To assess the value of a life-course approach to bioarchaeology, key life-course concepts (i.e., timing, context, linked lives and personal agency) are presented, followed by a discussion of the means through which stress experienced at specific periods of the life-course can be evaluated in skeletal remains (Cheverko 2021; Gowland 2018; Gowland 2015; Elder 1994). Then, previous research from both living and past populations is reviewed to demonstrate that the paradigm can clarify the relationships between life-course stress experience and outcomes (Jacob *et al.* 2019; Doyle *et al.* 2018; Mishra *et al.* 2010b; Kuh *et al.* 2003). Finally, the evolutionary theories advanced to explain the hypothesised adaptive benefits to phenotypic adaptations during periods of heightened plasticity are introduced (Gluckman *et al.* 2010; Skinner 2008; Kuzawa 2007; Jablonka *et al.* 1995).

2.2 Genetic and Environmental Influences

This section briefly highlights the extent to which genetic and environmental factors have been employed to explain outcomes in health, growth, morbidity and mortality. The unexplained variation in outcomes is, however, utilised to provide the rationale for investigating alternative approaches.

2.2.1 Genetics and Environment

Environmental factors and genetics have long been acknowledged as vital determinants of development, disease susceptibility and longevity (Davey Smith 2011; Peters *et al.* 2001). Much research has shown, for example, that deleterious environmental stimuli, such as exposure to toxicants or impoverished environments, can provoke rapid and damaging changes in affected individuals and populations (Davey Smith 2011: 537; Kuh and Ben-Schlomo 2004). In contrast, genomic alterations caused by mutations, genetic drift, stochastic processes and selective pressures usually occur more gradually over a longer period of time and produce relatively stable growth and disease profiles (Stinson 2012: 9; Wright 1982). Cumulatively, environmental and genetic explanations of growth and development as well as morbidity and mortality can account for many of the short and long-term variations in ontogeny and pathology in past and present populations (Buikstra 2019: 14; Agarwal 2016: 131; Stinson *et al.* 2012: 19; Barker 2012: 187; Davey Smith 2011: 537).

The archaeological application of this understanding has been inconsistent, however. The interrogation of genetic mutations and hereditary transmission of disease in past populations has only recently become feasible, and is still inhibited by the technical difficulties in extracting aDNA from diagenetically degraded materials (Willmott *et al.* 2020: 189; Stone and Ozga 2019: 183-185) and it is rarely possible to distinguish kinship

groups in skeletal samples using other methods (Voong *et al.* 2017). The focus, therefore, of many bioarchaeological investigations has been on the impact of environmental factors. Contextualising palaeoepidemiological explorations with environmental observations began in the early 20th century (Buikstra 2019: 14; Waldron 1994: 1-4; Hooton 1930), but the scope of such projects expanded after the publication of *Paleopathology and the Origins of Agriculture* (Cohen and Armelagos 1982). This influential study collated global analyses of osteological stress markers with the aim of assessing whether, and if so to what extent, the transition to an agricultural economy affected disease prevalence rates. It demonstrated that the agricultural transition, with its concomitant transformations of social and physical environments, negatively impacted childhood development and evidenced a widespread and sustained decline in health (Klepinger 1983; Cohen and Armelagos 1982).

Many subsequent bioarchaeological investigations also focused upon how differences in environments affected health. For example, "*The Backbone of History. Health and Nutrition in the Western Hemisphere"* (Steckel and Rose 2002) and "*The Backbone of Europe. Health, Diet, Work and Violence over Two Millennia"* (Steckel *et al.* 2019) explored the health of skeletal samples derived from a variety of temporal and social settings. Again, a suite of osteological variables was used to document stress experienced from childhood through to maturity and produce individual indices of "health" which could be collated for comparisons between samples (Steckel *et al.* 2019; Steckel *et al*. 2002). Environmental pressures were investigated by considering variables such as climate, socially-influenced patterns in activity and settlement complexity. In the latter study, each sample was also placed into a broad time bracket, from pre-medieval (300-500 BC) through to the Industrial (1800-1900) period, so that trends in health (which generally declined) and socio-economic complexity could be charted over *circa*

two millennia (Steckel *et al.* 2019: 5-6; Steckel and Engel 2019). However, interactions between formative stressors and later-life outcomes were not always fully explored and, consequently, an "adult lifestyle" model of health has often prevailed in archaeology in which deleterious outcomes are often perceived as a result of later-life stressors and unrepresentative of health for the majority of life (DeWitte 2010; DeWitte and Wood 2008: 1436; Kuh *et al.* 2003: 778; Wood *et al.* 1992) (Figure 2.1).

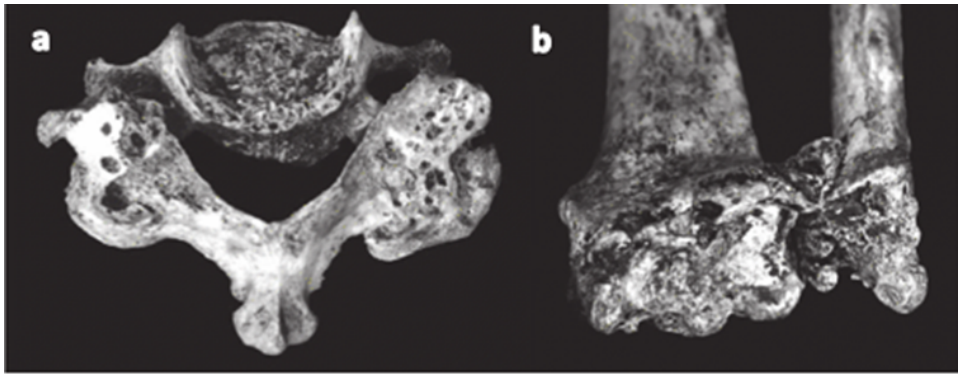

Figure 2.1 Eburnation on synovial joint surfaces, shown above on the vertebral superior articular facets (a) and distal radius and ulna (b), is diagnostic of osteoarthritis. The high prevalence of degenerative conditions such as osteoarthritis in archaeological samples has contributed to the "adult lifestyle" model of health in past research (Waldron 2019: 719-729; Kuh *et al.* 2003: 778; Ortner 2003: 557-558).

2.2.2 Alternative Perspectives

It has not always been accepted that genetics or adult environments were entirely responsible for growth and development as well as morbidity and mortality. Even in the late 19th century, for example, there was notable resistance to this idea in the scientific community. In 1899 the Edinburgh-based physician J. W. Ballantyne proposed in "*On Antenatal Therapeutics"* that the diets, environments and stressors affecting pregnant mothers (which included physical labour, industrial toxins as well as absinthe and cocaine) left their children "antenatally wounded, crippled, and diseased" (Reiss 1999; Ballantyne 1899: 889). Meanwhile, the psychiatrist H. Maudsley described F. Galton's views on genetic determinism as reductionist and incapable of accounting for the vast

array of variation observable in humans, stating that explanations of development must "go far deeper" (Davey Smith 2011: 545; Galton 1904; Maudsley 1904: 8).

More recently, a body of clinical literature has demonstrated that genetics and environment can be poor predictors of later-life outcomes (Davey Smith 2011). For instance, an extensive twin study quantified the genetic component to cancer risk, estimating genetic predisposition on a scale of 0 (no genetic component) through to 1 (genetically predetermined). The doubt/certainty associated with those estimates was articulated through confidence intervals (CIs) which express the range of values estimates are expected to fall between if a population is re-sampled (Lichtenstein *et al.* 2000: 79-80). Even though it was found that there was a greater concordance of risk in monozygotic versus dizygotic twins, estimates of genetic predetermination and their CIs were low. Prostate cancer had the highest estimate, for instance, but only reached 0.42 [95% CI: 0.29, 0.50], while for several cancers it was estimated that genetics played no part in susceptibility (Davey Smith 2011: 541; Lichtenstein *et al.* 2000: 82-83). Moreover, when Vineis and Fecht (2018) explored the environmental influences on carcinogenesis, they suggested that overall, only 16% [95% CI: 7%, 41%] of cancer deaths are the result of environmental exposures. Even after accounting for methodological differences and possible error (Davey Smith 2011: 544; Heinzl *et al.* 2005), these results suggest that genetic and environmental explanations in isolation incompletely explain morbidity and mortality and other factors must be at play.

2.2.3 Summary

Genetics and later-life environment cannot fully explain or predict later-life outcomes (Vineis and Fecht 2018; Davey Smith 2011; Lichtenstein *et al.* 2000). Many long-held understandings about growth and development as well as morbidity and mortality in past populations are therefore likely to be incomplete (DeWitte and Wood 2008: 1436; Wood *et al.* 1992; Klepinger 1983; Cohen and Armelagos 1982). The following section examines the potential of life-course theory to address this problem.

2.3 The Life-Course Approach

The life-course approach, though originating in sociology, has led to new understandings that can bridge the gaps in explanations of ontogeny and pathogenesis (Hodson and Gowland 2020: 45; Gowland 2015; Barker 2012; Kuh *et al.* 2004). This approach focuses on assessing the cumulative effects of experiences and their relation to social, historical and cultural setting; the individual, both in terms of their biology and social identity, represents the sum total of these contextually defined experiences (Agarwal 2016: 131; Giele and Elder 2013: 22; Mayer 2002: 2). The following section discusses the development of the life-course approach and identifies the paradigm's salient features.

2.3.1 Life-course Factors

The life-course approach has its origin in early- to mid-20th century longitudinal cohort studies, and though developments in the field have not led to a unified theory, several points of consensus have emerged (Cheverko 2021: 60-61; Hendricks 2012: 226; Mayer 2009: 2-3; Macmillan 2005: 4; Crosnoe and Elder 2004: 645). It is generally accepted, for instance, that life-course trajectories are shaped by experiences grounded in

four factors: *context*; *links to others*; *personal agency* and *timing* (Cheverko 2021: 61; Jacob *et al.* 2019; Giele and Elder 2013: 9-10; Hendricks 2012: 229; Shanahan 2000; Elder 1994; Giele 1988) (Figure 2.2).

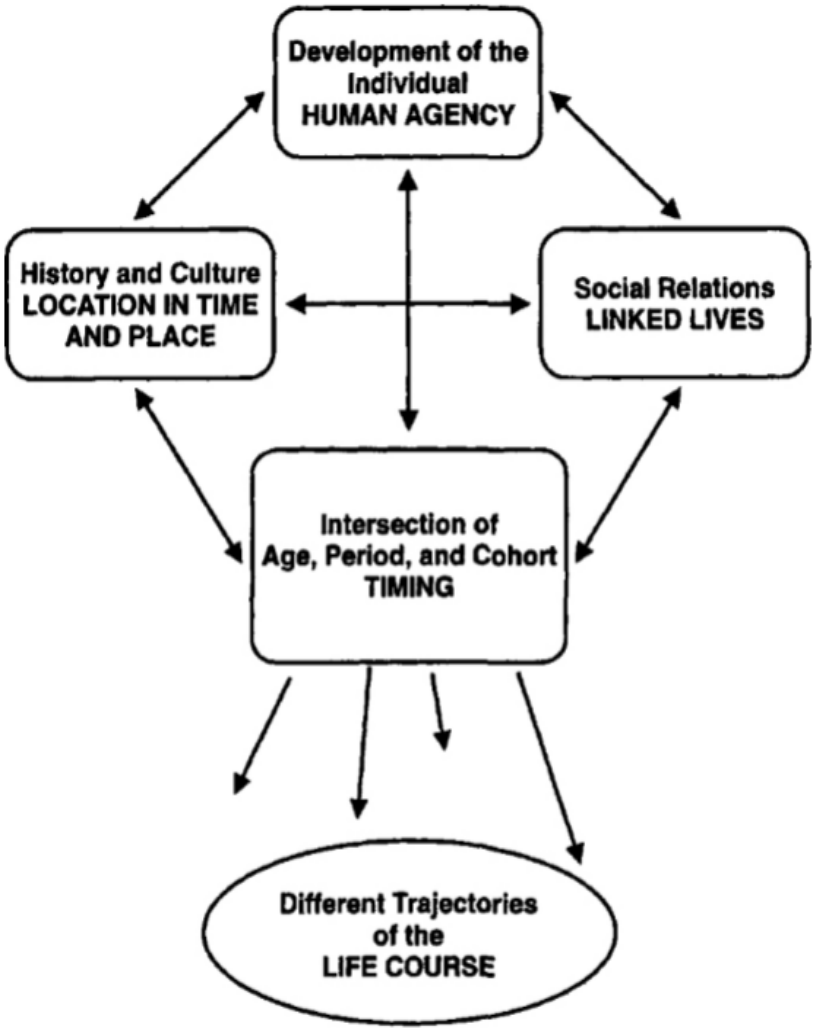

Figure 2.2 Theory suggests the timing of experiences is key to outcomes (Giele and Elder 2013: 11).

Context, or the specific setting inhabited by an individual/sample/population, has been repeatedly shown to pattern life-course trajectories. Factors such as historical milieu, geographic location, cultural behaviours and technological sophistication all therefore contribute to the character of a person's life (Cheverko 2021: 61; Giele and Elder 2013: 9-10; Hendricks 2012: 229-230). Meanwhile, although the concept of "linked lives" was

initially used to suggest that people acquired behavioural cues and access to resources through social interactions, as life-course theory has permeated into other disciplines the impact of biological connections has become an area of interest (Cheverko 2021: 61; Gowland 2015; Giele and Elder 2013: 10; Hendricks 2012: 229; Kuh *et al.* 2004; Elder 1994). In contrast, personal agency refers to the ability of individuals to adapt in order to achieve advantageous outcomes, sometimes despite their environment or connections to others (Cheverko 2021: 61; Giele and Elder 2013:10; Shanahan 2000: 670-671). While evaluating rehabilitation and recidivism, Laub and Sampson (2003) illustrated, for example, that though the effects of early experiences could usually be tracked over the life-course, they did not always predetermine later attainments or exert a continuous, unmodifiable pressure; through autonomous choices, developmental trajectories could be altered and even reversed (Laub and Sampson 2003: 10).

The timing of life-course events, while acknowledged as important, has become a subject of debate (Jacob *et al.* 2019; Hendricks 2012: 228) Some scholars emphasise that early-life events exercise a disproportionate force in shaping life-course trajectories (e.g., Gowland 2015). Others are more sceptical; Hauser and Sweeney (1997) went so far as to state that "there is scant evidence that the direct effects of poverty last beyond entry into adulthood," and suggested that any effects that formative events have on later-life outcomes are indirect and filtered through subsequent experiences (Hendricks 2012: 228). Giele and Elder (2013:10), in contrast, propose that the other three life-course factors coalesce through the "funnel of timing" with *critical periods*, or times at which experiences or stress exposures provoke the greatest responses, being particularly important. Even though not all sociologists agree upon the relative significance of the aforementioned factors, it is clear that they are to a greater or lesser extent interdependent (Cheverko 2021: 60-61; Giele and Elder 2013; Hauser and Sweeney 1997).

2.3.2 Holistic Profiles and Life-course Models

Disentangling the interplay of factors in development can be facilitated by considering the nature of the experience in question. Experiences can be considered as *causal*, *mediating* or *modifying* factors in life-course outcomes depending on whether they directly contribute to a result or in some way alter or transform the effects of a causal event/process (Kuh *et al.* 2003: 779). To return to the last example, Laub and Sampson (2003) reported that, when operating in the critical period of childhood, contextual factors such as socioeconomic status and access to education were causal factors in criminality. The effects of these contextually defined factors were, however, malleable; in many cases incarceration, for example, either moderated or entrenched certain behaviours. For some individuals, personal agency and social links led to behavioural modifications that completely altered their lives, with familial and spousal links appearing to be particularly powerful (Kuh *et al.* 2003; Laub and Sampson 2003). Life-course outcomes can therefore be viewed as the result of a complex coalescence of influences that operate over the entire life-course rather than bounded segments of it (Giele and Elder 2013; Mishra *et al.* 2010b; Kuh *et al.* 2003).

Because of this complexity it is accepted that the success of a life-course study is predicated on creating "holistic" and multidimensional profiles (Crosnoe and Elder 2002). Teasing out the complex interactions that occur continuously throughout the life-course between individuals, groups and their context can only be achieved after collecting a broad range of variables which reflect experiences at critical periods and outcomes throughout life (Gowland 2015; Crosnoe and Elder 2002). It has, however, been cautioned that the magnitude of an experience affects the severity of outcomes as well as the ability of investigators to detect relationships between them (Macmillan 2005: 8). Events such as the Great Depression, for instance, variably influenced educational

aspiration, parenthood and marriage; those having suffered the worst showing a tendency to establish families and seek financial security earlier than those less severely affected (Giele and Elder 2013: 5; Macmillan 2005: 8). As such, the variables chosen to track life-course trajectories must be sufficiently sensitive to register perturbations in order to avoid generating data that projects a distorted view of life-course dynamics (Macmillan 2005: 8; Crosnoe and Elder 2002).

Models are another useful aspect of the life-course approach. Models can illustrate a temporal sequence of exposures and possible interactions between factors that lead to a later outcome (Jacob *et al.* 2019: 1-2; Mishra *et al.* 2010b; Kuh *et al.* 2003: 778). They can consider critical periods and various factors, facilitating clarity when attempting to disentangle the interplay of life-course experiences (Kuh *et al.* 2003: 779). While some life-course models are relatively simple, others are highly sophisticated and attempt to explain dynamic, cumulative and synergistic relationships (Mishra *et al.* 2010b: 94; Kuh *et al.* 2003: 779-781). The more nuanced models predict pathways that link multiple formative exposures to an outcome that reflects an accumulation of lifetime experiences (Ben-Shlomo and Kuh 2002). Due to the complexity of interrelationships between experiences and outcomes, there are great benefits to modelling them quantitatively (Jacob *et al.* 2019; Kim 2015; Laub and Sampson 2013; Kuh *et al.* 2003: 778). For instance, Doyle *et al.* (2018), employed Structural Equation Modelling to investigate the connections between racial disparities, interpersonal relationships, the experience of discrimination and feelings of well-being in later-life which had been previously identified through qualitative research in order to infer the relative significance of each factor to later-life health (Doyle and Molix 2014; Subramanian *et al.* 2005; Amato and Booth 2001).

2.3.3 Summary

By employing a life-course approach it is possible to view outcomes as the result of experiences associated with several interacting factors operating at key periods (Cheverko 2021; Giele and Elder 2013; Laub and Sampson 2013). The paradigm facilitates the disentangling of said experiences so that dynamic processes can be clearly modelled and articulated, but the success of a life-course approach is dependent on, and possibly limited by, a researcher's ability to capture the effects of experiences at critical periods of life (Jacob *et al.* 2019; Doyle *et al.* 2018; Kim 2015; Kuh *et al.* 2003; Crosnoe and Elder 2002).

2.4 An Archaeology of the Life-course

For a life-course approach to be applied to past populations, signals from specific periods of life must be identifiable in skeletal remains. This section explores the means through which bioarchaeologists conventionally chart stress over the life-course and the ramifications of frequently encountered interpretative problems.

2.4.1 Stress Markers: Osteological Records of Experience

The skeleton can yield a wealth of information about life experiences in the form of stress markers. The information stress markers provide, however, can often be ambiguous. Except for teeth (Section 3.4.4), bones continuously remodel and the vestiges of stress can be obscured or completely lost (Brickley *et al.* 2020; Lynnerup and Klaus 2019). There is thus no guarantee that what is evident in the skeleton is a full and accurate record of the stresses experienced during life. Thankfully, several stress markers can be linked (with varying degrees of precision) to specific periods of life and these have proven to be essential in the application of life-course theory (Cheverko 2021: 69-70;

Gowland 2015). However, if not carefully selected, skeletal observations convey more information about the consequences of events and processes at specific periods of life at the expense of others, providing an unbalanced record of stress (Cheverko 2021: 69-70; DeWitte and Wood 2008: 1436; Kuh *et al.* 2003: 778).

Unfortunately, the period of early life is difficult to assess archaeologically; the fragile bones of foetuses and perinates survive poorly in the archaeological record and constitute a biased sample of non-survivors, while the most durable tissues that develop in *in utero* – deciduous teeth – are exfoliated in childhood, so are not present in skeletally mature remains (Halcrow *et al.* 2018: 85; DeWitte and Stojanowski 2015: 416-418; AlQahtani *et al.* 2010; Wood *et al.* 1992: 349). On the other hand, stress experience in infancy and childhood is preserved through CO and LEH (Figure 2.3). CO is caused by an expansion of the red blood cell-producing diploe (i.e., red marrow) at the expense of the outer table which is resorbed leading to a sieve-like appearance (Brickley 2018: 899; Walker *et al.* 2009: 111). Diploic expansion is an attempt to produce more functioning red blood cells when deficiencies in key constituent parts (e.g., iron, vitamin B12 and folic acid) mean there are insufficient red blood cells. As red marrow turns to yellow during later childhood and becomes less capable of producing red blood cells, CO is indicative of stress experienced prior to approximately 10 years (Brickley 2018: 898-899; Walker *et al.* 2009: 111). Unlike CO, which can only be associated with childhood generally and becomes obscured in later-life due to bone turnover, horizontal LEH result from an alteration to normal enamel mineralisation leading to "depressed" perikymata which, as permanent teeth develop throughout infancy and childhood without later remodelling, form a sequential record of stress events to *circa* the twelfth year (Bereczki *et al.* 2019: 175; Kinaston *et al.* 2019: 753-756; Guatelli-Steinberg 2016; Holt *et al.* 2012; AlQahtani *et al.* 2010; Smith *et al.* 2010; AlQahtani 2009; Reid and Dean 2006). Both lesions have a

variety of causes. LEH are linked to episodes of systemic stress caused by, *inter alia*, undernutrition and malnutrition, economic transitions and disease (Bereczki *et al.* 2019: 175; Kinaston *et al.* 2019: 753-756; Guatelli-Steinberg 2016; Hillson 2005: 170; Hillson 1996: 167-166), while CO is connected to genetic predisposition, haemorrhage, prolonged dietary insufficiency or an inability to digest the dietary factors needed to maintain a healthy balance of red cells (Papathanasiou *et al.* 2019: 198). Thus, both can be regarded as strong indicators of childhood stress but, given the multiplicity of potential causes, they are non-specific.

Figure 2.3 LEH (a) and CO (b) evidence childhood stress.

Growth deficits and delays to qualitative skeletal changes can also be used to explore the long-term consequences of stress. Although individuals can exhibit rapid catch-up growth before epiphyseal end plates fuse and prevent further growth, developmental deficits may persist into maturity, potentially as a result of endocrine reprogramming leading to an insensitivity to growth hormones or an incapability to produce these hormones in sufficient volume (Agarwal 2016: 134; Sharma *et al.* 2016; Vaiserman 2015; Liu *et al.* 2009: 740). In a modern population, Hwang (2014), for example, found that 10-15% of subjects that experienced intrauterine growth restriction

did not compensate for reduced early-life growth postnatally. It is likely that the larger bones of the lower-limb (which grow over a longer period) are especially sensitive (Pomeroy *et al.* 2012; Wadsworth *et al.* 2002). Regarding qualitative changes, stress can alter the age of initiation and subsequent tempo of puberty (Lewis 2020; Hwang 2014). Investigations of medieval and post-medieval osteological assemblages have, for instance, suggested that menarche and pubertal completion occurred much later than in modern populations because of elevated environmental stress (DeWitte and Lewis 2020; Gowland *et al.* 2018; Lewis *et al*. 2016). Differences in skeletal growth profiles and pubertal tempo have therefore been utilised to investigate the long-term impacts of stress experienced prior to reaching skeletal maturity, especially during adolescence (e.g., DeWitte and Lewis 2020; Lewis *et al.* 2016; Newman 2016).

Later-life stress can be explored through a variety of skeletal markers, but clinical studies linking formative stress and later-life metabolism and inflammation suggest that those associable with an underlying physiology are especially useful for a life-course approach. To illustrate, inflammatory conditions such as PD have been associated with several metabolic illnesses (e.g., cardiovascular disease and diabetes) whose origins lie in developmental stress (Barker 2012; Lockhart *et al.* 2012; Andriankaja *et al.* 2010). Making similar connections in skeletal samples is difficult, however. While bioarchaeologists have linked PD and PNBF (DeWitte and Bekvalac 2011; DeWitte and Bekvalac 2010), both of which have an inflammatory aetiology (Roberts 2019; Roberts and Buikstra 2019; Steckel *et al.* 2019: 418; Crespo *et al.* 2016: 145; Ogden 2008: 288; Weston 2008), inferring that skeletal stress markers can be employed to explore underlying physiology, robustly connecting these later-developing lesions with prior stress experience has proven challenging and remains an area of active research (Crespo *et al.* 2021; Franklin and Nystrom 2021; Crespo *et al.* 2016).

2.4.2 The Osteological Paradox and Heterogenous Frailty

When exploring stress experience in skeletal remains, the *Osteological Paradox* must be considered. First formally expounded in a paper by Wood *et al.* (1992) and reviewed more recently by DeWitte and Stojanowski (2015), these works highlight a profound interpretative dilemma. Namely, it cannot be assumed that the absence of a stress marker is evidence of an absence of stress, or that the presence of a stress marker is evidence of ill-health. In fact, it can be just as plausible to argue that stress markers are indicative of an ability to endure adversity (DeWitte and Stojanowski 2015: 405; Wood *et al.* 1992: 356-357). One way of mitigating this problem it to explore heterogenous *frailty*, or differences in susceptibility to risk factors that increase morbidity and mortality between, for example, sex and age cohorts (DeWitte and Stojanowski 2015: 399; Wood *et al.* 1992: 357; DeWitte 2010: 8; Vaupel 1988: 277).

Exploring differentials in frailty between sex and age cohorts present quite different problems. For instance, the estimation of sex in skeletally immature remains is near impossible through non-destructive methods and technically challenging with biomolecular tests (e.g., Inskip *et al.* 2019; Stewart *et al.* 2017). However, though there is a growing unease within the field concerning the use of binary categories with arguments being made that they reinforce unquestioned views of biological normalcy (DuBois and Shattuck-Heidorn 2021; Eliot *et al.* 2020; Gettler 2016), sex can be estimated with relative accuracy and ease in mature skeletons and provides a useful and accessible parameter through which to explore patterns of frailty and variation (DeWitte 2010; White and Folkens 2005: 385-397; Loth and Henneburg 1996; Schwatrz 1995; Buikstra and Ubelaker 1994: 15-20; Stinson 1985; Ferembach *et al.* 1980, Phenice 1969).

In contrast, exploring age is methodologically challenging in mature remains, but relatively simple when assessing immature skeletons due to the strong correlations

between chronological age and developmental changes (e.g., AlQahtani *et al.* 2010; Schaefer *et al.* 2009; Hoppa 1992). For both mature and immature remains, stages of age-related skeletal change are typically interpreted with reference to known age-at-death samples (e.g., Buckberry and Chamberlain 2002; Brooks and Suchey 1990; Todd 1920). However, for mature remains, due to the plethora of factors that can affect the ageing process and variously impact different osteological indicators of age, it is more common to take a multifactorial approach in which several age-estimation methods are applied (Garvin and Passalacqua 2012; Baccino *et al.* 1999). It is then customary to aggregate results and place individuals into broad age-groups (e.g., "18-25 years", "25-35 years", "35-45 years" and "45+ years"), with a final opened-ended category reflecting the fact that degenerative changes become increasingly influenced by factors other than age (Boldsen *et al.* 2021: 7-24; O'Connell 2018; Buckberry 2015: 327; White and Folkens 2005: 384; O'Connell 2004; Kemkes-Grottenthaller 2002: 58-61; Buikstra and Ubelaker 1994). Unfortunately, the process is vulnerable to a range of biases. Osteologists, for instance, have a habit of overpopulating the middle age categories (Buckberry 2015: 327; Gowland 2007: 158), while reference samples can skew results through a phenomenon known as "age mimicry." As many samples are forensically-derived, young adults are over-represented and there is a greater probability that individuals of unknown age share morphological attributes with the overrepresented younger cohort (Milner *et al.* 2021: 142; Buckberry 2015; Hoppa and Vaupel 2002b; Usher 2002; Katz and Suchey 1986; Todd 1920). For these reasons and the tendency for ageing systems to end with a "45+" or "50+" category, there is a common misperception that life was almost universally short in past populations, despite primary documents (where available) demonstrating otherwise (Boldsen *et al.* 2021: 21-23; Gowland 2007: 156-158; Hoppa and Vaupel 2002b; Molleson *et al.* 1993; Mackenzie 1827: 730-735).

In short, the traditional approach to age estimation in skeletally mature remains gives vague, and sometimes debateable, estimates inhibiting effective explorations of age-related frailty (Boldsen *et al.* 2021: 7-24; Buckberry 2015; Konigsberg and Frankenberg 2013: 163-168; Hoppa and Vaupel 2002b; Bocquet-Appel and Masset 1996; Konigsberg and Frankenberg 1992). Given that age-at-death itself is a key indicator of resilience and precise age estimates underpin a life-course approach, bioarchaeologists are unsurprisingly encouraged to adopt more sophisticated methods (Boldsen *et al.* 2021; Cheverko 2021: 70; Buckberry 2015).

2.4.3 Summary

Assessing stress experience through skeletal remains is possible, but beset by complicating factors. The skeleton reflects stressors from different times of life to varying degrees with early-life experience and later-life physiology particularly difficult to discern through conventional methods (Cheverko 2021; Halcrow *et al.* 2018; Agarwal 2016). Meanwhile the generation of robust and accurate estimates of age (or lack thereof) determine how effectively heterogenous frailty can be explored (Boldsen *et al.* 2021; Cheverko 2021; DeWitte and Stojanowski 2015: 399; Gowland 2015; Wood *et al.* 1992). Consequently, bioarchaeologists are being encouraged to employ and develop innovative solutions to circumvent these limitations (e.g., Boldsen *et al.* 2021; Cheverko 2021; Buckberry 2015).

2.5 DOHaD and the Life-course Approach

Despite limitations, the life-course approach has been applied with great success, notably in the formulation of the Developmental Origins of Health and Disease (DOHaD) Hypothesis (Barker 2012). This section reviews and evaluates how the key life-course factors previously identified have been employed in explorations of morbidity and mortality in past and present populations in order to justify the continued implementation of the paradigm.

2.5.1 Timing: The Critical Early-life Period

DOHaD's foundations lie in a seemingly counterintuitive phenomenon: the rising prevalence of chronic diseases in populations experiencing increasing prosperity (Barker and Osmond 1986: 1077). To investigate this paradox, Barker and Osmond (1986) contrasted infant mortality between 1921-1925 with adult cause-of-death between 1969-1978 in specific geographic regions. For many conditions it was found that adult morbidity was strongly correlated with neonatal mortality; stomach cancer, for example, had the highest correlation coefficient of 0.82 (Barker and Osmond 1986: 1077-1079). Although this seminal study did not follow specific individuals over their entire life-course and instead used geographic cohorts (i.e., residents of a particular region) from a time characterised by increasing population mobility (i.e., the residents of the regions studied changed to a greater or lesser extent over time) (Bashford and McAdam 2014; Bland 2006; Hoppa 2002: 12), follow-ups rigorously scoured medical records to link early and later-life data in the same individuals and related groups (Armelagos *et al.* 2009: 262; Syddall *et al.* 2005). Twin studies, for instance, have reported significant within-pair differences in later-life outcomes associable with differences in birth weight, despite shared genes and home environment (Armelagos *et al.* 2009: 261; Poulter *et al.*

1999), while analyses of Dutch Famine survivors found that foetuses exposed to undernutrition in mid-to-late gestation were significantly shorter and lighter at birth and in later-life had a higher risk of cardiovascular, respiratory and metabolic morbidity as well as higher mortality rates up to 50 years of age (Roseboom *et al.* 2001: 95; Roseboom *et al.* 2000; Lopuhaa *et al.* 2000; Ravelli *et al.* 1998).

Comparable findings have been reported by bioarchaeologists. In Japanese Jomon-period samples, it was found that individuals who developed LEH earlier acquired more defects throughout life and were likely to have died younger in comparison to those that developed their first defect later (Temple 2014: 541). DeWitte and Wood (2008) further reported that even in the most virulent epidemics, mortality was affected by childhood stress; they estimated that during the Black Death, individuals who experienced systemic stress between the ages of *circa* 1-6 years, evidenced by mandibular canine LEH, were at a 2.9 times higher risk than those without these indicators of developmental stress (DeWitte and Wood 2008: 1438). Overall, these findings suggest that influences experienced during development can alter life-course trajectories, provoking life-history trade-offs that increase morbidity and mortality (Temple 2014; Newman and Gowland 2016; Temple 2012; Temple 2007). Although difficult to investigate in skeletal samples, clinical and bioarchaeological evidence suggests that prenatal and early-postnatal life is an especially sensitive critical period in which environmental stressors can significantly influence, or programme, later-life phenotype (i.e., there is high *plasticity* in early life) (Barker 2012; Armelagos *et al.* 2009: 262; Barker and Osmond 1986: 1081; Holland Jones 2005).

More variability is perhaps evident in the archaeological record than the clinical, however. Perinatal and immature skeletons at archaeological sites, which frequently display LEH and other indicators of hardship suggest that early-life perturbations may

have completely circumscribed the life-course, possibly either due to differences in the levels of environmental stress experienced or the relative ineffectiveness of sociocultural and medical buffering systems (e.g., Newman and Gowland 2016: 226; Armelagos *et al.* 2009: 264; White 1978). Clearly, clinical analogues cannot substitute or replace direct interrogation of skeletal remains when investigating stress experience in past populations.

2.5.2 Linked Lives: The Maternal Lineage

The investigation of links between mother and dependent child is another aspect of the life-course perspective that has been particularly valuable. It is also being increasingly acknowledged that connections with grandparents (and potentially beyond) may be important (Gowland 2018; Gowland 2015). For instance, Kaati *et al.* (2002) found that grandparental access to food was a predictor of diabetes mortality in grand-offspring. Meanwhile, in Guatemalan communities, infants whose grandmothers received nutritional supplements were generally better developed, having higher birth weights and lengths, than peers whose grandmothers did not receive supplementation (Susser *et al.* 2012: 579; Stein *et al.* 2008). Similar patterns can be seen in victims of the Dutch Famine, as women who were themselves unborn foetuses during the famine gave birth to smaller offspring (Susser *et al.* 2012: 579; Kuzawa 2007: 656; Lumey 1992).

The fact that three generations can be negatively affected by one episode of deprivation is a product of reproductive life histories. In the reproductive system of female mammals, gametogenesis begins and ends during foetal development, with all primary ova formed prior to birth (Betts *et al.* 2017: 1294; Thayer and Kuzawa 2011: 798; Kierszenbaum 2006). As such, the stress experienced by a pregnant female also affects life-course trajectories in the gestating foetus, and if that foetus is female, the cells developing in the foetal ovary (Susser *et al.* 2012: 579; Gluckman *et al*. 2007: 7). An

outcome influenced in such a way would be considered a manifestation of a mitotically-stable *intergenerational* phenotype (Thayer and Kuzawa 2011: 798; Skinner 2008). There is, however, a growing body of experimental evidence to suggest that stressors in the maternal line can produce meiotically-stable, *transgenerational* (or *ancestral*) phenotypes that are perpetuated through sexual reproduction in which no direct exposure to an environmental stimulus is necessary to produce a phenotype associated with that stimulus (Lu *et al.* 2019; Van Winkle and Ryznar 2018; D'Urso and Brickner 2014; Susser *et al.* 2012; Thayer and Kuzawa 2011: 798; Gluckman *et al.* 2010: 13; Kierszenbaum 2006; Jablonka *et al.* 1995; Galler *et al.* 1994; Galler and Seelig 1981). Although research into paternal influences on health and disease are demonstrating its importance, the maternal line is generally considered more influential (e.g., Soubry 2018; Soubry *et al.* 2014; Kaati *et al.* 2002). Thus, when considering linked lives, researchers are beginning to reflect not just on the proximate connections suggested by Elder (1994) but also ancestral links, particularly in the maternal lineage (Gowland 2018; Gowland 2015).

Assessing maternally-mediated ancestral influences on life-course outcomes in bioarchaeological samples without medical records, however, is challenging. In rare cases, such as historical cemeteries with detailed burial registers (e.g., Molleson *et al.* 1993: 123-130) or where aDNA analyses are available (e.g.,Voong *et al.* 2017), it may be possible to identify several generations of one family. Yet, in general, links between maternal and offspring stress experience can only be confidently made in bioarchaeology through the observation of osteological markers whose occurrence is attributable to a period of time when an individual is developing *in utero* or breastfeeding (Brickley *et al.* 2020: 34-35; Newman 2016: 81; Newman and Gowland 2016: 226; Sibley *et al.* 1992),

and the influence of the ancestral maternal lineage is necessarily more tenuous regardless of their clinically and experimentally inferred importance (Gowland 2015: 534-535).

2.5.3 Context: Environmental Imprints

It has been argued that environments can induce specific life-course outcomes. In modern populations, such as the Dutch Famine cohort, in addition to growth deficits, environmental stress was linked to specific pathological sequelae (e.g., cardiovascular, respiratory and metabolic disease) (Roseboom *et al.* 2000; Lopuhaa *et al.* 2000; Ravelli *et al.* 1998). Similarly, a bioarchaeological comparison between the low-status and highly-stressed Cross Bones skeletal assemblage and the middle-class Bow Baptist cemetery found that despite a similar prevalence of non-specific stress markers (i.e., LEH), the skeletons at Cross Bones had a far higher prevalence of scorbutic lesions and evidence of infectious disease (Newman and Gowland 2016: 221-224). In fact, the distinctiveness of certain patterns has led M. Skinner and colleagues to hypothesise that responses to environmental stressors are unique and akin to a fingerprint which persists throughout life (Nilsson *et al.* 2018; Skinner 2008).

This increasing appreciation of site-specific responses is shaping clinical and bioarchaeological research. For instance, in Betsinger and DeWitte's (2020) "*The Bioarchaeology of Urbanization: The Biological, Demographic, and Social Consequences of Living in Cities"* authors were encouraged to explore the local factors that contributed to variability between sites and even create their own definitions of rural and urban. From more nuanced comparisons it has been suggested that fluid, transitional contexts are potentially more impactful to health and development. For instance, in the early-20th century, heart disease was more prevalent in higher socioeconomic groups than lower socioeconomic groups, before the situation was reversed in the later-20th century

(Marmot *et al.* 1978). Barker and Osmond (1986: 1081) theorised that this was because the higher-status groups were exposed to and impacted by socioeconomic transitions earlier. Meanwhile in skeletal samples it has been found that stress markers are more common in rapidly changing contexts such as those experiencing industrialisation (Hodson and Gowland 2020; Newman 2016: 249). Consequently, there is a growing move away from employing broad categorisations (e.g., urban and rural) which can obscure important details by glossing over differences in favour of emphasising commonalities.

2.5.4 Personal Agency

Individual agency has rarely been considered by clinical epidemiologists and bioarchaeologists. For those who wish to understand sickness and well-being at a populational level, it has been argued that individual case studies are of limited value (Davey Smith 2011). Moreover, when utilising skeletal remains it is unlikely that the limited range of osteological reactions possess the sensitivity to unambiguously express individualised shifts in life-course trajectory (Wood *et al.* 1992; Martin and Armelagos 1979: 571). So, even though personal agency has been shown to exert sufficient force to dramatically alter life-courses and case studies can provide illustrative examples (Chapter 8) (Giele and Elder 2013: 9-10; Davey Smith 2011; Laub and Sampson 2003; Shanahan 2000: 670-671), this line of enquiry is infrequently pursued and is likely only available through the collection of high-resolution qualitative data, such as that obtained through extensive interviewing or the construction of osteobiographies (e.g., Roffey *et al.* 2018; Mihanovic *et al.* 2017; Laub and Sampson 2003).

2.5.5 Summary

The life-course paradigm has added novel insights into the understanding of health and development with timing, context and linked lives proving useful interpretative constructs (Gowland 2018; Gowland 2015; Giele and Elder 2013; Hendricks 2012). When bioarchaeologists have taken a life-course approach, these tools have been used to explore the interactions between stressors operating throughout life more completely (Klaus 2014; DeWitte and Wood 2008: 1436), which represents a significant improvement on previous archaeological investigations which at times struggled to integrate data relating to both early- and later-life stress (Steckel *et al.* 2019; Steckel and Rose 2002; Cohen and Armelagos 1982). Further developments may be forthcoming if stressors can be linked more substantively to the late-foetal and early-postnatal period.

2.6 Evolutionary Perspectives

The maternally-mediated intergenerational and potentially ancestral/transgenerational influences on life-course outcomes have encouraged explorations of the evolutionary significance behind early-life programming (Cheverko 2021; Gluckman *et al.* 2007; Kuzawa 2007; Wells 2007; Jablonka *et al.* 1995). Evolutionary models are generally beneficial as they enable a more holistic consideration of biological factors and facilitate hypothesis generation and data interpretation (Agarwal 2016: 130-131; Klaus 2014: 294; Steadman 2018: 4; Waldron 1994: 4-5). This final section briefly describes the evolutionary understanding of early-life plasticity, its role in life-course trajectories and how this can be incorporated into bioarchaeology.

2.6.1 The Thrifty Phenotype

One of the earliest attempts to explain from an evolutionary standpoint the increases in morbidity and mortality associated with early-life stress was the Thrifty Phenotype Theory (Hales and Barker 2013; Hales and Barker 2001). A "thrifty" phenotype is a suite of outcomes adapted to an environment in which resources are scarce and periods of nutritional insufficiency and hardship are expected (Armelagos *et al.* 2009: 264; Gluckman *et al.* 2007: 2; Neel 1962). In such conditions it is proposed that during foetal growth and early infancy the development of vital organs, such as the brain, is prioritised while long-term investments in somatic, endocrine and immunological trajectories are reduced; in highly selective contexts this constraint enhances survival of early-life adversity, but reduces long-term fitness (Hales and Barker 2013: 1218; Wells 2012: 230). In this model the mother acts as a conduit, through intrauterine provisioning and later breastfeeding, for nutritional and hormonal cues (Pittet *et al.* 2017; Gluckman *et al.* 2007: 3). Phenotypic responses may, however, be counterproductive in many cultures as diet and activity patterns are modified for pregnant women to the extent that they often do not accurately reflect normal environmental stressors (i.e., there is low *fidelity* between maternal cues and environment) and so adaptations based around maternal cues may prove maladaptive (Gluckman *et al.* 2010: 10; Jablonka *et al.* 1995). Temple's (2014) bioarchaeological study supported this theory, finding that earlier experience of systemic stress (inferred by LEH presence) was associated with earlier age-at-death, suggesting that survival during ontogeny had been ensured at the expense of longevity. Despite support such as this, the theory is problematic. Although it can explain the increases in mortality and morbidity noticed by Barker and Osmond (1986) in populations that were increasing in prosperity with reference to low fidelity between the developmental and

later-life environment, it cannot account for the transgenerational transmission of phenotype (Susser *et al.* 2012; Roseboom *et al.* 2001).

2.6.2 Constraint and Maternal Capital

In the Thrifty Phenotype Model, the mother plays a relatively straightforward role as a medium through which environmental cues/stressors are channelled. Alternative theories have postulated more complicated relationships in which mothers actively shape offspring ontogeny, even to the point of constraining offspring growth and development (Lu *et al*. 21019; Wells 2012; Charnov 1997; Charnov 1991). The Maternal Capital Model, for instance, proposes that mothers and their offspring have a dynamic relationship, in which mothers balance investment in offspring with their own survival and continued reproductive success (Wells 2012: 231-234; Charnov 1997; Trivers and Willard 1973). As such, Wells (2003) theorised that when resources are scarce, mothers constrain provisioning, causing offspring developmental stress. Constraint may be behavioural (Fujita *et al.* 2012), but can also be physiological; in primates the composition of breastmilk is modulated in relation to maternal nutritional demands, for example (Pittet *et al.* 2017). On initial inspection this theory projects a parsimonious view of maternal support, but maternal signals cueing an offspring phenotype that is tailored to a level of investment that the mother can provide enhances offspring survival. Furthermore, if maternal signals represent a lifetime of ecological conditions, they may buffer against short-term environmental deprivations (Wells 2012: 232; Wells 2007: 335). Support for this theory in human studies is limited (Fujita *et al.* 2012; Cameron and Dalerum 2009), however, and it may be that maternal constraint is better evidenced in non-human animals with quicker reproductive cycles and multiple offspring per birth (Lu *et al.* 2019; Pittet *et al.* 2017; Robert and Braun 2012; Sibly and Brown 2009; Trivers and Willard 1973).

2.6.3 Predictive Adaptive Responses

The Predictive Adaptive Response (PAR) Theory states that phenotypic alterations can either be immediately or predictively adaptive (Gluckman *et al.* 2010; Gluckman *et al.* 2007; Bateson *et al.* 2004). Immediately adaptive reactions to stress lead, in essence, to outcomes similar to Hales and Barker's (2001) thrifty phenotype, with adaptations maximising the probability of short-term survival (Gluckman *et al.* 2007: 3). In contrast, predictive adaptations stem from a "forecast" of environmental conditions (Bateson *et al.* 2004). As mothers, to a large extent, sustain offspring on energetic reserves accumulated over a lifetime, the predictive cues offspring receive can be conceived of as a long-term record of ecological conditions, stretching back to when the mother herself was maternally-dependent and influenced by her own mother's accumulation of experiences (Gluckman *et al.* 2010: 9-11; Gluckman *et al.* 2007: 4-7; Wells 2007: 335). Predictive adaptations are, as such, compatible with the idea of persistent ancestral/transgenerational phenotypes (Susser *et al.* 2012; Skinner 2008), and adaptively beneficial as they promote outcomes less likely to be influenced by seasonal stressors (Kuzawa 2007: 655). Predictive cues, however, could result in a phenotypic "inertia" that produces an ancestral/transgenerational phenotype that would be innately maladaptive in rapidly transforming, unprecedented contexts (Gluckman *et al.* 2010: 10; Kuzawa 2007: 655; Jablonka *et al.* 1995: 133). Although phenotypic inertia may explain the seemingly paradoxical phenomenon of poor health in improving but transforming contexts (e.g., Barker and Osmond 1986), the PAR theory is generally thought to be characterised by overall increasing quality in phenotypic outcomes (Figure 2.4) which is at odds with the picture of centuries of health deterioration in European populations between the early medieval to Industrial periods presented by Steckel *et al.* (2019).

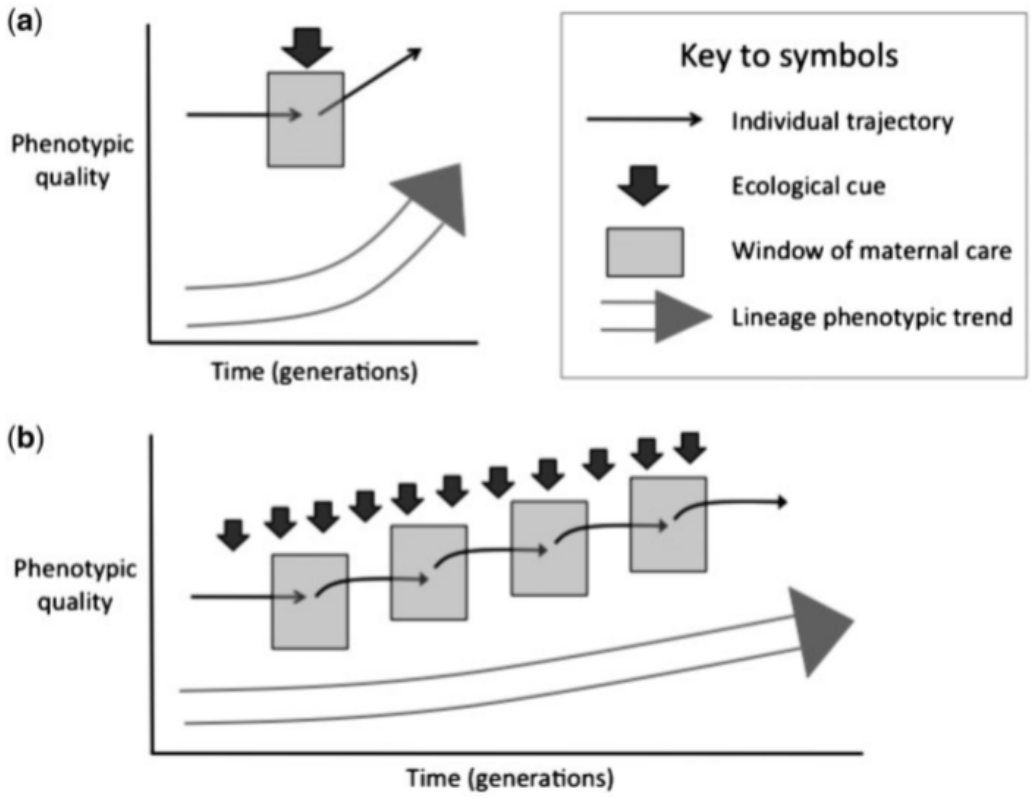

Figure 2.4 It has been theorised that maternal-mediated environmental cues provoke phenotypic adaptations in early life that predict later conditions, increasing the quality of later-life outcomes over successive generations (Wells 2012: 232).

2.6.4 Summary

Various theories regarding the evolutionary significance of early-life plasticity have been proposed (Wells 2012; Gluckman *et al.* 2010; Kuzawa 2007; Jablonka *et al.* 1995). All have merits, but also limitations in their capacity to explain observed phenomena and it may be that specific theories are more or less applicable to different species (Pittet *et al.* 2017; Robert and Braun 2012; Sibly and Brown 2009; Trivers and Willard 1973). The Thrifty Phenotype theory is supported by several human studies, both clinical and bioarchaeological in nature, but the PAR model best accounts for transgenerational outcomes (Hales and Barker 2013; Wells 2012; Gluckman *et al.* 2010; Kuzawa 2007; Jablonka *et al.* 1995).

2.7 Conclusion

This review of the literature has several primary conclusions of significant relevance to this thesis. Firstly, phenotypic outcomes reflect adaptations to stressors from physical and sociocultural environments (Gowland 2015; Susser *et al.* 2012; Skinner 2008; Selye 1973). Hence, in order to understand the characteristics that define an individual or population it is necessary to thoroughly contextualise study samples (Hendricks 2012; Crosnoe and Elder 2002). Secondly, evidence suggests the period of greatest phenotypic plasticity is relatively short, beginning periconception and ending in the first years of life: the period of maternal dependence (Gowland 2015; Agarwal 2016; Barker 2012). As such, the mother enacts a pivotal role in conveying physiologically cues that encourage alterations to phenotype affecting outcomes in growth and development as well as morbidity and mortality (Barker 2012; Kuzawa 2007; Jablonka *et al.* 1995). The central argument, therefore, is that maternally-mediated environmental influences experienced during early life are fundamental to life-course trajectories. It is hypothesised that through a combination of traditional and innovative techniques, it will be possible to construct multidimensional osteological profiles to explore the interactions of early- and later-life stressors and contribute to the archaeological understanding of past lives (Gluckman *et al.* 2010; Gluckman *et al.* 2007).

Chapter 3: Dental Development and Morphology

3.1 Introduction

Teeth are complex structures whose development is well-regulated. Yet it has also been demonstrated that subtle differences in morphological expression – especially in the crowns of multi-cusped teeth – can result from environmental stressors which, due to the chronological predictability of dental growth, can be linked to specific developmental periods (Lynnerup and Klaus 2019; Irish 2016a; Brook 2009; Hillson 2005; Tucker *et al.* 2004; Dempsey and Townsend 2001; Scott and Turner 1997). To explore these themes, this chapter first introduces basic dental anatomy and the associated descriptive terminology (Irish 2016a; Ungar 2016; Hillson 2005; Scott and Turner 1997; Carlsen 1987; Wood *et al.* 1983). Next, distinctions between dental fields are briefly discussed, as is the timing of odontogenesis (Cuozzo 2016; Irish 2016a; Lease 2016; AlQahtani *et al.* 2010; Smith *et al.* 2010; AlQahtani 2009; Hillson 2005; Koppe and Swindler 2004). From this it becomes clear that first permanent molars develop during the period of early-life that the previous chapter hypothesised was critical to developmental trajectories (i.e., from the late-foetal period through to the first postnatal year). Finally, after evaluating the patterning cascade model of molar crown development, it is proposed that stress-induced disruptions ripple across the multi-layered molecular networks that control cusp formation to produce a phenotype embodying genetic and environmental inputs which is then preserved through enamel formation (Stojanowski *et al.* 2017; Riga *et al*. 2014; Hunter *et al.* 2010; Brook 2009; Tucker *et al.* 2004; Salazar-Ciudad and Jernvall 2002; Dempsey and Townsend 2001; Koppinen *et al.* 2001; Jernvall and Jung 2000; Jernvall and Thesleff 2000; Jung *et al.* 1998).

3.2 Dental Anatomy

3.2.1 Definitions and Terminology

Every tooth has root and crown elements separated by a constricted neck or cervical region and is composed of three different hard tissues: dentine, cementum, and enamel (Lynnerup and Klaus 2019: 52; Irish 2016a: 88; Hillson 2005: 9; Scott and Turner 1997: 20) (Figure 3.1). Dentine is highly mineralised, retaining just enough elasticity to absorb biting forces (Tang *et al.* 2016: 204; Shahmoradi *et al.* 2014; Berkovitz *et al.* 2009). In the root, dentine is enclosed in an avascular cementum layer (Lynnerup and Klaus 2019: 53; Lease 2016: 95; Nanci 2013). Cementum is slightly less mineralised and serves as an attachment site for the collagenous periodontal ligament which, along with gingival tissue, anchors the root in the mandibular and maxillary alveolar processes (Harris 2016: 150; Tang *et al.* 2016: 211; Lease 2016: 95; Irish 2016a: 88). The crown is dentine capped with enamel. Being *circa* 96% inorganic apatite crystals, enamel is inert (Lynnerup and Klaus 2019: 52; Antoine and Hillson 2016: 223). Crowns are an interface at which an organism's skeletal structure directly interacts with its environment; consequently, crown size and morphology vary greatly, reflecting a variety of evolutionary pressures and modifications (Lynnerup and Klaus 2019: 52; Ungar 2016; Cuozzo 2016; Delezene 2016; Martinón-Torres and Bermúdez de Castro 2016). Within each tooth there are also two border areas where different tissues meet: the cemento-enamel junction (CEJ), located at the neck, is the point of contact between root cementum and the crown enamel; and the dentino-enamel junction (DEJ), within the crown, where the enamel cap abuts the underlying dentine (Lease 2016; Irish 2016a: 88). At a tooth's centre is a pulp chamber housing blood and lymphatic vessels, as well as nerves that reach into the dentine; the soft tissues in the pulp chamber make a tooth a

functional and sensory organ (Lynnerup and Klaus 2019: 52; Legge and Hardin 2016: 191; Irish 2016a: 89; Luukko *et al.* 2011).

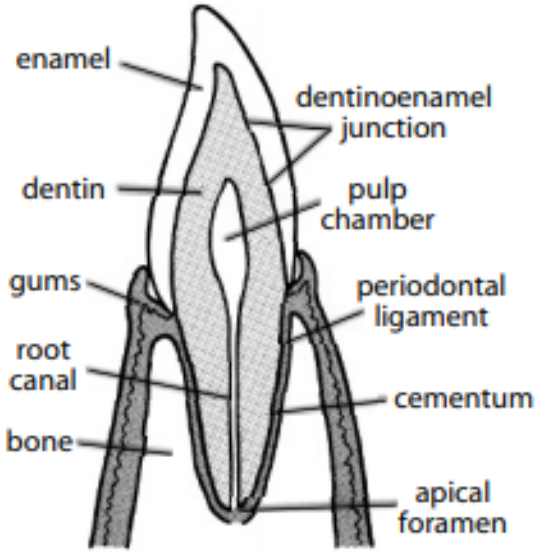

Figure 3.1 Tooth anatomy (White *et al.* 2012: 104).

A suite of terms (Figure 3.2) is used to orientate and describe teeth. The terms *mesial* and *distal* respectively refer to the portion of a tooth that is closest and farthest from the sagittal, or midline, plane. *Interproximal*, or *approximal*, interchangeably refer to the mesial or distal contact points between adjacent teeth. *Coronal* references the crown; the portion of crown which opposes, or *occludes* with, another tooth is known the *incisal* surface in anterior teeth or the *occlusal* surface in posterior teeth (e.g., molars). The *apex* of a tooth is the tip of the root most distant to the crown. The aspect of a tooth facing the tongue is referred to as *lingual*, while the surface which comes into contact with the soft tissues of the face is termed the *labial* surface in the anterior dentition or the *buccal* surface in the posterior dentition (Irish 2016a: 89; Hillson 2005: 9-11; Scott and Turner 1997: 15-16; Massler and Schour 1956). Teeth are arrayed in a parabolic arch formed by the opposing alveolar processes of the maxilla and mandible (i.e., the upper and lower jaw respectively); each arch is known as an *isomere* (Irish 2016a: 90; Scott and Turner

1997: 15-16). Although the maxillary and mandibular isomeres possess the same number of teeth in the same dental classes, the teeth are morphologically and developmentally distinct (Irish 2016a: 88-90). Both the mandible and maxilla are divided along the sagittal plane into *antimeres*; the left and right antimere reflect one another and their growth is regulated by the same genes (Irish 2016a: 89-90; Graham *et al.* 2010: 467).

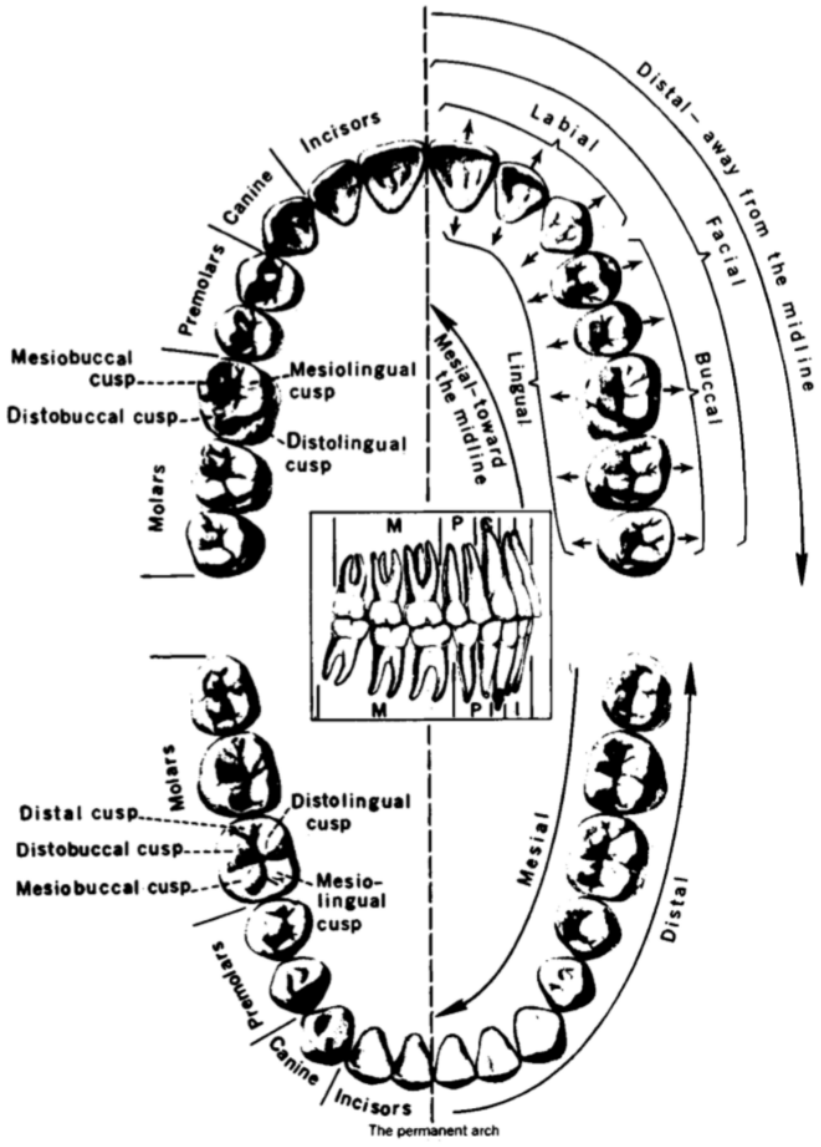

Figure 3.2 Positional terms used to describe dental fields and the relative position of each tooth within the dental arch. Image after Massler and Schour (1956) and taken from Scott and Turner (1997: 17).

3.2.2 Dental Fields

Humans are *diphyodonts* and *heterodonts*. As diphyodonts, humans have two sets of teeth (deciduous and permanent), while heterodonty means that teeth can be divided into several different classes, referred to as *metameres*, which include: incisor, canine, premolar and molar metameres (Irish 2016a: 89-90; Ungar 2016: 27; Hillson 2005). In each antimere of the deciduous dentition there are two incisors, one canine and two molars; in the permanent dentition there are two incisors, one canine, two premolars and three molars. Shorthand notation, with a few variations, has been developed to facilitate identification of individual teeth (Irish 2016a: 90; Hillson 2005: 12). The method described here is commonly applied and is used throughout this thesis. In the deciduous dentition, "d" is followed by the initial letter of the tooth field, say "m" in the case of a molar, with a number added to identify its position in that field (Irish 2016a: 90; Hillson 2005: 12). So, "dm1" refers to deciduous first molars collectively. In permanent teeth, an uppercase letter denotes dental field. In order to distinguish maxillary and mandibular isomeres, a superscript is added to a maxillary tooth denoting its relative position in the field, while a subscript is used for mandibular teeth (Irish 2016a: 90; Hillson 2005: 12). Thus, the first permanent maxillary molar is "M^1" and its mandibular counterpart is "M_1".

The occlusal surfaces of teeth are composed of several distinct features that include *ridges*, *cusps*, *fissures* and *fovea*. Incisors and canines have a single cusp, while premolars and molars are multi-cusped. In the latter teeth, cusps are separated by fissures (which may be called *grooves* or *sulci* in the most pronounced cases) and where two or more fissures meet, a fovea forms (sometimes called *pits* or *depressions*) (Scott *et al.* 2016: 248; Lease 2016; Scott *et al.* 2016; Ungar 2016: 30; Scott and Turner 1997: 20-21; Carlsen 1987). Incisors are located mesial to all other teeth and their spatulate crowns facilitate cutting and slicing during mastication, while the conical-shaped single cusps on

canines enables puncturing (Cuozzo 2016: 42; Lease 2016: 102-104; Hillson 2005; Koppe and Swindler 2004: 368; Scott and Turner 1997: 20; Carlsen 1987). Premolars are a tooth in the permanent dentition which replace deciduous molars. Although premolar shape varies, with some being more caniniform and others molarised, both maxillary and mandibular premolars usually have two cusps either separated by a fissure (P^1) or connected by a ridge (P_1), one of which in situated lingually and the other buccally (Delezene 2016; Lease 2016: 104-105; Martinón-Torres and Bermúdez de Castro 2016).

The occlusal surfaces of human molars, in contrast to the other teeth, are relatively flat; cusps do not form cutting edges, and show only moderate differences in elevation (Lease 2016: 106-107). This morphology is different to that seen in many other mammals; for example: the molars of insectivores possess exaggerated, sharp ridges that connect the buccal cusps; enlarged and jutting cusps are often found in carnivorous mammals; while infolding ridges, interspersed with depressions, fuse the molar cusps together in many herbivores (Cuozzo 2016: 44; Hillson 2005: 15-18). Humans, meanwhile possess a *bunodont* pattern with low and rounded cusps that is often associated with the necessary mobility at the temporomandibular joint to elevate, depress, protrude and retract the jaw; this set of characteristics collectively permits the crushing, grinding and shearing of the diverse foodstuffs associated with an omnivorous diet (Nystrom 2019: 26; Cuozzo 2016: 44; Hillson 2005: 17-18). This basic patterning in crown morphology, in addition to root traits, can be used to identify and categorise teeth and is indicative of highly conserved but functional evolutionary adaptations (Cuozzo 2016; Irish 2016a; Lease 2016; Hillson 2005; White and Folkens 2005: 127-152; Koppe and Swindler 2004; Scott and Turner 1997: 20-24).

3.2.3 Developmental Schedule

The timing of tooth growth, or *odontogenesis*, is remarkably stable, even under adverse environmental pressures. H. M. Liversidge and colleagues, for example, have shown that there is little variance in timing between stressed and unstressed groups. This was demonstrated through a cross-sectional comparison of over two thousand Sudanese subadults grouped according to whether their body mass index and height-for-age were indicative of chronic malnutrition according to World Health Organisation standards (Elamin and Liversidge 2013). Radiographic assessment of permanent crown and root growth was graded following the developmental stages of Moorrees *et al.* (1963) and it was found that individuals whose body proportions suggested long-term under nourishment did not differ significantly from the unstressed group in the mean age at which they entered a particular dental developmental stage or the mean length of time spent in that stage (Elamin and Liversidge 2013: 2-4). Comparative studies between populations have further shown that developmental schedule is generally consistent across populations. Liversidge *et al.* (2006), for instance, reported that dental maturation among populations of mainly European descent distributed globally was uniform, while Liversidge (2011) found that, even if female maturation schedules were slightly ahead of males, developmental rates between groups of differing ancestry were comparable.

In specific instances, however, studies show that the timing of odontogenesis can vary between individuals, possibly in response to exogenous stimuli. For instance, although Liversidge and Marsden (2010) estimated that there was a 0.945 probability of being at least 18 if M3 crown and root growth was complete, M3 maturation was observed to occur as early as 16 years of age in some individuals and as late as 24 years in others. In addition, full development of the mandibular canine is related to physiological cues and developmental schedules that are potentially influenced by

environmental stressors. Chertkow (1980), for example, noted that mandibular canine root completion did not occur until after peak velocity in pubertal development had been achieved. In a study that compared medieval and modern samples, Lewis *et al.* (2016) reported that although both groups initiated pubertal changes at a comparable age, medieval samples progressed through skeletal and dental indicators of pubertal maturation at a slower rate. Even though secular change could explain this difference (Eiben and Mascie-Taylor 2003), Lewis *et al.* (2016) suggested that stress, including but not necessarily limited to poor nutrition and infection, was responsible.

The earliest forming deciduous crowns are evident in the fifth week post-conception and all deciduous teeth, as well as first permanent molars, begin to form before birth, but crown formation continues throughout infancy and childhood, and for the M3 is not complete until an individual approaches maturity (Brickley *et al.* 2020: 345; Antoine and Hillson 2016: 223-234; Harris 2016: 145; AlQahtani *et al.* 2010; AlQahtani 2009; Christensen and Kraus 1965; Kraus and Jordan 1965). Due to this chronological consistency and span, teeth provide a highly accurate means of estimating age in immature individuals and, given the capacity of biological structures to embody environmental signals, opportunities for researchers to ask questions about specific periods of development (King *et al.* 2018; Halcrow *et al.* 2017; AlQahtani *et al.* 2010; AlQahtani 2009; Moorrees *et al.* 1963; Ubelaker 1989). As such, various projects have employed incremental isotopic analyses to explore themes such as diet and migration over the period of infancy to childhood (e.g., Craig-Atkins *et al.* 2018; King *et al.* 2018; Hemer and Evans 2018; Hemer 2014), while others have utilised defects in enamel and dentine formation (e.g., LEH) as indicators of early-life stress perturbations (Primeau *et al.* 2015; Holt *et al.* 2012; Reid and Dean 2006). Researchers assessing high-resolution histological sections, for instance, have been able to identify the neonatal line – a stress

accentuated striation coincident with birth – in human and hominoid teeth, including maxillary and mandibular first permanent molars, and by using striae counts that correspond to circadian rhythms in enamel deposition, estimate postnatal lifespan (Brickley *et al.* 2020: 344-345; Smith *et al.* 2010).

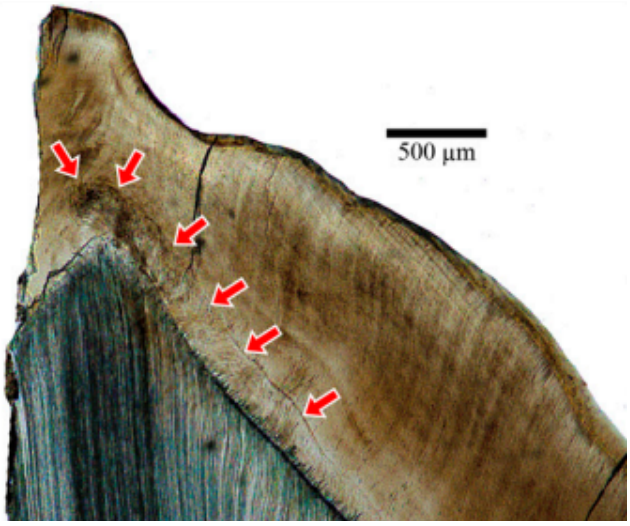

Figure 3.3 A sectioned M_1 with the neonatal line highlighted (Kelley and Schwatz 2009: 1036)

3.2.4 Summary

From this review, firstly it is apparent that tooth structure is complex but functional. Thus, teeth can be differentiated into various fields, each of which is characterised by a function and a set of role-specific morphological adaptations. Secondly, as the timing of odontogenesis is comparable across populations, dental materials can act as a window onto specific periods of development, largely free from geographic, historic or cultural biases (AlQahtani *et al.* 2010; Smith *et al.* 2010; AlQahtani 2009). Crucially, the formation of M1s spans a period critical in determining life-course trajectories – the foetal and early-postnatal period – and it may therefore be posited that the analysis of this tooth can be used to make inferences regarding the dynamics affecting individuals and populations during this time (King *et al.* 2018; Halcrow *et al.* 2017; Primeau *et al.* 2015; Smith *et al.* 2010).

3.3 Molar Crowns

To expand upon the previous section, the morphological features that define molars are described in more detail. To fully explore the range of molar variation, attention is paid to morphological traits that occur both more and less commonly. To facilitate this, further terminology and a brief history of its development is introduced.

3.3.1 Morphology

An M^1 possesses four cusps arranged in rhomboid-like shape (Ungar 2016: 30; Scott and Turner 1997: 16-19; Wood *et al.* 1983). The names used to identify these cusps were introduced by H. F. Osborn (1888b) and form part of a body of work conducted by himself (Osborn 1907, 1897, 1888b, 1888a) and his predecessor E. D. Cope (1888, 1874). The Cope-Osborn model proposed that the three main cusps in the both maxillary and mandibular molars were homologous. In archaic mammals, according to Osborn, maxillary molars were originally composed of a single cusp, the *protocone*; later, two more cusps developed buccally – the *paracone* and *metacone* – to form a *trigon* which was well-adapted to processing a diverse range of foodstuffs. Cope and Osborn further asserted a fourth cusp, the *hypocone*, formed later on a shelf called the *talon*. This configuration of maxillary cusps (Figure 3.4) has the protocone placed in the mesiolingual portion of the tooth, opposite the mesiobuccal paracone; the metacone is distobuccal and the hypocone is distolingual (Ungar 2016: 29-30; Hillson 2005: 14-17; Scott and Turner 1997: 16-17).

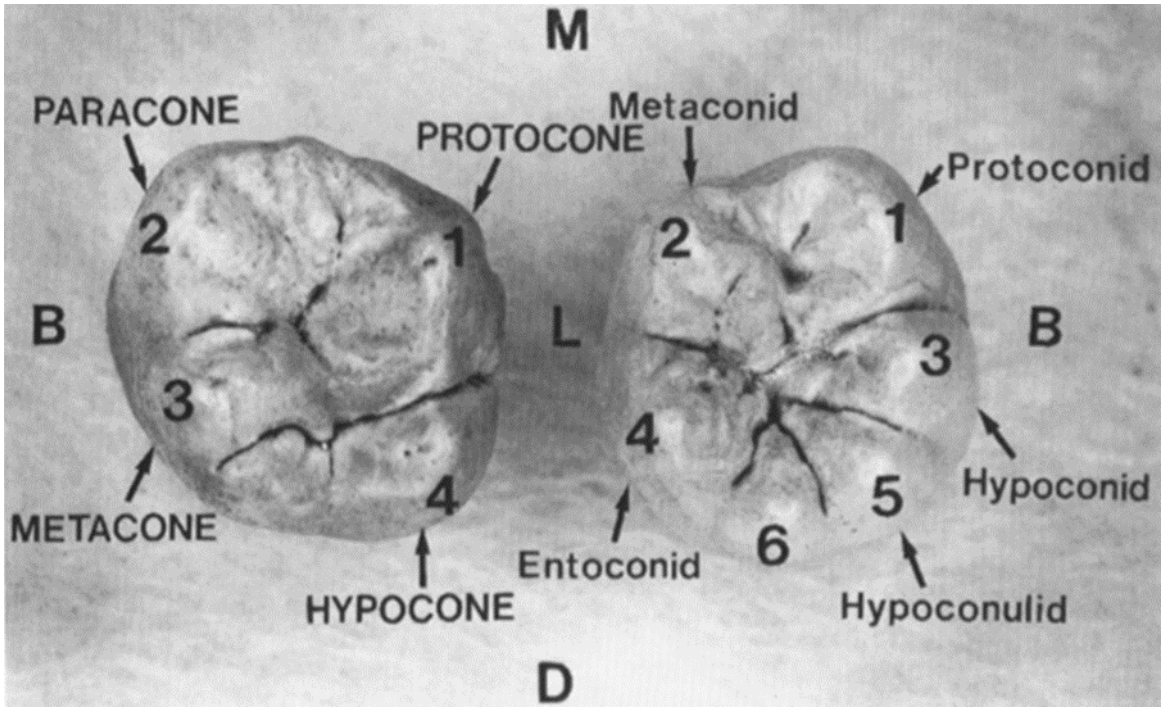

Figure 3.4 The names and numbers of molar cups. On the left is an M^1 with its four cusps labelled while on the right is an M_1 with five main cusps plus a supernumerary Cusp 6. M= mesial, D= distal; L= lingual; B= buccal (Scott and Turner 1997: 18).

Although, the M_1 has four major and one minor cusp arranged in a roughly rectangular pattern (Ungar 2016: 30; Scott and Turner 1997: 16-19; Wood *et al.* 1983), Osborn (1888b) hypothesised a similar evolutionary pathway was followed, and added the suffix "id" to the names of the cusps to distinguish between isomeres. So, in the mandible, the *protoconid* was the first cusp to develop, followed by the *paraconid* (which was to be later lost) and *metaconid* to form a trigonid; however, unlike in the maxilla, these later cusps were rotated lingually. A later *talonid* formed distally on which three cusps developed – the *entoconid*, *hypoconid* and *hypoconulid*. This places the protoconid mesiobuccally and the metaconid mesiolingually; the hypoconid is distobuccal and opposite the distolingual entoconid; most distal of all and relatively sagittal is the hypoconulid (Ungar 2016: 29-30; Gómez-Robles *et al.* 2011; Hillson 2005: 14-17; Scott and Turner 1997: 16-17). Several of the assumptions made by the Cope-Osborn model have transpired to be incorrect, however. For example, the original maxillary molar cusp

was the paracone, and, more importantly for comparative studies, isomeric opposites are not homologous. Despite this, the naming conventions have persisted and are widely employed to identify and describe basic molar morphology (Ungar 2016: 29-30; Hillson 2005: 14-17; Scott and Turner 1997: 16-17; Wood *et al.* 1983; Gregory 1916).

As previously mentioned, molars also possess a common pattern of ridges, fissures and fovea. A *sagittal fissure* with *mesial* and *distal fovea* divides the mesial and buccal cusps of an M^1. The sagittal fissure is intersected by *buccal* and *lingual fissures* that separate the mesial and distal cusps. Connecting the maxillary protocone and hypocone, and interrupting the sagittal fissure to a greater or lesser extent, is an oblique ridge – the *crista obliqua* (Hillson 2005: 276-277; Robinson *et al.* 2002; Wood *et al.* 1983). Similarly, on an M_1 the lingual and buccal cusps are divided by a long, centrally-located fissure, the *mesial longitudinal fissure*, which is initiated mesially and terminates distally with the *mesial* and *posterior fovea*. The mesial longitudinal fissure is punctuated three more times: first when it forms a junction with the *mesiobuccal fissure* which divides the metaconid and entoconid; again, when it is intersected by the *lingual fissure* that separates the protoconid and hypoconid; and finally, at the point where it meets the *distobuccal fissure*, which runs between the entoconid and the hypoconulid (Gómez-Robles *et al.* 2011; Hillson 2005: 276-277; Wood *et al.* 1983).

To exclusively focus upon the pattern of homologous molar features would, however, under-represent their variability (Hunter and Guatelli-Steinberg 2016; Scott *et al.* 2016; Scott and Turner 1997; Turner 1970). For instance, molars are noted for supernumerary features such as Carabelli's cusp (Figure 3.5). This cusp, which when observed is located on the lingual aspect of the M^1 protocone, shows a distinct ancestral bias in presence (Irish 2016b: 269; Scott and Turner 1997: 318-324; Townsend and Brown 1981; Von Carabelli 1842). Furthermore, when expressed, it can be detectable as

anything ranging from a small depression through to a well-developed feature that significantly distorts the occlusal outline (Martinón-Torres and Bermúdez de Castro 2016: 70; Scott *et al.* 2016: 250; Swindler 2002: 160-161; Scott and Turner 1997: 24-25). Variation in trait morphology is not limited to the presence or absence of supernumerary cusps, however. In European populations – which are noted for dental "simplification" – it is not uncommon for major cusps to be reduced, or sometimes even lost in the distal arcade (Hunter and Guatelli-Steinberg 2016: 492; Scott *et al.* 2016: 252; Turner 1970). In Western European populations, for instance, although the hypoconulid is present on the vast majority of M_1, it is absent in 71.1% of individuals on the M_2 (Scott and Turner 1997: 322). Given this inherent variability, evaluations of molar morphology require a careful selection of methods if comparisons are to be made within and between populations.

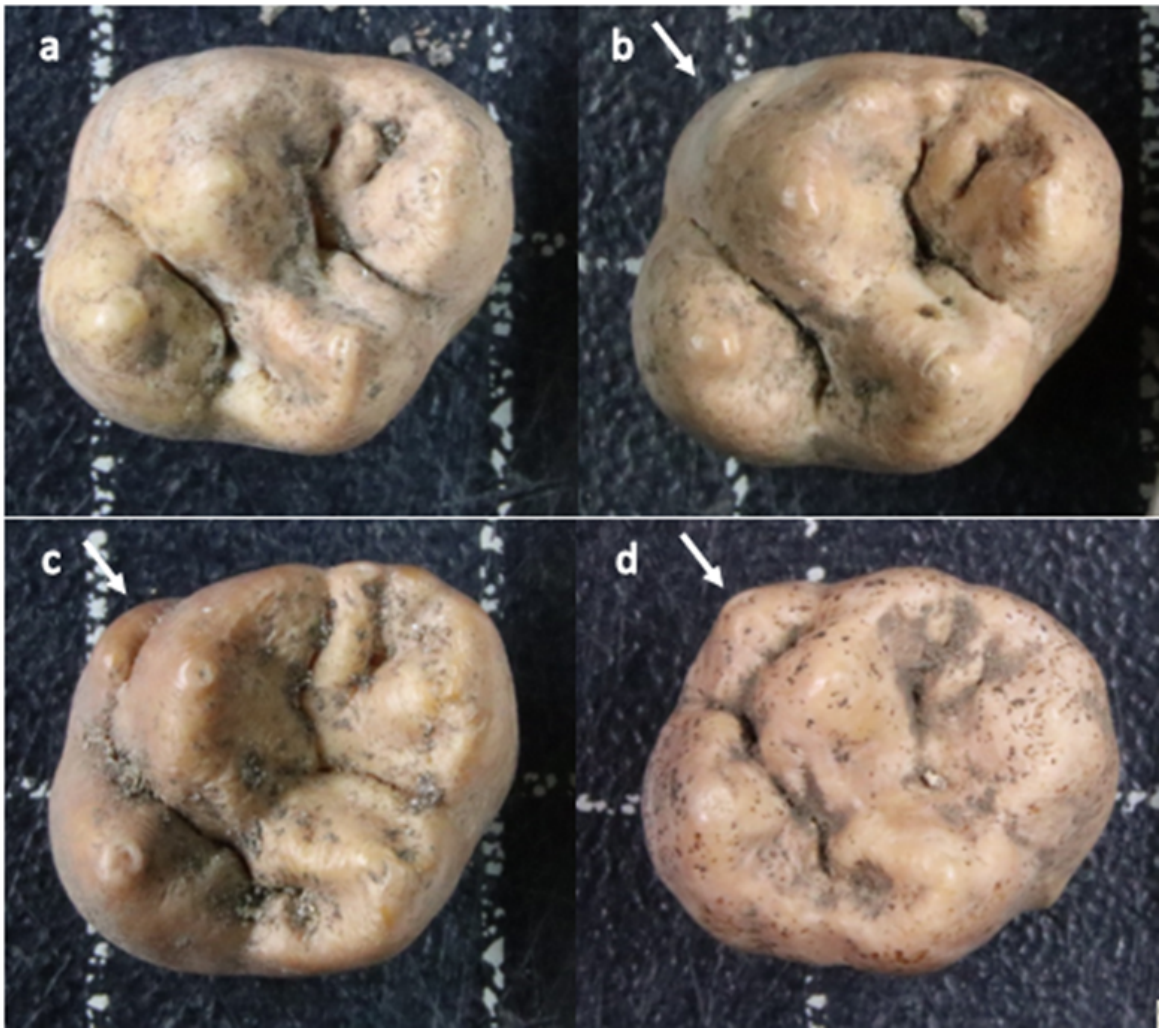

Figure 3.5 Carabelli cusps are variably expressed. They may be absent (a), present as a groove (b), a small cusp (c) or a large cusp which alters the tooth's occlusal outline substantially. Expression also varies throughout the dental arcade with Carabelli cusps, and supernumerary traits in general, being more common and distinct mesially than distally.

It has also been debated to what extent morphological characteristics may be expressed differently on the crown's occlusal surface and at the DEJ. Studies, for instance, have reported that supernumerary cusps and ridges observable on the DEJ can be absent, or "enameled over", on the corresponding occlusal enamel surface (OES) (Bailey *et al.* 2011; Scott and Turner 1997: 87-89; Korenhof 1982; Korenhof 1961; Korenhof 1960; Sakai *et al.* 1967; Kraus 1963). This is particularly problematic as the morphogenetic events which determine dental shape occur at the dental epithelium which is most directly preserved at the DEJ (Hunter and Guatelli-Steinberg 2016: 493) (Section

3.4.1). However, in the most comprehensive study of the issue, using microCT scans Bailey *et al.* (2011) found that there was generally agreement between the presence and absence of features on the occlusal enamel surface and the DEJ. In a sample of various hominids, a Spearman rank correlation coefficient quantified concordance at r_s=0.91 (discussed further in Section 4.2.2) (Bailey *et al.* 2011: 513-515).

3.3.2 Summary

In sum, there exists a basic pattern of features in molars – four major cusps on the M^1 and five on M_1 separated by fissures, ridges and fovea – which are common to all human populations and homologous between antimeres (Hillson 2005; Scott and Turner 1997; Wood *et al.* 1983). The anatomical features which define molars are also interrelated; fovea form where fissures intersect, and fissures develop where cusps grow next to one another (Scott *et al.* 2016: 250; Scott and Turner 1997: 24-25). These similarities, however, belie a vast array of non-homologous morphological variants (Irish 2016b; Martinón-Torres and Bermúdez de Castro 2016: 70; Swindler 2002: 160-161; Scott and Turner 1997; Townsend and Brown 1981). Therefore, it is hypothesised that molar crowns can be best explored through procedures capable of evaluating both homologous and non-homologous morphological features.

3.4 Molar Crown Formation

The extent to which variations in molar morphology are the result of endogenous programming and external stimuli has, however, been debated (e.g., Hughes and Townsend 2013; Jernvall and Jung 2000; Brook 2009). This section describes odontogenesis and critically reviews research conducted on the role of genes and environmental signals on the development of coronal features in molars.

3.4.1 Stages of Tooth Development

The embryonic mouth forms after a process of cell proliferation and apoptosis as well as tissue infolding which gives rise to primitive maxillary and mandibular arches, known as the dental lamina. The laminae are composed of a layer of epithelial cells covering mesenchyme (Hillson 2005: 208). Although a continuous process, crown formation can be divided into three broad stages – the *bud*, *cap* and *bell* stages – that are characterised by cell production and differentiation that lead to morpho- and histodifferentiation (Harris 2016: 145; Scott and Turner 1997: 76). It is during the bud stage (sometimes referred to as the *initiation* phase), that a swelling of epithelial cells, the presumptive enamel organ, penetrates the lamina and a pocket of ectomesenchymal cells forms beneath it to become the dental papilla – together this structure is the tooth germ. For the earliest forming permanent teeth this occurs at approximately sixteen weeks *in utero*, while for later growing teeth this process begins postnatally (Antoine and Hillson 2016: 224; Harris 2016: 146-147; Hillson 2005: 208; Hillson 1996: 118). Cell proliferation during the cap stage (alternatively known as *morphogenesis*), leads to a differentiation of the enamel organ into four distinct layers: the *outer enamel epithelium*; the *stellate reticulum*; the *stratum intermedium*; and the *inner enamel epithelium* (Figure 3.6). The enamel organ is further separated from the dental papilla by a basement

membrane; formation of this membrane, is a morphological milestone as the outline of crown shape and size are largely determined by this structure (Antoine and Hillson 2016: 224; Harris 2016: 147; Scott and Turner 1997: 77; Simmer *et al.* 2010; Butler 1956: 33-34). It is also in the cap stage that a primary enamel knot forms in the stellate retinaculum at the formative cusp apex; in multi-cusped teeth the primary knot creates secondary knots which go onto form secondary cusp apices (Harris 2016: 147; Jernvall and Jung 2000: 178; Jernvall *et al.* 1994). Finally, during the bell stage (or *histogenesis*), dentine formation at the inner enamel epithelium forms a template for subsequent enamel deposition (Antoine and Hillson 2016: 224; Harris 2016: 147-148).

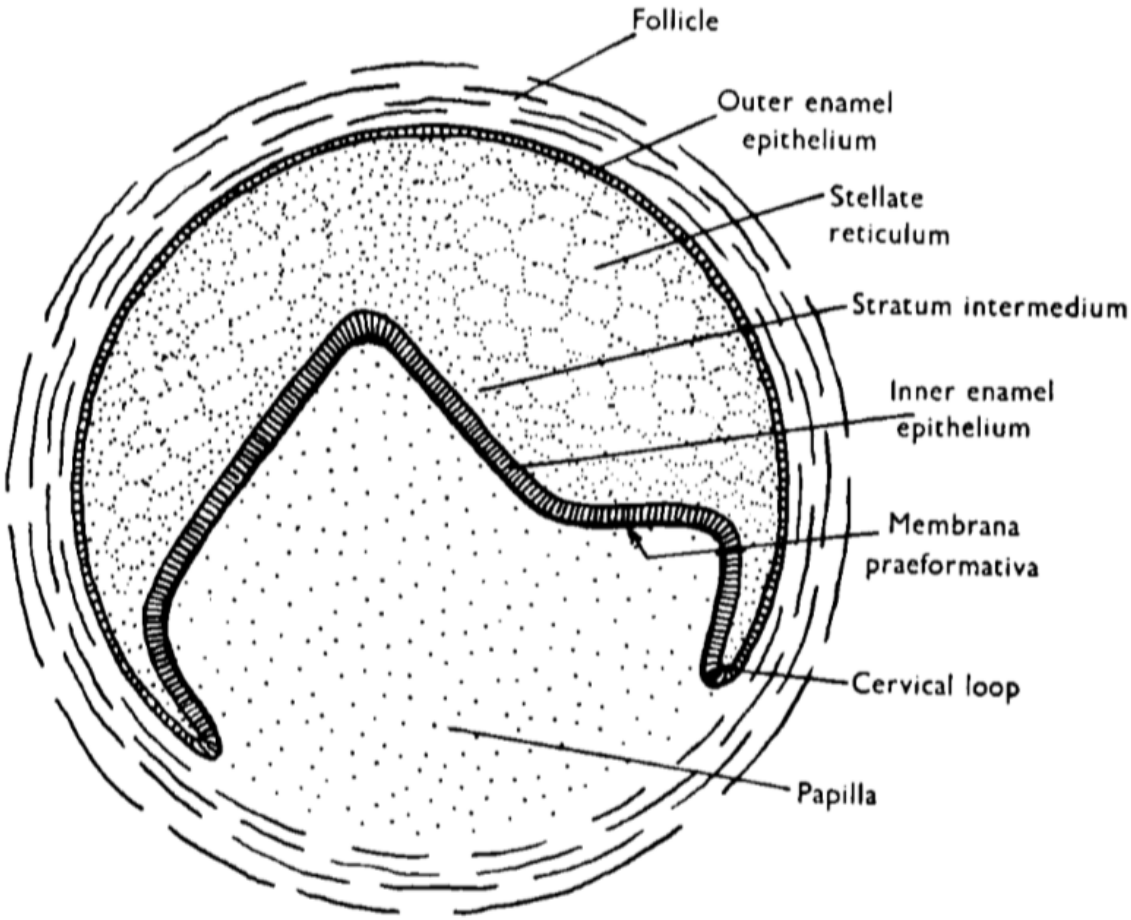

Figure 3.6 The anatomy of the developing tooth germ in cross section (Butler 1956: 33).

3.4.2 Genetics and The Patterning Cascade Model of Cusp Development

Genes play a central role in the development of dental morphology, providing the rationale for employing dental traits in biodistance analyses and which is demonstrated by twin studies (Hughes and Townsend 2013: 56-57; Irish 2011; Hasegawa *et al.* 2010; Irish 1998; Irish 1997; Alt and Vach 1995; Alt and Vach 1993; Turner 1990; Scott 1980). Townsend and colleagues, for example, have evaluated the relationship between expression of a Carabelli cusp on the M^1 in dizygotic (DZ) and monozygotic (MZ) twins, and consistently found that there are higher correlations between MZ twins, with trait heritability estimated to between *circa* 80-90% (Hughes and Townsend 2011; Townsend and Martin 1992). Research exploring the genetic mechanisms which control dental development has, nevertheless, suggested that the role of genes is not simple, but dependent upon many interactions in multi-layered systems that generate a great deal of variability in multi-cusped teeth, such as molars. Even though this is still an active field, it has emerged that hundreds of genes from several gene groups are expressed in the underlying mesenchyme of the dental papilla and the primary enamel knot (Lynnerup and Klaus 2019: 53; Brook *et al.* 2014; Tamura and Nemoto 2016; Rizk *et al.* 2013: 139; Brook 2009; Holland *et al.* 2007; Tucker *et al.* 2004; Jernvall and Jung 2000).

Though a full rendition of the physiological mechanisms that influence gene expression in the early stages of dental growth is beyond the scope of this thesis, the activities and interactions of a group of genes known as Fibroblast growth factors (*Fgfs*) are given as an illustrative example. Thanks to the research emanating from collaborative projects, in which J. Jernvall, P. Thesleff and I. Kettunen have important roles, a good deal is known about the presence and role of *Fgfs* and their interactions with other gene families, such as the Sonic hedgehog (*Shh*), Bone morphogenic protein (*Bmp*), and Wingless-integrated (*Wnt*) groups (Du *et al.* 2018; Jernvall and Jung 2000; Jernvall and

Thesleff 2000; Kettunen *et al.* 2000; Kettunen *et al.* 1998; Jernvall *et al.* 1994). It appears that four *Fgf*s in particular are noteworthy in dental morphogenesis: *Fgf3*; *Fgf4*; *Fgf9*; and *Fgf10*. Expression of these genes is complex: some are found only in the mesenchyme (*Fgf10*) or the enamel knot (*Fgf4* and *Fgf9*) while others occur in both (*Fgf3*); three are present from the bud stage (*Fgf3*, *Fgf4* and *Fgf9*), while one is not expressed until the cap stage (*Fgf10*). Though growth is not solely regulated by *Fgf* genes, the protein products of *Fgf*s stimulate cell division and initial development of the tooth germ; their spatial and chronological patterning ensure that growth is unequal and partially accounts for variations in cusp elevation and size (Jernvall and Jung 2000; Jernvall and Thesleff 2000; Kettunen *et al.* 2000; Kettunen *et al.* 1998; Jernvall *et al.* 1994). As they are expressed in the primary enamel knot, this biological landmark has been implicated as a key signalling centre for tooth germ development (Jernvall and Jung 2000: 177) (Figure 3.7).

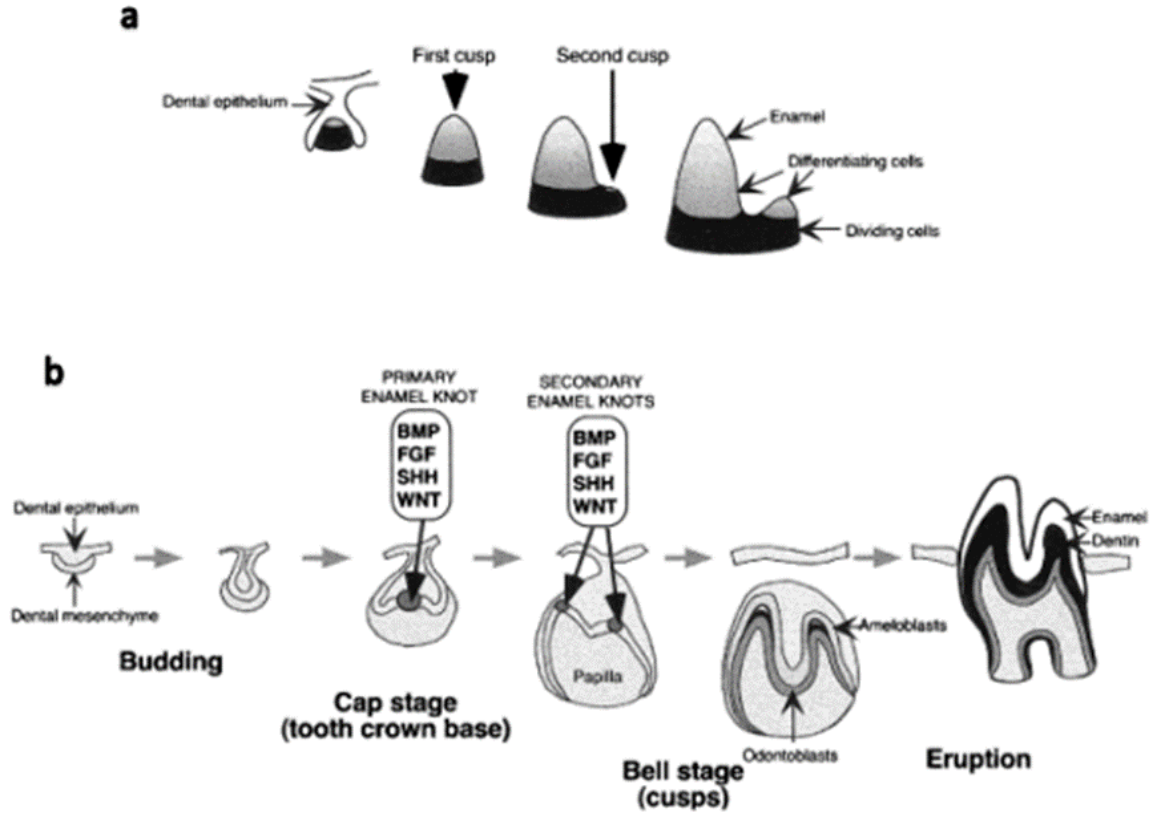

Figure 3.7 Processes involved in cusp patterning (Jernvall and Jung 2000: 176). During the cap stage, cusps form because of unequal cell growth on the inner enamel epithelium (shaded) promoted by signals from enamel knots (a). The stages and signals crucial for cusp growth (b).

Fibroblast growth factors do not, however, operate independently and the growth of the primary and secondary enamel knots – in a process comparable to that observed in the spacing of feather primordia – appears to be determined by a combination of stimulatory and inhibitory genes in a reaction-diffusion mechanism in the late cap and early bell stages (Liu *et al.* 2008: 219; Jernvall and Jung 2000: 179; Jernvall and Thesleff 2000). Jung *et al.* (1998), for example, found that proteins produced by *Fgf* in conjunction with *Shh* genes at primary signalling centres stimulated local tissue development, before also promoting the production and diffusion of *Bmp* genes. As *Bmp* protein products inhibit the activation of *Fgf* and *Shh* genes and spread diffusely, the appearance of new centres of growth is initially inhibited. However, *Bmp* products eventually reduce production of *Fgf* and *Shh* in the signalling centre from which they originate and thus ultimately stimulate the appearance of new sites of development. Activation of *Bmp*s, furthermore, is thought to increase mesenchymal receptivity to genes of the *Wnt* group which are essential to tissue growth and thus permit secondary knot appearance (Du *et al.* 2018; Tamura and Nemoto 2016; Liu *et al*. 2008; Klein *et al.* 2006; Jernvall and Jung 2000: 176; Jernvall and Thesleff 2000: 22). In sum, each enamel knot in its early development suppresses the initiation of other knots, however, towards the periphery of the inhibition field there is the potential for new knots, and therefore cusps, to form (Figure 3.8). Consequently, the size and spatial relationships between enamel knots (later cusps) are the result of multi-layered and interactive gene networks which are most evident in larger, multi-cusped teeth (Lynnerup and Klaus 2019: 53; Tamura and Nemoto 2016; Riga *et al.* 2014: 398; Rizk *et al.* 2013: 139; Hunter *et al.* 2010: 1; Brook 2009; Salazar-Ciudad and Jernvall 2002; Jernvall and Jung 2000). This explanation of cusp development is known as the Patterning Cascade Model (PCM) (or the Salazar-Ciudad

and Jernvall Model) (Hunter *et al.* 2010; Brook 2009; Salazar-Ciudad and Jernvall 2002; Jernvall and Jung 2000).

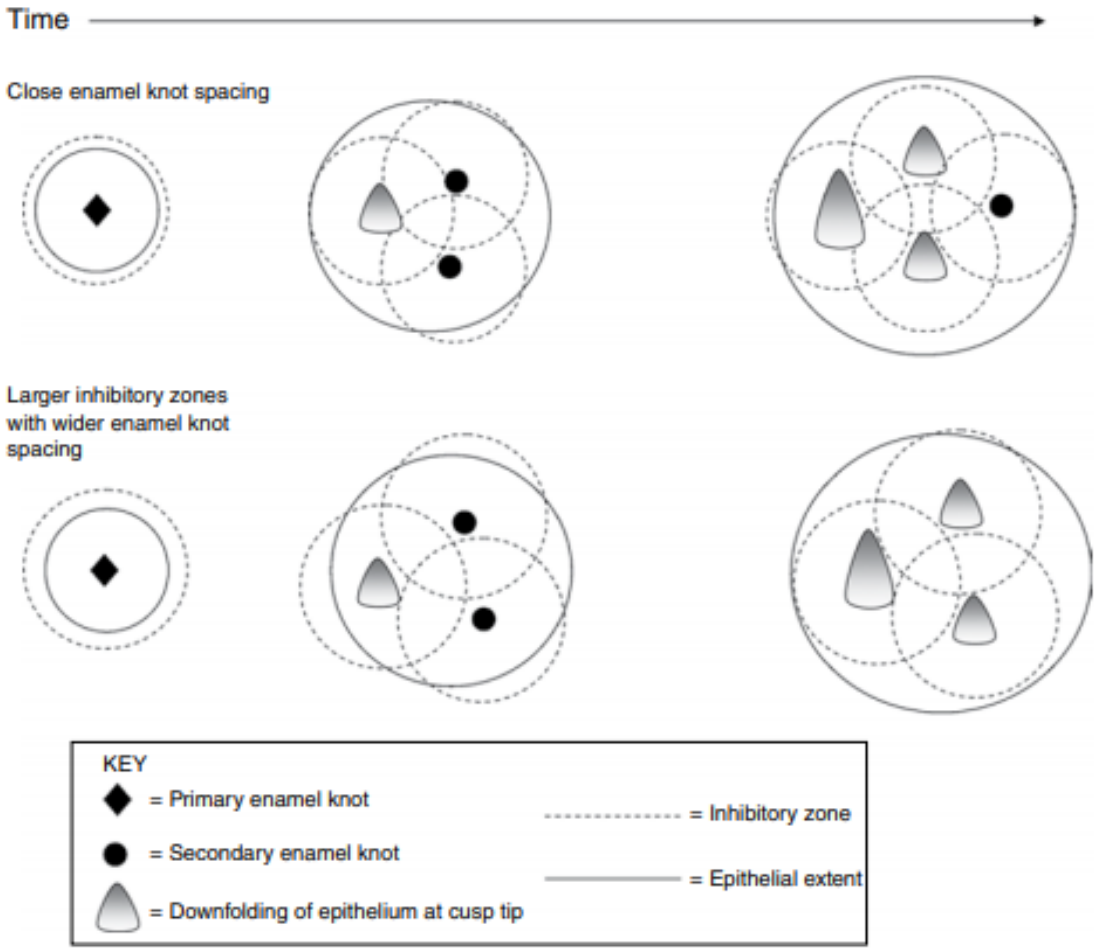

Figure 3.8 The Patterning Cascade Model of morphogenesis. The top row shows the growing dental epithelium with closely spaced enamel knots at three successive time points. After the primary enamel knot forms, secondary enamel knots develop only when the dental epithelium expands beyond the primary knot's inhibitory zone. Further knots may grow past the inhibitory field of the secondary knots. The bottom row illustrates the same process, however, larger inhibitory zones around enamel knots prevent or reduce the formation of further knots and therefore cusps (Hunter and Guatelli-Steinberg 2016: 489).

Much of the research that has led to the development of this theory has been carried out on mice, and its applicability to humans – and even other mammals – may be questioned. Nonetheless, it has been possible to test the expectations of this model by observation and results suggest that a cascade of molecular events does indeed determine cusp development in humans too (Hunter *et al.* 2010; Hlusko and Mahaney 2009: 6; Harris 2007; Kondo and Townsend 2006; Townsend *et al.* 2003; Salazar-Ciudad and

Jernvall 2002; Jernvall and Jung 2000). For instance, Hunter *et al.* (2010: 2) tested assumptions of the PCM by predicting a negative trend relating to the distances between main cusps and the presence of additive crown traits (i.e., when distances between the main cusps were small, there would be greater development of supernumerary cusps). From 376 M^1s, tooth and cusp area were calculated, intercusp distances were measured between the four main cusps (protocone, paracone, metacone and hypocone), and Carabelli cusp trait development was graded ordinally on a scale of 0-7 (absent to well-developed) (Hunter *et al.* 2010: 6). Hunter *et al.* (2010: 3-6) found that there was a significant negative correlation between Carabelli cusp development and mean intercusp distances and that Carabelli cusp area was also negatively related to mean intercusp distances. These results suggested that closely packed enamel knots during morphogenesis, indicated by reduced intercusp distances, provided conditions that increased the likelihood of new enamel knots breaking free of inhibitory fields and developing on the periphery of the tooth germ (Hunter *et al.* 2010: 5-6). Subsequent studies also revealed that the development of Carabelli cusps positively covaried with the development of other accessory cusps, further suggesting that cusp growth is the result of a single integrated mechanism, namely the PCM (Hunter and Guatelli-Steinberg 2016: 491; Moormann *et al.* 2013).

3.4.3 Stress and the Patterning Cascade

As with any complicated process involving both synergistic and antagonistic signals, the development of enamel knots and cusps is vulnerable to external interferences. Furthermore, with an iterative and interlinked nature, it is expected that "errors" ripple down the developmental cascade, increasing polymorphisms (Riga *et al.* 2014: 399; Jernvall 2000). As such, knock-out studies in animal subjects have found that where expression of a particular gene has been completely suppressed experimentally,

cusps or entire teeth are absent or abnormally formed, producing a phenotype comparable to that of a congenital disorder (Brook 2009; Tucker *et al.* 2004). Although more subtle, stress-induced alterations are difficult to chart experimentally, it is possible to infer the relative contributions of genetics and environmental stressors through studies of the final crown size and the morphological patterning of cusps (Riga *et al.* 2014; Brook 2009; Townsend *et al.* 2009; Tucker *et al.* 2004; Koppinen *et al.* 2001).

Results of such projects consistently suggest that environmental stressors influence morphogenesis. In twins, Dempsey and Townsend (2001) discovered that unique environmental factors generally accounted for 8-29% of variation in mesiodistal (MD) and buccolingual (BL) crown diameters. Environmental influences were strongest in molars, however, especially the M^1 where heritability in size was only estimated to be between 56-61% (Dempsey and Townsend 2001: 690). Similarly, Stojanowski *et al.* (2017) reported that average heritability for MD crown diameters was 51% in related individuals from the historic Gullah population. Heritability was much lower, however, in M^1 (46%) and M_1 (22%) diameters, and for the latter was not even significant, indicating the strong influence of non-genetic factors (Stojanowski *et al.* 2017: 509-510). Although the differences between heritability estimates in Dempsey and Townsend (2001) and Stojanowski *et al.* (2017) could be the result of differing methodologies, they may also relate to each sample's stress levels; the Gullah were politically and economically marginalised and therefore exposed to elevated socioenvironmental pressures (Stojanowski *et al.* 2017; Guatelli-Steinberg *et al.* 2006). Meanwhile, in a morphological analysis, Riga *et al*. (2014) used a stress indicator (LEH), to separate an historic sample into stressed and unstressed groups to test the hypothesis that developmental errors were transmitted down the cascade of reactions that occur during odontogenesis. To achieve this, the later forming main (metacone and hypocone) and accessory (Cusp 5, parastyle

and Carabelli's trait) M^1 cusps were graded ordinally. Findings showed greater variability in cusp development among the stressed group – e.g., in the unstressed group M^1 Carabelli traits were graded between 0-4, but 0-7 for the stressed (Riga *et al*. 2014: 400). When results were visualised, the output showed that unstressed individuals formed a cluster, whereas, the stressed group were diffusely distributed (Riga *et al*. 2014: 401).

Taken together, this evidence supports the PCM's picture of cusp development as ''a cascade of epigenetic events'' (Hunter *et al.* 2010: 5; Townsend *et al.* 2003: 355). In multi-cusped teeth it is posited that the spatial relationships of enamel knots at the inner enamel epithelium are result of multi-layered and iterative genetic relationships which are vulnerable to environmental cues (Hunter *et al.* 2010; Salazar-Ciudad and Jernvall 2002; Jernvall and Jung 2000). Due to the interrelated and sequential nature of enamel knot growth, stressors are not compartmentalised and their influences flow throughout the process of morphogenesis, with the consequence that later cusp and crown morphology embodies an accumulation of contextually influenced polymorphisms; unsurprisingly, this appears to be most pronounced in the teeth with most cusps – first permanent molars (Stojanowski *et al.* 2017; Riga *et al*. 2014; Dempsey and Townsend 2001; Jernvall and Jung 2000; Jernvall and Thesleff 2000; Jung *et al.* 1998). Though the mechanism theorised to be responsible for mediating genetic and environmental influences in teeth has been difficult to experimentally manipulate, it appears that the PCM is responsive to general physiological stress rather than specific stimuli (Nilsson *et al.* 2018; Vaiserman 2015; Brook 2009; Skinner 2008; Tucker *et al.* 2004; Koppinen *et al.* 2001; Escós *et al.* 2000: 331; Selye 1973).

3.4.4 Amelogenesis

The formation of enamel, or *amelogenesis*, which occurs in the bell phase, is part of a relatively well-understood process of cell differentiation which occurs once the underlying cusp pattern and crown form have been established (Tamura and Nemoto 2016: 78; Brook 2009: S6; Jernvall and Jung 2000: 180; Jernvall and Thesleff 2000; Jung *et al.* 1998). Amelogenesis, which can be separated into overlapping *production* and *maturation* phases, is undertaken by specialist cells, known as ameloblasts, that differentiate from the internal enamel epithelium. Ameloblasts are tall, columnar secretory cells that are arranged in rows and lay down an enamel matrix in the production phase (Antoine and Hillson 2016: 224; Hillson 2005: 155). Initially, enamel matrix is a near equal mix of water, protein and hydroxyapatite crystals. The crystals have different alignments which results in a prismatic enamel structure that can be divided into easily demarcated rods (Antoine and Hillson 2016: 224; Hillson 2005: 155; Ten Cate 1998; Boyde 1989; Boyde 1976). As a result of this prismatic structure, the movement of the enamel forming front remains visible in the mature enamel through the presence of darker coloured *striae of Retzius*, which can be observed most easily on the labial surfaces of the anterior dentition as a series of grooves known as *perikymata* (Lynnerup and Klaus 2019: 753; Hillson 2005: 161-163; Risnes 1984; Retzius 1837) (Figure 3.9).

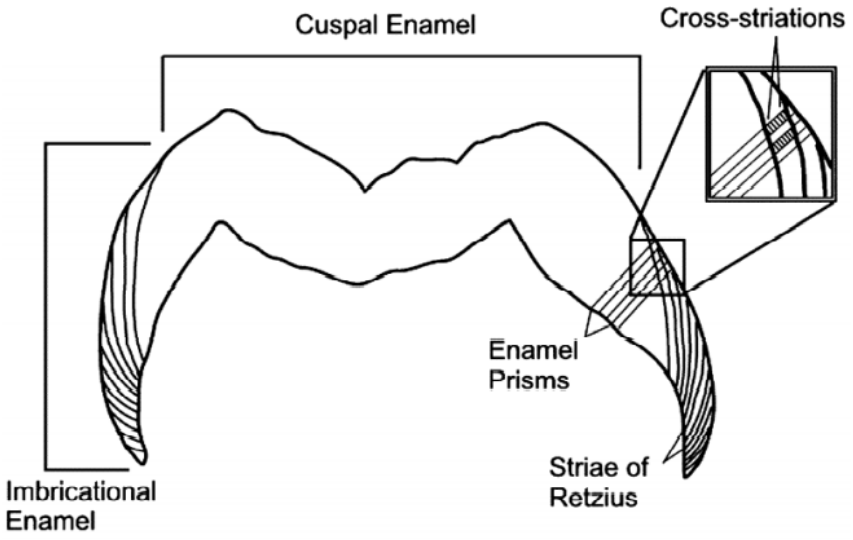

Figure 3.9 Section of a molar tooth illustrating the various divisions and incremental structures found within the enamel matrix (Smith *et al.* 2003).

Under a microscope, even finer *cross striations* can be seen in the enamel prisms of transversely sectioned teeth which preserve a record of the circadian rhythms of enamel deposition (Hillson 2005: 159-160; Antoine *et al.* 1999; Dean 1998). The cusp tips, being analogous to centres of ossification in bone, are formed first with successive dome-like increments of enamel laid down to form what is referred to as *cuspal enamel* (Brickley *et al.* 2020: 344; Hillson 2005: 161-163; Butler 1956: 41). Once full cusp height is achieved, the ameloblasts at the apex enter the maturation phase, whereby the organic and water content of the matrix is gradually reduced and hydroxyapatite crystals increase in number and size. Meanwhile, the active front of matrix production becomes sleeve-like and moves apically – to produce what is called *imbricational* or *lateral enamel* – in order to complete crown formation, which is finalised when the last-formed enamel in the cervical region is mineralised (Brickley *et al.* 2020: 344; Antoine and Hillson 2016: 225; Hillson 2005: 155-163). Once the maturation phase is complete, though attrition can obscure and erode crowns, dental materials do not remodel and

remain completely inert (Brickley *et al.* 2020; Lynnerup and Klaus 2019; Hillson 2005; Nystrom *et al.* 2004; Smith 1984).

3.4.5 Summary

The spatiotemporal patterning of enamel knots is determined by a multi-layered and iterative genetic mechanism that is susceptible to environmental influences. As enamel knot patterning forms a blueprint for cusp position and size as well as the locational relationships between cusps, final crown morphology reflects a cascade of stress-influenced processes (Stojanowski *et al.* 2017; Riga *et al.* 2014; Hunter *et al.* 2010; Townsend *et al*. 2002; Dempsey and Townsend 2001; Jernvall and Jung 2000; Jernvall and Thesleff 2000; Jung *et al.* 1998). Although these processes occur in the cap and early bell phase of dental morphogenesis, they are transformed into durable features through amelogenesis in the later bell phase (Stojanowski *et al.* 2017; Riga *et al*. 2014). Excepting wear, dental crown morphology, therefore, preserves a "fossilised" record of stress-induced polymorphic errors; as previously stated, in the case of first permanent molar crowns this is evidence of foetal and early-postnatal experiences (Halcrow *et al.* 2017; Antoine and Hillson 2016; Smith *et al.* 2010; Nystrom *et al.* 2004; Conroy and Kuykendall 1995: 121; Smith 1984).

3.5 Conclusion

After introducing dental anatomy and establishing the terminology employed to describe and compare dental materials, this review has three pertinent findings (Lynnerup and Klaus 2019; Irish 2016a; Hillson 2005; Scott and Turner 1997; Carlsen 1987). Firstly, after discussing dental fields and the timing of dental development, it can be concluded that first permanent molar growth spans the period believed to be critical to determining life-course trajectories in growth and development as well as morbidity and mortality

(i.e., early life) (King *et al.* 2018; Halcrow *et al.* 2017; Primeau *et al.* 2015; Smith *et al.* 2010). Secondly, by describing molars in greater detail, it has been established that the coronal surface of molars is morphologically complex, being composed of many interrelated traits – cusps, fissures, and fovea – and, while there is a core of homologous features, there are also many non-homologous structures (Hunter and Guatelli-Steinberg 2016; Irish 2016b; Scott *et al.* 2016; Hillson 2005; Scott and Turner 1997; Turner *et al.* 1991; Carlsen 1987; Turner 1970). Finally, after evaluating theoretical and empirical evidence, it can be concluded that the spatiotemporal disposition of crown features are likely determined by a complex physiological mechanism which is vulnerable to external stimuli that ripple across the developmental process to produce alterations to coronal phenotype that are fossilised during amelogenesis (Stojanowski *et al.* 2017; Riga *et al.* 2014; Hunter *et al.* 2010; Brook 2009; Salazar-Ciudad and Jernvall 2002; Dempsey and Townsend 200; Jernvall and Jung 2000; Jernvall and Thesleff 2000; Jung *et al.* 1998). It is therefore hypothesised that the complex morphology of M1 crowns offer a window onto the stressors experienced during foetal and early-postnatal life that is best assessed by methods that can evaluate and compare both homologous and non-homologous features.

Chapter 4: Evaluating Dental Morphology

4.1 Introduction

Traditionally, teeth have been assessed through "non-metric" traits and linear measurements (e.g., Barrett *et al.* 2012; Guatelli-Steinberg *et al.* 2006; Scott and Turner 1997). By critically evaluating these approaches it is shown that they lack the reliability and sensitivity to quantify the complexities of dental morphology accurately and precisely (Pilloud *et al.* 2019; Edgar and Rautman 2016; Tyrrell 1999; Nichol and Turner 1986). Following this, with reference to dental case studies (e.g., Kenyhercz *et al.* 2014; Benazzi *et al.* 2011a; Gómez-Robles *et al*. 2011), geometric morphometric (GM) methods are introduced and it is argued that Procrustean techniques represent an improved means of assessing dental morphology (Dryden and Mardia 1998; Bookstein 1991). Next, three forms of bilateral asymmetry are defined, with fluctuating asymmetry (FA) explored in greater detail due to its association with stress (Graham and Ozener 2016; Klingenberg 2015; Graham *et al.* 2010; Van Valen 1962). Finally, it is demonstrated that although dental FA has been employed to investigate socioenvironmental stressors in bioarchaeology, the means employed have been relatively simple and not – despite early calls to do so – substantively linked to measures of stress across the life-course (Barrett *et al.* 2012; Perzigian 1977; Bailit *et al.* 1970). To articulate the viability of Procrustean techniques to fill this research gap, examples are drawn from other disciplines of how FA has been employed as a predictor of later-life outcomes (e.g., Weisensee 2013; Radwan *et al.* 2003; Klingenberg and McIntyre 1998). By establishing the merit of taking a Procrustean approach to investigating FA here, it is possible to discuss the methods employed in data analysis in more detail in Chapter 7.

4.2 Traditional Approaches

4.2.1 History, Development and Successes

Although the analysis of linear measures and angles as well as less standard techniques such as dontoglyphics and Moiré contourography have been employed (the former focusing on features with negative relief such as fissures and the latter employing photographic techniques to produce relief maps of the occlusal surface), the non-metric traits defined by the Arizona State University Dental Anthropology System (ASUDAS) are by far the most popular and widely used method of assessing dental morphology (Irish 2016a; Irish 2016b; Scott 2016; Hughes and Townsend 2013; Tyrrell 2000; Scott and Turner 1997; Turner *et al.* 1991; Zubov and Khaldeeva 1979; Zubov 1977; Zubov 1968). The ASU system treats morphological features as discrete (present/absent) or quasi-continuous (graded on an interval scale) (Scott and Turner 1997; Tyrrell 2000), and has its roots in descriptive works stretching back to the 19th and early-20th century (Gregory 1922; Hrdlicka 1921; Gregory 1916; Von Carabelli 1842). Efforts toward coordinated systemisation, which continued for much of the latter half of the 20th century, were initiated in 1956 when A. A. Dahlberg lamented the lack of standardisation and produced a series of exemplar plaster plaques (Scott 2016: 8) (Figure 4.1). Although Soviet researchers were very active in the field (e.g., Zubov and Khaldeeva 1979; Zubov 1968), much of what was widely produced and persists today comes from Dahlberg and allied researchers (e.g., C. G. Turner and G. R. Scott) associated with Arizona State University (Scott 2016; Kelley and Larsen 1991; Turner *et al.* 1991).

The ASU system remains a popular method because of its practical benefits – e.g., data collection does not require specialist equipment, can be undertaken quickly, and the suite of traits observed can be individualised for each study (Irish and Scott 2016; Delezene 2016; Plavcan 2012; Irish 2011; Tyrrell 1999: 104-105; Irish 1998; Irish 1997;

Turner 1990). Consequently, the ASU system has successfully been used to qualitatively describe dental phenotype (Irish *et al.* 2018; Clement and Hillson 2013; Delezene 2016; Ungar *et al.* 2008; Scott *et al.* 2005; Wood and Abbott 1983). For instance, after observing that *Australopithecus sediba* possessed a diverse "mosaic" of ASUDAS traits, it was proposed that the species occupied an intermediary cladistic niche between *Homo* and east African australopiths (Irish *et al.* 2013; Berger *et al.* 2010). Moreover, a variety of quantitative methods have been employed to evaluate ASU traits. Cladograms and cluster analyses have been popular in the exploration of phylogenetic similarity, while classificatory procedures and distance statistics have proven useful in exploring biological affinities (Irish *et al.* 2018; Scott *et al.* 2018; Irish *et al.* 2017; Nikita 2015; Edgar 2013; Irish *et al.* 2013; Irish 2010; Edgar 2005; Smith 1972; Mahalanobis 1936). Smith's (1972) Mean Measure of Divergence (MMD), for example, was employed to evaluate morphological affinities between Egyptian samples dating from the Neolithic to post-dynastic period with findings suggesting a high degree of gene flow and populational continuity until the Hellenistic period (Irish 2006: 537-539). In short, the ASU system's broad applicability accounts for its continued usage and the commitment many researchers have shown to improving it (e.g., Pilloud *et al.* 2019; Scott *et al.* 2018; Irish 2010; Turner *et al.* 1991).

Figure 4.1 An ASUDAS reference plaque showing the ordinal grading of the M_1 hypoconid (i.e., cusp 5).

4.2.2 Pitfalls and Limitations

Practitioners have, nonetheless, become more aware of the system's limitations. As most traits are graded along an ordinal scale, then binarised into a presence/absence score at predefined breakpoints, results can become distorted (Scott and Turner 1997; Turner *et al.* 1991; Dahlberg 1956). In an evaluation of ridge expression at the DEJ and OES (Section 3.3.1), Bailey *et al.* (2011) found in humans the largest discrepancy in expression was between grades 1 and 2, with absence being determined at ≤1 and presence at ≥2. Thus, when results are dichotomised, the discordance between trait expression at the DEJ and OES may be exaggerated, even though a correlation coefficient of 0.77 indicated a strong correspondence between features apparent on the DEJ and occlusal surface when graded ordinally (Bailey *et al.* 2011: 513). Furthermore, although grade simplification is intended to reduce inter-observer error, its subjectivity can yield large discrepancies in trait frequencies between observers (Hasegawa *et al.* 2010; Nichol and Turner 1986; Mizoguchi 1985: 508). Lloyd Jones (1994), for example, reported the M^1 hypocone to be ubiquitously present in the Queensfield Farm assemblage, while Tyrrell (1999) found it to be present on only 28.3% of individuals. More concerning are low estimates of intra-observer reliability (Pilloud *et al.* 2019; Edgar and Rautman 2016; Tyrrell 1999). Nichol and Turner (1986), for instance, estimated intra-observer reliability in the grading of the M_1 protostylid to be 0.083, while Pilloud *et al.* (2019: 952) found this trait to achieve an intraclass correlation coefficient (ICC) of only 0.018 [95% CI: 0.065, 0.16].

Additionally, the quantitative methods employed to assess dental non-metric traits have come under increasing scrutiny and criticism. The statistical power of distance statistics, such as MMD, is questionable and there is a lack of consensus as to when divergences from central tendency are significant (Irish *et al.* 2018: 4; Alsoleihat 2013;

Irish 2010; Riani *et al.* 2009; Dos Santos Dias and Kageyama 1998; Leese and Main 1994). Additionally, there has been a great deal of variability in the selection of traits for analysis; morphological traits that occur either very frequently or rarely have been considered of "no biological meaning" and often removed from analyses (Irish *et al.* 2018: 4; Harris and Sjovold 2004: 91). In essence, the very flexibility of the ASU system, and the methods frequently employed in conjunction with it, means that projects are often not comparable. Moreover, when using the ASU system and associated quantitative techniques, it is impossible to visualise morphological patterns and changes in shape, inhibiting an intuitive understanding of morphological differences (Rizk *et al.* 2013: 126; Adams *et al.* 2004: 5; Rohlf 1999: 198).

4.2.3 Summary

As a rubric through which to describe morphological characteristics, the ASU system has been remarkably successful, however, quantitative analyses which have been conducted on ordinally and categorically graded traits have been criticised for poor reliability, distortive results, lack of standardisation in statistical methodology, and an inability to visually represent shape variance (Pilloud *et al.* 2019; Irish *et al.* 2018; Scott *et al.* 2018; Edgar and Rautman 2016; Irish and Scott 2016; Bailey *et al.* 2011; Irish 2011; Tyrrell 1999; Irish 1998; Irish 1997; Turner *et al.* 1991; Turner 1990; Nichol and Turner 1986).

4.3 Geometric Morphometrics and Dental Anthropology

4.3.1 The Revolution in Morphometrics

In the latter decades of the twentieth century a fundamental shift occurred in the way morphological analyses were conducted. Various methods, now collectively known as geometric morphometrics (GM), were developed that can capture and retain shape geometry – the information that is invariant after *translation*, *rescaling* and *rotation* – in both two and three dimensions (Rizk *et al.* 2013: 126; Small 1996: 6; Adams *et al.* 2004: 5). These developments – which have contributed to a "revolution in morphometrics" – have been made possible through the increased availability in technologies related to data collection (e.g., imaging and scanning hardware), processing (e.g., software to digitise outlines and landmarks) and post-processing analysis (Robinson 2005; Adams *et al.* 2004; Bookstein 1991). Broadly speaking, GM techniques can be categorised as either landmark or outline (Rizk *et al.* 2013: 127; Robinson 2005: 21; Dryden and Mardia 1998: 305-306).

4.3.2 Landmark Methods and Procrustean Analyses

A landmark is a site that corresponds within and between populations. Landmarks can be characterised according to two different criteria. The first has three categories of landmarks: anatomical, mathematical, and pseudo-landmarks. An anatomical landmark is a biologically meaningful and homologous point. Mathematical landmarks are geometrically located – e.g., the point of highest curvature. Pseudo-landmarks are artificial points placed either between anatomical and mathematical landmarks or around an outline (Dryden and Mardia 1998: 3-4; Lohmann 1983). Alternatively, landmarks can be defined as Type I, II or III. Type I landmarks are usually anatomical and located at discrete structural juxtapositions; in dental materials this includes fissure junctions, fovea and cusp apices. Type II landmarks are defined by local properties, such as maximal

curvature or depression; although many mathematical landmarks could be defined as Type II, so could aspects of dental anatomy like the deepest point of a fovea or apex of a cusp. Type III landmarks (often the least reliably located) are at found at extremal points, and are usually mathematical or pseudo-landmarks; in dental materials, for example, a landmark placed at the maximum mesial extremity (Dryden and Mardia 1998: 4-5; Bookstein 1991: 63-66). Landmarks, regardless of category or type, form the basis of non-coordinate and coordinate-based GM methods (Dryden and Mardia 1998; Bookstein 1991).

Non-coordinate based landmark methods, such as Euclidean Distance Matrix Analysis (EDMA), often calculate inter-landmark distances to explore shape. Such techniques have not, however, found lasting popularity within the field of dental anthropology (Robinson 2005: 29; Lele 1993; Lele and Richtsmeier 1991; Lele 1991). Although several projects have successfully employed non-coordinate methods, the procedures have been criticised for low statistical power, difficulties encountered when trying to visualise results, and the disproportionate effect larger objects can have on average shape (Rizk 2013: 128; Robinson 2005; Olejniczak *et al.* 2004; Liu *et al.* 2001; Rohlf 2000). The coordinate-based method of Procrustes analysis, by contrast, has proven to be a far more popular tool for the evaluation of dental morphology. Procrustes analysis is a superimposition technique (Figure 4.2), in that Cartesian *x*-*y* coordinate configurations describing the position of landmarks are overlain through an optimisation process – such as a Generalised Procrustes Analysis (GPA) – that relocates, rescales and rotates coordinate matrices to minimise differences between configurations due to location, size and orientation (Robinson 2005: 32-38; Adams *et al.* 2004: 6; Dryden and Mardia 1998: 84-92; Gower 1975).

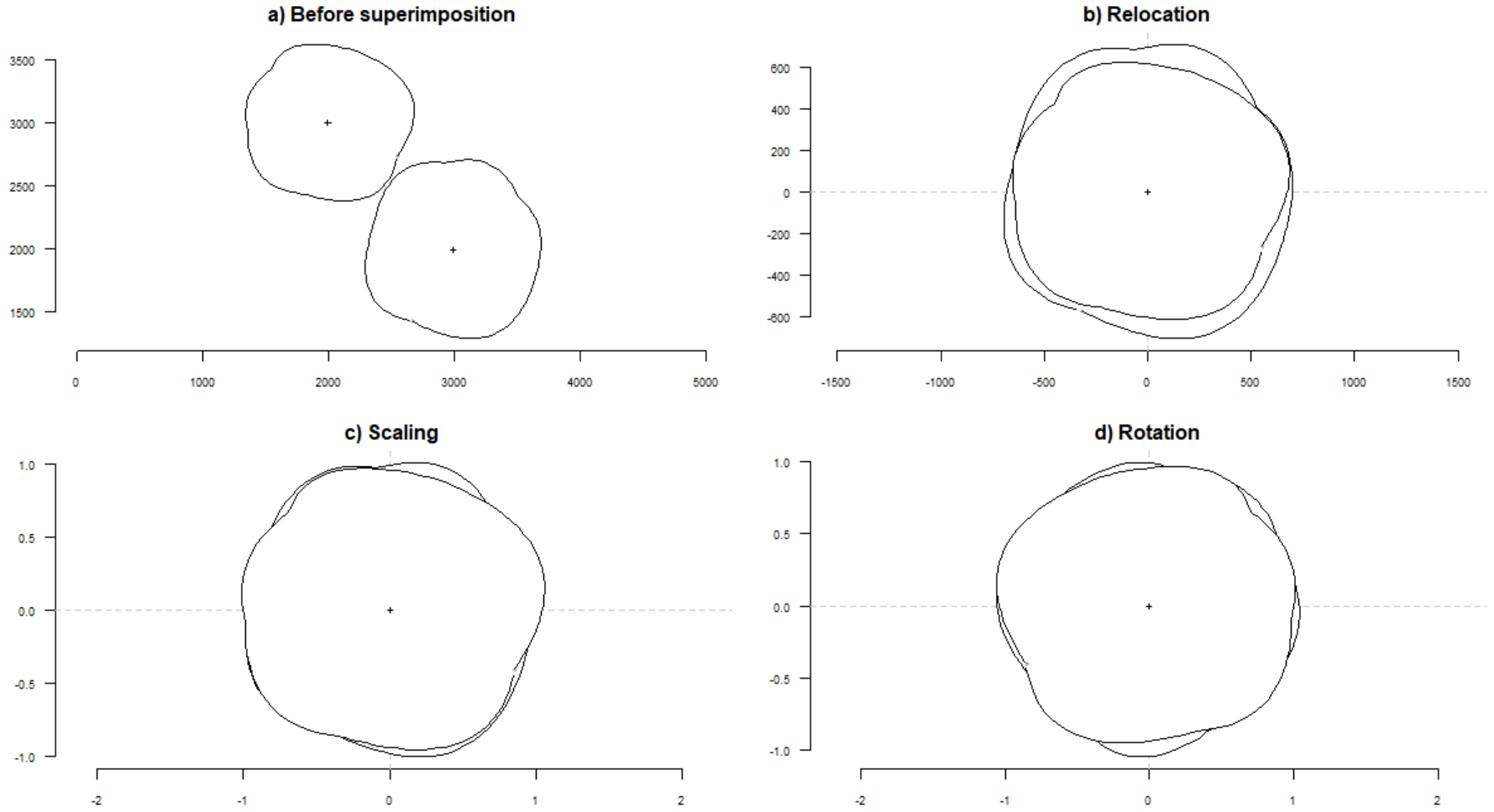

Figure 4.2 An example of Procrustes superimposition in which two M_1 shapes have been taken from their original positions (a), recentred at (0,0) to remove locational differences (b), then adjusted to remove differences due to size (c) and orientation (d). Note that outlines have been used to illustrate the process more clearly.

After being transformed through Procrustes superimposition, coordinates are regarded as points in Kendall's shape space, a non-Euclidean, multi-dimensional and non-linear space (Klingenberg 2020: 338-339; Robinson 2005: 38; Adams *et al.* 2004; Kendall 1984). The magnitude of differences between shapes (as represented by revised coordinate configurations) in Kendall's shape space is expressible as distances (e.g., found as the root sum of squared differences between coordinate configurations) (Bookstein 1991: 268-269). However, the distance between shapes is affected by superimposition methods. For example, if a partial Procrustes superimposition is performed on two shapes and both configurations are scaled to unit centroid size – centroid size being the square root of the sum of the squared Euclidean distances from each landmark to the configurations central point – the distance between them, known as the the partial Procrustes distance (d_P), is greater than if a full Procrustes superimposition is performed (Klingenberg 2020: 337-338; Dryden and Mardia 2016: 69-71; Mitteroecker *et al.* 2013; Dryden and Mardia 1998: 63-65; Bookstein 1991: 93-94). In the latter approach, which produces a full Procrustes distance (d_F), distances between shapes are reduced further as only the target shape is scaled to unit centroid size, while the other is scaled so that it matches as closely as possible the target configuration (Klingenberg 2020: 337-338; Dryden and Mardia 2016: 69-72; Dryden and Mardia 1998: 63-65).

Fortunately, the differences between the distances are minimal in most biological cases and to circumvent the need for special methods to deal with the non-Euclidean geometry, analyses can be conducted after objects have been projected into tangent linear space (Klingenberg 2020: 337-338; Dryden and Mardia 2016: 88-95; Robinson 2005: 38; Kent and Mardia 2001: 469; Rohlf 1999: 205; Dryden and Mardia 1998: 63-71). An illustrative metaphor through which to visualise the relationship between shape and tangent linear space is that of a sphere (Kendall's shape space) resting on a piece of paper

(tangent linear space) – in the same way that a cartographer takes coordinates from a globe and plots them on a two-dimensional map, so points in shape space may be projected onto the tangent plane (Robinson 2005: 96) (Figure 4.3). This necessarily leads to a degree of distortion, but if variation in shape is small (usually the case in biological datasets), then Euclidean distances between points in tangent linear space provide a good approximation of the non-Euclidean distances in Kendall's shape space (Dryden and Mardia 2016: 88-95; Robinson 2005: 38; Kent and Mardia 2001: 469; Rohlf 1999: 205; Dryden and Mardia 1998: 71). Projection therefore permits descriptive and inferential investigation through standard multivariate methods which, when compared to alternative GM methods, have high statistical power, enabling a wide variety of hypotheses to be tested effectively (Robinson 2005: 38; Rohlf 2000; Rohlf 1999: 205; Dryden and Mardia 1998: 151-160).

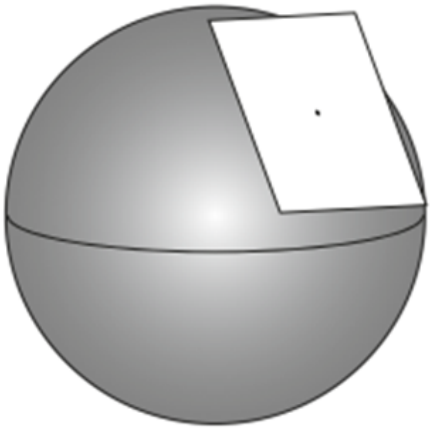

Figure 4.3 A convenient way in which to appreciate the relationship between Kendall's shape space and tangent linear space is by comparing the former to a spherical object, such as a globe, and the latter to a flattened representation of that object like a map (Klingenberg 2016: 121).

Application of Procrustean methods to dental materials has demonstrated that they can produce a wealth of information. For instance, to evaluate ancestral differences, Kenyhercz *et al.* (2014) placed landmarks at molar cusp apices and transformed the raw coordinate data through Procrustes superimposition. As well as finding that in most of the

cases Discriminant Function Analysis of M1 configurations correctly predicted ancestry, plots from Principal Components Analysis (PCA) showed that differences between groups were manifested in the displacement of major cusps in specific directions (Kenyhercz *et al.* 2014). Furthermore, when a subset of 25 teeth were digitised a second time for repeatability tests, no significant differences in coordinate locations between replicates was found (Kenyhercz *et al.* 2014: 270-271). This, and similar cases, have indicated that in comparison to the ASU system, Procrustean methods produce more data with greater reliability, and, consequently, their use is increasing (e.g., Rizk 2013; Benazzi *et al.* 2011a; Gómez-Robles *et al*. 2011; Gómez-Robles *et al.* 2008; Gómez-Robles *et al*. 2007).

4.3.3 Outline Methods and Sliding Semi-Landmarks

The ability to evaluate outlines is also essential for dental morphologists as outline data can compensate for a major restriction inherent in landmark methods. Specifically, it is possible with an outline to evaluate – to varying degrees – some non-homologous morphological features (i.e., supernumerary cusps) (Scott *et al.* 2016; Scott and Turner 1997; Carlsen 1987). The initial step in an outline analysis is to digitise coordinate points around an edge that corresponds between objects (Robinson 2005: 48; Adams *et al.* 2004: 6). In an outline with no clearly defined characteristics, however, ensuring points correspond is difficult to achieve and a variety of methods have been developed in response to this problem (Robinson 2005: 48; Adams *et al.* 2004: 6). Some early projects fitted points where equally spaced radii originating from a central point or landmark intersected the outline (Figure 4.4), while others added points where there was a change of angle (Adams *et al.* 2004: 6). These methods are, however, better suited to simple shapes, necessitating that more sophisticated approaches, such as Eigenshape and Fourier analysis, be applied to dental materials (Bailey and Lynch 2005; Robinson 2005; Adams

et al. 2004; Polly 2003; Rohlf 1986; Lohmann 1983). Fourier analysis, for instance, decomposes an outline into a series of harmonics, with the length of the truncated series dictating the resolution to which the outline is described. Each retained harmonic in the series contains coefficients that define outlines in terms of angle frequencies and magnitude which, when normalised for unit size, can be used in standard multivariate tests (Benazzi *et al.* 2011a; Bailey and Lynch 2005: 271; Robinson 2005: 52; Dryden and Mardia 1998: 305-306).

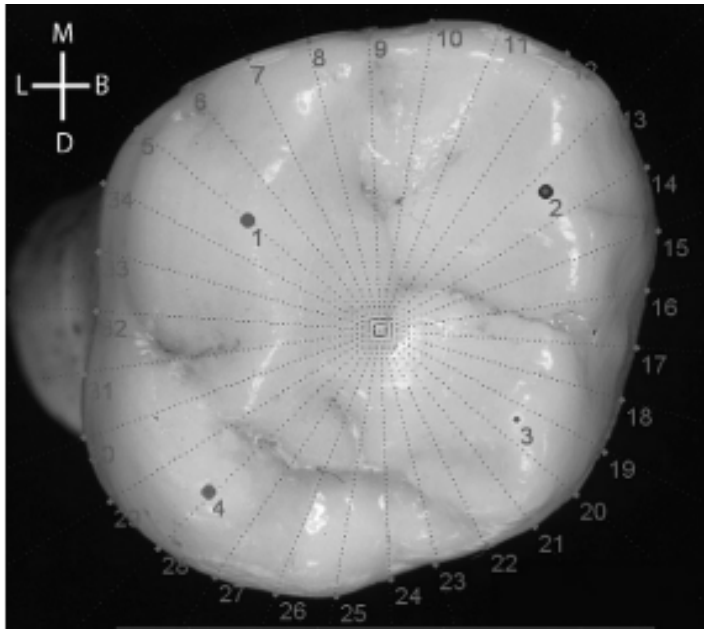

Figure 4.4 An M^1 defined by four landmarks at cusp apices and points along the outline whose locations were defined by equally spaced radii originating from a central point (Gómez-Robles *et al.* 2007: 275).

The use of both Eigenshape and Fourier analysis by dental morphologists has been modest and, when applied, have not alway performed as well as expected (Irish and Scott 2016; Scott and Irish 2013; Bailey and Lynch 2005: 274; Hillson 2005; Bailey 2002). This may reflect methodological problems. For instance, the outline rotation that takes place in Eigenshape analysis has been criticised for creating an arbitrary mathematical homology between shapes rather than a meaningful biological one (Bookstein 1991: 47; Rohlf 1986: 846; Full and Ehrlich 1986), while it has been argued that Fourier analysis

ignores the relative positions of points along the outline, thereby losing significant information (Robinson 2005: 52; Adams *et al.* 2004: 10; Rohlf 1986: 847-848). Furthermore, given that teeth are well-supplied with landmarks, methods that only quantify outline variation are at a significant disadvantage (Rizk *et al.* 2013; Benazzi *et al.* 2011a; Bailey and Lynch 2005).

Morphometricians have, however, developed semi-landmark methods through which the benefits of both Procrustean and outline techniques can be integrated. A semi-landmark is an *x*-*y* coordinate point located along an outline which can be compared to a corresponding semi-landmark in a superimposed configuration. In order to ensure semi-landmarks are comparable between configurations, two approaches have been devised. Either a least-squares procedure is used to reduce the Procrustes distance between them or bending energy (the idealised energy it would take to manipulate configurations onto one another) is minimised (Bookstein and Ward 2013; Benazzi *et al.* 2011a; Robinson 2005; Bookstein 1997). Although in samples where differences between shapes are expected to be small there is unlikely to be a great deal of difference between the two, reducing bending energy is generally preferable (Gunz and Mitteroecker 2013: 106). When the Procrustes distance is reduced, positional changes are not influenced by other landmarks or semi-landmarks and the final position of a semi-landmark may therefore overlap or pass that of another in violation of anatomical reality. Whereas, in order to minimise bending energy, semi-landmarks "slide" along a line tangent to the chord between points adjacent to the semi-landmark being slid; semi-landmarks cannot therefore move beyond adjacent landmarks/semi-landmarks and results more closely approximate real-world relationships (Bookstein and Ward 2013; Gunz and Mitteroecker 2013: 106-107; Zelditch *et al*. 2012: 123-124; Bookstein 1997; Duchon 1976). It is thus possible to overcome the ambiguities of outline landmark placement without

compromising on the statistical power achieved with Procrustean methods (Robinson 2005: 146; Adams *et al.* 2004: 8; Rohlf 2000; Bookstein 1997). For dental morphologists this means that morphological commonalities (i.e., homologous landmarks) and idiosyncratic features such as supernumerary cusps can to some extent be evaluated simultaneously.

4.3.4 Summary

GM techniques, in comparison to the ASU system, produce results that can be explored through standardised multivariate tests and, due to the preservation of spatial relationships, readily visualised (Rizk *et al.* 2013; Robinson 2005; Adams *et al.* 2004; Dryden and Mardia 1998; Bookstein 1991). Of these, Procrustean techniques can assess homologous features as well as shape outline and therefore appear to be the most suitable for application in the field dental anthropology (Kenyhercz *et al.* 2014; Rizk 2013; Benazzi *et al.* 2011a; Gómez-Robles *et al*. 2011; Robinson 2005; Rohlf 2000; Rohlf 1999; Dryden and Mardia 1998; Bookstein 1997; Bookstein 1991).

4.4 The Theory of Asymmetry

4.4.1 Asymmetry in Bilateria

As symmetrical development generally requires less energetic expenditure than asymmetric growth, many forms of symmetry exist. Symmetries are created through the repetition of component parts via a transformation, or combination of transformations, which include *reflection*, *rotation*, *translation* and *scaling* (Klingenberg 2015: 844-845; Graham *et al.* 2010: 469; Savriama and Klingenberg 2011). Bilateral symmetry, which involves reflection about a median plane, is especially common and many organisms can be included in the *bilateria* clade (Klingenberg 2015: 844-846; Namigai *et al.* 2014;

Graham *et al.* 2010: 467-471; Beloussov 1998). There are two types of bilateral symmetry: *object* and *matching* (Figure 4.5). In object symmetry, the structure itself is bilaterally symmetric, with the axis of reflection passing directly through it (e.g., the cranium). In contrast, matching bilateral symmetry involves two separate copies of a structure placed either side of an axis of reflection which does not pass through either structure (e.g., antimeric teeth) (Graham and Ozener 2016; Klingenberg 2015: 848; Graham *et al.* 2010: 475).

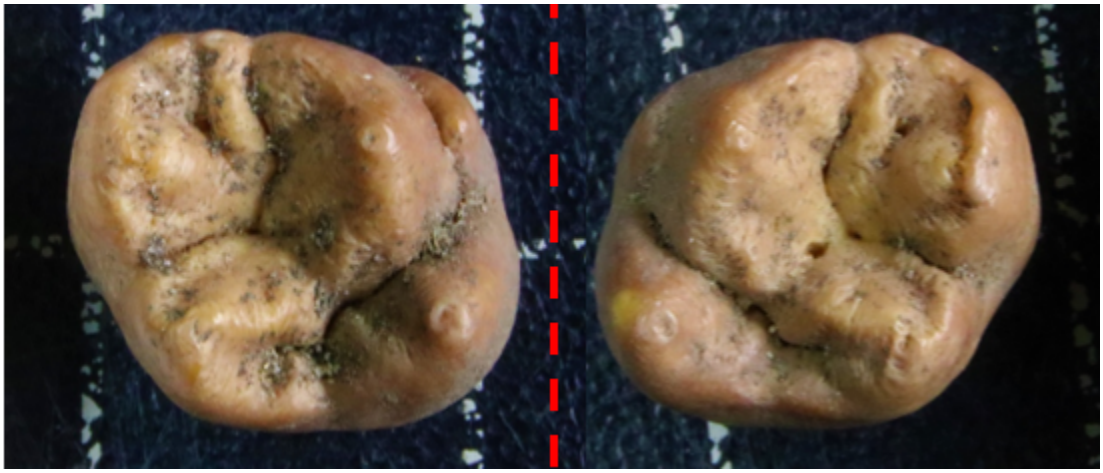

Figure 4.5 Paired objects, such as these left and right M^1s, have matching symmetry; they exist either side of an axis of symmetry (red line) about which one can be reflected for comparative purposes.

In bilaterians, although symmetrical growth begins during earliest embryonic development, deviations from perfect symmetry are normal and asymmetry, at its most basic level, can be expressed as the difference between sides (i.e., left minus right) (Klingenberg 2015; Namigai *et al.* 2014: 459; Graham *et al.* 2010: 472). The scientific study of bilateral asymmetry has a long history (e.g., Mather 1953; Ludwig 1932; Bateson 1892), but in 1962 L. Van Valen published a paper in *Evolution* that has become the conceptual cornerstone of research into the subject. It defined three categories of asymmetry: *directional asymmetry*, *antisymmetry* and *fluctuating asymmetry* (Klingenberg 2015: 850-855; Graham *et al.* 2010: 473-474; Van Valen 1962: 125).

Importantly, though asymmetries exist on an individual level, identification of which form of asymmetry is present requires reference to patterns of asymmetry observed in a sample or population (Klingenberg 2015; Graham *et al.* 2010; Palmer *et al.* 1993; Bookstein 1991: 267-270; Van Valen 1962).

4.4.2 Broken Symmetries: Directional Asymmetry and Antisymmetry

For a trait to be directionally asymmetric there must be a consistent tendency at the sample or population level for the preferential development of either the left or right side (Klingenberg 2015: 851; Graham *et al.* 2010: 474; Van Valen 1962: 125-126). The location of internal organs in many animals are prime examples of directionally asymmetric traits. In humans, the cardiovascular system displays many directionally asymmetric features; the heart, for example, is typically located on the left side of the body (Klingenberg 2015: 851; Gosling *et al.* 2002; Van Valen 1962: 126). Despite being asymmetric, this side bias in location and development is entirely normal, healthy and observable in the vast majority of the population. Deviations away from this pattern are in fact not only rare but often associated with increased morbidity and mortality. For example, *situs ambiguus* is an autosomal recessive condition leading to an anatomical abnormality where an organ is placed on the opposite side of the body to that which it is usually expressed; in the case of the heart, specifically referred to as dextrocardia, this can lead to a suite of cardiovascular ailments as well as overall poor health (Klingenberg 2015: 851; Sutherland and Ware 2009). Many genes and molecular processes have been implicated in the embryonic differentiation of left and right sides in bilateria; these developmental mechanisms appear to be present in distantly related bilaterians, suggesting that certain directionally asymmetric traits are highly conserved (Klingenberg 2015: 851; Coutelis *et al.* 2014; Namigai *et al.* 2014).

Antisymmetry, by contrast, is a pattern of asymmetry in which left-sided and right-sided forms are equally common (Klingenberg 2015: 854; Palmer 2005: 360). Whereas directional asymmetry is largely the result of genetic determinism, it appears as though antisymmetry is the result of external influences on phenotype which cause either a sinistral or dextral form to develop (Klingenberg 2015: 854; Palmer 2005: 360). Antisymmetry is not readily evident in humans, but can be seen in a variety of plants and animals (Klingenberg 2015: 853); in crossbill finches, the sides to which the upper and lower bill cross is conspicuously asymmetric but random and evenly distributed (Palmer 2005: 360; Neville 1976). When evaluating phenotype at the sample level with a univariate measure of left-right differences, it is canonically accepted that directionally asymmetric traits produce a unimodal and skewed distribution, while antisymmetry produces a bimodal or, in more subtle cases, a platykurtic distribution (i.e., a broad distribution with negative kurtosis and thin tails) (Klingenberg 2015: 855; Graham *et al.* 2010: 474; Palmer 2005: 360; Van Valen 1962: 126) (Figure 4.6). It has, however, been cautioned that asymmetries may not be this easy to distinguish in multivariate or composite measures and that distributional assumptions should be treated cautiously (Klingenberg 2015: 853). Despite their differences, both directional asymmetry and antisymmetry are referred to as "broken symmetries" (Graham *et al.* 2010: 474).

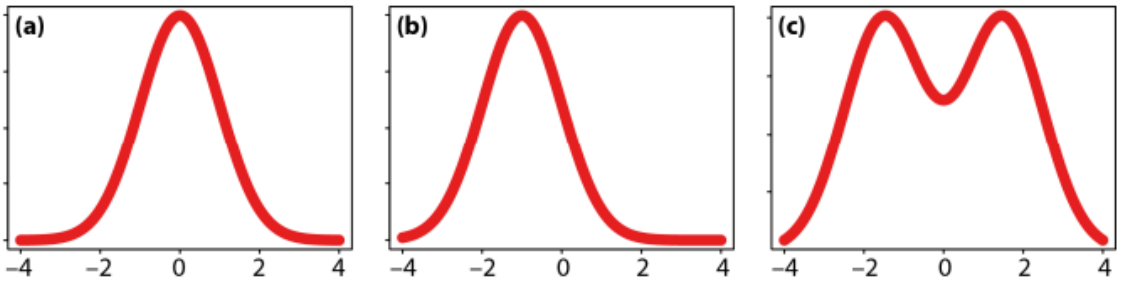

Figure 4.6 The distributions proposed by Van Valen of fluctuating (a) and directional asymmetry (b) as well as antisymmetry (c) in a signed univariate measure (Klingenberg 2015: 852).

4.4.3 Fluctuating Asymmetry

In the absence of a directional bias in development, left and right sides of bilaterian organisms are controlled by the same genetic mechanisms, so a "target phenotype" with perfect symmetry should develop (Klingenberg 2015: 852; Graham *et al.* 2010: 474; Van Valen 1962: 126). This, however, is rarely the case as stressors cause departures from perfect symmetry (Graham *et al.* 2010: 496). Stress-induced deviations from perfect symmetry are random and not deterministic in which side they affect; divergences from the target phenotype are, therefore, equally likely to manifest on either side – i.e., the effects of stress on symmetry fluctuates between left and right (Klingenberg 2015: 852; Graham *et al.* 2010: 474; Van Valen 1962: 126). The definition outlined in this paragraph is fundamental to understanding FA and its use as a marker of developmental stress and therefore also key to appreciating the methodological choices made during data collection/analysis and the interpretations presented in the thesis.

This relatively simple explanation for deviations in symmetry, however, belies several complications. For instance, many researchers have contended that fluctuating asymmetry – when quantified through a signed continuous variable such as left-right differences in a linear measure (e.g., MD or BL diameters) – should have a normal distribution with a mean of zero and therefore be easily distinguishable (Klingenberg 2015: 852; Graham *et al.* 2010: 474; Van Valen 1962: 126). Although this idea is often repeated and appealing (Palmer 1994: 348-349; Van Valen 1962: 129), it presupposes stressors provoke an additive and independent phenotypic response, which cannot be guaranteed in many biological structures (Graham and Ozener 2016: 176; Klingenberg 2015: 852; Graham *et al.* 2010: 507). Though adjustments can be made to accommodate non-normal distributions, the situation may be further complicated by the fact that, although the molecular interactions of genes have proven to be especially susceptible to

exogenous influences, stress can be manifested at a variety of biological levels (e.g., molecular, cellular, etc.) (Graham *et al.* 2010: 497; Raser and O'Shea 2005; Elowitz *et al.* 2002; McAdams and Arkin 1999; McAdams and Arkin 1997; Palmer 1994: 339). Moreover, it should also not be forgotten that fluctuating asymmetry is a pattern resulting from a process; its assessment is therefore only a proxy for that process and inferences pertaining to the parent mechanism must be made with the appropriate reservation (Palmer 1994: 339).

Despite complications, fluctuating asymmetry has been used to gauge the impact of environmental stress on phenotype. It does not have a direct and unambiguous relationship with environmental stimuli, however (Graham *et al.* 2010: 495-496). *Developmental homeostasis* is, by and large, a highly *canalised* process in that it is a well-regulated and stable affair in which somatic resources are allocated to precisely maintain developmental trajectories despite disruptions (Klingenberg 2015: 891; Graham *et al.* 2010: 495-496; Visser *et al.* 2003; Waddington 1957; Schmalhausen 1949). Disruptions to development can be caused by either environmental stressors, called *perturbations*, or independently occurring intrinsic stochastic deviations, known as *fluctuations*; the combined effect of perturbations and fluctuations is referred to as *developmental noise* (Klingenberg 2015: 892; Graham *et al.* 2010: 496; Nicolis and Prigogine 1989). Developmental noise can be mitigated and its impact minimised by an organism's faculty to *buffer* or "the ability to absorb changes … and still persist" – this has also been referred to as *resilience* (Graham *et al.* 2010: 496; Holling 1973: 17). Developmental stability is, therefore, influenced by endogenous fluctuations and buffering systems as well as exogenous stressors. The opposite of stability is *developmental instability* – the inability to correct for disruptions and conserve developmental homeostasis; as this typically occurs at the molecular level, instability has

been viewed as the "'play' in the epigenetic machine" (Graham *et al.* 1998: 2; Waddington 1957). Fluctuating asymmetry is therefore a measure of instability and, as such, it is an aggregate, and potentially subtle, measure that conceals complex dynamics in systemic physiology (Graham and Ozener 2016: 163; Klingenberg 2015: 892; Graham *et al.* 2010: 496-497; Escós *et al.* 2000: 331; Selye 1973).

Given the association of fluctuating asymmetry with instability and resilience, it has also been used to imply individual *fitness*, or an organism's ability to survive adversity and reproduce in its natural environment (Graham and Ozener 2016: 172; Klingenberg 2015: 893; Graham *et al.* 2010: 506; Orr 2009: 531). Attempts to assess fitness through asymmetry have met with varying success, however, and in some cases, there appears to be scant relationship between asymmetry and growth, mortality and reproductive success (Graham and Ozener 2016: 172; Klingenberg 2015: 893; Graham *et al.* 2010: 502; Bjorksten *et al.* 2000; Van Dongen *et al.* 1999). One possible explanation for these ambiguous results, is that fluctuating asymmetry is typically a measure made with reference to a sample, while fitness pertains to an individual's outcomes (Graham and Ozener 2016: 172; Klingenberg 2015: 893; Graham *et al.* 2010: 506; Orr 2009: 531). Although it is possible to compute individual FA indices, not all methods are equally effective. For example, simple left-right differences in univariate measures are often found to be an inadequate indicators of an organism's overall fitness, while combining scores from several traits for a composite measure is problematic due to the differential responsiveness of various biological tissues to developmental instability (Klingenberg 2015: 893; Zelditch *et al.* 2012: 364-369; Graham *et al.* 2010: 506; Palmer and Strobeck 2003: 319). In contrast, multivariate measures, although not perfect – realistically most multivariate traits are composed of several developmental sub-units for which covariation is high, with molar cusps a prime example (Jernvall and Jung 2000; Jernvall and Thesleff

2000; Jung *et al.* 1998) – avoid the inherent complications of simple and composite indices and likely provide a more meaningful evaluation of instability in the developing organism.

4.4.4 Summary

Although asymmetry at its most simple can be measured as the magnitude of difference between left and right sides, studies of asymmetries developing during the ontogenetic process must take into account several factors. There are, for instance, three forms of asymmetry, one of which – fluctuating asymmetry – represents developmental instability. Instability is the aggregation of random intrinsic fluctuations and external stressors as well as the organism's ability to buffer against physiological deviations to sustain developmental precision (Klingenberg 2015: 892; Graham *et al.* 2010: 496-501; Palmer 2005; Van Valen 1962). Consequently, measuring FA can be challenging and likely best achieved through multivariate quantifications with results reflecting organismal fitness and providing a coarse measure of stress experienced during development (Graham and Ozener 2016: 163; Klingenberg 2015: 892; Graham *et al.* 2010: 496-501; Palmer 1996; Palmer 1994; Holling 1973: 17).

4.5 Evaluating Asymmetry

4.5.1 Dental Anthropology, Bioarchaeology and Traditional Methods

There has been a surprising dearth of morphological studies of dental fluctuating asymmetry. The deficit, however, can be accounted for by the unsuitability of the ASU grading system for the task. Choice of traits, for instance, is problematic; low frequency traits can cause an unduly high level of antimerically concordant absence, artificially reducing quantifications of FA, while the selection of high frequency traits has the

opposite effect (Scott and Turner 1997: 98-99; Saunders and Mayhall 1982: 796). Further complications have been encountered with the recording of traits. When traits are graded as present/absent, tooth morphology has appeared more symmetric than is the case and the situation is only modestly mitigated by retention of ordinal grades (Scott and Turner 1997: 98-99; Saunders and Mayhall 1982; Scott 1980; Baume and Crawford 1980). Dietz (1944), for example, found a presence/absence asymmetry of a mere 2.2% for Carabelli cusp expression, but this increased when using a four-grade scale to 7%. In sum, the ASU system is insufficiently sensitive to register the small deviations in symmetry associated with FA and, as such, fluctuating asymmetry in dental materials has usually been investigated through simple linear measurements.

Early projects to take advantage of Van Valen's (1962) theoretical clarifications, were undertaken by Bailit *et al.* (1970) and Perzigian (1977). Both studies found that dental FA, quantified through left-right differences in linear measures (i.e., MD and BL diameters) (Figure 4.7), was higher in populations for which there was evidence of deprivation. In the case of the living populations studied by Bailit *et al.* (1970) this evidence was in the form of contemporary records. For Perzigian's (1977) past populations, factors such as the seasonal availability of food were employed to estimate relative stress experience (Parmalee and Klippel 1974; Webb 1946). Interestingly, Bailit *et al.* (1970: 631-636) found a low heritability estimate (h^2 2-5%) when contrasting FA between related individuals, while Perzigian (1977: 83) reported that when a sample was divided according to estimated stature, those above the mean estimated height had significantly lower ranked FA scores in MD measurement than those below. Somewhat contentiously, whilst Townsend and Brown (1980) also found low correlations between related and unrelated individuals, further suggesting fluctuating asymmetry was not the result of heritable predisposition, unlike either Bailit *et al.* (1970) or Perzigian (1977)

they reported significant differences between sexes in dental FA. Cumulatively, these studies hint that there may be substantial connections between dental FA, environmental stress and later-life outcomes that operate independently of genetic constraints, but they also highlight that for many years results were inconsistent and incomparable.

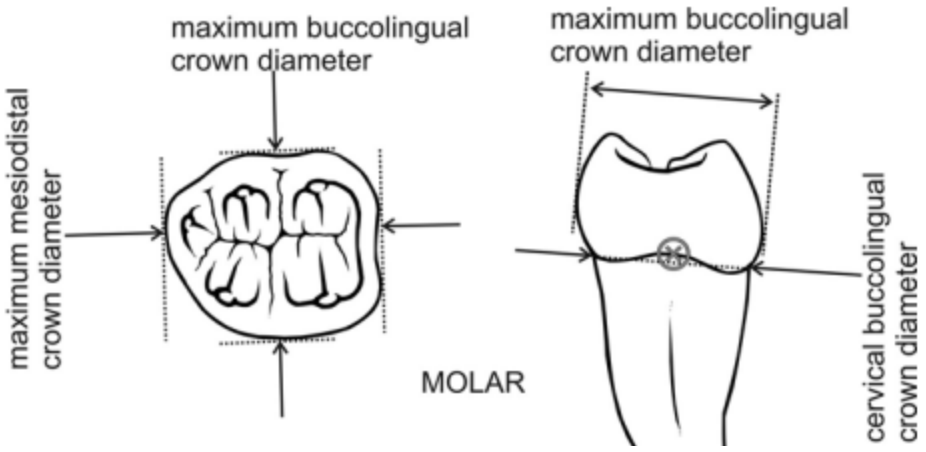

Figure 4.7 Measurements traditionally employed to assess the dentition (Hillson 2005: 261).

In order to increase comparability and statistical sensitivity, Palmer and Strobeck (1986), expanding on Leamy (1984), proposed that a two-way, mixed-model Analysis of Variance (ANOVA) with repeated measurements could be employed to decompose asymmetric variation (Section 7.4.1). This was beneficial as it can be expected that overall variance in a sample is attributable to several factors (i.e., differences within as well as between individuals), the interaction of those factors and also observer error (Murrar and Brauer 2018; Klingenberg and McIntyre 1998) (Table 4.1). The procedure is not, however, without its shortcomings. Specifically, a significant interaction between the two main effects identifies "non-directional asymmetry" which encompasses fluctuating asymmetry and antisymmetry, rather than FA in isolation (Palmer 1994; Palmer and Strobeck 1986). Nevertheless, checks can be conducted to ascertain whether the non-directional component to asymmetry is in fact associable with fluctuating asymmetry or antisymmetry (e.g., by assessing the distribution of left-right differences)

(Guatelli-Steinberg *et al.* 2006: 429; Klingenberg and McIntyre 1998: 1368) (Section 7.4.1), and the method has become a standard part of the statistical toolkit through which FA is analysed. Barrett *et al.* (2012) employed the ANOVA procedure to compare Neanderthals and modern humans, for example. By comparing FA in BL diameters among teeth that develop at specific ages, they were able to theorise that Neanderthals were either exposed to greater environmental stressors or were less capable of buffering against them and that cultural choices, such as infant and childhood diet, affected developmental instability (Barrett *et al.* 2012: 201). The clarity of these results prompted Barrett *et al.* (2012: 203) to describe the two-way, mixed-model ANOVA as, "a useful and straightforward means for comparing levels of developmental stress between populations."

Effects	df	MS	Expected Mean Squares	Source of Variation
individual (ind)	$J-1$	MS_J	$\sigma_m^2 + M(\sigma_i^2 + S\sigma_j^2)$	individual variation
side	$S-1$	MS_S	$\sigma_m^2 + M(\sigma_i^2 + (\frac{J}{S-1})\sum\alpha^2)$	directional asymmetry
ind x side	$(S-1)(J-1)$	MS_{SJ}	$\sigma_m^2 + M\sigma_i^2$	non-directional asymmetry
ind x side x replicate	$SJ(M-1)$	MS_{error}	σ_m^2	error

Table 4.1 The variance components of the two-way, mixed model ANOVA as presented by Palmer and Strobeck (1986: 405). $\sum\alpha^2$ is the fixed side variance; σ_j^2 is the variance attributable to individual differences; σ_i^2 is variance associated with non-directional asymmetry (including fluctuating asymmetry) reflecting variation between sides among individuals; σ_m^2 is variation due to measurement error. J=individuals; S=sides (i.e., two); and M=replicates. Note, this table replicates the original notation while the application of this approach detailed in Chapter 7 employs notation developed for this project.

Even though these investigations of FA by dental anthropologists very successfully demonstrated that there appears to a be a robust relationship between FA and environmental adversity as well as established a rubric around which FA can be explored

in dental remains, they also illuminate possible directions for future research (Barrett *et al.* 2012; Guatelli-Steinberg *et al.* 2006). For example, Bailit *et al.* (1970: 635-636) stated, "Clearly, it will be necessary to relate the degree of fluctuating asymmetry in the dentition to more conventional measures of fitness such as morbidity, mortality, and fertility. Only when this relationship is firmly established can interpopulation differences in asymmetry be considered biologically meaningful." Although this comment was made more than 50 years ago – and links between dental FA, growth and health in past populations have been articulated (e.g., Hagg *et al.* 2017; Weisensee 2013; Hoover and Matsumura 2008) – there is still scope to investigate these connections more rigorously. Fortunately, GM methods can help to fill this information gap.

4.5.2 Asymmetry and Procrustean Methods

GM approaches to quantifying FA have been employed most extensively in disciplines such as ecology and biology (Klingenberg 2015; Zelditch *et al.* 2012; Graham *et al.* 2010). Aside from the general benefits of GM methods, two Procrustean techniques pertinent to this thesis have proven especially advantageous and these have formed the basis for many subsequent GM analyses of FA (Klingenberg 2015; Graham *et al.* 2010). These are introduced here and discussed in more technical detail in Section 7.4.1.

The first innovation relates to the extension by Goodall (1991) of the ANOVA model to Procrustes coordinates. As Procrustes superimposition is based on a sum of squares algebra, morphological differences from a mean configuration can be decomposed in a manner analogous to differences from a grand mean in the conventional ANOVA. One of the earliest projects to make use of the Procrustes ANOVA was a study of tsetse fly wing shape by Klingenberg and McIntyre (1998). The question that motivated this study was the subject of a then unresolved debate; specifically, whether

fluctuating asymmetry results from a disruption to normal somatic growth – a crucial assumption in the use of FA as an indicator of developmental instability – or from special developmental processes (Klingenberg and McIntyre 1998: 1363; Palmer 1996; Markow 1995). Wing venation patterns provided a framework for the placement of homologous anatomical landmarks which were subjected to Procrustes superimposition. The following Procrustes ANOVA showed highly significant levels of both individual variation as well as fluctuating asymmetry. Furthermore, Mantel tests conducted on covariance matrices of individual variation and left-right differences rejected the null hypothesis of dissimilarity, suggesting that fluctuating asymmetry represented a disruption to normal developmental processes and was a valid marker of developmental instability (Klingenberg and McIntyre 1998: 1372-1373). Moreover, PCA identified that landmarks in the anterior and posterior wing compartments were near-equally affected by FA, suggesting morphological integration (Graham *et al.* 2010: 507; Klingenberg and Zaklan 2000; Klingenberg and McIntyre 1998: 1368-1370). The success of this pioneering project and others like it have proved that the two-way, mixed-model ANOVA advocated by Palmer and Strobeck (1986), can be applied just as readily to Procrustes-aligned landmark data (Klingenberg 2015; Zelditch *et al.* 2012; Graham *et al.* 2010; Palmer and Strobeck 2003; Klingenberg and McIntyre 1998: 1366; Edgington 1995; Palmer 1994; Good 1994; Goodall 1991).

The second development of interest, is the partitioning of asymmetries in coordinate matrices to produce an individual multivariate measure of FA (Figure 4.8). Although several different approaches have been proposed (e.g., Klingenberg and Monteiro 2005), that outlined by Bookstein (1991: 267-270) has proven to be the most frequently advocated. Bookstein's (1991) approach was first illustrated with reference to asymmetry in wing venation patterns. At its simplest, the Procrustes coordinates of left and right landmark configurations are subtracted from one another, and then the square

root of the summed and squared differences is found to give an individual measure of overall or "raw" asymmetry – this is the Procrustes distance between two shapes. This calculation can be further refined by considering mean left and right shapes in order to filter directional asymmetric variance and produce an individual index of FA (Zelditch *et al.* 2012: 364-369; Palmer and Strobeck 2003: 319; Klingenberg and McIntyre 1998: 1375; Smith *et al.* 1997; Bookstein 1991: 268-269). Though results have not always been unambiguous, an individual measure has facilitated the exploration of FA as a predictor of life-course outcomes (Klingenberg 2015; Zelditch *et al.* 2012; Van Dongen and Gangestad 2011; Graham *et al.* 2010; Klingenberg and Monteiro 2005; Møller 1999; Waynforth 1998). For instance, Radwan *et al.* (2003) found significant relationships between individual measures of FA, growth and reproductive success in insects, while Weisensee (2013) employed cranial FA to explore links between childhood stress and later-life mortality in a known cause-of-death 19th-20th century Portuguese skeletal sample. In the latter project, when individual measures of FA were averaged, higher mean FA scores were observed in individuals that died of degenerative metabolic diseases (such as cardiovascular disease and diabetes) related in modern populations to developmental stress than those whose causes-of-death was related to infectious or neoplastic pathology (Weisensee 2013: 415).

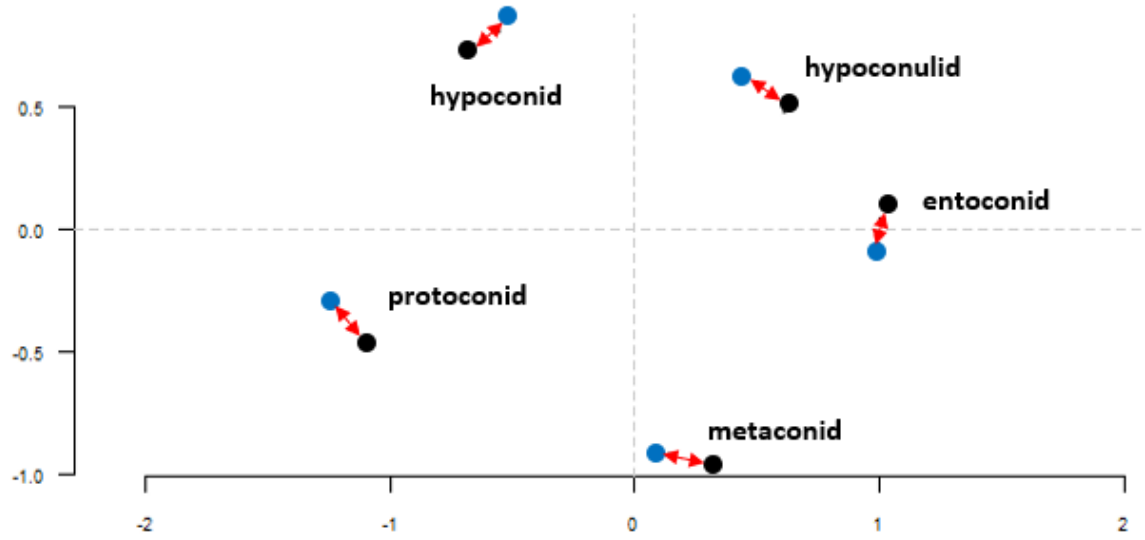

Figure 4.8 After reflecting the left side to make shapes comparable, the total Procrustes distance between left (blue) and right (black) M_1 configurations composed of landmarks at the main cusps is found as the root sum of squared distances (visualised as the red lines) between all homologous landmarks of Procrustes-aligned coordinate matrices. The coordinate configurations illustrated here are examples drawn from the data collected by this project.

4.5.3 Summary

Early studies of dental FA were comparatively simple, so although connections were made between dental FA and environmental adversity, questions were left unanswered. However, with increasing methodological sophistication and standardisation, bioarchaeologists have become capable of testing more complex hypotheses regarding the significance of dental phenotypic variation (Barrett *et al.* 2012; Guatelli-Steinberg *et al.* 2006; Scott and Turner 1997: 98-99; Palmer 1994; Palmer and Strobeck 1986; Leamy 1984; Perzigian 1977; Bailit *et al.* 1970). As of yet, however, the potential of GM evaluations of asymmetry in archaeologically recovered teeth has not been fully explored, despite the successes seen elsewhere (Zelditch and Swiderski 2018; Klingenberg 2015; Zelditch *et al.* 2012; Graham *et al.* 2010; Klingenberg and McIntyre 1998; Bookstein 1991). Additionally, even though Bailit *et al.* (1970) emphasised its critical importance early on, there have been few attempts to substantively link the early-life stress embodied in dental materials with later-life health outcomes.

4.6 Conclusion

This chapter has reviewed the methods and theory that underpin the evaluation of dental morphology as well as how shape variation can be employed to infer stress experience. From this, it can be concluded first that in certain circumstances – such as comparisons between paired teeth – the ASU system does not represent an appropriate means of evaluating morphological variation and that geometric morphometric methods fulfil this role much better. In particular, Procrustean techniques have the capacity to evaluate homologous and – to an extent – non-homologous features (Pilloud *et al.* 2019; Irish *et al.* 2018; Edgar and Rautman 2016; Kenyhercz *et al.* 2014; Rizk 2013; Benazzi *et al.* 2011a; Gómez-Robles *et al*. 2011; Robinson 2005; Dryden and Mardia 1998; Scott and Turner 1997; Bookstein 1991). Secondly, although fluctuating asymmetry is an aggregate measure that reflects environmental perturbations and an organism's physiological ability to maintain or buffer developmental homeostasis, due to its strong association with exogenous stimuli it can also act as a coarse proxy for stress experience (Graham and Ozener 2016; Klingenberg 2015; Graham *et al.* 2010; Palmer 1996; Palmer 1994; Holling 1974). Finally, past research demonstrates that Procrustean evaluations of asymmetry can be utilised to estimate the magnitude of developmental instability experienced by individuals as well as samples, then subsequently employed to explain later-life health outcomes and explore developmental mechanisms (Zelditch and Swiderski 2018; Klingenberg 2015; Zelditch *et al.* 2012; Graham *et al.* 2010; Radwan *et al.* 2003; Klingenberg and Zaklan 2000; Klingenberg and McIntyre 1998). The conclusions of this literature review therefore establish the rationale for adopting certain statistical procedures to interpret data and permit Chapter 7 to be a more technically focused discussion of the GM methods employed.

Chapter 5: Materials

5.1 Introduction

Materials for this study were derived from four archaeological skeletal assemblages . The largest and oldest of these was recovered from the Black Gate cemetery at Newcastle-upon-Tyne where most of the burials date to between the 8th and 11th centuries (Nolan *et al.* 2010). Two collections originate from the later medieval period (broadly the 11th to 15th centuries); the larger from All Saints' Church, York and the smaller from the cemetery of St Lawrence's Church, Warwick (McIntyre and Bruce 2010; Bruce 2003; Gethin n.d.; Hill n.d.). One post-medieval assemblage from St Hilda's Church, South Shields was also included (Raynor *et al.* 2009). These are referred to as the Black Gate, York Barbican, Warwick and South Shields assemblages respectively.

As it is posited that contextually-specific cues are crucial in life-course development, this chapter provides background data for the skeletal materials analysed by reviewing previous research (archaeological, historical and osteological) that has examined sociocultural and environmental setting as well as health and disease within the assemblages. This enables similarities and differences between sites to be highlighted, thereby facilitating later discussions on the impact (or lack thereof) of contextually unique factors on life-course experiences and outcomes.

The final section of this chapter details the sampling procedure through which skeletal individuals included in the study were selected. Comparisons are made between the study sample and the full skeletal assemblages. This leads onto a discussion of unavoidable demographic biases resulting from dental wear and availability.

5.2 The Black Gate Cemetery, Newcastle-upon-Tyne

5.2.1 Background

The cemetery is located on a promontory overlooking a bridging point of the Tyne (Figure 5.1). The first evidence for occupation is in the Roman period, when a fort (*Pons Aelius*) situated along Hadrian's Wall was constructed in the late-2nd or early-3rd century. The fort fell into disuse in the late-4th to early-5th century, after which the local population began to repurpose the buildings along with their constituent materials (Nolan *et al.* 2010: 155-162; Snape and Bidwell 2002a: 251; Snape and Bidwell 2002b). The exact processes which led to the development of a more permanent settlement during the early medieval period are unknown, and the first unequivocal documentary reference to the site does not occur until the 12th century when the arrival of William I to "a place formerly called 'Moneccestre' and now called New Castle" in 1072 is recorded (Nolan *et al.* 2010: 157; Raine 1838: 20-21). Given the possible monastic connection, it has been proposed that a community with a parish church grew around a religious centre during the period of economic and political stability experienced in Northumbria in the mid to late-7th century (Nolan *et al.* 2010: 156; Walker 1976: 63-67). Artefacts found during excavation (e.g., brooches) are stylistically consistent with this hypothesis as are the results of radiocarbon analyses conducted on the cemetery's human skeletal materials (Nolan *et al.* 2010: 156-157; Lucy 1999: 39). The cemetery likely remained in continuous use until 1080 when an earthwork castle was constructed on it and after which burial within the bailey was likely restricted to the new Norman social elite (Nolan *et al.* 2010: 157).

Figure 5.1 The locations from which the study's four samples derive (the Black Gate and South Shields collections both originating from the Tyneside region).

5.2.2 Excavations and Osteological Analysis

Modifications to the castle throughout the later medieval and post-medieval periods caused significant damage to the early medieval cemetery and the skeletal remains did not fare much better during archaeological investigations in the early 20th century (Nolan *et al.* 2010: 157-159; Richardson 1852: 28-29). The first known excavation of the area in 1929 focused upon exposing the Roman fort and neglected to document properly the human skeletal remains, treating them as an inconvenient layer through which to cut (Nolan *et al.* 2010: 159). The earliest attempts to record the cemetery were initiated in 1973 in response to planned landscaping and maintenance of the medieval castle. Burials were first encountered in 1977 and by 1992 when excavations ended, over six hundred individual inhumations along with further disarticulated deposits had been uncovered, revealing one of the largest known early medieval Christian cemeteries in the north-east of England (Nolan *et al.* 2010: 148). The duration of the project and the constraints of the site did, however, impose limitations on subsequent analyses. Excavations took place over a period that saw great advances in archaeological

methodology and trenches were located in separate areas across the site. These factors resulted in disconnected "islands" of excavation in which the stratigraphy was variably recorded, a problem compounded by the later loss of records (Nolan *et al.* 2010: 149-152). Consequently, a clear phasing of successive burial generations could rarely be inferred (Nolan *et al.* 2010: 159-160).

The early analysis of the osteological remains and graves was similarly *ad hoc*. Several investigators were employed over the various seasons of excavation and it initially appeared that the site was quite idiosyncratic (Boulter and Rega 1993; Anderson 1989; Anderson 1988). Most notably there was early evidence of a sex bias which it was speculated could have been the result of the site's association with a monastic community and then a Norman garrison (Boulter and Rega 1993: 8). Due to the significance of the assemblage, however, efforts have been made to synthesise data (Nolan *et al.* 2010) and, since deposition at Sheffield's Department of Archaeology, the assemblage has been the subject of numerous investigations that have included all 643 skeletons (e.g., Mahoney Swales 2019; Mahoney Swales 2012). This process has been facilitated by the good preservation of the osteological remains – 511 (79.5%) of the skeletons exhibit only slight cortical erosion (Mahoney Swales 2019: 200). It has emerged that 202 (31.4%) individuals were skeletally immature and 441 mature (68.6%). Of the mature skeletons, Mahoney Swales (2019: 202) could estimate sex for 351 individuals with 173 (49.3%) estimated to be female and 178 (50.7%) male. The near equal sex proportion suggests that the early supposition of a sex bias was likely the consequence of spatial differentiation in burial location – 70.6% of the adult burials in the area around the church were males, for instance (Mahoney Swales 2019: 202). Similarly, though some seasons of excavation found few immature remains (Boulter and Rega 1993: 9), overall it appears that the site had an attritional mortality profile in which there is a high number of infant fatalities, a

low number of deaths among older children, teenagers and young adults, and an increase in mortality throughout maturity (Mahoney Swales 2019: 202; Gowland and Chamberlain 2005: 146).

The occurrence and frequency of palaeopathological lesions has also been the subject of substantial research. The observation of severe hypoplastic defects in first permanent molars has been used to suggest the presence of congenital syphilis in the population and, in one case, this was supported by the presence of diffuse periosteal new bone formation (Nolan *et al.* 2010: 251). Though this diagnosis has not been universally accepted, the severity of the defects does highlight that, for some individuals at least, developmental stress could be substantial and potentially associated with systemic infection. Interestingly, when LEH and CO were assessed by Mahoney Swales using a life-course approach, similar frequencies were found throughout the cemetery and it was inferred that the early-life experience for most was relatively uniform (Mahoney Swales 2019: 215). Moreover, stature estimates ranged between 157 cm and 183 cm for males and 147 cm to 170 cm for females which is comparable to contemporary assemblages in the northeast (Nolan *et al.* 2010: 251; Anderson *et al.* 2005: 486), suggesting that the growth outcomes of the population were not unusual for the time and region.

Mahoney Swales (2019: 216) also identified two interesting patterns regarding the frequency of lesions thought to be related to occupation. Firstly, in addition to one male with a depressed fracture and cut-marks on the cranium (Nolan *et al.* 2010: 251-252), long bone and clavicular fractures were frequent in skeletons with elaborate burials (e.g., stone cists). As it has been suggested that farming in the early medieval period resulted in a higher prevalence of fractures, it was posited that involvement in agriculture may have been associated with higher social status which led to a funerary rite that required a greater investment of time and resources (Mahoney Swales 2019: 216). Secondly, higher

rates of maxillary sinusitis were also found amongst males with elaborate burials and it was speculated that these individuals may have been employed in specialist tasks such as metalworking which exposed them to higher concentrations of airborne contaminants, but led to higher social status (Mahoney Swales 2019: 216). Consequently, it was conjectured that early medieval Northumbria was relatively egalitarian and that status was, in part at least, attained in maturity through occupation and activity rather than inherited (Mahoney Swales 2019: 216; Mahoney Swales 2012: 416).

5.3 St Hilda's Church, South Shields

5.3.1 Background

The coastal town of South Shields is situated in the northeast of England on the banks of the Tyne, approximately 3 miles downstream of Newcastle-upon-Tyne. The earliest evidence of occupation is Iron Age settlement activity located beneath the Roman fort of *Arbeia* (Raynor *et al.* 2011: 10; Breeze 2006: 115). The fort, which was the most easterly extension of Hadrian's Wall, was active as a garrison and supply post between the mid-2nd to the late-4th centuries, after which it likely became the site of an early-medieval royal residence. These lands were gifted to the Abbess (and later saint) Hild in 648 CE. By the early-15th century a parish church dedicated to St Hilda had been established to serve the hamlet of South Shields which had come into being in the 13th century as a fishing and salt processing community and grew into a small but prosperous port and market town (Raynor *et al.* 2011: 10-11; Breeze 2006: 115-118; Finden 1838: 15; Mackenzie 1834 31; Surtees 1820: 94-104). Further economic expansion occurred during the Industrial Revolution due to maritime connections and the locality's coal-rich geology (Newman 2016: 95; Roberts *et al.* 2016: 40; Raynor *et al.* 2011: 9; Hodgson 1903). During the 19th century South Shields grew into an urban centre with a shipyard as well as port, glass and chemical factories, a gas works and colliery (Raynor *et al.* 2011: 106; Fordyce 1857: 722-723) (Figure 5.2). Productivity was not only fuelled by access to natural resources and a distribution network, but as towns such as South Shields became ever more prosperous, they drew in economic migrants, providing a ready pool of labour (Panayi 1995; Friedlander 1992; Ravenstein 1885). Unsurprisingly, the impact of rapid industrialisation became the subject of much concern and in 1845 an investigation was launched which found that the town was

'*generally enveloped in a dense atmosphere of smoke, from the coal-pit, glass-works and other manufactories… Besides these, there are a great many steam-boats continually plying on the river, which constantly emit great quantities of smoke; and westerly winds, which prevail here… bring down upon the place the smoke of the numerous works situated on the Tyne… Complaints have been made of the effects of the gases emitted from the alkali chemical works which exist here... The exhalations from these works have been found injurious…*' (Report of the Commissioners 1845: 185).

St Hilda's church was affected by the town's expansion. The churchyard had to provide for the whole community and with an ever-expanding population of parishioners, most of whom were employed as labourers in local industries, the cemetery soon became overcrowded (Raynor *et al.* 2011: 11; Salmon 1856: 64; Mackenzie 1834: 31). Despite efforts to build-up and expand the cemetery on several occasions, like many urban cemeteries it was closed by the 1855 Burials Act and only a limited number of interments in family plots occurred after that date (Raynor *et al.* 2011: 15; Fordyce 1857: 715; Salmon 1856: 64).

Figure 5.2 South Shield's position on the banks of the Tyne meant that by the 19th century the town was surrounded by chemical and glass works, smelting plants, collieries and docks. Detail from the 1863 Ordnance Survey; this work is based on data provided through www.VisionofBritain.org.uk and uses historical material which is copyright of the Great Britain Historical GIS Project and the University of Portsmouth.

5.3.2 Excavation and Osteological Investigations

In response to development, rescue excavations in a portion of the cemetery that was in use from the mid-18th century until its closure were carried out between 2006-2007 (Raynor *et al.* 2011: 6). Through stratigraphic phasing, three burial horizons were identified. The lower burial horizon, which predates 1816, contained 49 skeletons and a charnel deposit (Raynor *et al.* 2011: 32-35). The intermediate horizon held nine skeletons and six charnel deposits and is associated with an attempt between 1816 and 1818 to raise the cemetery with ballast and debris (Raynor *et al.* 2011: 35; Salmon 1856: 17). A further 97 articulated skeletons and 22 charnel deposits came from the main trench of the upper horizon along with 43 skeletons and 5 charnel deposits from a subsidiary trench; this layer was deposited from 1818 to the cemetery's closure in 1855 (Raynor *et al.* 2011: 35-43).

In total, the osteological analysis identified 204 individual skeletons from the burials and commingled charnel deposits. Of these, 87 (42.6%) were skeletally immature and 117 (57.4%) mature (Raynor *et al.* 2011: 76). Though intercutting made completeness variable, preservation was good; 91 (77.8%) of the mature skeletons were well-preserved, for instance (Raynor *et al.* 2011; Brickley 2018: 7). Among the mature cohort, sex could be estimated for 103 individuals: 52 (50.5%) were estimated to be female and 51 (49.5%) male. Estimated statures were within a few centimetres of those from contemporary assemblages; mean male stature was estimated to be 171 cm with a range of 149-181 cm while the estimated female mean stature was 159 cm with a range of 149-174 cm (Raynor *et al.* 2011: 47). Moreover, mortality data largely conformed to a pattern expected in a pre-antibiotic population without proper obstetric provision (Chamberlain 2000: 105). For instance, 54 (62.1%) of the 87 immature skeletons were neonates or preterm skeletons while another 14 (16.7%) individuals were thought to have died between 1-5 years of age

(Raynor *et al.* 2011: 76-77) after which mortality decreases until later adulthood (Raynor *et al.* 2011: 76-77). There was also a notably higher ratio of females (3:1) in the 'young adult' and 'young-prime adult' age categories, suggesting cohort specific dangers such as pregnancy and childbirth may have affected length of life (Raynor *et al.* 2011: 44-46).

Pathological lesions were also recorded to explore patterns of health and disease within the population. To facilitate this, where feasible, prevalence rates were contrasted to published data (Raynor *et al.* 2011). Notable similarities existed with other industrial assemblages. For example, of the 1,289 observable permanent teeth, 250 (19.4%) were affected by LEH which is comparable to contemporary sites such as the Newcastle Infirmary and St Martin's in-the-Bull Ring, Birmingham which had prevalence rates of 17.0% and 27.9% respectively (Raynor *et al.* 2011: 50-53; Boulter *et al.* 1998; Brickley *et al.* 2006). This suggests that childhood stress experience within the South Shields population was congruent with that of other industrial cities. It may be also be possible that susceptibility to proinflammatory conditions – such as infectious diseases – was typical for an 18th to 19th century site; 27 (23.1%) mature skeletons exhibited signs of non-specific bone inflammation, which is comparable to the post-medieval ranges reported by Roberts and Cox (2003: 344). However, with three mature skeletons (2.6%) exhibiting signs suggestive of syphilis and a further three (2.6%) possibly affected by tuberculosis, the crude prevalence rates of these specific infections among skeletally mature individuals more closely matched those found at hospital sites (Raynor *et al.* 2011: 68-69; Roberts and Cox 2003: 339-341; Boulter *et al.* 1998). Further non-specific and specific lesions imply site-specific perturbations to health relatable to lifestyle and environment. Raynor *et al.* (2011: 64) report that 95 (86.4%) out of 110 skeletons at St Hilda's with one or more surviving vertebrae showed evidence of spinal joint disease, which is often linked to occupational stress and labour. This is much higher than the

10-14% range post-medieval Britain found by Roberts and Cox (2003: 352), and exceeds rates from other working-class industrial sites; 56.6 % of the skeletons from St Luke's, Islington showed evidence of spinal degeneration, for example (Raynor *et al.* 2011: 65; Boyle *et al.* 2005: 241). The high prevalence of maxillary sinusitis (17.5% of skeletons were affected compared to a post-medieval average of 6.9%) and possible case of "phossy jaw", both of which are linked to air quality and environmental pollutants, may be further markers of industrialisation and chemical contamination of the environment (Roberts *et al.* 2016: 44; Marx 2008), suggesting that economic development came at the expense of respiratory health.

5.4 St Lawrence's, Warwick

5.4.1 Background

The site of St Lawrence's Church is located within the modern city of Warwick, but would have occupied agricultural land outside of the medieval settlement (Stephens 1969; Gethin n.d.) (Figure 5.3). It is not known when the church first came into existence, but in 1123 it was gifted along with seven other religious houses, which included a priory and leprosarium, to the newly established St Mary's collegiate church (Gethin n.d.: 6). St Mary's functioned as the parish church of Warwick and, like other medieval collegiate churches, fell beyond diocesan jurisdiction meaning that it could administer its considerable holdings independently (Willoughby 2012: 331; Proudfoot 1983: 231; Gethin n.d.). As such, St Lawrence's formed part of a localised religious network within the Warwick area.

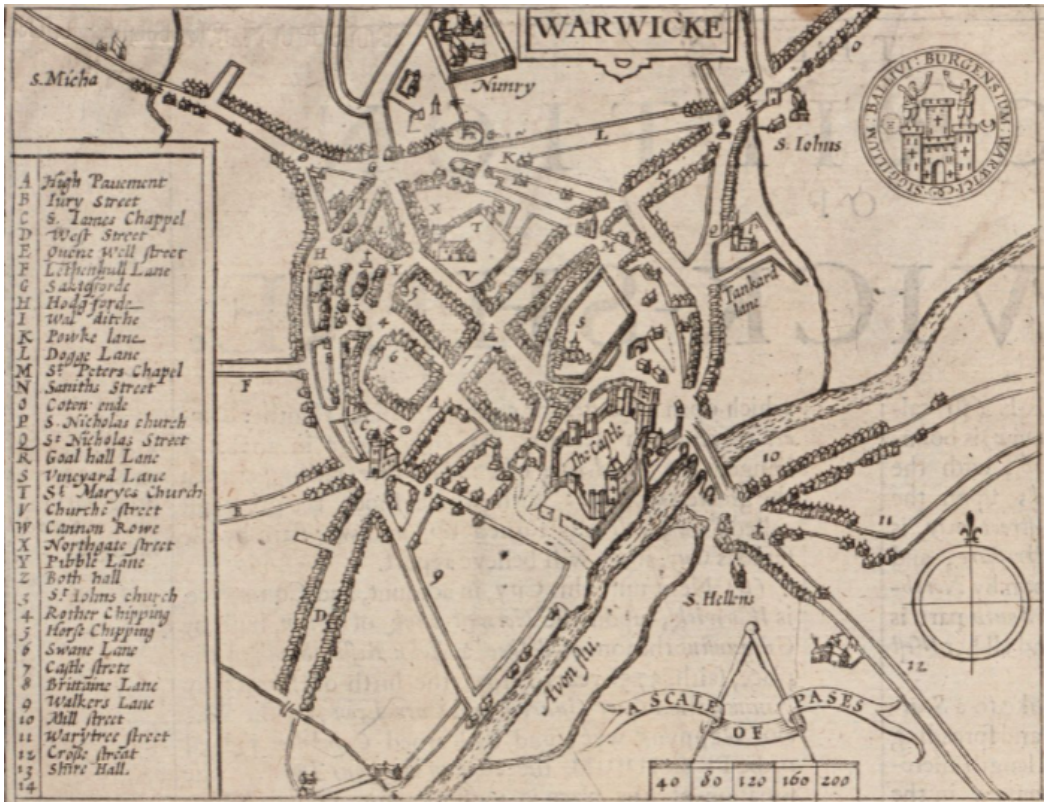

Figure 5.3 Detail of Warwick from Speed (1610). St Lawrence's was in the pastoral lands to the south of the city.

Documentary data for Warwickshire (e.g., Domesday Book and the Hundred Rolls) suggest an expanding population and economy from the 11th-13th centuries (John 1997). This growth was most pronounced in the northern part of the county (in which Warwick is located), which had previously been forested-covered and sparsely populated (John 1997: 42; Harley 1958: 18). Like many of Warwickshire's churches, St Lawrence's church expanded over this period and historical texts describe it as possessing structural flourishes (e.g., a steeple) that imply an investment beyond the strictly functional (Proudfoot 1983: 232; Gethin n.d.: 8). This period of prosperity seems to have been short lived, however, as the coming of the 14th century heralded dramatic changes for the county. Though some postulate the Black Death epidemic of 1348-1350 as the cause, others theorise that the area was either approaching or exceeding carrying capacity before this and that a combination of environmental and anthropogenic factors tipped the region beyond sustainability (Slavin 2013; John 1997: 41; Proudfoot 1983; Harley 1958: 18; Gethin n.d.). Certainly, throughout England and Wales extreme weather events – torrential rain, flooding and freezing winters – from 1314 to 1317, led to crop failures and food shortages which, exacerbated by food hoarding and aggressive price rises, culminated in the Great Famine (Slavin 2013). At a local level, Warwickshire seems to have been badly affected as it appears that agricultural production was already struggling to keep pace with demographic growth and there was a consequent decline in Warwickshire's population and a concomitant dip in church maintenance (John 1997: 41; Proudfoot 1983; Harley 1958: 18; Gethin n.d.). The parish of St Lawrence's was almost certainly a victim of these adverse times and in the latter 14th century, the dilapidated St Lawrence's was ordered to close along with several other small local churches (Gethin n.d.: 15).

5.4.2 Excavations and Osteological Analysis

The site was initially excavated in 2009 by Archaeology Warwickshire with results summarised by Gethin (n.d.) in an as yet unpublished report. The architectural and material finds conform to the picture presented by the documentary evidence. The oldest piece of masonry found was a Norman capital while the nave is likely to be the earliest portion of the church exposed by the excavators (Gethin n.d.: 8). The nave was constructed of rough sandstone blocks covered with white mortar; decorative embellishment must have been present though as stone fragments were painted white with traces of red, black and yellow (Gethin n.d.: 8). The north aisle was a later addition, in all probability made at a time of greater affluence; the walls were wider and constructed of higher quality stonework than those of the nave (Gethin n.d.:14). Further excavations were conducted in 2015 (Hill n.d.: 1); little information is currently available on the archaeological findings, but the scope of the project appears to have been limited and not resulted in anything that would contradict the inferences drawn from the previous excavations. Both seasons encountered graves from the churches' cemetery which for the most part were organised into rows with substantial intercutting (Hill n.d.: 1). By the end of excavations in 2010, 174 skeletons along with 59 deposits of disarticulated remains had been found (Newman 2019: 1; Gethin n.d.: 10-13); 22 more burials were uncovered in 2015 (Hill n.d.: 1-2). The skeletons were analysed separately with results contained in two unpublished reports by Newman (2019) and Hill (n.d.) which are synthesised here.

In total, 196 skeletons have been recovered and analysed (Newman 2019: 1; Hill n.d.: 1). Although preservation varied over the site, both reports indicate that most skeletons were highly fragmented (Newman 2019: 19; Hill n.d.: 2), probably as a result of intercutting. Of the 174 skeletons in which skeletal maturity could be determined, 63 (36.2%) were immature and 111 (63.8%) mature (Newman 2019: 17-18; Hill n.d: 7-10).

Sex could be estimated for 72 mature skeletons; 34 (47.2%) mature skeletons were estimated to be female, compared to 38 (52.8%) males (Newman 2019: 19; Hill n.d.: 2). Age estimation for 122 skeletons, revealed two mortality peaks. The first of these was in childhood with 55 (45.1%) individuals estimated to have died before 11 years of age. Then, after a decline in mortality during adolescence and early adulthood, a second peak develops and 58 (47.5%) individuals from the sample are estimated to have died after 26 years of age (Newman 2019: 19). Mean female stature was estimated to be 159 cm with a range of 150-167 cm, while estimated mean male stature was 169 cm with a range of 161-179 cm (Newman 2019: 20); these are consistent with female and male averages (159 cm and 171 cm respectively) for late medieval Britain (*circa* 1050-1550) (Roberts and Cox 2003: 248). Overall, the pattern described is consistent with a normal living population – e.g., near-equal sex ratio and close-to-average statures.

A more recent research project by Nolan (2019) has suggested the mortality profile was unusual, however. Nolan (2019) employed a transition analysis to estimate age-at-death more precisely (Section 7.2.3.1.1), and found that the mortality peaks for individuals <10 years and >70 years were higher than expected when compared to a normal attritional or catastrophic mortality profile. As famines typically impact the more vulnerable members of a community (i.e., the youngest and oldest), it was argued the population suffered a period of severe resource scarcity leading to deaths directly through starvation as well as indirectly through suppressed immune response and increased disease susceptibility (Nolan 2019: 47-50; Yaussy *et al.* 2016). This supposition seems credible when viewed alongside the palaeopathological evidence from the osteological reports. Newman (2019: 10-15) noted two skeletons with diffuse but largely symmetrical PNBF. Hypertrophic osteoarthropathy (HOA) – often a secondary condition associated with chronic pulmonary conditions (e.g., lung cancer, pulmonary tuberculosis) (Grauer

2019: 503; Binder and Saad 2017; Mays and Taylor 2002) – was suggested as a potential differential diagnosis. Hill (n.d.) also identified a skeleton with elongated and distally thinned phalanges consistent with tuberculous dactylitis (Roberts and Buikstra 2019: 339) as well as the fusion of nine thoracic vertebrae along with centrum destruction leading to severe anterior kyphosis (Figure 5.4). The abnormal curvature of the spine was identified as Pott's disease (tuberculous spondylitis), which is virtually pathognomonic of tuberculosis and often results from the haematogenous spread of the disease – usually from the lungs (Roberts and Buikstra 2019: 327; Hill n.d.: 4; Garg and Somvanshi 2011: 445). These cases suggest a population in which chronic disease (possibly the consequence of resource insufficiency) played a major role in determining life-course outcomes.

Figure 5.4 Vertebral body collapse and severe thoracic kyphosis in SK 34 (Hill n.d.: 5).

5.5 All Saints' Church, York ("The Barbican")

5.5.1 Background

The cemetery of All Saints' Church is located immediately outside the medieval walls of York (McIntyre and Bruce 2010: 32; Bruce 2003: 8). Situated at the confluence of the rivers Ouse and Foss (Figure 5.5), York was founded in 71 CE (Campbell 2009: 4; Bruce 2003: 9). What was initially a military and administrative centre developed into one of the largest cities in Roman Britain (McIntyre 2015: 413-415; Bruce 2003: 9). The city remained an important centre in the post-Roman period and was the capital of Northumbria in the 7th century (Bruce 2003: 10; Toswell 2000). From the mid-8th to mid-10th century, York thrived; there is archaeological evidence for a mint and craft production, as well as the incorporation of the city into an international network of trade (Lund and Sindbaek 2021; Bruce 2003: 10; Sindbaek 2007). However, after being first absorbed into the unified English kingdom, following several revolts the city was laid waste during the early Norman period (Bruce 2003: 10; Kappelle 1979). Despite this, medieval York remained a focal point for production and trade during the 12th-15th centuries; artisans (e.g., masons, goldsmiths and glass painters) practised their crafts, grain and wool was stored in the city for export to Europe, while both staples (e.g., fish and shellfish) as well as luxury products (e.g., spices and wine) were imported (Goldberg 2019: 163; Mahoney Swales 2012: 220; Barrett *et al.* 2004: 619-621; Tilliot 1961: 84-106). Given the abundance of material wealth, the city grew into a busy and sometimes overcrowded hub (Goldberg 2019: 175; Watts 2011: 570; Dyer 1989). Though the church may have an earlier origin, it is in this later period that All Saint's is first mentioned as a gift to Whitby Abbey in the 11th century. The church was closed with the Abbey in the mid-16th century, however, and effectively faded from the historical record

with the site being used for the construction of a cattle market in the 1820's (McIntyre and Bruce 2010: 32; Bruce 2003: 5-10).

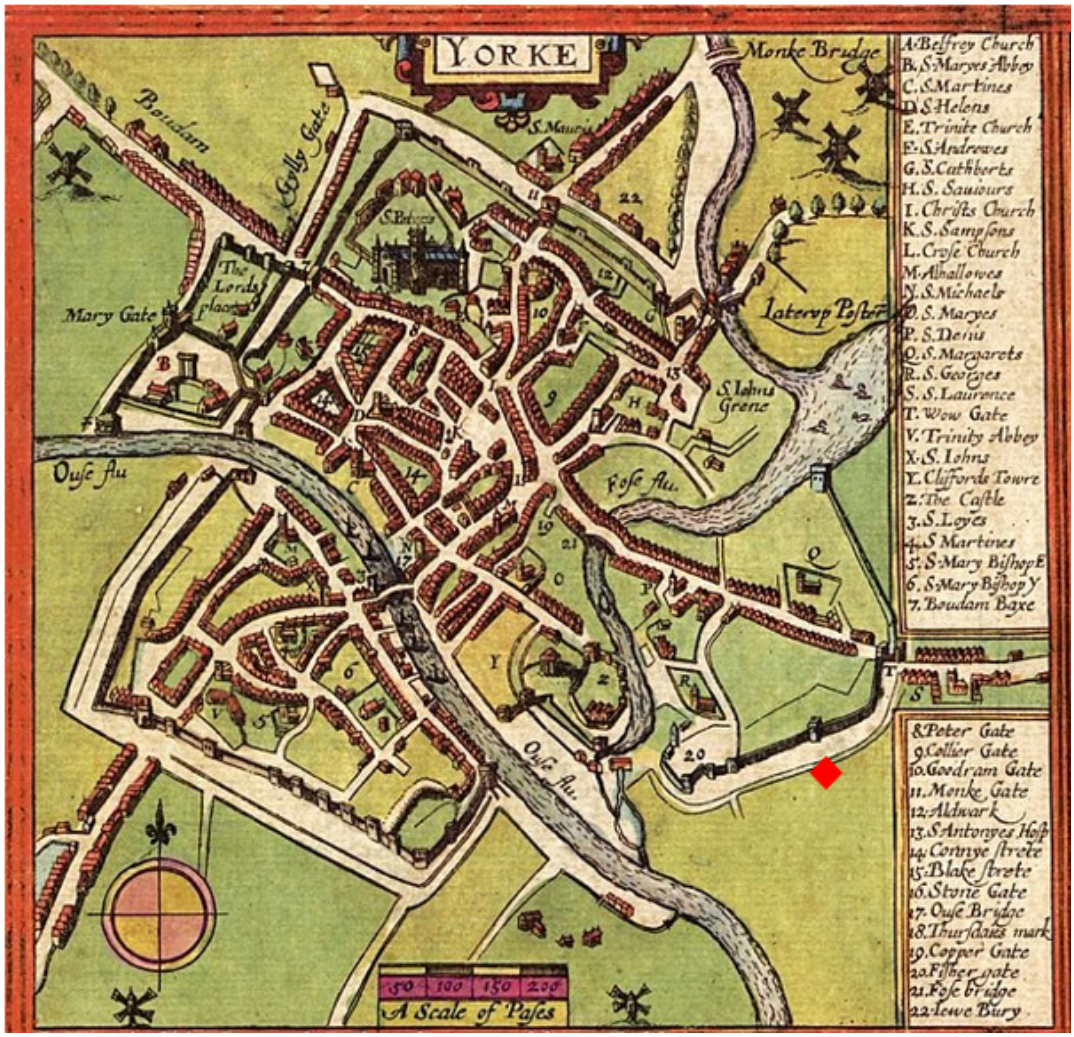

Figure 5.5 John Speed's (1611) map of York. Despite its recent closure, All Saints' Church had already begun to fade from memory and is not marked. The church's approximate location has been added in red.

5.5.2 Excavations and Osteological Analysis

In 2003 an archaeological investigation was initiated in the presumed area of the "lost" church (Bruce 2003: 5). Fourteen trenches were dug uncovering the foundations of the church, a variety of ceramics and building materials dated to the Roman and medieval period and, in three trenches, 31 articulated human skeletons as well as large quantities of disarticulated remains (Bruce 2003: 24). Due to the density of burials and intercutting it

was believed that the cemetery had been in use for a substantial period and that further excavation would reveal a large cemetery (Bruce 2003: 53). More extensive archaeological investigation between 2007-2008 uncovered over six hundred skeletons so that in total 667 individuals were recovered (McIntyre and Bruce 2010). It was noted that not all skeletons conformed to the same burial pattern, however, and that some likely originated from different eras of York's long history. Specifically, a cluster of seven inhumations in the northwest corner of the site were orientated on an approximately north-south axis, suggesting a non-Christian burial – an inference supported by the discovery of grave goods (e.g., rings and brooches) dated to the Roman period (McIntyre and Bruce 2010: 33). A further 113 skeletons were discovered closely packed into ten mass graves. It is likely that they are the skeletons of soldiers that died during the siege of York in 1644 – later osteological analyses found most of these skeletons belonged to younger mature males, adding weight to this interpretation (McIntyre 2016; McIntyre and Bruce 2010: 36). Due to the small number of the Roman remains and the demographically-biased nature of the mass graves, these skeletons were excluded from analysis in this study.

The remaining 547 skeletons followed a common west-east alignment but with substantial truncation of graves believed to be the result of prolonged use of the area without burial markers. Despite a scarcity of artefactual finds to independently confirm the cemetery's period of use, due to the burial alignment and vicinity to the medieval church it is believed that these are Christian era inhumations dating approximately to the 11th-16th century (McIntyre and Bruce 2010: 33-34; Bruce 2003: 10-11). As a result of grave intercutting and post-medieval construction (i.e., the cattle market), most of the skeletons are only partially present – 235 (42.9%) are less than 25.0% complete (McIntyre n.d.: 12) (Figure 5.6). Nevertheless, preservation was generally good, with

little or no surface degradation for most of the recovered bones (McIntyre n.d.: 14). Three hundred and sixty-four (66.5%) of the skeletons were mature; for 334 of these, sex could be estimated, revealing an approximately equal sex distribution: 162 (48.5%) were estimated to be female and 172 (51.5%) male (McIntyre n.d.: 17). The average female stature was estimated to be 159 cm while the average estimated male stature was 170 cm (McIntyre n.d.: 16); these values fall very close to female and male averages (159 cm and 171 cm respectively) for late medieval Britain (*circa* 1050-1550) (Roberts and Cox 2003: 248). Among the mature skeletons, mortality peaks in the 35-49 years age category. For the skeletally immature cohort, mortality declines after a high in the early postnatal period (McIntyre n.d.: 20). From this it has been surmised that medieval burials in the Barbican assemblage represent a normal living population with an attritional mortality profile (Gowland and Chamberlain 2005: 146; McIntyre n.d.: 20).

Figure 5.6 Osteological assessments of the York Barbican assemblage have been complicated as a result of grave cutting by extensions to the medieval church (a) and later structures, such as the cattle market, as well as intermingling of remains (b) from prolonged cemetery usage. Images from Bruce and McIntyre (2010).

Several interesting findings have also emerged from more in-depth analysis of the assemblage and its archaeological context (McIntyre n.d.; Bruce 2003). For instance, leprosy was present in the population. Five skeletons (four females and one male) have lesions (such as resorption of the anterior maxillary alveolus and rounding of the nasal aperture) that are likely the result of prolonged *Mycobacterium leprae* infection (McIntyre n.d.: 50). As leprosy is usually transferred when in close proximity to sufferers for extended periods (Kelmelis *et al.* 2020: 175; Barreto *et al.* 2014), this further suggests that the densely populated cemetery reflected the living conditions of many residents (McIntyre n.d.: 50; McIntyre and Bruce 2010: 33-34; Bruce 2003: 10-11). Aside from infectious disease, it has also been proposed that physical activity and traumatic events influenced life experiences. Regarding the former, both males and females had high rates of lesions that can, among other things, be associated with intense or chronic physical strain; there is ample evidence for dislocation as well as fracture and 45% of the skeletons had some form of joint degeneration (McIntyre n.d.: 24-42). The observation of a likely puncture wound in the right ilium of one female skeleton has also been used to imply that trauma was not always accidental, but sometimes the result of violence (McIntyre n.d.: 32). Meanwhile, the find of a female skeleton with the remains of a perinate in the pelvic region with its head orientated toward the pubic symphysis has been interpreted as evidence of obstetric fatality and poignantly illustrates the dangers for both mother and child during pregnancy and birth – though, due to the presence of LEH, tibial PNBF and generally small stature of the female, it has been suggested that stress during the mother's development may have been a complicating factor (McIntyre n.d.: 78; Bruce 2003: 53).

5.6 Sample Selection and Implications

As dental wear was the key determinant to inclusion, certain biases were created in the study's skeletal sample when compared to the full assemblages (Table 5.1-Table 5.2). Specifically, individuals needed to possess antimeric M1s in sufficiently good condition that the occlusal outline was clear and homologous points identifiable. This is obviously limiting when studying past populations in which diets were generally abrasive, causing rapid attrition of enamel and destruction of coronal features (Hillson 2005: 214-215) (Figure 9.13). Thus the skeletons analysed in this project represent a subsample of the assemblages discussed throughout this chapter so far. To illustrate, although over six hundred skeletons were recovered from Black Gate (Nolan *et al.* 2010: 148), only 84 could be assessed. Similarly, 33 individuals were analysed from South Shields, 30 from Warwick and 73 from York Barbican. Inevitably some degree of disparity between the estimates of stress experience for the sample and the actual living population can be expected, especially as mean shapes are influenced by sample size and this project relied heavily upon measures derived from means (Sections 7.4 and 7.5) (Cardini *et al.* 2019; Cardini *et al.* 2015; Cardini and Elton 2007). Moreover, as dental wear is age-progressive, a disproportionately large number of mature skeletons were excluded. Returning to the Black Gate assemblage, Mahoney Swales (2019) found that 68.6% of individuals were skeletally mature while, in contrast, only 56.0% of the Black Gate skeletons in the project's sample were. The requirement for well-preserved teeth therefore led to a bias towards the inclusion of younger, skeletally immature individuals and the likelihood of being excluded from the sample increased with age – it was noted, for instance, that only five of the 217 skeletons in the sample were associated with point estimates of age greater than 60 years (Section 8.2.1).

Site		Immature	Mature	Reference
Black Gate	sample	37 (44.0%)	47 (56.0%)	
	full assemblage	202 (31.4%)	441 (68.6%)	Mahoney Swales 2019
South Shields	sample	14 (42.4%)	19 (57.8%)	
	full assemblage	87 (42.6%)	117 (57.4%)	Raynor *et al.* 2011
Warwick	sample	20 (69.0%)	9 (31%)	
	full assemblage	63 (36.2%)	111 (63.8%)	Newman 2019; Hill n.d.
York Barbican	sample	33 (47.1%)	37 (52.9%)	
	full assemblage	183 (33.5%)	364 (66.5%)	McIntyre n.d.

Table 5.1 Frequency of skeletally immature and mature individuals recovered from each site as well as included in the study sample.

Site		Female	Male	Reference
Black Gate	sample	12 (35.3%)	22 (64.7%)	
	full assemblage	173 (49.3%)	178 (50.7%)	Mahoney Swales 2019
South Shields	sample	5 (35.7%)	9 (64.3%)	
	full assemblage	52 (50.5%)	51 (49.5%)	Raynor *et al.* 2011
Warwick	sample	4 (58.3%)	3 (48.7%)	
	full assemblage	34 (47.2%)	38 (52.8%)	Newman 2019; Hill n.d.
York Barbican	sample	15 (50%)	15 (50%)	
	full assemblage	162 (48.5%)	172 (51.5%)	McIntyre n.d.

Table 5.2 Frequency of females and males among the skeletally mature individuals for whom sex could be estimated from each assemblage as well as included in the study sample. Note the bias towards males in the samples from Black Gate and South Shields.

Figure 5.7 Dental wear, which is very common in past populations as shown above, necessitated the exclusion of many skeletons from the sample, especially those associated with older individuals.

Given that frequencies of stress marker presence often vary between immature and mature cohorts (e.g., Blakey and Armelagos 1985), thus implying significant disparities in stress experience between non-survivors and survivors, the estimates of early-life stress generated from the sample likely distort experiences endured by the living population. Moreover, as up until approximately three years of age M1s remain covered by the alveolar bone (Figure 9.14a), and without resorting to destructive methods were largely unobservable through the methods detailed in Chapter 7, the immature cohort analysed here underrepresented the youngest skeletons. Given the high perinatal/infant mortality rates in past populations, the near-exclusion of this subset further skewed results (Newton 2015: 218; Pozzi and Ramiro Fariñas 2015: 55; Vallin 1991). One might wonder whether the stress experience of individuals that did not manage to survive this period of life significantly differed from the immature cohort generally. For example, do they represent orphans that did not benefit from postnatal maternal support or was maternal buffering insufficient to mitigate the most extreme stressors? Moreover, some individuals most severely affected by early-life stress were likely excluded by the methodology's reliance on configurations containing homologous landmarks (Chapter 7). That is, a small number of skeletons could not be included due to gross dental defects rendering their occlusal surface highly irregular and incomparable. Individuals from Black Gate and Warwick, for example, had gross hypoplasia possibly related to the transplacental transmission of infection from mother to foetus (Roberts and Buikstra 2019: 399; Ortner 2003: 595; Aufderheide and Rodríguez-Martín 1998: 405-406) (Figure 9.14b). For the purposes of assessing maternally-mediated early-life stress (especially severe stress), such individuals would likely have been very informative.

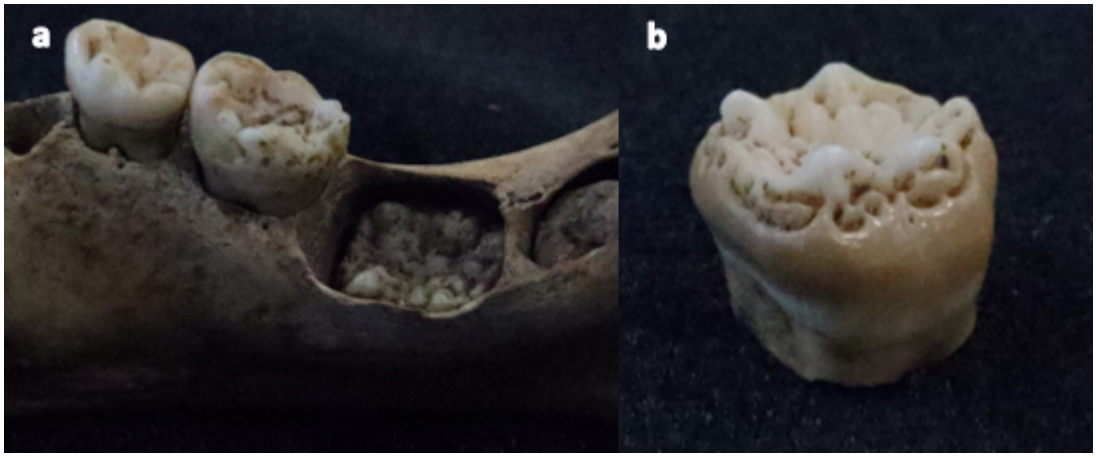

Figure 5.8 M1s from BG 477. The right M_1 was not assessable because it was still lodged in the alveolar process (a). Even if it were free, the gross enamel defects which affect both teeth, and are most clearly seen on the left tooth (b), make it impossible to apply methods reliant on identifying homologous landmarks.

Meanwhile, the underrepresentation of older mature skeletons due to dental wear probably impacted the exploration of early-life stress on later-life frailty. Many chronic later-life diseases associated with early-life programming typically have a late age of onset (e.g., the risk of coronary heart disease increases dramatically after 60) (e.g., Rodgers *et al.* 2019: 1; Barker 2012; Yazdanyar and Newman 2009; Roseboom *et al.* 2000; Barker and Osmond 1986). As most of these conditions do not typically produce osteological signs, it might be argued that the inclusion of larger numbers of mature skeletons would not be overly fruitful. However, such pathologies increase frailty and mortality generally (e.g., Mozaffarian *et al.* 2016; Sanchis-Gomar *et al.* 2016: 6; Roseboom *et al.* 2001); age-at-death distributions in older mature individuals would therefore have likely been of interest. To summarise, although unavoidable, the requirement for well-preserved M1s rendered certain parts of the life-course obscure.

5.7 Conclusion

The assemblages of the study sample represent a variety of time periods, geographic regions and scales of urban development. The Black Gate cemetery can be characterised as early-medieval (*circa* 500-1000 CE), the York Barbican and Warwick collections date to the late medieval period (*circa* 1000-1500 CE), while the South Shields sample is from the industrial period (Steckel *et al.* 2019: 7). Although categorising samples by period in such a way can be reductionist – in that it implies relatively dramatic, universal breaks in the historical record, rather than variable and gradual transitions – it does facilitate comparisons between sites and with published data (Steckel *et al.* 2019: 1-10).

Three of the sites (Black Gate, York Barbican and South Shields) are located in the northeast of England, while Warwick is central. The York Barbican and South Shields sites can be described as urban (i.e., settlements of high population density, market economy, etc), although urban environments in the medieval and industrial periods were substantially different (e.g., in types of industry present and their environmental impact) (DeWitte and Betsinger 2020: 2-21). The Black Gate and Warwick sites are more rural in nature. The Black Gate cemetery likely served as a focal point for surrounding rural communities, while the church of St Lawrence's, although located close to Warwick, was associated with a small parish beyond the town's walls surrounded by arable land (Mahoney Swales 2012; Nolan *et al.* 2010; Boulter and Rega 1993; Stephens 1969; Gethin n.d.).

From past osteological analyses and research projects it can be implied that the osteological collections associated with each site are a fairly representative sample of a living population – there are no substantial sex biases, attritional mortality is present

(although mortality among more vulnerable individuals may have been higher at Warwick) and stature ranges appear comparable to contemporary sites (Newman 2019; Nolan 2019; Raynor *et al.* 2011; Gowland and Chamberlain 2005: 146; Gethin n.d.; McIntyre n.d.). A variety of factors have been identified as important to life-course trajectories; some of these are site-specific (e.g., airborne industrial pollutants at South Shields), while others, such as physically-arduous adult life-styles, appear to be more ubiquitous (Newman 2019; Raynor *et al.* 2011; Gethin n.d.; McIntyre n.d.).

Although early-life stress has been discussed in previous research, fluctuating asymmetric variance in first permanent molars has never been quantified in any of these populations. An assessment of M1 asymmetry with these materials therefore permitted not only the trial of an original method for inferring maternally-mediated early-life stress in past human populations, but also the exploration of stress experience over many centuries and across a variety of contexts and, importantly, with reference to themes such as environmental change and economic development. It was thus possible to generate new perspectives about the contextually dependent factors that shaped life-courses at each site, and explore themes that have the capacity to provide valuable information on issues that affect both modern and past groups. The fundamental requirement for erupted and relatively well-preserved M1s did, however, prove challenging. So, although the full skeletal assemblages represent normal living populations fairly well, the individuals included in this study represent a biased sample. Specifically, perinates and infants along with many older individuals were excluded from the analysis.

Chapter 6: Methods – Osteological

6.1 Introduction

The following chapter details the methods employed to generate osteological profiles that include demographic and palaeopathological data. In many cases, these techniques are relatively well-known (e.g., the traits employed to estimate sex). However, in other instances a choice has been made between competing methods (such as the adoption of a Bayesian approach to adult age estimation) or the reasoning behind the selection may not be obvious (for instance, periodontal disease was assessed to explore underlying physiology rather than diet). Consequently, as well as describing the methods utilised (to permit replication of the experimental protocol, if desired), the rationale behind their use is also expounded. In conjunction with the Procrustean index of fluctuating asymmetry (Chapter 7), these variables enable stress experience to be charted across the life-course so that within and between-group patterns can be quantitatively investigated.

6.2 Demographic Profiles

The observations collected to generate age and sex data are largely well-recognised and widely employed due to their inclusion in reference texts (e.g., Brickley and Mitchell 2017; Brickley and McKinley 2004). However, as life-course research has shown that mortality is related to early-life stress, additional consideration was given to methods of age-at-death estimation, especially in older individuals for whom a more quantitatively refined approach was sought (Temple 2014; DeWitte and Wood 2008; Roseboom *et al.* 2001).

6.2.1 Sex Estimation

Dimorphic osteological traits in the skull and pelvis, such as the greater sciatic notch (Figure 6.1), were assessed to estimate sex (Table 6.1). These morphological characteristics exist on a spectrum of expression and were scored along a 5-grade scale; grade 1 is often described as "female", 2 as "female?", 3 as "indeterminate", 4 as "male?" and 5 as "male" (e.g., Ferembach *et al.* 1980: 518). All features present were graded and the median grade employed as a summary estimate. Individuals with summary estimates of grades 1-2 were combined into a "female" group, 4-5 into a "male", while sex was considered indeterminate for remains with a grade of 3 (White and Folkens 2005: 385-397; Buikstra and Ubelaker 1994: 15-20). Given that these categorisations were derived entirely from osteological observations, the resulting estimate was of *skeletal sex*.

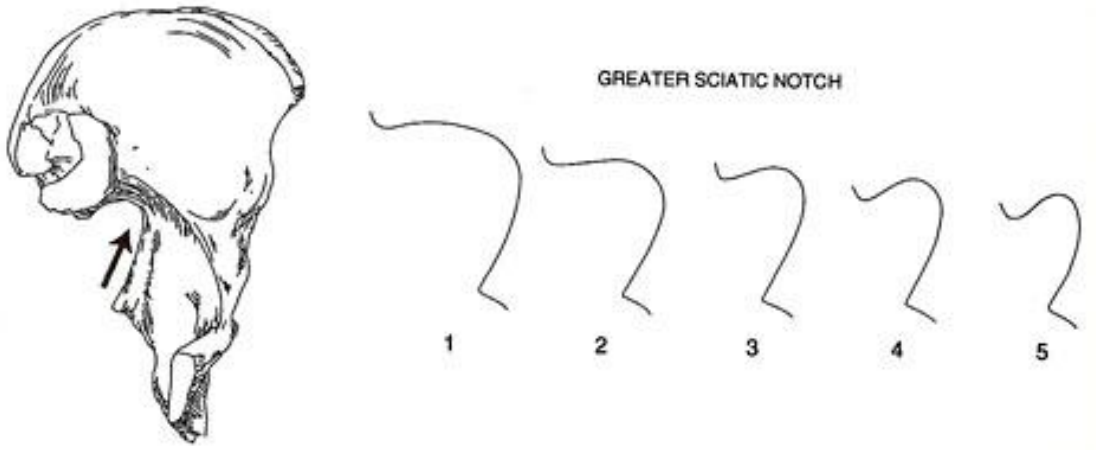

Figure 6.1 Dimorphic traits, such as the greater sciatic notch shown above, were graded along a scale of 1-5, with 1 and being typical of female and 5 male morphologies (Buikstra and Ubelaker 1994: 18).

Dimorphic Traits	Description	
Pelvis	Female	Male
Ventral arc (anterior pubic ridge sweeping inferolaterally)	Present	Absent
Subpubic concavity	Concave inferior pubic ramus	Straight (or slightly concave) inferior pubic ramus
Ischiopubic ramus (medial aspect)	Sharp ridge	Flat, broad, blunt
Iliac crest	Flat, less distinct S-shape	Accented S-shape
Greater sciatic notch	Wide, open, U-shaped	Narrow, V-shaped
Obturator foramen	Triangular, sharp rims	Oval, rounded rims
Preauricular sulcus	Deep and well defined	Absent
Cranium		
Nuchal crest	Smooth or slight traces of nuchal lines	Large, well-defined ledge/hook
Mastoid process	Small, minimal projection	Large, width/length much greater than external auditory meatus
Supraorbital margin	Palpably sharp, distinct edge	Thich border, blunt, rounded border
Glabella	Minimal expression, rounded frontal bone	Rounded prominence, often with well-defined supraorbital ridges
Mandible		
Mental eminence	Little or minimal eminence	Pronounced, can dominate anterior mandible
Gonial angle	Eversion absent	Pronounced eversion/flare
Ramus angle	Shallow angle	Near right angle, flexed ramus
Ramus flexion	Minimal/absent	Accentuated

Table 6.1 Morphological features of the pelvis and cranium employed to estimate skeletal sex (White and Folkens 2005: 385-397; Loth and Henneburg 1996; Schwatrz 1995; Buikstra and Ubelaker 1994: 15-20; Ferembach *et al.* 1980, Phenice 1969). Features are expressed on a spectrum and, for brevity, the descriptions above represent what has been termed as "female" and "male" or, in other words, the most distinct manifestations of skeletal sex (i.e., on a 5-grade scale, these would correspond to grades 1 and 5).

Although, biomolecular tests are becoming progressively more accessible (i.e., aDNA and enamel peptide analyses) and they provide the most accurate means of assessing genetic sex from osteological remains (Inskip *et al.* 2019; Stewart *et al.* 2017), they were not available for use in this case. Additionally, the requirement for destructive sampling would have limited sample size. As the accuracy with which sex can be estimated from skeletal morphology is high – e.g., Phenice (1969: 300), reported a 96% accuracy rate based upon the assessment of three pelvic features – it is unlikely that the reliance on skeletal traits was a major drawback.

Sex was not estimated in immature remains. Although skeletally immature remains evidence sexual dimorphism, it is subtle and difficult to assess (Klales and Burns 2017; Schutkowski 1993). Consequently, accuracy when estimating sex before the attainment of maturity through the observation of morphological features is low (Klales and Burns 2017; Schutkowski 1993).

6.2.2 Age Estimation through Dental Development

Age-at-death estimation in younger individuals can be achieved in several ways. The appositional growth of long bones and fusion of epiphyses, for example, are relatively well-regulated and, under ideal circumstances, it is possible to estimate age with confidence to within a few years. However, as males and females grow and mature skeletally at different rates (Figure 6.2), these methods are confounded by an inability to reliably estimate sex in immature remains (Section 6.2.1). Furthermore, as malnutrition and disease can cause delays in growth and epiphyseal fusion, the projection of developmental schedules derived from modern populations onto archaeological samples (which often exhibit signs of adversity) has been shown to over-estimate age (Schaefer *et al.* 2009; Coqueugniot and Weaver 2007; Smith 2007; Scheuer and Black 2000; Hoppa 1992; Gindhart 1973; Maresh 1970). The formation and eruption of teeth is, in contrast, highly correlated with chronological age and follows a predictable pattern that is comparable within and between populations with only small variations between sexes and groups of different ancestry – an exception being C_1 root completion (Section 7.3.2) (Antoine and Hillson 2016: 223; Harris 2016: 145; Lewis *et al.* 2016; Elamin and Liversidge 2013; AlQahtani *et al.* 2010; Liversidge and Marsden 2010; Liversidge *et al.* 2006; Chertkow 1980; Christensen and Kraus 1965; Kraus and Jordan 1965; Moorrees *et al.* 1963).

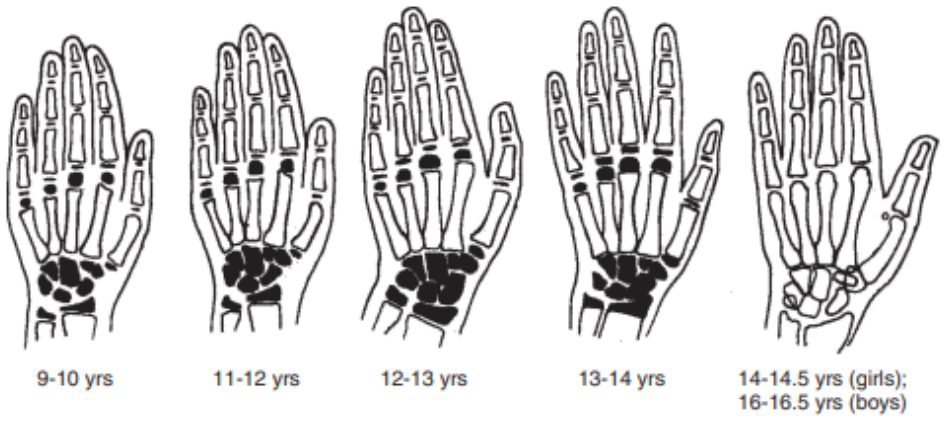

Figure 6.2 The fusion of epiphyses, such as those found distally in metacarpals and proximally in phalanges, varies according to sex, with males reaching maturity later than females (Schaefer *et al.* 2009: 227).

Several atlases of dental growth have been published to estimate age, but use of the London Dental Atlas (AlQahtani *et al.* 2010) (Figure 6.3) is becoming increasingly widespread. Being developed from a sample of 176 pre- and early-postnatal skeletal remains from historical known age-at-death collections and 528 radiographs from living participants to give a total sample size of 704 individuals, one major benefit of the London Atlas is its representativeness. From this sample, for the period between the second and twenty-fourth year, dental growth was assessed from radiographs associated with 24 living participants (with an equal sex ratio) per year (e.g., between 2 and 3 years of age, dental development was assessed through radiographs from 12 females and 12 males, and so on). Such a large sample with verifiable provenance compares favourably with earlier atlases. For instance, it is not definitively known from what sample Schour and Massler's (1941) atlas was developed, though anatomical and radiographic data from as few as 26 or 29 individuals has been conjectured (AlQahtani *et al.* 2010: 484; Smith 1991). Thus, the atlases of Schour and Massler (1941) and Ubelaker (1989), have large gaps, especially in the teenage years (Ubelaker 1989: 64; Schour and Massler 1941: 1154).

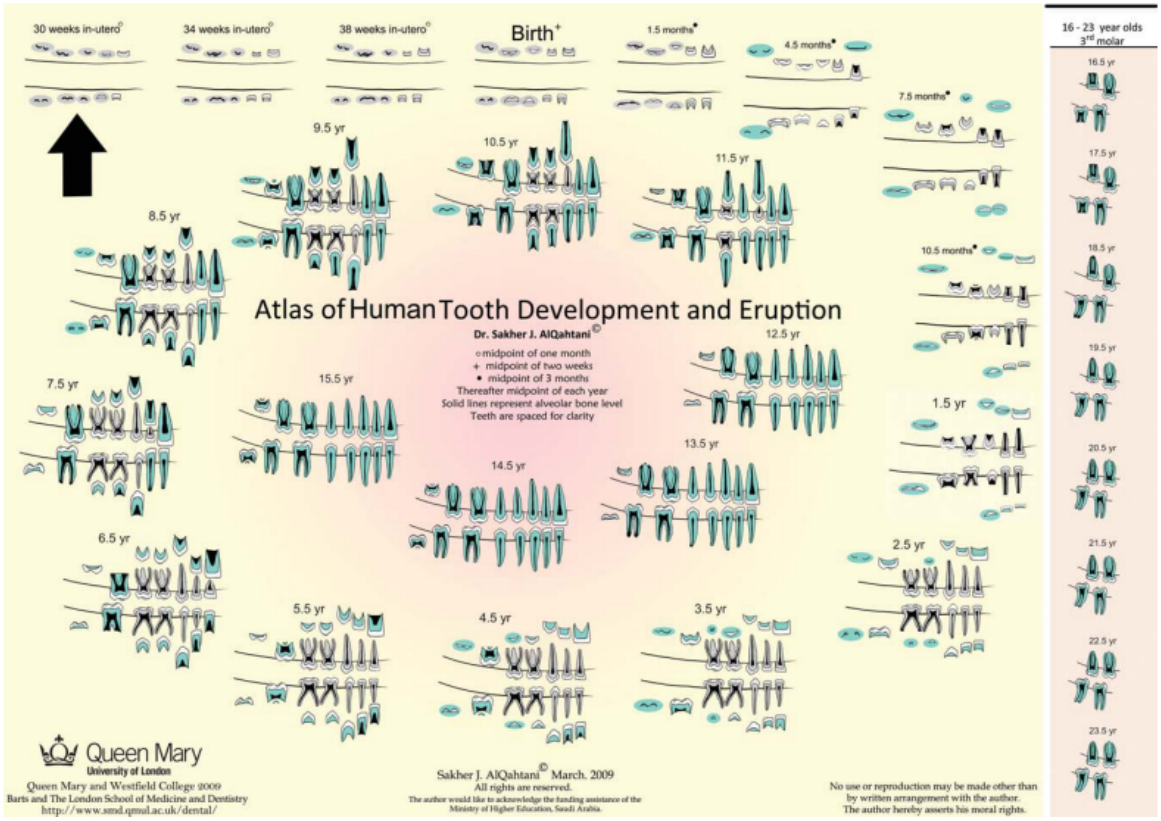

Figure 6.3 The London Dental Atlas (AlQahtani *et al.* 2010).

Although the accuracy of age estimates decreases with advancing age, unsurprisingly when these three atlases were tested (AlQahtani *et al.* 2010; Ubelaker 1989; Schour and Massler 1941), the London Dental Atlas performed best. Thus, in a sample of 1,506 individuals with documented age, it was found that the difference between recorded age and that estimated through the London Atlas was +0.08 years for individuals aged 1.0-1.9 years, increasing up to -1.83 for individuals aged 23.0-23.9 years. The mean difference overall between estimated and actual age for the London Atlas was only -0.10 years, compared to -0.76 and -0.80 years for the Schour and Massler (1941) and Ubelaker (1989) atlases respectively. Moreover, for ages 1 through to 18 years, the differences between estimated and recorded age for the Schour and Massler (1941) and Ubelaker (1989) atlases were statistically significant ($p<0.05$), while for the London Atlas they were not (AlQahtani *et al.* 2014). In sum, the London Dental Atlas offers the most accurate and precise method of assessing chronological age in immature

skeletal remains. Estimating age through the dentition alone had a further advantage for the present study, as long bone growth could be used as a physiological stress marker (i.e., growth attributable to age could be estimated by comparing bone lengths to dental age and residual variance then explored to infer the impact of stress on growth).

As a consequence, rather than estimating age through a variety of less accurate techniques (e.g., diaphyseal length) and subjectively balancing results, available teeth were compared to the London Dental Atlas and the mean age was calculated to give an estimate of *dental age* as a proxy for chronological age (AlQahtani *et al.* 2014: 71). Although this approach introduces certain biases (e.g., the timing of dental development is more variable in some teeth than others) (AlQahtani *et al.* 2014: 77), it has been proven to facilitate explorations of the impact of developmental stress on later-life outcomes (e.g., Lewis *et al.* 2016; Shapland and Lewis 2013). Uncertainty in estimates was acknowledged by recording the range of possible ages implied by dental development.

6.2.3 Evaluating Senescent Changes to Estimate Age

To estimate age-at-death in skeletons with fully developed dentition, a transition analysis was conducted to interpret stages of age-related change in late-fusing epiphyses and immobile joints. This section describes the analytical method through which transitions between stages of change were modelled to estimate age and then details the variables on which this procedure was conducted.

6.2.3.1 The Transition Analysis: TA^3

To address concerns associated with the traditional approach to age-at-death estimation in mature remains (Section 2.4), the Rostock Manifesto was published in "*Paleodemography. Age Distributions from Skeletal Samples*" (Hoppa and Vaupel 2002a). This recommends that stages of age-related change are validated in appropriate reference

samples so that models can be developed to estimate $Pr(c|a)$ – the probability (Pr) of observing a particular suite of characteristics (c) given age (a). To mitigate age mimicry and better estimate age in the oldest of the old, it emphasises the importance of setting parameters, such as the expected upper limits of life span (ω) *a priori*, through the utilisation of an age distribution – $f(a)$. Through this it is possible to calculate the *conditional probability* of an individual expressing a particular set of characteristics given their age, which, when adjusted for the integrated *marginal probability* of observing those characteristics at all possible ages, gives $Pr(a|c)$, or the *posterior probability* of age-at-death given those observations (Lynch 2007: 23; Hoppa and Vaupel 2002b: 1-5). This application of Bayes theorem is expressed as

$$Pr(a|c) = \frac{Pr\,(c|a)f(a)}{\int_0^{\omega} Pr\,(c|a)f(a)\mathrm{d}a}.$$

A transition analysis has become a popular option through which to translate this theory into practice (e.g., Boldsen *et al.* 2021; Getz 2020; DeWitte and Yaussy 2019; Getz 2017). Although accomplishable in various ways (e.g., Sasaki and Kondo 2016; Tangmose *et al.* 2015; Konigsberg and Frankenberg 2013: 163-168; Konigsberg and Herman 2002), in the current study the Transition Analysis 3 (TA^3) program was employed (specifically version 0.8.0 available at www.statsmachine.net/software). By assuming that stages $i = 1,\ldots,n$ are a non-overlapping series through which progression is unidirectional and sequential, in TA^3 the probabilistic relationship between age and the stages of change in a reference sample are estimated through a generalised linear model with a logit link function $exp\,(.)\,/(1 + exp(.))$ (Milner *et al.* 2021: 140; Getz 2020: 4-6; Konigsberg and Frankenberg 2013: 164; Boldsen *et al.* 2002: 82). Thus, for the *j*th individual in a sample of $j = 1, \ldots, n$ skeletons the probability trait y is at stage i, for example, is $Pr\left(y_j = i|\, a_j\right) = \Delta(\alpha + \beta a_j)$ where a_j is the individual's age-at-death and

Δ represents the inverse of the model's link function (Getz 2020: 4-6; Boldsen *et al.* 2002: 82). The model's α and β coefficients are estimated by Maximum Likelihood. The mean age of transition from one stage to the next is calculated as α/β with a standard deviation of $3^{-1/2}\pi/\beta$ (Konigsberg and Frankenberg 2013: 164; Boldsen *et al.* 2002: 82). Though unrealistic, for practical purposes if it is assumed that the probability distribution that age lies between 15 and 110 years is uniform (Milner and Boldsen 2012: 100), the probability density function for age conditional on an individual being in the *i*th stage of a trait is therefore

$$f(a|y_j = i) = \frac{Pr(y_j = i|a)}{\int_{15}^{110} Pr(y_j = i|x)\mathrm{d}x}.$$

As the proportionality of the equation's denominator is a constant (Boldsen *et al.* 2002: 85), the likelihood function is given as $L(a|y_j = i) \propto Pr(y_j = i|a)$. When multiple traits from $k = 1,\ldots, m$ are used, this is extended to

$$L(a|y_j = i) = \prod_{k=1}^{m} L(a|y_{jk} = i_k)$$

to produce a probability distribution (Getz 2020: 7; Boldsen *et al.* 2002: 85-86). Although the underlying assumption of independence of traits is acknowledged as a limitation of this approach, the value of a maximising this function provides the maximum likelihood estimate for age-at-death in the *j*th skeleton (Getz 2020: 7; Boldsen *et al.* 2002: 85). A likelihood-based 95% CI can be read from the curve, allowing the point estimate to be supplemented by an indication of uncertainty (Getz 2020: 6; Konigsberg and Frankenberg 2013: 164; Boldsen *et al.* 2002: 85). The input variables assessed through this procedure are described in the following section.

6.2.3.2 Input Variables: Grading Stages of Change

The variables chosen for interpretation through the transition analysis were carefully selected and included a range of late-fusing epiphyses and degenerative changes at immobile joints (Table 6.2). Regarding the latter, joints can be treated as a single integrated unit or a suite of component traits. To better capture the varying stages of change throughout joints, each was divided into component traits (Kemkes-Grottenthaller 2002: 57-58). Stages of age-related change were graded with reference to images and descriptions in Milner *et al*. (2019).

Traits	Stage (graded)			
Late fusing epiphyses	0	1	2	3
Spheno-occipital synchondrosis	Open	Closed	N.A.	N.A.
L1 superior epiphyseal ring	NF	PF	RL	FF
L1 inferior epiphyseal ring	NF	PF	RL	FF
L5 superior epiphyseal ring	NF	PF	RL	FF
L5 inferior epiphyseal ring	NF	PF	RL	FF
S1 and S2 fusion	Gap ≤10 mm	Gap >10 mm	Closed	N.A.
Medial clavicle	NF	PF	RL	FF
Auricular surface				
Inferior surface porosity	Absent	Present	N.A.	N.A.
Superior posterior iliac exostoses	Smooth	Exostoses	N.A.	N.A.
Inferior posterior iliac exostoses	Smooth	Exostoses	N.A.	N.A.
Posterior exostoses	Absent	Discontinuous	Continuous	N.A.
Pubic symphysis				
Symphyseal collar	Absent	Present	N.A.	N.A.
Symphyseal relief	Billows	Residual	Flat	N.A.
Superior protuberance	Serrated	Knob	Flat	N.A.
Ventral margin	Serrated	Rampart	Rim	Breakdown
Dorsal margin	Serrated	Flattened	Rim	Breakdown

Table 6.2 Stages of change at selected traits. Epiphyses were scored as either: not fused (NF), partially fused (PF), fused but with visible remnant line (RL), fully fused (FF). Exostoses were defined as bony protuberances. On bilateral traits, both left and right sides were recorded when present. Descriptions are summaries of those provided in Milner *et al*. (2019).

This specific selection of traits can be justified for several reasons. In younger adults, late-fusing epiphyses (e.g., the medial clavicle) can be assessed to estimate age-at-death to within a relatively small timeframe, while they serve as a useful benchmark (akin to a *terminus post quem*) for older individuals (Schaefer *et al.* 2009; Scheuer and Black 2000). Meanwhile, immobile joints (e.g., the pubic symphysis)

express senescent modifications that can be utilised to infer age even after skeletal maturity has been reached (Buckberry and Chamberlain 2002; Gosling *et al.* 2002; Brooks and Suchey 1990; Katz and Suchey 1986; McKern and Stewart 1957; McKern 1956; Todd 1920) (Figure 6.4). Thus, given the observed changes occur across the lifespan, it is possible to estimate age throughout maturity (Milner *et al.* 2021: 148). As deviations to the normal relationship between age and skeletal change are unpredictable (i.e., they may be localised or dispersed), the "entire skeleton" method was employed to mitigate the effects of random biases in the age estimation process (Milner *et al.* 2021: 140-142; Gowland 2007: 157; Todd 1920: 288).

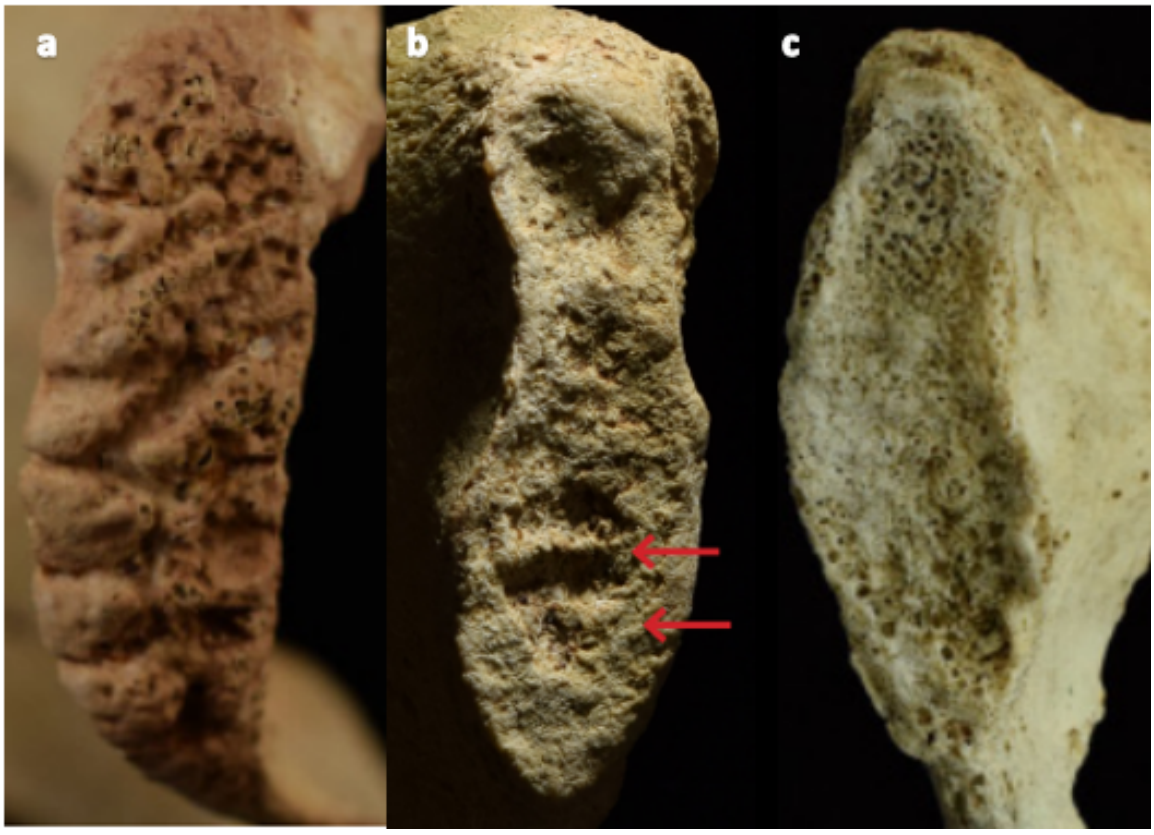

Figure 6.4 An example of stages of age-related change (i.e., from billowed relief to flat/irregular) on one component trait (the articular surface) of the pubic symphysis. A billowed symphyseal surface was graded "0" (a); when the symphyseal face was largely flat, but with evidence of residual billows (i.e., two consecutive grooves, as indicated by red arrows) relief was graded "1" (b); when the symphyseal face was flat or irregular with a defined rim, relief was scored "2" (c). Images from Milner *et al.'s* (2019:75-76) "Trait Manual".

6.2.4 Summary

The estimation of sex and age with the methods described represent the most effective and accurate means available without resort to destructive techniques (Inskip *et al.* 2019; Stewart *et al.* 2017). It is acknowledged that for age especially, results are suggestive of broader patterns only; that is, individual point estimates of age are subject to a range of biases, but collectively they can be employed to investigate sample-level trends in mortality (Getz and Byrnes 2021; DeWitte 2018: 5). As such, although the methods are not free from uncertainties and it should be emphasised that results are regarded as estimates of skeletal sex and age (Milner *et al.* 2021; Boldsen *et al.* 2002: 82), they enabled a rigorous investigation of differential frailty and the effect of early-life stress on lifespan (DeWitte and Stojanowski 2015; Wood *et al.* 1992).

6.3 Development and Later-life Stress Experience

This section focuses on the recording protocols employed in the collection of data related to developmental and later-life stress experience. The osteological characteristics described below are all stress-responsive in some way and, just as importantly, their development can be tied to certain periods of the life-course. They thus enable stress experience to be charted throughout life (Cheverko 2021: 69-70; Gowland 2015).

6.3.1 Non-specific Childhood Stress Indicators

As previously discussed (Section 2.4), CO and LEH of the permanent dentition develop during childhood in response to general physiological stress (Bereczki *et al.* 2019: 175; Kinaston *et al.* 2019: 753-756; Brickley 2018: 899; Guatelli-Steinberg 2016; Walker *et al.* 2009: 111; Hillson 2005: 170; Hillson 1996: 167-166). Thus, these lesions were employed to investigate stress experience for the period immediately after early-life maternal dependence.

CO, or porosity in the orbital vaults, forms before red marrow turns to yellow prior to approximately 10 years of age (Brickley 2018: 898-899; Walker *et al.* 2009: 111). CO was graded after Steckel *et al.* (2019: 403-404) (Table 6.3). Active and healed lesions were distinguished through an assessment of the pore edges; sharply defined edges were recorded as active lesions, while edges with a softer, remodelled shape were deemed to be healed (Walker *et al.* 2009: 111) (Figure 6.5). By recording the extent of porosity and separating active from healed lesions it was possible to assess an individual's resilience (i.e., the ability to recover or correct physiological functioning following a metabolic perturbation) (Steckel *et al.* 2019: 403-404; Graham *et al.* 2010: 496; Walker *et al.* 2009; Holling 1973: 17).

Grade	Description of Orbit
x	No orbits present for observation
0	Porosity absent with at least one orbit observable
1	Fine pores present, but covering ≤ 1cm²
2	Pores covering ≥ 1cm² of orbit

Table 6.3 Grading of CO after Steckel *et al.* (2019: 403-404).

Figure 6.5 An example of an orbit showing Grade 2 CO. Note that the pore edges are also rounded suggesting a healed/healing lesion.

Horizontal LEH were macroscopically assessed in the permanent anterior and posterior dentition (Figure 6.6a). A relatively strict recording protocol was employed: LEH were scored present when distinct trough-like grooves extended the full width of the tooth surface. Though this conservative approach inevitably meant that less-pronounced striations were not recorded, it ensured that false-positives through the counting of accentuated perikymata (known as "false hypoplasia") were avoided and the defects recorded were more likely to have a pathological origin (Guatelli-Steinberg 2003: 311; Hillson 1996: 167-166; Goodman and Rose 1990: 67). Additionally, defects in the form of pits, planes and vertical grooves were not recorded, as the aetiology and recording methods are less clear (Hillson 2005: 170; Hillson 1996: 167-166) (Figure 6.6b).

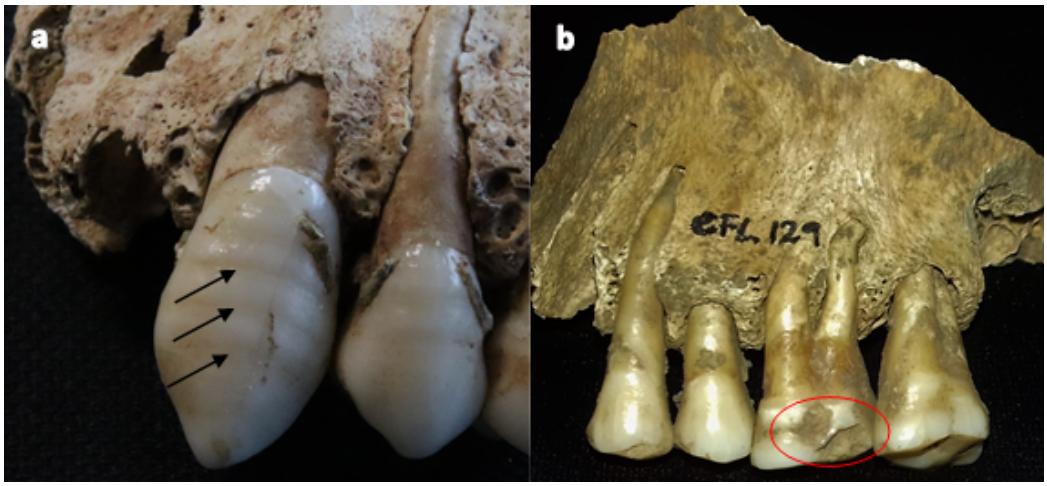

Figure 6.6 A left C^1 with LEH (indicated by arrows), easily identifiable through their trough-like appearance (a). M^1 with pit-like hypoplastic defects (highlighted with red oval) (b).

Using Primeau *et al.'s* (2015) atlas (Figure 6.7), LEH formation age was estimated by subdividing teeth into chronologically comparable zones (each rounded to the one decimal place and 0.9 years in length, beginning in the first year and going up to 11.9 years). When defects were matched on multiple teeth, it was taken as evidence of an episode of elevated stress experience (i.e., rather than a prolonged exposure); it was thus

possible to approximate the chronology and frequency of stress events between infancy and the twelfth year (Primeau *et al.* 2015; Temple *et al.* 2012; Hillson 2005: 171-174; Blakey and Armelagos 1985). Attempts were not made, however, to evaluate hypoplasia depth and infer the severity of stress experience. Defect depth is influenced by location and the same stressor may produce defects of varying size in different teeth making comparability problematic (Hillson 2005: 171-174; Goodman and Rose 1990: 65).

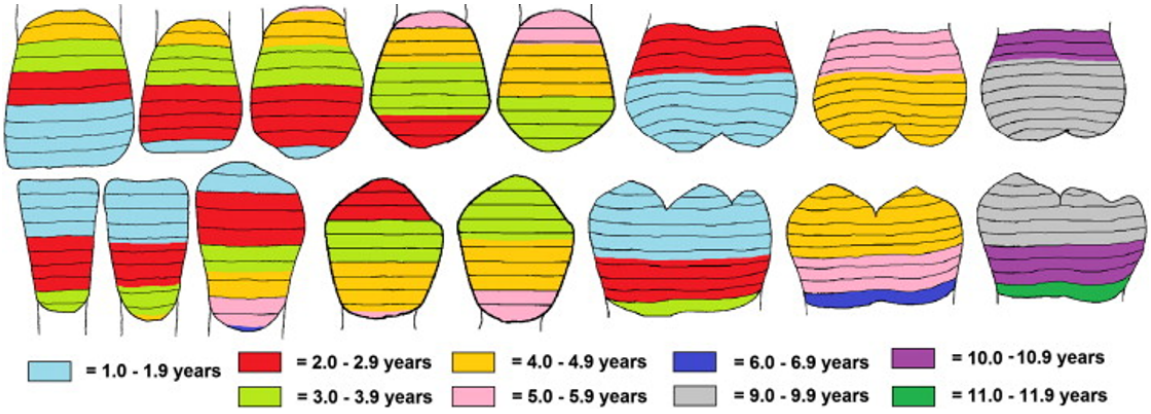

Figure 6.7 Atlas used to estimate the age of LEH defect formation from Primeau *et al.* (2015).

6.3.2 Skeletal Growth and Development

Somatic growth encompasses many complex processes and stress experienced during an individual's formative years can elicit growth deficits which can persist into maturity (Newman 2016; Hwang 2014; Gowland 2015; Liu *et al.* 2009; Wadsworth *et al.* 2002). Long bones (i.e., femora, tibiae, fibulae, humeri, ulnae and radii) were therefore measured in immature and mature remains. Using a standard osteometric board, the maximum length of long bones was recorded to the nearest millimetre (mm) after the conventions established in "*Standards for Data Collection from Human Skeletal Remains*" (Buikstra and Ubelaker 1994: 69-84). In immature long bones with unfused epiphyses, the maximum diaphyseal length was taken, while for skeletally mature individuals the length with epiphyses was recorded (Figure 6.8); diaphyseal and epiphyseal lengths were compared separately.

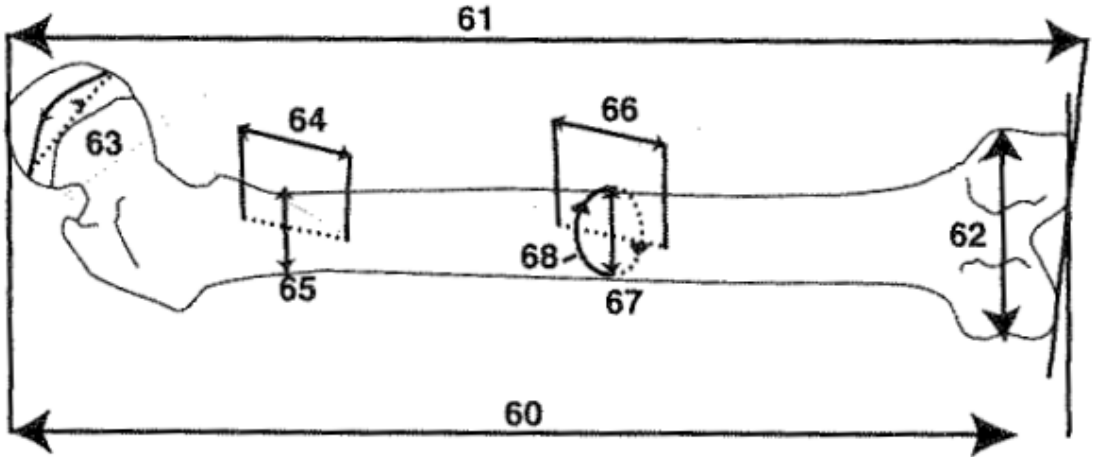

Figure 6.8 Femoral measurements. Maximum femoral length (number 60) is the distance from the femoral head's most superior point to the condyle's most distal. Image taken from Buikstra and Ubelaker (1994: 83).

As the initiation and completion of puberty are influenced by environmental stress (DeWitte and Lewis 2020; Gowland *et al.* 2018; Lewis *et al*. 2016), pubertal stage was estimated following Shapland and Lewis's (2013) method. This method assesses five skeletal sites that have previously been used to categorise pubertal development in living subjects (Table 6.4). For example, a number of the observations – e.g., cervical vertebrae maturation (CVM) – have been employed clinically to determine the appropriacy of surgical intervention based upon an individual's pubertal stage, and as such have passed rigorous and repeated testing to ensure reliability and accuracy (Zhang *et al.* 2008; Baccetti *et al.* 2005; Scoles *et al.* 1987; Hägg and Taranger 1982; Chertkow 1980; Grave and Brown 1976; Demirjian *et al.* 1973; Hewitt and Acheson 1961a; Hewitt and Acheson 1961b). An individual was assigned to a stage when three or more observations were concordant – if this could not be achieved, pubertal stage was recorded as indeterminate.

Stage	Description	C_1	Hook of Hamate	Phalanges and Upper Limb	Iliac Crest	CVM
Initiation (1)	Growth of sexual organs and hormonal changes	Root 1/2 to 3/4 complete	Hook absent	Proximal epiphysis of 2nd metacarpal narrower than shaft; distal radius unfused	Epiphysis not present	1
Acceleration (2)	Increased body mass and emergence of secondary sexual characteristics.	Root complete to apex 1/2	Hook appearing or increased	2nd phalangeal metaphysis and epiphyses of equal width; distal radius unfused	Epiphysis 50% complete; unfused	2
Peak Height Velocity (3)	Sexual characteristics and shift towards adult body mass become obvious	Apex complete	Hook complete	Increased width of 2nd proximal phalanx; distal radius unfused; proximal ulna and humeral capitate fusing/fused	Epiphysis 50-75% complete; unfused	3
Deceleration (4)	Menstruation and ovulation in females	Apex complete	Hook complete	Capping of phalangeal epiphyses; distal radius unfused	Epiphysis 75-100% complete; non/partial union	4-5
Maturation (5)	Regular ovulation in females and appearance of sexual maturity	Apex complete	Hook complete	Fusing of 3rd metacarpal proximal epiphysis; distal radius partially fused	Epiphysis 100% complete; partial union	5-6
Completion (6)	Fully mature	Apex complete	Hook complete	Phalanges and distal radius fused	Fusion complete	6

Table 6.4 Adapted from Lewis *et al.* (2016: 51). C^1 mineralisation graded after Demirjian *et al.* (1973), hook completion follows Shapland and Lewis (2013), while CVM is scored after Baccetti *et al.* (2005).

Pubertal stage was assessed in individuals estimated to have been between nine and 25 years of age (Sections 6.2.2 and 6.2.3). Bioarchaeological investigations, historical records, and clinical literature defined these age parameters. In both modern and past populations puberty is generally initiated *circa* 10 years of age, though in rare instances for severely stressed females, initiation may begin up to a year earlier (Lewis 2020; DeWitte and Lewis 2020; Lewis 2018). On the other hand, evidence suggests that pubertal completion may have been delayed (potentially up to the twenty-fifth year) due

to stress in past populations (Lewis 2020; DeWitte and Lewis 2020; Lewis 2018; Lewis *et al*. 2016; Eiben and Mascie-Taylor 2003; Ibáñez *et al.* 2000).

6.3.3 Later-life Physiology

Early-life stress has been associated with alterations to later-life physiology (Sharma *et al.* 2016; Vaiserman 2015; Hwang 2014; Liu *et al.* 2009). To investigate the potential long-term consequences of early-life stress, it is therefore necessary to make observations indicative of later physiological state.

Although periodontal disease has traditionally been used to investigate the effects of factors such as diet on oral health (Larsen 1997: 77), the recognition that it is the result of a local inflammatory response to pathogenic bacteria (e.g., *Porphyromonas gingivalis*) has led to a re-evaluation of its interpretation and it is increasingly being explored as a proxy for a later-life proinflammatory physiology (Crespo *et al.* 2021; Crespo *et al.* 2016; Lockhart *et al.* 2012; DeWitte and Bekvalac 2011; DeWitte and Bekvalac 2010; Andriankaja *et al.* 2010; Ogden 2008: 288). As PD is characterised by age-progressive degeneration of the alveolar margin, one method of assessing the presence and extremity of the disease has been to measure the distance from the CEJ to the alveolar border (Trombley 2019: 259; DeWitte and Bekvalac 2010: 344). However, as teeth erupt continuously throughout life in response to dental wear this technique is not reliable and qualitative methods have proven more consistent (DeWitte and Bekvalac 2010: 345; Ogden 2008: 290; Kerr 1988). The descriptive criteria shown in Table 6.5 were utilised to categorise alveolar morphology in the region of each molar, diagnose the presence or absence of periodontal disease and, when present, infer severity (Figure 6.9).

Grade	Description of Alveolar Crest	Diagnosis
x	No observation possible	N.A.
0	Alveolar bone meets tooth at a knife-edged acute angle	No disease
1	Alveolar margin is blunt, flat-topped with a slight rim	Mild PD
2	Rounded and porous margin, with a trough 2-4 mm deep	Moderate PD
3	Ragged and porous with an irregular trough ≥5 mm deep	Severe PD

Table 6.5 Grading of PD after Ogden (2008: 293).

Figure 6.9 Note the alveolar recession throughout the molar region and formation of a trough between the alveolar margin and tooth root in the M_2 and M_3. These morphological features are associated with PD; the trough is indicative of progression to Grade 2 of Ogden's (2008) schemata.

Periosteal new bone formation (PNBF) is the manifestation of an inflammatory response of the periosteum to a pathological process. It is frequently associated with systemic infectious disease – this connection becomes more robust when PNBF is expressed diffusely or bilaterally (Roberts 2019; Roberts and Buikstra 2019; Steckel *et al.* 2019: 418; DeWitte and Wood 2008: 1439; Weston 2008). Given the relatively high frequencies with which this lesion is seen in pre-antibiotic archaeological contexts, the assessment of periosteal new bone formation is a viable means of evaluating an underlying proinflammatory physiology and, when properly contextualised, exploring immunocompetence and environmental pathogen load.

PNBF on long bones and skulls was systematically recorded and distinction was made between active and healed lesions to assess an individual's ability to recover from systemic or localised assault (Marques *et al*. 2019: 137; DeWitte 2014a: 263; Weston 2008: 51-52). A lesion with a woven, porous or disorganised appearance is typical of a process active at time-of-death (though it cannot be assumed that the lesion is related to death) and potentially diminished resilience (i.e., an inability to recover or persist despite physiological perturbations). Meanwhile, plaques of lamellar bone with either a well-organised and striated or dense, sclerotic appearance are indicative of healing and a resolved inflammatory response as well as resilience (Graham *et al.* 2010: 496; Weston 2008: 51-52; Holling 1973: 17) (Figure 6.10). In addition to activity, distinctions were made between unilateral and bilateral lesions. Weston's (2008) grading rubric was used to assess the extent/severity of PNBF (Table 6.6).

Figure 6.10 An example of PNBF formation in a tibial diaphysis; the close-up shows a combination of dense, sclerotic and well-organised, striated lamellar bone indicative of a healed lesion.

Grade	Description
x	No observation possible
0	Normal bone surface
1	Isolated elevated plaque or plaques covering <33% of the bone surface
2	As above covering 33-66% of the bone surface
3	Uniform elevation of >66% of the bone surface with little increase in diameter
4	As above with elevation of more than 2-3 mm

Table 6.6 Grading of PNBF after Weston (2008: 51).

6.3.4 Differential Diagnoses

Even though many palaeopathological lesions are not pathognomonic of a particular condition, the patterning of morbid changes as well as inferred pathogenesis can suggest specific causal diseases, especially when contextualised (Mays 2020; Roberts 2019; Roberts and Buikstra 2019; Mitchell 2017; Weston 2008; Ortner 2003). When making a diagnosis, the first step was to identify and describe all abnormal bone changes (both bone growth and loss) and infer potential pathogenic mechanisms (Klaus and Lynnerup 2019: 81). Comparisons were then made between the constellation of observed lesions, as well as their most likely aetiology, to standard diagnostic manuals, such as "*Ortner's Identification of Pathological Conditions in Human Skeletal Remains*" edited by Buikstra (2019) and Aufderheide and Rodriguez-Martin's (1998) "*The Cambridge Encyclopaedia of Human Paleopathology*". In order to appreciate more comprehensively variation in disease susceptibility and expression, where necessary reference was also made to case studies in which the role of specific sociocultural and environmental influences had been investigated through either historical, archaeological or medical data (Mitchell 2017; Roberts *et al.* 2016). Alternative hypotheses were systematically explored and, where possible, excluded so that the resulting diagnosis was the most likely explanation for any observed pathological change (Klaus and Lynnerup 2019: 81). Regardless of the rigour of the process, not all diagnoses could be made with comparable certitude. Therefore, the adaptation to the Istanbul Terminological Framework proposed

by Appleby *et al.* (2015: 20) was employed to explicitly acknowledge the degree of confidence associated with each diagnosis.

Certainty	Criteria
Not consistent	The lesion(s) could not have been caused by the condition(s) described
Consistent with	The lesion(s) could have been caused by the condition(s) described, but it is non-specific and there are many other possible causes
Highly consistent	The lesion(s) could have been caused by the condition(s) described, and there are few other possible causes
Typical of	That the lesion(s) is usually found with this type of condition(s), but there are other possible causes
Diagnostic of	The lesion(s) could not have been caused in any way other than by the condition(s) described (i.e., it is pathognomonic)

Table 6.7 The adaptation of the Istanbul Terminological Framework employed to express diagnostic certainty/uncertainty (Klaus and Lynnerup 2019: 81; Appleby *et al.* 2015: 20).

Taking this evidence-based diagnostic process enabled a contextually informed exploration of the social and environmental influences on health (Mays 2020: 91-93; Klaus and Lynnerup 2019: 81-82). Additionally, to form an impression of the specific conditions that may have contributed to ill-health at a wider populational level, data from individual skeletal remains was collated to recognise the epidemiologic 'footprint' of various diseases. That is, even if a condition is not identifiable confidently in a single skeleton, suggestive markers throughout an assemblage can be employed to infer the presence of a specific disease within a sample (Rothschild 2021; Klaus and Lynnerup 2019: 81). Moreover, as osseous responses to stress are only manifested skeletally when an individual can endure said insult to health, somewhat paradoxically, osteological lesions and diagnoses of specific conditions are an indicator of lived experience (rather than cause-of-death) (DeWitte and Stojanowski 2015; Temple 2014; Armelagos *et al.* 2009: 264; Wood *et al*. 1992; White 1978). This multi-scalar approach (incorporating individual diagnoses and sample-level patterns), thus permitted inferences to be made regarding the conditions experienced at each site.

Certain pathological conditions were considered of greater significance than others. Entheseal and degenerative joint change was not recorded as there is little connection with early-life stress, with both largely related to senescent processes, activity and weight (Milner *et al.* 2018; Niinimäki and Baiges Sotos 2013; Jurmain *et al.* 2012; Niinimäki 2012; Cardoso and Henderson 2010; Molnar 2006; Jurmain 1980). Similarly, evidence of fungal disease, parasite infection, circulatory disorders and skeletal dysplasia was not specifically sought; some are rare while others are exceptionally difficult to identify in skeletal remains (e.g., parasite infection) and, with the possible exception of circulatory problems, there is little basis to suggest a link between these pathologies and early-life stress (Grauer and Roberts 2019; Reinhard and Camacho 2019; Grauer 2019; Lewis 2019).

Neoplastic lesions, in contrast, were recorded as these have been linked to developmental stress and skeletal fluctuating asymmetry in modern and past populations (Weisensee 2013; Swerdlow *et al.* 1997), as were congenital defects due to their association with the developmental process (Lewis 2019: 585). Particular attention was paid to the identification of bacterial infections as their presence and prevalence represents the intersection of an individual's immune competence, biosocial buffering systems and a pathogen's interaction with its environment (Roberts and Buikstra 2019: 375). Thus, evidence of trauma was noted because of the potential for secondary bacterial infections rather than its relationship to injury (Redfern and Roberts 2019: 224). Additionally, metabolic diseases linked to deficiency (e.g., scurvy and rickets) were considered of special interest. As well as a growing body of research suggesting that dependent offspring gut microbiota (and therefore capacity to absorb nutrients) are influenced by maternal cues in early-life (Chong *et al.* 2018; Cong *et al.* 2016; Caricilli and Saad 2013; Brown *et al.* 2012), past research has implicated early life and childhood

nutritional shortages as critical to life-course trajectories (Brickley and Mays 2019: 532-539; Newman 2016: 110-111; Mays 2014; Geber and Murphy 2012; Van der Merwe *et al.* 2010; Mahoney-Swales and Nystrom 2009; Maat 2004).

6.3.5 Calculating Frequencies

Prevalence rates are a widely employed measure of lesion frequency. In a palaeopathological context there are two commonly applied ways in which prevalence rates are calculated (Sanogo *et al.* 2014; Waldron 1994: 42-43). Crude prevalence rate (CPR) is found as the percentage of individuals with a lesion, while true prevalence rate (TPR) is the percentage of skeletal elements/teeth with a lesion divided by the number of elements/teeth where an observation was possible (Waldron 1994: 42-43). As is often the case, both were calculated and distinctions made clear. These measures are useful as contrasting lesion frequency between groups (e.g., sites and sexes) is an important way of exploring the sociocultural, environmental and biological influences on development and stress experience as well as heterogenous frailty. For example, through a contextualised comparison of sites it is possible to infer the impact of social and environmental factors on life-course outcomes. Such data is crucial in assessing the relative significance of early-life stress in determining life-course trajectories.

6.3.6 Summary

The skeletal observations selected provided information pertaining to stress experienced throughout life. In some cases lesions can be attributed to relatively circumscribed stress events (i.e., matched LEH), while others are more reflective of prolonged experiences (e.g., CO and PD) (e.g., Primeau *et al.* 2015; Temple *et al.* 2012; Ogden 2008). As such, it was possible to explore the impact of acute and chronic stress exposure. Differentiation of active and healed lesions was used to infer resilience and the

ability to buffer against stress (Marques *et al*. 2019; DeWitte 2014a: 263; Walker *et al.* 2009; Weston 2008). Skeletal markers indicative of a proinflammatory state were included in the hope of bridging one of the gaps in the clinical and archaeological understandings of early-life stress and its effect on health (Barker 2012; Lockhart *et al.* 2012; Andriankaja *et al.* 2010). The multidimensional pathological profiles constructed were therefore an attempt to chart stress as completely as possible and when viewed holistically could be used to investigate life-history trade-offs in response to maternally-mediated early-life stress (Pittet *et al.* 2017; Wells 2012; Charnov 1997; Charnov 1991).

6.4 Conclusion

At the core of the methods described in this chapter lies a suite of dental and skeletal observations. These methods were carefully selected so that life-course outcomes could be assessed and stress experience chronicled from early childhood through to maturity (Gowland 2015; Agarwal 2016; Armelagos *et al.* 2009). They thus permitted the creation of holistic profiles through which statistical connections could be drawn and rigorously investigated to illuminate life-course dynamics and explore themes such as differential frailty and resilience (Jacob *et al.* 2019; Mishra *et al.* 2010b; DeWitte 2010; DeWitte and Wood 2008; Kuh *et al.* 2003; Roseboom *et al.* 2001; Vaupel 1988; Barker and Osmond 1986; Stinson 1985). Although an element of uncertainty is almost ubiquitously attached to inferences drawn from skeletal remains, efforts have been made to achieve as much precision as possible without compromising accuracy and to acknowledge the degree of confidence attached to estimates (e.g., when generating probability distributions of age for mature skeletons, 95% CIs were recorded as well as point of estimates) (Milner *et al.* 2021; Klaus and Lynnerup 2019: 81; Appleby *et al.* 2015; Klaus 2014; Wood *et al.* 1992). In the following chapter the geometric

morphometric processes employed to investigate M1 FA, and therefore enable a more comprehensive study of stress over the life-course, are detailed.

Chapter 7: Methods – Geometric Morphometric

7.1 Introduction

This chapter introduces the techniques through which M1 fluctuating asymmetry was quantified as a proxy for early-life stress (i.e., that experienced by maternally-dependent offspring). This includes a description of photographic and digitisation procedures, Procrustes analysis and tangent space inference. The results of a pilot study conducted to evaluate error in the data acquisition procedure are also presented and the implications discussed. It is then illustrated how Procrustes-aligned coordinate configurations can be handled to isolate fluctuating asymmetric variance. This includes the procedures through which deviations from symmetry were decomposed at the sample level and an individual measure of fluctuating asymmetry calculated. Also described is the suite of statistical techniques employed to explore the individual measure of asymmetry which, when analysed in conjunction with osteological variables representing later-life experience (Chapter 6), is used to infer the role of early-life stress in defining life-course trajectories.

7.2 A Procrustean Approach to Exploring Early-Life Stress

This section details the method through which the homologous occlusal features and M1 outlines were captured and transformed through Procrustean techniques. A brief description of the tangent space inference and the statistical packages used is also given.

7.2.1 Data Acquisition: Imaging and Landmark Digitisation

To produce images of M1 occlusal surfaces, a Canon EOS 250D DSLR camera with an AET-CS Auto Extension Tube was set to take JPEG images and affixed to a Kaiser Copy Stand (alignment was checked with spirit levels). To be compatible with the

focal parameters of the macro lens, camera height was adjusted to ensure that each tooth was 22 cm from the camera's focal point (Uzunov *et al.* 2015; Dukić 2014). This further mitigated parallax, or the distortion of an image resulting from the object being placed too close to the camera (Mullins and Taylor 2002). To ensure stability, individual teeth and those embedded in cranial and mandibular fragments were held in place with modelling clay. When maxillary teeth were associated with complete crania, a polystyrene ring was used to stabilise the crania (Figure 7.1a-b). The horizontal alignment of the CEJ was ensured with a laser spirit level (Cucchi *et al.* 2011: 15; Gómez-Robles *et al.* 2008; Gómez-Robles *et al.* 2007), and a grid and cross pattern on the camera screen was used to assist in the final location of each tooth directly below the lens's centre point. To provide scale, a ruler was placed next to the tooth and parallel to the camera lens. To enhance depth of field and clarity, the camera's aperture was fixed to f 32; ISO and shutter speed were varied as necessary to accommodate differences in the colouration and reflectiveness of each tooth (Uzunov *et al.* 2015). After each picture was taken, image quality was assessed and the tooth was completely removed from position before the imaging process was repeated to produce replicate measures.

Images were transferred to a laptop computer for processing. So that the left and right sides could be compared in the superimposition process, the left was reflected by flipping it along the horizontal axis by 180˚ in Microsoft Paint (Zelditch and Swiderski 2018: 28-29). The digital images were saved in a folder under unique codes that defined the skeleton, side and replicate number. So that landmarks and an outline could be digitised for each image in the freely available R application *Stereomorph* (Figure 7.1c), an assortment of files and folders was created to function as a working directory. This included text documents that specified the number and names of landmarks to be applied,

the start and end point of the outline, and a folder in which landmark and outline data were stored as a text document for each image post-digitisation.

Figure 7.1 Examples of stabilising loose teeth for imaging with modelling clay (a) and complete crania with a polystyrene ring (b) as well as the user interface of *Stereomorph*, with a ruler used to provide scale (c).

In *Stereomorph*, landmarks were located at anatomically homologous points which included fissure junctions, fovea and cusp apices (Figure 7.2 and Table 7.1-Table 7.2). An outline was drawn around each tooth's occlusal surface and then subsampled by semi-landmarks. The point at which the lingual fissure crossed the outline was used to locate the first semi-landmark while the remaining semi-landmarks were placed

automatically at equally spaced distances around the outline (Adams *et al.* 2021: 123-124; Olsen 2015; Olsen and Westneat 2015; Robinson *et al.* 2002; Wood *et al.* 1983). When occlusal wear had eroded the cusp apex, exposed patches of dentine were used to estimate original apical position (Figure 7.3a). Similarly, when the mesial or distal aspects of the outline were damaged by interproximal wear, the original border was approximated by reference to overall crown shape and contour (Kenyhercz *et al.* 2014; Benazzi *et al.* 2011b: 349; Gomez-Robles *et al.* 2007: 275-276; Wood and Engleman 1988: 3) (Figure 7.3b). To provide scale, ruler points were digitised.

No.	Description
1	The centre of the mesial fovea, at the most mesial extension of the sagittal fissure
2	The intersection of the sagittal fissure by the buccal fissure
3	The intersection of the sagittal fissure by the lingual fissure
4	The centre of the distal fovea located at the most distal extension of the sagittal fissure
5	Paracone apex
6	Metacone apex
7	Protocone apex
8	Hypocone apex

Table 7.1 Maxillary first permanent molar landmarks.

No.	Description
1	The centre of the mesial fovea, at the most mesial extension of the longitudinal fissure
2	The intersection of the longitudinal fissure by the mesiobuccal fissure
3	The intersection of the longitudinal fissure by the lingual fissure
4	The intersection of the longitudinal fissure by the distobuccal fissure
5	The distal fovea located at the most distal extension of the longitudinal fissure and, when present, its intersection with the buccal and lingual foveal fissures
6	Protoconid apex
7	Hypoconid apex
8	Metaconid apex
9	Entoconid apex
10	Hypoconulid apex

Table 7.2 Mandibular first permanent molar landmarks.

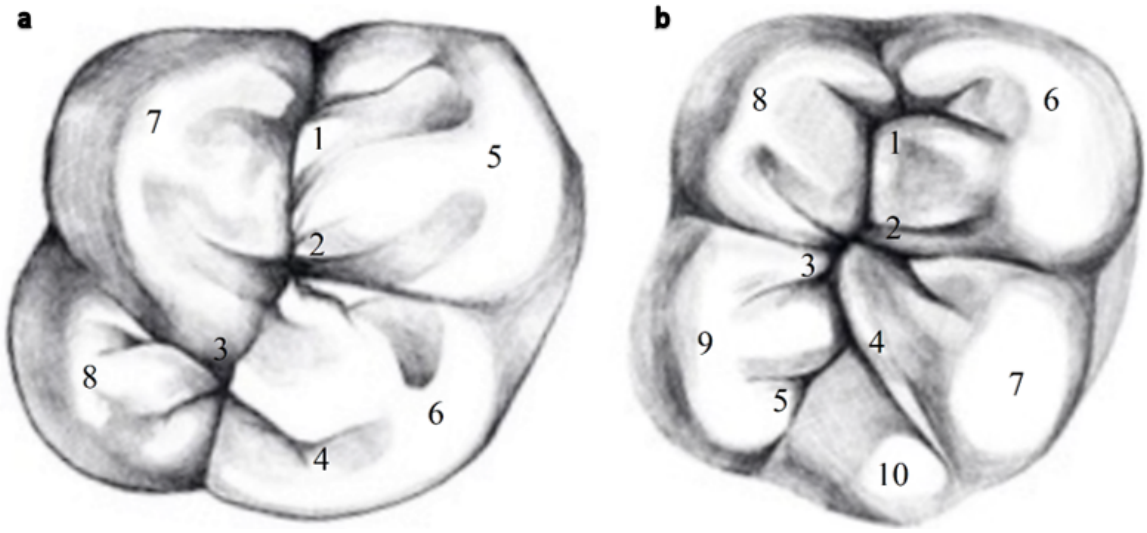

Figure 7.2 Maxillary (a) and mandibular (b) first permanent molars with landmarks (see Tables 7.1 and 7.2 for landmark descriptions). Illustrations orientated with mesial at the top and buccal to the right.

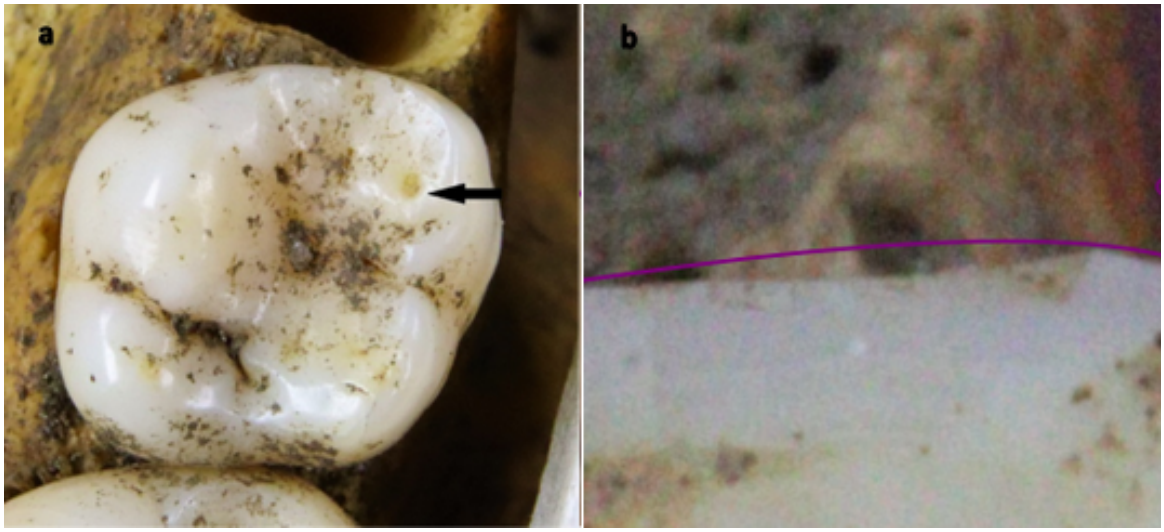

Figure 7.3 Exposed patches of dentine (highlighted by arrow) were used to locate the position of worn apices (a). For teeth with chips and interproximal wear facets, the outline (in purple) was estimated through reference to surviving border curvature (b).

At the end of the digitisation process, the occlusal surface of each tooth was represented by a k x m matrix (X) of Cartesian coordinates points, such as

$$X = \begin{pmatrix} x_1 & y_1 \\ x_2 & y_2 \\ \vdots & \vdots \\ x_k & y_k \end{pmatrix}$$

where k was the number of landmarks and semi-landmarks and m the number of dimensions. As points along the x and y axis were digitised, $m = 2$. The ordering of coordinate points corresponded exactly between configurations, and coordinate matrices $X_1, \ldots, X_n$ were collated into a k x m x n data array.

7.2.2 Centroid Size

In order to investigate factors such as the impact of allometry on fluctuating asymmetry, it was useful to define size. Centroid size (S) is a widely accepted and popular measure. For configuration X, centroid size is given as

$$S = \|CX\| = \sqrt{\sum_{i=1}^{k}\sum_{j=1}^{m}(X_{ij} - \bar{X}_j)^2}$$

where X_{ij} is the (i,j)th point of X, the mean of the jth dimension is $\overline{X_j} = \frac{1}{k}\sum_{i=1}^{k} X_{ij}$, C is the centring matrix $I_k - \frac{1}{k}1_k 1_k^T$, and $\|X\| = \sqrt{trace(X^T X)}$ is the Euclidean norm, while I_k is the k x k identity matrix and 1_k is the k x 1 vector of ones (Dryden and Mardia 2016: 34; Dryden and Mardia 1998: 24). Centroid size is therefore the square root of the sum of squared Euclidean distances of each landmark from the configuration's centroid (i.e., central point), the location of which is calculated by averaging x and y coordinates (Klingenberg 2016: 120; Robinson 2005: 26), and is alternatively expressed as

$$S = \sqrt{\sum_{i=1}^{k}\|(X)_i - \bar{X}\|^2}$$

where $(X)_i$ is the ith row of $X(i = 1,\ldots, k)$ and $\overline{X} = (\overline{X}_1,\ldots, \overline{X}_m)$ is the centroid (Dryden and Mardia 2016: 34; Dryden and Mardia 1998: 24).

7.2.3 Sliding Semi-landmarks

Of the Cartesian points in configurations $X_1, ..., X_n$, semi-landmarks $j = 1, ..., q < k$ were initially placed equidistant around each tooth's outline. As this placement was achieved only through reference to outline length, semi-landmarks were not comparable between subjects. From the methods through which semi-landmarks can be manipulated to achieve a point-to-point correspondence, it was decided to minimise bending energy for the benefits described in Section 4.3.3. Bending energy is reduced in superimposed configurations by initially treating landmarks and semi-landmarks in the same way to find a mean shape. To align outlines more smoothly to the mean, each semi-landmark is then slid along a line tangent to the outline at that point (Figure 7.4); as the outline's contour is not known, the tangent is estimated as a line parallel to a segment connecting points adjacent to the semi-landmark being slid (e.g., Zelditch *et al.* 2012: 123; Perez *et al.* 2006: 770). For example, in configuration $X_i = (X_{ix}, X_{iy})^T$ containing semi-landmarks $j = 1, ..., q < k$, semi-landmarks are slid along tangent direction $u_j = (u_{jx}, u_{jy})^T$ with $\|u_j\| = 1$. In the resulting configuration matrix $Y_i = (Y_{ix}, Y_{iy})^T$, semi-landmarks have novel positions $Y_j = (Y_{jx}, Y_{jy})^T$ (Dryden and Mardia 2016: 368; Robinson 2005: 181; Dryden and Mardia 1998: 261; Bookstein 1997). The new location of Y_j is

$$Y_j = X_j + t_j u_j, \quad j = 1, ..., q.$$

As the bending energy is given by

$$Y^T diag\left(B_e, B_e\right) Y = Y^T B_2 Y$$

where the bending energy matrix B_e depends only on the old configuration $X_i, i = 1, ..., k$ and B_2 is the tensor product, then $Y = Y^0 + Ut^T$ where Y^0 is

$$Y^0 = \begin{pmatrix} X_{1x}, \dots, X_{qx}, & Y_{q+1,x}, \dots, Y_{kx} \\ X_{1y}, \dots, X_{qy}, & Y_{q+1,y}, \dots, Y_{ky} \end{pmatrix}^T,$$

U is a $2k$ x q matrix

$$U = \begin{pmatrix} diag(u_{Ix}, \dots, u_{qx}) \\ diag(u_{Iy}, \dots, u_{qy}) \\ 0_{2k-2q,q} \end{pmatrix}$$

and $t = (t_1, ..., t_q)^T$. To minimise bending energy

$$(Y^0 + Ut^T)^T B_2 (Y^0 + Ut^T)^T,$$

with respect to t an iterative procedure was taken where the starting value of $u_j = (X_{j+1} - X_{j-1})/\|X_{j+1} - X_{j-1}\|$ (Dryden and Mardia 2016: 368; Dryden and Mardia 1998: 261; Bookstein 1997). After each iteration, configurations were superimposed again; if the new mean configuration differed from the previous, the procedure was repeated until the mean shapes of successive iterations converged and it could be assumed that shape differences between outlines was not due to the initial, extrinsically defined spacing of semi-landmarks (Zelditch *et al.* 2012: 123; Gunz and Mitteroecker 2013: 106-107).

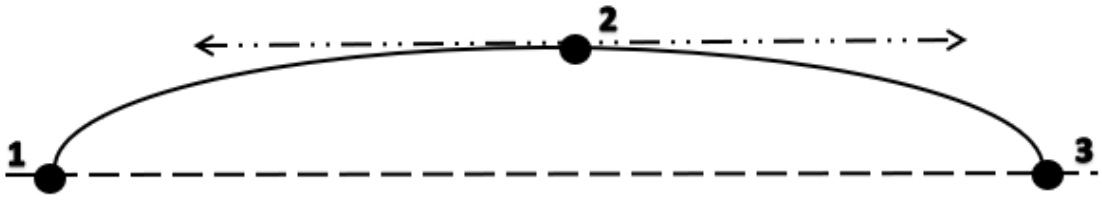

Figure 7.4 To minimise bending energy, all landmarks and semi-landmarks are superimposed to compute mean shape. As the outline (solid line) is treated as unknown, in the case of semi-landmark 2, sliding occurs on a line tangent (dashed/dotted line) to the segment (dashed line) connecting adjacent points (i.e., 1 and 3) (Dryden and Mardia 2016: 368; Zelditch *et al.* 2012: 123; Dryden and Mardia 1998: 261; Bookstein 1997).

Note that the convention of referring to coordinate configurations as X_i is retained, despite the fact that they have been revised and differ from their original state, as this notation is well-established. Thus, throughout the following sections and thesis generally, configurations are referred to as X_i rather than Y_i.

7.2.4 Generalised Procrustes Analysis

A full Generalised Procrustes Analysis was carried out on the *k* x *m* x *n* data array of revised coordinate configurations (i.e., with semi-landmarks in their new locations) to explore shape variation about the sample average. For configurations X_i, a model for the 'population' of shapes is

$$X_i = \beta_i(\mu + E_i)\Gamma_i + 1_k\gamma_i^T$$

where E_i are the matrices of independent errors, μ is the mean shape configuration and the "nuisance" parameters for scale, rotation and translation are represented as β_i, Γ_i and γ_i (Robinson 2005: 76; Dryden and Mardia 1998: 88; Gower 1975). To remove nuisance parameters, an iterative approach was adopted in which locational differences between shapes were first removed by translating all superimposed coordinate configuration's centroid points to a common origin at (0,0). Then, the first configuration was employed as a target or consensus shape around which all other configurations were scaled and rotated through a least-squares optimisation algorithm. Following the initial fit, an average shape was computed and employed as the target for a subsequent round of fitting. This iterative process was repeated until the average shapes produced by successive rounds ceased to differ due to the sum of squared Euclidean distances between configurations X_1,…, X_n having been minimised (Adams *et al.* 2021: 49; Dryden and Mardia 2016: 134; Robinson 2005: 36-37; Dryden and Mardia 1998: 87-91; Gower 1975). If γ is a translation vector of

length *m*, β>0 is a scale parameter, and Γ is an orthogonal rotation matrix, the process of a full GPA transforms configurations relative to one another to minimise the total sum of squares for each parameter value

$$G(X_1, \ldots, X_n) = \sum_{i=1}^{n} \left\| (\beta_i X_i \Gamma_i + 1_k \gamma_i^T) - \mu \right\|^2,$$

so that the squared full Procrustes distance (d_F^2) between configurations in the set, say X_a and X_b for example, is

$$\min_{\gamma,\beta,\Gamma} \left\| \frac{X_a}{\|X_a\|} - (\beta \frac{X_b}{\|X_b\|} \Gamma + 1_k \gamma^T) \right\|^2 = \min_{\gamma,\beta,\Gamma} \left\| \frac{X_b}{\|X_b\|} - (\beta \frac{X_a}{\|X_a\|} \Gamma + 1_k \gamma^T) \right\|^2$$

The full Procrustes fit for X_i is then

$$X_i^P = \hat{\beta}_i X_i \hat{\Gamma}_i + 1_k \hat{\gamma}_i^T, \; i = 1, \ldots, n$$

where $\hat{\beta}_i$, $\hat{\Gamma}_i$ and $\hat{\gamma}_i$ are the minimising parameters.

The resulting Procrustes-aligned *x*-*y* configurations in which locational, scaling and rotational differences are minimised, are thus registered to a common coordinate system in Kendall's shape space (Adams *et al.* 2021: 49; Zelditch and Swiderski 2018: 46-47; Sherrat 2014: 19-22; Robinson 2005: 37; Dryden and Mardia 1998: 87-92; Bookstein 1997; Bookstein 1991; Kendall 1984; Gower 1975). As is usual, configurations were subsequently projected into tangent linear space about a "pole" – the average shape or [μ] – for the purposes of inferential exploration (Dryden and Mardia 2016: 88-95; Robinson 2005: 97-98; Kent and Mardia 2001: 469; Rohlf 1999: 205; Dryden and Mardia 1998: 71). As discussed previously (Section 4.3.2), the differences between

configurations in shape and tangent linear space are minimal, thus if X_a and X_b are closely related configurations in shape space and υ_a and υ_b are their tangent plane coordinates,

$$\|v_a - v_b\| \approx d_F(X_a, X_b).$$

As such, it was possible to employ standard statistical methods based on Euclidean distances between coordinates in the tangent plane (Dryden and Mardia 2016: 88-95; Robinson 2005: 98; Kent and Mardia 2001: 469; Dryden and Mardia 1998: 151-173).

7.2.5 Implementation of Transformations

The aforementioned transformations of coordinate configurations were carried out in *Geomorph*, an R package written by Dean Adams and colleagues (e.g., Adams *et al.* 2021). This frequently used and updated package is found in the CRAN repository. It has been applied in a variety of settings to produce articles that have been published in a broad selection of peer reviewed journals and is supported by a plethora of user manuals and a Google group in which members can directly and openly correspond with the package's authors (Adams *et al.* 2021; Zelditch and Swiderski 2018; Sherrat 2014; Zelditch *et al.* 2012). The use of *Geomorph* also streamlines data acquisition and processing. For instance, due the increasing integration of the package with *Stereomorph*, it is possible with the function *readland.shapes* to take the raw scaled coordinate data created in *Stereomorph* and define coordinate points as either landmarks or semi-landmarks so that the *Geomorph* functions treat them appropriately (Adams *et al.* 2021: 117-119). Furthermore, although the calculation of centroid size, sliding of semi-landmarks, and registration of coordinate configurations through GPA are separate steps, they are all accomplished through *Geomorph*'s *gpagen* function (Adams *et al.* 2021: 49-51). *Geomorph* further facilitates the handling of practical problems such as missing data and digitisation errors. As such, before performing GPA, a linear regression

model was employed to predict missing landmark values; realistically, this was rarely employed as individual differences account for the greatest proportion of variation in molar morphology and landmarks estimated with reference to the average position in the sample have the capacity to inflate individual estimates of FA. After registration, the *plotOutliers* function identified abnormal configurations. Initially, several notable deviations were detected; these were the result of imaging and digitisation errors (e.g., switching landmarks) and, in these cases, new images were produced and coordinate configurations amended (Adams *et al.* 2021; Zelditch and Swiderski 2018: 40; Sherrat 2014: 16-18; Dryden and Mardia 1998: 288) (Figure 7.5).

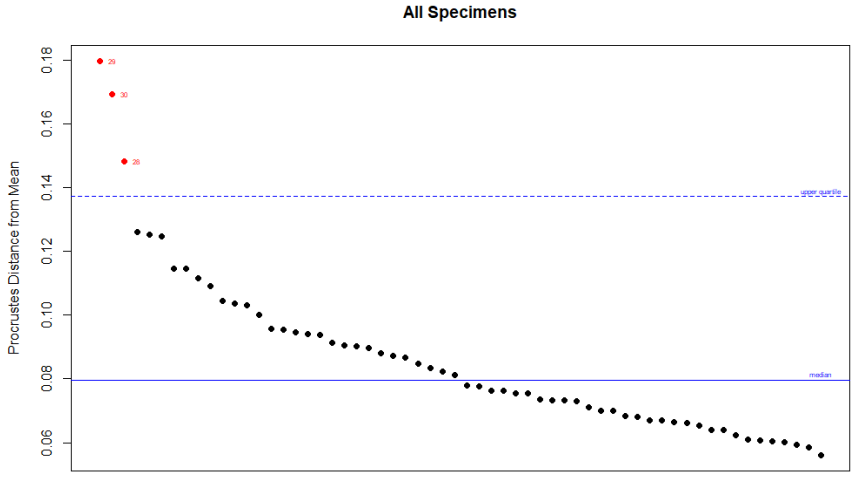

Figure 7.5 Errors in alignment, orientation and subsequent digitisation were identified through the *plotOutliers* function in *Geomorph* which graphically highlights outlying configurations in red.

7.2.6 Summary

The above method is a means through which M1 occlusal morphology can be defined. Although the procedures are complex, the development of packages such as *Geomorph* and *Stereomorph* in the statistical environment R means that they are an accessible and practical option (Adams *et al.* 2021; Zelditch and Swiderski 2018; Olsen 2015; Olsen and Westneat 2015). By targeting M1s, which develop perinatally, it was possible to quantify morphological variation associated with a specific time of life.

7.3 Pilot Study

Before data collection began, two issues were explored. Firstly, the question of how many semi-landmarks should be used to sample the outline and, secondly, to what extent intra-observer error in the imaging and digitisation processes affected the analysis. As Principal Components Analysis played a key role in answering these questions, this section begins with a description of this exploratory procedure. The teeth evaluated during the pilot study were selected from individuals originating from the South Shields collection with minimally worn M1 occlusal surfaces. Replicate measures were taken of each tooth, with replicates being produced on separate days. The analytical procedures detailed here were conducted after each tooth had been recorded five times.

7.3.1 Principal Components Analysis

As dental morphological features are functionally, developmentally and genetically linked, complex patterns of variation and covariation between shape variables can be expected (Zelditch *et al.* 2012: 136). Principal Components Analysis (PCA) makes these patterns easier to interpret by generating new variables (i.e., PCs) that sum to the same total variance as the original variables, but are independent linear combinations of them (e.g., Zelditch *et al.* 2012: 136-146). The first step to finding PCs is to calculate the sample covariance matrix (S_v) for the tangent space configurations v_i, ..., v_n as

$$S_v = \frac{1}{n}\sum_{i=1}^{n}(v_i - \bar{v})(v_i - \bar{v})^T$$

where $\bar{v} = \frac{1}{n}\sum v_i$. When $M = 2k - 4$ is the dimension of the shape space, the $p = min(n - 1, M)$ non-zero eigenvectors of S_v are the principal components ψ_1,…, ψ_p and the magnitude of variance explained by them is given by the corresponding

eigenvalues $\lambda_1,\ldots, \lambda_p$ (Dryden and Mardia 2016: 150-152; Zelditch *et al.* 2012: 144; Robinson 2005: 102; Dryden and Mardia 1998: 47-49). The PC score for the *i*th configuration on the *j*th component is

$$s_{ij} = \psi_j^T\left(v_i - \bar{v}\right),\ i = 1, ..., n; j = 1, ..., p.$$

while the percentage of variability captured by the *j*th PC ($j = 1, ..., p$) is

$$\frac{100\lambda_j}{\sum_{j=1}^{p}\lambda_j}.$$

PCA thus made it possible to simplify complex data and facilitate an exploration of morphological variability (Dryden and Mardia 2016: 152; Zelditch *et al.* 2012: 136-150; Robinson 2005: 102; Dryden and Mardia 1998: 47-49.

7.3.2 Determining Semi-landmark Number

The number of semi-landmarks needed to describe an outline effectively is an issue to which there is no ready answer. Investigators must achieve a balance between under-sampling, which would lead to insufficient morphological data being captured, and the loss of statistical power associated with over-sampling (Dryden and Mardia 2016: 369). Consequently, there has been a great deal of variability in how many semi-landmarks have been used to define M1 outlines. For example, Gómez-Robles used 30 semi-landmarks in an early paper but 39 in a later one (Gómez-Robles *et al.* 2011; Gómez-Robles *et al.* 2007), while Benazzi *et al.* (2011b) employed as few as 16 outline points. This confusing situation is partially the result of the differing nature of the projects; each venture imposes a unique set of requirements and investigators must determine how many points are appropriate for the specific project in question (Bardua *et al.* 2019: 18-19; Watanabe 2018; Gunz and Mitteroecker 2013: 104-105).

To decide how many semi-landmarks to employ, five antimeric M^1 and M_1 pairs were replicated five times (for a total of 50 M^1 and M_1 coordinate configurations), as discussed above. Outlines were then sampled by 10, 20, 30 and 40 semi-landmarks. Coordinate configurations were subjected to a PCA and the first two PCs were plotted to find the point at which additional semi-landmarks no longer caused perceptible alterations and presumably ceased to contribute useful information (Bardua *et al.* 2019: 19; Watanabe 2018: 2). The plots from these analyses showed visually appreciable differences in configurations with 10 and 20 semi-landmarks, but little alteration beyond that (Figure 7.6). As a result, it was decided to define outlines with 20 semi-landmarks in subsequent tests. Although the decision was subjective, the number appeared to capture morphological variation in sufficient detail and provided enough points to visually interpret data in a meaningful manner, whilst mitigating against the introduction of redundant information.

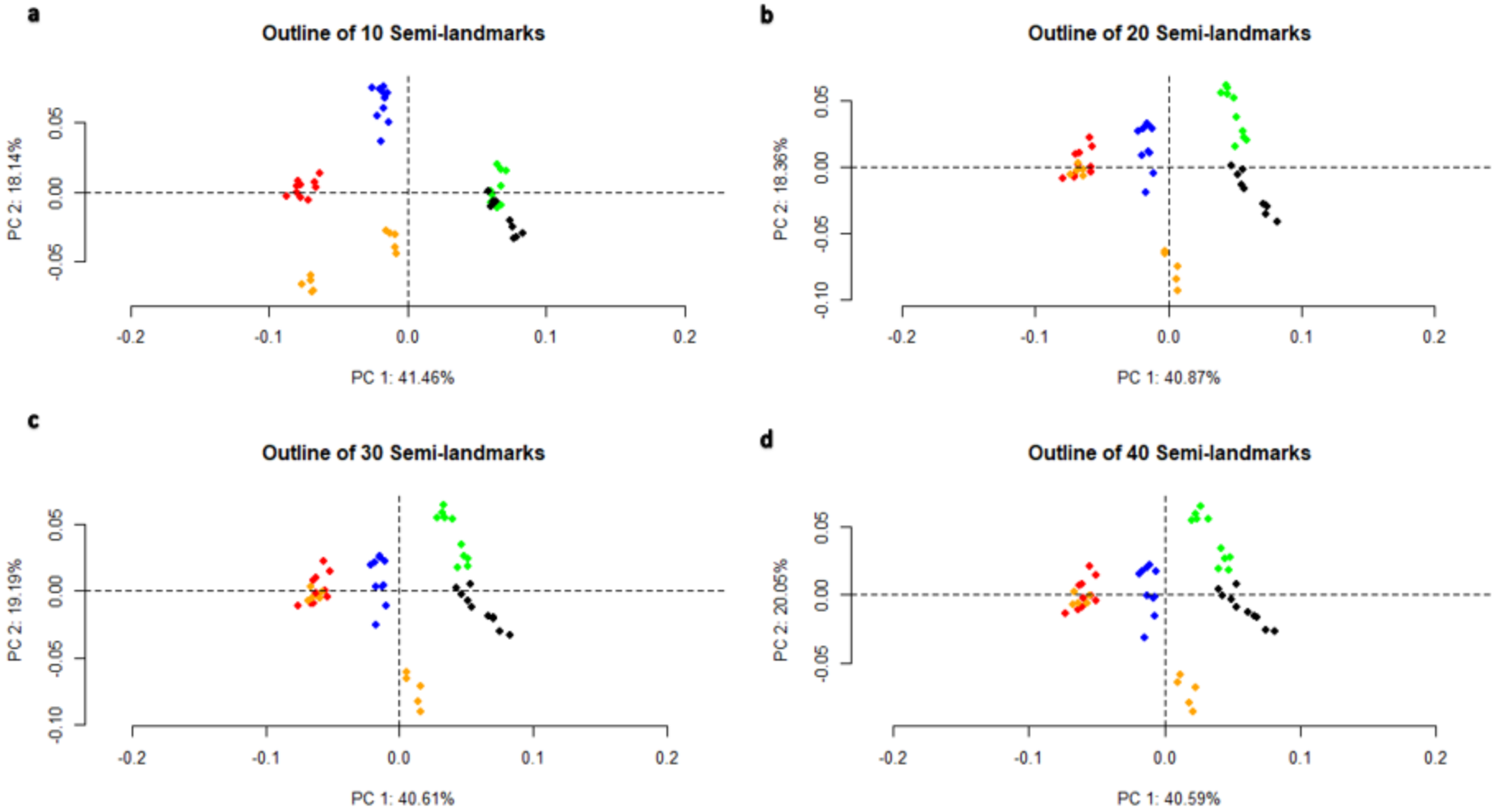

Figure 7.6 Plots of first two PCs of M^1 configurations with 10 (a), 20 (b), 30 (c) and 40 (d) semi-landmarks. Colours represent individuals, each of which was represented by five left and five right replicate configurations.

7.3.3 Error, Reliability and Replicate Measures

Methodological validity was dependent upon several factors that are easily influenced by operator error. These include: the orientation and alignment of teeth prior to imaging, as well as the placement of landmarks in the digitisation process (Fruciano *et al.* 2017; Shearer *et al.* 2017: 11; Robinson 2005: 110-145; Singleton 2001: 553-554; Arnqvist and Martensson 1998). Consequently, identifying sources of error and quantifying overall reliability was deemed essential so that the method could be tested, revised and refined. This is especially crucial when analysing dental fluctuating asymmetry as variance is always expected to be relatively small and therefore likely to be obscured easily by methodological irregularities (Fruciano *et al.* 2017; Klingenberg 2015; Graham *et al.* 2010). Multiple methods have been devised to evaluate error and reliability. Though varied in nature, these techniques revolve around exploring differences in replicate measurements.

Prior to initiating data collection, to assess error and intra-observer agreement, five replicate measures were taken from ten maxillary and mandibular M1s each representing five antimeric pairs (the same sample used in Section 7.3.2). Landmarks (eight for the M^1 and ten for the M_1) and an outline (sampled by 20 semi-landmarks) were digitised for each tooth. Semi-landmarks were slid and configurations adjusted by GPA. Following this, the locations of discrepancies in landmark and semi-landmark placement were identified, while overall methodological reliability and the relative contribution of fluctuating asymmetry and error to morphological variance were quantified.

7.3.3.1 Locations of Error

To test the consistency of landmark placement, the distances between a landmark's mean position and the landmark's location in each replicate were calculated.

This procedure gives an intra-landmark distance that measures dispersion (Shearer *et al.* 2017: 11; Kenyhercz *et al.* 2014; Rohlf 2003: 668; Singleton 2001: 553-554). When determined after performing Procrustes superimposition, sliding semi-landmarks and projecting shapes into tangent linear space, intra-landmark distances can be used to evaluate persistent locational discrepancies (Shearer *et al.* 2017: 11; Robinson 2005: 117; Singleton 2001: 553-554). In two-dimensional shape configurations with an *x* and *y* coordinate, the distance between the mean point (i.e., $\bar{x}$ and $\bar{y}$) for landmark *i* and the same landmark in the *j*th configuration is calculated as

$$\sqrt{((x_{ij} - \bar{x}_i)^2 + (y_{ij} - \bar{y}_i)^2)}.$$

For each tooth, a mean shape was computed from five GPA-aligned replicates. Following this, intra-landmark distances between coordinate points in every replicate and the mean configuration were calculated. Distances were visually compared through boxplots (Figure 7.7). This revealed that the distance between replicate measures and the mean shape was least at the intersection of fissures located centrally and most at cusp apices, while semi-landmarks occupied a middle ground. A robust, non-parametric Kruskal-Wallis test was employed to compare intra-landmark distances; differences were significant in both the M^1 (H=241.335, df=27, $p<0.001$, $\eta^2=0.16$) and M_1 sample (H=178.755, df=29, $p<0.001$, $\eta^2=0.10$), with large and moderate effect size respectively (Cohen 1988). In both instances, *post hoc* pairwise comparisons using Dunn's test with Bonferroni adjusted significance thresholds showed that significant dissimilarities existed between landmarks located centrally along the sagittal (in the M^1) and longitudinal fissures (in the M_1) and landmarks at cusp apices as well as semi-landmarks on the outline.

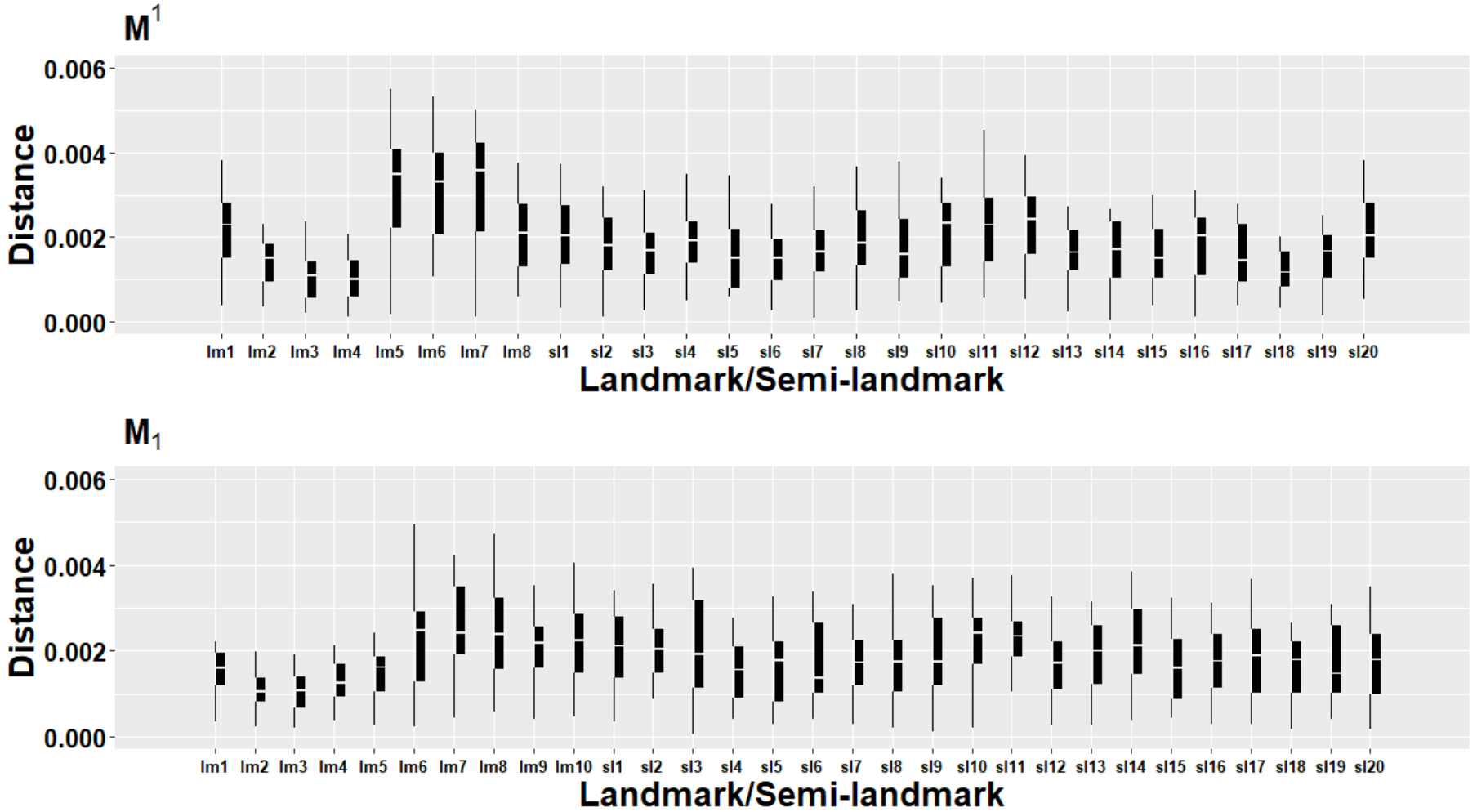

Figure 7.7 Boxplots showing the Procrustes distances between landmarks and semi-landmarks in replicate measures and mean M^1 (a) and M_1 (b) configurations. "*lm*" and "*sl*" are abbreviations of *landmark* and *semi-landmark* respectively; landmark order follows that established in Table 7.1 and Table 7.2. Note that the landmarks that deviate the least from their mean position and show little variance are located at distinct anatomical points along centrally-located fissures.

There are two likely explanations for these results. Firstly, as fissure junctions represent the definite juxtaposition of two anatomical structures, they are more clearly identifiable, Type I landmarks. In contrast, cusp apices are placed at the maximal height of each cusp (Type II landmarks) and, in two-dimensional images especially, they are less distinct. In this interpretation the inconsistent identification of landmarks underlies error. Alternatively, landmarks located further away from the image's central point of focus were affected to a greater degree by variation in alignment than landmarks located centrally. In either case it might be expected that semi-landmarks placed most peripherally on an outline without any clearly defined features would produce the greatest intra-landmark distances. However, as the location of semi-landmarks on the outline is initially mathematically determined they are less influenced by human error and differences are then reduced through both the sliding process and Procrustes fit (Benazzi *et al.* 2011b: 349; Robinson 2005: 112-114). On balance, it seems plausible that a combination of both factors (identification error and alignment inconsistency) accounts for the observed variances in intra-landmark distances. Nevertheless, it should be noted that although these differences were significant, they do not necessarily represent a magnitude of error that could confound results and, consequently, error relative to fluctuating asymmetry is explored in Section 7.3.3.3.

7.3.3.2 Reliability: Correlation Coefficients

Robinson (2005) developed a novel means of appraising overall methodological reliability from repeated measures in a GM context by decomposing morphological variation into uncorrelated variables through PCA. This is achieved after performing a GPA, by comparing the mean PC scores through an ANOVA design to calculate an intra-class correlation coefficient (ICC) (Robinson 2005: 117-121; Shrout and Fleiss 1979). Since Shrout and Fleiss (1979) first proposed computing an ICC through an

ANOVA, it has become a popular method of exploring how reliably "judges" score "subjects"; results are expressed between a range of 0.0 and 1.0, reflecting no correlation through to perfect correlation between replicate measures (Koo and Li 2016; Robinson 2005: 117; Fleiss 1986; Shrout and Fleiss 1979). There are several variants, but as intra-observer reliability was being questioned, a two-way, mixed effects test of absolute agreement in a single observer was conducted on the PC scores of two, three and five replicates (i.e., two replicate measures were initially taken, then a third and so on) of Procrustes-aligned landmark and semi-landmarks configurations for the sample of ten M^1s and M_1s (Koo and Li 2016: 157; McGraw and Wong 1996: 32-34; Fleiss 1986; Shrout and Fleiss 1979). Mean PC scores were organised into a table. With a fixed rater (i.e., judge), each column was analogous to a summary of a single judge's score for each tooth and each row a different tooth (i.e., subject). Based on the expected mean squares an ICC was calculated as

$$ICC = \frac{MS_r - MS_e}{MS_r + \frac{MS_c - MS_e}{n}}$$

where MS_r is the mean square for rows (variance between teeth), MS_c is the mean square for columns (variance between replicates), and MS_e is the mean square of the residual variance attributable to error and n is the number of subjects (McGraw and Wong 1996: 36). To test statistical significance, an F value was calculated as $F = MS_r/MS_e$ and compared to an F distribution (McGraw and Wong 1996: 39). Results are presented in Table 7.3.

Though qualitative descriptors of reliability are somewhat arbitrary, they are convenient and can be used to articulate confidence in the method being evaluated (Liljequist *et al.* 2019; Koo and Li 2016; Robinson 2005: 128; Shoukri *et al.* 2004: 270;

Cicchetti 1994; Donner and Eliasziw 1987). According to the relatively parsimonious conventions of Koo and Li (2016) the overall reliability achieved in the placement of landmarks in both three and five replicate measures, being greater than 0.9 in both M1s, was "excellent." The ICC score for two replicate measures of the M_1 was also excellent. For the M^1, however, two replicate measures fell below this threshold – though it should be noted that a score of 0.808 is still considered "good" and was statistically significant. These results suggest that variation between replicates is small in comparison to variation between individuals and that an analysis of three replicate measures achieves excellent reliability.

Tooth	Intraclass Correlation	*F* test and Significance			
		Value	df 1	df 2	p
M^1					
5 replicates	0.983	57.7	9	36	< 0.001
3 replicates	0.973	37.0	9	18	< 0.001
2 replicates	0.808	5.20	9	9	0.01
M_1					
5 replicates	0.980	48.8	9	36	< 0.001
3 replicates	0.972	35.8	9	18	< 0.001
2 replicates	0.947	18.8	9	9	< 0.001

Table 7.3 ICCs with landmarks and an outline of 20 semi-landmarks.

7.3.3.3 Error Relative to Fluctuating Asymmetry

Thus far, error has been discussed without reference to FA, and though this has been informative, it needed to be demonstrated that observer error did not obscure the small variances typically associated with fluctuating asymmetry. As previously discussed (Section 4.5), the two-way, mixed model ANOVA quantifies the relative variance in a sample attributable to each term, including error. This comparative measure was used to infer whether measurement error was sufficiently low to enable an effective exploration of fluctuating asymmetry (Klingenberg 2015: 868-870; Graham *et al.* 2010: 487-489; Arnqvist and Martensson 1998: 83-85; Palmer 1994: 353-355; Bailey and Byrnes 1990; Palmer and Strobeck 1986: 403-406; Leamy 1984).

As the previous tests inferred that "excellent" repeatability was achieved with three repeated measures, three replicates were taken from five M^1 and M_1 bilateral antimeric pairs (i.e., to give a total of thirty maxillary and mandibular replicates; these were the same replicates employed in Section 7.3.3.2). The Procrustes-aligned coordinates (both landmarks and an outline of 20 semi-landmarks) were then evaluated through a Procrustes ANOVA (Section 7.4.1). The output provided several pertinent statistics. In the M^1, fluctuating asymmetry accounted for 22.2% of morphometric variance; though small relative to individual variation (68.4%), this was much higher than variation due to measurement error (5.0%) and, consequently, there was a high ratio of fluctuating asymmetry to error (F=22.209) (Table 7.4). Although FA contributed less to overall morphometric variance (14.6%) in the M_1, the ratio of fluctuating asymmetry to measurement error was similar (F=19.056) and it appeared that the reduction in the percentage of overall variation associable with FA was due to an increase in inter-individual variation (76.6%) (Table 7.5).

Effects	df	SS	MS	R^2	F	p
ind	4	0.120	0.030	0.684	3.089	0.677
side	1	0.008	0.008	0.044	0.795	0.627
ind x side	4	0.039	0.010	0.222	22.209	<0.001
error	20	0.009	0.001	0.050		
Total	29	0.176				

Table 7.4 Procrustes ANOVA evaluating asymmetric shape variation in a sample of 5 M^1 pairs. A Randomised Residual Permutation Procedure (RRPP) with 1000 permutations was used to determine significance (Adams *et al.* 2021; Adams and Collyer 2018; Collyer and Adams 2018).

Effects	df	SS	MS	R^2	F	p
ind	4	0.123	0.030	0.766	5.261	0.538
side	1	0.008	0.008	0.050	1.377	0.403
ind x side	4	0.023	0.005	0.146	19.056	<0.001
error	20	0.006	0.001	0.038		
Total	29	0.160				

Table 7.5 Procrustes ANOVA evaluating asymmetric shape variation in a sample of 5 M_1 pairs. A Randomised Residual Permutation Procedure (RRPP) with 1000 permutations was used to determine significance (Adams *et al.* 2021; Adams and Collyer 2018; Collyer and Adams 2018).

7.3.3.4 Summary

Through the calculation of intra-landmark distances, it was possible to identify the locations and infer the causes of error. It appears that inconsistencies in alignment as well as problems in identifying less clearly juxtaposed landmarks are a source of methodological error (Fruciano *et al.* 2017; Shearer *et al.* 2017: 11; Robinson 2005: 117; Singleton 2001: 553-554; Arnqvist and Martensson 1998). However, after decomposing morphometric variance into uncorrelated PCs and computing ICCs, it was found that the method was highly repeatable; specifically, an average of three replicates achieved "excellent" intra-observer reliability (Liljequist *et al.* 2019; Koo and Li 2016; Robinson 2005: 117-121; Cicchetti 1994; Donner and Eliasziw 1987; Fleiss 1986; Shrout and Fleiss 1979). Finally, it was demonstrated that fluctuating asymmetry exceeds measurement error by a factor of *circa* 20. Based on these results, it was decided that in the project's data acquisition phase three replicates of each tooth would be collected. One proviso when using replicate measures is that error at every stage of the data acquisition process must affect each replicate (Arnqvist and Martensson 1998). Therefore, for each replicate, the tooth being evaluated was removed from its setting before being repositioned, rephotographed and re-digitised. When an individual measure was needed (i.e., when exploring the relationship between FA and later-life stress in individuals), these replicates were used to compute a mean shape (Section 7.4.2).

7.4 Evaluating Fluctuating Asymmetry

This section first details the ANOVA procedure through which tangent space distances were decomposed to explore asymmetry in the sample. Next, the steps taken to produce an individual measure of fluctuating asymmetry are described.

7.4.1 Goodall's *F* and the Procrustes ANOVA

In a sample of n coordinate configurations $X_1,\ldots, X_n$, when it is assumed that configurations are isotropic normal perturbations about a mean, to test the null hypothesis of $H_0: \mu = \mu_0$ against the alternative hypothesis of $H_1: \mu \neq \mu_0$, Goodall's F can be approximated from squared distances in tangent linear space (d_v^2) as

$$F = (n-1)n\frac{d_v^2\,(\mu_0, \bar{\mu})}{\sum_{i=1}^{n} d_v^2\,(X_i, \bar{\mu})} \sim F_{M,(n-1)M}$$

where $\bar{\mu}$ is the full Procrustes estimate of mean shape and is calculated as the arithmetic mean of each coordinate point (Dryden and Mardia 1998: 90), and $M = km - m - m(m-1)/2 - 1$. For large values of F, the null hypothesis H_0 can be rejected (Dryden and Mardia 2016: 197-198; Robinson 2005: 106; Dryden and Mardia 1998: 161; Goodall 1991: 314).

Regarding asymmetric variance, the sum of square (SS) distances in tangent space between configurations can be decomposed as

$$\sum_{p=1}^{P}\sum_{b=1}^{B} d_U^2\left(x_{pb}, \bar{\bar{x}}\right) = B\sum_{p=1}^{P} d_U^2\,(\bar{x}_p, \bar{\bar{x}}) + P\sum_{b=1}^{B} d_U^2\,(\bar{x}_b, \bar{\bar{x}}) + \sum_{p=1}^{P}\sum_{b=1}^{B} d_U^2\left(x_{pb}, \bar{x}_p + \bar{x}_b - \bar{\bar{x}}\right)$$

where individuals $p = 1, \ldots, P$ are associated with sides $b = 1,\ldots, B$, where $B = 2$ so that x_{pb} is side b of the pth individual and $\bar{x}_p$ and $\bar{x}_b$ are individual and side means and $\bar{\bar{x}}$ is

the grand mean. The sums on the right-hand side of the equation respectively account for: individual variation, directional asymmetry, and non-directional asymmetry (Savriama and Klingenberg 2011: 5). As variation can be partitioned through a sums of squares procedure, with differences between shapes found as the squared tangent coordinate differences summed across all coordinates of all landmarks, it is possible to employ an ANOVA procedure to calculate *F* (Savriama and Klingenberg 2011; Klingenberg 2015: 869; Klingenberg and McIntyre 1998).

As previously discussed in Section 4.5, a two-way, mixed model ANOVA has become an essential step in the sample-level evaluation of asymmetry. Variation is explored about two main factors: a between-subjects random effect and a within-subjects fixed effect. Also accounted for is the synergistic interaction of factors and, when replicate measures are taken, the residual variance attributable to error (McKillup 2012: 147-150; Zelditch *et al.* 2012: 228-240; Field 2005: 393-432). The random between-subjects effect (*ind*), or variation between individuals, was found as the sum of square differences (i.e., squared tangent space distances) between average individual shapes (i.e., the individual mean calculated from all replicate measures) and the grand mean shape (Table 7.6). The fixed within-subject effect (*side*) quantified variation in the sample attributable to a side bias, that is directional asymmetry, and was computed as the summed difference between the sample's average left and right-side shapes and the grand mean shape. The interaction between the two main effects (*ind x side*) quantified the contribution of individual left-right differences to overall variance and measured non-directional asymmetry (in simple terms, in the ANOVA design this is the variance in squared tangent space distances left unexplained by individual variation and sample-level side biases). Variation due to error was calculated as the summed differences between each replicate and the corresponding individual's mean left or right configuration (Adams

et al. 2021: 6-10; Murrar and Brauer 2018; Zelditch and Swiderski 2018; Klingenberg 2015: 869-870; Zelditch *et al.* 2012: 364-366; Graham *et al.* 2010: 487-489; Klingenberg and McIntyre 1998; Palmer and Strobeck 1986: 407-408). In order that this process could be achieved in *Geomorph*'s *bilat.symmetry* function, vectors were supplied to specify which individual, side and replicate each configuration represented as well as an argument to denote that the structures have matching symmetry (i.e., teeth are paired organs reflected about a midline axis; refer to Section 4.4) (Adams *et al.* 2021: 6-10; Sherrat 2014: 23-25).

Effect	SS	df	MS
ind	$CB\sum_{p=1}^{P} d_{\upsilon}^{2}(\bar{x}_{p}, \bar{\bar{x}})$	$P - 1$	$SS_{ind}/(P - 1)$
side	$CP\sum_{b=1}^{B} d_{\upsilon}^{2}(\bar{x}_{b}, \bar{\bar{x}})$	$B - 1$	$SS_{side}/(B - 1)$
ind x side	$C\sum_{p=1}^{P}\sum_{b=1}^{B} d_{\upsilon}^{2}(\bar{x}_{pb}, (\bar{x}_{p} + \bar{x}_{b} - \bar{\bar{x}}))$	$(P - 1)(B - 1)$	$SS_{ind\ x\ side}/(P - 1)(B - 1)$
error	$\sum_{c=1}^{C}\sum_{p=1}^{P}\sum_{b=1}^{B} d_{\upsilon}^{2}(x_{pbc}, \bar{x}_{pb})$	$PB(C - 1)$	$SS_{error}/PB(C - 1)$
Total	$\sum_{c=1}^{C}\sum_{p=1}^{P}\sum_{b=1}^{B} d_{\upsilon}^{2}(x_{pbc}, \bar{\bar{x}})$	$PBC - 1$	

Table 7.6 The ANOVA procedure, developed from that presented in Chapter 4, through which the differences (measured as squared tangent space distances) between shapes (defined above) was computed to decompose asymmetric variation. As three replicate measures were taken, $c = 1, ..., C$ where $C = 3$ (Section 7.3).

The SS values are divided by their respective degrees of freedom to give the mean square (MS) for each term, while dividing the *SS* for each effect by the total *SS* gave an R^2 value which represented the proportion of variation attributable to each term (Adams *et al.* 2021: 111). To determine significance for the interaction term (i.e., non-directional asymmetry) an *F*-value was computed as $F = MS_{ind\ x\ side}/MS_{error}$ (Zelditch and

Swiderski 2018; Klingenberg 2015: 869-870; Zelditch *et al.* 2012: 240; Graham *et al.* 2010: 487-489; Klingenberg and McIntyre 1998). To avoid the need to make normality assumptions, significance testing was done non-parametrically through a residual randomisation permutation procedure (RRPP) in *Geomorph* (Collyer *et al.* 2015; Collyer 2015; Klingenberg 2015: 869-870; Graham *et al.* 2010: 487-489; Klingenberg and McIntyre 1998; Good 1994; Edgington 1995; Palmer and Strobeck 1986: 407-408). In RRPP, residuals from null linear models are randomised and added to the fitted values to generate random pseudovalues. By doing this repeatedly, an empirical sampling distribution of ANOVA statistics is produced (Collyer and Adams 2018: 1773; Adams and Collyer 2015: 824-825; Zelditch *et al.* 2012: 215-217; Anderson and Ter Braak 2003). Thus, the *F*-values for the observed effects are compared to the distribution of many values and deemed significant when they fall beyond the 95th percentile.

Contingent upon significant results, coordinate configurations were investigated further to discern whether the non-directional component to asymmetry was likely the result of random deviations from symmetry (i.e., was the interaction term identifying significant fluctuating asymmetry or antisymmetry). For each M1 landmark and semi-landmark plots of signed left-right differences were visually examined and tested for kurtosis. If antisymmetry was present, scatter plots would reveal two clusters while histograms and density plots would display a bimodal or platykurtic distribution (Balzeau *et al.* 2012: 2; Silva *et al.* 2012: 561-564; Guatelli-Steinberg *et al.* 2006: 249; Radwan *et al.* 2003: 502; Debat *et al.* 2001: 425-426; Klingenberg and McIntyre 1998: 1368).

7.4.2 Individual Measures of Fluctuating Asymmetry

Fluctuating asymmetry was investigated further by isolating the directional and fluctuating components according to the procedures outlined by Bookstein (1991) and Klingenberg and McIntyre (1998). The directional component to asymmetry (D) is computed as the difference between the overall sample's mean left $(\overline{x\text{-}y}_L)$ and right configuration $(\overline{x\text{-}y}_R)$ (Oxilia *et al.* 2021: 5; D. Adams, personal communication, 21st May 2020; Zelditch *et al.* 2012: 364-369; Palmer and Strobeck 2003: 319; Klingenberg and McIntyre 1998: 1375; Smith *et al.* 1997; Bookstein 1991: 269). The matrix $D = (d_{ij})$, where $i = 1, ..., k$ and $j = 1, ..., m = 2$, is given as

$$D = \overline{x\text{-}y}_L - \overline{x\text{-}y}_R$$

By subtracting the directionally asymmetric component to asymmetry (the matrix D) from the difference between the individual left (x-y_L) and right (x-y_R) coordinate configurations (in this case, individual left and right configurations were replicate averages), it is possible to obtain a k x m matrix of x-y coordinates for individuals $p = 1, ..., P$ that reflects the component of morphological variance attributable to fluctuating asymmetry. For the pth individual this is calculated as

$$A_p = \big((x\text{-}y_{pL}) - (x\text{-}y_{pR})\big) - (D).$$

The computation of A_p is performed by the *bilat.symmetry* function and the adjusted coordinate matrices can be found by calling up *FA.component* (Adams *et al.* 2021: 6-10; D. Adams, personal communication, 21st May 2020).

To calculate a univariate index of the overall magnitude of fluctuating asymmetry (a_p), from A_p configurations the square root of the sum of squares is found to give

$$a_p = \sqrt{\sum_{i=1}^{k}\sum_{j=1}^{m} A_p^2}.$$

As an unsigned individual estimate of fluctuating asymmetry, a_p scores are amenable to standard univariate tests (Oxilia *et al.* 2021: 5; Lazić *et al.* 2015: 48-49; Zelditch *et al.* 2012: 364-369; Palmer and Strobeck 2003: 319; Klingenberg and McIntyre 1998: 1375; Smith *et al.* 1997; Palmer 1994: 356-358; Bookstein 1991: 269). They were therefore used to explore statistically (Section 7.5) the relationships between fluctuating asymmetry, demographic cohorts and the osteological data employed to infer later-life stress (Chapter 6). This individual measure of FA thus enabled an exploration of the links between early and later-life stress experience and themes such as heterogeneous frailty, developmental tempo and selective mortality/morbidity.

7.4.3 Summary

The method described is a procedure for identifying fluctuating asymmetry through GM methods, determining significance and then, if appropriate, computing an individual index of fluctuating asymmetry (Zelditch *et al.* 2012: 364-369; Klingenberg and McIntyre 1998: 1375; Smith *et al.* 1997; Bookstein 1991: 268-269). As this was computed for M1s which form perinatally, it can be employed as a proxy for early-life stress, contrasted between groups and compared to measures of later-life stress in a life-course approach to health and development.

7.5 Asymmetry: Between and Within-group Patterns

With early-life stress estimated through an index of fluctuating asymmetry (i.e., a_p scores) and later-life stress experience charted through other pathological lesions (Chapter 6), it was possible to explore differences in life-course experiences between groups and the influence stress experienced at specific periods had on later frailty (i.e., subsequent vulnerability to stressors) and final outcomes (e.g., estimated age-at-death, long bone length, etc). The statistical procedures used to accomplish this are detailed here. Unfortunately, this requires the reuse of some notation; where this occurs, it is made clear.

7.5.1 Differences Between Groups

Before undertaking any tests, a_p scores were visually checked (e.g., through boxplots and density plots) to ensure that groups produced comparable distributions. When normally distributed (or when approximate normality could be achieved by transformation), parametric tests were employed (Van Pool and Leonard 2010: 172; Field 2005: 72).

When two groups were being compared parametrically, a two-tailed, two-sample *t*-test was employed to ascertain whether mean values were significantly different. In order to avoid assuming equal variances between groups, Welch's correction was employed in which *t* is computed as

$$t = \frac{\bar{x}_1 - \bar{x}_2}{\sqrt{\frac{s_1^2}{n_1} + \frac{s_2^2}{n_2}}},$$

where $\bar{x}_1$ and $\bar{x}_2$ are the means of the first and second groups which have variances s_1^2 and s_2^2 and are n_1 and n_2 data points in size respectively (McKillup 2012: 118-120; Field 2005: 298). Degrees of freedom are approximated as

$$df = \frac{\left(\frac{s_1^2}{n_1} + \frac{s_2^2}{n_2}\right)^2}{\frac{s_1^4}{n_1^2(n_1 - 1)} + \frac{s_2^4}{n_2^2(n_2 - 1)}}.$$

Significance can then be determined by comparing the t value to a *t*-distribution with the corresponding degrees of freedom (McKillup 2012: 120). When significant, the magnitude of the difference between groups was expressed through Cohen's d. When variance between groups is not assumed equal, this is found as

$$d = \frac{\bar{x}_1 - \bar{x}_2}{\sqrt{(s_1^2 + s_2^2)/2}}.$$

For three or more groups with comparable variances, comparisons were made with a one-way ANOVA. In this procedure, the sum of squares accounted for by between-group differences (SS_b), that is the extent to which differences among groups could account for total variation, is found as

$$SS_b = \sum_{i=1}^{k} n_i \, (\bar{x}_i - \bar{\bar{x}})^2$$

where is $\bar{x}_i$ the mean of the *i*th group which has n observations, there are $i = 1, \ldots, k$ groups, and $\bar{\bar{x}}$ is the grand mean of all groups combined (McKillup 2012: 147-150; Field 2005: 320-321). The model's mean square (MS_b) is found by dividing SS_b by degrees of freedom equal to $k - 1$. The residual sum of squares (SS_r), essentially within-group variation attributable to factors not explained by between-group difference, is given as

$$SS_r = \sum_{i=1}^{k} (x_{ik} - \bar{x}_k)^2$$

and converted to the within group mean squares (MS_r) by dividing SS_r by $n - k$ degrees of freedom. An F ratio is found as MS_b/MS_r and compared to an F distribution (Field 2005: 319-324). When $p<0.05$, to find which groups differed significantly, pairwise tests were made by comparing all combinations of groups in what were essentially *t*-tests; to mitigate against Type 1 error, Bonferroni adjusted significance thresholds were used (i.e., α was divided by the number of comparisons) (Dinno 2015: 299; McKillup 2012: 162; Field 2005: 339). Additionally, an effect size statistic (ω^2) was calculated. Conveniently, this statistic is computed from the terms used to determine significance (Field 2005: 358), so that

$$\omega^2 = \frac{MS_b - MS_r}{MS_b + ((n-1)MS_r)}.$$

Had the assumptions necessary for parametric tests not been met, non-parametric equivalents would have been considered (Tomczak and Tomczak 2014; Van Pool and Leonard 2010: 172; Field 2005: 72; Rosenthal 1991: 19; Dunn 1964).

7.5.2 Predicting Life-course Outcomes

With a quantification of fluctuating asymmetry (i.e., a_p scores) acting as a proxy for maternally mediated early-life stress and further variables reflecting later experiences (e.g., matched LEH presence) and outcomes (e.g., age-at-death), it was possible to infer statistically in archaeologically recovered remains the extent to which early-life stress defined the life-course and the significance of this critical period relative to others. This section describes the specific procedures utilised.

For continuous dependent variables (such as estimated age-at-death) a linear model was employed to describe the relationship between dependent variable y and predictor variables $x_1, ..., x_n$. Such a linear model may be conceptualised as a plane of best fit and is summarised by two statistics: α the point at which each x_i is 0 and the plane intercepts the y axis; and β coefficients that describe the slope of the plane (McKillup 2012: 246; Field 2005: 146). The interaction effect between predictors on y was also considered. In a hypothetical model which includes two predictors and an interaction between them, the regression equation would be

$$y = \alpha + \beta_1 x_1 + \beta_2 x_2 + \beta_3 x_1 x_2.$$

Various diagnostic statistics were used to evaluate the model. A t-statistic, for example, was calculated for each β coefficient by dividing the coefficient by its standard deviation. When compared to a t-distribution this statistic inferred whether the coefficient's contribution to the model was significantly different from zero (McKillup 2012: 251-258; Field 2005: 151). The statistical significance of the overall regression model was detected in the same way as a single-factor ANOVA. Firstly, total variation in the dependent variable was calculated as $SST = \sum_i^n (y_i - \bar{y})^2$, that is the sums of squared distances between the ith observed value and the grand mean, denoted as and y_i and $\bar{y}$ respectively. The SST was then partitioned into components either explained or unexplained by the regression model. The sums of squares explained for by the regression (SSR) was the difference between $\hat{y}$ – the point estimated by the regression plane – and $\bar{y}$, and is given as $SSR = \sum_i^n (\hat{y}_i - \bar{y})^2$. The residual unexplained variation (SSE), sometimes referred to as the "error" of the model, was calculated as the difference between y_i and $\hat{y}$,

so $SSE = \sum_{i}^{n}(y_i - \hat{y}_i)^2$. SSR and SSE were then divided by their degrees of freedom to give the mean squares (MS) for these two sources of variation. An F ratio was calculated as

$$F = \frac{MS_{regression}}{MS_{residual}}$$

and used to assess the model's statistical significance. The quality of the regression was further measured through the coefficient of determination (R^2), calculated as

$$R^2 = \frac{SSR}{SST}$$

and is the proportion of variation explained by the model (McKillup 2012: 251-258; Field 2005: 148-150).

In the case that y was a binary variable, logistic regression was used. In this instance an iteratively reweighted least squares method for Maximum Likelihood Estimation produced the intercept and coefficients of the regression model (Field 2005: 218-221). Given independent predictor values $x_1, ..., x_n$, the model was used to predict the probability of being in a particular category as

$$log[p/(1 - p)] = \alpha + \beta_1 x_1 + \beta_2 x_2, ..., \beta_n x_n$$

where p is the probability of being in one category and $1 - p$ is the probability of being in the other. Like the *t*-values in linear regression, *z*-scores were calculated to evaluate whether each coefficient's contribution to the model was significantly different from zero. The overall fit and significance of the model was calculated through McFadden's pseudo-R^2, given as

$$R^2_{McFadden} = \frac{\log\left(L_{fitted}\right)}{\log\left(L_{null}\right)}$$

where L_{fitted} denotes the maximised likelihood value for the fitted model, and L_{null} is the corresponding value for the null model – a model with only an intercept and no covariates. These two values are respectively analogous to SSR and SST, making this version of the pseudo-R^2 statistic closely related to the R^2 value calculated when performing linear regression – hence, it was chosen in preference to the alternatives. To evaluate whether the model was statistically significant a χ^2 value was calculated as $2[\log\left(L_{fitted}\right) - \log\left(L_{null}\right)]$. To obtain a p value, this was referenced to a χ^2 distribution where the degrees of freedom were equal to the number of parameters in the fitted model (the intercept and the β coefficients) minus the number of parameters in the null model (the intercept only) (Field 2005: 222; Long 1997: 104-106). Coefficients and standard errors were also employed to calculate odds ratios and their confidence intervals to indicate the relative risk associated with each input variable (Szumilas 2010; Gelman and Hill 2007; Field 2005: 717-718; Waldron 1994: 74-85).

In archaeological projects, factors beyond investigator control influence sample size. This is particularly pronounced in studies of teeth as the coarse diets, poor oral hygiene and extra-masticatory wear evidenced in past societies all contribute to diminished sample sizes (Larsen 1997: 169; Smith 1984). Limitations in sample size have obvious implications for the sensitivity of statistical procedures such as regression analyses. To mitigate these to some extent, regression models contained a minimum of 10 cases for every predictor variable (Field 2005: 172-173). Although larger samples are needed to detect relationships with small effect size (Field 2005: 172-173; Green 1991), the parameters employed took into account the practical limitations encountered when

dealing with osteological assemblages and permitted the overall fit of the models as well as the contribution of individual predictors to be evaluated. As the primary focus of the thesis was on assessing the impact of early-life stress on life-course trajectories/outcomes, before full models were constructed, relationships between FA scores and outcome variables were explored. M^1 and M_1 a_p scores were entered into separate regression procedures, thus maximising the amount of data in each analysis (i.e., models were not constrained to observations from individuals with FA values from both M1s). From there, to explain outcomes as thoroughly as possible, regression models were constructed containing all factors; at this stage, models thus incorporated site, sex, skeletal maturity and stress marker presence alongside FA scores. To refine models, a backwards elimination process was implemented in which non-significant variables (i.e., $p>0.05$) were removed sequentially, beginning with the variable with the highest p value. The model was refit after each removal, until only significant predictors were retained (Gelman and Hill 2007: 69; Field 2005: 212-213). Final models therefore accounted for outcome variables as best as possible and, when FA scores were retained, implied the importance of early-life stress in life-course outcomes.

7.5.3 Summary

With fluctuating asymmetry summarised in a univariate score amenable to standard tests it was possible to investigate differences in life-course experiences between groups and the influence stressors experienced at specific periods of life had on subsequent frailty (i.e., vulnerability to later stressors) and outcomes (e.g., attainment of skeletal maturity, long bone length, etc).

7.6 Conclusion

These methods represent an attempt to investigate the impact of stress experience during a critical period of development (i.e., the period of maternal dependence in early life) (Agarwal 2016; Gowland 2015; Armelagos *et al.* 2009). Specifically, Procrustean techniques were used to define M1 occlusal morphology, which forms during the period in question, and quantify fluctuating asymmetry (Adams *et al.* 2021; Zelditch and Swiderski 2018; Dryden and Mardia 2016: 197-198; Klingenberg 2015; Graham *et al.* 2010). The reliability of this method was established through a pilot study which, after evaluating differences between replicate measures, found that intra-observer error accounted for a small proportion of variation in relation to fluctuating asymmetry (Koo and Li 2016; Robinson 2005: 117-121). Furthermore, it has been demonstrated that a univariate summary of FA can be computed, thus making it possible through standard statistical techniques to explore within and between group variation in early-life stress experience and infer the role played by early-life stress in defining later-life frailty and life-course outcomes (Zelditch *et al.* 2012: 364-369; Klingenberg and McIntyre 1998: 1375; Smith *et al.* 1997; Bookstein 1991: 268-269). In the following chapter, the observations generated by the data collection process as well as the results of statistical testing are presented.

Chapter 8: Results

8.1 Introduction

This chapter is divided into three sections. First, the osteological data is explored. The demographic profile and pathological characteristics of the sample are investigated with reference to factors shown to influence and explain stress experience and life-course outcomes in modern and archaeological samples: site, sex and somatic maturity. Hypotheses are also generated as to how the impact of other factors (such as early-life stress) may be investigated in the dataset. In the second section, results from morphometric procedures are presented, including the decomposition of variance into different forms of asymmetry. Fluctuating asymmetry is investigated in detail; the occlusal locations more susceptible to stress-induced deviations to symmetry are identified and the impact of size on asymmetric variance is quantified. Fluctuating asymmetry is then contrasted and compared between groups to explore demographic patterns in stress experience. Finally, the utility of fluctuating asymmetry and other variables as predictors of later-life experiences and outcomes (e.g., length-of-life, growth, etc.) are evaluated with reference to the hypotheses generated in the first section. It was therefore possible to infer the extent and nature of the impact maternally-mediated early-life stress and other factors had on the life-course. Where necessary, attention is also drawn to results which may have been affected by the sampling biases discussed in Section 5.6.

8.2 The Osteological Data

8.2.1 Demographic Overview

In total, the skeletal remains of 217 individuals were analysed. Eighty-four skeletons (38.7%) came from the Black Gate collection, making the site the single largest contributor to the sample. Seventy (32.3%) individuals originated from the York Barbican excavations, 33 (15.2%) from South Shields and 30 (13.8%) from Warwick. One hundred and twelve (51.6%) were skeletally mature, while 104 (48.1%) were skeletally immature. Skeletal sex could be estimated for 85 (39.2%) individuals. Among these skeletons, 36 (42.4%) were female and 49 (57.6%) were male (Figure 8.1).

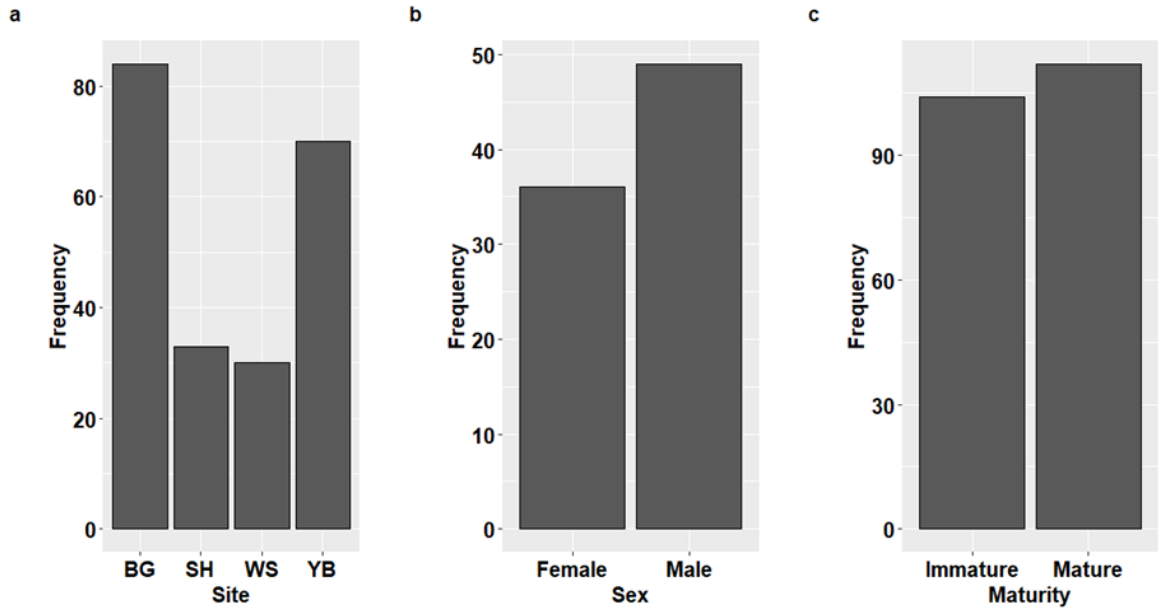

Figure 8.1 The frequency of skeletons from Black Gate (BG), South Shields (SH), Warwick (WS) and York (YB) (a), females and males (b), as well as skeletally immature and mature individuals (c).

Site-specific biases were evident in the demographic composition of the sample. For example, although there was a relatively even sex ratio among the skeletons from York Barbican and Warwick, the nine (64.3%) males from South Shields and 22 (64.7%) from Black Gate constituted a much larger percentage of the skeletons from those sites (Figure 8.2a). Differences were also noted in the relative frequencies of immature and

mature skeletons. Of the 29 skeletons from Warwick in which skeletal maturity could be established, 20 (69.0%) were immature. In contrast, the 37 (44.0%) immature skeletons from Black Gate, 14 (42.4%) from South Shields and 33 (47.1%) from York Barbican formed a much smaller proportion of those samples (Figure 8.2b). On the basis of this, it could be speculated that the structure and representativeness of the assemblages had been affected by either 1) incomplete cemetery excavation and choice of burial location or 2) substantial site-specific differentials in mortality between groups. However, past research has established that the frequency of immature and mature skeletons as well as females and males from each assemblage was comparable (Chapter 5) (e.g., Mahoney Swales 2019; Newman 2019; Raynor *et al.* 2011; McIntyre n.d.). It was therefore hypothesised that the demand for relatively well-preserved M1s had affected sampling.

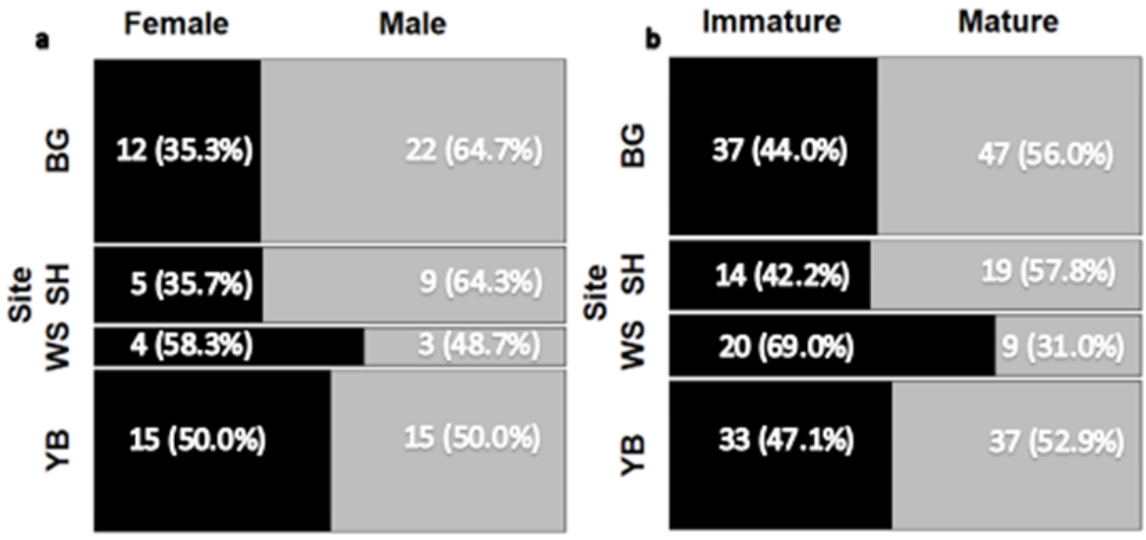

Figure 8.2 Mosaic plots representing the relative proportions of females and males (a) as well as skeletally mature and immature individuals (b) at each site with the area inside each box reflecting sample size. The numbers and percentages of females/males and immature/mature skeletons at each site are also given.

Age-at-death could be estimated for 183 individuals. To facilitate clarity and acknowledge that there is an inherent uncertainty associated with estimates of dental and skeletal age, estimates were used to place individuals into five-year age categories (Figure 8.3). This revealed a bimodal mortality distribution. The first, and highest, peak was

among skeletally immature individuals between 5.1-20.0 years and the second in mature individuals aged between 50.1-60.0 years. As highlighted previously (Section 5.6), these age distributions underrepresented perinates/infants and older individuals.

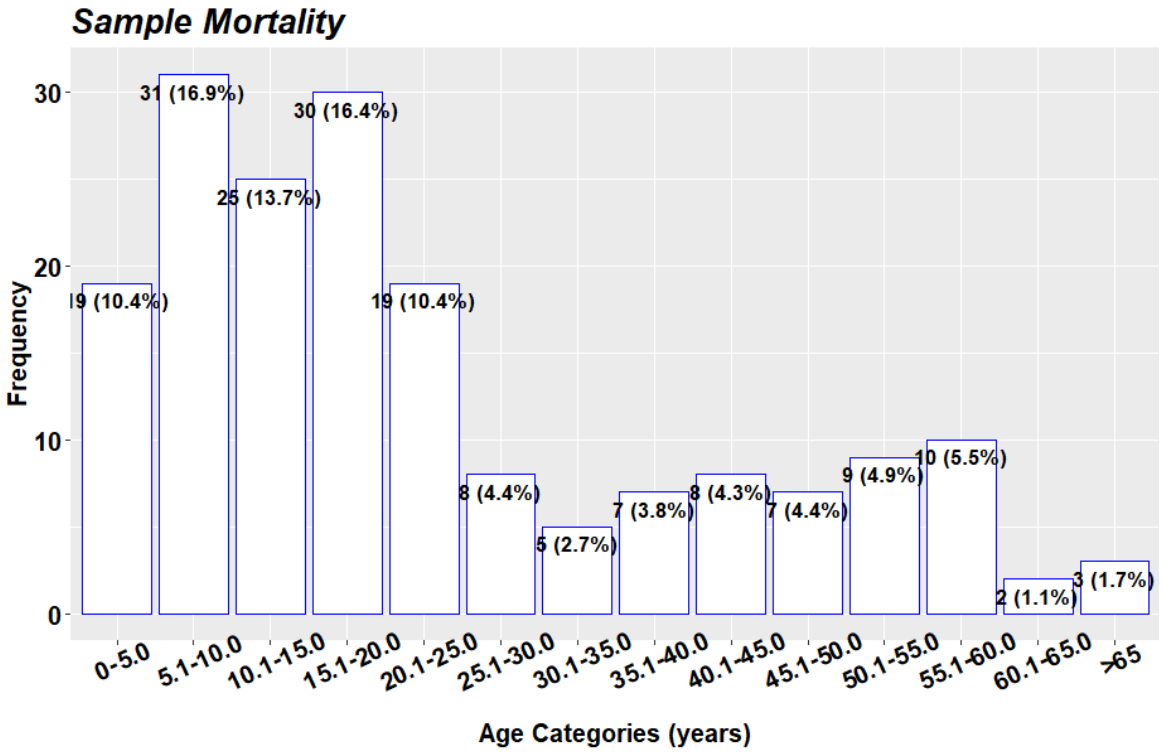

Figure 8.3 Mortality profile of the overall sample after age-at-death estimates were aggregated into five-year age categories. Tabulated frequencies can be found in Appendix 2.

Variations to the mortality distribution were evident when sites and sexes were compared. For example, the peak in immature mortality was more pronounced in the Warwick sample, in which 13 (52.0%) individuals were estimated to have died between 5.1-10.0 years of age. In contrast, in the South Shields and York Barbican assemblages, the peak in mortality among immature skeletons was later (i.e., it occurred in the 15.1-20.0 year category rather than the 5.1-10 or 10.1-15.0 year categories) (Figure 8.4). Meanwhile, the distinction between earlier and later peaks in mortality was less visible in the skeletons from the Black Gate assemblage. In summary, although sampling strategy may have affected assemblage representation, the general mortality patterns conformed to expectations (Gowland and Chamberlain 2005: 146). Subtle between-site variations did,

however, suggest that site-specific influences could have impacted mortality and length of life.

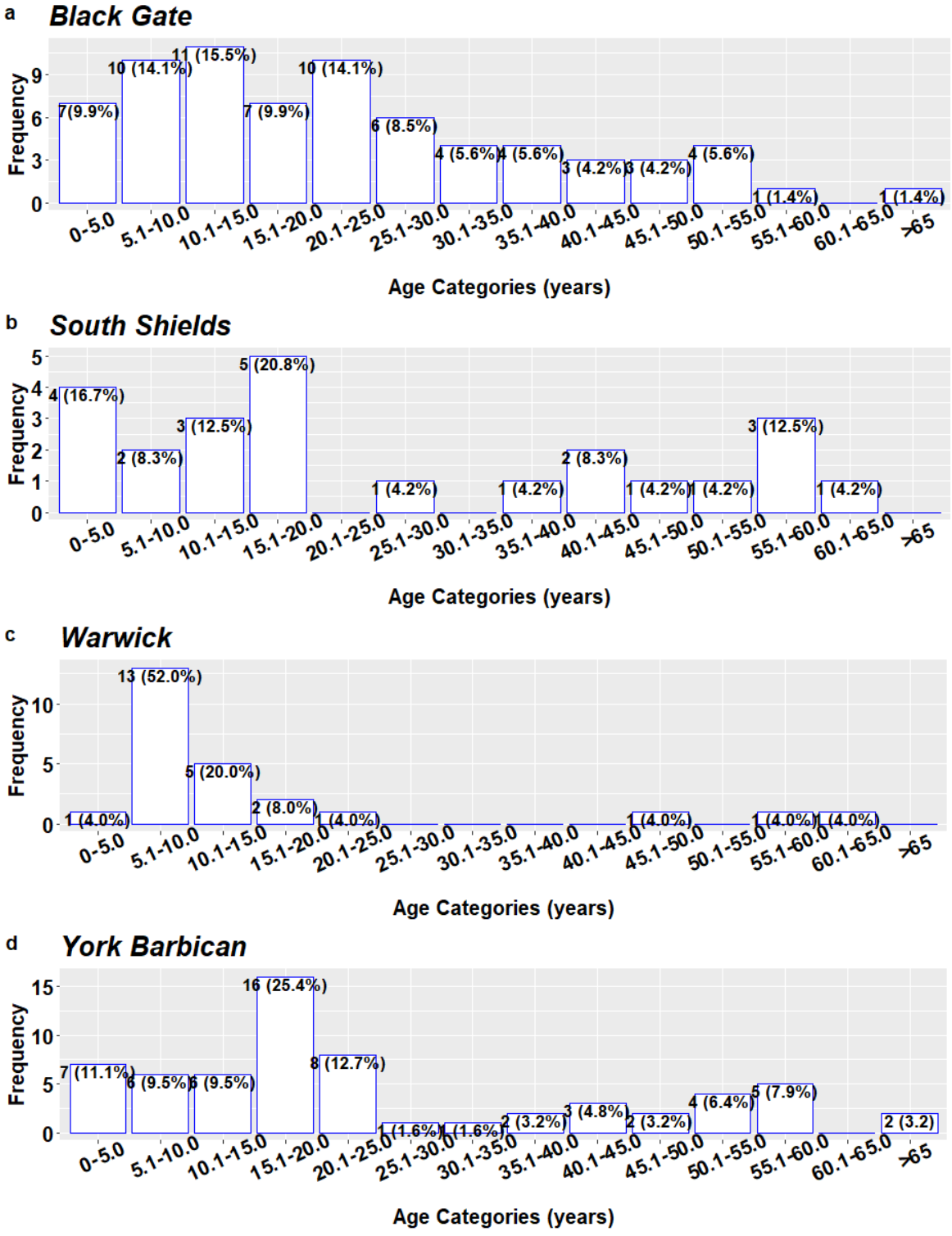

Figure 8.4 Mortality profiles associated with Black Gate (a), South Shields (b), Warwick (c) and the York Barbican (d). Tabulated frequencies can be found in Appendix 2.

Among the mature skeletons for whom sex could be estimated, there was an increased risk of mortality between the fiftieth and sixtieth years. For males the most dramatic peak in mortality, however, occurred between 20.1-25.0 years with 10 (25.6%) males – 6 of whom come from the Black Gate collection – falling into this age category. In comparison, the highest frequency of females – 7 (23.3%) – were to be found in the 55.1-60.0 years category (Figure 8.5). Again, the general pattern (i.e., increasing mortality risk in later maturity) is consistent with expectations (Gowland and Chamberlain 2005: 146). However, the noticeable difference between females and males in early adulthood suggested that 1) sampling biases may have skewed normal mortality patterns (i.e., higher female mortality during reproductive years) and 2) that sex-related differentials in life expectancy needed to be explored further.

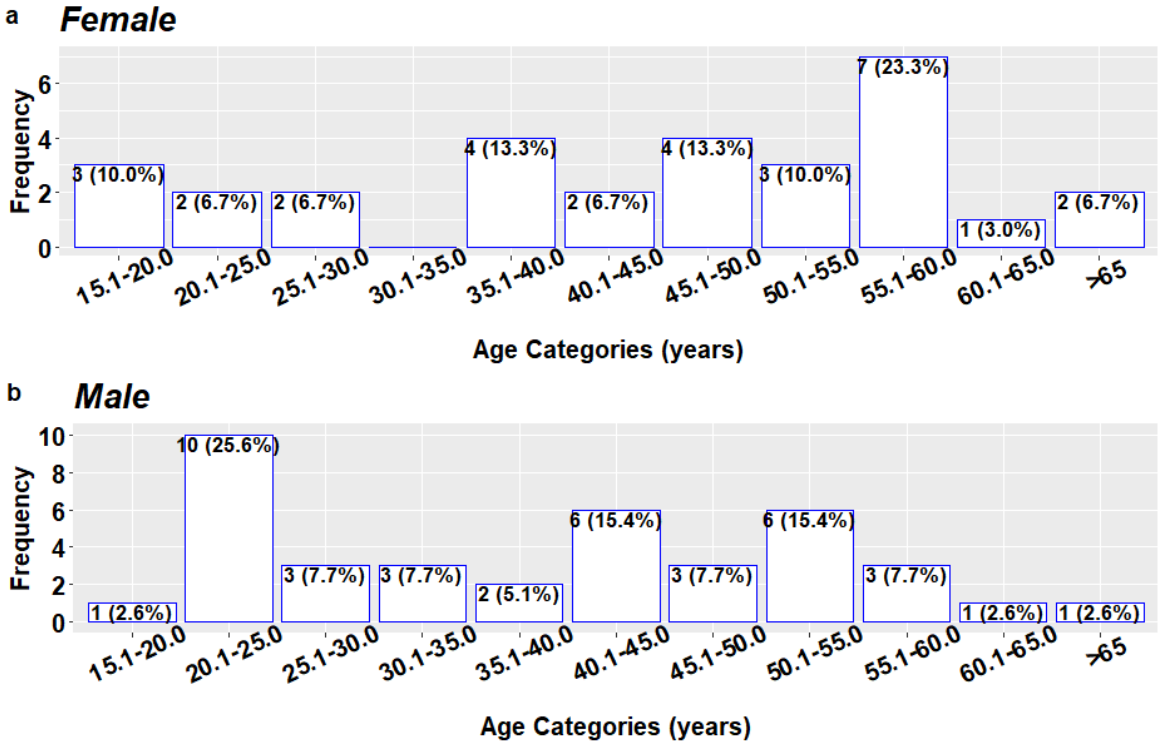

Figure 8.5 Mortality profiles associated females (a) and males (b). Tabulated frequencies can be found in Appendix 2.

8.2.2 Skeletal Proxies for Growth and Development

Seventy-three mature skeletons had measurable long bones. The humerus was the best represented element with 58 skeletons having either one or both humeri. Femora and tibiae were somewhat less common and measurements could only be taken from 42 and 40 skeletons respectively. Thirty-eight individuals produced radial measurements while 33 had ulnar. Just 14 mature skeletons had complete fibulae. For the sake of brevity, the key patterns identified in these measurements are described here with support from selected figures, while full tabulated summaries and further illustrations are provided in Appendix 2.

As expected, females had shorter bones than males. Although subtle differences between sites were observed, it was noted that when long bone lengths were contrasted between sites, points of central tendency were close and interquartile ranges generally overlapped. Furthermore, when lengths were compared with reference to site and sex at the same time, it was found that sex biases contributed to the differences observed between sites. For example, although humeri were on average longer at South Shields, of the eight individuals from the site with humeral measurements, six were males (Figure 8.6). In sum, sexual dimorphism appeared to be the most influential factor in the lengths of mature long bones and differences attributable to other factors were likely to be small in comparison.

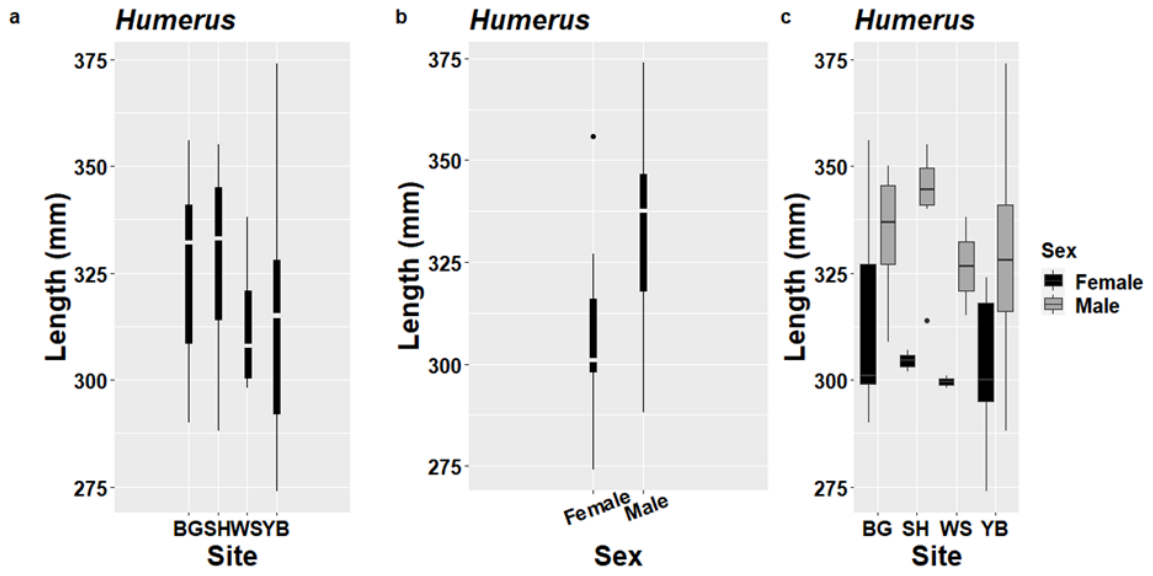

Figure 8.6 Boxplots comparing humeral measurements between sites (a), females and males (b) and with reference to both factors (c).

There was a strong relationship between age and variables representing growth and development in skeletally immature individuals. Diaphyseal lengths, for instance, increased with estimated age (Figure 8.7). Similarly, for the 41 individuals for whom puberty could be assessed, pubertal tempo appeared age-dependent. Interestingly, a large proportion of immature individuals (45.6%) with an estimate of pubertal stage perished during PHV, the period when developmental changes occur at an increasingly rapid rate with secondary sexual characteristics and dimorphism becoming more pronounced (Lewis 2020; Lewis *et al.* 2016: 51). It was also observed that for some, maturity was delayed. SK 268 from the Black Gate collection, for instance, was allocated to Stage 3 (as their iliac crest and distal ulna were unfused) even though, with an ADBOU age estimate of 21.0 years (95% CI [15.1, 29.0]), they were likely in their early twenties and the stage's mean age was notably lower (14.9 years) (Table 8.1). Consequently, it was hypothesised that factors other than age were influencing growth and development and that passage through PHV (Stage 3) was possibly a critical biological threshold.

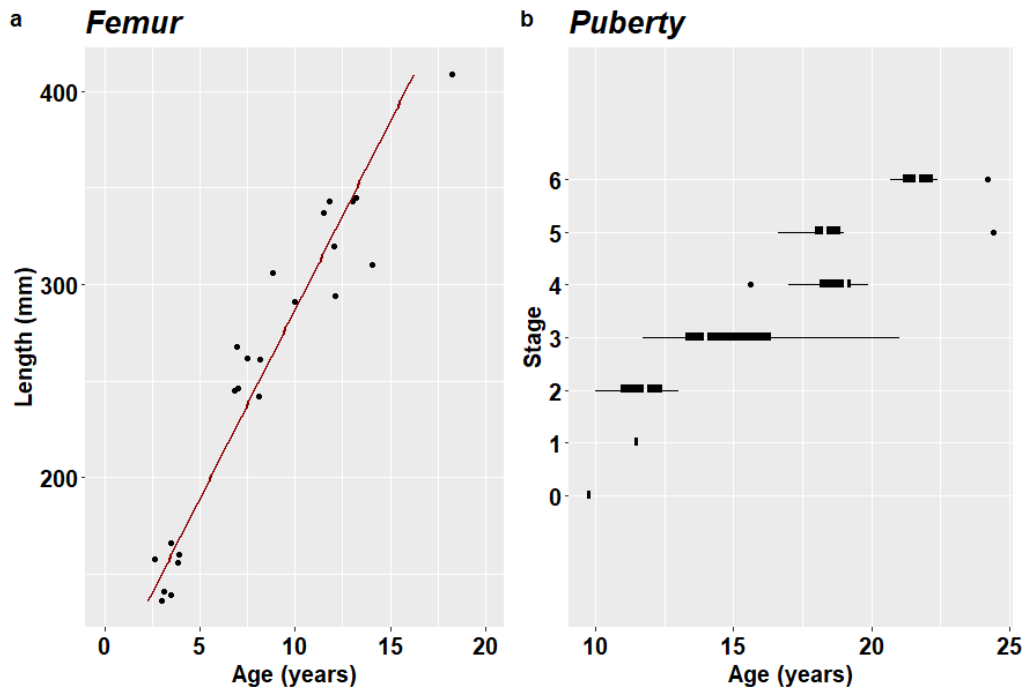

Figure 8.7 A scatterplot comparing femoral diaphyseal length (see Appendix 2 for other elements) and estimated age (a). Boxplot demonstrating the age-related patterns in pubertal development (b).

Stage	No.	Mature/Immature	Min Age	Mean Age	Max Age	Std dev Age
0	1	0/1	9.79	9.79	9.79	NA
1	1	0/1	11.5	11.5	11.5	NA
2	3	0/3	10.0	11.6	13.0	1.5
3	15	0/15	11.7	14.9	21.0	2.7
4	9	2/7	15.6	18.9	22.2	1.8
5	6	5/1	16.6	19.1	24.4	2.7
6	6	6/0	20.7	21.8	24.2	1.3

Table 8.1 Age-related trends in pubertal tempo (age in years).

8.2.3 Pathology

8.2.3.1 Linear Enamel Hypoplasia: Childhood Stress

Every skeleton in the sample (217) could be assessed for LEH and in total 4,033 teeth were observed. One hundred and forty-three (CPR=65.9%) skeletons had one or more LEH, while 631 (TPR=15.7%) teeth were affected. LEH could be chronologically matched across teeth in 112 (CPR=51.6%) individuals and, with some skeletons exhibiting multiple matched defects, 187 matched defects were recorded. When the frequency of matched LEH was tabulated for age categories, a dramatic increase in incidence was found to have occurred after 1.0-1.9 years, suggesting individuals were

buffered until that point, after which they experienced an increased volume or intensity of stress episodes which later declined around the fifth year of life (Figure 8.8).

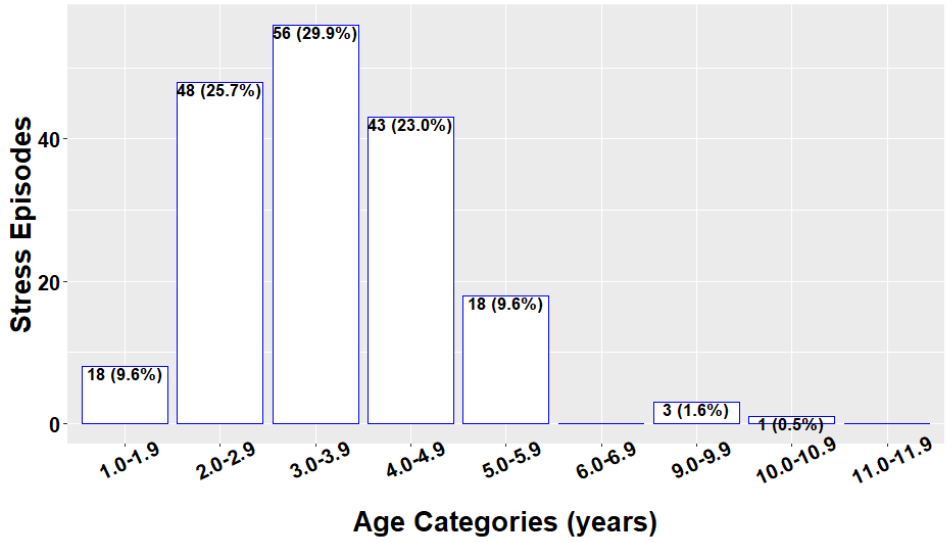

Figure 8.8 With defects matched across multiple teeth, it was possible to infer stress episodes at specific periods. This bar graph gives the frequency and percentage of episodes attributed to each age category.

Between-site differences were detected in LEH prevalence (Figure 8.9). Only 13 (CPR=39.4%) skeletons and 37 (TPR=7.0%) teeth from South Shields were affected, while there was a crude prevalence of 70.0-74.0% in the Black Gate, Warwick and York Barbican samples. Despite similarities in crude prevalence (i.e., percentage of skeletons affected) to Black Gate and York Barbican, it was noted however that there was a higher true prevalence of LEH in the Warwick sample with 118 (TPR=22.1%) teeth affected (Table 8.2). There was also a higher percentage of individuals from Warwick with chronologically matched LEH (Table 8.4). When the timing of matched defects was contrasted between sites, the increase in frequency after 1.0-1.9 years was most apparent in the Warwick sample, but less pronounced in the York Barbican skeletons (Figure 8.10). Given the association of LEH with childhood adversity, it was hypothesised that significant differences in stress experience during this period were shaped by site-specific influences.

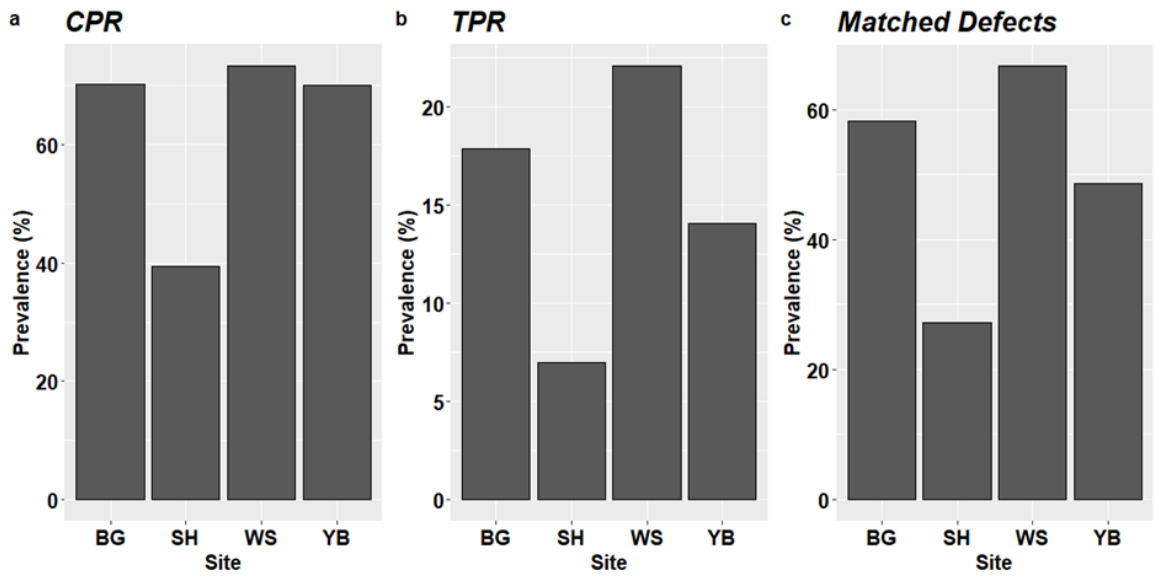

Figure 8.9 A between-site comparison of LEH crude (a) and true (b) prevalence rates as well as the prevalence of matched LEH (c).

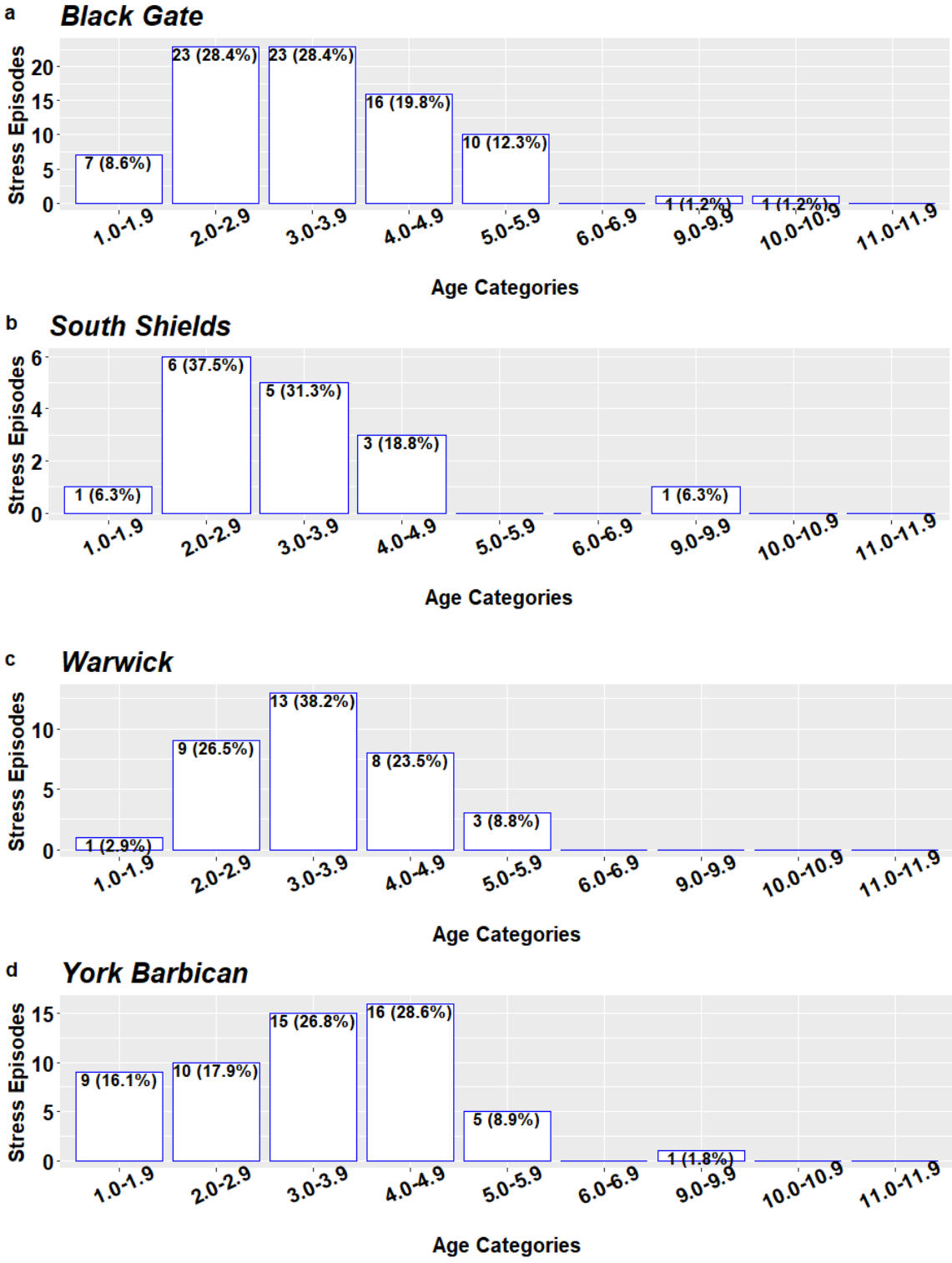

Figure 8.10 The distribution of stress episodes across age categories inferred through matched LEH in the Black Gate (a), South Shields (b), Warwick (c) and York Barbican (d) assemblages.

Site	LEH Absent (CPR)	LEH Present (CPR)	Total
BG	20 (29.8%)	59 (70.2%)	84
SH	20 (60.6%)	13 (39.4%)	33
WS	8 (26.7%)	22 (73.3%)	30
YB	21 (30.0%)	49 (70.0%)	70

Table 8.2 Frequency of skeletons with LEH by site.

Site	LEH Absent (TPR)	LEH Present (TPR)	Total
BG	1228 (82.1%)	268 (17.9%)	1496
SH	493 (93.0%)	37 (7.0%)	530
WS	416 (77.9%)	118 (22.1%)	559
YB	1265 (85.9%)	208 (14.1%)	1503

Table 8.3 Frequency of teeth with LEH by site.

Site	Matched Defect Absent (CPR)	Matched Defect Present (CPR)	Total
BG	35 (41.7%)	49 (58.3%)	84
SH	24 (72.7%)	9 (27.3%)	33
WS	10 (33.3%)	20 (66.7%)	30
YB	36 (51.4%)	34 (48.6%)	70

Table 8.4 Frequency of skeletons with chronologically matched LEH by site.

When sexes were compared, males had higher prevalence rates of LEH than females (Figure 8.11). Among the 49 male skeletons, 40 (CPR=81.6%) had LEH compared to 25 (CPR=69.4%) out of 36 females. Similarly, of the 1,123 teeth associated with male skeletons, 209 (TPR=18.6%) had observable LEH, while only 101 (TPR=12.3%) of the 819 teeth from females did. A greater number of males also had chronologically matched LEH; 36 (CPR=71.4%) males were affected, compared to 18 (CPR=50.0%) females. However, a smaller proportion of the male skeletons developed matched LEH in the youngest age category (1-1.9 years) (Figure 8.12). The consistently higher prevalence of LEH among males suggested substantial differentials in frailty during childhood attributable to sex.

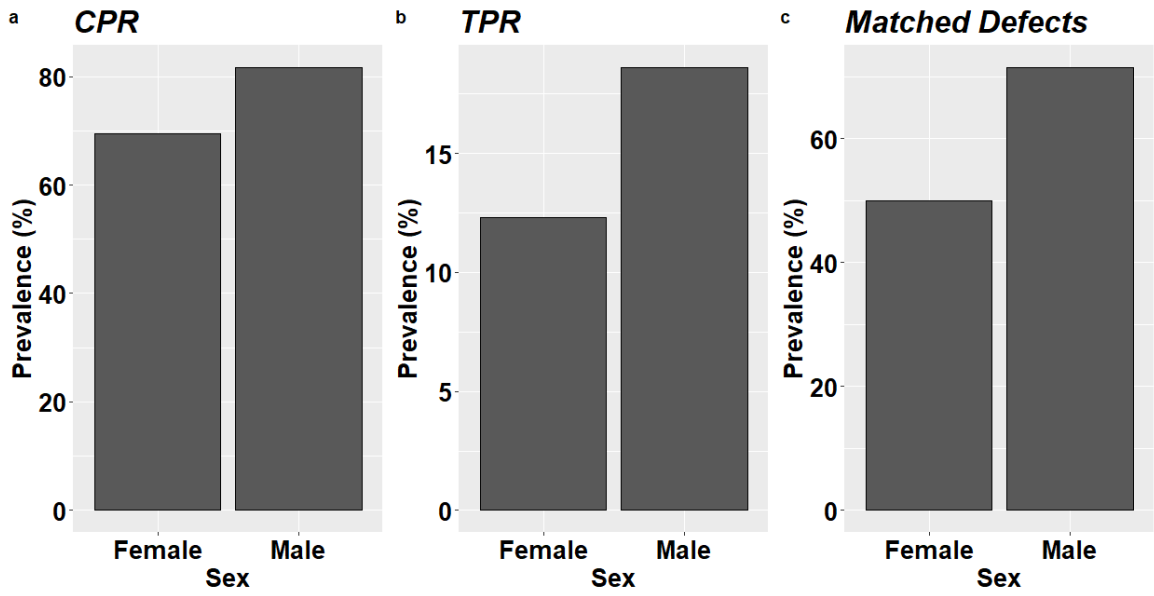

Figure 8.11 A comparison of LEH crude (a) and true (b) prevalence as well as the prevalence of chronologically matched LEH (c) between females and males.

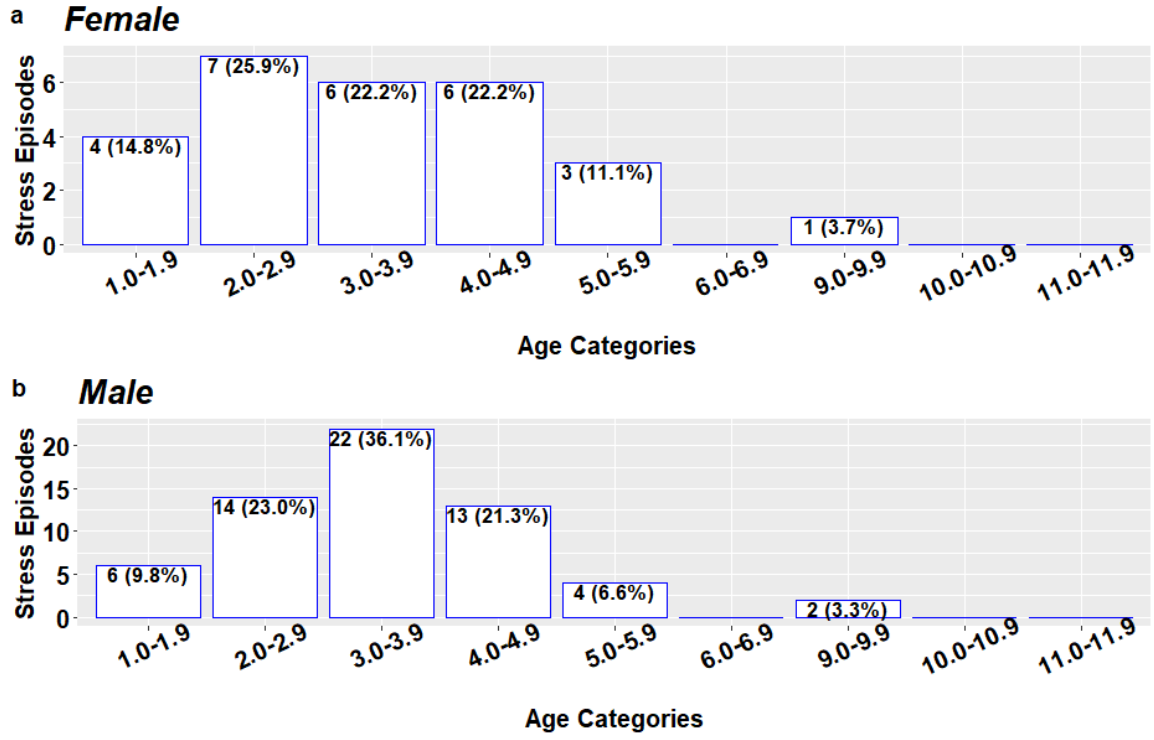

Figure 8.12 The distribution of stress episodes across age categories inferred through matched LEH in females (a) and males (b).

Disparities in prevalence rates between mature and immature skeletons were ambiguous. In total, 112 mature and 104 immature skeletons, associated with 2,495 and 1,534 teeth respectively, were assessed. With 81 (CPR=72.3%) mature skeletons

exhibiting LEH compared to 61 (CPR=58.6%) immature, there was a higher proportion of mature individuals with LEH. Similarly, a greater number of mature individuals had chronologically matched LEH; 62 (CPR=55.4%) mature skeletons were affected while only 49 (CPR=47.1%) immature were. Nonetheless, more teeth from immature skeletons had LEH; 356 (TPR=14.3%) teeth from mature skeletons had LEH while 273 (TPR=17.7%) teeth from immature individuals were affected. This suggested a complicated relationship between childhood stress, resilience and development/survival. Despite these differences, the chronological occurrence of the stress episodes inferred through matched LEH was not dissimilar between groups (Figure 8.13), both of which followed the more general pattern described previously.

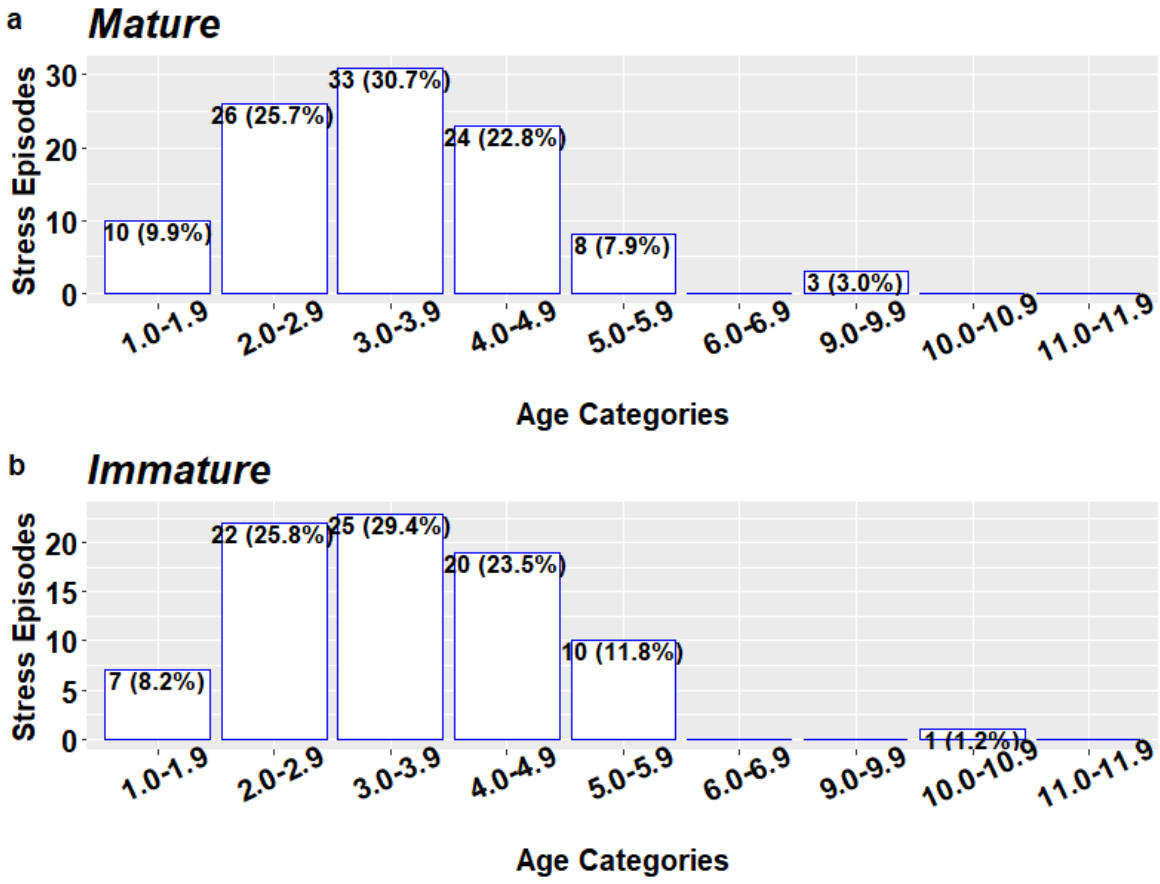

Figure 8.13 The distribution of stress episodes across age categories inferred through matched LEH in mature (a) and immature groups (b).

8.2.3.2 Cribra Orbitalia

One hundred and sixty-eight skeletons had observable orbits. Of these, 89 (CPR=53.0%) had CO. The true prevalence rate was similar, with 147 (TPR=49.0%) of 300 orbits affected, indicating that most lesions were bilateral. Among the individuals with CO, 64 (CPR=71.9%) had lesions with an inactive/healed appearance (i.e., pores were rounded), while 25 (CPR=28.1%) had lesions likely associated with an active or mixed process (i.e., sharp-edged pores were present). Thus, for most individuals CO was not likely associated with an active pathological disruption to normal bone formation/maintenance.

Substantial between-groups differences were noted in the prevalence and nature of CO. With 14 (CPR=60.9%) and 34 (CPR=65.4%) individuals exhibiting CO respectively, the Warwick and York Barbican assemblages had much higher prevalence rates than Black Gate and South Shields (Table 8.5 and Figure 8.14). The most severe CO was also seen in the skeletons from Warwick and York Barbican (Table 8.6). When mature and immature individuals were compared, severity was comparable between groups but differences in prevalence rates and lesion activity were notable. From the 92 mature skeletons with observable orbits, 32 (CPR=34.8%) had CO but only four of these (CPR=12.5%) had active/mixed lesions. Meanwhile, CO was far more common in the skeletally immature cohort; of the 76 skeletons with assessable orbits, 57 (CPR=75.0%) had CO, 21 of whom (CPR=36.8%) had active lesions (Figure 8.15). It was, as such, surmised that site-specific influences and age-related susceptibility affected vulnerability to metabolic deficiency and that, in addition to prevalence, severity and activity are informative when attempting to identify factors associated with CO development.

Site	CO Absent (CPR)	CO Present (CPR)	Total
BG	37 (52.9%)	33 (47.1%)	70
SH	15 (65.2%)	8 (34.8%)	23
WS	9 (39.1%)	14 (60.9%)	23
YB	18 (34.6%)	34 (65.4%)	52

Table 8.5 Frequency of skeletons with CO by site.

Site	Grade 1 CO (CPR)	Grade 2 CO (CPR)	Total
BG	16 (48.5%)	17 (51.5%)	33
SH	7 (87.5%)	1 (12.5%)	8
WS	8 (57.1%)	6 (42.9%)	14
YB	16 (47.1%)	18 (52.9%)	34

Table 8.6 Severity of lesions in skeletons with CO.

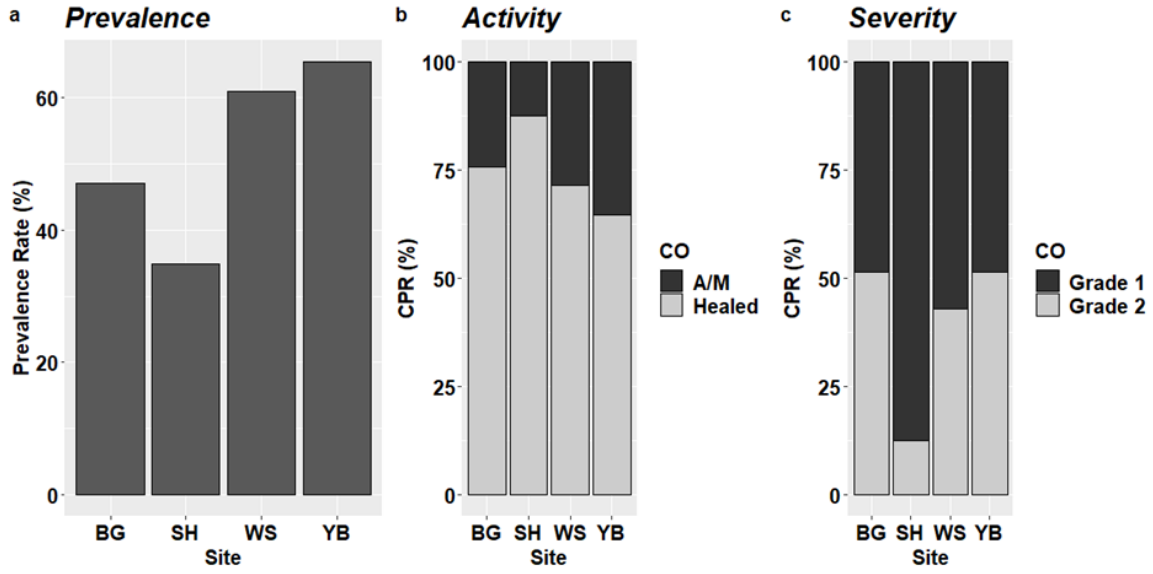

Figure 8.14 A comparison of crude prevalence rates between sites (a) and, among the individuals with CO, the proportion of active/mixed (A/M) and healed lesions (b) as well as the severity of lesions (c).

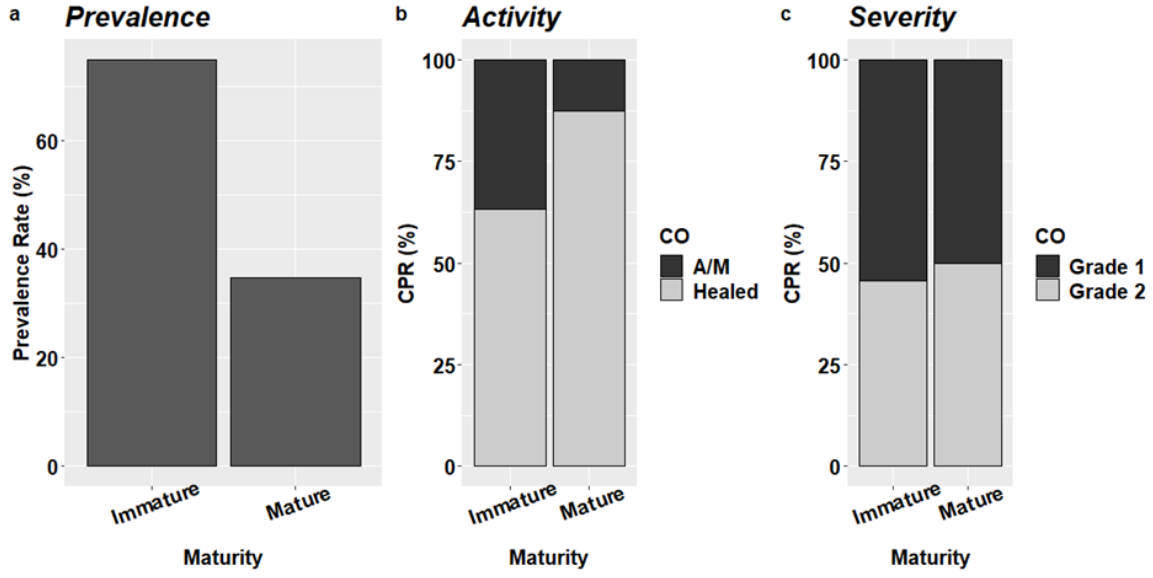

Figure 8.15 A comparison of crude prevalence rates between skeletally immature and mature individuals (a) and, among the individuals with CO, the proportion of active/mixed (A/M) and healed lesions (b) as well as the severity of lesions (c).

8.2.3.3 Periodontal Disease

All skeletons in the sample (217) could be assessed for PD and in total the alveolar regions associated with 1,018 molars were observed. Ninety-seven (CPR=44.7%) individuals exhibited some degree of alveolar degeneration indicative of PD and 377 (TPR=37.0%) tooth sockets were affected. Of the 97 skeletons with PD, 76 (CPR=78.3%) manifested the mildest markers of pathological degeneration (i.e., a blunt and flat-topped alveolar margin with a slightly raised rim), 19 (CPR=19.6%) had moderate signs, and only two (CPR=2.1%) were affected by the most severe osteological indicators.

A subtle site-related pattern was noted in the prevalence of PD (Figure 8.16). There was a higher prevalence of PD at South Shields, for example, with 17 (CPR=51.5%) skeletons and 87 (TPR=51.5%) alveolar sockets affected (Table 8.7-Table 8.8). When considering severity, however, site differences were more pronounced. South Shields stood out as the only site where most skeletons with PD had moderate-to-severe, rather than mild, signs of the condition (Table 8.9). By contrast, there was little difference in the crude prevalence of PD between females and males, with the condition being common for both sexes. From the 36 females associated with 232 alveolar sockets, 28 (CPR=77.8%) skeletons and 138 (TPR=59.5%) sockets were afflicted. Similarly, PD affected 149 (TPR=50.0%) alveolar sockets from 39 (CPR=79.6%) males out of a potential 49 skeletons with 298 assessable sockets. The severity of expression was also generally similar between sexes, with mild cases being far more common, with the only real difference being that two (CPR=5.1%) males had severe PD while no females expressed such advanced alveolar degeneration (Table 8.10). In sum, differences between sites appeared more important in PD prevalence than sex differentials. It was also

speculated that when determining the influence of other factors on PD development, severity of expression may be a more sensitive indicator than presence/absence.

Site	PD Absent (CPR)	PD Present (CPR)	Total
BG	46 (55.9%)	38 (46.1%)	84
SH	16 (48.5%)	17 (51.5%)	33
WS	19 (63.3%)	11 (36.7%)	30
YB	39 (55.7%)	31 (44.3%)	70

Table 8.7 Frequency of skeletons with PD absent and present by site.

Site	PD Absent (TPR)	PD Present (TPR)	Total
BG	226 (65.9%)	117 (34.1%)	343
SH	82 (48.5%)	87 (51.5%)	169
WS	72 (60.0%)	48 (40.0%)	120
YB	261 (67.6%)	125 (32.4%)	386

Table 8.8 Frequency of teeth with surrounding alveolar bone with PD by site.

Site	Mild PD (CPR)	Moderate PD (CPR)	Severe PD (CPR)	Total
BG	33 (86.8%)	5 (13.6%)	0 (0.0%)	38
SH	7 (41.2%)	9 (52.9%)	1 (5.9%)	17
WS	9 (81.8%)	2 (18.2%)	0 (0.0%)	11
YB	27 (87.1%)	3 (9.7%)	1 (3.2%)	31

Table 8.9 Severity of lesions in skeletons with PD.

Site	Mild PD (CPR)	Moderate PD (CPR)	Severe PD (CPR)	Total
Female	22 (78.6%)	6 (21.4%)	0 (0.0%)	28
Male	28 (71.8%)	9 (23.1%)	2 (5.1%)	39

Table 8.10 Severity of lesions in females and males with PD.

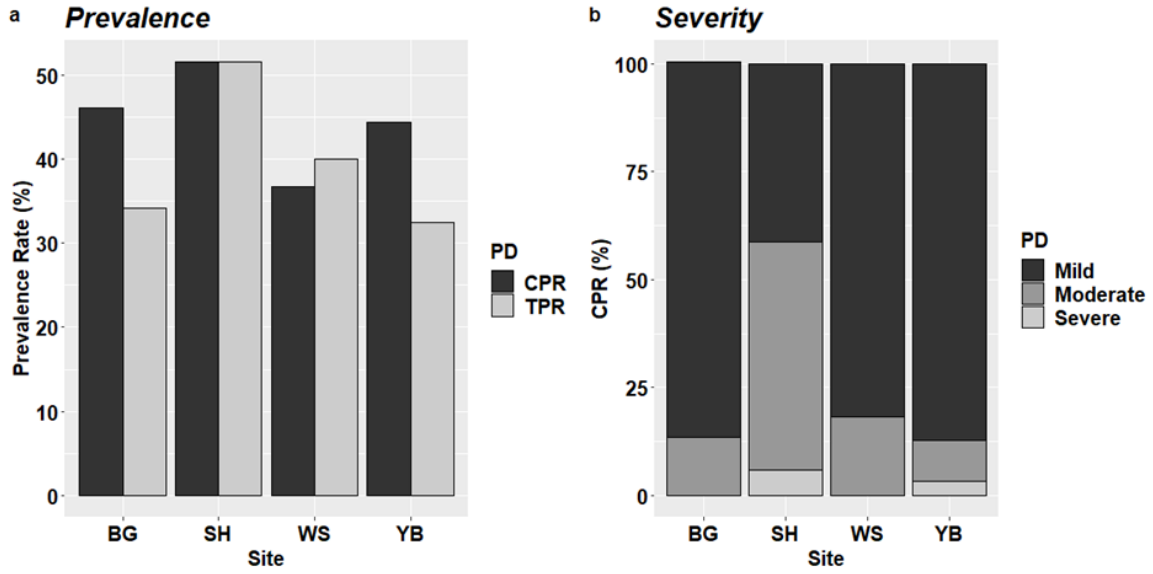

Figure 8.16 A comparison of crude and true prevalence rates between sites (a) as well as severity in the individuals with PD (b).

Emphatic differences in the prevalence of PD were observed between skeletally immature and mature individuals (Figure 8.17). Observations could be taken from the alveolar regions surrounding 677 molars in 112 skeletally mature individuals. Of these, 82 (CPR=73.2%) had PD and the bone surrounding 340 (TPR=50.2%) molars was affected. The alveolar bone surrounding 341 molars from 104 skeletally immature individuals was also assessed. In contrast to the mature cohort, where most skeletons had PD, only 15 (CPR=14.4%) immature skeletons and the alveolar crests surrounding 37 molars (TPR=10.9%) showed evidence of PD. Additionally, except for one individual with moderate PD (CPR=6.7%), all immature skeletons with PD exhibited mild signs of the condition. By comparison, a larger number of the mature skeletons with PD had moderate-to-severe signs of PD; 18 (CPR=21.9%) had moderate and two (CPR=2.4%) severe. PD therefore showed strong age-related trends with the condition becoming more common and more severe with advancing age.

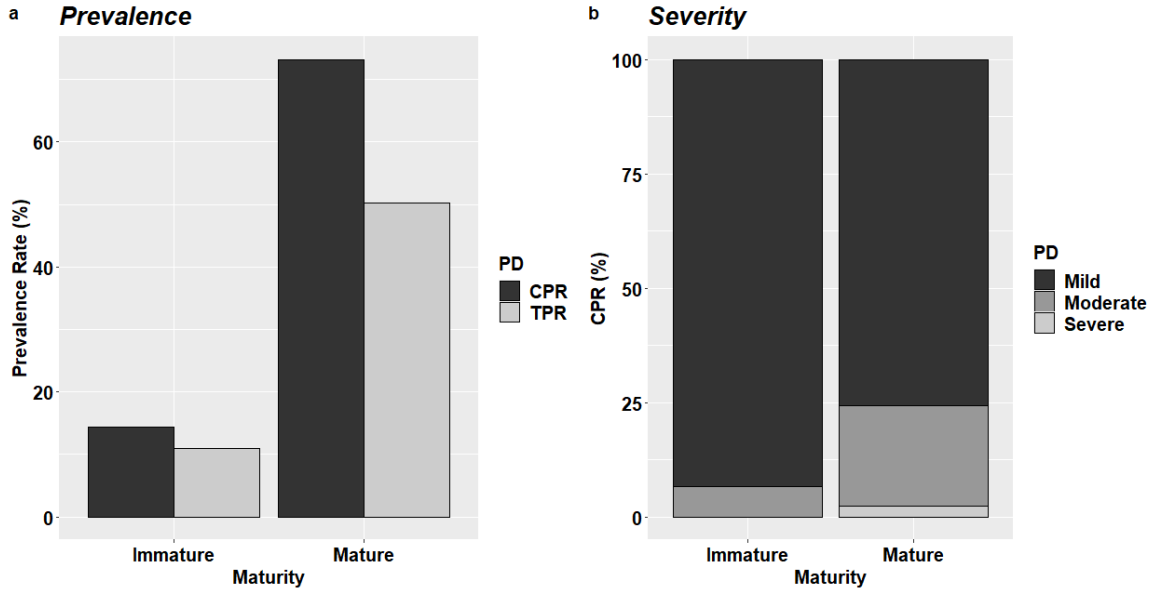

Figure 8.17 A comparison of crude and true prevalence rates between mature and immature skeletons (a) as well as severity in the individuals with PD (b).

8.2.3.4 Periosteal New Bone Formation

It was possible to assess the presence and absence of PNBF in 199 individual skeletons and 1,489 skeletal elements (long bones and skulls). Fifty-six (CPR=28.1%) skeletons and 157 bones (TPR=10.5%) exhibited plaques of PNBF. Of the individuals with PNBF, 38 (CPR=67.9%) had lesions with an active or mixed appearance, while 18 (CPR=32.1%) had inactive/healed lesions. There was a higher frequency of less well-developed lesions; 40 (CPR=71.4%) individuals had Grade 1 PNBF, 12 (CPR=21.4%) had Grade 2, while three (CPR=5.4%) had Grade 3 lesions and one (CPR=1.8%) had Grade 4. In 46 cases it could be determined whether PNBF was distributed unilaterally or bilaterally; in 34 (CPR=73.9%) individuals, lesions were observed bilaterally.

Differences in the prevalence and nature of PNBF were noted between sites (Figure 8.18). For instance, with 28 (CPR=41.2%) individuals affected, York Barbican had the highest crude prevalence of PNBF (Table 8.11). However, with only 12 (CPR=57.1%) individuals expressing lesions bilaterally, a mere 63 (TPR=12.5%) bones were affected and the true prevalence of PNBF among the York Barbican assemblage was not as extreme as the crude rate might have implied (Table 8.12). Moreover, among the individuals with PNBF, the skeletons from York Barbican generally had relatively mild periosteal reactions that were more likely to be inactive than at other sites; for example, 22 (CPR=78.5%) skeletons had Grade 1 PNBF, and only a small minority had more severe lesions (Table 8.13-Table 8.14). In contrast, although the crude prevalence of PNBF among the Warwick skeletons was lower, the site was associated with the highest true prevalence rate with 27 (TPR=16.1%) out of 168 bones affected. Additionally, with five (CPR=83.3%) out of six individuals with active or mixed reactions the assemblage had a relatively low rate of healed lesions and all the Warwick skeletons with PNBF

expressed it bilaterally (Table 8.15). The data therefore inferred site-specific influences affected susceptibility to PNBF and lesion development.

Site	PNBF Absent (CPR)	PNBF Present (CPR)	Total
BG	63 (80.8%)	15 (19.2%)	78
SH	21 (75.0%)	7 (25.0%)	28
WS	19 (76.0%)	6 (24.0%)	25
YB	40 (58.8%)	28 (41.2%)	68

Table 8.11 Frequency of skeletons with PNBF absent and present by site.

Site	PNBF Absent (TPR)	PNBF Present (TPR)	Total
BG	592 (92.8%)	49 (7.2%)	641
SH	159 (89.8%)	18 (10.2%)	177
WS	141 (83.9%)	27 (16.1%)	168
YB	440 (87.5%)	63 (12.5%)	503

Table 8.12 Frequency of bones with PNBF absent and present by site.

Site	Grade 1 (CPR)	Grade 2 (CPR)	Grade 3 (CPR)	Grade 4 (CPR)	Total
BG	10 (66.6%)	4 (26.7%)	1 (6.7%)	0 (0.0%)	15
SH	4 (57.1%)	1 (14.3%)	1 (14.3%)	1 (14.3%)	7
WS	4 (66.6%)	2 (34.4%)	0 (0.0%)	0 (0.0%)	6
YB	22 (78.5%)	5 (17.9%)	1 (3.6%)	0 (0.0%)	28

Table 8.13 Severity of lesions in skeletons with PNBF.

Site	Healed PNBF (CPR)	Active/Mixed (CPR)	Total
BG	6 (40.0%)	9 (60.0%)	15
SH	1 (14.3%)	6 (85.7%)	7
WS	1 (16.7%)	5 (83.3%)	6
YB	10 (35.7%)	18 (64.3%)	28

Table 8.14 Frequency of skeletons with PNBF that had active/mixed lesions compared to healed by site.

Site	PNBF Unilateral (CPR)	PNBF Bilateral (CPR)	Totalal
BG	2 (14.3%)	12 (85.7%)	14
SH	1 (20.0%)	4 (80.0%)	5
WS	0 (0.0%)	6 (100.0%)	6
YB	9 (42.9%)	12 (57.1%)	21

Table 8.15 Frequency of skeletons with PNBF that had unilateral and bilateral lesions by site.

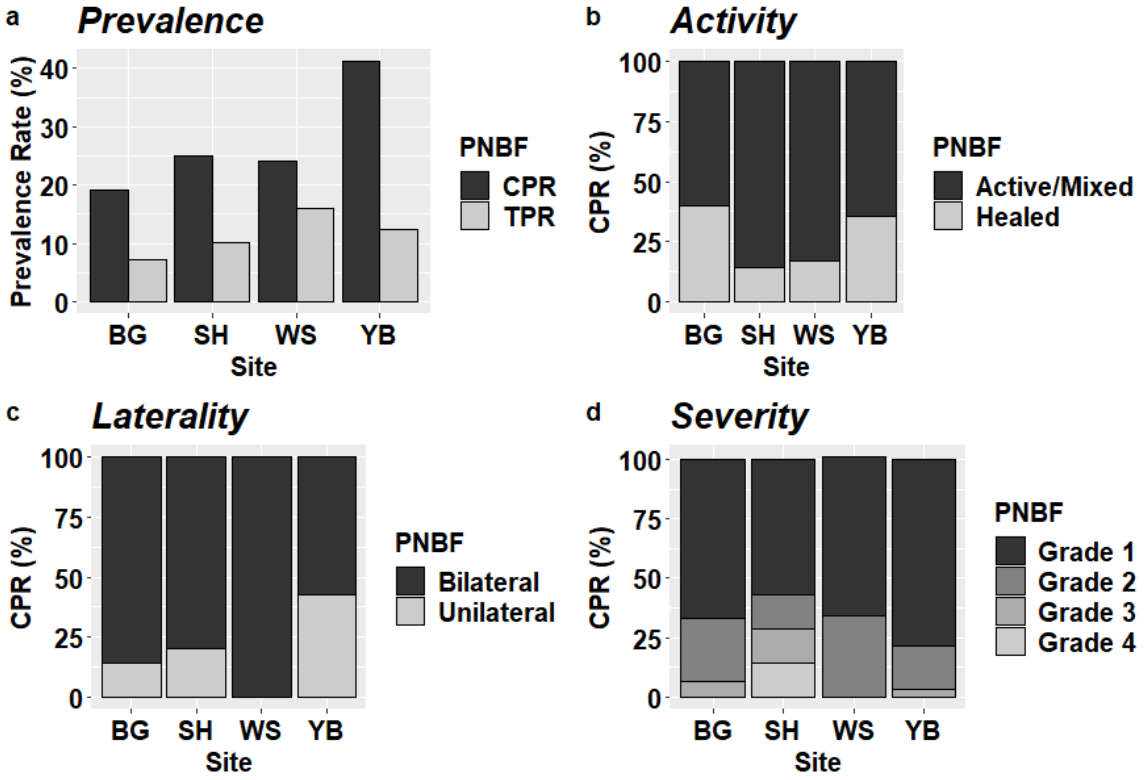

Figure 8.18 A comparison of crude and true prevalence rates between sites (a) as well as the activity (b), distribution (c) and severity (d) of PNBF in those individuals with lesions.

Differences between sexes in PNBF prevalence were varied. For example, although nine (CPR=25.7%) of a possible 35 females were affected compared to 18 (CPR=40.0%) of 45 males, true prevalence rates were near-equal. Specifically, of the 300 bones (i.e., long bones and skulls) from female skeletons, 33 (TPR=11.0%) were affected, while of the 404 bones from males, 53 (TPR=13.1%) exhibited PNBF. Moreover, it was not possible to discern whether the sex differences in the rates of active and severe PNBF were meaningful or an artefact of sample size (Table 8.16-Table 8.17).

Sex	Healed PNBF (CPR)	Active/Mixed (CPR)	Total
Female	3 (34.4%)	6 (66.6%)	9
Male	9 (50.0%)	9 (50.0%)	18

Table 8.16 Frequency of skeletons with PNBF that had active/mixed lesions compared to healed by sex.

Sex	Grade 1 (CPR)	Grade 2 (CPR)	Grade 3 (CPR)	Grade 4 (CPR)	Total
Female	6 (66.7%)	2 (22.2%)	1 (11.1%)	0 (0.0%)	9
Male	10 (55.6%)	6 (33.3%)	2 (11.1%)	0 (0.0%)	18

Table 8.17 Severity of lesions in skeletons with PNBF by sex.

Differences in PNBF prevalence between mature and immature skeletons were complicated. That is, although true prevalence rates were close to identical, there was a moderately higher crude prevalence of PNBF among mature individuals. Specifically, 102 skeletally mature individuals with a total of 875 bones could be assessed for PNBF, with 92 (TPR=10.5%) bones and 32 (CPR=30.4%) skeletons exhibiting lesions. Meanwhile, even though 63 (TPR=10.6%) bones out of 614 from immature skeletons were affected, only 25 (CPR=25.8%) individuals from 97 were recorded with PNBF. Between-group disparities of varying magnitude emerged when lesion patterning was contrasted between individuals with PNBF (Figure 8.19). For instance, although active lesions were common in both cohorts, 22 (CPR=88.0%) immature skeletons with PNBF had active/mixed lesions compared to 16 (CPR=51.6%) mature skeletons. A moderately higher proportion of immature individuals with PNBF also had bilateral lesions. From the 17 immature and 29 mature skeletons where lesion distribution was assessable, 14 (CPR=82.3%) immature individuals had bilateral PNBF in comparison to 20 (CPR=69.0%) mature skeletons. The severity of lesions was, however, generally greater in skeletally mature individuals (Table 8.18). It was thus believed that aside from age-related trends, the impact of factors on PNBF development may become more obvious when the severity, distribution and activity of lesions are considered.

Maturity	Grade 1 (CPR)	Grade 2 (CPR)	Grade 3 (CPR)	Grade 4 (CPR)	Total
Mature	20 (64.5%)	8 (25.8%)	3 (9.7%)	0 (0.0%)	31
Immature	20 (80.0%)	4 (16.0%)	0 (0.0%)	1 (4.0%)	25

Table 8.18 Severity of lesions in skeletally mature and immature individuals with PNBF.

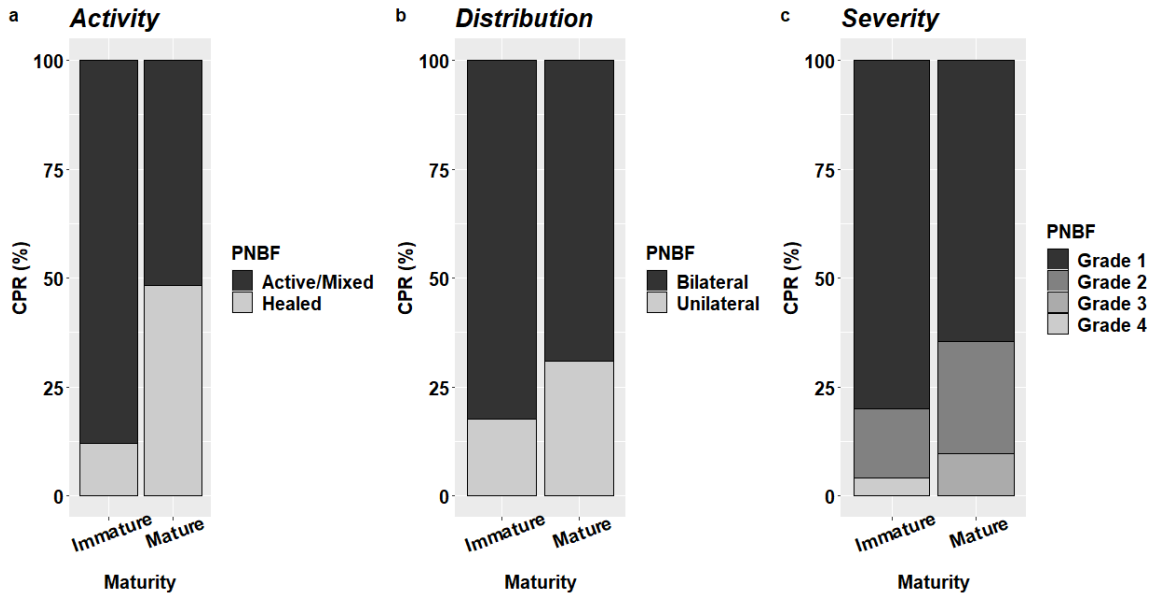

Figure 8.19 A comparison of activity (a), distribution (b) and severity (c) of PNBF between skeletally mature and immature individuals with lesions.

8.2.3.5 Specific Conditions: Infectious Diseases

In addition to the non-specific indicators of stress described so far, specific infectious conditions could be identified in eight individuals (CPR=3.8%) based upon a constellation of skeletal signs (Table 8.19).

For some conditions, site-specific patterns were evident. Among the 30 Warwick skeletons, there were two individuals (CPR=6.7%) with diffuse, active and largely symmetrical PNBF. In a previous osteological analysis by Newman (2019), it was postulated that these lesions were the result of hypertrophic osteoarthropathy (HOA); this diagnosis is supported by reference to clinical and palaeopathological case studies (Grauer 2019: 503; Binder and Saad 2017; Mays and Taylor 2002). One (CPR=3.3%) of these skeletons (SK 357) also had extensive active PNBF on the pleural rib surfaces (Figure 8.20), with the left ribs between the second and tenth positions affected most, and small cavities of the anterior surface of contiguous lower thoracic and upper lumbar vertebrae. For several reasons, it is proposed that these changes are *consistent with*

pulmonary tuberculosis. Firstly, rib lesions (specifically PNBF on the pleural surfaces, with a focus on the left side) have a significant association with pulmonary TB (Davies-Barrett *et al.* 2019: 540; Santos and Roberts 2006; Santos and Roberts 2001; Roberts *et al.* 1994: 172). Secondly, comparable vertebral body changes have been positively linked to tuberculosis through pathogen DNA screening (Nelson *et al.* 2020). HOA is also a secondary condition associated with pulmonary diseases like TB (Grauer 2019: 503; Binder and Saad 2017: 59; Mays and Taylor 2002; Santos and Roberts 2001: 41). Regarding TB, pathognomonic signs of the disease have been found in skeletons from the Warwick assemblage (Hill n.d.: 4) and, given its communicable nature, it was believed reasonable to assume that other individuals in the living community were also infected.

Site	Skeleton (*profile*)	Diagnosis	Summary of Lesions
BG	187 (*immature; 14 years*)	Leprosy (*typical of*)	Rounded edges to the nasal aperture; possible resorption of nasal spine and the anterior maxillary alveolar; pitted palate; PNBF on the mandible; bilateral femoral and tibial PNBF.
SH	80.1 (*immature; 19.9 years, 95% CI [18.6, 19.9]*)	Osteomyelitis (*diagnostic of*)	The right femur appears to have been fractured in two places and healed in incorrect alignment; a mixture of dense sclerotic and porous PNBF cover most of right femur which also has a cloaca on the posterior distal shaft on the popliteal surface; to a lesser extent, the distal left femur also affected by dense, well-organised PNBF.
WS	357 (*immature; 19.0 years*)	Hypertrophic Osteoarthropathy (*typical of*)	Active PNBF found: bilaterally on the femora, tibiae, fibulae, humeri, ulnae and tarsal and metatarsals; right radius; superior to the acetabulum on the blade of the right ilium - left too degraded to assess; supraspinous fossa of the right scapula. PNBF largely symmetric in nature.
		Pulmonary TB (*consistent with*)	Active PNBF on the pleural surfaces (vertebral ends and in some cases the length of the shaft) of 8 out of 11 surviving left ribs positionally located between the second and tenth ribs. Right ribs less severely affected; 5 of 12 show PNBF, but in isolated plaques. Cavitation of anterior bodies of T10-L2.
	589 (*mature female; 60.7 years, 95% CI [33.5, 89.1]*)	Hypertrophic Osteoarthropathy (*consistent with*)	Active PNBF found: in plaques on the pleural surfaces on the left and right ribs in the range of the second to tenth ribs; bilaterally on the proximal ulnae, distal radii and ilia just superior to the acetabulum; unilaterally in the supraspinous fossa of the right scapula, subscapular fossa of the left scapula, left metacarpals 1 and 2.
YB	4079 (*immature, 18.5 years*)	Leprosy (*typical of*)	Resorption of the nasal spine inferior nasal border which has a saddle-like appearance; maxillary alveolar processes in the region of the incisors also resorbed – i.e., rhinomaxillary syndrome (RMS); palatal bones are extremely pitted; spicules of bone in both maxillary sinuses; heavy build-up of calculus. Lower limb absent.
	3586 (*mature male*)	Leprosy (*consistent with*)	Resorption of nasal spine and along the inferior nasal border; slight recession of maxillary alveolar process in the region of the anterior dentition - i.e., possible early-stage RMS; pitted palate; PNBF on the palate and in maxillary sinuses; heavy build-up of calculus. Lower limb absent.
	3329 (*mature female; 56.3 years, 95% CI [25.4, 87.9]*)	Leprosy (*typical of*)	Resorption of nasal spine and maxillary alveolar processes in the region of the incisors i.e., RMS; pitted palate. Bilateral mixed PNBF on the tibiae and fibulae.
		Brodie's Abscess (*typical of*)	Large (33mm width) perforating lesion on the right ilium surrounded by a rim of PNBF – on the medial surface, PNBF extends across the iliac crest. On the right proximal femur (i.e., the region closest to the abscess), mixed PNBF affects the lesser trochanter, gluteal tuberosity and proximal half of the linea aspera.
	2708 (*immature; 19.5 years*)	Osteomyelitis (*diagnostic of*)	Right rib, just medial to tubercle, is infected. Active PNBF on a right rib, just medial to tubercle, with 3 cloacae. Rib shaft and sternal end unaffected. Three other right ribs also have plaques of active PNBF between the head and angle. Fragmentation precluded precise seriation of affected ribs, but all between the third and tenth position.

Table 8.19 Specific infectious conditions identified at each site with a brief summary of lesions used in diagnoses.

Figure 8.20 Plaques of porous PNBF (highlighted with red arrows) located on the visceral surface of a left rib from SK 357 at vertebral (a) and sternal ends (b). Also, small cavities on the anterior surface of T10 body (c).

Four skeletons showed signs of leprosy. These diagnoses (which varied in certainty between cases that were *consistent with* and *typical of* leprosy) were mainly made on the basis of morphological changes around the nasal aperture and maxillary alveolar region (Figure 8.21), which further suggested these individuals had lepromatous or near-lepromatous leprosy (Roberts and Buikstra 2019: 368; Roffey 2012: 216; Ortner 2003: 264; Andersen and Manchester 1992: 122). Most of these cases (3) originated from York. Unfortunately, due to the high frequency of grave truncation in the York Barbican assemblage (Section 5.5.2), postcranial markers were absent in two of these skeletons and the range of secondary infections that are usual in leprosy could not be explored to add further support to the diagnoses. For SK 3329, however, there was abundant evidence of an inflammatory response to a chronic infection in the postcranial skeleton. On SK 3329's right ilium, for instance, a roughly circular lesion surrounded by well-organised PNBF

completely perforated the iliac crest (Figure 8.21). Although several diseases are known to cause 'punched out' lesions (e.g., TB and multiple myeloma), the rim of PNBF along with a mixture of new and sclerotic bone on the associated proximal femur (Figure 8.21) are typical of a Brodie's Abscess – a sign of hematogenous iliac osteomyelitis often the result of staphylococcal infection (Behara *et al.* 2017; Ogbonna *et al.* 2017; Beslikas *et al.* 2005; Beaupré and Carroll 1979).

Even though none of these skeletons exhibited the well-developed *facies leprosa* (rhinomaxillary syndrome) that is unambiguously diagnostic of advanced lepromatous leprosy, collectively they presented compelling evidence that *Mycobacterium leprae* infection was a significant disease risk in medieval York. This threat was probably compounded by secondary infections (osteomyelitis being one example) that often affect sufferers of leprosy (Roberts and Buikstra 2019: 363-368; Ortner 2003: 263-272). In fact, as diagnostically suggestive changes to the facial skeleton only occur after severe and chronic infection and are absent in the milder and less clearly visible response to the disease (tuberculoid leprosy) (Roberts and Buikstra 2019: 368; Roffey 2012: 216; Ortner 2003: 264; Boldsen 2001: 380; Andersen and Manchester 1992: 122), it can be reasonably speculated that the crude prevalence for leprosy in the York Barbican sample (CPR=4.3%) is likely an underestimate for the living population which would have also included asymptomatic and mildly symptomatic cases.

In addition to highlighting the presence of infectious pathogens at sites, the skeletons diagnosed with specific conditions raise further questions. Firstly, what environmental and cultural factors made certain contexts more amenable to pathogens? Secondly, at these sites, where likely most of the population was exposed to communicable diseases, why did some individuals contract them and not others?

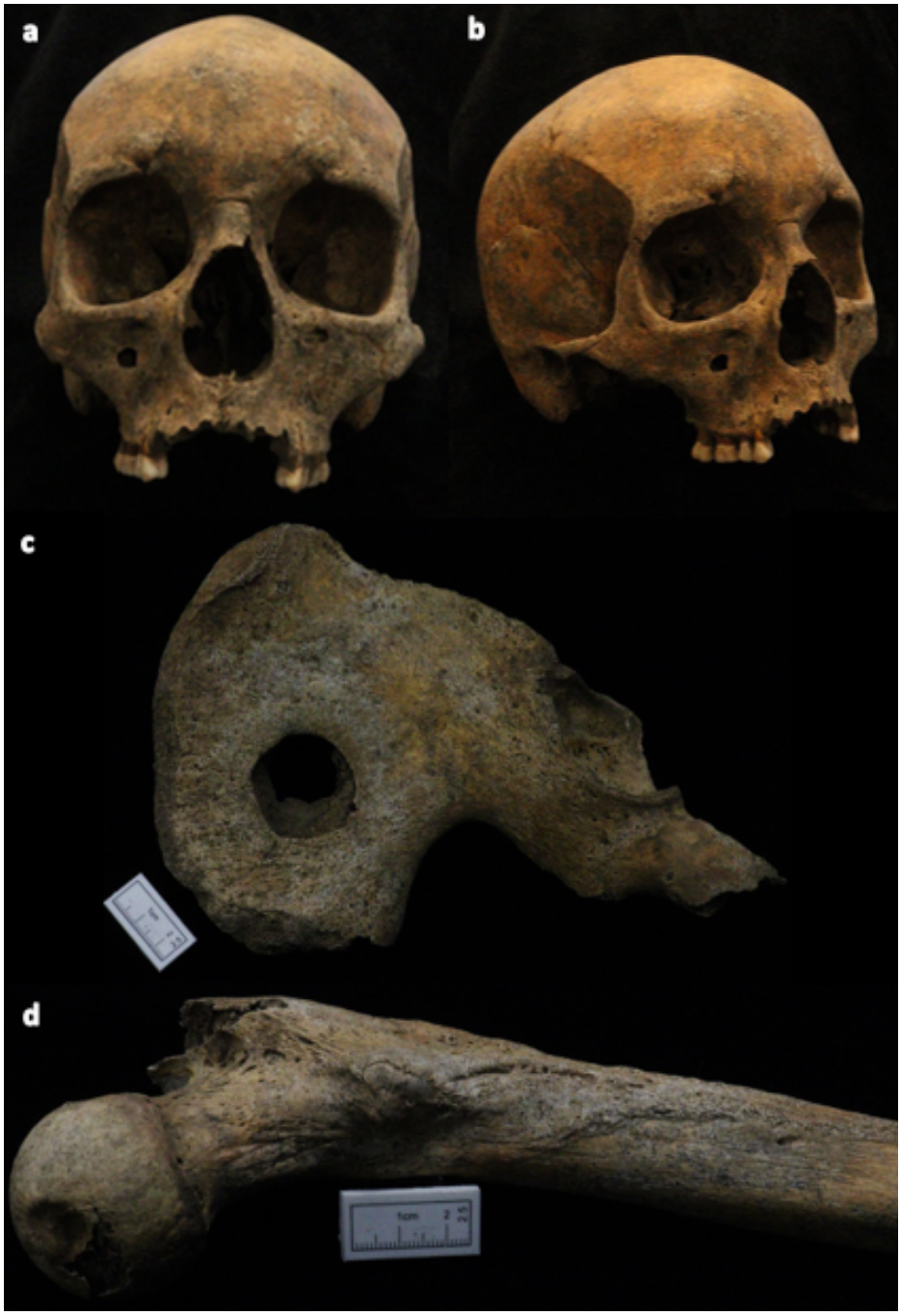

Figure 8.21 SK 3329 from the York Barbican collection. In the nasal region it is possible to see rounding of the inferior border and widening of the aperture as well as loss of the spine; there is also resorption of the anterior maxillary alveolus (a and b). Also present are a large perforating lesion in the ilium (c) and mixed PNBF on the proximal aspect of the posterior surface of the right femur (d).

8.2.3.6 Specific Conditions: Metabolic Diseases

Seven (CPR=3.2%) skeletons had signs suggesting that in life they suffered from a specific metabolic disease (Table 8.20). Although the unequivocal diagnosis of any specific metabolic condition is challenging, the distribution and supposed pathogenesis of the observed lesions can be related to vitamin C deficiency (Figure 8.22). For example, some of the most frequently observed lesions were at sites of muscle attachment where, in individuals suffering from a chronic and severe lack of vitamin C, blood vessels haemorrhage leading to periosteal inflammation and PNBF or capillarisation and subsequent porosity (Brickley and Mays 2019; Newman 2016: 110; Snoddy *et al.* 2016; Mays 2014; Geber and Murphy 2012; Mahoney-Swales and Nystrom 2009; Mays *et al.* 2006; Pinhasi *et al.* 2006; Ortner 2003: 383-404). Similarly, the periosteal lesions seen in two individuals (SK 203 and SK 3936), may well be associated with haemorrhaging in the orbital region which can be caused by vitamin C deficiency (Damini *et al.* 2021; Cheah *et al.* 2020; Brickley and Mays 2019: 534-536; Newman 2016: 110; Billoir *et al.* 2012; Saha *et al.* 2012; Mahoney-Swales and Nystrom 2009). As such, it was proposed that the suite of pathological markers in each case was *consistent with* a diagnosis of scurvy. As all but one individual within this group were skeletally immature, it was inferred that age played a key role in vulnerability to or capacity to manifest the signs of metabolic disease. Diagnosable lesions not discussed here are presented in Appendix 3.

Site	Skeleton (*profile*)	Diagnosis	Summary of Lesions
BG	478 (*immature, 3.5 years*)	Scurvy (*consistent with*)	Porosity bilaterally at muscle attachment sites, including: the greater wings of the sphenoid; posterior cranium; supraspinous fossae of the scapulae; ulnar tuberosities. Cortical fraying (especially on the proximal and distal humeri and femora). Flaring of the distal femoral metaphyses. Curvature of the tibiae. CO – active/mixed.
	203 (*immature, 3.5 years*)	Scurvy (*consistent with*)	Porosity bilaterally on the greater wings of the sphenoid and palate. Porosity in the right scapula supraspinous fossae - left scapula not present. CO – active/mixed. PNBF in the left orbit.
	278 (*immature*)	Scurvy (*consistent with*)	Bilateral porosity at muscle attachment sites, such as: the greater wings of the sphenoid between pterygoid plates and supraspinous fossae of the scapulae – notably more apparent in the right scapula. Bilateral plaques of PNBF on the distal anterior femora (active/mixed) and tibiae (active). Fraying of the inferior femoral metaphyses as well as tibial superior and inferior metaphyses. CO – healed.
SH	539 (*immature, 3.1 years*)	Scurvy (*consistent with*)	Porosity on the cranial vault, especially near the external occipital protuberance and around the foramen magnum, but also on the palate and right maxillary alveolar process. Porosity surrounding nutrient foramina in the supraspinous fossa of the scapula – more extensive on the right side. Bilateral active PNBF around the gonial angle of the mandible, in the region of the insertion of the *Masseter* muscle. CO – active/mixed.
WS	570 (*immature, 13.8 years*)	Scurvy (*consistent with*)	Porosity at muscle attachment sites, including: the medial surface of the mandibular ramus bilaterally; the right greater wing of the sphenoid (left absent); the area surrounding the posterior aperture of the foramen rotundum – these pores were rounded in appearance. Although little of the right supraspinous fossa of the scapula has survived (left completely absent), it was filled with fine pores. CO – healed. LEH – one stress episode inferred from these, estimated to have occurred between 5-5.9 years of age.
YB	2469 (*immature, 3.0 years*)	Scurvy (*consistent with*)	Porosity at muscle attachment sites, including: the left greater wing of the sphenoid; the supraspinous fossa of the left scapula (right damaged); bilaterally inferior to the coronoid process of the ulnae. Bilateral, active PNBF was present at the insertion of several sites of muscle attachment, such as: the insertion of the *Masseter* muscle at the mandibular gonial angle; the origin of the medial head of *Triceps* on the posterior surface of the humeri distal to the radial groove. Fraying also on the proximal and distal left femur and tibia (right absent). Orbits absent.
	3936 (*mature*)	Scurvy (*consistent with*)	Active PNBF on the right mandibular ramus laterally and medially – at insertions of *Masseter* and *Medial Pterygoid* – and on medial aspect of coronoid process at the insertion of the *Lateral Pterygoid*. Only fragments of the right condyle survive, but a plaque of PNBF was present on the neck. The left side of the mandible had PNBF on the medial aspect of the coronoid process and lateral condylar neck. PNBF was also observed in both orbits (so extensively that CO could not be assessed). LEH – four stress episodes inferred from these, estimated to have occurred between 1-1.9, 2-2.9, 4-4.9 and 9-9.9 years of age.

Table 8.20 Specific metabolic conditions identified at each site with a brief summary of lesions used in diagnoses.

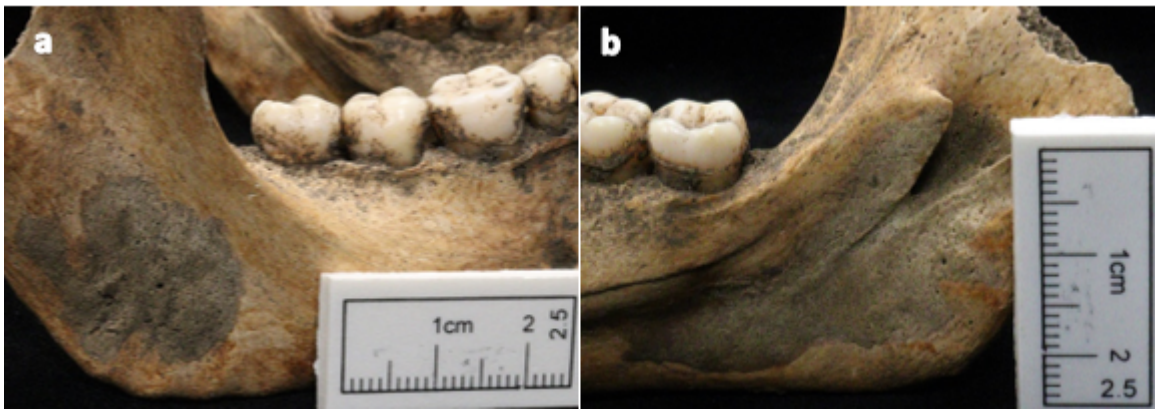

Figure 8.22 PNBF on the mandibular ramus of SK 3936 from York Barbican at insertion sites of the *Masseter* (a) and *Medial Pterygoid* muscles and at the mandibular foramen through which the maxillary artery and the inferior alveolar vein pass (b). The plaques of periosteal new bone are consistent with an inflammatory response to haemorrhaging of blood vessels and at attachment sites of muscles subjected to repetitive use (e.g., muscles of mastication), as is observed in individuals with weakened blood vessels due to vitamin C deficiency.

8.2.3.7 Summary

The osteological data has been explored to reveal several patterns in mortality and the prevalence of pathological markers. These have established that site and sex as well as age-related susceptibility play key roles in stress marker development and, crucially, that relationships between factors may be discernible when the nature of the stress marker is considered (e.g., mild versus severe). Therefore, when attempting to infer the impact of early-life stress on life-course outcomes in the final section of this chapter, fluctuating asymmetry is not just contrasted between individuals with and without pathological markers, but also between individuals with particular characteristics of lesion development.

8.3 Asymmetry

This section describes asymmetric variation in the 154 M^1 and 148 M_1 pairs assessed. In addition to identifying the presence of FA in tooth morphology, variation at specific landmarks is compared to investigate where stress-induced deviations to symmetry may be more likely to develop as well as the relationship between M^1 and M_1 FA, thus facilitating a later discussion of developmental mechanisms. Additionally, to explore a potential confounding effect, the relationship between size and FA is scrutinised. Once fluctuating asymmetry has been described in isolation, it is explored with reference to the grouping factors discussed in the previous section.

8.3.1 Finding Asymmetries

The decomposition of morphological variation through a Procrustes ANOVA (Table 8.21-Table 8.22) indicated that by far the greatest proportion of variance (*circa* 83%) in both M1s was explained by differences between individuals. Permutation procedures also found greater differences between left and right sides than expected in both the M^1 ($p=0.003$) and M_1 ($p=0.008$). These fixed left-right biases (i.e., directional asymmetry) accounted for only a minor amount of variation (i.e., *circa* 0.3%), but did justify the further adjustment of coordinate configurations (Section 6.4.2) to remove variance due to directional asymmetry. Highly significant interactions ($p=0.001$) between individuals and sides revealed the presence of non-directional asymmetry. Importantly, variation between replicates (i.e., error due to intra-observer inconsistency) accounted for a small percentage of variation (*circa* 2%) in both M1s, so was unlikely to obscure variance due to non-directional asymmetry. This is especially important when investigating fluctuating asymmetry, as both error and FA represent random effects (Klingenberg 2015: 868-869; Graham *et al.* 2010: 486-487). In fact, *F* values indicated

that M^1 non-directional asymmetry explained in excess of twenty-six times more variation than error (F=26.411); for the M_1 this increased to greater than thirty-six times (F=36.107). Non-directional asymmetry, although significant in both teeth, was slightly better evinced in the M_1 with R^2 scores being marginally higher. Crucially, when the signed left-right differences for each M1 landmark and semi-landmark were examined, there was no evidence of antisymmetry (i.e., there was no clustering in scatter plots, while histograms and density plots revealed peaked rather than platykurtic distributions) (Figure 8.23). This finding is consistent with previous research which has not found antisymmetry in human teeth (e.g., Guatelli-Steinberg *et al.* 2006: 249), and it was therefore assumed that the non-directional component to asymmetry identified by the Procrustes ANOVA was in fact fluctuating asymmetry (Balzeau *et al.* 2012: 2; Silva *et al.* 2012: 561-564: Radwan *et al.* 2003: 502; Debat *et al.* 2001: 425-426; Klingenberg and McIntyre 1998: 1368).

Effects	df	SS	MS	R^2	*F*	p
ind	153	3.530	0.023	0.833	5.854	0.781
side	1	0.011	0.011	0.002	2.862	0.003
ind x side	153	0.603	0.004	0.142	26.411	0.001
error	616	0.091	<0.001	0.021		
Total	923	4.237				

Table 8.21 M^1 Procrustes ANOVA. Significance determined through RRPP with 1000 permutations.

Effects	df	SS	MS	R^2	*F*	p
ind	147	4.507	0.031	0.826	5.362	0.977
side	1	0.014	0.014	0.003	2.406	0.008
ind x side	147	0.841	0.006	0.154	36.107	0.001
error	592	0.094	<0.001	0.017		
Total	887	5.455				

Table 8.22 M_1 Procrustes ANOVA. Significance determined through RRPP with 1000 permutations.

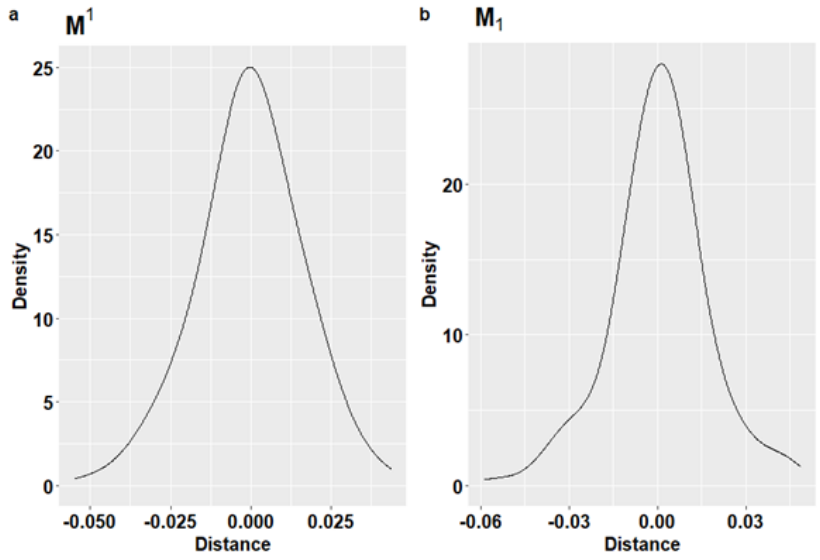

Figure 8.23 Plots of left-right differences in the location of the first landmark in M^1 (a) and M_1 (b) configurations (i.e., the centre of the mesial fovea, located at the most anterior extension of the sagittal and longitudinal fissures respectively). The peaked, rather than broad or bimodal distributions, suggested that the significant *ind*side* interaction in the Procrustes ANOVA was due to fluctuating asymmetry rather than antisymmetry.

8.3.2 Fluctuating Asymmetry: Adjusted Coordinate Matrices

To explore assumptions associated with the PCM of dental development and the impact stress has upon it (Salazar-Ciudad and Jernvall 2002; Jernvall and Jung 2000) (Section 3.4.3), A_{pij} configurations were examined to identify the locations at which fluctuating asymmetric variance was most evident. It was found that when the complex variation in coordinate matrices was simplified through PCA, that variance was largely dispersed throughout configurations; for example, it took 15 and 19 PCs to capture ≥95% of variation in the M^1 and M_1 covariance matrices. The first two PCs were, however, influenced to a greater extent by semi-landmarks located along the outline and landmarks positioned at fissure junctions and pits (i.e., points at the periphery of cusps). The eigenvectors of the third and fourth PCs by contrast had higher correlations between cusp apices, especially those of the distal cusps. Meanwhile, the mesial cusps (paracone and protocone in the M^1 and the protoconid and metaconid in the M_1) were relatively stable.

These patterns could be appreciated best visually. As such, the configurations with the most extreme differences in each PC (i.e., the shapes that contributed the minimum and maximum variance to each component were used as reference and target shapes) were plotted and vector displacements compared (Figure 8.24). These procedures suggested that fluctuating asymmetric variance predominantly manifested at the edges of cusps, and that when cusps apices did vary, the distal cusps were more likely to be affected than the mesial.

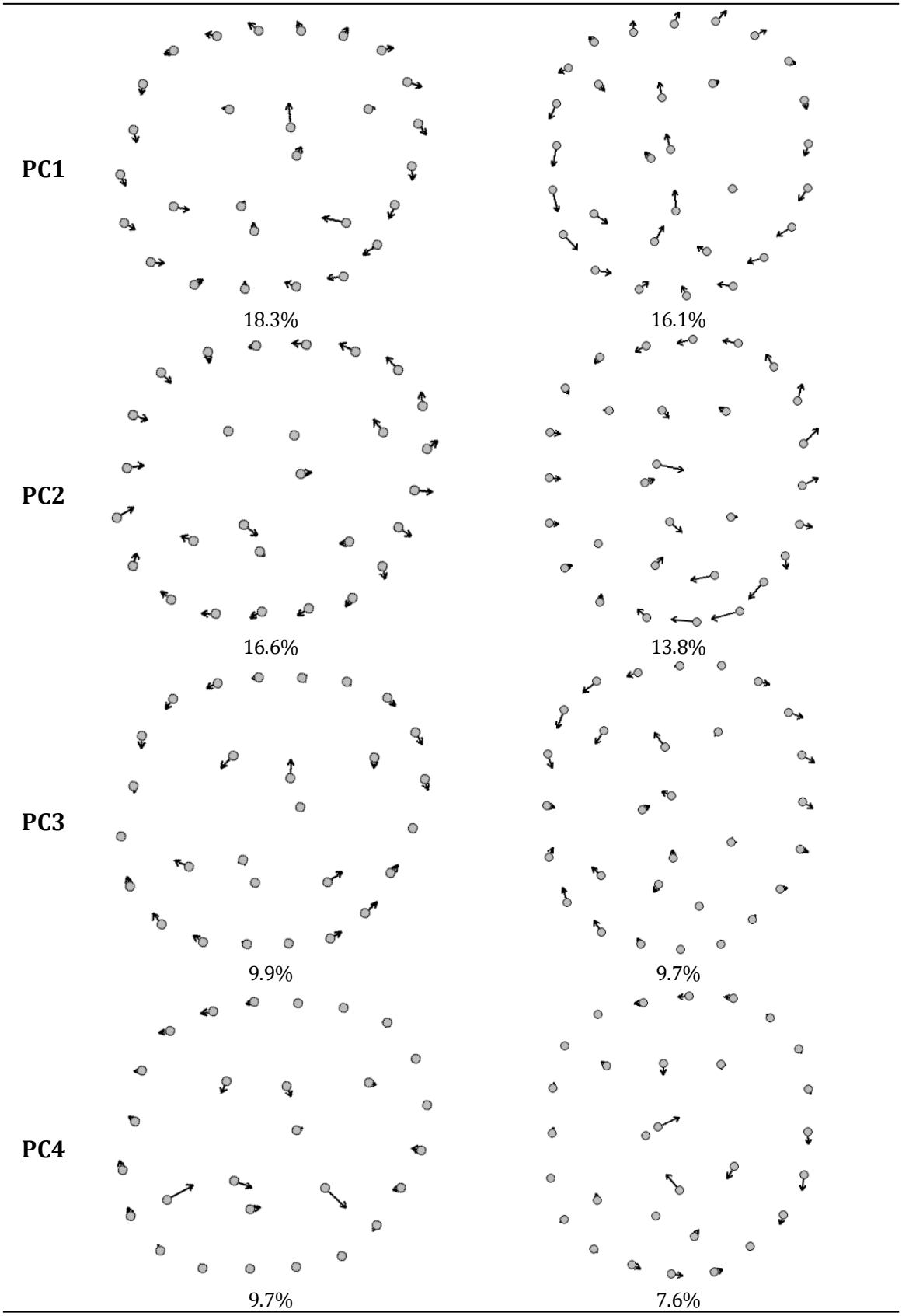

Figure 8.24 Vector displacements (length and orientation of line indicate magnitude and direction) between reference (individual with least variance) and target (individual with most variance) shapes in the first four PCs. Percentages correspond to the proportion of variation accounted for by each PC. Mesial is up.

Although reconstructing *in vivo* processes from patterns identified in inert materials is challenging and must be done with caution, these findings are consistent with assumptions associated with the PCM. Specifically, it appears stress-induced morphological variance is most apparent in later-forming occlusal features while those forming earlier (e.g., cusps apices – especially those located mesially) are more stable. This supports the hypothesis that the processes responsible for the development of occlusal traits in multi-cusped teeth is sequential and interlinked in nature and that stress ripples down the various physiological interactions to provoke a cascade of developmental errors (Riga *et al.* 2014: 399; Salazar-Ciudad and Jernvall 2002; Jernvall and Jung 2000). These findings also suggest that the extent to which stress is embodied must be considered when attempting to chart stress experience across the life-course (Section 9.4).

8.3.3 Fluctuating Asymmetry: Exploring Univariate Scores

To further explore FA, the distributions of unsigned univariate scores were investigated (Table 8.23 and Figure 8.25). When M1 a_p scores were plotted, density and quantile-quantile plots indicated peaked or 'light-tailed' and positively skewed distributions, potentially influenced by outlying values. Density plots also revealed a second, smaller peak within the right tail of each distribution, suggesting two distinct groups within the sample. It was also noted that the differences between individual M1 a_p scores were small; given the arbitrary nature of the registration process, this reflects computational mechanics rather than real-world disparities in stress experience (Zelditch and Swiderski 2018: 46-47; Dryden and Mardia 1998: 87-92).

These distributional and scaling characteristics required consideration. It was decided that when subjecting a_p scores to quantitative procedures, the scaled natural

logarithm would be used. After logarithmic transformation, scores better approximated a normal distribution, facilitating parametric testing (Van Pool and Leonard 2010: 216). Meanwhile, scaling mitigated against the computational difficulties associated with exploring small differences (Grus 2015). In order to scale scores, the sample mean was subtracted from each individual a_p value to centre scores, then centred scores were divided by the sample's standard deviation; scaled vectors therefore had a mean of 0 and a standard deviation of 1 (Grus 2015). Overall, these procedures made a_p scores more amenable to subsequent quantitative testing and were applied in all statistical procedures (summary tables are derived from untransformed data for reference).

Tooth	No.	Min	Q1	Median	Mean	Q3	Max	Std dev
M^1	154	1.000369	1.000790	1.001176	1.001304	1.001776	1.003410	0.000678
M_1	148	1.000477	1.001253	1.001738	1.001891	1.002566	1.003846	0.000812

Table 8.23 A summary of a_p scores.

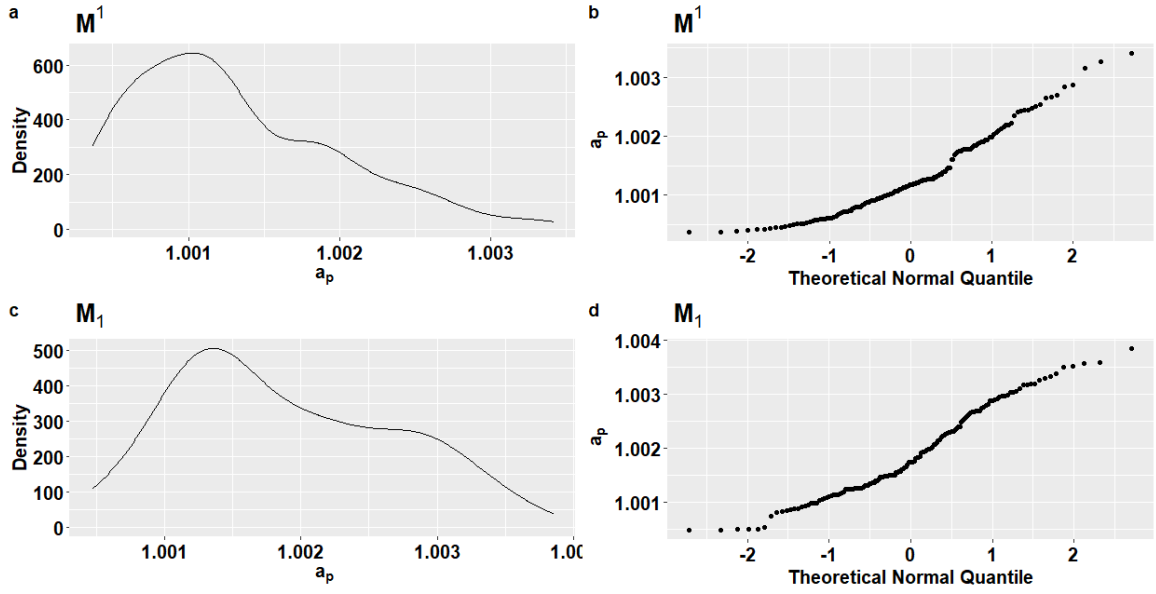

Figure 8.25 Density (a) and quantile-quantile plots (b) of M^1 (a-b) and M_1 a_p scores (c-d).

Among the 85 individuals for whom both maxillary and mandibular M1s could be assessed, linear regression detected a relationship between logged and scaled M_1 a_p scores and the corresponding M^1 value ($F(1,83)=15.57$, p=<0.001, $R^2=0.148$) (Figure 8.26).

Although the R^2 value associated with the model indicated only a moderate proportion of variability had been explained, overall the result inferred a connection between the processes that led to stress-induced deviations to symmetry in each isomere and that M^1 and M_1 a_p scores likely reflected the same underlying causal factors (i.e., non-specific stress). Furthermore, to evaluate the possibility that FA was either affected by or the result of size asymmetry (i.e., the allometric effect in which shape variation increases with size), the relationship between a_p scores and left-right difference of centroid size was explored (Klingenberg 2015: 896; Klingenberg and McIntyre 1998: 1368) (Table 8.24-Table 8.25 and Figure 8.27). Regression tests found no significant relationship between either scaled M^1 ($F(1,152)=1.436$, $p=0.233$) or M_1 a_p scores ($F(1,146)=1.034$, $p=0.319$) and size asymmetry. In summary, size was not a predictor of the univariate measure of FA employed, and an allometric effect was unlikely to have a meaningful impact on analyses.

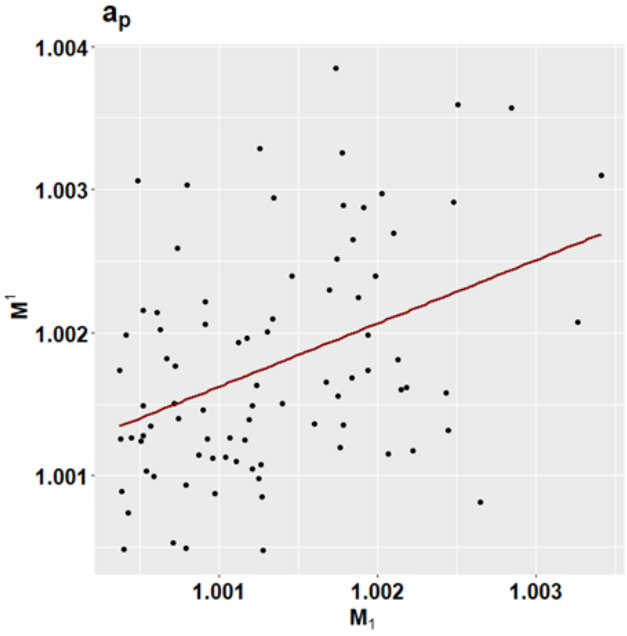

Figure 8.26 The relationship between M^1 and M_1 a_p scores with a line of best fit plotted. Regression tests inferred a positive linear connection between scores.

Tooth	No.	Min	Q1	Median	Mean	Q3	Max	Std dev
M^1	924	23.49	25.35	26.10	26.20	27.04	30.03	1.19
M_1	888	23.64	25.74	26.46	26.53	27.28	30.11	1.16

Table 8.24 Summary of centroid size from all replicates.

Tooth	No.	Min	Q1	Median	Mean	Q3	Max	Std dev
M^1	154	0.000624	0.122740	0.256641	0.318606	0.470529	1.149850	0.246908
M_1	148	0.002028	0.151919	0.318877	0.372857	0.561840	1.569290	0.287740

Table 8.25 Individual differences in left-right centroid size.

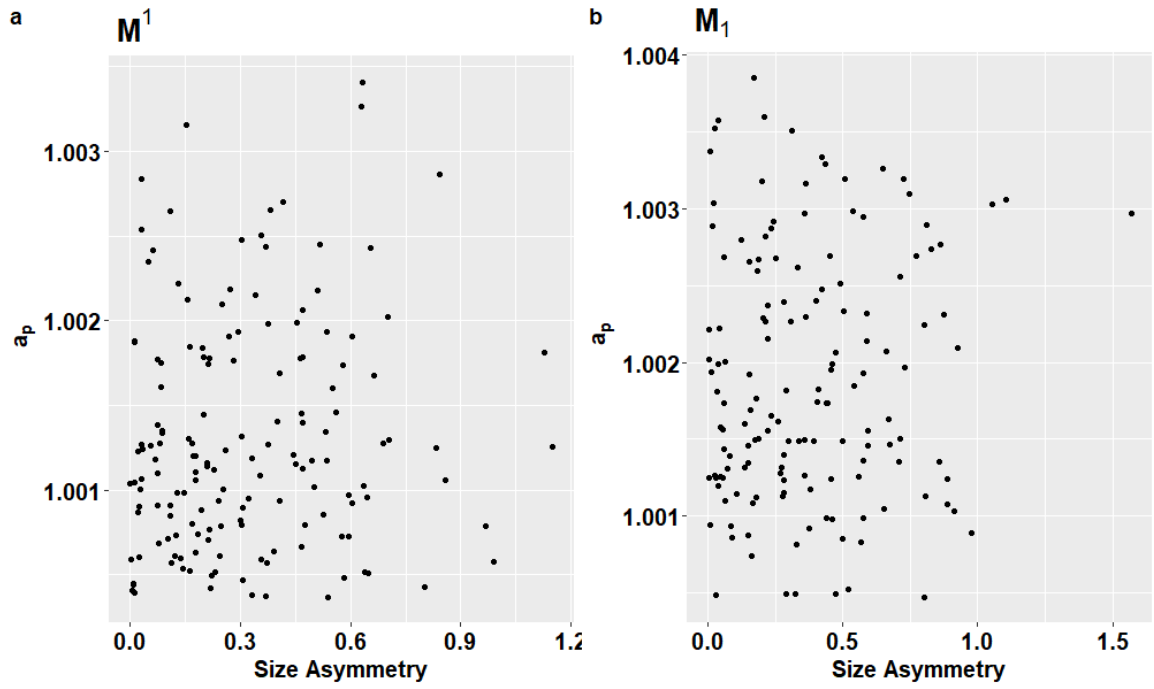

Figure 8.27 Left-right differences in centroid size plotted against M^1 (a) and M_1 (b) a_p scores. No significant linear relationship was detected between scaled a_p scores and size.

8.3.4 Between-group Comparisons: Site, Sex and Skeletal Maturity

The following section explores between-groups differences in FA through a_p scores. Thus, individual measures of FA are contrasted between sites and sexes as well as mature and immature skeletons. Through this it was possible to investigate and identify differences that may imply significant disparities between stress experience.

Subtle between-site differences in FA were noted (Table 8.26-Table 8.27). Even though interquartile ranges overlapped, Warwick had the highest average M^1 and M_1 a_p scores. The most visually appreciably difference in plotted scores was in M^1 a_p values

which showed that those associated with York Barbican were much lower than those from Warwick assemblage (Figure 8.28). Statistical testing on scaled scores supported these observations. After checking underlying assumptions and removing an outlying value from the York Barbican assemblage, an ANOVA found significant differences between sites in scaled M^1 a_p scores (F(3,149)=7.703, p=<0.001) with moderate effect size (ω^2 =0.12). Post-hoc pairwise comparisons with Bonferroni adjusted thresholds inferred significant differences between the Warwick and the Black Gate (p=0.007), South Shields (p=0.018) and York Barbican assemblages (p=<0.001). Despite this, between-site differences in M_1 a_p scores were insignificant (F(3,144)=0.776, p=0.509).

Site	No.	Min	Q1	Median	Mean	Q3	Max	Std dev
BG	60	1.000369	1.000816	1.001156	1.001330	1.001820	1.003155	0.000720
SH	23	1.000472	1.000906	1.001227	1.001295	1.001714	1.002417	0.000529
WS	17	1.000521	1.001344	1.001874	1.001908	1.002428	1.003410	0.000807
YB	54	1.000384	1.000638	1.001031	1.001090	1.001275	1.002447	0.000523

Table 8.26 A comparison of M^1 a_p scores between sites.

Site	No.	Min	Q1	Median	Mean	Q3	Max	Std dev
BG	52	1.000477	1.001253	1.001776	1.001837	1.002310	1.003591	0.000731
SH	22	1.001032	1.001491	1.001707	1.002075	1.002617	1.003846	0.000818
WS	27	1.000497	1.001426	1.001985	1.001995	1.002507	1.003570	0.000798
YB	47	1.000487	1.001115	1.001491	1.001805	1.002729	1.003522	0.000903

Table 8.27 A comparison of M_1 a_p scores between sites.

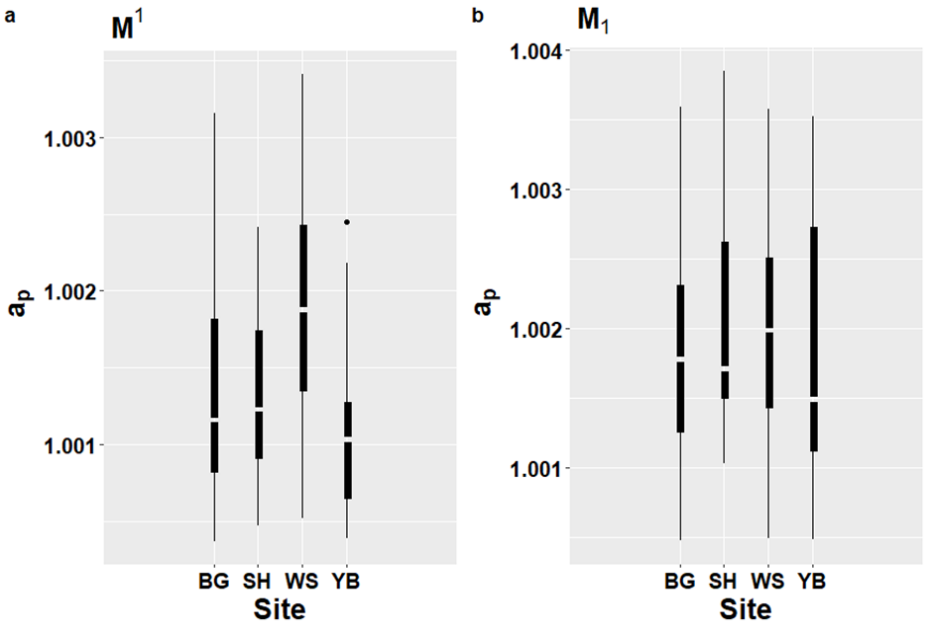

Figure 8.28 A comparison of M^1 (a) and M_1 (b) a_p scores between sites.

Differences in FA between females and males were not readily discernible (Table 8.28-Table 8.29). Points of central tendency in a_p scores were comparable and ranges (interquartile and maximal) overlapped, for example (Figure 8.29). This impression was reinforced through statistical testing which found no significant differences between groups in scaled M^1 (t=-0.600, df=55.98, p=0.551) or M_1 scores (t=-1.399, df=57.75, p=0.167).

Sex	No.	Min	Q1	Median	Mean	Q3	Max	Std dev
Female	29	1.000369	1.000609	1.001041	1.000983	1.001273	1.001904	0.000413
Male	32	1.000384	1.000586	1.000925	1.001060	1.001358	1.002447	0.000580

Table 8.28 A comparison of M^1 a_p scores between sexes.

Sex	No.	Min	Q1	Median	Mean	Q3	Max	Std dev
Female	26	1.000477	1.001106	1.001371	1.001448	1.001897	1.003058	0.000610
Male	34	1.000493	1.001240	1.001411	1.001694	1.002271	1.003373	0.000751

Table 8.29 A comparison of M_1 a_p scores between sexes.

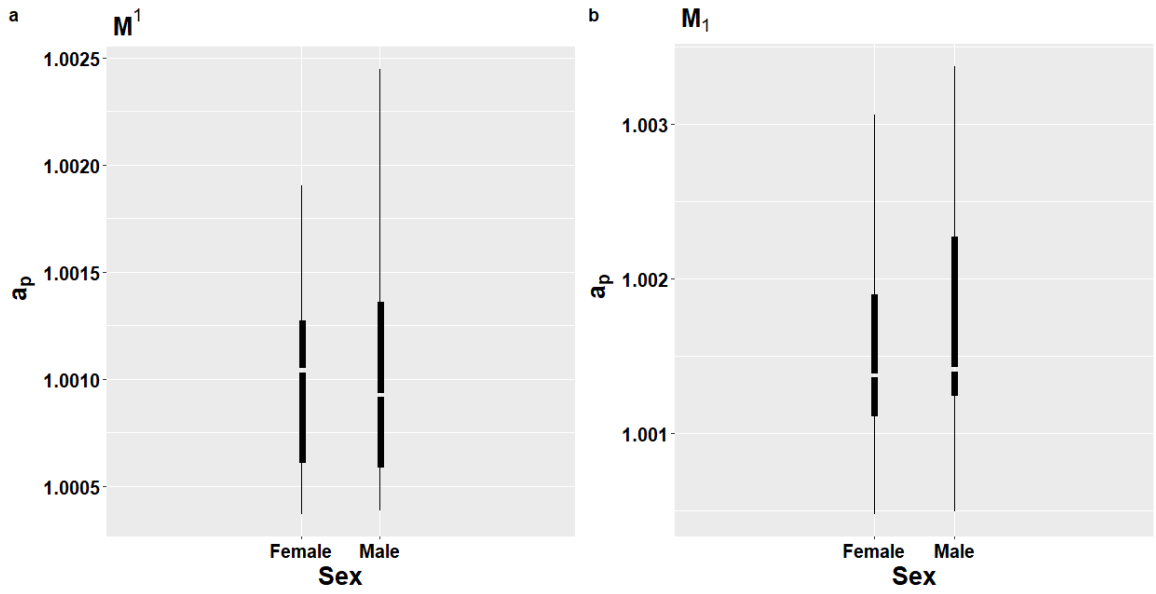

Figure 8.29 A comparison of M^1 (a) and M_1 a_p scores (b) between females and males.

When a_p scores were contrasted between skeletally mature and immature individuals, it was observed that the immature cohort had higher scores for both M1s (Table 8.30-Table 8.31 and Figure 8.30). After removing an outlying value from the skeletally mature group, a *t*-test on scaled M^1 a_p scores produced significant results (t=5.202, df=128.4, p=<0.001) with large effect size (Cohen's d=-0.848). Similarly, differences in M_1 a_p scores were significant (t=3.159, df=136.1, p=0.002) with a medium effect size (Cohen's d=-0.526). These results were believed important for three reasons. Firstly, it was speculated that the comparatively high frequency of immature skeletons in the Warwick sample may have influenced the significant differences in M^1 a_p scores between this and other sites. Secondly, it was hypothesised that the disparity in FA between skeletally mature and immature groups accounted for the bimodal distribution in scores noted in Section 8.3.3. Thirdly, and most importantly, it also seemed reasonable to propose that there were substantial differences in maternally mediated early-life stress experience between the mature and immature individuals.

SK	No.	Min	Q1	Median	Mean	Q3	Max	Std dev
Mature	79	1.000369	1.000608	1.000969	1.001056	1.001301	1.002447	0.000512
Immat	75	1.000421	1.000998	1.001349	1.001566	1.002113	1.003410	0.000734

Table 8.30 A comparison of M^1 a_p scores between individuals at different stages of skeletal development.

SK	No.	Min	Q1	Median	Mean	Q3	Max	Std dev
Mature	77	1.000477	1.001143	1.001492	1.001688	1.002215	1.003373	0.000723
Immat	70	1.000497	1.001469	1.001960	1.002102	1.002757	1.003846	0.000851

Table 8.31 A comparison of M_1 a_p scores between individuals at different stages of skeletal development.

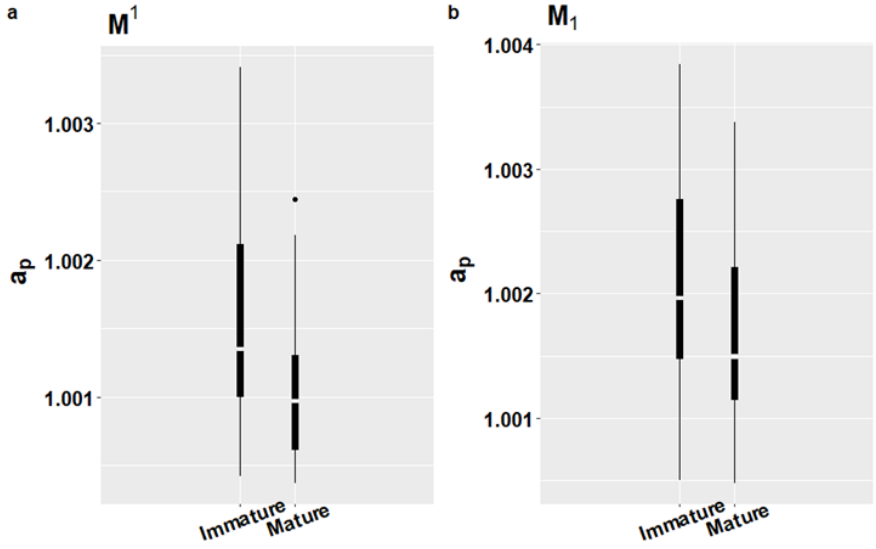

Figure 8.30 M^1 (a) and M_1 a_p scores (b) contrasted between mature and immature skeletons.

8.3.5 Summary

Significant asymmetries were successfully detected in M1 morphology. Directional asymmetry accounted for a small percentage of morphological variance in comparison to non-directional asymmetry. Further tests indicated that the non-directional component to asymmetry was the result of fluctuating asymmetry (rather than antisymmetry). Points at the periphery of cusps, along the outline and central fissure appeared more vulnerable to stress-induced deviations to symmetry than cusp apices. Importantly, measurement error was marginal and size had no significant impact on FA. When measures of FA (i.e., a_p scores) were contrasted between groups, sex biases were absent and differences between sites were subtle. Despite this, significant and

medium-to-large differences in scaled M^1 and M_1 a_p scores were detected between the skeletally mature and immature cohorts, with the latter category associated with the higher FA. It was therefore speculated that stress experienced during early life may have influenced length of life, but that site-specific stressors and sex differentials in frailty either played a minimal role in stress experience or were successfully mediated.

8.4 Defining the Life-course

This final section investigates to what extent fluctuating asymmetry (as a proxy for maternally-mediated early-life stress) can be used to predict later-life stress experience and outcomes. As part of this, the hypotheses generated in the initial investigation of osteological data in Section 8.2 are tested. As discussed previously, regression analysis played a key role in this process. After ascertaining whether FA scores could explain outcome variables, models containing further predictors (e.g., site, skeletal maturity, pathological lesions, etc) were constructed. Of these, only those models chosen using the backwards elimination process described in Section 7.5.2 have been presented. By taking this approach it was possible to quantitatively model life-course dynamics and infer the importance of early-life stress signals transmitted across the mother-child nexus in relation to factors such as context, sex and age and their combined impact on frailty and resilience.

8.4.1 Length of Life

As there were significantly higher M1 a_p scores in the skeletally immature cohort it was hypothesised, with reference to past research (e.g., Roseboom *et al.* 2001; Barker and Osmond 1986; Blakey and Armelagos 1985), that early-life stress affected mortality.

To investigate further, linear regression analyses were employed; as age estimates were not normally distributed, they were log transformed. As it was suspected that the strength or nature of the relationship between early-life stress and mortality would be different in the immature and mature cohorts, they were treated separately.

8.4.1.1 Length of Life in the Skeletally Mature Group

Regression procedures failed to detect a significant linear relationship between age estimates and scaled M^1 ($F(1,57)=2.176$, p=0.146) and M_1 a_p scores ($F(1,56)= 0.871$, p=0.355) (Table 8.32-Table 8.33), although slope coefficients and plots of age estimates against FA values suggested that a slight negative trend may exist. The inability to discern a statistically significant connection between FA and age-at-death in the mature cohort was somewhat surprising given clinical studies have established substantial differentials in later-life morbidity and mortality resulting from early-life adversity (e.g., Roseboom *et al.* 2001: 95; Roseboom *et al.* 2000; Lopuhaa *et al.* 2000; Ravelli *et al.* 1998). It is speculated that the underrepresentation of older mature skeletons in the study sample may have limited the ability to detect similar patterns here.

	Coefficient	Std error	*t*	p
Constant	3.523	0.059	59.76	<0.001
M^1 a_p	-0.108	0.071	-1.475	0.146

Table 8.32 Regression of log transformed estimates of age-at-death in skeletally mature individuals with scaled M^1 a_p scores as a predictor variable.

	Coefficient	Std error	*t*	p
Constant	3.582	0.057	62.51	<0.001
M_1 a_p	-0.058	0.062	-0.933	0.355

Table 8.33 Regression of log transformed estimates of age-at-death in skeletally mature individuals with scaled M_1 a_p scores as a predictor variable.

Age-at-death in the mature cohort was in fact much better predicted by sex, PD, PNBF and the interaction of the latter two pathological lesions ($F(4,58)=10.54$, p=<0.001, $R^2=0.38$) (Table 8.34). Unsurprisingly, even this improved model was unable to account

for variation in age completely as demonstrated by residual plots (Figure 8.31). The model did, however, reveal factors which contributed to significant differentials in length of life. As the response variable (i.e., estimated age) had been log transformed and was not in its natural units, to infer relative risk from coefficient values, these were exponentiated, one was subtracted from this number and then multiplied by 100 (Gelman and Hill 2007). From this it was found that males were estimated to have a length of life 23.2% (95% CI [9.9, 34.6]) shorter than females. PD and PNBF, being degenerative diseases associated with advancing age (e.g., Ogden 2008: 288-293; Larsen 1991: 77-78) (Section 8.4.3), were both positive predictors of estimated age-at-death. However, the interaction of the two produced a negative coefficient which suggested that, in comparison to individuals without either lesion, there was a 49.7% (95% CI [23.1, 67.1]) reduction in estimated length of life for skeletally mature individuals with both. Aside from reiterating well-established sex differentials in life expectancy and the previously inferred degenerative nature of PD and PNBF, these results alluded to a connection between PD and PNBF and hinted that their combined presence was perhaps symptomatic of an underlying pathological state that increased mortality risk in later-life.

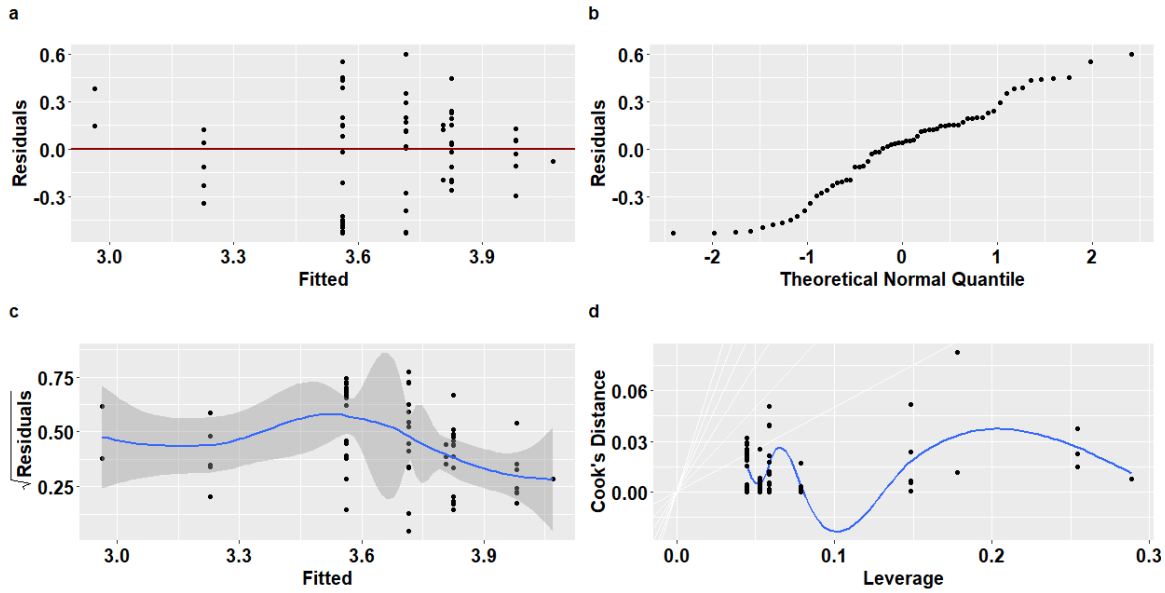

Figure 8.31 Diagnostic plots of residuals from the regression analysis in which sex, PNBF, PD and the interaction of the latter two variables were employed to model age in the skeletally mature cohort. Residual variance is plotted against the model's line of best fit (red line) (a); residuals compared to a normal distribution (b); a scale-location plot to assess homoscedasticity (c); Cook's distances to identify outlying points.

	Coefficient	Std error	*t*	p
Constant	3.228	0.118	27.461	<0.001
Sex (Male)	-0.264	0.080	-3.304	0.002
PNBF (Present)	0.841	0.195	4.320	<0.001
PD (Present)	0.596	0.129	4.625	<0.001
PNBF*PD	-0.687	0.212	-3.238	0.002

Table 8.34 Regression of log transformed estimated age-at-death in skeletally mature individuals with significant predictors.

8.4.1.2 Length of Life in the Skeletally Immature Group

Within the skeletally immature group, there was a significant positive linear trend between estimated age-at-death and scaled M^1 ($F(1,70)=7.455$, p=0.008, $R^2=0.08$) as well as M_1 a_p values ($F(1,66)=4.391$, p=0.040, $R^2=0.05$) (Table 8.35-Table 8.36). An increase in scaled M^1 and M_1 a_p scores by one unit (which, after scaling, represented one standard deviation) were associated with an estimated 19.5% (95% CI [4.9, 36.1]) and 12.1% (95% CI [0.6, 24.9]) increase in length of life respectively. Although this is somewhat counterintuitive when it is recalled that older and skeletally mature individuals were associated with reduced FA (and low R^2 scores suggested other factors played critical roles in determining length of life in the immature cohort), it implied that elevated

early-life stress may have been beneficial to survival during development (discussed further in Section 9.3). The strength of this relationship varied between sites, however. Among the immature skeletons from Warwick, for example, there was only a weak relationship between M_1 a_p scores and age-at-death, while there was no evidence of a positive association between M^1 FA and age in the assemblage (Figure 8.32).

	Coefficient	Std error	*t*	p
Constant	2.136	0.075	28.57	<0.001
M^1 a_p	0.178	0.065	2.730	0.008

Table 8.35 Regression of log transformed estimates of age-at-death in skeletally immature individuals with scaled $M^1 a_p$ scores as a predictor variable.

	Coefficient	Std error	*t*	p
Constant	2.278	0.057	39.72	<0.001
M_1 a_p	0.114	0.054	2.096	0.040

Table 8.36 Regression of log transformed estimates of age-at-death in skeletally immature individuals with scaled M_1 a_p scores as a predictor variable.

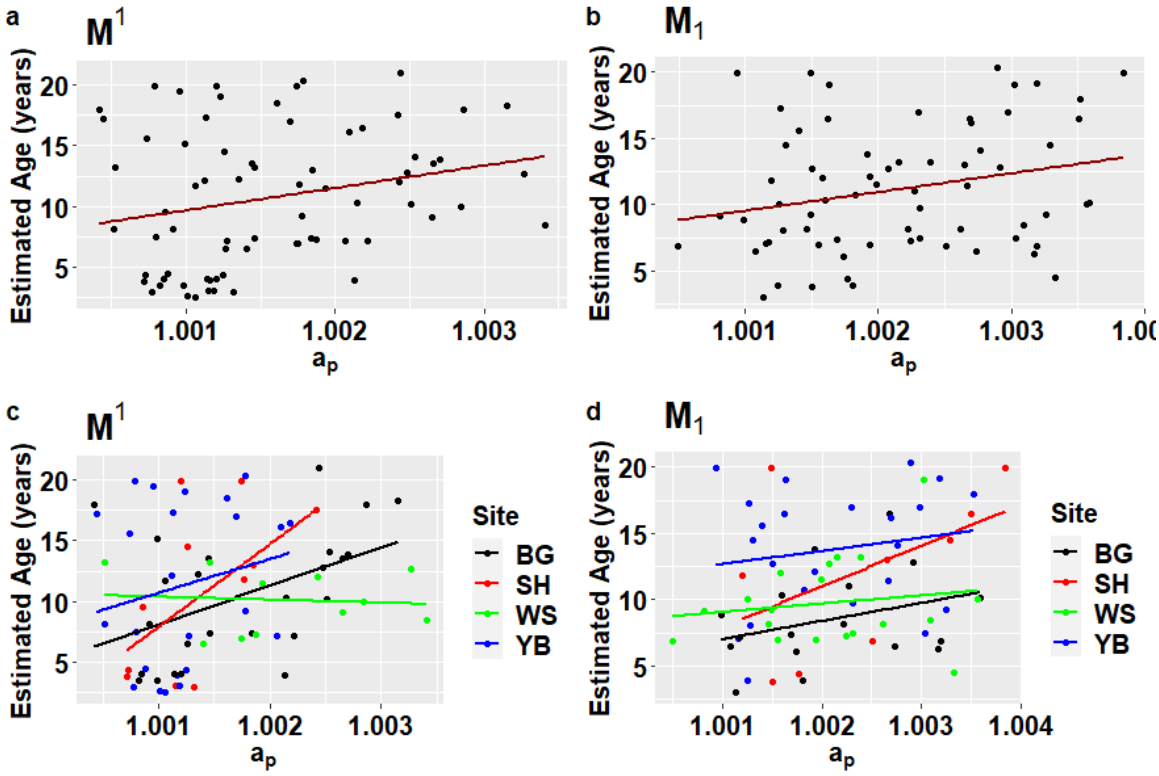

Figure 8.32 The generally positive linear relationship between estimated age in the immature cohort and fluctuating asymmetry are represented in the upper panels (a and b), while in the lower (c and d), sites have been differentiated.

Despite being significant predictors, a_p scores could only explain a small proportion of variation in age-at-death estimates (i.e., $R^2 \leq 0.08$) and regression models were improved with the addition of further independent variables. In the M_1 sample, in addition to a_p values, immature age-at-death was predicted by chronologically matched LEH and site ($F(5,62)=9.994$, p=<0.001, $R^2=0.40$). Regression coefficients indicated that immature individuals with matched LEH were estimated to have lived 53.9% (95% CI [28.8, 83.9]) longer than those without and that skeletally immature individuals from York Barbican were predicted to live 53.1% (95% CI [21.7, 92.7]) longer than those from Black Gate. In the M^1 sample, scaled a_p values, chronologically matched LEH and the interaction between the two made significant contributions to the model ($F(3,67)=15.97$, p=<0.001, $R^2=0.39$). Although for both main effects coefficients indicated a positive correlation with age-at-death, the negative coefficient of the interaction term suggested that a one-unit increase in a_p scores and the presence of matched LEH were estimated to have reduced length of life by 34.8% (95% CI [17.9, 48.2]) (Table 8.37-Table 8.38).

	Coefficient	Std error	*t*	p
Constant	1.853	0.080	23.07	<0.001
$M^1 a_p$	0.377	0.089	4.258	<0.001
Matched LEH (Present)	0.706	0.128	5.520	<0.001
$M^1 a_p$ * Matched LEH	-0.428	0.115	-3.715	<0.001

Table 8.37 Regression of log transformed estimates of age-at-death in skeletally immature individuals with scaled $M^1 a_p$ scores and additional predictor variables.

	Coefficient	Std error	*t*	p
Constant	1.856	0.095	19.56	<0.001
$M_1 a_p$	0.101	0.043	2.330	0.023
Matched LEH (Present)	0.431	0.089	4.828	<0.001
Site (SH)	0.296	0.149	1.985	0.052
Site (WS)	0.074	0.121	0.611	0.543
Site (YB)	0.426	0.115	3.686	<0.001

Table 8.38 Regression of log transformed estimates of age-at-death in skeletally immature individuals with scaled $M_1 a_p$ scores and additional predictor variables.

Given that the skeletally mature cohort had already been associated with a higher prevalence of LEH (Section 8.2.3.1), the positive contribution made by matched LEH to models could indicate that its presence is a marker of robustness (i.e., the capacity to endure stress) (Graham *et al.* 2010: 496; Holling 1973: 17). On on the other hand, as in both models higher a_p scores and matched LEH presence were associated with a longer length of life, it might be inferred that elevated early-life and childhood stress had a positive effect on survival during development. However, as the interaction of the two in the M^1 sample suggested a reduction in length of life, it supported the hypothesis posed in Section 8.2.3.1 that there was a complicated relationship between the volume and intensity of stress experience and later outcomes. When plotting residuals against predicted values, it was noted that variance decreased moderately as age increased. However, quantile-quantile plots suggested that residuals approximated a normal distribution. So, although factors not included influenced length of life within the skeletally immature cohort, the model was reasonably good and R^2 scores indicated a considerable proportion of variation (39-40%) had successfully been explained, inferring the patterns identified were meaningful (Figure 8.33-8.34). It was, however, wondered if the relationship between perinates/infant age-at-death and FA would conform to the same pattern. Unfortunately, due to the sampling procedure, this cohort was not well-represented in the sample (Section 5.6).

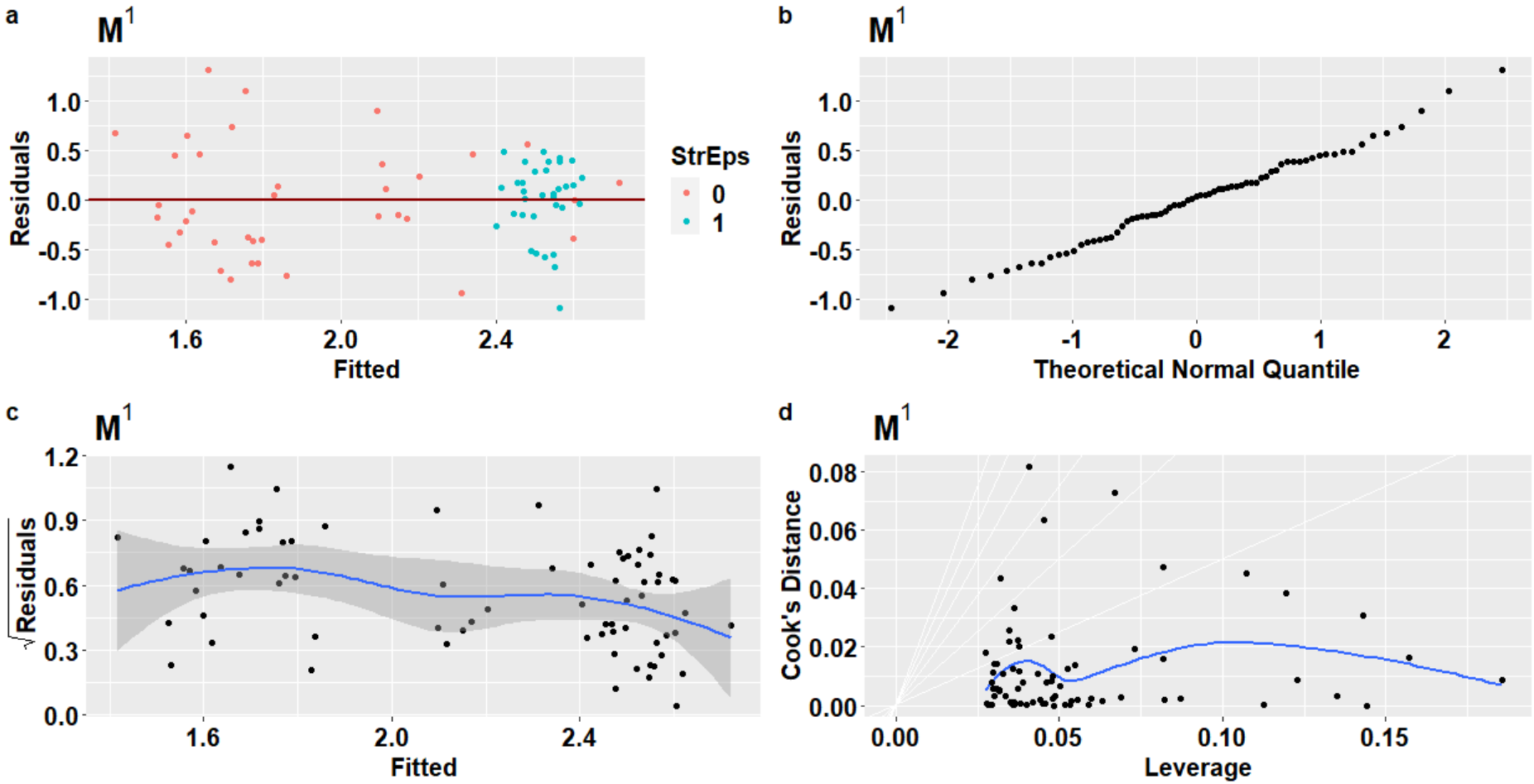

Figure 8.33 Diagnostic plots of residuals from the improved regression model for the M[1] sample in which scaled a_p scores, chronologically matched LEH and the interaction of the two have been used to predict age among skeletally immature individuals. Residual variance is plotted against the model's line of best fit (red line) with individuals identified as to whether matched LEH were absent (0) or present (1) (a); residuals compared to a normal distribution (b); a scale-location plot to assess homoscedasticity (c); Cook's distances employed to identify outlying residuals.

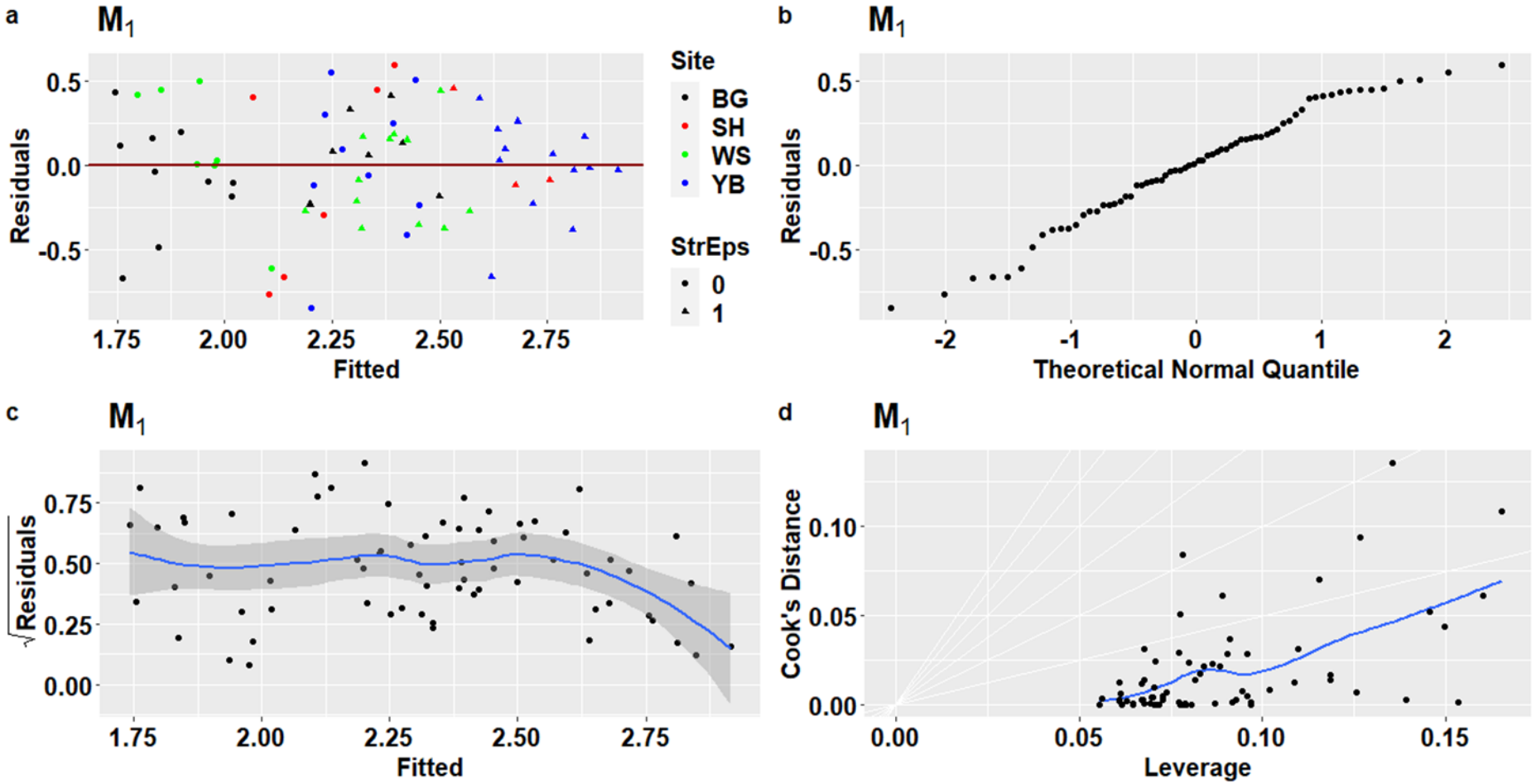

Figure 8.34 Diagnostic plots of residuals from the improved regression model for the M_1 sample in which scaled a_p scores, site and the presence of chronologically matched LEH have been used to predict age among skeletally immature individuals. Residual variance is plotted against the model's line of best fit (red line) with individuals identified according to site and whether matched LEH were absent (0) or present (1) (a); residuals compared to a normal distribution (b); a scale-location plot to assess homoscedasticity (c); Cook's distances employed to identify outlying residuals.

8.4.2 Growth and Development

Strong sex and age-related patterns in growth and development were inferred in Section 8.2.2, but suggestions have been made that other factors may also have been influential. Regression procedures were therefore employed to investigate further.

8.4.2.1 Mature Long Bone Lengths

Fluctuating asymmetry proved to be a poor predictor of long bone growth and M1 a_p scores failed to make significant contributions to regression analyses. For example, despite the fact that tibial growth is often regarded as comparatively stress-sensitive (e.g., Pomeroy *et al.* 2012), scaled M^1 ($F(1,24)=0.239$, $p=0.629$) and M_1 a_p scores ($F(1,26)=0.568$, $p=0.458$) could not be employed to explain variance in tibial length. As such, contrary to expectations, no substantial connection was detected between osteological measures of mature growth and FA, inferring that growth outcomes were not determined by early-life stress signals transmitted across the mother-child nexus.

In contrast, sex and chronologically matched LEH explained growth outcomes much better (although too few intact fibula were present for this element to be explored effectively). Sex was a predictor in all models, while matched LEH presence made a significant contribution to those for femoral, tibial and humeral length (Table 8.39-Table 8.43). As expected, coefficients demonstrated that sexual dimorphism had the greatest impact on long bone lengths – e.g., male femora were estimated to have been 53.9 mm (95% CI [40.1, 67.9]) longer than female femora. Nevertheless, it was found that matched LEH presence predicted shorter bone lengths. For instance, matched LEH presence was associated with a reduction in tibial length by 17.6 mm (95% CI [3.0, 32.3]). Overall, these models accounted for long bone lengths reasonably well, explaining 49-64% of variation. As posited in Section 8.2.2, sexual dimorphism was the most significant factor.

However, the contribution of matched LEH to models suggested that elevated childhood stress was associated with reduced growth in the larger skeletal elements.

	Coefficient	Std error	*t*	p
Constant	429.823	6.720	63.958	<0.001
Sex (Male)	53.989	6.934	7.786	<0.001
Matched LEH (Present)	-22.441	7.317	-3.067	0.004

Table 8.39 Femoral length was predicted by sex and matched LEH ($F(2,33)=31.49$, p=<0.001, $R^2=0.64$).

	Coefficient	Std error	*t*	p
Constant	347.093	6.222	55.782	<0.001
Sex (Male)	44.577	7.314	6.094	<0.001
Matched LEH (Present)	-17.623	7.314	-2.409	0.023

Table 8.40 Tibial length was predicted by sex and matched LEH ($F(2,28)=18.69$, p=<0.001, $R^2=0.54$).

	Coefficient	Std error	*t*	p
Constant	316.324	4.917	64.338	<0.001
Sex (Male)	32.020	5.358	5.976	<0.001
Matched LEH (Present)	-19.523	5.430	-3.595	<0.001

Table 8.41 Humeral length was predicted by sex and matched LEH ($F(2,39)=20.41$, p=<0.001, $R^2=0.49$).

	Coefficient	Std error	*t*	p
Constant	222.933	2.666	83.619	<0.001
Sex (Male)	26.867	3.770	7.126	<0.001

Table 8.42 Radial length was predicted by sex only ($F(1,28)=50.78$, p=<0.001, $R^2=0.63$).

	Coefficient	Std error	*t*	p
Constant	237.545	3.419	69.488	<0.001
Sex (Male)	29.749	4.387	6.781	<0.001

Table 8.43 Ulna length was predicted by sex only ($F(1,26)=45.98$, p=<0.001, $R^2=0.63$).

8.4.2.2 Diaphyseal Lengths and Developmental Tempo

Unsurprisingly, regression models demonstrated that age best explained diaphyseal lengths in the skeletally immature cohort (though again there were too few whole fibulae for this element to be included in analyses). Except for the femur and tibia, R^2 values from regression analyses indicated that >90% of variation was accounted for by age alone (Table 8.44-Table 8.48). Femoral diaphyseal lengths were, however, better explained with the incorporation of matched LEH presence into the model; other factors (i.e., age) being held constant, individuals with matched LEH were estimated to have femora that were shorter by 31.5 mm (95% CI [3.7, 59.3]). Similarly, tibial length was more accurately modelled through the inclusion of a stress marker; PNBF presence was associated with an age-independent growth deficit of 18.3 mm (95% CI [1.9, 34.8]).

Although the addition of these terms to the regression models only increased the percentage of variation explained from 91% to 93% in the case of the femur and 89% to 91% for the tibia, they do account for a substantial proportion (*circa* 20-30%) of variance not attributable to differences in age. It was therefore inferred that lower limb growth during development was vulnerable to elevated childhood stress.

	Coefficient	Std error	*t*	p
Constant	94.556	11.111	8.510	<0.001
Age	20.500	1.563	13.112	<0.001
Matched LEH (Present)	-31.502	13.891	-2.268	0.034

Table 8.44 Regression of femoral diaphyseal length on age and matched LEH presence (F(2,20)=142.7, p=<0.001, R^2=0.93).

	Coefficient	Std error	*t*	p
Constant	95.17	8.726	10.91	<0.001
Age	13.81	0.902	15.31	<0.001
PNBF (Present)	-18.33	8.241	-2.220	0.037

Table 8.45 Regression of tibial diaphyseal length on age and PNBF presence (F(2,21)=117.3, p=<0.001, R^2=0.91).

	Coefficient	Std error	*t*	p
Constant	85.38	5.855	14.58	<0.001
Age	11.89	0.500	23.76	<0.001

Table 8.46 Regression of humeral diaphyseal length on age (F(1,23)=564.7, p=<0.001, R^2=0.95).

	Coefficient	Std error	*t*	p
Constant	67.73	5.484	12.35	<0.001
Age	8.250	0.524	15.73	<0.001

Table 8.47 Regression of radial diaphyseal length on age (F(1,21)=247.5, p=<0.001, R^2=0.92).

	Coefficient	Std error	*t*	p
Constant	68.84	6.900	9.975	<0.001
Age	9.593	0.706	13.59	<0.001

Table 8.48 Regression of ulna diaphyseal length on age (F(1,11)=184.6, p=<0.001, R^2=0.94).

When attempting to ascertain which factors influenced pubertal development, cases were identified which suggested early-life stress may have influenced tempo. For example, SK 268, the individual highlighted previously as evidencing a substantial delay in maturation, had an M^1 a_p score of 1.002436 (after log transformation and scaling, this produced a standardised score of 1.67) which fell beyond the upper quartile of M^1 values. However, the search for statistical connections between stress markers and pubertal stage was not successful. There were too few individuals in each stage to treat them separately, necessitating that categories were collapsed. Assigning skeletons to either a 'pre-PHV' or

'post-PHV' group, however, resulted in a dramatic loss of resolution and it is suspected this confounded further quantitative exploration.

However, as several skeletally immature individuals were associated with age estimates that inferred they were in their twenties (i.e., an age when long bone epiphyses would normally be fused), it was theorised that the attainment of maturity more generally was affected by other factors (e.g., early-life stress) in addition to age. Binary logistic regression was performed to investigate further. Unsurprisingly, age alone was a highly significant predictor of whether an individual was skeletally mature or not (χ^2=258.0, p=<0.001, R^2=0.86) (Table 8.49). However, it was also found that M_1 scores made a significant contribution to the model (χ^2=184.96, p=<0.001, R^2=0.91), with coefficients demonstrating that higher a_p scores were associated with the immature cohort (Table 8.50). Interactions between the two factors were not significant and the presence of matched LEH also failed to make a significant contribution to the model. A comparison of McFadden's R^2 indicated that although age on its own could accounted for the majority of variation in skeletal development, the addition of M_1 a_p scores to the model helped to explain *circa* 5% more variation. Although M^1 scores were not a significant predictor of maturity, they also produced a negative coefficient (-1.223). Overall, this consistently suggested that early-life stress influenced delays to somatic development.

	Coefficient	Std error	*z*	p
Constant	-17.591	4.380	-4.017	<0.001
Age	0.896	0.224	3.991	<0.001

Table 8.49 Logistic regression with estimated age predicting whether an individual was skeletally immature (0) or mature (1).

	Coefficient	Std error	*z*	p
Constant	-19.086	6.103	-3.127	0.002
Age	0.971	0.308	3.149	0.002
M_1 a_p	-1.621	0.773	-2.098	0.036

Table 8.50 Logistic regression with estimated age and scaled M_1 a_p scores predicting whether an individual was skeletally immature (0) or mature (1).

8.4.3 Later-life Stress Experience: Comorbidities, Resilience and Frailty

Early-life stress has been implicated in later-life ill-health (e.g., Gowland 2015; Barker 2012). To further investigate, binary logistic regression was employed to ascertain whether FA is associated with other stress markers and whether a_p scores can be employed to predict either their presence or absence. As it was hypothesised in Section 8.2.3 that factors influencing stress marker development beyond site, sex and age/maturity may be more clearly detected through the distribution, severity and activity of lesions, these characteristics were also considered.

8.4.3.1 LEH Presence

Through binary logistic regression, it was found that LEH presence could not be predicted with scaled M^1 (χ^2=0.358, p=0.550) or M_1 a_p scores (χ^2=0.10, p=0.920). The presence or absence of LEH could, to an extent, be explained by site (χ^2=11.649, p=0.008, R^2=0.04) with coefficients inferring a 72.4% (95% CI [35.0, 88.3]) reduction in the relative risk of developing LEH for individuals at South Shields in comparison to those at Black Gate (Table 8.51). Similarly, the presence of chronologically matched LEH was not predicted by scaled M^1 (χ^2=2.966, p=0.085) or M_1 a_p scores (χ^2=0.162, p=0.687). However, in addition to site, sex also made a significant contribution to the regression model (χ^2=203.7, p=<0.001, R^2=0.67). Again, there were significant differences between the South Shields and Black Gate assemblages and an odds ratio of 2.83 (95% CI [1.03, 7.80]) inferred that males were at a higher risk of developing matched LEH than females (Table 8.52). As this model accounted for a substantial proportion of variation (i.e., *circa* 67%), it supported the suppositions advanced in Section 8.2.3 that site-specific influences shaped differentials in frailty and that males were more vulnerable to childhood stress.

	Coefficient	Std error	*z*	p
Constant	0.859	0.239	3.598	<0.001
Site (SH)	-1.289	0.429	-3.007	0.002
Site (WS)	0.153	0.477	0.321	0.748
Site (YB)	-0.011	0.354	-0.032	0.974

Table 8.51 Regression of LEH absence (0) and presence (1) on site.

	Coefficient	Std error	*z*	p
Constant	0.750	0.506	1.486	0.137
Site (SH)	-2.390	0.754	-3.170	<0.001
Site (WS)	-0.885	0.902	-0.982	0.326
Site (YB)	-0.837	0.581	-1.440	0.150
Sex (Male)	1.040	0.507	2.051	0.040

Table 8.52 Regression of chronologically matched LEH absence (0) and presence (1) on site.

8.4.3.2 Periodontal Disease

Higher M^1 a_p scores (χ^2=4.160, p=0.041, R^2=0.02) were associated with PD absence (Table 8.53). However, the model could only account for a small proportion of variation (i.e., *circa* 2%) and there was no significant relationship between PD and M_1 a_p scores (χ^2=1.452, p=0.228). As it had been established that PD was more commonly recorded in mature skeletons, who also generally had significantly lower FA, it seemed likely that the relationship between M^1 a_p scores and PD absence was specious. Skeletal maturity was better able to predict PD presence (χ^2= 82.40, p=<0.001, R^2=0.28) (Table 8.54), with an odds ratio of 16.2 (95% CI [8.04, 32.7]) suggesting that degeneration of the alveolar margin was an age-dependent process with older, mature individuals being more vulnerable.

	Coefficient	Std error	*z*	p
Constant	-0109	0.164	-0.668	0.504
M^1 a_p	-0.339	0.170	-1.993	0.046

Table 8.53 Regression of PD absence (0) and presence (1) on scaled M^1 a_p scores.

	Coefficient	Std error	*z*	p
Constant	-1.781	0.279	-6.380	<0.001
Maturity (mature)	2.786	0.351	7.930	<0.001

Table 8.54 Regression of PD absence (0) and presence (1) on skeletal maturity (i.e., whether an individual was skeletally immature or mature).

As it was speculated in Section 8.2.3.3 that exploring the severity of PD expression may be informative, skeletons absent PD were grouped with those that only expressed mild signs of the disease, while moderate and severe cases were combined. When binary logistic regression was performed to discern which factors predicted the presence of the more severe manifestations of the stress marker, it was found that in addition to age, the presence of PNBF and site were also significant explanatory variables (χ^2=73.759, p=<0.001, R^2=0.53) (Table 8.55). Odds ratios of 6.55 (95% CI [1.54, 27.8]) and 9.25 (95% CI [1.70, 50.2]) suggested the chances of developing moderate-to-severe PD were significantly higher for individuals with PNBF and those originating from South Shields. This analysis implied that contextual factors influenced severity of expression and that PD and PNBF were either associated with shared risk factors or the same underlying pathological processes.

	Coefficient	Std error	*z*	p
Constant	-5.798	1.016	-5.709	<0.001
Age	0.074	0.018	4.032	<0.001
PNBF (Present)	1.879	0.723	2.600	0.009
Site (SH)	2.225	0.846	2.630	0.008
Site (WS)	0.404	1.104	0.366	0.714
Site (YB)	-1.460	0.957	-1.525	0.127

Table 8.55 Regression of PD presence, when absent and mild cases are grouped together (0) and moderate and severe cases combined (1), on various factors.

8.4.3.3 Metabolic Deficiency: Cribra Orbitalia and Scurvy

Maturity and site were significant predictors of CO presence (χ^2=34.91, p=<0.001, R^2=0.15) (Table 8.56), as speculated in Section 8.2.3.2. An odds ratio of 0.17 (95% CI [0.08, 0.35]) indicated that in comparison to skeletally immature individuals the risk of mature skeletons exhibiting CO were significantly lower and that age-related vulnerability was key in lesion development. An odds ratio of 2.31 (95% CI [1.01, 5.26]) further suggested that the population of York Barbican was at a higher risk of developing CO than that of Black Gate.

	Coefficient	Std error	z	p
Constant	0.992	0.340	2.721	0.007
Maturity (mature)	-1.775	0.361	-4.913	<0.001
Site (SH)	-0.480	0.545	-0.880	0.379
Site (WS)	0.098	0.542	0.182	0.856
Site (YB)	0.837	0.412	2.031	0.042

Table 8.56 Regression of CO absence (0) and presence (1) on skeletal maturity and site .

Higher a_p scores were also generally found to be associated with CO presence (Table 8.57-Table 8.58). While a significant association could not be found between CO and M_1 a_p scores (χ^2=1.325, p=0.249), scaled M^1 a_p values were significant predictors of lesion presence (χ^2=5.355, p=0.021, R^2=0.03) with a positive coefficient indicating that higher M^1 FA was associated with an increased risk of developing CO (Table 8.59). This observation should be interpreted cautiously, however. As CO can only develop in skeletally immature individuals (Brickley 2018: 898) and early-life stress was believed to significantly increase mortality risk for this cohort, the connection between high a_p scores and CO may be spurious. Despite this, among the individuals with CO, the upper range and mean a_p scores were higher for the group with active or mixed lesions (Table 8.60-Table 8.61). In this instance, however, statistical significance was not achieved with scaled M^1 a_p scores (χ^2=0.178, p=0.673) but with M_1 scores and skeletal maturity (χ^2= 23.544, p=<0.001, R^2=0.37) (Table 8.62); an odds ratio of 4.89 (95% CI [1.78, 13.4]) inferred a one-unit increase in M_1 a_p scores was associated with a significantly higher risk of individuals exhibiting active lesions. In sum, the relationship between FA and CO was variable, but did hint at connections between maternally-mediated early-life stress, metabolic deficiency and resilience.

CO	No.	Min	Q1	Median	Mean	Q3	Max	Std dev
Absent	58	1.000396	1.000672	1.001065	1.001162	1.001347	1.002863	0.000600
Present	70	1.000384	1.000853	1.001202	1.001447	1.001936	1.003410	0.000766

Table 8.57 A summary of M^1 a_p scores for individuals without and with CO.

CO	No.	Min	Q1	Median	Mean	Q3	Max	Std dev
Absent	53	1.000477	1.001239	1.001496	1.001731	1.002315	1.003330	0.000756
Present	55	1.000497	1.001311	1.001764	1.001903	1.002477	1.003591	0.000804

Table 8.58 A summary of M_1 a_p scores for individuals without and with CO.

	Coefficient	Std error	z	p
Constant	0.193	0.182	1.065	0.288
M^1 a_p	0.413	0.185	2.229	0.026

Table 8.59 Regression of CO absence (0) and presence (1) on M^1 a_p scores.

CO	No.	Min	Q1	Median	Mean	Q3	Max	Std dev
A/M	19	1.000421	1.000995	1.001162	1.001510	1.002140	1.003410	0.000820
Healed	51	1.000384	1.000767	1.000124	1.001423	1.001921	1.003266	0.000752

Table 8.60 A summary of M^1 a_p scores for individuals with active/mixed (A/M) and healed CO.

CO	No.	Min	Q1	Median	Mean	Q3	Max	Std dev
A/M	15	1.001249	1.001972	1.002693	1.002571	1.003135	1.003591	0.000795
Healed	40	1.000497	1.001169	1.001538	1.001653	1.002004	1.003033	0.000657

Table 8.61 A summary of M_1 a_p scores for individuals with active/mixed (A/M) and healed CO.

	Coefficient	Std error	z	p
Constant	-0.805	0.439	-1.836	0.066
M_1 a_p	1.587	0.504	3.150	0.002
Maturity (mature)	-2.801	1.234	-2.270	0.023

Table 8.62 Regression of active/mixed (0) and healed CO (1) on scaled M_1 a_p scores and skeletal maturity.

When specific metabolic conditions were considered in relation to FA, it was found that a_p scores were usually lower among individuals diagnosed with scurvy (Table 8.63-Table 8.64 and Figure 8.35). Although the small number of individuals involved demands cautious interpretation, these results suggested that the chances of surviving severe metabolic deficiency long enough to develop diagnostic skeletal lesions may have been enhanced if developmental stress was low. This further supports the notion of a link between early-life experience and resilience.

Disease	No.	Min	Q1	Median	Mean	Q3	Max	Std dev
Absent	148	1.000369	1.000792	1.001186	1.001313	1.001778	1.003410	0.000679
Present	6	1.000396	1.000782	1.000903	1.001079	1.001110	1.002351	0.000672

Table 8.63 A summary of M^1 a_p scores for individuals diagnosed with scurvy.

Disease	No.	Min	Q1	Median	Mean	Q3	Max	Std dev
Absent	146	1.000477	1.001261	1.001740	1.001910	1.002584	1.003846	0.000801
Present	2	1.000487	1.000489	1.000492	1.000492	1.000494	1.000497	0.000695

Table 8.64 A summary of M_1 a_p scores for individuals diagnosed with scurvy.

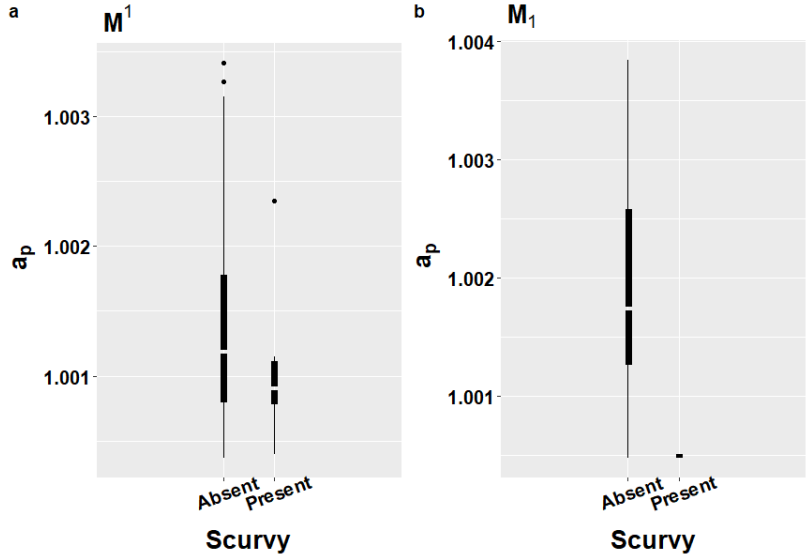

Figure 8.35 A comparison of M^1 (a) and M_1 a_p scores (b) between individuals with evidence of a scurvy in comparison to those without.

8.4.3.4 Periosteal New Bone Formation and Specific Infection

The presence or absence of PNBF could not be predicted with scaled M^1 (χ^2=0.137, p=0.711) or M_1 a_p scores (χ^2=1.255, p=0.262). Estimated age and site were in contrast significant predictors of PNBF presence (χ^2=37.171, p=<0.001, R^2=0.16) (Table 8.65). While increasing age was associated with an increased risk of developing PNBF, an odds ratio of 2.63 (95% CI [1.17, 5.91]) inferred the chances of skeletons exhibiting PNBF were also significantly higher in the York Barbican assemblage than the Black Gate. Site-specific influences and age therefore seem to affect vulnerability to PNBF.

	Coefficient	Std error	z	p
Constant	-1.971	0.394	-5.002	<0.001
Age	0.024	0.009	2.562	0.010
Site (SH)	0.490	0.561	0.874	0.382
Site (WS)	0.502	0.576	0.871	0.384
Site (YB)	0.968	0.404	2.393	0.012

Table 8.65 Regression of PNBF absence (0) and presence (1) on age and site.

Age was also a predictor of PNBF activity (χ^2=9.997, p=0.002, R^2=0.14) with positive coefficients inferring older individuals were more likely to be associated with healed/inactive lesions (Table 8.66). Though perhaps influenced by the moderately higher rates of active lesions in the immature cohort and its association with elevated a_p scores, there also appeared to be a relationship between FA and lesion activity. Although the association was not sufficiently distinct to achieve statistical significance with either M^1 (χ^2=1.823, p=0.177) or M_1 (χ^2=3.347, p=0.067) scores, as noted with CO, higher average a_p scores were found among the individuals with active lesions and lower average scores were seen among those with healed/inactive lesions. As well as justifying the speculation that important patterns may be discerned in the characteristics (e.g., activity and distribution) of periosteal lesions, these results again linked early-life experience with resilience and the ability to recover from perturbations to health (Table 8.67-Table 8.68 and Figure 8.36).

	Coefficient	Std error	z	p
Constant	-1.930	0.651	-2.965	0.003
Age	0.038	0.0170	2.229	0.026

Table 8.66 Regression of active/mixed (0)and healed PNBF (1) on age.

PNBF	No.	Min	Q1	Median	Mean	Q3	Max	Std dev
A/M	28	1.000396	1.000792	1.001192	1.001343	1.001642	1.002840	0.000695
Healed	10	1.000384	1.000628	1.000986	1.001034	1.001273	1.002185	0.000529

Table 8.67 A summary of M^1 a_p scores for individuals with active/mixed (A/M) and healed PNBF.

PNBF	No.	Min	Q1	Median	Mean	Q3	Max	Std dev
A/M	25	1.000487	1.001463	1.002329	1.002188	1.002946	1.003846	0.000932
Healed	12	1.000477	1.000882	1.001424	1.001604	1.002341	1.002882	0.000859

Table 8.68 A summary of M_1 a_p scores for individuals with active/mixed (A/M) and healed PNBF.

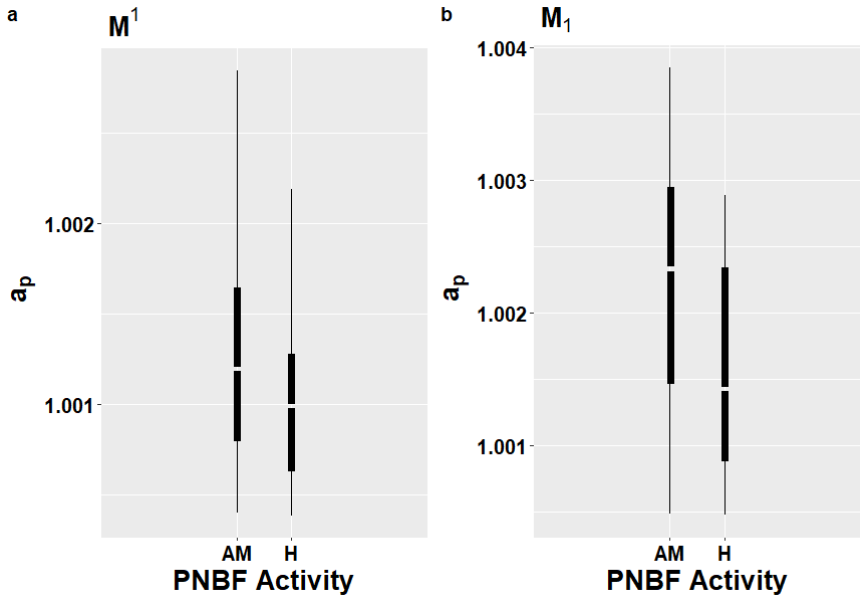

Figure 8.36 A comparison of a_p scores between individuals with active/mixed (A/M) and inactive, healed (H) PNBF.

Further patterns between FA and PNBF emerged when the distribution of lesions was considered. Despite small sample sizes inhibiting the detection of a statistically significant association between scaled M^1 (χ^2=1.882, p=0.170) or M_1 (χ^2=2.220, p=0.136) scores and PNBF distribution, higher a_p scores were found among individuals with bilaterally rather than unilaterally distributed PNBF (Table 8.69-Table 8.70 and Figure 8.36). Again though, the association of the immature cohort with slightly higher rates of bilateral PNBF as well as elevated FA should not be forgotten as a potentially complicating factor. Despite this caveat, given the appreciably higher FA among individuals with bilateral PNBF and the connection between diffuse periosteal reactions and chronic systemic infection (Roberts 2019; Roberts and Buikstra 2019; Steckel *et al.* 2019: 418; DeWitte and Wood 2008: 1439; Weston 2008), it is suggested that maternally-mediated early-life stress was connected to infection in later-life. This supposition was supported by the discovery that the individuals diagnosed with specific

infections also had higher average a_p scores than those without (Table 8.71-Table 8.72 and Figure 8.37).

PNBF	No.	Min	Q1	Median	Mean	Q3	Max	Std dev
Unilateral	8	1.000567	1.000867	1.001007	1.001027	1.001146	1.001610	0.000321
Bilateral	25	1.000384	1.000770	1.001335	1.001390	1.002098	1.002840	0.000767

Table 8.69 A summary of M^1 a_p scores for individuals with unilaterally and bilaterally distributed PNBF.

PNBF	No.	Min	Q1	Median	Mean	Q3	Max	Std dev
Unilateral	7	1.000493	1.001052	1.001349	1.001561	1.002195	1.002593	0.000783
Bilateral	23	1.000477	1.001477	1.002394	1.002175	1.002914	1.003846	0.001005

Table 8.70 A summary of M_1 a_p scores for individuals with unilaterally and bilaterally distributed PNBF.

Infection	No.	Min	Q1	Median	Mean	Q3	Max	Std dev
Absent	147	1.000369	1.000791	1.001175	1.001302	1.001779	1.003410	0.000680
Present	7	1.000574	1.000869	1.001335	1.001362	1.001674	1.002539	0.000671

Table 8.71 A summary of M^1 a_p scores for individuals diagnosed with a specific infection.

Infection	No.	Min	Q1	Median	Mean	Q3	Max	Std dev
Absent	144	1.000477	1.001253	1.001736	1.001878	1.002523	1.003591	0.000792
Present	4	1.000497	1.001696	1.002562	1.002367	1.003232	1.003846	0.001436

Table 8.72 A summary of M_1 a_p scores for individuals diagnosed with a specific infection.

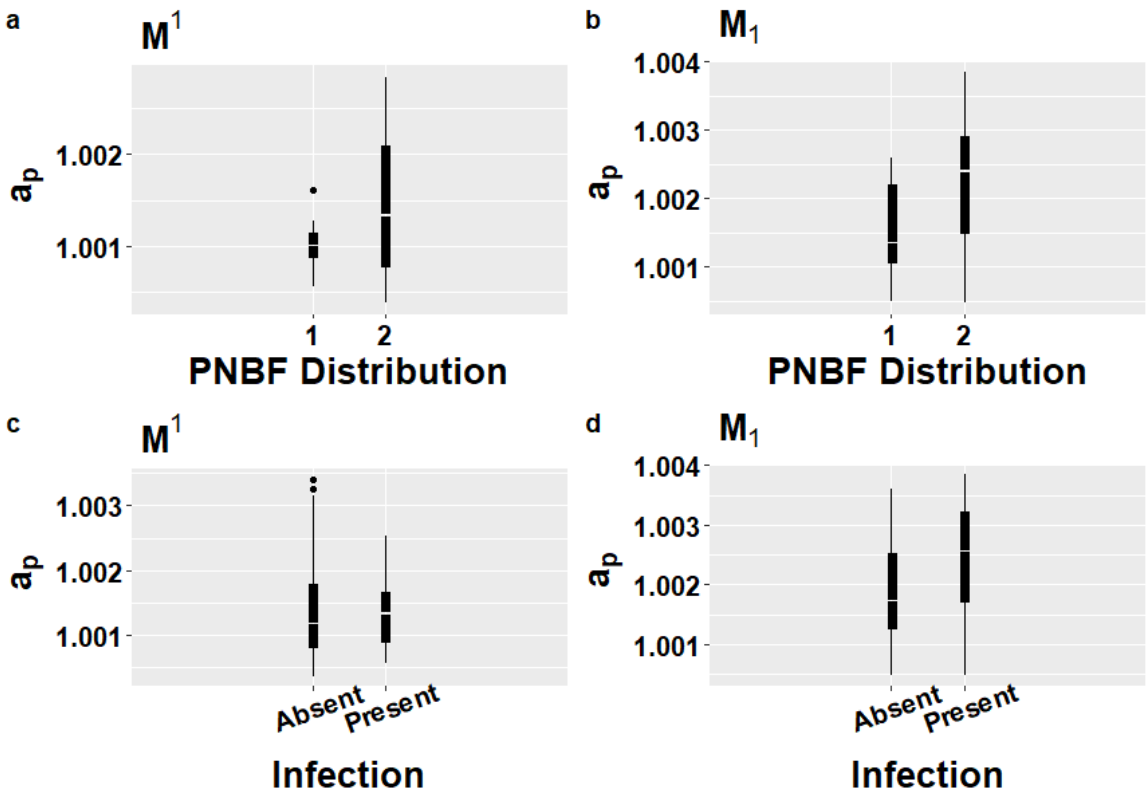

Figure 8.37 A comparison of a_p scores between individuals with unilateral (1) and bilaterally (2) distributed PNBF (a-b) as well as those with evidence of a specific infectious disease (c-d).

8.5 Conclusion

From the osteological data, several demographic and pathological patterns emerged. Some were site-specific, such as the indicators of severe non-specific stress and evidence of infectious disease at Warwick. Differences between sexes were also observed; for instance, LEH were more common amongst males, while females lived longer. Meanwhile, CO and PD were associated with skeletally immature and mature cohorts respectively. Consequently site, sex and age were effective predictors of many stress markers.

Fluctuating asymmetry was successfully identified and isolated. It was also possible to explore the locations at which stress-induced deviations to symmetry were discovered and quantify the impact of potentially confounding variables. Differences between sites and sexes in measures of fluctuating asymmetry were found to be slight, while the disparity between skeletally immature and mature cohorts was more pronounced. The age-related trends within the immature group indicated a complicated relationship between early-life stress and survival. Moreover, elevated early-life stress may have delayed the attainment of skeletal and sexual maturity. There was, however, little evidence of a direct connection between FA and skeletal growth which was instead accounted for by sex and age, although childhood stress episodes may have caused lasting growth deficits. Subtle but consistent differences were inferred in the asymmetry scores of individuals with healed and active pathological lesions plus specific conditions and chronic systemic infection, suggesting that early-life experience impacted later-life frailty and resilience.

This points towards several themes of discussion, including: 1) the factors that define life-course trajectories, especially the role mothers played in mediating

environmental stressors, 2) the impact stressors experienced during critical periods have on specific life-course outcomes and their potential adaptive significance, 3) the developmental mechanisms through which early-life stress is embodied, and 4) the limitations in the method developed for this project and potential means through which it could be improved.

Chapter 9: Discussion

9.1 Introduction

This chapter begins by discussing the contextually dependent environmental and sociocultural factors underlying stress and the role mothers played in mediating early-life stress for dependent offspring. This leads onto an exploration of the impact stressors experienced during critical periods had on life-course trajectories and the potential adaptive benefits of stress experienced during periods of phenotypic plasticity. The developmental mechanisms through which stress is embodied are also discussed, with reference to how these affect the accuracy of M1 FA as a proxy for early-life stress. Finally, the constraints encountered by the project are evaluated along with their implications, and suggestions for future improvements are made.

9.2 Life-course Factors

As discussed in Chapter 2, life-course theorists have postulated that context and links between individuals influence outcomes (e.g., Giele and Elder 2013: 9-10; Hendricks 2012: 229-230; Kuh *et al.* 2004; Elder 1994). Empirical research has supported this claim, demonstrating that 1) environments imprint themselves on their inhabitants (e.g., Nilsson *et al.* 2018; Skinner 2008), 2) early life is the time when external stimuli have the greatest impact (e.g., King *et al.* 2012; Roseboom *et al.* 2001; Lopuhaa *et al.* 2000; Ravelli *et al.* 1998) and 3) that mothers act as intermediaries between dependent offspring and the world (Cheverko 2021: 61; Agarwal 2016; Gowland 2015; Richardson *et al.* 2014). This section investigates the connections identified in this project between sociocultural environment, stress experience, and the mother-child nexus.

9.2.1 Context: Environmental Imprints

To begin with, the extent to which site-specific influences imprinted themselves on the skeleton is discussed. Consideration is also made of the sociocultural dynamics that may have mitigated, modulated or magnified stress experience.

9.2.1.1 Black Gate

Three skeletally immature individuals from Black Gate exhibited lesions *consistent with* a diagnosis of scurvy. This indicates that portions of the population endured severe nutritional deficiency during childhood over a sufficiently long period of time for osteological markers of specific metabolic disease to develop (Brickley and Mays 2019; Newman 2016: 110; Snoddy *et al.* 2016; Mays 2014; Geber and Murphy 2012; Mahoney-Swales and Nystrom 2009; Mays *et al.* 2006; Pinhasi *et al.* 2006; Ortner 2003: 383-404). Although the lesions are to an extent indicative of survival despite chronic insufficiency (DeWitte and Stojanowski 2015: 405; Wood *et al.* 1992: 356-357), the supposition of severe metabolic stress among a subset of the sample also helps to explain the patterns noted in the prevalence of another marker of childhood metabolic stress, namely CO. Specifically, even though the more severe, Grade 2 lesions were relatively common among the individuals with CO (CPR=51.5%), CO was less frequently encountered at Black Gate (CPR=47.1%) than other sites. In fact, an odds ratio of 2.31 (95% CI [1.01, 5.26]) indicated that individuals from York Barbican were at a significantly greater risk of developing CO. From the evidence it can be inferred that, although potentially severe when experienced, metabolic insufficiency was comparatively uncommon. As it has been posited that the site was a focal point for a collection of rural settlements (Mahoney Swales 2012; Nolan *et al.* 2010: 249; Boulter and Rega 1993: 8), it is speculated that periods of severe deficiency in a small number of individuals could relate to seasonal availability of food with shortages potentially left unmitigated due to

lack of socioeconomic connectivity within a dispersed network of communities. Despite this, average M1 a_p scores were similar to those from South Shields and York Barbican, LEH crude prevalence (CPR=70.2%) rate was comparable to those calculated for the Warwick and York Barbican and the percentage of individuals exhibiting matched LEH (CPR=58.3%) was considerably lower than at Warwick (CPR=66.7%). Therefore, for the majority of the Black Gate sample, early life and childhood stress experience appears to have been relatively unexceptional.

The osteological evidence could also be construed as suggesting that later-life stress was not as pronounced for the population in comparison to the other sites assessed here. The lowest crude (CPR=19.2%) and true prevalence rates (TPR=7.2%) for PNBF were found in the Black Gate assemblage and an odds ratio of 2.63 (95% CI [1.17, 5.91]) inferred skeletons from York Barbican were significantly more likely to exhibit such lesions. The lowest rates of active PNBF (CPR=60.0%) were also found in the Black Gate sample and Grade 4 lesions were not observed at all. Cumulatively, this suggested periosteal reactions were more likely to be resolved before becoming severe than at other sites inferring greater resilience and, given that healed lesions have been associated with enhanced survival (e.g., DeWitte 2014b), decreased mortality risk. Similarly, the true prevalence of PD was relatively low (TPR=34.1%), the most severe manifestations of the disease were completely absent, and an odds ratio of 9.25 (95% CI [1.70, 50.2]) suggested that individuals from South Shields were at a significantly higher risk of developing PD. As both stress markers had a significant association with age and skeletal maturity, it appears that older individuals within the Black Gate population were relatively resilient in the face of later-life physiological perturbations.

The fact that individuals from Black Gate are in large part responsible for the spike in mortality among males in their early-to-mid-twenties was therefore slightly incongruous. However, as it has been hypothesised that in more highly stressed contexts frailer individuals perish before reaching maturity (Zoëga and Murphy 2016: 580), it is proposed that among the skeletons that reached maturity at Black Gate there were frailer members of the living population that would not have survived elsewhere. As it has been theorised that the community was relatively egalitarian and that status was acquired in life (i.e., through involvement in agriculture or craft production) (e.g., Mahoney Swales 2019: 216; Mahoney Swales 2012: 416), it is tempting to speculate that less pronounced structural inequalities created an environment that promoted health for most of the population (Galtung 1969). This conjecture must be treated cautiously, however, as the supposition of an egalitarian community was made based on funerary investment and the variety in burial type and grave goods suggests this was not determined by a single set of conventions (Nolan *et al.* 2010: 204-223). Signals derived from the funerary evidence may therefore be mixed and generalisations based on them could be overly simplistic.

9.2.1.2 South Shields

The osteological evidence could suggest, if interpreted without reference to the Osteological Paradox (discussed two paragraphs below), that the individuals from South Shields had the least stressful childhoods. South Shields was the only assemblage where ≤70% of the skeletons exhibited LEH (CPR=39.4%) and had by far the lowest prevalence of matched LEH presence (CPR=27.3%). It was estimated through regression analyses that there was a 72.4% (95% CI [35.0, 88.3]) reduction in the relative risk of developing LEH if individuals came from South Shields rather than Black Gate. Similarly, CO was comparatively uncommon (CPR=34.8%), especially when compared to Warwick and York Barbican where the crude prevalence rates exceeded 60%. These low prevalence

rates are surprising given that past research has evidenced a significant increase in LEH prevalence during the Industrial period in many European samples (Bereczki *et al.* 2019: 182-184) and historical sources indicate the environment at South Shields was very poor (Figure 9.1). For instance, records talk of factories emitting "injurious" fumes which covered the town in a pall of smoke (Report of the Commissioners 1845: 185). This likely contributed to maxillary sinusitis rates that were more than twice as high as the average for post-medieval cities as well as conditions such as phossy jaw (Roberts *et al.* 2016: 44; Raynor *et al.* 2011; Marx 2008). Nevertheless, it is unlikely that the prevalence rates of childhood stress markers presented here are underestimates; previous analyses have also found low rates of developmental stress markers such as LEH and CO (e.g., Newman *et al.* 2019; Raynor *et al.* 2011: 53-79).

Figure 9.1 The Tyneside area was home to a mixture of industries which included shipping, chemical refineries and collieries. The stress markers observed in the South Shields assemblage show evidence of this potentially noxious and high stress environment in skeletally mature individuals but not their immature counterparts. Image available from: https://northumbrian-words.com/2019/03/25/the-rags-to-riches-poet/.

Conversely, skeletally mature, older individuals at South Shields appear to have been relatively frail. As above, due to their association with skeletal maturity and

advancing age (Section 8.4.3), PD and PNBF are used to illustrate a later-life vulnerability to stress. Among the individuals with PNBF, those from South Shields had the highest rates of active lesions (CPR=85.7%) as well as the highest prevalence of the most severe Grade 3 (CPR=14.3%) and Grade 4 lesions (CPR=14.3%). Additionally, PD affected more individuals (CPR=51.5%) and alveolar sockets (TPR=51.5%) at South Shields than any other site and it was the only assemblage where more skeletons were affected by moderate-to-severe (CPR=58.8%) manifestations of the lesion than mild (CPR=41.2%). In fact, the odds of developing moderate-to-severe PD were 9.25 (95% CI [1.70, 50.2]) times greater at South Shields than Black Gate. Moreover, in addition to the one diagnosis of osteomyelitis, past research has identified syphilis and tuberculosis among adults in the full assemblage at rates higher than might be expected outside of hospital sites (Raynor *et al.* 2011: 68-69; Roberts and Cox 2003: 339-341; Boulter *et al.* 1998). As mentioned in Section 5.3.2, the rate of degenerative changes in the spine also exceeded the post-medieval average (Raynor *et al.* 2011: 64; Roberts and Cox 2003: 352). In sum, the skeletally mature population from South Shields were subjected to a variety of degenerative conditions, often with little evidence of healing (Crespo *et al.* 2021; Crespo *et al.* 2016; DeWitte and Bekvalac 2011; DeWitte and Bekvalac 2010; Ogden 2008: 288). This suggests a lifestyle that increased frailty in later-life and decreased resilience (DeWitte and Stojanowski 2015: 399; Wood *et al.* 1992: 357; DeWitte 2010: 8; Vaupel 1988: 277).

The incongruity between a supposed low-stress childhood and higher stress later-life has confounded past palaeopathological investigations and generated several possible explanations. With reference to the Osteological Paradox, previously it has been proposed that the children in the assemblage died as a result of acute perturbations to health before stress markers could develop (Newman *et al.* 2019: 116-117; Newman

2016: 198-199). The perception that stress experience during this stage of life was relatively low is therefore a consequence of osteological insensitivity and the cohort actually represents a group of highly stressed non-survivors (DeWitte and Stojanowski 2015: 416-418; Wood *et al.* 1992: 349). It has also been speculated that the town's role as a port gave children greater access to nutritional resources and, unlike in many other industrial cities, when they undertook work it was in outdoor activities such as ship-building which were putatively healthier than working in industries like cotton manufacturing (Newman *et al.* 2019: 116-117; Newman 2016: 198-199; Raynor *et al.* 2011: 106). Neither of these hypotheses is completely satisfying, however. If the population of South Shields was exposed to such extreme environmental stressors, M1 a_p scores should reflect that to some degree and this was not the case. Meanwhile, given contemporary descriptions of the harmful industrial pollutants that affected the air quality in South Shields and the Tyneside region (e.g., Report of the Commissioners 1845), it is wondered to what extent employment outdoors represented a significantly healthier mode of living than indoor work.

It is hypothesised here that post-medieval economic migration contributed to the apparent disconnect between childhood and later-life stress. During the Industrial Revolution, manufacturing cities underwent rapid expansion that could only be sustained through migration (Panayi 1995: 35; Friedlander 1992; Redford and Chaloner 1976: 132-137; Ravenstein 1885: 199). South Shields was no exception and by the 19th century the town was the home to a considerable number of incomers (Bland 2006: 68; Panayi 1995: 163). As well as adult migrants, rural children often relocated to urban centres to undertake apprenticeships and find employment (Gowland *et al.* 2018: 45; Pelling 1994; Sharpe 1991; Report of the Commissioners 1833: 12). Though the shift may have brought economic possibilities, it was often deleterious to health. Contemporaries observed that

"chronic diseases" and "irregular developments" were often seen after the "child from an agricultural district . . . blooming with rosy health, full of vitality, is transported to a crowded town . . . [where] it is exposed to miasmatic evaporations, shut up in a narrow street, its home is damp and cold, its food poor and badly cooked. . ." (Gaskell 1836: 157-158). It is thus proposed that young, healthy migrants supplemented the town's population and had their health transformed and diminished by the hazardous environment and demands of industrial labour – which even at the time was described as "exceedingly prejudicial to life" – leaving them vulnerable and less resilient to subsequent stressors (Buckley *et al.* 2021: 549; Buckley 2021; Sledzik and Sandberg 2002: 185-207; Gaskell 1836: 220). Given the quoted historical sources and that osteological investigations have found similar rates of childhood stress markers in other industrial assemblages (Raynor *et al.* 2011: 50-53; Boulter *et al.* 1998; Brickley *et al.* 2006) (Section 5.3.2), this explanation may be generalisable to other post-medieval sites. Whichever explanation (or combination thereof) is true, from a life-course perspective the assemblage clearly articulates that life-course outcomes are not always dependent on developmental experiences.

9.2.1.3 Warwick

The data suggest that the population of medieval Warwick endured high levels of stress which negatively impacted life-course outcomes. Although likely influenced by the higher relative frequency of immature skeletons (who generally had elevated FA), the only significantly higher a_p scores among sites were associated with M^1s from Warwick skeletons ($F(3,149)=7.703$, p=<0.001). Furthermore, a greater percentage of skeletons (CPR=73.3%) as well as teeth (TPR=22.1%) from Warwick exhibited LEH than other sites and more individuals had matched LEH (CPR=22.1%). Moreover, CO prevalence at Warwick (CPR=60.9%) was only marginally exceeded by that among the skeletons from

York Barbican (CPR=65.4%). Early-life and childhood stress therefore appear to have been highest at Warwick, potentially because of repeated episodes of stress. This interpretation is consistent with previous work which theorised that, due to the over-exploitation of the region's natural and agricultural resources, the population was left especially vulnerable to the calamities (e.g., the Great Famine, livestock diseases, the Black Death) that affected Britain generally in the late-13th to 14th century (Slavin 2013; Gethin n.d.; John 1997; Proudfoot 1983; Harley 1958) (Figure 9.2). It is proposed therefore that exploitative sociocultural practices contributed to early-life and childhood stress which increased mortality during periods of vulnerability (i.e., during development and among the oldest individuals) noted in previous studies (Nolan 2019). However, the over-representation of immature skeletons from the site (i.e., 69.0% of skeletons from Warwick assessed by this project were immature compared to 36.2% in the entire assemblage) and the association of that cohort with higher a_p scores mean that inferences regarding early-life experience are made cautiously (Newman 2019; Hill n.d.).

Figure 9.2 Increasing agricultural production and environmental degradation (i.e., clearing of forest) along with a rising population is thought to have left medieval Warwickshire vulnerable to the disasters that impacted Britain and continental Europe in the 14th century. Image from the Luttrell Psalter available from: https://thehistoryjar.com/2020/07/22/medieval-field-measurements/.

Although it is difficult to assess health in maturity from a sample in which most individuals are skeletally immature, later-life stress was also likely elevated. For example,

although the crude prevalence of PNBF was moderate (CPR=24.0%) in comparison to other sites, Warwick's true prevalence was highest (TPR=16.1%) suggesting that periosteal reactions were diffuse when present. Furthermore, all individuals affected had bilaterally expressed PNBF and there was a high rate of active/mixed lesions (CPR=83.3%). This patterning of periosteal lesions suggests that systemic physiological stress, possibly as a result of chronic infection, was a relatively common risk at Warwick and, as lesions were often unresolved, resilience was low (Roberts 2019; Roberts and Buikstra 2019; Steckel *et al.* 2019: 418; DeWitte and Wood 2008: 1439; Weston 2008). Similarly, the two cases of active specific infection in the skeletons assessed by this project and the identification of tuberculosis in the wider assemblage (Newman 2019: 10-15; Hill n.d.: 4-5), indicate that even though individuals survived with infection, they experienced disease for a prolonged period (i.e., long enough for skeletally diagnostic signs to develop) without healing rather than at discrete stages of the life-course after which recovery was achieved.

It is likely that social influences on life-course outcomes were more negative than positive. Specifically, there was a profound gap between lower and higher status groups during the medieval era which became especially pronounced between *circa* 11th-14th centuries. During this period, structural inequalities were created, perpetuated and justified through laws and religious doctrines which curtailed the freedoms and opportunities of the lower social strata (Abels 2009; Hatcher 1994: 10; Galtung 1969). Various statutes, for instance, limited the maximum wages of labourers (Clark 2007: 117; Cohn 2007; Hatcher 1994: 10-11; Poos 1983). Despite this, sources indicate that local elites at times made efforts to alleviate the hardships faced by the wider population. At Warwick in the 12th century local aristocrats established several religious houses which included a leprosarium that likely provided care for the sick, destitute and infirm

generally (Gethin n.d.: 6; Roffey 2012: 205; Sweetinburgh 2004). Nevertheless, after several were gifted to Warwick's collegiate church, in spite of popular protest, the ecclesiastical authorities closed a number of small parish churches (including St Lawrence's) in the 14th century, possibly to consolidate their fiscal assets (Gethin n.d.: 15). It can thus be surmised that social support was not reliably available and therefore likely inadequate to provide for a population that lived through a series of disasters that spanned generations. In fact, the entrenched structural inequalities potentially magnified stress experience for individuals of lower social status at Warwick.

9.2.1.4 York Barbican

As All Saints' Church cemetery was in use during the same period as St Lawrence's, it is reasonable to assume that the York Barbican sample was exposed, to a greater or lesser extent, to the same range of nation-wide catastrophes that impacted Warwick. Thus, both would have been affected by the extremes in weather (e.g., freezing winters) experienced across England and Wales between 1314-1317 and which caused crop failures leading to the Great Famine (Slavin 2013). Likewise, the Great Bovine Pestilence (1319-1350), which was responsible for an estimated 62% mortality in bovine livestock between 1319-1320 alone and depleted the availability of meat and dairy products, would have affected both locations (Slavin 2012: 1240-1242). Given nutritional insufficiency has been cited as a potential causal agent in CO development (e.g., Papathanasiou *et al.* 2019: 198; Geber and Murphy 2012: 516; Goodman and Martin 2002: 27-29; Stuart-Macadam 1992: 39), the high rates of CO among the skeletons from Warwick (CPR=60.9%) and York Barbican (CPR=65.4%) may be evidence for these periods of food shortage causing heightened metabolic stress.

Despite being exposed to these stressors, the York Barbican population appears to have been well-buffered during early life and childhood. York Barbican's average M1 a_p scores fell below those from elsewhere, suggesting the population experienced the lowest levels of early-life stress. Similarly, the only site to be associated with a lower true prevalence of LEH and fewer skeletons with matched LEH was South Shields, inferring that childhood stress was also relatively moderate, especially when compared to contemporary Warwick. Based on these observations, it is hypothesised that, in addition to maternal influences (Section 9.2.2), the York Barbican sample benefitted from further buffering mechanisms. It is conjectured that the city's function as a centre of trade allowed it access to resources that offset local food shortages (Goldberg 2019: 163; Mahoney Swales 2012: 220; Barrett *et al.* 2004: 619-621; Tilliot 1961: 84-106) (Figure 9.3). Although transported foodstuffs would not have the same nutritional quality as fresh produce and may not have been able to support normal metabolic functioning, they would likely have modulated the worst stress events (Newman 2016: 178; Sharpe 2012: 1478). This theory could explain the high rates of CO coupled with the evidence of low early-life and childhood stress.

Figure 9.3 Medieval York by Ridsdale Tate (1914). Although a high population density likely promoted infectious diseases prevalence, as a centre of commerce, craft production and administrative power, York's population may well have had access to resources that enabled it to better buffer against the adversities it faced in the 14th century.

There is also evidence that later-life stress was influenced by sociocultural factors. The highest rates of PNBF, a lesion associated with increasing age, were found among the individuals from York Barbican (CPR=41.2%) while an odds ratio of 2.63 (95% CI [1.17, 5.91]) suggested that skeletons from the site were significantly more likely to have PNBF than those from Black Gate. Although the population was at a higher risk of developing PNBF, as the site was associated with the lowest rate of PD (CPR=3.2%) it does not seem that this frailty was due to a physiological predisposition towards an inflammatory response. Moreover, York Barbican produced the lowest rates of bilateral (CPR=57.1%) and greater-than-Grade 1 lesions (CPR=21.5%); the rate of active/mixed PNBF was also relatively low (CPR=64.3%), being only marginally higher than Black Gate's (CPR=60.0%). Overall, the patterning of PNBF among the York Barbican skeletons contrasted starkly with that seen at Warwick (where the diffuse, bilateral and active lesions were used to imply the presence of chronic systemic stress, possibly resulting from infection) and therefore required an alternative explanation.

As traumatic injury was relatively common in medieval Britain (e.g., Dittmar *et al.* 2021; Grauer and Miller 2017; Grauer and Roberts 1996), the high frequency of PNBF in the York Barbican assemblage may have been secondary to localised trauma, the effects of which could have been mitigated through care to reduce the rate of systemic sequelae (Dittmar *et al.* 2023; Grauer and Roberts 1996). This explanation is consistent with past research on York's lower status St. Helen-on-the-Walls assemblage. Analysis found that most traumatic fractures were well-aligned and subsequently healed without substantial deformity. This was interpreted as evidence of the availability of treatment by specialists for even the poorer inhabitants of the city (Grauer and Roberts 1996). It is unlikely, however, that the urban environment exerted a purely beneficial influence on health. Higher population densities, which were accentuated by the shared accommodation occupied by poorer residents (Goldberg 2019: 175), likely increased the risk of transmission of communicable diseases, potentially accounting for the cases of leprosy in the sample (CPR=4.3%) (Kelmelis *et al.* 2020: 175; Barreto *et al.* 2014).

9.2.1.5 Summary

Site-specific influences imprinted themselves on the skeletal remains of the populations that inhabited them. The Black Gate sample, for example, was likely affected by seasonal shortages that the socioeconomic networks of the agricultural community were not capable of mitigating (Mahoney Swales 2019; Mahoney Swales 2012; Nolan *et al.* 2010; Boulter and Rega 1993). Similarly, the sample from Warwick was unable to buffer the catastrophes that affected medieval Britain and were magnified by environmental degradation specific to the region (Slavin 2013; Gethin n.d.; John 1997; Proudfoot 1983; Harley 1958). Conversely, the trade networks into which urban York was integrated likely mitigated the impact of the events which affected rural Warwick so negatively, although high population densities would have increased the relative risk of

contracting a communicable infection (Goldberg 2019; Slavin 2013; Slavin 2012). The osteological data from industrial South Shields suggests that negative later-life outcomes were not the result of early-life or childhood adversity indicating that life-course trajectories were not necessarily deterministically imprinted on individuals by contextual influences during development. Reflecting on these trends, two points become apparent. Firstly, the ability to detect site-specific differences in stress experience effectively in osteological remains is dependent upon selecting assemblages from substantially different contexts. Secondly, it is also crucial to employ measures of stress and analytical methods that are sufficiently sensitive to register even subtle differences. The latter point is discussed further in Section 9.4.

9.2.2 Links: The Mother-Child Nexus

Continuing with the theme of crucial life-course factors, theory states that connections between individuals influence outcomes (Giele and Elder 2013: 10; Hendricks 2012: 229; Kuh *et al.* 2004; Elder 1994). Although social networks were explored initially, research on biological links has shown that mothers particularly shape the life-course by acting as intermediaries for contextual influences (Cheverko 2021: 61; Agarwal 2016; Gowland 2015). This section explores the role the mother-child nexus played in offspring development.

9.2.2.1 Maternal Buffering

Differences between sites in FA were at most minor. That is, there were no significant differences between sites in M_1 a_p scores (F(3,144)=0.776, p=0.509). Moreover, though significant, M^1 a_p scores (F(3,149)=7.703, p=<0.001) were only slightly higher in the Warwick assemblage and possibly influenced by biases in sampling (i.e., a relatively high frequency of immature skeletons). It could therefore be proposed

that either 1) M1 FA is an insensitive stress marker, 2) differences between sites in the nature and magnitude of stress were not as distinct as initially presumed or, 3) that stress was mitigated during early life. The latter interpretation is more likely when reference is made to previous research and the findings of this project which have established the unique characteristics of the sites studied (e.g., Slavin 2013; Raynor *et al.* 2011; John 1997). Similarly, although it could be argued that the strength of canalisation in dental growth and development prevents pronounced deviations to symmetry in response to site-specific stimuli, previous work has revealed significant FA differences between sites in other teeth (e.g., Barrett *et al.* 2012; Guatelli-Steinberg *et al.* 2006). It is therefore theorised that mothers protected dependent offspring whilst *in utero* and during early postnatal life (i.e., when M1 crowns are forming) to such an extent that deviations to normal development were much less pronounced than expected.

Further dental observations suggested maternal stress buffering continued until the beginning of childhood. Specifically, the frequency of chronologically matched LEH was low prior to the second year of life, after which there was a dramatic increase (Figure 9.4); only 9.6% of matched LEH were estimated to have formed before approximately 1.9 years of age compared to 25.7% and 29.9% in the 2.0-2.9 years and 3.0-3.9 years categories respectively. The disparity between the percentage of LEH forming before 1.9 years and after that point was most pronounced at Warwick, where only 2.9% of matched LEH were estimated to have formed before the second year. Given the extreme stressors associated with this site, this again pointed towards the influence of an effective early-life buffering mechanism. As isotopic data suggests that in many premodern societies weaning occurred around the second year (e.g., Stantis *et al.* 2020; Beaumont *et al.* 2015; Henderson *et al.* 2014; Haydock *et al.* 2013), it is proposed that mothers were physiologically protecting their offspring up until that point, after which weaned and

immunologically naive infants were more directly exposed to sociocultural and environmental stressors (Simon *et al.* 2015), and therefore more likely to suffer episodes of stress and consequently develop chronologically matched LEH. This is supported by the significant association of matched LEH with site through binary logistic regression (χ^2=203.7, p=<0.001, R^2=0.67), which inferred that stress episodes in childhood were influenced by exogenous, site-specific factors. A similar interpretation was made by Sandberg *et al.* (2014) who, after comparing both types of data, found that LEH frequency increased when isotope profiles inferred weaning occurred.

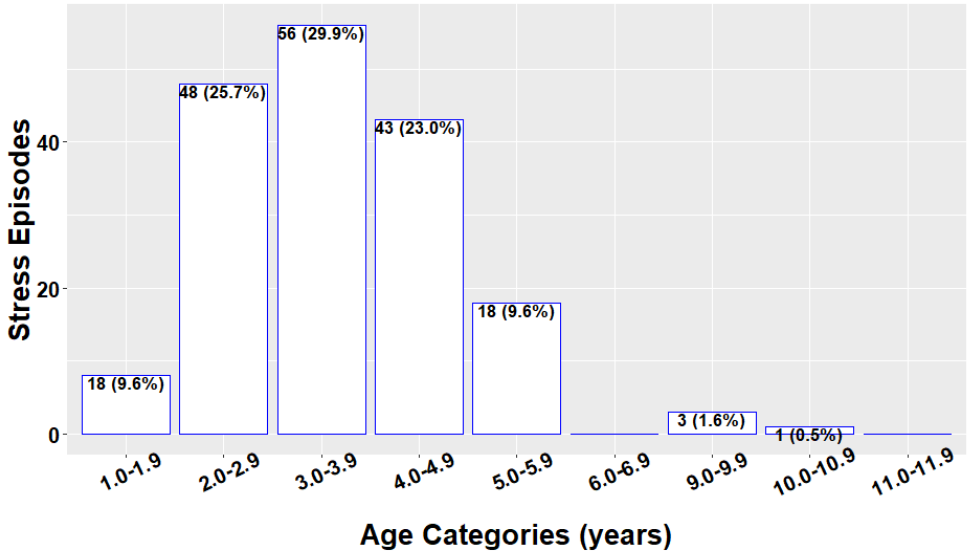

Figure 9.4 The sharp increase in matched LEH frequency after approximately the second year is thought to be due to the cessation of direct maternal support through weaning leading to elevated stress experience. The later decline (i.e., after the fifth to sixth year) is likely accounted for by immune maturation that occurs throughout childhood and eventually leads to a greater resistance to external perturbations to health (Simon *et al.* 2015).

Due to sex differentials in frailty, males likely benefitted more from maternal buffering. Given well-established sex biases in frailty (e.g., DeWitte 2010; Stinson 1985), the association of males with various pathological lesions was expected. For example, a greater number of males (CPR=71.4%) had chronologically matched LEH than females (CPR=50.0%) and an odds ratio of 2.83 (95% CI [1.03, 7.80]) inferred that males were at a significantly greater risk of developing such defects. Moreover, a higher proportion of

males (CPR=40.0%) were affected by PNBF than females (CPR=25.7%). Overall, this strongly suggests that males were more vulnerable to episodes of childhood and later-life stress and, as length of life was estimated to have been 23.2% (95% CI [9.9, 34.6]) shorter for males, it is hypothesised that increased frailty throughout life contributed to earlier age-at-death. Despite this, there were no significant differences between females and males in either M^1 (t=-0.600, df=55.98, p=0.551) or M_1 a_p scores (t=-1.399, df=57.75, p=0.167) suggesting that males did not experience elevated levels of *in utero* or early-postnatal stress. This is consistent with past bioarchaeological studies which failed to detect sex differences in dental FA (e.g., O'Donnell and Moes 2020: 166; Perzigian 1977: 84; Bailit *et al.* 1970: 632). Furthermore, a smaller proportion of matched LEH formed before 1.9 years of age in males (9.8%) than females (14.8%). As the frequency of matched LEH increases more dramatically for males (i.e., it more than doubles to 23.0%) after the second year of life (Section 8.2.3.1), it is believed to be additional evidence of male offspring benefitting from maternal buffering during early life and then, due to their innate frailty, experiencing a greater frequency of stress episodes post-weaning.

9.2.2.2 A Mother's Health, the Maternal Lineage and Past Environments

The evidence suggests that, despite substantial disparities between sites (i.e., in sociocultural and environmental stressors), contextually-specific influences exerted surprisingly little impact on early-life stress experience. Given mothers appear to have moderated environmental stress during early-life, it is hypothesised that differences in FA were therefore connected to maternal condition (e.g., nutritional status and health) and the impact this had on buffering capacity.

Much previous research has inferred stress impacting the mother-child nexus relates to nutritional provisioning (e.g., Hales and Barker 2013; Roseboom *et al.* 2001; Chávez *et al*. 2000). Associating FA with nutritional status was, however, not possible. While areas of poorly mineralised dentine matrix have been observed in M1s and associated with vitamin D shortages, demonstrating that M1 malformation can be influenced by maternally-mediated nutritional deficiency, other factors (e.g., renal disease, autoimmune disorders and genetic predisposition) can also cause these defects (Brickley *et al.* 2020; D'Ortenzio *et al.* 2018). Similarly, as CO has often been employed as a "nutritional stress indicator" (e.g., Papathanasiou *et al.* 2019: 198; Geber and Murphy 2012: 516; Goodman and Martin 2002: 27-29; Stuart-Macadam 1992: 39), the elevated M1 a_p scores observed in individuals with active CO could support a connection between early-life stress and nutritional deficiency. However, CO may develop years after M1 formation is complete and be influenced by a diverse range of factors (O'Donnell *et al.* 2020; Brickley 2018; Antoine and Hillson 2016: 223-234; Harris 2016: 145; Walker *et al.* 2009; Weinberg and Miklossy 2008; Stuart-Macadam 1992; Weinberg 1984). Thus, connections between maternal access to nutritional resources and M1 FA, while reasonable, are speculative.

It has also been suggested that early-life stress is influenced by maternal health and well-being more generally (e.g., Gowland 2018; Gowland 2015: 533; Thayer and Kuzawa 2011: 800). Although health encompasses the subject of nutrition and maternal access to food influences offspring development (e.g., breastfeeding infants receive less nutritional support from malnourished mothers) (e.g., Gowland 2015: 533; Roseboom *et al.* 2001; Chávez *et al*. 2000), it may be affected by many factors. For example, Lee *et al.* (2020) found significant differentials in the risk of later-life ill-health among offspring along with a dose-response relationship based upon whether mothers had been host to an

active infection during pregnancy and, if so, its severity. It is therefore conjectured that differences in maternal health affected a mother's ability to buffer offspring from stressors (e.g., the immature cohort, in which FA was higher, may have had mothers that were in general less healthy). Unfortunately, it was not possible to substantiate this hypothesis more thoroughly as the collections assessed were not associated with the documentary data necessary to explore maternal health and fluctuating asymmetry is a non-specific stress marker. Overall, however, it seems reasonable to propose variance in FA between individuals is related to differences in maternal health status and access to nutritional resources and the impact these had on mediating contextual stressors. Early-life stress markers therefore also shed light on maternal condition as well as environmental stress load.

Additionally, it has been argued that maternal buffering and influences are not only determined by the mother's health and circumstances whilst pregnant/breastfeeding, but also environments experienced by the mother earlier in life as well as health in the maternal lineage. Given that later-life morbidity (such as susceptibility to inflammatory conditions and resilience) are influenced by early-life stress (Section 9.3.1.1), it can be contended that a mother's condition was in part dependent on her own maternally-mediated developmental experience (i.e., either during foetal development or breastfeeding). This is congruent with the concept of the intergenerational transmission of mitotically-stable phenotypes; that is, stressors influencing the mother can also affect their dependent offspring and, for female offspring developing *in utero*, their ova, thereby potentially impacting up to three generations (Gowland 2015; Thayer and Kuzawa 2011: 798; Skinner 2008). It has also been proposed that the maternal lineage can cue an ancestral/transgenerational phenotype (Gowland 2015: 534-535; Gluckman *et al.* 2010: 10; Kuzawa 2007: 655; Jablonka *et al.* 1995: 133). There is, however, growing

speculation regarding the validity of supposing highly-canalised, meiotically-stable ancestral/transgenerational phenotypes (i.e., those perpetuated through sexual reproduction without the requirement for direct exposure to a stressor) in humans (Lu *et al.* 2019; D'Urso and Brickner 2014; Susser *et al.* 2012; Thayer and Kuzawa 2011: 798; Gluckman *et al.* 2010: 13; Kierszenbaum 2006; Jablonka *et al.* 1995). Aside from the fact that the empirical support for such phenotypes is based upon studies from plants and animals with much quicker life-histories (Van Winkle and Ryznar 2018; Susser *et al.* 2012; Galler *et al.* 1994; Galler and Seelig 1981), theoretically it has been doubted that phenotypes programmed by signals reflecting an ancestral environment would be sufficiently responsive to the environmental shifts experienced and often provoked by comparatively long-lived species such as humans (Prince-Buitenhuys and Bartelink 2021; Lu *et al.* 2019; Horsthemke 2018; Fuentes *et al.* 2010). It may therefore not be safe to assume that the phenotypic inertia required for a meiotically stable transgenerational transmission of phenotype would be beneficial for humans (Hodson and Gowland 2020: 45; D'Urso and Brickner 2014; Thayer and Kuzawa 2011: 798; Gluckman *et al.* 2010: 10; Skinner 2008; Kuzawa 2007: 655; Holland Jones 2005; Jablonka *et al.* 1995: 133).

9.2.2.3 Summary

Although it was not possible to discern the influence of the ancestral maternal lineage in the shaping of a transgenerational phenotype, the importance of the mother-child connection and intergenerational influences in past populations was evaluated. Mothers mitigated against both environmental perturbations to development as well as innate differentials to those external stimuli. Maternal buffering likely persisted until approximately the second year of life when weaning frequently occurred in premodern populations (e.g., Stantis *et al.* 2020; Beaumont *et al.* 2015; Henderson *et al.* 2014; Haydock *et al.* 2013). It is proposed that variance between individuals in FA is

related to maternal health and well-being, with morbidity potentially impacted by her own maternally-mediated developmental experience, in addition to environmental stress-load; FA could therefore be employed to explore maternal condition as well as offspring early-life stress. Overall, it appears that maternal influences were highly beneficial. This is significant as it provides a counterpoint to clinical interpretations which at times portray the physiological cues impacting the mother-child nexus as largely deleterious to offspring health and development (e.g., Barker 2012; Roseboom *et al.*2001; Barker and Osmond 1986). This difference likely reflects disparities in the volume and intensity of stress experienced by past and modern populations.

9.3 Critical Periods, Life-course Models and Adaptive Perspectives

This section is divided into two parts. Firstly, different stages of the life-course are discussed to explore the implications and origins of stress experienced at that particular time of life. Interactions between stressors operating at different stages are also discussed and models employed to illustrate how it is believed stressors coalesced to shape the life-course. In the second part, themes such as the adaptive significance of phenotypic plasticity and life-course trade-offs are discussed along with evolutionary theory.

9.3.1 A Model of Stress

It has been found that certain stress markers can be confidently associated with early life, childhood/adolescence and later-life/maturity. The importance of each of these stages is evaluated and, for childhood and later-life, the factors potentially underlying stress are explored (refer to Section 9.2.2.2 for a discussion of maternal status as a source of early-life stress). The consequences of stress experienced at different stages is discussed as are the interactions of experiences occurring over the life-course.

9.3.1.1 Early Life

It has been proposed that stress-induced early-life alterations to physiological phenotype impact morbidity (Lu *et al.* 2019: 252; Gowland 2015: 533; McDade 2012: 17286; Monaghan 2007: 1637). As higher M1 a_p scores were seen among individuals with markers of inflammation and infection (Figure 9.5), the results of this project are congruent with this hypothesis. Although elevated FA and inflammatory/infectious lesions could result from the same underlying frailty, previous research suggests a causal relationship and that morbidity is embedded in early-life experience (e.g., Roseboom *et al.* 2001; Lopuhaa *et al.* 2000; Ravelli *et al.* 1998; Barker and Osmond 1987). Similarly, while the higher M1 a_p scores among individuals with bilateral and active PNBF as well as active CO could be influenced by the generally higher prevalence of these lesion characteristics and FA among immature skeletons (Table 9.1-9.2), the association may be indicative of early-life stress diminishing the physiological capacity to recover from subsequent perturbations. If this were the case, the higher prevalence of active lesions in the immature cohort could implicate early-life stress and its effect on resilience in reduced survivorship. Whilst acknowledging the logical pitfalls associated with proposing causality because one event precedes another, past research does support the latter interpretation (e.g., Tan *et al.* 2021; O'Donnell and Moes 2020). In sum, it is conjectured that elevated early-life stress increased morbidity, specifically a susceptibility to inflammatory conditions and infection, as well as possibly impairing recovery, raising mortality risk and reducing an individual's chances of surviving into maturity. Increased mortality due to a vulnerability to inflammatory conditions would also align well with the finding that the interaction of PNBF and PD predicted a significantly reduced length of life in the mature cohort (Section 8.4.1.1).

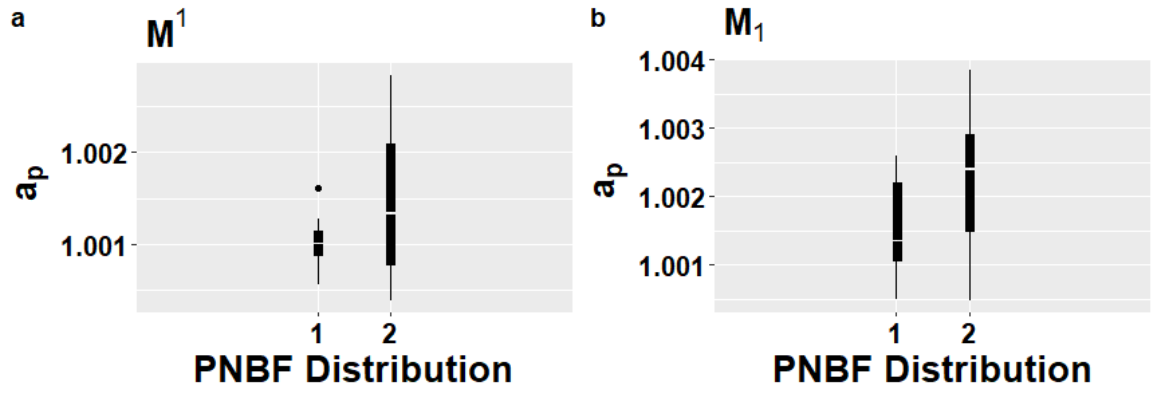

Figure 9.5 A comparison of M^1 (a) and M_1 a_p scores (b) between individuals with unilateral (1) and bilaterally (2) distributed PNBF (a-b) Although a coarse proxy for infection, bilateral PNBF evidences a systemic inflammatory response which can be caused by infectious pathogens. The higher FA among the group with bilateral PNBF therefore suggests a link between early-life stress and infection.

Maturity	PNBF Unilateral (CPR)	PNBF Bilateral (CPR)	Total
Mature	9 (31.0%)	20 (69.0%)	29
Immature	3 (17.6%)	14 (82.4%)	17

Table 9.1 A tabular comparison of the frequency of skeletally mature and immature individuals with PNBF that have unilateral and bilateral lesions.

Maturity	Healed PNBF (CPR)	Active/Mixed (CPR)	Total
Mature	15 (48.4%)	16 (51.6%)	31
Immature	3 (12.0%)	22 (88.0%)	25

Table 9.2 A tabular comparison of the frequency of skeletally mature and immature individuals with PNBF that have active/mixed lesions compared to healed.

Even if the pathological pathways are speculative, the finding that there were significant differences with moderate-to-strong effect size in M^1 (t=5.202, df=128.4, p=<0.001) and M_1 a_p scores (t=3.159, df=136.1, p=0.002) between skeletally immature and mature groups supports the supposition that early-life stress affected survival into maturity and is well-corroborated by past findings. In archaeological populations, for instance, individuals with LEH on deciduous and early-forming permanent dentition (i.e., teeth that develop prenatally and in early-postnatal life) often have significantly shorter lives than those without (e.g., Temple 2014: 541; Armelagos *et al.* 2009; Blakey and Armelagos 1985: 376), while clinical studies have linked severe *in utero* stress with

higher adulthood mortality risk (e.g., Roseboom *et al.* 2001: 95; Barker and Osmond 1986: 1077-1079). However, it is unlikely that early-life stress operated independently in defining mortality risk; a one-unit increase in scaled M^1 a_p scores as well as matched LEH presence was associated with a 34.8% (95% CI [17.9, 48.2]) reduction in length of life for immature individuals. It can therefore be inferred that stresses experienced throughout development accumulated to define mortality risk, though it is possible that early-life experience initiated a "chain of risk" in which experiences were linked and exposure to one raised the probability of others (Kuh *et al.* 2003: 779; Riley 1989; Rutter 1989) (Figure 9.6). Given that site and sex were predictors of matched LEH presence it is probable that site-specific factors and sex differentials in frailty modified the extent to which later stressors built upon earlier deleterious influences, however (DeWitte 2010; Kuh *et al.* 2003: 779; Riley 1989; Stinson 1985).

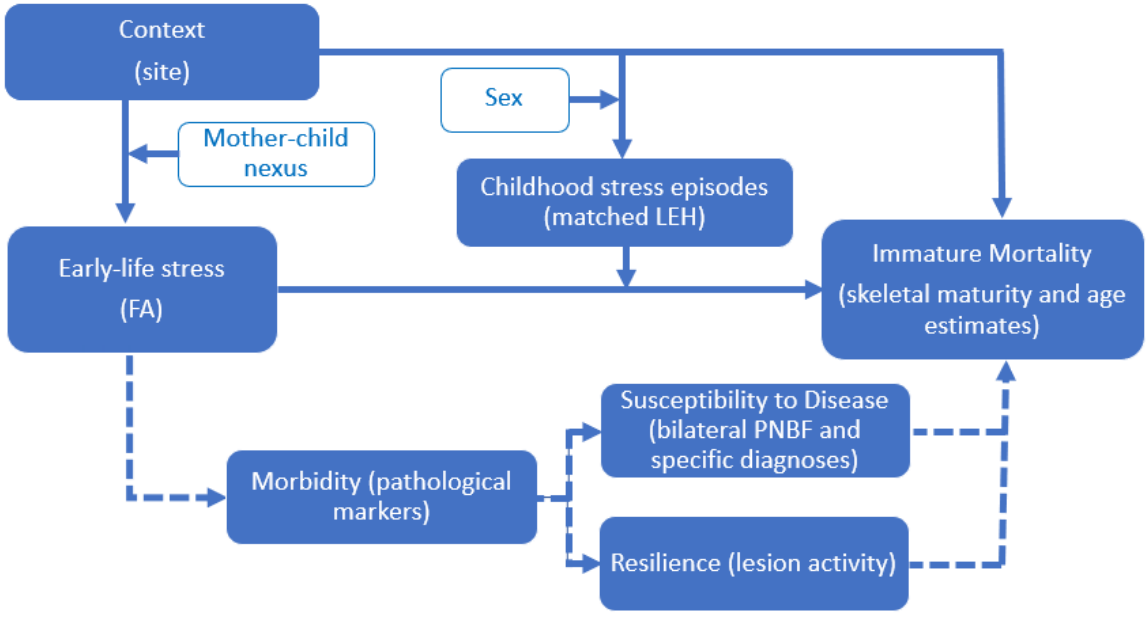

Figure 9.6 The hypothesised connections between stressors and mortality during immaturity. The proxies employed in analyses are given in brackets. Modifying factors are also highlighted (blue text in clear cells). Statistically significant relationships are indicated by solid lines; dashed lines show connections not tested through inferential methods, but suggested through descriptive statistics and past research. The latter are the pathways through which it is suspected early-life stress influences mortality.

Despite the aforementioned associations with morbidity and mortality in childhood and later-life, it is believed that early-life stress also promoted immediate survival. The significant positive correlations between M^1 ($F(1,70)=7.455$, p=0.008, $R^2=0.08$) and M_1 a_p scores ($F(1,66)=4.391$, p=0.040, $R^2=0.05$) and age-at-death estimates in the immature cohort may evidence this. To illustrate, a one-unit increase in scaled M^1 and M_1 a_p scores was associated with a 19.5% (95% CI [4.9, 36.1]) and 12.1% (95% CI [0.6, 24.9]) increase in length of life respectively. Even though the nature of the changes provoked by early-life stimuli which aided survival can only be conjectured from osteological remains, clinical data suggests that adaptations to physiological phenotype which increase susceptibility to later-life disease do in fact initially promote beneficial responses to health insults. It has been found that an aggressive inflammatory response to pathogen infection helps to contain the spread of disease, despite being associated with later increases in morbidity and mortality related to hyperinflammation (such as a higher risk of cardiovascular disease) (e.g., Tan *et al.* 2021; Gustine and Jones 2021; Oishi and Manabe 2018; Zietek and Rath 2016). This suggests that early life was critical in cueing adaptations to phenotype that, though associated with changes in later-life frailty and resilience which impacted mortality, were conducive to short-term survival (the theme of trade-offs is explored further in Section 9.3.2.1). In sum, the data suggests that stress experience during early life was exceptionally important in shaping life-course outcomes.

9.3.1.2 Childhood and Adolescence

Childhood was a time of increased vulnerability. The rise in matched LEH frequency after approximately the second year of life infers an escalation in the number of stress episodes experienced. This was likely a result of weaning and the concomitant cessation of direct nutritional and immunological support from mothers and intensified

exposure of offspring to sociocultural or environmental stressors (Stantis *et al.* 2020; Beaumont *et al.* 2015; Henderson *et al.* 2014; Sandberg *et al.* 2014; Haydock *et al.* 2013). It seems reasonable to assume that increased stress exposure also led to elevated mortality risk. This is corroborated by historical records which, although charting a declining trend by the 19th century, indicate that in industrialising England *circa* 25% of individuals died before their fifth year (Newton 2015: 218; Pozzi and Ramiro Fariñas 2015: 55; Vallin 1991). Risk likely diminished in later childhood, after approximately the fifth or sixth year of life, when the frequency of matched LEH also declines, due to the gradual maturation of the immune system throughout this period (Simon *et al.* 2015).

Aside from increased vulnerability, childhood is associated with high phenotypic plasticity (Gowland 2015: 530; Barker 2012: 186), and proxies for childhood stress can therefore be linked with later-life outcomes. Specifically, even though a great deal of variation in mature long bone lengths was explained by sex, significant negative correlations were observed with matched LEH presence in the largest long bones (i.e., the femur, tibia, fibula and humerus). For example, matched LEH presence predicted an estimated reduction in humeral length by 19.5 mm (95% CI [8.7, 30.7]). It is therefore speculated that the adverse childhood experiences causing the formation of chronologically matched LEH also reduced skeletal growth (Figure 9.7). However, it was found that in addition to age, M_1 a_p scores (χ^2=184.96, p=<0.001, R^2=0.91) were significant predictors of skeletal maturity. With coefficients inferring higher scores were associated with the immature cohort, it was hypothesised that early-life stress was implicated in developmental delays. It is possible that maturation was delayed due to health insults in adolescence, susceptibility to which was influenced by early-life stress and its association with increased frailty and decreased resilience. Alternatively, delays may have been programmed to allow immature individuals more time to both grow and

accrue the somatic resources necessary to successfully achieve maturation. Whichever is the case (these themes are explored further in Section 9.4), it suggests that childhood and adolescent growth and development was to a greater or lesser extent intertwined with maternally mediated early-life experiences.

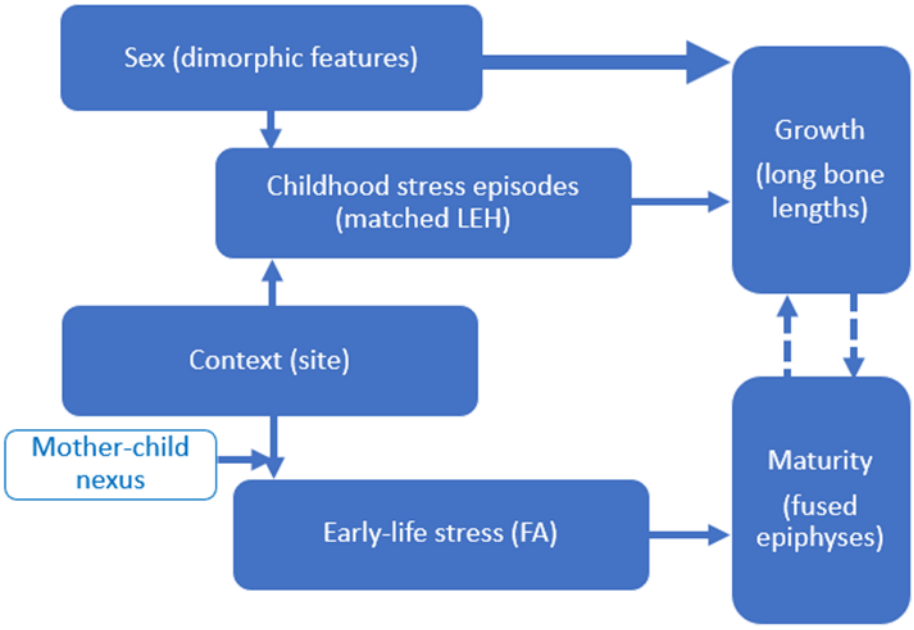

Figure 9.7 Although regression models did not indicate that sex, site and matched LEH presence interacted to impacted long bone growth, as matched LEH presence was predicted by sex and site, it is believed that innate sex differentials in vulnerability had the capacity to mediate sociocultural/environmental stressors (DeWitte 2010; Kuh et al. 2003: 779; Rutter 1989; Stinson 1985). Meanwhile, with M1 a_p scores predicting whether individuals had attained skeletal maturity or not, it seems likely that maternally-mediated early-life stress influenced developmental tempo with delays potentially creating greater opportunities for catch-up growth to occur and somatic resources to be accumulated.

It has been hypothesised that the leading causes of childhood stress in the past included metabolic stress linked to malnutrition/undernutrition (e.g., Newman 2016: 16; Geber and Murphy 2012; Horrell and Oxley 2012) and infection (e.g., Hayward *et al.* 2016; Crimmins and Finch 2006; Finch and Crimmins 2004). As CO was common amongst immature skeletons (CPR=75.0%), metabolic stress appears to have been a widespread problem for younger and skeletally immature individuals. However, the

perception that dietary deficiency was relegated to or most keenly felt by the young is likely influenced by differentials in the responsiveness of bone to metabolic stressors (Brickley 2018: 898-899; Walker *et al.* 2009: 111). So, although an odds ratio of 0.17 (95% CI [0.08, 0.35]) demonstrated that there were significantly fewer mature skeletons with CO (CPR=34.8%), this may only reflect the fact that older skeletons were less likely to manifest the osteological signs of metabolic stress. Similarly, a reduction in requirements for energetic/metabolic resources once growth and development have been completed may account for the lower rate of active/mixed lesions in mature (CPR=12.5%) compared to immature skeletons (CPR=36.8%) (Brickley and Mays 2019: 532; Newman 2016: 110-111; Ortner 2003: 386-387). In sum, although poor dietary provisioning likely did contribute to metabolic disease, with the evidence at hand it is not possible to say that malnutrition/undernutrition was predominantly a childhood affliction.

In contrast, there is better evidence to support the hypothesis that infection was a greater risk during childhood and adolescence (Hayward *et al.* 2016; Crimmins and Finch 2006; Finch and Crimmins 2004). While specific diagnoses were generally rare (CPR=3.8%), six of the eight individuals for whom a particular infection could be identified were skeletally immature. Although all these individuals were associated with age estimates indicating they likely died in their mid-to-late teens, given the time diagnostic lesions take to form (Roberts and Buikstra 2019: 368; Roffey 2012: 216; Ortner 2003: 264; Boldsen 2001: 380; Andersen and Manchester 1992: 122), their initial experience of disease may have been much earlier in life (i.e., in childhood). Furthermore, although a coarse proxy for infection (Roberts 2019; Roberts and Buikstra 2019; Steckel *et al.* 2019: 418; DeWitte and Wood 2008: 1439; Weston 2008), bilateral PNBF was more common among the subset of immature individuals with lesions (CPR=82.3%) than mature skeletons with PNBF (CPR=69.0%). There was also a higher rate of active/mixed

lesions among immature skeletons with PNBF (CPR=88.0%) compared to mature individuals (CPR=51.6%) and it was found that age was a significant predictor of lesion healing (χ^2=9.997, p=0.002, R^2=0.14) with older individuals more likely to have healed lesions. Although not conclusive, this data supports the theory that childhood and adolescent mortality and morbidity were impacted by infection (Hayward *et al.* 2016; Crimmins and Finch 2006; Finch and Crimmins 2004).

9.3.1.3 Maturity and Later-life

Thus far it has been posited that early-life and childhood stress contributed to a range of life-course outcomes that persisted into or affected individuals even after skeletal maturity had been attained (e.g., susceptibility to infection, final growth, etc). Previous research has also demonstrated that even in past populations where adult life-ways could be exceptionally onerous, links can still often be found between formative experiences and outcomes that are seemingly disconnected (e.g., Wilson 2014). This is not always apparent, however. Most notably, it was found that while the early-life and childhood experiences of individuals from South Shields appear to have been relatively stable (e.g., LEH prevalence rates were low), the sample exhibited signs of chronic, later-life disease (e.g., the highest rates of moderate-to-severe PD). It was suggested that the discrepancy between stress experience at different life-course stages was the result of a relatively well-buffered childhood followed by a harmful later-life environment (Section 9.2.1.2). Comparable results have been reported elsewhere. For example, historic American military samples have shown higher prevalence rates for activity-related osteological modifications and younger average age-at-death compared to non-military groups, but generally less evidence of early-life/childhood stress – i.e., recruits selected for their robusticity had their health diminished and life expectancy shortened (Sledzik and Sandberg 2002: 185-207). Although these examples may promote an “adult lifestyle”

model of health, they suggest that early-life and childhood experience exercised a variable pressure in past lives (Giele and Elder 2013: 5; Macmillan 2005: 8; Laub and Sampson 2003).

As the combined presence of inflammatory lesions (i.e., PNBF and PD) in mature skeletons predicted a 49.7% (95% CI [23.1, 67.1]) reduction in estimated length of life, it is inferred that later-life physiology was generally important in defining mortality risk for older individuals (Figure 9.8). This is consistent with clinical research which has proposed localised and non-fatal inflammatory lesions such as PD as well as chronic and potentially fatal metabolic conditions like cardiovascular disease are symptomatic of a pathological physiology (Rachlani *et al.* 2017; Lockhart *et al.* 2012; Andriankaja *et al.* 2010). A plethora of factors have been implicated in the development of such a physiological phenotype. For example, diets high in sugar and fats as well as exposure to environmental pollutants are risk factors (Rachlani *et al.* 2017; Lockhart *et al.* 2012; Andriankaja *et al.* 2010). This may explain why the prevalence of PD was so high at post-medieval South Shields (CPR=51.5%). During the post-medieval period, sugar consumption increased by 83% between 1814-1832 (Newman 2016: 60; Gaskell 1836: 118-119) and, with the proliferation of factories and evermore readily tobacco, exposure to respiratory toxins became more frequent. Gaskell (1836), for instance, reports that the air in industrial centres was "injurious in a very marked way" and that "tobacco is very largely consumed by male and female labourers indiscriminately". As South Shields was overshadowed by a "dense atmosphere of smoke" and osteological reports have identified skeletons with pipe-smoking notches (Eastlake 2013: 49; Raynor *et al.* 2011: 55; Report of the Commissioners 1845: 185), these problems certainly affected the town. Thus, the causes of stress experienced by skeletally mature individuals are likely in many cases to have been influenced by contextually specific factors.

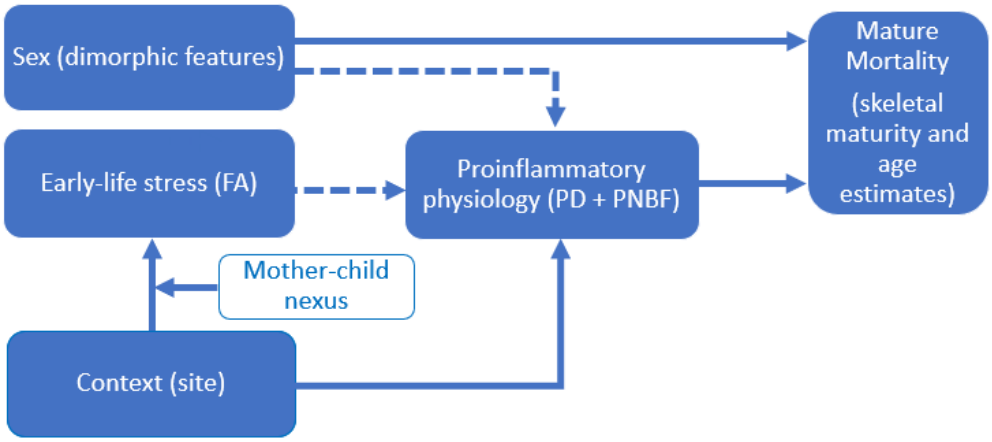

Figure 9.8 The hypothesised life-course model employed to explain mortality risk in the skeletally mature cohort. The proxies employed are given in brackets. Modifying factors are also highlighted (blue text in clear cells). Statistically significant relationships are indicated by solid lines; dashed lines show connections not tested through inferential methods, but suggested through descriptive statistics and past research.

Contextually specific influences were not, however, the only factors to impact later-life morbidity and mortality. Given that previous investigations have established that many skeletons in the assemblages studied showed signs of degenerative joint disease (Chapter 5), it seems highly likely that adult activity and occupation affected later-life morbidity and well-being in past populations generally (e.g., Mahoney Swales 2019; Raynor *et al.* 2011; McIntyre n.d.). Moreover, sex influenced outcomes in maturity. Even though alterations to physiological phenotype have been linked to early-life stress here and in past research (Crespo *et al.* 2021: 78; Crespo *et al.* 2016; DeWitte 2014b; Barker 2012; Lockhart *et al.* 2012; Andriankaja *et al.* 2010), as males have been found to be more vulnerable to inflammatory responses (Roberts and Buikstra 2019: 364; Lockhart *et al.* 2012: 2524; Andriankaja *et al.* 2010: 255; Shiau and Reynolds 2010), sex differentials in frailty likely contributed to risk (DeWitte 2010; Stinson 1985). Male frailty may explain why sex was a significant predictor of age-at-death among skeletally mature individuals with males estimated to have lives 23.2% (95% CI [9.9, 34.6]) shorter than females. Previous studies have, however, also inferred age-specific risks among females, speculating that these are associated with pregnancy. That is, at South Shields there was a

higher-than-expected frequency of deaths among young adult females while in the York Barbican assemblage there is a young female who appears to have died around the time of childbirth (Section 5.5.2) (Raynor *et al.* 2011: 44-46; McIntyre n.d.: 78; Bruce 2003: 53). Overall, as social categorisations of sex could also have influenced, *inter alia*, occupation, access to education and resources (Stewart 2011: 481-482; Sledzik and Sandberg 2002; Van Staa *et al.* 2001: 517-522; Cockburn 1991), it seems reasonable to propose that sex became more important to life-course experiences and outcomes after maturity was attained.

It should not, however, be forgotten that mortality could have been related to less predictable circumstances. Although the surrounding events are impossible to reconstruct, among the Black Gate and York Barbican assemblages there were skeletons with evidence of peri-mortem sharp force trauma and it has been speculated that their deaths resulted from intentional violence (Nolan *et al.* 2010: 251-252; McIntyre n.d.: 32) (Figure 9.9). The fact that similar trauma was not more common indicates that violence was likely not a widespread societal problem and that these individuals were possibly the victims of actions unrelated to broader contextual trends.

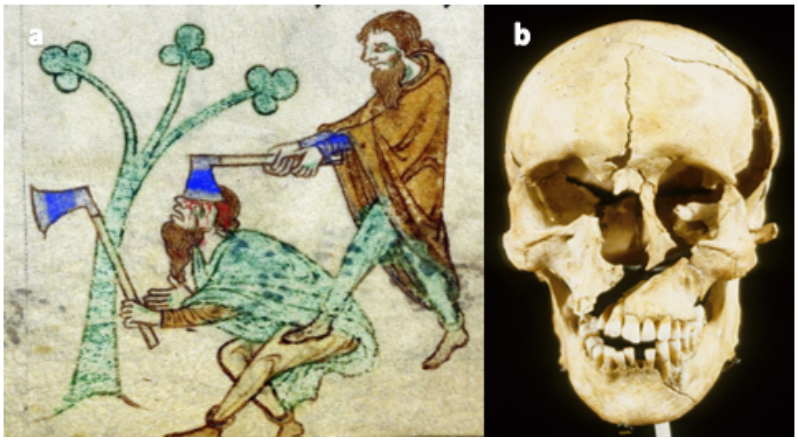

Figure 9.9 An image from the medieval Topographia Hibernica (available at: http://irisharchaeology.ie/2015/11/a-violent-death-in-early-medieval-meath/) depicting a fatal attack (a) and the osteological evidence of such an act (b) (Fiorato *et al.* 2000). Although analyses do not suggest violence was common, for some individuals it was more significant than subtle forces acting over the life-course.

9.3.1.4 Summary

Initially, the effects of stress at different stages of the life-course were explored and, where not discussed previously, the origins of stress were hypothesised. From this it emerged that early-life experience was likely critical in influencing survival beyond an individual's formative years and into physical maturity as well as later-life frailty and resilience. Meanwhile, stresses during childhood seemingly either constrained or programmed reduced somatic growth. Although discerning the underlying causes of stress was challenging, it is suggested that differences in early-life stress could be related to nutritional deficiency and variance in maternal health while episodes of infection contributed to childhood adversity (e.g., Hayward *et al.* 2016; Hales and Barker 2013; Gluckman *et al.* 2010; Gluckman *et al.* 2007; Crimmins and Finch 2006; Finch and Crimmins 2004; Bateson *et al.* 2004). Mortality among skeletally mature individuals was impacted by unique environmental factors as well as sex and the association of inflammatory lesions with reduced length of life is in line with the supposition that physiological phenotype affects later-life morbidity. By considering connections between life-course phases it was possible to discern how entangled they were. Although it cannot be implied that distant events were at the root of all outcomes, it appears that stressors experienced during periods of heightened phenotypic plasticity (i.e., early-life and childhood) can initiate a chain of risk in which harmful influences accumulate to shape outcomes in growth and development as well as health and longevity (Cheverko 2021: 61; Giele and Elder 2013:10; Davey Smith 2011; Kuh *et al.* 2003: 779; Sledzik and Sandberg 2002; Shanahan 2000: 670-671; Rutter 1989).

9.3.2 Adaptive Perspectives on Stress and Plasticity

In the previous section it was suggested that stressors experienced at particular stages of the life-course had programmed outcomes, some of which could be considered positive (to an extent) while others were negative. This section reviews these inferences to more directly address the subjects of phenotypic plasticity, life-course trade-offs and adaptive significance.

9.3.2.1 The Thrifty Phenotype: Short-term Benefits and Later Trade-offs

Elevated maternally-mediated early-life stress negatively impacted development and length of life. The significantly higher M^1 (t=5.202, df=128.4, p=<0.001) and M_1 a_p scores (t=3.159, df=136.1, p=0.002) among the skeletally immature group intimates that early-life stress shortened the life-course. Given this finding, it may be wondered how stress experienced during periods of phenotypic plasticity may confer adaptive advantages. Such a position becomes tenable, however, when the relationship between length of life and M1 FA is considered in the immature cohort. Within this group, there was a significant (although modest) positive correlation between a_p scores and age-at-death estimates. That is, the regression of age on M^1 and M_1 scores produced coefficients of 0.178 and 0.114 respectively which, when exponentiated, inferred that a one-unit increase in scaled a_p scores predicted an estimated 19.5% (95% CI [4.9, 36.1]) and 12.1% (95% CI [0.6, 24.9]) increase in length of life. Although the broad CIs of these estimates and low R^2 values associated with the regressions (Section 8.4.1.2) encourages a cautious interpretation, among "non-survivors" it seems that stress experienced in early life was linked to adaptations that enhanced chances of survival in the short-term but decreased it long-term. Due to the associations between higher M1 a_p scores and inflammatory lesions (i.e., active and bilateral PNBF), it was cautiously hypothesised that

these adaptations involved the programming of a highly active (potentially aggressive) physiological phenotype (Section 9.3.1.1). This is consistent with the Thrifty Phenotype Hypothesis which proposes adaptations during periods of plasticity maximise the chances of immediate survival at the expense of trade-offs in later-life morbidity and mortality (Hales and Barker 2013; Armelagos *et al.* 2009; Hales and Barker 2001).

It was also noted that some individuals experienced delays in pubertal development, and it is believed that early-life experience influenced physical maturation. SK 268 from Black Gate, for example, despite being dentally mature (i.e., M3s were fully formed and in occlusion) and possessing an ADBOU age estimate suggesting they were in their early twenties, was thought to only be in Stage 3 of puberty inferring they had not yet achieved sexual maturation (Lewis *et al.* 2016: 51; Shapland and Lewis 2013). Other aspects of their development also appear to have been slowed. For instance, although senescent changes in the pelvis were present (i.e., exostoses on the ilium), SK 268's distal ulnar and humeral epiphyses as well as iliac crest were unfused (these would generally fuse during adolescence) (Schaefer *et al.* 2009; Scheuer and Black 2000). Given SK 268's higher-than-average M1 FA, delays could be related to early-life experience (Section 8.4.2.2). Although age and pubertal stage estimates are subject to error and individual case studies should be treated cautiously, binary logistic regression demonstrated that, in addition to age, M_1 a_p scores (χ^2=184.96, p=<0.001, R^2=0.91) were significant predictors of skeletal maturity within the sample, adding weight to the hypothesis of stress-related delays. Despite negative connotations, it can however be argued that developmental delays are not entirely disadvantageous. Although stalled sexual maturation could have impacted reproductive life-histories, delays in epiphyseal fusion may have provided extra time for catch-up growth to compensate for deficits or allowed individuals the opportunity to accrue sufficient somatic resources to pass through the physiologically

demanding and stressful process of maturation (Kralick and McGrath 2021; Pittet *et al.* 2017; Agarwal 2016: 134; Ellison and Reiches 2012: 90; Fujita *et al.* 2012; Hinde 2009; Kinoshita *et al.* 2003: 110; Tanner and Whitehouse 1980). Although speculative, this again implicates stress in the catalysation or programming of short-term benefits (i.e., longer growth period) at the expense of later trade-offs (i.e., shortened reproductive period).

Broadly, this supposition is supported by the finding that the lengths of several skeletal elements (the femur, tibia and humerus) were negatively correlated with matched LEH presence. As matched LEH act as a proxy for a stress event rather than a prolonged exposure (Hassett 2012: 560-561; Temple *et al.* 2012: 1639; Temple 2007; Hillson 2005: 169) (Section 6.3.1), it seems plausible to suggest that the association between childhood stress and persistent growth deficits may not be indicative of the same underlying harmful experience. Furthermore, if the presence of matched LEH and reduced skeletal dimensions were the consequence of a continuous stress exposure preventing catch-up growth, then it could be expected that there would be a similar relationship between matched LEH presence and diaphyseal lengths, which was not generally the case (matched LEH only predicted reduced femoral diaphyseal length). These findings could therefore suggest that growth deficits associated with childhood stress are indicative of programmed constraint, again aligning well with the Thrifty Phenotype hypothesis which posits that in poor environments growth is modulated to match resource availability (Agarwal 2016: 134; Barker and Lampl 2013: Barker 2012: 186). Although this inference is made tentatively, similar results have been found in living populations. For instance, anthropometric comparison by Pomeroy *et al.* (2012) between two genetically similar groups exposed to substantially different levels of developmental stress found that head proportions showed the smallest size differences followed by autopod (i.e., hand and foot)

dimensions, while long bones (specifically the ulna and tibia) evidenced the greatest differences. Pomeroy *et al.* (2012), with reference to the Thrifty Phenotype Hypothesis, proposed that a trade-off in constrained long bone growth had been made to protect development in areas of specialist and critical functioning (i.e., the brain, hands and feet), essentially prioritising the features most likely to enhance survival at the expense of other later-life outcomes

9.3.2.2 Alternative Theories: PARs and Maternal Capital

Although the Thrifty Phenotype theory is a popular explanation of the significance of developmental plasticity, others have been expounded. The hypothesis of Predictive Adaptive Responses has, for example, received considerable attention. In short, a PAR is a phenotypic change that is not immediately beneficial and advantages are felt in later-life (Gluckman *et al.* 2010: 9; Gluckman *et al.* 2007: 4; Wells 2007: 335). However, the evidence produced by this project strongly suggests that responses to early-life stress were beneficial in the short-term and linked to negative long-term consequences. For instance, although inflammatory responses to infection indicate a strong immune response, it has been suggested that early-life stress induced a shift towards a pathological hyper-inflammatory phenotype and increased morbidity/mortality (Crespo *et al.* 2021: 78; Crespo *et al.* 2016; DeWitte 2014b; Barker 2012; Lockhart *et al.* 2012; Andriankaja *et al.* 2010). Furthermore, while it is possible that the positive linear relationship between a_p scores and age estimates among the immature skeletons indicates a predictive adaptation (Lu *et al.* 2019: 254), the significantly higher FA among the group points compellingly to the conclusion that phenotypic adaptations to early-life stress were eventually associated with unambiguously negative later-life outcomes (i.e., non-survival). Moreover, as humans are noted for manipulating environments in processes of construction and reconstruction (e.g., Prince-Buitenhuys and Bartelink 2021; Wells 2012: 232; Fuentes *et*

al. 2010), to the extent that it has been hypothesised that such actions are highly conserved behavioural characteristics (Wells 2012: 232; Fuentes *et al.* 2010), it may be doubted how well later-life environment can be predicted and consequently the value of predictive adaptations (Lu *et al.* 2019).

The Maternal Capital Model is also an unlikely explanation of developmental adaptations. Although maternal constraint in resource allocation could plausibly induce a phenotype associated with short-term benefits – e.g., maternal nutritional regulation could enable greater accuracy in the matching of growth outcomes to resource availability (Wells 2012: 231; Wells 2007: 235) – the data gathered here does not support this. If mothers were constraining offspring provisioning to maximise their own success, it would be expected that between-site differences in FA would be commensurate with the stresses operating in those contexts (i.e., in harsher environments, mothers would reduce offspring investment and FA would increase). However, differences in M1 FA between assemblages were largely insignificant, despite the prevalence of later forming stress markers inferring substantial between-site disparities in stress experience (Section 9.2.1). Therefore, in conjunction with the evidence of maternal buffering and post-weaning increases in stress (Section 9.2.3), it is hypothesised that mothers protected their offspring from environmental adversity, rather than modulating resource allocation in response to it. However, to fully explore (and therefore exclude) the Maternal Capital Model, it would be necessary to access data on maternal age, social status, access to nutritional resources, number and sex of offspring as well as number of previous births in order to evaluate the most appropriate investment strategy for individual mothers (Pittet *et al.* 2017; Fujita *et al.* 2012; Wells 2012: 231-234; Charnov 1997; Charnov 1991; Trivers and Willard 1973).

9.3.2.3 Contradictions and Complications: Cue or Stressor?

From the discussion so far, it can be surmised that the skeletons with the lowest a_p scores were either the youngest immature individuals or those that had reached skeletal maturity. This seemingly odd occurrence may be accounted for by the degree to which early-life and later-life conditions matched. For example, if an individual were to experience low environmental stress during development and they continued to inhabit a rich milieu throughout life (i.e., there was high fidelity between environments), then it would be expected that the traces of early-life stress (e.g., M1 FA) would be low and that proxies for later-life fitness (e.g., length of life) would suggest positive outcomes because the phenotype programmed during development matched well with the demands of later conditions (Gluckman *et al.* 2010: 10; Monaghan 2007: 1638; Jablonka *et al.* 1995). This patterning of experiences and outcomes is sometimes called the "silver spoon" effect (Lu *et al.* 2019: 252; Monaghan 2007: 1638; Stamps 2006).

In contrast, if an individual experienced a later-life environment which was substantially different from their developmental one (i.e., there was low fidelity), then the match between the phenotype programmed during development and later-life environment would likely be poor (Gluckman *et al.* 2010: 10; Monaghan 2007: 1637-1638; Jablonka *et al.* 1995). This may account for the immature individuals with low a_p scores but who died early in childhood and also the lack of a positive linear relationship between M1 a_p scores and age estimates among Warwick's immature skeletons. Warwickshire was subjected to increasingly unsustainable agricultural exploitation between the 11-13th centuries, rendering it vulnerable to natural disasters that decimated human as well as life-stock populations and devastated the area's fragile economy (Slavin 2013; John 1997: 41; Proudfoot 1983; Harley 1958: 18; Gethin n.d.).

Given this instability, it can be expected that there was a potential for very low fidelity between maternal cues and the environments inhabited by offspring (Gluckman *et al.* 2010: 10; Jablonka *et al.* 1995). This is consistent with clinical studies which have found that even positive changes in circumstances can be associated with negative outcomes. For example, when individuals endure an impoverished developmental period in which nutritional shortages are common, metabolic changes relating to insulin sensitivity and body fat regulation occur that increase the risk of diabetes and cardiovascular disease if later environments are resource rich (e.g., Hales and Barker 2013; Hales and Barker 2001; Roseboom *et al.* 2001: 95; Barker and Osmond 1987).

In this section, the term cue and stressor have become collocated at points. It has been proposed that environmental stress cues phenotypic adaptations that promote success, with the data from this and other projects suggesting that short-term survival is prioritised (e.g., DeWitte 2014b; Temple 2014; Roseboom *et al.* 2001: 95; Barker and Osmond 1987). Thus, the stimuli that impact the mother-child nexus both contain information on and are a product of environmental stressors. However, cues that catalyse changes maximising the chances of short-term survival may result in a phenotype that is suboptimal in later-life. Essentially, phenotypic alterations cued by stress make the "best of a bad job" and it is not expected that the costs of experiencing adversity can be completely offset (Lu *et al.* 2019: 252; Monaghan 2007: 1637). It is also likely that the magnitude of stress experienced was important in determining how beneficial cues were. To elaborate, although higher M1 a_p scores were correlated positively with length of life in the immature cohort, the negative coefficient of the interaction in the regression model between M^1 scores and matched LEH predicted a 34.8% (95% CI [17.9, 48.2]) reduction in length of life with a one-unit increase in scaled a_p scores and the presence of matched LEH. Consequently, while the terms cue and stressor may be interchangeable to an extent,

the volume and intensity of experience was likely key in defining the exact impact of stressors (Gowland 2015: 533; Richardson *et al.* 2014).

9.3.2.4 Summary

The association of elevated FA with later age-at-death estimates in skeletally immature individuals suggests that stressors experienced during early life catalysed adaptations which enhanced chances of short-term survival. Immediate benefits seem to have come at the expense of long-term trade-offs, however. The significantly higher FA among immature skeletons infers that heightened early-stress likely delayed somatic development and eventually contributed to earlier age-at-death. The association of higher FA with inflammatory lesions, indicators of chronic disease and active pathological lesions also suggests the programming of a hyper-inflammatory physiology which, despite initial benefits, was associated with increased morbidity and mortality risk. The connection between matched LEH presence and reduced long bone lengths is also consistent with the theory that developmental stress contributed to programming developmental tempo and growth profiles. Overall, results support the Thrifty Phenotype Hypothesis as an explanation for the evolutionary significance of phenotypic plasticity, however, given the observational rather than experimental nature of the evidence gathered any inferences are conjectural and tentative.

9.4 Embodying Stress: The Challenges of Skeletal Assessments

With a few notable exceptions (e.g., Davey Smith 2011; Laub and Sampson 2003; Sledzik and Sandberg 2002), much past research could be construed as suggesting that there is a direct and unambiguous causal connection between early-life stress and later-life experiences and outcomes (e.g., Dancause *et al.* 2011; Roseboom *et al.* 2001; Lopuhaa *et al.* 2000; Ravelli *et al.* 1998; Barker and Osmond 1987). However, when searching for correlations and associations between archaeologically durable osteological proxies for stress throughout the life-course, the statistical signals identified were often faint. As this thesis focuses upon employing M1 FA as a proxy for maternally-mediated stress, this section begins by discussing the mechanisms through which early-life stress is embodied on the M1 occlusal surface. This is contrasted to other processes through which maternally-mediated stress is embodied. Finally the effectiveness of the skeletal proxies for later-life stress and outcomes are discussed.

9.4.1 Error, Algorithms and the Patterning Cascade

Although it might be argued that the aforementioned subtle statistical connections could have been influenced by methodological inaccuracy, Procrustes ANOVA results indicated that error was small (i.e., accounting for *circa* 2% of variance). As the production of each replicate measure required the repetition of every stage in the data acquisition process, it can be assumed that the estimate of error is accurate, implying the techniques employed to quantify FA were reliable and consistently applied. Therefore, rather than focusing on observer error, the processes through which stress induced dental variation is manifested and the impact this has when employing M1 FA as a proxy for early-life stress are discussed.

In Chapter 3 it was proposed that empirical evidence supported the Patterning Cascade Model (PCM) of dental development (Hunter *et al.* 2010; Brook 2009; Salazar-Ciudad and Jernvall 2002; Jernvall and Jung 2000). Thus, the spatial relationships between the features found on multi-cusped teeth are thought to be the result of a network of genes that interact through a series of feedback loops across which disruptions to development ripple to affect later-forming traits (Lynnerup and Klaus 2019: 53; Tamura and Nemoto 2016; Riga *et al.* 2014: 398; Rizk *et al.* 2013: 139; Hunter *et al.* 2010: 1; Brook 2009; Salazar-Ciudad and Jernvall 2002; Jernvall and Jung 2000). The patterns in variation noted in this project are consistent with this hypothesis (Figure 9.10). Specifically, PCA revealed that fluctuating asymmetric variation in occlusal morphology was not easily summarised by a small number of orthogonally rotated eigenvectors composed of highly correlated variables. Thus, instead of variation being isolated in specific features, it was dispersed across the occlusal surface, as would be expected if developmental errors were the result of integrated and iterative processes (Hunter *et al.* 2010; Townsend *et al.* 2003: 355; Salazar-Ciudad and Jernvall 2002; Jernvall and Jung 2000). Despite this diffuse pattern, when vector displacements were compared between the shape configurations with the most extreme differences in each PC, differences were more apparent among semi-landmarks located along the outline as well as landmarks positioned at fissure junctions and pits. Cusp apices showed less variation, but distal cusps were more vulnerable to deviations to symmetry than the earlier-forming mesial ones. This further supports the PCM as it implies that stress-induced developmental perturbations caused a cascade of reactions that flowed down chains of interactions with later-forming regions affected to a greater extent (Hunter *et al.* 2010: 5; Townsend *et al.* 2003: 355).

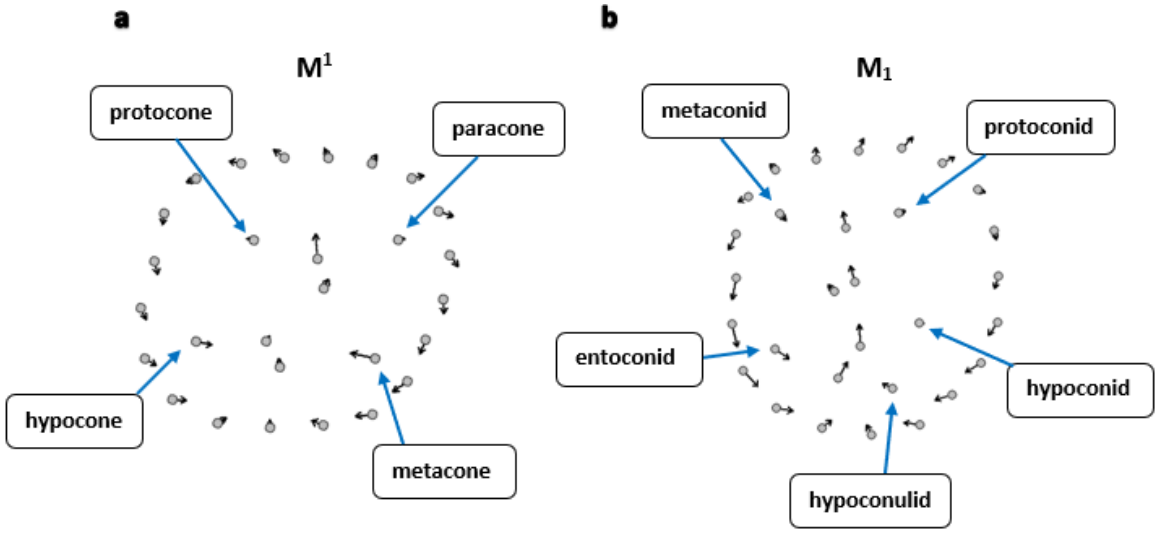

Figure 9.10 Vector displacements between reference (individual with least variance) and target (individual with most variance) shapes in the first PC of variation in A_p configurations (mesial is up). Greater FA variation is found on the periphery of cusps while earlier forming mesial cusps vary least.

Although the patterns discerned through PCA are consistent with the theoretical expectations associated with the PCM, the interpretation is not itself free from uncertainties. Firstly, without direct experimental control, it is impossible to establish that the patterns observed in inert dental materials are the consequence of a cascade of bimolecular reactions (Lynnerup and Klaus 2019: 52; Antoine and Hillson 2016: 223; Hunter *et al.* 2010; Brook 2009; Salazar-Ciudad and Jernvall 2002; Jernvall and Jung 2000). Secondly, the least-squares algorithm used in the Procrustes registration process has been noted to spread variation among nearby landmarks and this likely contributed to the dispersed patterning of variation to some degree (Klingenberg 2021; Klingenberg 2013; Klingenberg and McIntyre 1998: 1366-1367; Chapman 1990: 260). However, the results found here are comparable to those reported elsewhere which are free of the complications imposed by Procrustes registration. For example, Hunter *et al.* (2010: 5) inferred that the negative correlation between distances among the main M^1 cusps and Carabelli cusp size (graded non-metrically) was the result of developmental perturbations inhibiting growth of the main enamel knots and therefore leading to increased potential

for growth on the occlusal periphery. Similarly, Riga *et al*. (2014) found significantly more variability in the ASU graded development of accessory cusps located along the occlusal outline among individuals with evidence of stress (LEH presence). In sum, it seems unlikely that the patterns identified by this project and described here are entirely the result of computational idiosyncrasies and at worst genuine patterns of variation were accentuated. This does, however, lead to further questions regarding the use of M1 occlusal FA as a proxy for early-life stress which are discussed in the following section.

9.4.2 M1 FA, Early-life Stress and the Osteological Paradox

The multi-layered and iterative pathways through which the spatial patterning of molar cusps is determined suggests that developmental errors could produce non-additive effects (Riga *et al.* 2014: 398; Hunter *et al.* 2010: 1; Brook 2009; Salazar-Ciudad and Jernvall 2002; Jernvall and Jung 2000; Jernvall 2000: 2645). This may in part have contributed to the skewed distribution of untransformed M1 a_p scores and outlying values that could not be accounted for by error. Allometry, or the effect of shape variation increasing with size due to the difficulties associated with maintaining developmental canalisation in larger structures, was also considered as a potential confounding factor. However, as regression tests found no significant relationship between M^1 ($F(1,152)=1.436$, $p=0.233$) or M_1 a_p scores ($F(1,146)=1.034$, $p=0.319$) and size asymmetry, it seems unlikely that allometry affected the distribution of FA scores. It is more plausible to suggest that individuals with outlying FA values were either exposed to stressors that went beyond the normal range of experience. Or, alternatively, that stressors endured at key points during the cascade of biomolecular interactions that characterise the PCM reverberated across the various feedback loops and disproportionately affected

phenotype (e.g., if the development of the primary enamel knot were to be affected by stress, it would impact the growth of multiple secondary knots).

If the latter interpretation is correct, then the extent to which stressors are embodied in M1s varies depending upon when stress is experienced. So, although it was possible to offset the statistical challenges associated with exploring non-normal distributions through transformations, it remains an open question as to how accurately M1 a_p scores reflect early-life stress. The situation becomes more problematic when it is recalled that fluctuating asymmetry is more accurately described as a measure of developmental instability rather than stress *per se*. As such, FA is influenced by the volume of developmental noise (itself an aggregate of exogenous stressors and intrinsic stochastic processes) as well as stability in the developmental process which is determined by an organism's ability to buffer developmental noise and maintain developmental homeostasis (Graham and Ozener 2016: 163; Klingenberg 2015: 892; Graham *et al.* 2010: 496-497; Escós *et al.* 2000: 331; Graham *et al.* 1998: 2; Nicolis and Prigogine 1989; Holling 1973: 17; Selye 1973; Waddington 1957). More simply put, FA is the sum of everything negatively impacting development minus the organism's capacity to offset these deleterious influences.

This raises the issue of the Osteological Paradox. As healthier persons are more capable of maintaining developmental homeostasis they embody stressors to a lesser degree than frailer individuals. Conversely, differing levels of stress could be embodied to the same extent based upon differences in robustness (e.g., a highly-stressed healthy individual may develop similar stress markers to a less robust individual enduring lower stress) (DeWitte and Stojanowski 2015: 405; Wood *et al.* 1992: 356-357). Consequently, M1 a_p scores can only be considered a coarse proxy for early-life stress that reflect, to an

unquantifiable degree, a variety of hidden processes and biases. This complication likely accounts for the difficulties past researchers have had in discerning direct and unambiguous relationships between FA and other measures of health and fitness (e.g., Hoover and Matsumura 2008: 474; Møller 1999; Bailit *et al.* 1970: 635-636). When discussing maternally-mediated stress, this issue is magnified as both mother and offspring have the capacity to offset developmental perturbations.

9.4.3 Alternative Methods or Invisible Imprints?

As M1 a_p scores are an imperfect stress measure, it may be wondered if viable alternatives exist. The "stress hormone" cortisol is potentially a means of assessing general physiological responses to adversity. Cortisol is regulated by the Hypothalamic-Pituitary-Adrenal (HPA) axis. The hypothalamus is an executive region of the brain formed by a collection of nuclei that modulates homeostasis via regulation of the anterior lobe of the pituitary gland (Lewis 2019: 567; Betts *et al.* 2017: 563). When exposed to a stressor, the hypothalamus produces corticotropin-releasing hormone (CRH) which is detected by the pituitary gland (Carrera *et al.* 2020: 2; Quade *et al.* 2020: 2; Edwards and Boonstra 2018; Betts *et al.* 2017: 705; Jung *et al.* 2011). CRH stimulates the pituitary's anterior lobe to secrete adrenocorticotropic hormone (ACTH) which, when encountered by the adrenal glands, stimulates the production of cortisol (Lewis 2019: 567; Betts *et al.* 2017: 747-749). Exposure to cortisol has been associated with various life-course outcomes (e.g., shortened reproductive life-history and suppressed immunocompetence) (Carrera *et al.* 2020: 2; Lu *et al.* 2019: 253; Betts *et al.* 2017: 760; Houtepen *et al.* 2016; Thayer and Kuzawa 2014). The HPA axis is thus a mechanism which directly controls physiological responses to exogenous stimuli and therefore cortisol levels should provide a good indicator of stress experience. The extent to which cortisol concentrations can be investigated archaeologically is debatable, however. Webb

et al. (2010) successfully detected and analysed cortisol levels in hair samples, demonstrating that HPA activation can be directly assessed to reconstruct short-term life-histories. However, the attempt to reconstruct early-life stress experience by Quade *et al.* (2020) met with mixed results; while cortisol was successfully identified in dental materials, concentrations were low and not all teeth produced measurable results. Overall, the viability of assessing cortisol concentrations and directly evaluating HPA activation is still uncertain in skeletal remains.

Epigenetic processes which alter genome expression and are stress-responsive may also provide alternative measures of early-life stress to M1 a_p scores. These processes include modifications to the proteins (histones and chromatin) around which DNA is spooled and organised, the activity of non-coding RNA at "enhancer" loci and the addition of methyl compounds which act as repressors (Vaiserman 2015: 255; D'Urso and Brickner 2014; Aalto and Pasquinelli 2012; Choi and Friso 2010: 9-12; Kim *et al.* 2010) (Figure 9.11). Studies demonstrate that these processes (especially methylation) are responsible for durable outcomes associated with early-life experience. For instance, in a study of pregnant Québécois women affected by the 1998 ice storms (Cao-Lei *et al.* 2014: 2; King *et al.* 2012: 274; Lechat 1979), it was found that objective measures of maternal stress (e.g., time without power) predicted offspring outcomes such as birth weight and length, childhood body mass index and teenage insulin secretion (Dancause *et al.* 2013; Dancause *et al.* 2012; King *et al.* 2012: 274-282; Dancause *et al.* 2011). Moreover, when assessed a decade later, a strong dose-response relationship was detected between measures of maternal stress and offspring DNA methylation (Cao-Lei *et al.* 2014). Importantly, the assessment of epigenetic modifications is becoming more plausible in archaeological contexts. Islands of methylation in sequenced DNA have now been identified in millenia-old remains and the problems associated with degradation and

contamination are not as restrictive as they once were (Briggs *et al.* 2010; Green *et al.* 2009; Pruvost *et al.* 2005; Höss *et al.* 1996). However, despite this, the methods require equipment that is beyond the scope of most bioarchaeological projects and, aside from a small number of case studies, the detection of epigenetic alterations is still currently considered to be on the "frontiers" of the discipline (Klaus 2014; Green *et al.* 2009).

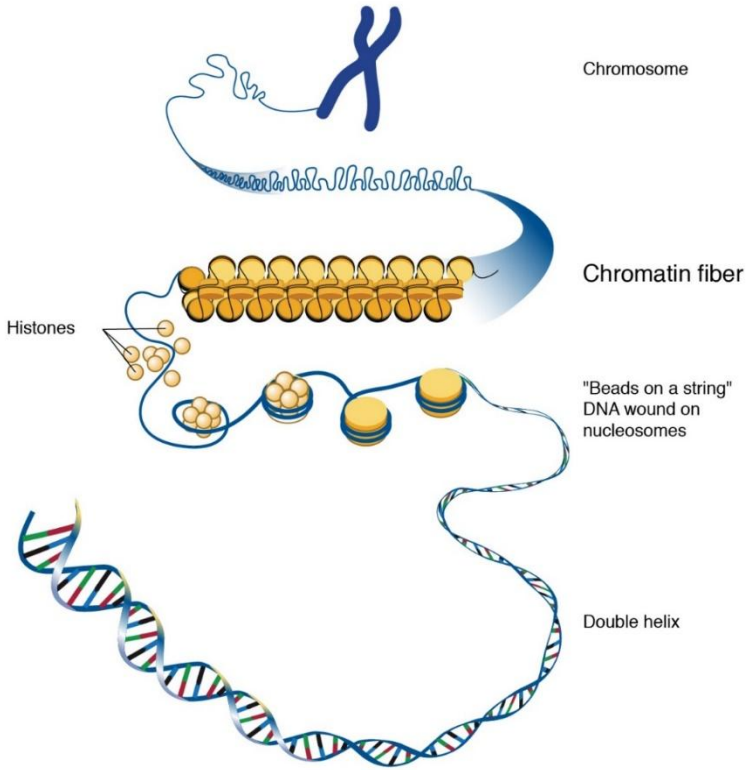

Figure 9.11 The length of DNA strands is disproportionate to cell size and so they are organised around several proteins (chromatin and histones). Stress-induced modifications to these proteins or the addition of chemical repressors can alter DNA expression and influences later-course outcomes (Vaiserman 2015; D'Urso and Brickner 2014; Aalto and Pasquinelli 2012; Choi and Friso 2010; Kim et al. 2010). Image available from: https://www.genome.gov/genetics-glossary/Chromatin.

As maternal influences define the gut microbiome of dependent offspring (Kapourchali and Cresci 2020; Chong *et al.* 2018; Cong *et al.* 2016; Caricilli and Saad 2013; Brown *et al.* 2012), evaluation of bacterial diversity may also be informative. Microbiota translocate from the maternal gut to the placenta and the colonisation of the foetal intestine is achieved through the ingestion of amniotic fluid which is initiated *circa*

the tenth week post-conception (Kapourchali and Cresci 2020: 387; Chong *et al.* 2018: 3). Shared bacterial DNA in mothers and breastfed infants further suggests that breast milk mediates the vertical transfer of microbial communities to the infant's gut postnatally (Chong *et al.* 2018: 3; Pannaraj *et al.* 2017). As a consequence of this transfer, a mother's health status and physiological condition influences the complexity and richness of the offspring microbiome until weaning age. An evolving body of research is beginning to explore the interplay between maternal influences, gut microbiome dysfunction, and health outcomes – thus far, dysbiosis has been associated with infant immune, intestinal and metabolic conditions (Kapourchali and Cresci 2020; Chong *et al.* 2018; Cong *et al.* 2016; Kundu *et al* 2017; Caricilli and Saad 2013; Brown *et al.* 2012). Archaeologically, it has been possible to explore gut microbiota through, for example, the analysis of sediments from occupation sites (e.g., Rampelli *et al.* 2021; Lugli *et al.* 2017; Santiago-Rodriguez *et al.* 2016). The analysis of gut microbiota is challenging if taking a life-course approach, however. Specifically, foetal and postnatal microbiome fluctuations may stabilise during infancy (Kapourchali and Cresci 2020: 389; Chong *et al.* 2018: 3; Cong *et al.* 2016: 303; Brown *et al.* 2012: 1095-1096), meaning that information relating to these periods is lost in most cases and the method is of limited use in generating information pertaining to the life-course trajectories among "survivors" (DeWitte and Stojanowski 2015: 416-418; Wood *et al.* 1992: 349).

In summary, cortisol levels, DNA methylation and gut microbiota richness are not only stress-responsive, they contribute to later-life outcomes. It is therefore arguable that they may provide more accurate predictors of life-course trajectories than M1 a_p scores; although M1 FA is symptomatic of early-life stress, it does not contribute to early-life programming. However, the requirement for expensive equipment means that their assessment in bioarchaeological investigations is currently limited. Moreover, the

methods through which they can be evaluated, while having gone beyond the purely theoretical, are still uncertain and have not been validated in large samples (e.g., Rampelli *et al.* 2021; Quade *et al.* 2020; Briggs *et al.* 2010). So, rather than considering these methods as more desirable alternatives to quantifications of M1 FA, it may be better to view them as complementary techniques whose results can be compared and contrasted in order to evaluate accuracy and sensitivity more comprehensively.

9.4.4 Proxies for Later Experience

From the past two sections it can be observed that, although responsive to the same experiences, the mechanisms through which early-life stress influences life-course trajectories (e.g., DNA methylation) and is preserved skeletally (i.e., dental fluctuating asymmetry) are different and this likely impacted the effectiveness of M1 a_p scores as predictors of life-course trajectories. It further raises the question of how effectively the other skeletal stress markers employed reflected later-life stress experience and so that is discussed here.

As is usual (e.g., Primeau *et al.* 2015; Temple *et al.* 2012; Blakey and Armelagos 1985), LEH were employed as a non-specific marker of episodes of childhood stress. Given the range of experimental studies in animals that have increased LEH prevalence through artificially induced metabolic deficiencies and physiological disturbances (e.g., Kreshover1960; Kreshover and Hancock 1956; Kreshover and Bear 1953a; Kreshover and Bear 1953b), this assumption seems safe. However, the identification of LEH macroscopically is difficult. It is possible, for example, for prevalence rates to be inflated through the inclusion in frequency counts of accentuated perikymata which, though visible on imbricational enamel and very similar to LEH, are not stress-induced (Hillson 1996: 167-166; Goodman and Rose 1990: 67). Consequently, two methods were

employed to mitigate this. Firstly, only "trough-like" depressions were counted and, secondly, LEH were matched across chronological zones (Primeau *et al.* 2015; Temple *et al.* 2012; Hillson 2005: 171-174; Goodman and Rose 1990: 70; Blakey and Armelagos 1985). Even with these measures, it is not possible to be certain that a depression on the surface of a tooth genuinely represents an underlying disruption to amelogenesis without histological examination (Hillson 1996: 167-166; Goodman and Rose 1990: 67). Despite this, results presented in this thesis are concordant with those of other projects. For instance, it has been found that the incidence of LEH increases past the period of early-life maternal-dependence and peaks in childhood (Temple 2014: 541; Temple *et al.* 2012: 1638; Armelagos *et al.* 2009: 267; Yamamoto 1992). It is therefore supposed that the record of stress reconstructed through matched LEH incidence reflects with relatively high accuracy the perturbations experienced during childhood that were sufficiently intense or prolonged to disrupt amelogenesis.

When assessing other proxies for childhood stress (i.e., CO and long bone lengths) a different suite of problems are encountered. The extent to which CO preserves a record of metabolic stress is debatable, for instance. CO is caused by the expansion of the red blood cell producing marrow and the concomitant atrophy of surrounding cortical and trabecular bone (Brickley 2018: 899; Jaffe 1972: 697). Yet, as the space available for red marrow expands throughout childhood (i.e., the diploë becomes larger), increased red blood cell production can be accommodated without expansion (Brickley 2018: 900). Consequently, the degree to which a metabolic stressor is embodied is not only determined by the intensity of the deficiency, but also age. Even when CO forms, as cortical bone can remodel and heal, lesions may be lost in part or completely (Steckel *et al.* 2019: 403-404; Brickley 2018: 900; Walker *et al.* 2009: 111). It is speculated these complicating factors may account for the fact that, unlike matched LEH presence, CO

presence failed to predict outcomes such as mature long bone lengths. Regarding long bones, as catch-up growth can compensate for deficits in skeletal development (through either increases in growth rate or extension of the period of time over which growth occurs), length variance may not be the best indicator of childhood/adolescent stress (Agarwal 2016: 134; Cameron 2012: 18-20; Bogin and Loucky 1997). In one relatively extreme clinical example, a deficit of approximately 6 years' growth was completely recovered once the subject had been diagnosed with severe coeliac disease and their diet was adjusted to facilitate nutritional absorption (Tanner and Whitehouse 1980). Thus, although it is believed that growth programming was identified in the regression models in which matched LEH presence predicted long bone length, long bone lengths in themselves likely poorly reflect developmental stress.

While remodelling can also obscure PNBF (Weston 2008: 51-52), other interpretative problems are associated with the lesion. Throughout the thesis, it has been proposed that bilateral lesions suggest the presence of a systemic inflammatory response to infection. While the palaeopathological literature supports this assertion (Roberts 2019; Roberts and Buikstra 2019; Steckel *et al.* 2019: 418; Weston 2008) (Figure 9.12), and it has been recognised that bilateral lesions are only a crude proxy for such, further discussion is warranted. Firstly, it must be acknowledged that certain conditions can produce bilateral PNBF without the influence of an infectious pathogen. For example, even though hypertrophic osteoarthropathy is noted for producing symmetrically distributed lesions and has been associated with infectious diseases such as TB, several non-infectious pathologies lead to secondary HOA (Grauer 2019: 503; Binder and Saad 2017; Mays and Taylor 2002). Moreover, high mechanical stresses can produce bilateral reactions on the periosteum of the lower limb (e.g., Drubach *et al.* 2001; Nielsen *et al.* 1991). It has been speculated that this has led to elevated levels of PNBF in past

populations, such as an assemblage of French Napoleonic soldiers in which most lower limb long bones (TPR=70%) exhibited PNBF (Marques *et al*. 2019: 161; Cerdá *et al.* 2003). Overall, while it can be said that PNBF is a robust embodiment of stress and that bilateral distributions are not unreasonably associated with an inflammatory response and an infectious aetiology, an element of caution must remain in the interpretation of periosteal lesions. For example, using the identification of HOA and the high prevalence of bilateral PNBF in the Warwick assemblage as evidence of infectious disease presence should be treated carefully.

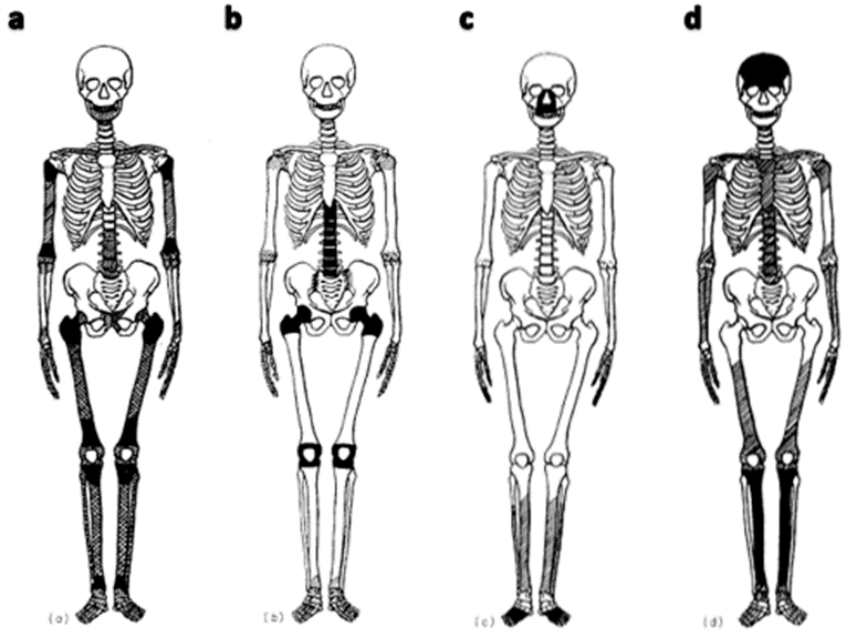

Figure 9.12 Shading illustrates the distributions of PNBF associated with osteomyelitis (a), tuberculosis (b) leprosy (c) and syphilis (d). Commonly affected sites are cross-hatched while the locations of diagnostic lesions are indicated by black (Rogers and Waldron 1989: 622-623). Note that bilateral distributions are common.

Moreover, although PD was employed to explore later-life physiology and inflammation, it is possible that it is indicative of senescence rather than pathological change. If so, the odds ratio of 16.2 (95% CI [8.04, 32.7]) inferring older, mature individuals were at a significantly higher risk of developing PD than immature ones may

just highlight normal, age-related deterioration of alveolar morphology. Comparable inferences have been made elsewhere. For instance, while entheseal change is known to be partly age-dependent (e.g., Niinimäki and Baiges Sotos 2013; Jurmain *et al.* 2012; Villotte and Knüsel 2012), it has emerged that modifications of a specifically inflammatory nature are significantly influenced by age (e.g., Moshrif *et al.* 2022; Bakirci *et al*. 2020). Yet, it is still possible that the more severe manifestations of inflammatory change are pathological. Polachek *et al.* (2017), for instance, reported that acute entheseal inflammation was not associated with advancing age but other risk factors (e.g., weight). This is consistent with the results of this project which found that moderate-to-severe PD was predicted by several variables in addition to age. However, further biases may complicate lesion interpretation. Physiological changes during pregnancy, for example, down-regulate immune function and, although these alterations re-adjust following birth, they leave pregnant females vulnerable to a variety of inflammatory pathogens and at a greater risk of PD (Wu *et al.* 2015; Borgo *et al.* 2014; Armitage 2000). As such, it appears that although PD can reflect physiological adaptations to stressors, these may be temporary. Furthermore, factors such as diet and oral hygiene are also critical in PD development and it is unlikely that the skeletal manifestations of the disease precisely reflect clinically recognised, soft-tissue symptoms (Kinaston *et al.* 2019: 771; Ogden 2008: 288; Armitage 2000: 162; Larsen 1997: 77-78).

Length of life is perhaps the most compelling indicator of whether an individual had managed to successfully endure stressors over the life-course. Consequently, the ability to accurately assess age-at-death is key to life-course and palaeoepidemiological research. As discussed in Chapter 6, in immature individuals age-at-death can be estimated with relative ease and precision through dental development (e.g., AlQahtani *et al.* 2010). The same cannot be said for the assessment of senescent changes in mature

skeletons. Although a transition analysis permits the generation of individual point estimates of age facilitating quantitative exploration (e.g., DeWitte 2018: 5), it is an imperfect technique. Aside from violating several assumptions (such as the independence of traits) (Getz 2020; Boldsen *et al.* 2002), testing of the TA^3 program in a known age-at-death population found that only in 70.8% of cases did known age fall within the point estimate's 95% CI (Getz and Byrnes 2021; DeWitte 2018: 5). Despite this, the program has outperformed traditional methods and TA^2 in terms of accuracy (Galimary and Getz 2021; Getz and Byrnes 2021) and likely represents the best means of approximating sample-level mortality patterns (Getz 2020: 7; DeWitte 2018: 5). In short, estimating age for the oldest of the old remains a persistent challenge for bioarchaeologists but fundamental to exploring connections between early-life and later-life morbidity – especially as many later-life pathological conditions associated with early-life adversity do not often produce skeletal lesions, but do increase mortality risk (e.g., Mozaffarian *et al.* 2016; Sanchis-Gomar *et al.* 2016: 6; Roseboom *et al.* 2001).

In sum, the efficacy with which the lesions chosen to reflect stress experience after the period of maternal dependence is variable. While LEH form a durable and chronologically reliable record of stress that can be interpreted with relative ease and accuracy (Primeau *et al.* 2015; Temple *et al.* 2012; Hillson 2005: 171-174; Goodman and Rose 1990), bone remodelling and age-related sensitivity makes CO a more obscure proxy for childhood metabolic stress (Steckel *et al.* 2019: 403-404; Brickley 2018; Walker *et al.* 2009). Similarly, even though bilateral PNBF is frequently associated with a well-progressed inflammatory response to infection, other chronic stressors may be implicated (Roberts 2019; Roberts and Buikstra 2019; Steckel *et al.* 2019: 418; Drubach *et al.* 2001; Nielsen *et al.* 1991). Meanwhile, whilst consistently linked to an inflammatory physiology and diseases influenced by early-life stress in the clinical

literature (e.g., Barker 2012; Lockhart *et al.* 2012; Andriankaja *et al.* 2010), the plethora of complicating factors make PD a perplexing non-specific embodiment of stress (Kinaston *et al.* 2019: 771; Armitage 2000: 162; Larsen 1997: 77-78). The estimation of age-at-death in skeletal remains continues to be a thorny subject: individual estimates of age are likely to be inaccurate, but the process of generating those estimates is becoming more objective and is capable of approximating sample-level mortality patterns which are key to bioarchaeological research (Getz 2020; DeWitte 2018; Buckberry 2015: 327; Gowland 2007: 158; Boldsen *et al.* 2002).

9.4.5 Summary

It is speculated that the relationships between M1 FA and later-life experiences were relatively subtle in part due to differences in the mechanisms through which stress is manifested. HPA axis mediated cortisol production, DNA methylation and gut microbial population are all influenced by maternally-mediated early-life experience and appear to have direct and causal relationships with later-life outcomes (Carrera *et al.* 2020; Kapourchali and Cresci 2020; Chong *et al.* 2018; Betts *et al.* 2017: 760; Houtepen *et al.* 2016; Cong *et al.* 2016; Vaiserman 2015; D'Urso and Brickner 2014; Thayer and Kuzawa 2014; Caricilli and Saad 2013; Brown *et al.* 2012; Choi and Friso 2010). Assessment of these processes is beyond most bioarchaeological projects, however, due to constraints in the archaeological survival of the imprints they leave and the accessibility of specialist equipment needed to observe what may endure (e.g., Rampelli *et al.* 2021; Quade *et al.* 2020; Briggs *et al.* 2010). By contrast, fluctuating asymmetry appears to be the result of a stress-responsive network of feedback loops (i.e., the PCM) through which dental morphology alone is determined and, which due to the nature of the cascading interactions, may not accurately reflect the underlying volume and intensity of stress experienced (Tamura and Nemoto 2016; Riga *et al.* 2014; Rizk *et al.* 2013; Hunter *et al.*

2010; Brook 2009; Salazar-Ciudad and Jernvall 2002; Jernvall and Jung 2000; Jernvall 2000: 2645). However, M1 FA represents an archaeologically durable proxy for maternally-mediated stress which can be effectively assessed through readily available equipment/software and conveniently summarised with M1 a_p scores. So, although a variety of factors (e.g., bone remodelling) have the capacity to obscure the connections between early-life events and subsequent outcomes, it is believed that meaningful signals do survive in the archaeological record and that these can be employed to disentangle the interactions between stressors experienced over the life-course.

9.5 Further Considerations and Future Improvement

In the previous section, the extent to which stress is embodied was explored to critically evaluate the utility of the osteological and dental stress markers employed and explain the sometimes-subtle quantitative connections between them. This final section evaluates further factors which influenced results. Attention is given to considerations relating to two and three-dimensional analyses, skeletal preservation and sample nature.

9.5.1 Two-dimensional and Three-dimensional Analysis

By describing and analysing M1 occlusal morphology in two rather than three dimensions it was possible to offset the demand for perfectly preserved and completely unworn teeth. That is, the position of features could be estimated in the *x*-*y* plane with some confidence even when (slightly) worn, but it is doubtful that the height of features along the z axis could have been accurately approximated. However, as teeth are three-dimensional structures, it seems highly unlikely that perturbations to the developmental cascade described by the PCM did not also affect the height of occlusal features (Jernvall and Jung 2000: 182; Jernvall 2000). It could therefore be contended that

important information was lost in the "flattening" of three-dimensional objects into two-dimensional coordinate configurations (Klingenberg 2015: 889).

The investigative value of three-dimensional analyses is, however, variable. The use of three-dimensional procedures has in the past been limited by the expense and availability of the necessary equipment. However, the requisite tools (e.g., micro computed tomography scanners) are becoming increasingly more commonplace and, as a result, a variety of studies have been conducted to test the benefits and limitations of three versus two-dimensional protocols (e.g., Wasiljew *et al.* 2020; Hendrick *et al.* 2019; Attard *et al.* 2018; Buser *et al.* 2018; Marcy *et al.* 2018; Benazzi *et al.* 2011a). These projects have met with mixed results. For example, Buser *et al.* (2018) and Wasiljew *et al.* (2020) both investigated cranial shape in fish through Procrustean techniques to explore within and between-group differences. Buser *et al.* (2018: 815) found generally smaller pairwise differences between groups in their two-dimensional dataset and hypothesised that this could be the result of variance being reduced through the loss of the *z* axis. Despite this, two and three-dimensional analyses supported the same hypotheses and small differences were only apparent where variability was predominantly located along the *z* axis (Buser *et al.* 2018). Similarly, Wasiljew *et al.* (2020) reported that two and three-dimensional procedures performed near-equally when comparing clustering of species and sexes after subjecting Procrustes-aligned configurations to PCA, and further went onto caution that the additional time and effort it took to produce three-dimensional data was restrictive. In sum, the gains associated with three-dimensional analyses are often marginal and practically costly.

When assessing teeth, further concerns emerge. Reflective enamel surfaces, for example, make direct scanning challenging. To work around this problem, fine powders can be applied to teeth to reduce their reflectiveness or moulds can be taken and then used

to produce replica casts. However, powders can confound later microwear analysis and the fabrication of moulds/casts is time consuming (Benazzi *et al.* 2011a: 311). Moreover, and with specific reference to fluctuating asymmetry, after performing a Procrustes ANOVA, Marcy *et al.* (2018: 9-10) found that measurement error accounted for a relatively high proportion of variation in a three-dimensional analysis and cautioned the small morphometric variances associated with fluctuating asymmetry may be lost or obscured in three-dimensional datasets. Even if these practical complications were to be overcome, it seems unlikely that contrasting the results of two and three-dimensional evaluations of M1 FA would be especially rewarding. As the PCM of dental development suggests that the morphogenesis of occlusal features is heavily influenced by distances between enamel knots and their inhibitory fields rather than differences in cusp height (e.g., Paul *et al.* 2017; Hunter *et al.* 2010; Jernvall and Jung 2000; Jernvall 2000), it is argued that the utilisation of two-dimensional procedures was theoretically appropriate. This is supported by various studies which have found that individual cusp form is dependent on the overall spatiotemporal patterning of cusps – e.g., Hunter *et al.* (2010) found that distances between main cusps could be used to predict the overall size of accessory cusps. In sum, it seems doubtful that the findings of a three-dimensional study would be substantially different from those generated by this two-dimensional project and, if differences in results did exist, it is likely that the increased statistical noise in a necessarily smaller sample would obscure patterns rather than clarify them (Bardua *et al.* 2019: 19; Watanabe 2018: 2; Paul *et al.* 2017).

9.5.2 Skeletal Completeness and Life-history Trade-offs

The paramount requirement for teeth caused complications when assessing other skeletal variables. To illustrate, even though the femur is the most robust long bone and it is generally better preserved archaeologically (White and Folkens 2005: 255), only 42 mature skeletons in the sample had femora while other less robust elements were better represented (e.g., 58 mature skeletons possessed one or both humeri). This idiosyncratic pattern is likely related to the practice of grave intercutting. In cemeteries in which grave markers were not used or where temporary markers were common, the position of burials was often lost (McIntyre and Bruce 2010: 34; Nolan *et al.* 2010: 151). Consequently, subsequent interments cut through older graves and the transection of skeletons is not uncommon; in the York Barbican assemblage, for instance, 42.9% of skeletons were less than a quarter complete (McIntyre n.d.: 12). As paired M1s were a requirement for inclusion in the project's sample, there was an obvious bias towards collecting data from skeletons in which the more superiorly located elements had survived. Consequently, it is believed this inhibited the identification of potentially subtle statistical connections between M1 a_p scores and long bone lengths, especially in the lower limb which is generally considered more sensitive to stress-induced growth disruptions (e.g., Pomeroy *et al.* 2012; Liu *et al.* 2009; Wadsworth *et al.* 2002).

It is speculated that the inability to effectively explore the relationship between stress and pubertal tempo was a greater loss to the project, however. Reproduction is widely regarded as an objective marker of success from an evolutionary perspective and a goal around which other aspects of life-history are organised and mediated (e.g., Gluckman *et al.* 2010: 8; Kuzawa 2007; Charnov 2001). It has also been posited theoretically and validated empirically that diverting energetic resources in order to achieve reproductive capacity and raise offspring is costly. Thus, in adverse environments

in which resources are constrained, various life-history trade-offs must be made to balance short and long-term demands. For example, young mothers that prioritise investment in offspring may inhibit their own growth and development and thereby diminish their long-term reproductive success (e.g., Pittet *et al.* 2017; Fujita *et al.* 2012; Hinde 2009; Charnov 2001; Charnov 1997; Charnov 1991). As it has also been speculated that sexual maturation and reproductive debut are malleable life-history traits responsive to contextual factors (e.g., Pittet *et al.* 2017: 14; Johnson 2003: 87-93; Bercovitch and Berard 1993) and that the method proposed by Shapland and Lewis (2013) has successfully identified variance in pubertal tempo likely in response to environmental stress (DeWitte and Lewis 2020; Gowland *et al.* 2018; Lewis *et al*. 2016), it was expected that age-independent relationships between stress markers and pubertal stage would be identifiable. However, due to the requirement for reasonably complete and well-preserved remains, pubertal stage could only be estimated for 41 skeletons – too few for a thorough quantitative exploration of pubertal tempo and stress experience.

Despite this, as it was hypothesised that elevated stress had led to delays in skeletal development (Section 9.4.2), it is believed that further investigation would be productive. Stress-induced alterations to developmental tempo could be explored in several ways. Firstly, while Shapland and Lewis (2013) include fusion stages of several epiphyses in their method, as somatic development is an integrated process (i.e., pubertal tempo is not unrelated to other aspects of growth and development) it is conjectured that more epiphyseal changes could be encompassed as well as long bone lengths (Malina *et al.* 2015; Ellison and Reiches 2012: 90; Morris *et al.* 2010), enabling a fuller assessment of skeletal changes – though this may hinge upon the accurate estimation of sex in immature remains. Secondly, in order to map relationships between observations and predict pubertal stage, it is supposed that a more statistically rigorous approach would be

beneficial. Given that a Bayesian approach has proven amenable to estimating age from reference collections through ordinally graded stages of senescent change (despite the somewhat unrealistic assumptions necessary to conduct a transition analysis) (e.g., Boldsen *et al.* 2021; Boldsen *et al.* 2002; Konigsberg and Frankenberg 2013), it is predicted that similar success could be achieved in estimating pubertal stage and attainment of life-history traits such as reproductive maturation.

9.5.3 Maternal Lineage, Maternal Condition and Documented Assemblages

Strong links have been found between later-life outcomes, early-life programming and the maternal lineage through both clinical observation (e.g., Susser *et al.* 2012; Stein *et al.* 2008; Kaati *et al.* 2002) and experimental research (e.g., Van Winkle and Ryznar 2018; Galler *et al.* 1994; Galler and Seelig 1981). Despite this evidence for intergenerational and transgenerational influences on early-life programming and later-life phenotype, the interpretations presented here suggest that maternal influences reflect cues relating to the immediate environment and potentially a mother's developmental conditions rather than an ancestral environment. Although there is some theoretical doubt as to the adaptive benefits of ancestral influences in longer-lived species such as humans (e.g., Lu *et al*. 21019; Horsthemke 2018; Wells 2007), the failure to find evidence for ancestral/transgenerational influences on life-course outcomes is also the consequence of the samples employed. The assemblages studied are characteristic of most archaeological samples in that the skeletons are largely devoid of personal identifying information so that familial connections cannot be made between individuals, while the chronological relationships between grave cuts were often unclear through a combination of intercutting, poor recording and incomplete stratigraphic analysis (McIntyre and Bruce 2010; Nolan *et al.* 2010; Raynor *et al.* 2009; Gethin n.d.). Consequently, it was not possible to trace stress experience across matrilineal kinship groups or broader cohorts

corresponding to generations. A small number of assemblages, such as the Spitalfields collection (Molleson *et al.* 1993: 123-130), do exist in which identifiable family groups are represented and these likely represent the best opportunity to explore bioarchaeologically matrilineal influences on life-course trajectories. Alternatively, cemeteries with clearly defined chronological deposits can produce assemblages that could be grouped into generational cohorts through which the links between ancestral stress and descendent outcomes may be discernible (e.g., Zoëga and Murphy 2016: 576).

Skeletal collections associated with more comprehensive records may also afford the chance to evaluate the impact of maternal life-history and fitness more thoroughly on offspring outcomes in past populations. A better understanding of mothers would likely prove invaluable to understanding offspring life-course trajectories. Primiparous mothers, for example, are subjected to greater physical stresses and are less capable of physiologically nurturing dependent offspring than mothers who have already given birth and breastfed (Morino *et al.* 2019; Pittet *et al.* 2017; Sharma *et al.* 2016; Fujita *et al.* 2012; Hinde 2009). Regarding physical stressors, first birth provokes a suite of biochemical reactions that enable morphological alterations in the pelvic girdle to facilitate childbirth and, although many of these are transitory in nature, others persist (Pany-Kucera *et al.* 2022; Morino *et al.* 2019; Huseynov *et al.* 2016). Similarly, though cellular apoptosis post-weaning reduces the number of secretory cells in the mammary gland, enough remain after first pregnancy to suggest that multiparous females are more capable of breastfeeding offspring (Lang *et al.* 2012; Matulka *et al.* 2007; Oakes *et al.* 2006). Unsurprisingly, offspring of primiparous mothers experience higher levels of morbidity and mortality (Sharma *et al.* 2016: 69; Sunderland *et al.* 2008). Aside from parity, a mother's own somatic development, social status and access to resources has been shown to affect offspring support. For instance, young mothers still growing

themselves do not have access to the same bodily reserves as mature mothers (Pittet *et al.* 2017; Tardif *et al.* 2001), while mothers with multiple offspring must divide their support (Hinde and Milligan 2011: 18; Tardif *et al.* 2001), and the availability of resources within the same environment can vary depending upon maternal social status (Pittet *et al.* 2017; Fujita *et al.* 2012). As such, it is hypothesised that access to detailed maternal life-history data has the capacity to unlock further within-group variation in maternally-mediated early-life experience and its impact on offspring life-course trajectories. However, for past populations, such predictions will likely go untested given the scarcity of such detailed data.

9.5.4 Summary

After reviewing comparative research, it is believed that the use of a two-dimensional protocol is a better option than a three-dimensional as it is supposed that the additional data would contribute statistical noise rather than novel information at the expense of sample size reduction. It was further speculated that low skeletal completeness inhibited a thorough exploration of the effects of stress upon skeletal growth and pubertal tempo. Finally, it was hypothesised that the inability to determine matrilineal connections between individuals in the sample inhibited a more thorough exploration of intergenerational cues and potentially obscured transgenerational influences on early-life programming and later-life phenotype.

Chapter 10: Conclusion

10.1 Research Aims

This study aimed to 1) develop a statistically-valid and precise method of quantifying FA in dentition from archaeological human remains, 2) use the data generated under aim 1 to examine exposure to physiological stress during early life, and 3) explore the impact of early-life stressors on life-course trajectories and later-life outcomes. In order to determine whether these aims have been achieved, the research questions outlined in the introductory chapter are reviewed.

10.2 Research Questions

1. Is dental fluctuating asymmetry a sensitive indicator of early-life stress?

Perturbations to developmental processes reflect the impact of external stressors, endogenous fluctuations and an organism's ability to buffer these insults and maintain developmental homeostasis. Given this interplay of factors, in paired structures in which the target phenotype has perfect bilateral symmetry, fluctuating asymmetry is a coarse proxy for stress experience during development rather than a sensitive indicator (Graham and Ozener 2016: 163; Klingenberg 2015: 892; Graham *et al.* 2010: 496-497; Escós *et al.* 2000: 331; Selye 1973; Holling 1973: 17). Despite this, recent bioarchaeological studies which have included dental FA have produced results in which the relationships between stressors, stress markers and outcomes align with theoretical and clinical expectations (e.g., O'Donnell and Moes 2020; Barker 2012; Barrett *et al.* 2012; Guatelli-Steinberg *et al.* 2006; Roseboom *et al.* 2001), validating the use of dental FA as marker of stress (imperfect as it may be). Importantly for a life-course approach, because odontogenesis is highly canalised chronologically, the timing of stress experience can be approximated

with a reasonable degree of accuracy; as first permanent molars crowns form during foetal and early-postnatal life, M1 occlusal FA reflects early-life stress experience (Klingenberg 2015; AlQahtani *et al.* 2010; Smith *et al.* 2010). M1 FA therefore presents an invaluable opportunity through which to explore life-course dynamics in past populations.

The robusticity of dental materials also renders dental FA an archaeologically durable stress marker (Barrett *et al.* 2012; Guatelli-Steinberg *et al.* 2006; Hillson 2005). Although dental wear and loss may make the assessment of older individuals challenging, as enamel does not remodel throughout life (Lynnerup and Klaus 2019: 52; Antoine and Hillson 2016: 223), assessments of M1 FA enable early-life stress experience to be evaluated in both skeletally immature and mature individuals. Moreover, as GM assessments of occlusal morphology do not require destructive sampling and can be implemented with equipment/software that is readily available for most (Adams *et al.* 2021; Olsen and Westneat 2015), M1 FA has the potential to be assessed in larger samples and more precisely without damaging human remains and limiting future research. Crucially, the consistency of results produced by more recent studies of dental FA (GM and traditional) and their correspondence with clinical analogues suggests that the methodological problems associated with early projects have to a large extent been overcome (e.g., O'Donnell and Moes 2020; Barker 2012; Barrett *et al.* 2012; Guatelli-Steinberg *et al.* 2006). In sum, M1 FA is an archaeologically durable and accessible proxy for early-life stress that can be measured reliably and which persists in the remains of survivors and non-survivors.

2. In past populations, to what extent did early-life stress determine life-course trajectories in growth, development, morbidity and mortality?

Somewhat surprisingly, it did not appear that early-life stress affected growth directly. Instead, childhood experience was implicated in perturbations to growth and it was hypothesised that deficits which persisted in skeletally mature individuals represented phenotypic reprogramming rather than a failure of catch-up growth (Agarwal 2016: 134; Cameron 2012: 18-20; Bogin and Loucky 1997; Tanner and Whitehouse 1980). Higher M1 FA was, however, associated with the immature cohort and within the sample there were individuals with elevated a_p scores that also evidenced delays in pubertal development. Potentially, elevated early-life stress delayed maturation so that growth could take place over a longer time in adverse environments, suggesting that early-life experience may have indirectly affected growth trajectories. It was further possible to make inferences regarding mortality and morbidity. These were based on the finding of significantly higher FA in the immature cohort in comparison to the mature skeletons, the positive correlation observed between immature age estimates and M1 a_p scores (the GM quantification of early-life stress), and the higher scores associated with inflammatory stress markers and active health insults. Together, this was taken to evidence the impact of adaptations (likely revolving around physiological phenotype) that increased the chances of short-term survival at the expense of later-life frailty, resilience and mortality risk. Overall, the data consistently support the Thrifty Phenotype Hypothesis (Hales and Barker 2013; Armelagos *et al.* 2009; Hales and Barker 2001).

3. Is it possible to infer which factors and dynamics created disparities in stress experience?

After reviewing the life-course approach it was theorised that contextually specific environmental and sociocultural influences were responsible for stress experience (Cheverko 2021: 61; Giele and Elder 2013: 9-10; Hendricks 2012: 229-230). This, in essence, appeared to be highly accurate. Past research had speculated that the Black Gate assemblage was associated with a dispersed and relatively egalitarian rural community (Mahoney Swales 2019; Mahoney Swales 2012; Nolan *et al.* 2010). It is believed that the generally moderate rates of stress markers and small number of skeletons with lesions consistent with scurvy evidence a reasonably equitable society with some members occasionally affected by seasonal resource availability. Given the contemporaneous accounts of 19th century South Shield's noxious environment (e.g., Salmon 1856; Report of the Commissioners 1845; Mackenzie 1834), it was unsurprising to find skeletal evidence of chronic later-life stress in the collection. What was perplexing, however, was the inference of relatively good childhood health. A variety of hypotheses have been developed to explain this, most of which revolve around child-labour practices in Industrial Britain and some specific to South Shields (Newman *et al.* 2019: 116-117; Newman 2016: 198-199; Raynor *et al.* 2011: 106). Meanwhile, the disasters of the 14th century, which included several famines and the Black Death, are thought to have contributed to the significantly higher levels of stress and mortality before maturity seen in the Warwick assemblage (Nolan 2019; Slavin 2013; John 1997; Proudfoot 1983; Harley 1958). Although high population density likely promoted the spread of infectious disease in the York Barbican population, the skeletal evidence suggests the community was relatively well-buffered by its commercial connections in terms of nutritional resources and possibly also in the provision of specialist care (Goldberg 2019; Grauer and

Roberts 1996; Tilliot 1961). Extrapolating from these case studies, it is posited that localised contexts uniquely imprint themselves upon the populations which inhabit them.

It was also predicted that mothers and the maternal lineage modified early-life experience (Cheverko 2021: 61; Gowland 2015; Giele and Elder 2013). The skeletal evidence strongly suggests that mothers very successfully mediated stress. Despite the distinct patterns in later-life stress experience, early-life stress as inferred through M1 FA was not generally significantly different between sites. As the frequency of stress episodes inferred through matched LEH also increased after the supposed cessation of breastfeeding (Primeau *et al.* 2015; Sandberg *et al.* 2014), it is theorised that mothers protected dependent offspring, providing a more stable developmental experience and that variance in offspring early-life experience is related to maternal condition and their ability to effectively mitigate stressors. Aside from buffering against harmful stressors, as early-life stress has been implicated in phenotypic programming for adaptive advantage (Pomeroy *et al.* 2012; Gluckman *et al.* 2010; Hales and Barker 2001), it seems that the mother-child nexus was also key to enhancing the likelihood of offspring survival in the short-term. This interpretation is significant because it contrasts with clinical understandings of the mother-child relationship which can, at times, characterise the stressors impacting this nexus as detrimental to offspring health and development (e.g., Barker 2012; Roseboom *et al.* 2001; Barker and Osmond 1986). As developmental experience appeared to be highly influential in later-life morbidity, it was also suggested a mother's own developmental experience would have impacted the level of support available to her own dependent offspring, supporting the concept of intergenerational health and mitotically-stable phenotypes (Gowland 2015; Thayer and Kuzawa 2011: 798; Skinner 2008). What was not apparent were ancestral/transgenerational influences. It may be that such influences are more important for organisms with quicker life-histories (Lu *et*

al. 2019; Van Winkle and Ryznar 2018; Susser *et al.* 2012). However, the inability to identify transgenerational relationships in archaeological samples prevented this theory being explored and will likely inhibit future investigations. Overall, the data suggests that mothers played a direct role in protecting offspring during the critical period of early life and stimulated phenotypic adaptations which were beneficial in the short-term but associated with increased morbidity and mortality later in life.

10.3 Summary

Returning once more to the project's aims, a statistically-valid and precise method of quantifying FA in the dentition of archaeologically recovered human remains was successfully developed, however, FA is not a precise measure of stress (Graham and Ozener 2016; Klingenberg 2015; Graham *et al.* 2010). Despite this M1 FA quantified through GM methods represents a durable and accessible proxy for maternally-mediated early-life stress (Lynnerup and Klaus 2019; Antoine and Hillson 2016; Smith *et al.* 2010) and, as such, is an extremely useful measure for bioarchaeologists taking a life-course approach. Consequently, by utilising the methods developed for this project along with a suite of osteological observations, it was possible to examine early-life stress exposure and its later-life impacts in past populations. From this investigation it was possible to show that localised contextual stressors imprinted themselves upon samples derived form past populations and that mothers mediated stress experience for dependent offspring and played a role in phenotypic adaptations that maximised the chances of immediate survival at the expense of increased frailty, decreased resilience and greater mortality risk in later-life.

More broadly the successes of this project help to reiterate the assertion made at the beginning of the thesis. That is, the capacity for bioarchaeological research to enhance

our collective understanding of the human experience through the assessment of skeletal tissues which embody both biological and cultural influences and preserve information otherwise lost to the historical record (Agarwal 2021; Cheverko *et al.* 2021; Buikstra 1977). Bioarchaeology and the findings emanating from the field should therefore be regarded as complementary to a range of disciplines and not viewed as a niche interest with limited significance.

10.4 Future Work

Aside from the recommendations made in Chapter 9 which largely related to difficulties identified in the specific approach taken here, several broader directions for future work emerge from the reflections on the project's aims and questions. One potential avenue of research is that of phenotypic programming. Although this is not novel, it is believed that more work could be done in the field of bioarchaeology to ascertain or reinterpret the extent to which later-life outcomes are determined by early-life and childhood experiences. For example, previous research has shown that developmental stress can be associated with reduced growth. In past work this has at times been viewed as a failure of catch-up growth to adequately compensate for deprivation-induced delays to development, but equally it could be the result of phenotypic reprogramming and the calibration of skeletal dimensions to be more sustainable in a resource-deprived environment (Agarwal 2016; Cameron 2012; Bogin and Loucky 1997; Tanner and Whitehouse 1980). Moreover, it has been inferred in clinical research that early-life stress causes alterations to physiological phenotype that influences morbidity concerning metabolic and inflammatory conditions (e.g., Barker 2012; Lockhart *et al.* 2012; Andriankaja *et al.* 2010). Attempts made here to link inflammatory lesions and M1 FA were promising but not conclusive. Although undoubtedly difficult when studying skeletal remains, it is speculated that more could be done to assess physiological

phenotype. Potentially, inflammatory modifications to joints and entheses could be assessed so that much more holistic multidimensional profiles could be created through which to explore an integrated phenotypic response to general physiological stress (Bakirci *et al*. 2020; Polachek *et al.* 2017; Selye 1973).

Regarding alterations to phenotype in response to stress, it is believed that the morphological data generated by this project can be investigated further. Patterns were identified which suggested that stress-induced deviations to bilateral occlusal symmetry in paired molars were manifested to a greater extent at the periphery of cusps and that mesial cusp apices were least affected. This supported the PCM which posits that, in multi-cusped teeth, cusps are developmental units whose growth is chronologically sequenced and linked through biomolecular feedback loops (Salazar-Ciudad and Jernvall 2002; Jernvall and Jung 2000). With support from past empirical research, it was therefore surmised that stress-induced developmental "errors" could ripple across these physiological networks, increasing morphological variation in later-forming occlusal features (Riga *et al.* 2014; Hunter *et al.* 2010; Jernvall and Jung 2000). This finding was important as it contributed to the discussion surrounding the sensitivity of M1 FA as a proxy for early-life stress. However, more research could be conducted to ascertain to what extent cusp development is integrated (Adams and Collyer 2019; Adams and Collyer 2016). The topic of developmental integration/modularity was not pursued in this project, which from the start focused upon the associations between stress experienced at different phases of the life-course and later-life outcomes, but continuing geometric morphometric investigations of the data gathered would likely provide valuable insights for the fields of dental anthropology and developmental biology.

It is also believed that the incorporation of historical sources, where possible, to a much greater extent would be valuable. To illustrate, although lived experience can be investigated through osteological remains alone and likely provides the only source of information for more chronologically distant epochs, the interpretation of skeletal patterns of stress exposure at South Shields was enriched using contemporary accounts (e.g., Fordyce 1857; Salmon 1856; Mackenzie 1834; Report of the Commissioners 1845). Though obtaining such data becomes increasingly challenging as the gulf in time widens and could necessitate a multidisciplinary approach engaging historians as well as osteologists, it is believed that the inclusion of more detailed data on contextually-specific sociocultural and environmental factors would add a great deal of inferential nuance. Moreover, information pertaining to site-specific practices concerning pregnant females and mothers with dependent offspring (e.g., whether diet and work were modified as a result of pregnancy or remained the same) would be invaluable in evaluating the impact of factors such as maternal condition and weaning age on the efficacy of maternal buffering.

Finally, it is recommended that more work be done to focus on the mothers in the mother-child dyad. As a consequence of the early formulation and articulation of the research questions, this thesis has largely focused upon the impact maternally-mediated stress had upon offspring development, life-course experiences and final outcomes. So, although maternal diet and health have been discussed, it has been in relation to the impact that they had upon their offspring. In contrast, other work has employed stress markers which form whilst maternally dependent to explore more directly the mother's health (e.g., Hodson and Gowland 2020; Beaumont *et al.* 2015; Gowland 2015). Given the competing demands placed upon mothers (i.e., the need to provision offspring and themselves) which increase vulnerability to stress and decrease resilience, mothers

represent a sensitive indicator of a society or culture's capacity to successfully buffer harmful influences. Although limited in sample size due to the destructive nature of sampling, incremental isotopic analyses of dental materials have been employed to investigate maternal stress experience, access to resources and the demands of reproduction/pregnancy/breastfeeding (e.g., Feuillâtre *et al.* 2022; Beaumont *et al.* 2015; Fuller *et al.* 2006: 51). It is proposed that a project which employs both the method developed here and isotopic testing on M1s has the potential to validate the association between M1 FA, offspring early-life stress experience and maternal diet and physiological status.

Bibliography

Aalto, A. P. and Pasquinelli, A. E. 2012. Small non-coding RNAs mount a silent revolution in gene expression. *Current Opinions in Cell Biology* 24: 333-340.

Abels, R. 2009. The Historiography of a Construct: "Feudalism" and the Medieval Historian. *History Compass* 7 (3): 1008-1031.

Adams, D. C. and Collyer, M. L. 2015. Permutation tests for phylogenetic comparative analyses of high-dimensional shape data: What you shuffle matters. *Evolution* 69 (3): 823-829.

Adams, D. C. and Collyer, M. L. 2016. On the comparison of the strength of morphological integration across morphometric datasets. *Evolution* 70: 2623-2631.

Adams, D. C. and Collyer, M. L. 2018. Multivariate Phylogenetic Comparative Methods: Evaluations, Comparisons, and Recommendations. *Systematic Biology* 67 (1): 14-31.

Adams, D. C. and Collyer, M. L. 2019. Comparing the strength of modular signal, and evaluating alternative modular hypotheses, using covariance ratio effect sizes with morphometric data. *Evolution* 73: 2352-2367.

Adams, D. C., Collyer, M. L., Kaliontzopoulou, A. and Baken, E. 2021. Geomorph: Software for geometric morphometric analyses. *R package version 4.0.0. https://cran.r-project.org/package=geomorph*.

Adams, D. C., Rohlf, F. J. and Slice, D. E. 2004. Geometric morphometrics: Ten years of progress following the 'revolution.' *Italian Journal of Zoology* 71 (1): 5-16.

Agarwal, S. C. 2016. Bone Morphologies and Histories: Life Course Approaches in Bioarchaeology. *Yearbook of Physical Anthropology* 159: 130-149.

Agarwal, S. C. 2021. What is normal bone health? A bioarchaeological perspective on meaningful measures and interpretations of bone strength, loss, and aging. *American Journal of Human Biology* 33: e23647.

Agresti, A. 2007. *An Introduction to Categorical Data Analysis, Second Edition*. New York: Wiley.

AlQahtani, S. 2009. *An Atlas of Dental Development and Eruption*. London: Queen Mary College, University of London.

AlQahtani, S., Hector, M. P. and Liversidge, H. M. 2010. Brief Communication: The London Atlas of Human Tooth Development and Eruption. *American Journal of Physical Anthropology* 142: 481-490.

AlQahtani, S., Hector, M. P. and Liversidge, H. M. 2014. Accuracy of Dental Age Estimation Charts: Schour and Massler, Ubelaker, and the London Atlas. *American Journal of Physical Anthropology* 154: 70-78.

Alsoleihat, F. 2013. A New Quantitative Method for Predicting Forensic Racial Identity Based on Dental Morphological Trait Analysis. *International Journal of Morphology* 31 (2): 418-424.

Alt, K. W. and Vach, W. 1993 Detection of Kinship Structures in Prehistoric Burial Sites Based on Odontological Traits. In J. Andresen, T. Madsen, and I. Scollar (eds). *Computing the Past - Computer Applications and Quantitative Methods in Archaeology*. Aarhus University Press. Pp. 287-292.

Alt, K. W. and Vach, W. 1995. Odontologic kinship analysis in skeletal remains: concepts, methods, and results. *Forensic Science International* 74: 99-113.

Amato, P. R. and Booth, A. 2001. The legacy of parents' marital discord: consequences for children's marital quality. *Journal of Personality and Social Psychology* 81: 627-638.

Anderson, M. J. 2006. Distance-Based Tests for Homogeneity of Multivariate Dispersions. *Biometrics* 62: 245-253.

Anderson, M. J. and Ter Braak, C. J. F. 2003. Permutation tests for multifactorial analysis of variance. *Journal of Statistical Computation and Simulation* 73 (2): 85-113.

Anderson, S. 1988. *The Human Skeletal Remains from Blackgate, Newcastle 1977–8*. Durham University Human Skeletal Research Unit, Department of Anthropology, University of Durham.

Anderson, S. 1989. *A comparative study of the human skeletal material from late first and early second millennium sites in the north-east of England*. Durham theses: Durham University. Available at Durham E-Theses Online: http://etheses.dur.ac.uk/6740/1/6740_4044.PDF

Anderson, S., Wells, C. and Birkett, D. 2005. The human skeletal remains. In R. Cramp. *Wearmouth and Jarrow Monastic Sites, Volume 1*. English Heritage. Pp 481-502.

Andriankaja, O. M., Sreenivasa, S., Dunford, R. and DeNardin, E. 2010. Association between metabolic syndrome and periodontal disease. *Australian Dental Journal* 55: 252-259.

Antoine, D. and Hillson, S. 2016. Enamel Structure and Properties. In J. D. Irish and G. R. Scott (eds). *A Companion to Dental Anthropology, First Edition*. London: Wiley. Pp 223-243.

Antoine, D. M., Dean, M. C. and Hillson, S. W. 1999. The periodicity of incremental structures in dental enamel based on the developing dentition of post-Medieval known-age children. In J. T. Mayhall and T. Heikinnen (eds). *Dental Morphology*. Oulu: Oulu University Press. Pp 48-55.

Appleby, J., Thomas, R. and Buikstra, J. E. 2015. Increasing confidence in palaeopathological diagnoses – application of the Istanbul Terminological Framework. *International Journal of Paleopathology* 8: 19-21.

Armelagos, G. J., Goodman, A. H., Harper, K. N. and Blakey, M. L. 2009. Enamel Hypoplasia and Early Mortality: Bioarchaeological Support for the Barker Hypothesis. *Evolutionary Anthropology* 18: 261-271.

Armitage, G. C. 2000. Bi-directional relationship between pregnancy and periodontal disease. *Periodontology* 61: 160-176.

Arnqvist, G. and Martensson, T. 1998. Measurement Error in Geometric Morphometrics: Empirical Strategies to Assess and Reduce its Impact on Measures of Shape. *Acta Zoologica Academiae Scientiarum Hungaricae* 44 (1-2): 73-96.

Attard, M. R. G., Sherratt, E., McDonald, P., Young, I., Vidal-García, M. and Wroe, S. 2018. A new, three-dimensional geometric morphometric approach to assess egg shape. *PeerJ* 6: e5052-e5052.

Aufderheide, A. C. and Rodríguez-Martín, C. 1998. *The Cambridge Encyclopedia of Human Paleopathology*. Cambridge: Cambridge University Press.

Baccetti, T., Franchi, L. and McNamara, J. 2005. The cervical vertebral maturation (CVM) method for the assessment of optimal treatment timing in dentofacial orthopedics. *Seminars in Orthodontics* 11: 119-129.

Baccino, E., Ubelaker, D. H., Hayek, L-A. C. and Zerilli, A. 1999. Evaluation of seven methods of estimating age at death from mature human skeletal remains. *Journal of Forensic Sciences* 44 (5): 931-936.

Bailey, R. C. and Byrnes, J. 1990. A New, Old Method for Assessing Measurement Error in Both Univariate and Multivariate Morphometric Studies. *Systematic Zoology* 39 (2): 124-130.

Bailey, S. E. and Lynch, J. 2005. Diagnostic differences in mandibular P4 shape between Neanderthals and anatomically modern humans. *American Journal of Physical Anthropology* 126: 268-277.

Bailey, S. E. 2002. A closer look at Neanderthal postcanine dental morphology. I. The mandibular dentition. *The Anatomical Record* 269: 148-156.

Bailey, S. E., Skinner, M. M. and Hublin, J-J. 2011. What Lies Beneath? An Evaluation of Lower Molar Trigonid Crest Patterns Based on Both Dentine and Enamel Expression. *American Journal of Physical Anthropology* 145: 505-518.

Bailit, H., Workman, P., Niswander, J., and MacLean, C. 1970. Dental Asymmetry as an Indicator of Genetic and Environmental Conditions in Human Populations. *Human Biology* 42 (4): 626-638.

Bakirci, S., Solmaz, D., Stephenson, W., Eder, L. Roth, J. and Aydin, S. Z. 2020. Entheseal Changes in Response to Age, Body Mass Index, and Physical Activity: An Ultrasound Study in Healthy People. *The Journal of Rheumatology* 47 (7): 968-972.

Ballantyne, J. W. 1899. On Antenatal Therapeutics. *The British Medical Journal* 889-893.

Balzeau, A., Gilissen, E. and Grimaud-Herve, D. 2012. Shared Pattern of Endocranial Shape Asymmetries among Great Apes, Anatomically Modern Humans, and Fossil Hominins. *PLoS ONE* 7 (1): e29581.

Bardua, C., Felice, R. N., Watanabe, A., Fabre, A-C. and Goswami, A. 2019. A Practical Guide to Sliding and Surface Semilandmarks in Morphometric Analyses. *Integrative Organismal Biology* 1 (1): 1-34.

Barker, D. J. P. 2012. The Developmental Origins of Health and Disease. *Public Health* 126: 186.

Barker, D. J. P. and Lampl, M. 2013. Commentary: the meaning of thrift. *International Journal of Epidemiology* 42: 1229-1230.

Barker, D. J. P. and Osmond, C. 1986. Infant Mortality, Childhood Nutrition and Ischaemic Heart Disease in England and Wales. *Lancet* 1 (8489): 1077-1081.

Barreto, J. G., Bisanzio, D., de Souza Guimarães, L., Spencer, J. S., Vazquez-Prokopec, G. M., Kitron, U. and Salgado, C. G. 2014. Spatial Analysis Spotlighting Early Childhood Leprosy Transmission in a Hyperendemic Municipality of the Brazilian Amazon Region. PLoS Neglected Tropical Diseases 8 (2): e2665.

Barrett, C, K., Guatelli-Steinberg, D. and Sciulli, P. W. 2012. Revisiting dental fluctuating asymmetry in Neandertals and modern humans. *American Journal of Physical Anthropology* 149 (2): 193-204.

Barrett, J. H., Locker, A. M. and Roberts, C. M. 2004. Dark Age economics revisited. *Antiquity* 78: 618-636.

Bashford, A. and McAdam, J. 2014. The Right to Asylum: Britain's 1905 Aliens Act and the Evolution of Refugee Law. *Law and History Review* 32 (2): 309-350.

Bateson, P., Barker, D., Clutton-Brock, T., Deb, D., D'Udine, B., Foley, R. A., Gluckman, P., Godfrey, K., Kirkwood, T., Mirazon Lahr, M., McNamara, J., Metcalfe, N. B., Monaghan, P., Spencer, H. G. and Sultan, S. E. 2004. Developmental plasticity and human health. *Nature* 430: 419-421.

Bateson, W. 1892. On numerical variation in teeth, with a discussion of the concept of homology. *Proceedings of the Zoological Society of London* 102-115.

Baume, R. M. and Crawford, M. H. 1980. Discrete dental trait asymmetry in Mexican and Belizean groups. *American Journal of Physical Anthropology* 52 (3): 315-321.

Beaumont, J., Montgomery, J. and Buckberry, J. and Jay, M. 2015. Infant Mortality and Isotopic Complexity: New Approaches to Stress, Maternal Health, and Weaning. *American Journal of Physical Anthropology* 157: 441-457.

Beloussov, L.V. 1998. *The Dynamic Architecture of a Developing Organism*. Dordrecht: Kluwer.

Benazzi, S., Coquerelle, M., Fiorenza, L., Bookstein, F., Katina, S. and Kullmer, O. 2011b. Comparison of Dental Measurement Systems for Taxonomic Assignment of First Molars. *American Journal of Physical Anthropology* 144: 342-354.

Benazzi, S., Fiorenza, L., Katina S., Bruner, E. and Kullmer, O. 2011a. Quantitative assessment of interproximal wear facet outlines for the association of isolated molars. *American Journal of Physical Anthropology* 144: 309-316.

Ben-Shlomo, Y. and Kuh, D. 2002. A life course approach to chronic disease epidemiology: conceptual models, empirical challenges, and interdisciplinary perspectives. *International Journal of Epidemiology* 31: 285-293.

Bercovitch, F. B and Berard, J. D. 1993. Life history costs and consequences of rapid reproductive maturation in female rhesus macaques. *Behavioral Ecology and Sociobiology* 32 (2): 103-109.

Bereczki, Z., Teschler-Nicola, M., Marcsik, A., Meinzer, N. J. and Baten, J. 2019. Growth Disruption in Children. Linear Enamel Hypoplasia. In R. H. Steckel, C. S. Larsen, C. A. Roberts and J. Baten (eds). *The Backbone of Europe. Health, Diet, Work and Violence over Two Millenia*. Cambridge: Cambridge University Press. Pp 175-197.

Berger, L., De Ruiter, D., Churchill, S., Schmid, P., Carlson, K. and Kibii, J. 2010. *Australopithecus sediba*: A New Species of Homo-Like Australopith from South Africa. *Science* 328 (5975): 195-204.

Berkovitz, B. K. B., Holland, G. R. and Moxham, B. J. 2009. *Oral Anatomy, Histology and Embryology*. Edinburgh: Mosby.

Betsinger, T. K. and DeWitte, S. N. 2020. *The Bioarchaeology of Urbanization: The Biological, Demographic, and Social Consequences of Living in Cities*. New York: Springer.

Betts, J. G., Desaix, P., Johnson, E., Korol, O., Kruse, D., Poe, B., Wise, J. A., Womble, M. and Young, K. A. 2017. *Anatomy and Physiology*. Houston: Rice University Press.

Binder, M. and Saad, M. 2017. Hypertrophic osteoarthropathy in a young adult male from Berber, Sudan (2nd–3rd century CE). *International Journal of Paleopathology* 18: 52-62.

Bjorksten, T., David, P., Pomiankowski, A. and Fowler, K. 2000. Fluctuating asymmetry of sexual and nonsexual traits in stalk-eyed flies: a poor indicator of developmental stress and genetic quality. *Journal of Evolutionary Biology* 13: 89-97.

Blakey, M. L. and Armelagos, J. G. 1985. Deciduous Enamel Defects in Prehistoric Americans from Dickson Mounds: Prenatal and Postnatal Stress. *American Journal of Physical Anthropology* 66: 371-380.

Bland, H. 2006. British Eugenics and 'Race Crossing': A Study of an Interwar Investigation. *New Formations* 60: 66-78.

Bocquet-Appel, J. P. and Masset, C. 1996. Paleodemography: Expectancy and False Hope. *American Journal of Physical Anthropology* 99: 571-583.

Bogin, B. and Loucky, J. 1997 Plasticity, political economy and physical growth status of Guatemala Maya Children Living in the United States. *American Journal of Physical Anthropology* 102:17-32.

Boldsen, J. l., Milner, G. R. and Ousley, S. D. 2021. Paleodemography: From archaeology and skeletal age estimation to life in the past. *American Journal of Biological Anthropology* 1-36.

Boldsen, J. l., Milner, G. R., Konigsberg, L. W. and Wood, J. W. 2002. Transition Analysis. A New Method for Estimating Age from Skeletons. In R. D. Hoppa and J. W. Vaupel (eds). *Paleodemography. Age Distributions from Skeletal Samples*. Cambridge: Cambridge University Press. Pp 73-106.

Bookstein, F. L. 1989. Principal Warps: Thin Plate Splines and the Decomposition of Deformations. *Transactions on Pattern Analysis and Machine Intelligence* 11: 567-585.

Bookstein, F. L. 1991. *Morphometric Tools for Landmark Data*. Geometry and Biology. Cambridge: Cambridge University Press.

Bookstein, F. L. 1996. Biometrics, Biomathematics and the Morphometric Synthesis. *Bulletin of Mathematical Biology* 58 (2): 313-365.

Bookstein, F. L. 1997. Landmark methods for forms without landmarks: localizing group differences in outline shape. *Medical Image Analysis* 1: 225-243.

Bookstein, F. L. and Ward, P. D. 2013. A modified Procrustes analysis for bilaterally symmetrical outlines, with an application to microevolution in Baculites. *Paleobiology* 39 (2): 214-234.

Borgo, P.V., Rodrigues, V. A. A., Feitosa, A. C. R., Xavier, K. C. B. and Avila-Campos, M. J. 2014. Association between periodontal condition and subgingival microbiota in women during pregnancy: A longitudinal study. *Journal of Applied Oral Science* 22 (6): 528-533.

Boulter, S. and Rega, E. 1993. *Report of Human Remains from Blackgate, Newcastle-Upon-Tyne.* Sheffield: Archaeological Research and Consultancy, University of Sheffield (ARCUS).

Boulter, S., Robertson, D. and Start, H. 1998. *The Newcastle Infirmary at the Forth, Newcastle Upon Tyne Volume II: The Osteology: People, Disease and Surgery, ARCUS*. Unpublished Report.

Boyde, A. 1976. Amelogenesis and the Structure of Enamel. In B. Cohen and I. R. H. Kramer (eds). *Scientific Foundations of Dentistry*. London: William Heinemann Medical Books. Pp 335-352.

Boyde, A. 1989. Enamel. In B. K. B. Berkovitz, A. Boyde, R. M. Frank, H. J. Höhling, B. J. Moxham, J. Nalbandian, and C. H. Tonge (eds). *Teeth*. New York: Springer. Pp 309-473.

Boyle, A., Boston, C. and Witkin, A. 2005. *The Archaeological Experience at St Luke's Church, Old Street, Islington*. Oxford Archaeology Report.

Breeze, D. J. 2006. *John Collingwood Bruce's Handbook to the Roman Wall*, Newcastle upon Tyne: John Nichols.

Brickley, M. B. 2018. Compiling a skeletal inventory: articulated inhumed bone. In P. D. Mitchell and M. Brickley (eds). *Updated Guidelines to the Standards for Recording Human Remains, Chartered Institute for Archaeologists/British Association of Biological Anthropology and Osteoarchaeology*, Institute of Field Archaeologists. Pp 7-9.

Brickley, M. B. 2018. Cribra orbitalia and porotic hyperostosis: A biological approach to diagnosis. *American Journal of Physical Anthropology* 167: 896-902.

Brickley, M. B. and Mays, S. 2019. Metabolic Disease. In J. E. Buikstra (eds). *Ortner's Identification of Pathological Conditions in Human Skeletal Remains*. London: Academic Press. Pp 531-566.

Brickley, M. B., Kahlon, B. and D'Ortenzio, L. 2020. Using teeth as tools: Investigating the mother–infant dyad and developmental origins of health and disease hypothesis using vitamin D deficiency. *American Journal of Physical Anthropology* 171: 342-353.

Brickley, M., Buteux, S., Adams, J., and Cherrington, R. 2006. *St Martin's Uncovered: Investigations in the Churchyard of St. Martin's-in-the-Bull Ring, Birmingham, 2001*. Oxford: Oxbow Books.

Briggs A. W., Stenzel, U., Meyer, M., Krause, J., Kircher, M. and Pääbo, S. 2010. Removal of deaminated cytosines and detection of in vivo methylation in ancient DNA. *Nucleic Acids Research* 38: e87.

Brook, A. H. 2009. Multilevel complex interactions between genetic, epigenetic and environmental factors in the aetiology of anomalies of dental development. *Archives of Oral Biology* 54S: S3-S17.

Brook, A. H., Jernvall, J., Smith, R. N., Hughes, T. E. and Townsend, G. C. 2014. The dentition: the outcomes of morphogenesis leading to variations of tooth number, size and shape. *Australian Dental Journal* 59 (1): 131-142.

Brooks, S. and Suchey, J. M. 1990. Skeletal age determination based on the os pubis: a comparison of the Ascadi-Nemeskeri and Suchey-Brooks methods. *Human Evolution* 5: 227-238.

Brown, K., DeCoffe, D., Molcan, E. and Gibson. D. L. 2012. Diet-Induced Dysbiosis of the Intestinal Microbiota and the Effects on Immunity and Disease. *Nutrients* 4: 1095-1119.

Bruce, G. 2003. *The Barbican Centre, York. OSA Report No: Osa03ev08*. Report on Archaeological Evaluation, On Site Archaeology.

Buckberry, J. 2015. The (mis)use of adult age estimates in osteology. *The Annals of Human Biology* 42 (4): 323-331.

Buckberry, J. L. and Chamberlain, A. T. 2002. Age estimation from the auricular surface of the ilium: a revised method. *American Journal of Physical Anthropology* 119: 231-239.

Buckley, G. 2021. Migrant vs. Native Health at Ancient Teotihuacan, Mexico (AD 1-550): Isotopes and Survival Analysis. [Presentation Abstract]. *(Un)natural Lives: BURG Conference 2021*.

Buckley, G., Storey, R., Longstaffe, F. J., Carballo, D. M., Hirth, K. G. and Renson, V. 2021. New Perspectives on Migration into the Tlajinga District of Teotihuacan: A Dual-Isotope Approach. *Latin American Antiquity* 32 (3): 536-556.

Buikstra, J. E. 1977. Biocultural Dimensions of Archeological Study: A Regional Perspective. In J. E. Buikstra and R. L. Blakely. *In Biocultural Adaptation in Prehistoric America*. Athens: University of Georgia Press. Pp 67-84.

Buikstra J. E. and Ubelaker D. H. 1994. *Standards for Data Collection from Human Skeletal Remains*. Arkansas: Twelfth Printing 2010.

Buikstra, J. E. 2019. A Brief History and 21st Century Challenges. In J. E. Buikstra (eds). *Ortner's Identification of Pathological Conditions in Human Skeletal Remains*. London: Academic Press. Pp 11-17.

Buikstra, J. E. 2019. *Ortner's Identification of Pathological Conditions in Human Skeletal Remains*. London: Academic Press.

Buser, T. J., And Sidlauskas, B. L. and Summers, A. P. 2018. 2D or Not 2D? Testing the Utility of 2D Vs. 3D Landmark Data in Geometric Morphometrics of the Sculpin Subfamily Oligocottinae (*Pisces; Cottoidea*). *The Anatomical Record* 301: 806-818.

Butler, P. M. 1956. The Ontogeny of Molar Pattern. *Biological Reviews* 31 (1): 30-69.

Cameron, E. Z. and Dalerum, F. 2009. A Trivers-Willard Effect in Contemporary Humans: Male-Biased Sex Ratios among Billionaires. *Plos* 4 (1): e4195.

Cameron, N. 2012. The Human Growth Curve, Canalization and Catch-Up Growth. In N. Cameron and B. Bogin (eds). *Human growth and development. Second Edition*. Amsterdam: Elsevier. Pp 1-22.

Campbell, D. B. 2009. *Roman Auxiliary Forts 27 BC-AD 378*. Oxford: Osprey Publishing.

Cao-Lei, L., Massart, R., Suderman, M. J., Machnes, Z., Elgbeili, G., Laplante, D. P., Szyf, M. King, S. 2014. DNA Methylation Signatures Triggered by Prenatal Maternal Stress Exposure to a Natural Disaster: Project Ice Storm. *PLoS ONE* 9 (9): e107653.

Cardini, A. and Elton, S. 2007. Sample size and sampling error in geometric morphometric studies of size and shape. *Zoomorphology* 126: 121-134.

Cardini, A., O'Higgins, P. and Rohlf, F. J. 2019. Seeing Distinct Groups Where There are None: Spurious Patterns from Between-Group PCA. *Evolutionary Biology* 46: 303-316.

Cardini, A., Seetah, K. and Barker, G. 2015. How many specimens do I need? Sampling error in geometric morphometrics: testing the sensitivity of means and variances in simple randomized selection experiments. *Zoomorphology* 134: 149-163.

Cardoso, F. A. and Henderson, C. Y. 2010. Enthesopathy formation in the humerus: Data from known age-at-death and known occupation skeletal collections. *American Journal of Physical Anthropology* 141 (4): 550-560.

Caricilli, A. M. and Saad, M. J. A. 2013. Diet-Induced Dysbiosis of the Intestinal Microbiota and the Effects on Immunity and Disease. *Nutrients* 5: 829-851.

Carlsen, O. 1987. *Dental Morphology*. Copenhagen: Munksgaard.

Carrera, S. C., Sen, S., Heistermann, M., Lu, A., Beehner, J. C. 2020. Low rank and primiparity increase fecal glucocorticoid metabolites across gestation in wild geladas. *General and Comparative Endocrinology* 293: 113494.

Cerdá, M. P., Feucht, M. and Blanco, V. J. D. 2003. Periostitis y marcadores ocupaciones en soldados franceses fallecidos durante la guerra de la Independencia en Valencia. In M. Campo and F. Robles (eds). *¿Dónde estamos? Pasado, Presente y Futuro de la Paleopatología*. Madrid: Universidad Autónoma de Madrid. Pp 420-429.

Chamberlain, A. 2000. Problems and Prospects in Palaeodemography. In M. Cox and S. Mays (eds). *Human Osteology in Archaeology and Forensic Science*. Cambridge: Cambridge University Press. Pp 101-106

Charnov, E. L. 1991. Evolution of life history variation among female mammals. *Proceedings of the National Academy of Science* 88: 1134-1137.

Charnov, E. L. 1997. Trade-off-invariant rules for evolutionarily stable life histories. *Nature* 387: 393-394.

Chávez A, Martinez C, Soberanes B. 2000. The effect of mal-nutrition on human development: a 24-year study of well-nourished and malnourished children living in a poor Mexican village. In A. H. Goodman, D. L. Dufour, G. H. Pelto (eds). *Nutritional anthropology: Biocultural perspectives on food and nutrition*. California: Mayfield Publishing Co. Pp 234-252.

Chertkow, S. 1980. Tooth mineralization as an indicator of the pubertal growth spurt. *American Journal of Orthodontics* 77: 79-91.

Cheverko, C. M. 2021. Life course approaches and life history theory: Synergistic perspectives for bioarchaeology. In C. M. Cheverko, J. R. Prince-Buitenhuys and M. Hubbe (eds). *Theoretical Approaches in Bioarchaeology*. Oxford: Routeledge. Pp 59-75.

Cheverko, C. M., Prince-Buitenhuys, J. R. and Hubbe, M. 2021. Theory in Bioarchaeology. In C. M. Cheverko, J. R. Prince-Buitenhuys and M. Hubbe (eds). *Theoretical Approaches in Bioarchaeology*. Oxford: Routeledge. Pp 1-14.

Choi, S-W. and Friso, S. 2010. Epigenetics: A New Bridge between Nutrition and Health. *Nutritional epigenetics* 1: 8-16.

Chong, C. Y. L., Bloomfield, F. H. and O'Sullivan, J. M. 2018. Factors Affecting Gastrointestinal Microbiome Development in Neonates. *Nutrients* 10: 274.

Christensen, G. J. and Kraus, B. S. 1965. Initial Calcification of Human Permanent First Molar. *Journal of Dental Research* 44: 1338-1342.

Cicchetti, D. V. 1994. Guidelines, criteria, and rules of thumb for evaluating normed and standardized assessment instruments in psychology. *Psychological Assessment* 6 (4): 284-290.

Clark, G. 2007. The long march of history: Farm wages, population, and economic growth, England 1209-1869. *Economic History Review* 60 (1): 97-135.

Clef, T. 2013. *Exploratory Data Analysis in Business and Economics: An Introduction Using SPSS, Stata, and Excel*. New York: Springer.

Clement, A. and Hillson, S. 2013. 'Do larger molars and robust jaws in early hominins represent dietary adaptation?' A New Study in Tooth Wear. *Archaeology International* 16: 59-71.

Cockburn, J. S. 1991. Patterns of Violence in English Society: Homicide in Kent 1560-1985. *Past and Present* 130: 70-106.

Cohen, J. 1988. *Statistical power analysis for the behavioral sciences*. Second Edition. Hillsdale: New Jersey.

Cohen, M. N. and Armelagos, G. J. 1982. *Paleopathology and the Origins of Agriculture*. Orlando: Academic Press.

Cohn, S. 2007. After the Black Death: Labour Legislation and Attitudes Towards Labour in Late-Medieval Western Europe. *Economic History Review* 60 (3): 457-485.

Collyer, M. L. 2015. ANOVAs and Geomorph. [online] *R-bloggers*. [Viewed 31st August 2020]. Available from: https://www.r-bloggers.com/anovas-and-geomorph/

Collyer, M. L. and Adams, D. C. 2018. RRPP: An R package for fitting linear models to high-dimensional data using residual randomization. *Methods in Ecology Evolution* 9: 1772-1779.

Collyer, M. L., Sekora, D. J. and Adams, D. C. 2015. A method for analysis of phenotypic change for phenotypes described by high-dimensional data. *Heredity* 115 (4): 357-365.

Commissioners, The. 1833. *Reports from the Commissioners on Conditions in Factories. Volume XXI. Parliamentary Papers*. London.

Commissioners, The. 1845 *Second report of the Commissioners for Inquiring into the State of Large Towns and Populous Districts, Appendix 2*. London.

Cong, X., Xu, W., Romisher, R., Poveda, S., Forte, S., Starkweather, A. and Henderson, W. A. 2016. Gut Microbiome and Infant Health: Brain Gut-Microbiota Axis and Host Genetic Factors. *Yale Journal of Biology and Medicine* 89: 299-308

Conroy. G. C. and Kuykendall. K. L. 1995. Paleopediatrics: Or When Did Human Infants Really Become Human? *American Journal of Physical Anthropology* 98: 121-131.

Cope, E. D. 1874. On the homologies and origin of the types of molar teeth in Mammalia educabilia. *Journal of the Academy of Natural Sciences* 8: 71-89.

Cope, E. D. 1888. On the tritubercular molar in human dentition. *Journal of Morphology* 2: 7-26.

Coqueugniot, H and Weaver, T. D. 2007. Brief Communication: Infracranial maturation in the skeletal collection from Coimbra, Portugal: New aging standards for epiphyseal fusion. *American Journal of Physical Anthropology* 134: 424-437.

Coutelis, J-B., González-Morales, N., Géminard, C. and Noselli, S. 2014. Diversity and convergence in the mechanisms establishing L/R asymmetry in metazoa. *EMBO Reports* 15: 926-937.

Craig-Atkins, E. F., Towers, J. and Beaumont, J. 2018. The role of infant life histories in the construction of identities in death: An incremental isotope study of dietary and physiological status among children afforded differential burial. *American Journal of Physical Anthropology* 167: 644-655.

Cramer, H. 1946. *Mathematical Methods of Statistics*. Princeton: Princeton University Press.

Crespo, F. A., Klaes, C. K., Switala, A. E. and DeWitte, S. N. 2016. Do leprosy and tuberculosis generate a systemic inflammatory shift? Setting the ground for a new dialogue between experimental immunology and bioarchaeology. *American Journal of Physical Anthropology* 162: 143-156.

Crespo, F. A., Rich, E., DeWitte, S. N. and Zuckerman, M. K. 2021. *Osteoimmunology as new frontier in treponemal infection: Setting the ground for bioarchaeological analysis and reconstruction of host immunological status using skeletal samples* [Presentation at the 48th Annual North American Meeting of the Paleopathology Association]. April [Viewed 7th April 2021].

Crimmins, E. M. and Finch, C. E. 2006. Infection, inflammation, height, and longevity. *Proceedings of the National of the Academy of Science* 103 (2): 498-503.

Crosnoe, R. and Elder, J. G. 2002. Successful Adaptation in the Later Years: A Life Course Approach to Aging. *Social Psychology Quarterly* 65: 309-328.

Crosnoe, R. and Elder, J. G. 2004. From childhood to the later years: Pathways of human development. *Research on Aging* 26: 623-654.

Cucchi, T., Hulme-Beaman, A., Yuan, J. and Dobney, K. 2011. Early Neolithic pig domestication at Jiahu, Henan Province, China: clues from molar shape analyses using geometric morphometric approaches. *Journal of Archaeological Science* 38 (1): 11-22.

Cuozzo, F. P. 2016. The Teeth of Prosimians, Monkeys, and Apes. In J. D. Irish and G. R. Scott (eds). *A Companion to Dental Anthropology, First Edition*. London: Wiley. Pp 37-51.

D'Ortenzio, L., Kahlon, B., Peacock, T., Salahuddin, H. and Brickley, M. 2018. The rachitic tooth: Refining the use of interglobular dentine in diagnosing vitamin D deficiency. *International Journal of Paleopathology* 22: 101-108.

D'Urso, A. and Brickner, J. H. 2014. Mechanisms of epigenetic memory. *Trends in Genetics* 30 (6): 230-236.

Dahlberg, A. A. 1956. *Materials for the Establishment of Standards for Classification of Tooth Characters, Attributes, and Techniques in Morphological Studies of the Dentition*. Chicago: University of Chicago [Unpublished item].

Dancause, K. N., Laplante, D. P., Fraser, S., Brunet, A., Ciampi, A., Schmitz, N. and King, S. 2012. Prenatal exposure to a natural disaster increases risk for obesity in 5 1/2 year old children. *Paediatric Research* 71: 126-131.

Dancause, K. N., Laplante, D. P., Oremus, C., Fraser, S., Brunet, A. and King, S. 2011. Disaster-related prenatal maternal stress influences birth outcomes: Project Ice Storm. *Early Human Development* 87: 813-820.

Dancause, K.N., Veru, F., Andersen, R. E., Laplante, D. P. and King, S. 2013. Under Review. Prenatal stress predicts insulin secretion in adolescence. *Early Human Development* 89 (9): 773-776.

Davey Smith, G. 2011. Epidemiology, Epigenetics and the "Gloomy Prospect": Embracing Randomness in Population Health Research and Practice. *International Journal of Epidemiology* 40 (3): 537-562.

De Visser, J. A. G. M., Hermisson, J., Wagner, G. P., Meyers, L.A., Bagheri-Chaichian, H., Blanchard, J. L., Chao, L., Cheverud, J. M., Elena, S. F., Fontana, W., Gibson, G., Hansen, T. F., Krakauer, D., Lewontin, R. C., Ofria, C., Rice, S. H., Von Dassow, G., Wagner, A. and Whitlock, M. C. 2003. Perspective: evolution and detection of genetic robustness. *Evolution* 57: 1959-1972.

Dean, M. C. 1998. A comparative study of cross striation spacings in cuspal enamel and of four methods of estimating the time taken to grow molar cuspal enamel in Pan, Pongo and Homo. *Journal of Human Evolution* 35: 449-462.

Debat, V., Alibert, P., David, P., Paradis, E. and Auffray, J-C. 2000. Independence between developmental stability and canalization in the skull of the house mouse. *Proceedings of the Royal Society. Biological Sciences* 267 (1442): 423sol-430.

Delezene, L. K. 2016. The Hominins 1: Australopithecines and Their Ancestors. In J. D. Irish and G. R. Scott (eds). *A Companion to Dental Anthropology, First Edition*. London: Wiley. Pp 52-66.

Demirjian, A., Goldstein, H. and Tanner, J. 1973. A new system of dental age assessment. *Human Biology* 45: 211- 227.

Dempsey, P. J. and Townsend, G. 2001. Genetic and environmental contributions to variation in human tooth size. *Heredity* 86: 685-693.

DeWitte, S. and Lewis, M. 2020. Medieval menarche: Changes in pubertal timing before and after the Black Death. *American Journal of Human Biology: The Official Journal of the Human Biology Council*: E23439.

DeWitte, S. N. 2010. Sex Differentials in Frailty in Medieval England. *American Journal of Physical Anthropology* 143 (2): 285-297.

DeWitte, S. N. 2014a. Health in Post-Black Death London (1350-1538): Age Patterns of Periosteal New Bone Formation in a Post-Epidemic Population. *American Journal of Physical Anthropology* 155: 260-267.

DeWitte, S. N. 2014b. Differential survival among individuals with active and healed periosteal new bone formation. *International Journal of Paleopathology* 7: 38-44.

DeWitte, S. N. 2018. Stress, sex, and plague: Patterns of developmental stress and survival in pre- and post-Black Death London. *American Journal of Human Biology* 30: e23073.

DeWitte, S. N. and Bekvalac, J. 2010. Oral Health and Frailty in the Medieval English Cemetery of St Mary Graces. *American Journal of Physical Anthropology* 142: 341-354.

DeWitte, S. N. and Bekvalac, J. 2011. The Association between Periodontal Disease and Periosteal Lesions in the St. Mary Graces Cemetery, London, England A.D. 1350-1538. *American Journal of Physical Anthropology* 146: 609-618.

DeWitte, S. N. and Betsinger, T. K. 2020. Introduction to the Bioarchaeology of Urbanization. In T. K. Betsinger and S. N. DeWitte (eds). *The Bioarchaeology of Urbanization: The Biological, Demographic, and Social Consequences of Living in Cities*. New York: Springer. Pp 1-21.

DeWitte, S. N. and Stojanowski, C. 2015. The Osteological Paradox 20 Years Later: Past Perspectives, Future Directions. *Journal of Archaeological Research* 23: 397-450.

DeWitte, S. N. and Wood, J. W. 2008. Selectivity of Black Death mortality with respect to preexisting health. *Proceedings of the National Academy of Science* 105 (5): 1436-1441.

DeWitte, S. N. and Yaussy, S. L. 2019. Sex differences in adult famine mortality in medieval London. *American Journal of Physical Anthropology* 171: 164-169.

Dietz, V. H. 1944. A Common Morphotropic Factor, the Carabelli Cusp. *Journal of the American Dental Association* 31: 784-789.

Dinno, A. 2015. Nonparametric pairwise multiple comparisons in independent groups using Dunn's test. *Strata Journal* 15 (1): 292-300.

Dittmar, J. M., Mitchell, P. D., Cessford, C., Inskip, S. A. and Robb, J. E. 2021. Medieval injuries: Skeletal trauma as an indicator of past living conditions and hazard risk in Cambridge, England. *American Journal of Physical Anthropology* 175: 626-645.

Dittmar, J. M., Mulder, B., Tran, A., Mitchell, P. D., Jones, P. M., Inskip, S. A., Cessford, C. and Robb, J. E. 2023. Caring for the injured: Exploring the immediate and long-term consequences of injury in medieval Cambridge, England. *International Journal of Paleopathology* 40: 7-9.

Donner, A. and Eliasziw, M. 1987. Sample size requirements for reliability studies. *Statistical Medicine* 6: 441-448.

Dos Santos Dias, L. A. and Kageyama, P. Y. 1998. Comparison Between Multivariate Methods Applied for the Evaluation of Genetic Divergence in Cacao (Theobroma cacao L.) *Brazilian Archives of Biology and Technology* 41 (2): 1-8.

Doyle, D. M. and Molix, L. 2014. Love on the margins: the effects of social stigma and relationship length on romantic relationship quality. Social Psychology and Personality Science 5: 102-110.

Doyle, D. M., Factor-Litvak, P. and Link, B. G. 2018. Modeling racial disparities in physical health via close relationship functioning: A life course approach. *Social Science and Medicine* 204: 31-38.

Drubach, L. A., Connolly, L. P., D'Hemecourt, P. A. and Treves, S. T. 2001. Assessment of the clinical significance of asymptomatic lower extremity uptake abnormality in young athletes. *The Journal of Nuclear Medicine* 42 (2): 209-212.

Dryden, I. L. and Mardia, K. V. 1998. *Statistical Shape Analysis*. Chichester: Wiley.

Dryden, I. L. and Mardia, K. V. 2016. *Statistical shape analysis, with applications in R: Second edition*. Chichester: Wiley.

Du, W., Du, W., and Yu, H. 2018. The Role of Fibroblast Growth Factors in Tooth Development and Incisor Renewal. *Stem Cells International* 2018: 7549160.

DuBois, L. Z. and Shattuck-Heidorn, H. 2021. Challenging the binary: Gender/sex and the bio-logics of normalcy. *American Journal of Human Biology* 33: e23623.

Duchon, J. 1976. Interpolation des fonctions de deux variables suivant le principe de la flexion des plaques minces. *RAIRO Analyse Numérique* 10: 5-12.

Dukić, Z. 2014. Depth of Field in Dental Photography and Methods for Its Control. *Serbian Dental Journal* 61 (3): 149-156.

Dunn, O. J. 1964. Multiple comparisons using rank sums. *Technometrics* 6 (3): 241-252.

Dyer, C. 1989. *Standards of Living in the Later Medieval Ages: Social Change in England c. 1200-1520*. Cambridge Medieval Textbook: Cambridge.

Eastlake, L. 2013. *Dental health in 18th and 19th Century Britain: A Comparative Analysis of the Coronation Street, Newcastle and St Bride's Church, London Assemblages*. Master's Thesis, University of Sheffield.

Edgar, H. J. H. 2005. Prediction of race using characteristics of dental morphology. *Journal of Forensic Science* 50 (2): 269-273.

Edgar, H. J. H. 2013. Estimation of ancestry using dental morphological characteristics. *Journal of Forensic Science* 58 (S1): S3-S8.

Edgar, H. J. H. and Rautman, A. L. M. 2016. Forensic Odontology. In J. D. Irish and G. R. Scott (eds). *A Companion to Dental Anthropology, First Edition*. London: Wiley. Pp 339-361.

Edgington, E. S. 1995. *Randomization Tests*. New York: Marcel Dekker.

Edwards, P.D. and Boonstra, R., 2018. Glucocorticoids and CBG during pregnancy in mammals: diversity, pattern, and function. *General and Comparative Endocrinology* 259: 122-130.

Eiben, O. G. and Mascie-Taylor, C. G. N. 2003. The Age at Menarche and the Social Status of the Family. *Történeti Demográfiai Évkönyve* 5-31.

Elamin, F. and Liversidge, H. M. 2013. Malnutrition Has No Effect on the Timing of Human Tooth Formation. *PLoS ONE* 8 (8): e72274.

Elder, G. H. 1994. Time, human agency, and social change: Perspectives on the life course. *Social Psychology* Quarterly 57: 4-15.

Eliot, L., Ahmed, A., Khan, H., and Patel, J. 2020. Dump the "dimorphism": Comprehensive synthesis of human brain studies reveals few male-female differences beyond size. *Neuroscience and Biobehavioral Reviews* 121: 667-697.

Ellison, P. T. and Reiches, M. W. 2012. Puberty. In N. Cameron and B. Bogin (eds). *Human growth and development. Second Edition*. Amsterdam: Elsevier. Pp 80-107.

Elowitz, M. B., Levine, A. J., Siggia, E. D. and Swain, P. S. 2002. Stochastic gene expression in a single cell. *Science* 297: 1183-1186.

Escós, J. M., Alados, C. L., Pugnaire, F. I., Puigdefábregas, J. and Emlen, J. M. 2000. Stress resistance strategy in arid land shrub: interaction between developmental instability and fractal dimension. *Journal of Arid Environments* 45: 325-336.

Ferembach, D., Schwidetzky, I. and Stloukal, M. 1980. Recommendations for age and sex diagnoses of skeletons. *Journal of Human Evolution* 9: 517-549.

Feuillâtre, C., Beaumont, J. and Elamin, F. 2022. Reproductive life histories: can incremental dentine isotope analysis identify pubertal growth, pregnancy and lactation? *Annals of Human Biology* 49 (3-4): 171-191.

Field, A. 2005. *Discovering Statistics Using SPSS, Second Edition*. London: SAGE Publications Ltd.

Finch, C. E. and Crimmins, E. M. 2004. Inflammatory exposure and historical changes in human life-spans. *Science* 305 (5691): 1736-1739.

Finden, W. 1838. *Views of the Ports, Harbours and Watering Places of Great Britain*. London: Charles Tilt.

Fiorato, V., Boylston, A. and Knüsel, C. 2000. *Blood Red Roses: The Archaeology of a Mass Grave from the Battle of Towton AD 1461*. Oxford: Oxbow.

Fordyce, F. 1857. *The History and Antiquities of the County Palatine of Durham, 2*. London: A Fullerton.

Franklin, E. and Nystrom, P. 2021. *Childhood stress and immune dysregulation: Considering a life-course approach for the assessment of frailty in skeletal remains* [Presentation at the 48th Annual North American Meeting of the Paleopathology Association]. April [Viewed 12th April 2021].

Fricke, F., Laffoon, J., Victorina, A. and Haviser, J. 2020. Delayed physical development in a first generation enslaved African woman from Pietermaai, Curaçao. *International Journal of Osteoarchaeology* 30: 43-52.

Friedlander, D. 1992. Occupational Structure, Wages, and Migration in Late Nineteenth-Century England and Wales. *Economic Development and Cultural Change* 40 (2): 295-318.

Friedlander, D., Schellekens, J., Ben-Moshe, E. and Keysar, A. 1995. Socio-Economic Characteristics and Life Expectancies in Nineteenth-Century England: A District Analysis. *Population Studies* 39 (1): 137-151.

Fruciano, C., Celik, M. A., Butler, K., Dooley, T., Weisbecker, V. and Phillips, M. J. 2017. Sharing is caring? Measurement error and the issues arising from combining 3D morphometric datasets. *Ecology and Evolution* 7: 7034-7046.

Fuentes, A., Wyczalkowski, M. A. and MacKinnon, K.C. 2010. Niche Construction through Cooperation: A Nonlinear Dynamics Contribution to Modeling Facets of the Evolutionary History in the Genus Homo. *Current Anthropology* 51 (3): 435-444.

Fujita, M., Roth, R., Lo, Y-J., Hurst, C., Vollner, J. and Kendell, A. 2012. In Poor Families, Mothers' Milk is Richer for Daughters than Sons: A Test of Trivers-Willard Hypothesis in Agropastoral Settlements in Northern Kenya. *American Journal of Physical Anthropology* 149: 52-59.

Fuller, B. T., Molleson, T. I., Harris, D. A., Gilmour, L. T. and Hedges, R. E. M. 2006. Isotopic Evidence for Breastfeeding and Possible Adult Dietary Differences from Late/Sub-Roman Britain. *American Journal of Physical Anthropology* 129: 45-54.

Full, W. E. and Ehrlich, R. 1986. Fundamental problems associated with "eigenshape analysis" and similar "factor" analysis procedures. *Mathematical Geology* 18: 451-463.

Galimany, J. and Getz, S. M. 2021. The Age-Informative Value of the Pubic Symphysis Compared to Other Skeletal Traits in a Chilean Sample Using Transition Analysis. *Proceedings of the American Academy of Forensic Sciences* 27: 55.

Galler, J. R. and Seelig, C. 1981. Home-orienting behavior in rat pups: The effect of 2 and 3 generations of rehabilitation following intergenerational malnutrition. *Developmental Psychobiology* 14: 541-548.

Galler, J. R., Tonkiss, J. and Maldonado-Irizarry, C. S. 1994. Prenatal Protein Malnutrition and Home Orientation in the Rat. *Physiology and Behavior* 55 (6): 993-996.

Galton, F. 1904. Eugenics: Its Definition, Scope, and Aims. *American Journal of Sociology* 10 (1): 1-25.

Galtung, J. 1969. Violence, Peace and Peace Research. *Journal of Peace Research* 6 (3): 167-191.

Garvin, H. M. and Passalacqua, N. V. 2012. Current practices by forensic anthropologists in adult skeletal age estimation. *Journal of Forensic Science* 57: 427-433.

Gaskell, P. 1836. *Artisans and Machinery: The Moral and Physical Condition of the Manufacturing Population Considered with Mechanical Substitutes for Human Labour*. London: John W. Parker.

Geber, J. and Murphy, E. 2012. Scurvy in the Great Irish Famine: Evidence of vitamin C deficiency from a mid-19th century skeletal population. *American Journal of Physical Anthropology* 148: 512-524.

Gelman, A. and Hill, J. 2007. *Data analysis using regression and multilevel/hierarchical models*. Cambridge: Cambridge University Press.

Gethin, B. n.d. *Interim Report on Archaeological Investigations at the site of St Lawrence's Church, 5 Stratford Road, Warwick, Warwickshire*. Unpublished Report.

Gettler, L. T. 2016. Becoming DADS: Considering the role of cultural context and developmental plasticity for paternal socioendocrinology. *Current Anthropology* 57 (S13): S38-S51.

Getz, S. M. and Byrnes, P. D. 2021. Testing the Traits of TA3: Setting a Baseline for Method Development and Performance. *Proceedings of the American Academy of Forensic Sciences* 27: 56.

Getz, S. M. 2017. *Improved Skeletal Age-At-Death Estimation and its Impact on Archaeological Analyses*. Ph.D. Thesis, Pennsylvania State University.

Getz, S. M. 2020. The use of transition analysis in skeletal age estimation. *Forensic Science* 2: e1378.

Gibson, M., and Mace, R. 2003. Strong Mothers Bear More Sons in Rural Ethiopia. *Proceedings: Biological Sciences* 270: S108-S109.

Giele, J. and Elder, G. H. 2013. Life Course Research: Development of a Field. In J. Giele, and G. Elder (eds). *Methods of Life Course Research: Qualitative and Quantitative Approaches*. Thousand Oaks: Sage. Pp 5-27.

Giele, J. Z. 1988. Gender and sex roles. In N. J. Smelser (eds). *The handbook of sociology.* Newbury Park: Sage. Pp 291-323.

Gindhart, P.S. 1973. Growth standards for the tibia and radius in children aged one month through eighteen years. *American Journal of Physical Anthropology* 39: 41-48.

Gluckman, P. D., Hanson, M. A. and Beedle, A. S. 2007. Early Life Events and Their Consequences for Later Disease: A Life History and Evolutionary Perspective. *American Journal of Human Biology* 19: 1-19.

Gluckman, P. D., Hanson, M. A. and Buklijas, T. 2010. A conceptual framework for the developmental origins of health and disease. *Journal of Developmental Origins of Health and Disease* 1 (1): 6-18.

Goldberg, J. 2019. Making the house a home in later medieval York. *Journal of Medieval History* 45 (2): 162-180.

Gómez-Robles, A., Martinon-Torres, M., Bermudez de Castro, J. M., Prado, L., Sarmiento, S. and Luis Arsuaga, J. 2008. Geometric morphometric analysis of the crown morphology of the lower first premolar of hominins, with special attention to Pleistocene Homo. *Journal of Human Evolution* 55 (4): 627-638.

Gómez-Robles, A., Martinon-Torres, M., de Castro, J. M. B., Margvelashvili, A., Batir, M., Arsuaga, J. L., and Martinez, L. M. 2007. A geometric morphometric analysis of hominin upper first molar shape. *Journal of Human Evolution* 53 (3): 272-285.

Gómez-Robles, A., Olejniczak, A. J., Martinón-Torres, M., Prado-Simón, L. and Bermúdez de Castro, J. M. 2011. Evolutionary Novelties and Losses in Geometric Morphometrics: A Practical Approach through Hominin Molar Morphology. *Evolution* 65 (6): 1772-1790.

Good, P. 1994. *Permutation tests: a practical guide to resampling methods for testing hypotheses*. New York: Springer-Verlag.

Goodall, C. 1991. Procrustes Methods in the Statistical Analysis of Shape. *Journal of the Royal Statistical Society Series B 53* (2): 285-339.

Goodman, A. H. and Martin. D. L. 2002. Reconstructing Health Profiles from Skeletal Remains. In R. H. Steckel and J. C. Rose (eds). *The Backbone of History. Health and Nutrition in the Western Hemisphere.* Cambridge: Cambridge University Press. Pp 11-60.

Goodman, A. H. and Rose, J. C. 1990. Assessment of systemic physiological perturbations from dental enamel hypoplasias and associated histological structures. *Yearbook of Physical Anthropology* 33: 59-110.

Gosling, J. A., Harris, P. F., Whitmore, I. and Willan, P. L. T. 2002. *Human Anatomy: Colour Atlas and Text*. Amsterdam: Elsevier Limited.

Gower, J. C. 1966. Some distance properties of latent root and vector methods used in multivariate analysis. *Biometrika* 53: 325-338.

Gower, J. C. 1975. Generalized Procrustes Analysis. *Psychometrika* 40 (1): 33-51.

Gowland, R. L. and Chamberlain, A. T. 2005. Detecting plague: palaeodemographic characterisation of a catastrophic death assemblage. *Antiquity* 79 (303): 146-157.

Gowland, R. L. 2007. Age, ageism and osteological bias: the evidence from late Roman Britain.', Journal of Roman Archaeology – *Supplementary Series* 65: 153-169.

Gowland, R. L. 2015. Entangled Lives: Implications of the Developmental Origins of Health and Disease Hypothesis for Bioarchaeology and the Life Course. *American Journal of Physical Anthropology* 158: 530-540.

Gowland, R. L. 2018. Infants and Mothers: Linked Lives and Embodied Life Courses. In S. Crawford, D. Hadley and G. Shepherd (eds). *The Oxford Handbook of the Archaeology of Childhood*. Oxford: Oxford University Press. Pp 104-123.

Gowland, R. L., Caffell, A., Newman, S. L., Levene, A. and Holst, M. 2018. Broken Childhoods: Rural and Urban Non-Adult Health during the Industrial Revolution in Northern England (Eighteenth–Nineteenth Centuries). *Bioarchaeology International* 2 (1): 44-62.

Graham, J. H. and Ozener, B. 2016. Fluctuating Asymmetry of Human Populations: A Review. *Symmetry* 8: 154.

Graham, J. H., Emlen, J. M., Freeman, D. C., Leamy, L. J. and Kieser, J. A. 1998. Directional asymmetry and the measurement of developmental instability. *Biological Journal of the Linnean Society* 64 (1): 1-16.

Graham, J. H., Raz, S., Hagit, H. and Nevo E. 2010. Fluctuating Asymmetry: methods, theory and applications. *Symmetry* 2: 466-495.

Grauer, A. L. 2019. Circulatory, Reticuloendothelial, and Hematopoietic Disorders. In J. E. Buikstra (eds). *Ortner's Identification of Pathological Conditions in Human Skeletal Remains*. London: Academic Press. Pp 491-530.

Grauer, A. L. and Miller, A. G. 2017. Flesh on the Bones: A Historical and Bioarchaeological Exploration of Violence, Trauma, Sex, and Gender in Medieval England. *Fragments* 6: 38-79.

Grauer, A. L. and Roberts, C. A. 1996. Paleoepidemiology, Healing and Possible Treatment of Trauma in the Medieval Cemetery of St. Helen-on-the-Walls, York, England. *American Journal of Physical Anthropology* 100 (4): 531-544.

Grauer, A. L. and Roberts, C. A. 2019. Fungal, Viral, Multicelled Parasitic and Protozoan Infections. In J. E. Buikstra (eds). *Ortner's Identification of Pathological Conditions in Human Skeletal Remains*. London: Academic Press. Pp 441-478.

Grave, K. and Brown, T. 1976. Skeletal ossification and the adolescent growth spurt. *American Journal of Orthodontics* 69: 611-619.

Green, R. 1991. How many subjects does it take to do a regression analysis? *Multivariate Behavioural Research* 26: 499-510.

Green, R. E., Briggs, A. W., Krause, J., Prufer, K., Burbano, H. A., Siebauer, M., Lachmann, M. and Pääbo, S. 2009. The Neandertal genome and ancient DNA authenticity. *European Molecular Biology Organization Journal* 28: 2494-2502.

Gregory, W. K. 1916. Studies on the evolution of Primates. I. The Cope-Osborn "theory of tritubercuIy" and the ancestral molar patterns of Primates. *Bulletin of the American Museum of Natural History* 35: 239-257.

Gregory, W. K. 1922. *The Origin and Evolution of the Human Dentition*. Baltimore: Williams and Wilkins.

Grus, J. 2015. *Data Science from Scratch First Principles with Python*. Sebastopol: O'Reilly.

Guatelli-Steinberg, D. 2003. Macroscopic and microscopic analyses of linear enamel hypoplasia in Plio-Pleistocene South African hominins with respect to aspects of enamel development and morphology. *American Journal of Physical Anthropology* 120: 309-322.

Guatelli-Steinberg, D. 2016. Dental Stress Indicators from Micro- to Macroscopic. In J. Irish and G. R. Scott (eds). *A Companion to Dental Anthropology*. Chichester: John Wiley. Pp 472-486.

Guatelli-Steinberg, D., Sciulli, P. and Edgar, H. J. H. 2006. Dental Fluctuating Asymmetry in the Gullah: Tests of Hypotheses Regarding Developmental Stability in Deciduous vs Permanent Teeth. *American Journal of Physical Anthropology* 129: 427-434.

Gunz, P. and Mitteroecker, P. 2013. Semilandmarks: a method for quantifying curves and surface. *Hystrix* 24 (1): 103-109.

Gustine, J. N. and Jones, D. 2021. Immunopathology of Hyperinflammation in COVID-19. *The American Journal of Pathology* 191 (1): 4-17.

Hagg, A. C., Van der Merwe, A. E. and Steyn, M. 2017. Developmental instability and its relationship to mental health in two historic Dutch populations. *International Journal of Paleopathology* 17: 42-51.

Hägg, U. and Taranger, J. 1982. Maturation indicators and the pubertal growth spurt. *American Journal of Orthodontics* 82: 299-309.

Halcrow, S. E., Tayles, N. and Elliot, G. 2018. The bioarchaeology of foetuses. In S. Hans, T. K. Betsinger and A. B. Scott (eds). *Anthropology of foetuses: Biology, culture and society*. Berghahn Books. Pp 83-111.

Hales, C. N. and Barker, D. J.P. 2001. The thrifty phenotype hypothesis. *British Medical Bulletin* 60: 5-20.

Hales, C. N. and Barker, D. J.P. 2013. Type 2 (non-insulin-dependent) diabetes mellitus: the thrifty phenotype hypothesis. *International Journal of Epidemiology* 42: 1215-1222.

Harley, J. B. 1958. Population Trends and Agricultural Developments from the Warwickshire Hundred Rolls of 1279. *The Economic History Review* 11 (1): 8-18.

Harris, E. F. 2007 Carabelli's trait and tooth size of human maxillary first molars. *American Journal of Physical Anthropology* 132: 238-246.

Harris, E. F. 2016. Odontogenesis. In J. D. Irish and G. R. Scott (eds). *A Companion to Dental Anthropology, First Edition*. London: Wiley. Pp 142-158.

Harris, E. F. and Sjovold, T. 2004. Calculation of Smith's mean measure of divergence for intergroup comparisons using nonmetric data. *Dental Anthropology* 17: 83-93.

Hasegawa, Y., Rogers, J., Scriven, G. and Townsend, G. C. 2010. Carabelli Trait in Australian Twins: Reliability and Validity of Different Scoring Systems. *Dental Anthropology* 23: 7-15.

Hassett, B. R. 2012. Evaluating sources of variation in the identification of linear hypoplastic defects of enamel: a new quantified method. *Journal of Archaeological Science* 39: 560-565.

Hatcher, J. 1994. England in the Aftermath of the Black Death. *Past and Present* 144: 3-35.

Hauser, R. M. and Sweeney, M. M. 1997. Does poverty in adolescence affect the life chances of high school graduates? In G. J. Duncan and J. Brooks-Gunn (eds). *Consequences of Growing Up Poor*. New York: Russell Sage Foundation. Pp 541-595.

Haydock, H., Clarke, L., Craig-Atkins, E., Howcroft, R. and Buckberry, J. 2013. Weaning at Anglo-Saxon Raunds: Implications for Changing Breastfeeding Practice in Britain Over Two Millennia. *American Journal of Physical Anthropology* 151: 604-612.

Hedrick, B. P. Antalek-Schrag, P., Conith, A. J., Natanson, L. J. and Brennan, P. L. R. 2019. Variability and asymmetry in the shape of the spiny dogfish vagina revealed by 2D and 3D geometric morphometrics. *Journal of Zoology* 308: 16-27.

Heinzl, H., Waldhor, T. and Mittlbock, M. 2005. Careful use of pseudo R-squared measures in epidemiological studies. *Statistics in Medicine* 24: 2867-2872.

Hemer, K. A. 2014. Are we nearly there yet? Children and migration in early medieval western Britain. In D. M. Hadley and K. A. Hemer (eds). Medieval Childhood: archaeological approaches. SSCIP Monograph 3. Oxford: Oxbow. Pp 131-144.

Hemer, K. A. and Evans, J. A. 2018. The contribution of stable isotope analysis to the study of childhood movement and migration. In D. M. Hadley, S. Crawford and G. Shepard (eds). Handbook of the Archaeology of Childhood. Oxford: Oxford University Press. Pp 505-520.

Henderson, R. C., Lee-Thorp, J. and Loe, L. 2014. Early Life Histories of the London Poor Using δ13C and δ15N Stable Isotope Incremental Dentine Sampling. *American Journal of Physical Anthropology* 154: 585-593.

Hendricks, J. 2012. Considering Life Course Concepts. *The Journals of Gerontology: Series B* 67 (2): 226-231.

Hewitt, D. and Acheson, R. 1961a. Some aspects of skeletal development through adolescence. I. Variations in the rate and pattern of skeletal maturation at puberty. *American Journal of Physical Anthropology* 19: 321-331.

Hill, D. n.d. *Assessment of the Human Remains from Stratford Road, Warwick (WR15).* Unpublished.

Hillson, S. 1996. *Dental Anthropology*. Cambridge: Cambridge University Press.

Hillson, S. 2005. *Teeth. Second Edition*. Cambridge: Cambridge University Press.

Hinde, K. 2009. Richer Milk for Sons but More Milk for Daughters: Sex-Biased Investment during Lactation Varies with Maternal Life History in Rhesus Macaques. *American Journal of Human Biology* 21: 512-519.

Hinde, K. and Milligan, L. A. 2011. Primate Milk: Proximate Mechanisms and Ultimate Perspectives. *Evolutionary Anthropology* 20: 9-23.

Hinzpetere, R. and Ponce de León, M. S. 2016. Developmental evidence for obstetric adaptation of the human female pelvis. *Proceedings of the National Academy of Sciences* 113 (19): 5227-5232.

Hlusko, L. and Mahaney, J. 2009. Quantitative Genetics, Pleiotropy, and Morphological Integration in the Dentition of *Papio Hamadryas*. *Evolutionary Biology* 36 (1): 5-18.

Hodder, I. 1982. Theoretical archaeology: A reactionary view. In I. Hodder (eds). *Symbolic and Structural Archaeology (New Directions in Archaeology)*. Cambridge: Cambridge University Press. Pp 1-16.

Hodgson, G.B. 1903. *The Borough of South Shields from the Earliest Period to the Close of the Nineteenth Century*. Newcastle-upon-Tyne: Andrew Reid.

Hodson, C. M. and Gowland, R. 2020. Like Mother, Like Child: Investigating Perinatal and Maternal Health Stress in Post-medieval London. In R. Gowland and S. Halcrow (eds). (2019). *The mother-infant nexus in anthropology: Small beginnings, significant outcomes*. Cham: Springer. Pp 39-64.

Holland Jones, J. 2005. Fetal programming: Adaptive life-history tactics or making the best of a bad start? *American Journal of Human Biology* 17 (1): 22-33.

Holland, P. W., Booth, H. A. F. and Bruford, E. A. 2007. Classification and nomenclature of all human homeobox genes. *BMC Biology* 5: 47.

Hollander, M. and Wolfe, D. A. 1973. *Nonparametric Statistical Methods*. New York: Wiley.

Holling, C. S. 1973. Resilience and stability of ecological systems. *Annual Review of Ecological Systems* 4: 1-23.

Holt, S., Reid, D. and Guatelli-Steinberg, D. 2012. Brief Communication: Premolar Enamel Formation: Completion of Figures for Aging LEH Defects in Permanent Dentition. *Journal of Dental Anthropology* 25: 4-7.

Hooton, E. A. 1930. *The Indians of Pecos Pueblo, a study of their skeletal remains*. New Haven: Yale University Press.

Hoover, K. C. and Matsumura, H. 2008. Temporal Variation and Interaction Between Nutritional and Developmental Instability in Prehistoric Japanese Populations. *American Journal of Physical Anthropology* 137: 469-478.

Hoppa, R. D. 1992. Evaluating Skeletal Growth: an Anglo-Saxon Example. *International Journal of Osteoarchaeology* 2: 275-288.

Hoppa, R. D. 2002. Paleodemography: Looking Back and Thinking Ahead. In R. D. Hoppa and J. W. Vaupel (eds). *Paleodemography. Age Distributions from Skeletal Samples.* Cambride: Cambridge University Press. Pp 9-28.

Hoppa, R. D. and Vaupel, J. W. 2002a. *Paleodemography. Age Distributions from Skeletal Samples*. Cambridge: Cambridge University Press.

Hoppa, R. D. and Vaupel, J. W. 2002b. The Rostock Manifesto for paeodeomography: the way from stage to age. In R. D. Hoppa and J. W. Vaupel (eds). *Paleodemography. Age Distributions from Skeletal Samples*. Cambridge: Cambridge University Press. Pp 1-8.

Horrell, S. and Oxley, D. 2012. Bringing home the bacon? Regional nutrition, stature, and gender in the industrial revolution. *Economic History Review* 65 (4): 1354-1379.

Horsthemke, B. 2018. A critical view on transgenerational epigenetic inheritance in humans. *Nature Communications* 9: 2973.

Höss, M., Jaruga, P., Zastawny, T. H., Dizdaroglu, M. and Pääbo, S. 1996. DNA damage and DNA sequence retrieval from ancient tissues. *Nucleic Acids Research* 24: 1304-1307.

Houtepen, L. C., Vinkers, C. H., Carrillo-Roa, T., Hiemstra, M., van Lier, P. A., Meeus, V., Branje, S., Heim, C. M., Nemeroff, C. B., Mill, J., Schalkwyk, L. C., Creyghton, M. P., Kahn, R. S., Joels, M., Binder, E. B. and Boks, M. P. M. 2016. Genome-wide DNA methylation levels and altered cortisol stress reactivity following childhood trauma in humans. *Nature Communications* 7: 10967.

Hrdlicka, A. 1921. Further studies of tooth morphology. *American Journal of Physical Anthropology* 4: 141-176.

Hughes, T. E. and Townsend, G. C. 2013. Twin and family studies of human dental crown morphology: genetic, epigenetic, and environmental determinants of the modern human dentition. In G. Scott and J. Irish (eds). *Anthropological Perspectives on Tooth*

Morphology: Genetics, Evolution, Variation. Cambridge: Cambridge University Press. Pp 31-68.

Hunt, S. 2005. *The Life Course: A Sociological Introduction*. Basingstoke: Palgrave Macmillan.

Hunter, J. P. and Guatelli-Steinberg, D. 2016. New Directions in Dental Development Research. In J. D. Irish and G. R. Scott (eds). *A Companion to Dental Anthropology, First Edition*. London: Wiley. Pp 487-498.

Hunter, J. P., Guatelli-Steinberg, D., Weston, T. C., Durner, R., Betsinger, T. K. 2010. Model of Tooth Morphogenesis Predicts Carabelli Cusp Expression, Size, and Symmetry in Humans. *PLoS ONE* 5 (7): e11844.

Hunter, R. G. 2012 Epigenetic effects of stress and cortisteroids in the brain. *Frontiers in Cellular Neuroscience* 6: 1-8.

Huseynova, A., Zollikofera, C. P. E., Coudyzerb, W., Gaschoc, D., Kellenbergerd, C.,

Hwang, I. T. 2014. Efficacy and safety of growth hormone treatment for children born small for gestational age. *Korean Journal of Paediatrics* 57 (9): 379-383.

Ibáñez, L., Ferrer, A., Marcos, M. V., Hierro, F. R. and De Zegher, F. 2000. Early Puberty: Rapid Progression and Reduced Final Height in Girls with Low Birth Weight. *Pediatrics* 106.5: E72.

Inskip, S. A., Scheib, C., Kivisild, T., Cessford, C., Wohns, A. W. and Robb, J. E. 2019. Evaluating Macroscopic Sex Estimation Methods using Genetically Sexed Archaeological Material: The Medieval Skeletal Collection from St John's Divinity School, Cambridge. *American Journal of Physical Anthropology* 168: 340-351.

Irish, J. D. 1997. Characteristic high- and low-frequency dental traits in Sub-Saharan African populations. *American Journal of Physical Anthropology* 102: 455-467.

Irish, J. D. 1998. Ancestral dental traits in recent Sub-Saharan Africans and the origins of modern humans. *Journal of Human Evolution* 34: 81-98.

Irish, J. D. 2010. The Mean Measure of Divergence: Its Utility in Model-Free and Model-Bound Analyses Relative to the Mahalanobis D^2 Distance for Nonmetric Traits. *American Journal of Human Biology* 22: 378-395.

Irish, J. D. 2011. Afridonty: the "Sub-Saharan African Dental Complex" revisited. *American Journal of Physical Anthropology* 144 (52): 174.

Irish, J. D. 2013. Afridonty. In G. Scott and J. D. Irish (eds). *Anthropological Perspectives on Tooth Morphology: Genetics, Evolution, Variation*. Cambridge: Cambridge University Press. Pp. 278-295.

Irish, J. D. 2016a. Terms and Terminology Used in Dental Anthropology. In J. D. Irish and G. R. Scott (eds). *A Companion to Dental Anthropology, First Edition*. London: Wiley. Pp 87-93.

Irish, J. D. 2016b. Assessing Dental Nonmetric Variation among Populations. In J. D. Irish and G. R. Scott (eds). *A Companion to Dental Anthropology, First Edition*. London: Wiley. Pp 265-286.

Irish, J. D. and G. R. Scott (eds). 2016. *A Companion to Dental Anthropology, First Edition*. London: Wiley.

Irish, J. D., Bailey, S. E., Guatelli-Steinberg, D., Delezene, L. K and Berger, L. R. 2018. Ancient teeth, phenetic affinities, and African hominins: Another look at where *Homo naledi* fits in. *Journal of Human Evolution. Journal of Human Evolution*: 1-16.

Irish, J. D., Guatelli-Steinberg, D., Legge, S. S., de Ruiter, D. J. and Berger, L. R. 2013. Dental Morphology and the Phylogenetic "Place" of *Australopithecus sediba*. *Science* 340 (12): 1233062/1- 1233062/4.

Irish, J. D., Lillios, K.T., Waterman, A. J., and Silva, A.M. 2017. "Other" possibilities? Assessing regional and extra-regional dental affinities of populations in the Portuguese Estremadura to explore the roots of Iberia's Late Neolithic-Copper Age. *Journal of Archaeological Science*: Reports 11: 224-236.

Irish, J.D. 2006. Who Were the Ancient Egyptians? Dental Affinities Among Neolithic Through Postdynastic Peoples. *American Journal of Physical Anthropology* 129: 529-543.

Jablonka, E., Oborny, B., Molnar, I., Kisdi, E., Hofbauer, J. and Czaran, T. 1995. The adaptive advantage of phenotypic memory in changing environments. *Philosophical Transactions: Biological Sciences* 350: 133-141.

Jacob, C. M., Cooper, C., Baird, J. and Hanson, M. 2019. *What quantitative and qualitative methods have been developed to measure the implementation of a life-course approach in public health policies at the national level?* Copenhagen: WHO Regional Office for Europe.

Jaffe, H. L. 1972. *Metabolic, degenerative, and inflammatory diseases of bones and joints*. Philadelphia: Lea and Febiger.

Jernvall J. 2000. Linking development with generation of novelty in mammalian teeth. *Proceedings of the National Academy of Sciences* 97: 2641-2645.

Jernvall, J. and Jung, H-S. 2000. Genotype, Phenotype, and Developmental Biology of Molar Tooth Characters. *Yearbook of Physical Anthropology* 43: 171-190.

Jernvall, J. and Thesleff I. 2000. Reiterative signaling and patterning during mammalian tooth morphogenesis. *Mechanisms of Development* 92: 19-29.

Jernvall, J., Kettunen, P., Karavanova, I., Martin, L. B. and Thesleff, I. 1994. Evidence for the role of the enamel knot as a control center in mammalian tooth cusp formation: non-dividing cells express growth stimulating Fgf-4 gene. *International Journal of Developmental Biology* 38: 463-469.

John, T. 1997. Population Change in medieval Warwickshire: Domesday Book to the Hundred Rolls of 1279-1280. *Local Population Studies* 59: 41-53.

Johnson, S. E. 2003. Life history and the competitive environment: trajectories of growth, maturation, and reproductive output among chacma baboons. *American Journal of Physical Anthropology* 120: 83-98.

Jung, C., Ho, J. T., Torpy, D. J. Rogers, A., Doogue, M., Lewis, J. G., Czajko, R. J. and Inder, W. J. 2011 A Longitudinal Study of Plasma and Urinary Cortisol in Pregnancy and Postpartum. *Journal of Clinical Endocrinology and Metabolism* 96 (5): 1533-1540.

Jung, H-S., Francis-West, P. H., Widelitz, R. B., Jiang, T-X., Ting-Berreth, S., Tickle, C., Wolpert, L. and Chuong, C-M. 1998. Local inhibitory action of BMPs and their relationships with activators in feather formation: implications for periodic patterning. *Developmental Biology* 196: 11-23.

Jurmain, R. 1980. The pattern of involvement of appendicular degenerative joint disease. *American Journal of Physical Anthropology* 53: 143-150.

Jurmain, R., Cardoso, F. A., Henderson, C. and Villotte, S. 2012. Bioarchaeology's Holy Grail: The Reconstruction of Activity. In A. L. Grauer (eds). *A Companion to Paleopathology*. London: Blackwell. Pp 531-552.

Kaati, G., Bygren, L. O. and Edvinsson, S. 2002. Cardiovascular and diabetes mortality determined by nutrition during parents' and grandparents' slow growth period. *European Journal of Human Genetics* 10: 682-688.

Kapourchali, F. R. and Cresci, G. A. M. 2020. Early-Life Gut Microbiome—The Importance of Maternal and Infant Factors in Its Establishment. *Nutrition in Clinical Practice* 35 (3): 386-405.

Kappelle, W. E. 1979. *The Norman Conquest of the North: the region and its transformation, 1000-1135*. Chapel Hill: University of North Carolina Press.

Katz, D. and Suchey, J. M. 1986. Age Determination of the Male Os Pubis. *American Journal of Physical Anthropology* 69: 427-435.

Kelmelis, K. S., Kristensen, V. R. L., Alexandersen, M. and Pedersen, D. D. 2020. Markets and Mycobacteria – A Comprehensive Analysis of the Influence of Urbanization on Leprosy and Tuberculosis Prevalence in Denmark (AD 1200–1536). In T. K. Betsinger and S. N. DeWitte (eds). *The Bioarchaeology of Urbanization. The Biological, Demographic, And Social Consequences of Living in Cities*. Cham: Springer. Pp 147-182.

Kemkes-Grottenthaller, A. 2002. Aging through the ages: historical perspectives on age indicator methods. In R. D. Hoppa and J. W. Vaupel (eds). *Paleodemography. Age Distributions from Skeletal Samples*. Cambridge: Cambridge University Press. Pp 48-72.

Kendall, D. G. 1984. Shape-manifolds, Procrustean metrics and complex projective spaces. *Bulletin of the London Mathematical Society* 16: 81-121.

Kent, J. and Mardia, K. 2001. Shape, Procrustes tangent projections and bilateral symmetry. *Biometrika* 88 (2): 469-485.

Kenyhercz, M. W., Klales, A. R. and Kenyhercz, W. E. 2014. Molar Size and Shape in the Estimation of Biological Ancestry: A Comparison of Relative Cusp Location Using Geometric Morphometrics and Interlandmark Distances. *American Journal of Physical Anthropology* 153: 269-279.

Kerr, N. W. 1988. A method of assessing periodontal status in archaeologically derived skeletal material. *Journal of Paleopathology* 2: 67-78.

Kettunen, P., Karavanova, I. and Thesleff, I. 1998. Responsiveness of developing dental tissues to fibroblast growth factors: expression of splicing alternatives of FGFR1, -2, -3, and of FGFR4; and stimulation of cell proliferation by FGF-2, -4, -8, and -9. *Developmental Genetics* 22: 374-385.

Kettunen, P., Laurikkala, J., Itäranta, P., Vainio, S., Itoh, N. and Thesleff, I. 2000. Associations of FGF-3 and FGF-10 with signalling networks regulating tooth morphogenesis. *Developmental Dynamics* 219: 322-332.

Kierszenbaum, A. L. 2006. Cell-cycle regulation and mammalian gametogenesis: a lesson from the unexpected. *Molecular Reproductive Development* 73 (8): 939-942.

Kim, T. K., Hemberg, M., Gray, J. M., Costa, A. M., Bear, D. M., Wu, J., Harmin, D. A., Laptewicz, M., Barbara-Haley, K., Kuersten, S., Markenscoff-Papadimitriou, E., Kuhl, D., Bito, H., Worley, P. F., Kreiman, G. and Greenberg, M. E. 2010. Widespread transcription at neuronal activity-regulated enhancers. *Nature* 465 (7295): 182-187.

Kim, Y-J. 2015. The Effect of Incarceration on Midlife Health: A Life-Course Approach. *Population Research and Policy Review* 34: 827-849.

Kinaston, R., Willis, A., Miszkiewicz, J., Tromp, M. and Oxenham, M. F. 2019. The Dentition: Development, Disturbances, Disease, Diet and Chemistry. In J. E. Buikstra (eds). *Ortner's Identification of Pathological Conditions in Human Skeletal Remains*. London: Academic Press. Pp 749-797.

King, C. L., Halcrow, S. E., Millard, A. R., Grocke, D. R., Standen, V. G., Portilla, M. and Arriaza, B. T. 2018. Let's talk about stress, baby! Infant-feeding practices and stress in the ancient Atacama Desert, Northern Chile. *American Journal of Physical Anthropology* 166: 139-155.

King, S., Dancause, K. N., Turcotte-Tremblay, A-M., Veru, F. and Laplante, D. P. 2012. Using Natural Disasters to Study the Effects of Prenatal Maternal Stress on Child Health and Development. *Birth Defects Research (Part C)* 96: 273-288.

Kinoshita, M., Moriyama, R., Tsukamura, H. and Maeda, K-I. 2003. A rat model for the energetic regulation of gonadotropin secretion: role of the glucose-sensing mechanism in the brain. *Domestic Animal Endocrinology* 25 (1): 109-120.

Klales, R. and Burns, T. L. 2017. Adapting and Applying the Phenice (1969) Adult Morphological Sex Estimation Technique to Subadults. *Journal of Forensic Sciences* 62 (3): 747-753.

Klaus, H. D. 2014. Frontiers in the Bioarchaeology of Stress and Disease: Cross-Disciplinary Perspectives from Pathophysiology, Human Biology, and Epidemiology. *American Journal of Physical Anthropology* 155: 294-308.

Klaus, H. D. and Lynnerup, N. 2019. Abnormal Bone: Considerations for Documentation, Disease Process Identification, and Differential Diagnosis. In J. E. Buikstra (eds). *Ortner's Identification of Pathological Conditions in Human Skeletal Remains*. London: Academic Press. Pp 59-87.

Klein, O. D., Minowada, G., Peterkova, R., Kangas, A., Yu, B. D., Lesot, H., Peterka, M., Jernvall, J., and Martin, G. R. 2006. Sprouty genes control diastema tooth development via bidirectional antagonism of epithelial-mesenchymal FGF signaling. *Developmental Cell* 11 (2): 181-190.

Klepinger, K. L. 1983. Review: Paleopathology and the origins of agriculture. *American Journal of Physical Anthropology* 71 (1): 126-127.

Klingenberg, C. P. 2015. Analysing Fluctuating Asymmetry with Geometric Morphometrics: Concepts, Methods, and Applications. *Symmetry* 7: 843-934.

Klingenberg, C. P. 2016. Size, shape, and form: concepts of allometry in geometric morphometrics. *Development Genes and Evolution* 226: 113-137.

Klingenberg, C. P. 2020. Walking on Kendall's Shape Space: Understanding Shape Spaces and Their Coordinate Systems. *Evolutionary Biology* 47: 334-352.

Klingenberg, C. P. and McIntyre, G. S. 1998. Geometric Morphometrics of Developmental Instability: Analyzing Patterns of Fluctuating Asymmetry with Procrustes Methods. *Evolution* 52 (5): 1363-1375.

Klingenberg, C. P. and Monteiro, L. R. 2005. Distances and directions in multidimensional shape spaces: Implications for morphometric applications. *Systematic Biology* 54: 678-688.

Klingenberg, C. P. and Zaklan, S. D. 2000. Morphological Integration between Developmental Compartments in the Drosophila Wing. *Evolution* 54 (4): 1273-1285.

Knudson, A. 1971. Mutation and cancer: statistical study of retinoblastoma. *Proceedings of the National Academy of Science* 68: 820-823.

Kondo, S. and Townsend, G. C. 2006. Associations between Carabelli trait and cusp areas in human permanent maxillary first molars. *American Journal of Physical Anthropology* 129: 196-203.

Konigsberg, L. W. and Frankenberg, S. R. 1992. Estimation of age structure in anthropological demography. *American Journal of Physical Anthropology* 89: 235-256.

Konigsberg, L. W. and Frankenberg, S. R. 2013. Bayes in Biological Anthropology. *American Journal of Physical Anthropology* 57: 153-184.

Konigsberg, L. W. and Hermann, N. P. 2002. Markov chain Monte Carlo Estimation of hazard model parameters in paleodemography. In R. D. Hoppa and J. W. Vaupel (eds). *Paleodemography. Age Distributions from Skeletal Samples*. Cambridge: Cambridge University Press. Pp 222-242.

Koo, T. K. and Li, M. Y. 2016. A Guideline of Selecting and Reporting Intraclass Correlation Coefficients for Reliability Research. *Journal of Chiropratic Medicine* 15 (2): 155-163.

Koppe, T. and Swindler, D. R. 2004. Metric sexual dimorphism in the deciduous teeth of Old World monkeys. *Annals of Anatomy* 186: 367-374.

Korenhof C. A. W. 1982. Evolutionary trends of the inner enamel anatomy of deciduous molars from Sangiran (Java, Indonesia). In B. Kurte (eds). *Teeth: form, function and evolution*. New York: Columbia University Press. Pp 350-365.

Korenhof, C. A. W. 1960. *Morphogenetical aspects of the human upper molar*. Utrecht: Uitgeversmaatschappij Neerlandia.

Korenhof, C. A. W. 1961. The enamel-den tin border: a new morphological factor in the study of the (human) molar pattern. *Koninklijke Nederlandse Akademie van Wetenschappen* 64: 639-664.

Kralick, A. E. and McGrath, K. 2021. More severe stress markers in the teeth of flanged versus unflanged orangutans (*Pongo* spp.). *American Journal of Physical Anthropology* 176: 625-637.

Kraus, B. S. 1963. Morphogenesis of deciduous molar pattern in man. In D. R. Brothwell (eds). *Dental Anthropology*. New York: Pergamon. Pp 87-104.

Kraus, B. S. and Jordan, R. E. 1965. *The Human Dentition before Birth*. London: Lea and Febiger.

Kreshover, S. J. 1960. Metabolic disturbances in tooth formation. *Annals of the New York Academy of Sciences* 85: 161-167.

Kreshover, S. J. and Clough, O. W. 1953b. Prenatal influences on tooth development: Part II. Artificially induced fever in rats. *Journal of Dental Research* 32: 565-572.

Kreshover, S. J. and Hancock, J. A. 1956. The effect of lymphocytic choriomeningitis on pregnancy and dental tissues in mice. *Journal of Dental Research* 35: 467-483.

Kreshover, S. J., Clough, O. W. and Bear, D. M. 1953a. Prenatal influences on tooth development: Part I. Alloxan diabetes in rats. *Journal of Dental Research* 32: 246-261.

Kuh, D., and Ben-Shlomo, Y. 2004. Introduction. In D. Kuh, Y. Ben-Shlomo, and S. Ezra (eds). *A Life Course Approach to Chronic Disease Epidemiology*. Oxford: Oxford University Press. Pp 1-14.

Kuh, D., Ben-Shlomo, Y. and Ezra, S. 2004. *A Life Course Approach to Chronic Disease Epidemiology*. Oxford: Oxford University Press

Kuh, D., Ben-Shlomo, Y., Lynch, J., Hallqvist, J. and Power, C. 2003. Life Course Epidemiology. *Journal of Epidemiology and Community Health* 57 (10): 778-783.

Kundu, P., Blacher, E., Elinav, E. and Pettersson, S. 2017. Our Gut Microbiome: The Evolving Inner Self. *Cell* 171: 1481-1493.

Kuzawa, C. W. 2007. Developmental Origins of Life History: Growth, Productivity, and Reproduction. *American Journal of Human Biology* 19: 654-661.

Lang, S. L. C., Iverson, S. J. and Bowen, W. D. 2012. Primiparous and multiparous females differ in mammary gland alveolar development: implications for milk production. *The Journal of Experimental Biology* 215: 2904-2911.

Larsen, C. S. 1997. *Bioarchaeology. Interpreting behaviour from the human skeleton*. Cambridge: Cambridge University Press.

Laub, J. H. and Sampson, R. J. 2003. *Shared Beginnings, Divergent Lives: Delinquent Boys to Age 70*. Cambridge: Harvard University Press.

Laub, J. H. and Sampson, R. J. 2013. Integrating Quantitative and Qualitative Data. In J. Giele, and G. Elder (eds). *Methods of Life Course Research: Qualitative and Quantitative Approaches*. Thousand Oaks: Sage. Pp 213-230.

Lazić, M. M., Carretero, M. A., Crnobrnja-Isailović, J. and Kaliontzopoulou, A. 2015. Effects of Environmental Disturbance on Phenotypic Variation: An Integrated Assessment of Canalization, Developmental Stability, Modularity, and Allometry in Lizard Head Shape. *The American Naturalist* 185: 44-58.

Leamy, L. 1984. Morphometric studies in inbred and hybrid house mice. V. Directional and fluctuating asymmetry. *American Naturalist* 123: 579-593.

Lease, L. R. 2016. Anatomy of Individual Teeth and Tooth Classes. In J. D. Irish and G. R. Scott (eds). *A Companion to Dental Anthropology, First Edition*. London: Wiley. Pp 94-107.

Lechat, M. F. 1979. Disasters and public health. *Bulletin of the World Health Organisation* 57 :11-17.

Lee, Y. H., Cherkerzian, S., Seidman, L.J., Papandonatos, G. D., Savitz, D. A., Tsuang, M. T., Goldstein, J. M., Buka, S. L. 2020. Maternal Bacterial Infection During Pregnancy and Offspring Risk of Psychotic Disorders: Variation by Severity of Infection and Offspring Sex. *American Journal of Psychiatry* 177: 66-75.

Leese, M. N. and Main, P. L. 1994. The Efficient Computation of Unbiased Mahalanobis Distances and their Interpretation in Archaeometry. *Archaeometry* 36 (2): 307-316.

Legge, S. S. and Hardin, A. M. 2016. In J. D. Irish and G. R. Scott (eds). *A Companion to Dental Anthropology, First Edition*. London: Wiley. Pp 191-203.

Lele, S. 1991. Some comments on coordinate-free and scale-invariant methods in morphometrics. *American Journal of Physical Anthropology* 85: 407-417.

Lele, S. 1993. Euclidean Distance Matrix Analysis (EDMA): Estimation of mean form and mean form difference. *Mathematical Geology* 25: 573-602

Lele, S. and Richtsmeier, J. 1991. Euclidean distance matrix analysis: a coordinate-free approach for comparing biological shapes using landmark data. *American Journal of Physical Anthropology* 86: 415-427.

Lewis, M. 2007. *The Bioarchaeology of Children: Perspectives from Biological and Forensic Anthropology*. Cambridge: Cambridge University Press.

Lewis, M. 2017. Fetal paleopathology: an impossible discipline? In S. Han, T. K. Betsinger and A. B. Scott (eds) T*he Anthropology of the Fetus: Biology, Culture, and Society.* New York: Berghan. Pp 112-131.

Lewis, M. 2018. Children in Bioarchaeology: methods and interpretations. In A. Katzenberg and A. Grauer (eds). *Biological Anthropology of the Human Skeleton*. New York: Academic Press. Pp 119-143.

Lewis, M. 2019. Congenital and Neuromechanical Abnormalities of the Skeleton. In J. E. Buikstra (eds). *Ortner's Identification of Pathological Conditions in Human Skeletal Remains*. London: Academic Press. Pp 585-614.

Lewis, M. 2019. Endocrine Disturbances. In J. E. Buikstra (eds). *Ortner's Identification of Pathological Conditions in Human Skeletal Remains*. London: Academic Press. Pp 567-584.

Lewis, M. 2019. Skeletal Dysplasias and Related Conditions. In J. E. Buikstra (eds). *Ortner's Identification of Pathological Conditions in Human Skeletal Remains*. London: Academic Press. Pp 615-718.

Lewis, M. 2020. *Assessing puberty stage* [online workshop]. Puberty and Adolescent Growth Workshop [Viewed 17th July 2020]. Available from: https://www.reading.ac.uk/archaeology/research/Projects/puberty-adolescence-bioarchaeology.aspx

Lewis, M., Shapland, F. and Watts, R. 2016. On the Threshold of Adulthood: A New Approach for the Use of Maturation Indicators to Assess Puberty in Adolescents from Medieval England. *American Journal of Human Biology* 28: 48-56.

Lichtenstein, P., Holm, M. V., Verkasalo, P. K., Iliadou, A., Kaprio, J., Koskenvuo, M., Pukkala, E., Skytthe, A. and Hemminki, K. 2000. Environmental and heritable factors in the causation of cancer. *New England Journal of Medicine* 343: 78-85.

Liljequist, D., Elfving, B. and Skavberg Roaldsen, K. 2019. Intraclass correlation – A discussion and demonstration of basic features. *Plos ONE* 14 (7): e0219854.

Liu, F., Chua, E. Y., Watt, B., Zhang, Y., Gallant, N. M., Andla, T., Yang, S. H.,Lu, M-M., Piccolo, S., Schmidt-Ullrich, R., Taketo, M. M., Morrisey, E. E., Atit, R., Dlugosz, A. A. and Millar, S. E. 2008. Wnt/β-catenin signaling directs multiple stages of tooth morphogenesis. *Developmental Biology* 313 (1): 210-224.

Liu, J., Tan, H, and Jeynes, B. 2009. Is Femur Length the Key Height Component in Risk Prediction of Type 2 Diabetes Among Adults? *Diabetes Care* 32 (4): 739-740.

Liu, W., Hlusko, L., and Zheng, L. 2001. Morphometric analysis of hominoid lower molars from Yuanmou of Yunnan Province, China. *Primates* 42: 123-134.

Liversidge, H. M. 2011. Similarity in dental maturation in two ethnic groups of London children. *Annals of Human Biology* 38: 702-715.

Liversidge, H. M. and Marsden, P. H. 2010. Estimating age and the likelihood of having attained 18 years of age using mandibular third molars. *British Dental Journal* 209: E13.

Liversidge, H. M., Chaillet, N., Mörnstad, H., Nyström, M., Rowlings, K., Taylor, J. and Willems, G. 2006. Timing of Demirjian tooth formation stages. *Annals of Human Biology* 33: 454-470.

Lloyd-Jones, J. 1994. Measuring biological affinity among populations: a case study of Romano-British and Anglo-Saxon populations. In J. Hugget and N. Ryan (eds). Computer Applications and Quantitative Methods in Archaeology. *BAR International Series* 600: 69-73.

Lockhart, P. B., Bolger A. F., Papapanou, P. N, Osinbowale, O. E., Trevisan, M. A., Levison, M. W., Taubert, K. L, Newburger, J. H., Gornik, H. R., Gewitz, M. C., Wilson, W. M., Smith, S. and Baddour. L. 2012. Periodontal Disease and Atherosclerotic Vascular Disease: Does the Evidence Support an Independent Association? *A Scientific Statement from the American Heart Association 125* (20): 2520-544.

Lohmann, G. P. 1983. Eigenshape analysis of microfossils: A general morphometric procedure for describing changes in shape. *Mathematical Geology* 15: 659-672.

Long, J. S. 1997. *Regression Models for Categorical and Limited Dependent Variables*. London: Sage.

Lopuhaa, C. E., Roseboom, T. J., Osmond, C., Barker, D. J. P., Ravelli, A. C. J., Bleker, O. P., van der Zee, J. S. and van der Meulen, J. H. P., 2000. Atopy, lung function and obstructive airways disease in adults after prenatal exposure to the Dutch famine. *Thorax* 55: 555-561.

Loth, S. R. and Henneberg, M. 1996. Mandibular ramus flexure: a new morphological indicator of sexual dimorphism in the human skeleton. *American Journal of Physical Anthropology* 99: 473-485.

Lovejoy, C. O., Meindl, R. S., Pryzbeck, T. R. and Mensforth, R. P. 1985. Chronological Metamorphosis of the Auricular Surface of the Ilium: A New Method for the Determination of Adult Skeletal Age at Death. *American Journal of Physical Anthropology* 68: 15-28.

Lu, A., Petrullo, L., Carrera, S., Feder, J., Schneider-Crease, I. and Snyder-Mackler, N. 2019. Developmental responses to early-life adversity: Evolutionary and mechanistic perspectives. *Evolutionary Anthropology* 28: 249-266.

Lucy, S. 1999. Changing Burial Rites in Northumbria AD 500-750. In J. Hawkes and S. Mills (eds). *Northumbria's Golden Age*. Stroud: Sutton Publishing. Pp 12-43.

Ludwig, W. 1932. *Das Rechts-Links Problem im Tierreich und beim Menschen*. Berlin: Springer.

Lugli, G. A., Milani, C., Mancabelli, L., Turroni, F., Ferrario, C., Duranti, S., Van Sinderen, D. and Ventura, M. 2017. Ancient bacteria of the Ötzi's microbiome: a genomic tale from the Copper Age. *Microbiome* 5: 5.

Lumey L H. 1992. Decreased birthweights in infants after maternal in utero exposure to the Dutch famine of 1944– 1945. *Paediatric and Perinatal Epidemiology* 6: 240-253.

Lund, J. and Sindbaek, S. 2021. Crossing the Maelstrom: New Departures in Viking Archaeology. *Journal of Archaeological Research* 29: 1-61.

Luukko, K., Kettunen, P., Fristad, I. and Berggreen, E. 2011. Structure and Functions of the Dentin-Pulp Complex. In K. M. Hargreaves, S. Cohen and L.H. Berman (eds). *Cohen's Pathways of the Pulp*. St. Louis: Elsevier. Pp 452-503.

Lynch, S. M. 2007. *Introduction to Applied Bayesian Statistics and Estimation for Social Scientists*. New York: Springer.

Lynnerup, N. and Klaus, H. D. 2019. Fundamentals and Human Bone and Dental Biology: Structure, Function and Development. In J. E. Buikstra (eds). *Ortner's Identification of Pathological Conditions in Human Skeletal Remains*. London: Academic Press. Pp 35-58.

Maat, G. J. R. 2004. Scurvy in adults and youngsters: the Dutch experience. A review of the history and pathology of a disregarded disease. *International Journal of Osteoarchaeology* 14: 77-81.

Mackenzie, E. 1827. *A descriptive and historical account of the town and country of Newcastle including the borough of Gateshead*, Newcastle: Mackenzie and Dent.

Mackenzie, E. 1834. *A historical, topographical and descriptive view of the County Palatine of Durham, 1*, Durham: Mackenzie and Dent.

Macmillan, R. 2005. The Structure of the Life Course. Classic Issues and Current Controversies. *Advances in Life Course Research* 9: 3-24.

Mahalanobis, P. C. 1936. On the generalized distance in statistics. *Proceedings of the National Institute of Science India* 2: 49-55.

Mahoney Swales, D. 2012. *Life And Stress: A Bio-Cultural Investigation into the Later Anglo-Saxon Population of the Black Gate Cemetery, Newcastle-Upon-Tyne*. PhD Thesis, The University of Sheffield.

Mahoney Swales, D. 2019. A biocultural analysis of mortuary practices in the later Anglo-Saxon to Anglo-Norman Black Gate Cemetery, Newcastle-upon-Tyne, England. *International Journal of Osteoarchaeology* 29: 198-219.

Mahoney-Swales, D. and Nystrom, P. 2009. Skeletal Manifestations of Non-Adult Scurvy from Early Medieval Northumbria: The Black Gate Cemetery, Newcastle-upon-Tyne. In M. E. Lewis and M. Clegg (eds). *Proceedings of the Ninth Annual Conference of the British Association for Biological Anthropology and Osteoarchaeology*. Oxford: BAR Publishing. Pp 31-41.

Malina, R. M., Rogol, A. D., Cumming, S. P., Coelho e Silva, M. J. and Figueiredo, A. J. 2015. Biological maturation of youth athletes: assessment and implications. *British Journal of Sports Medicine* 49: 852-859.

Manly, B. F. J. 1994. *Multivariate Statistical Methods: A Primer (Second Edition)*. Boca Raton: Chapman and Hall.

Mantel, N. and Haenszel, W. 1959. Statistical Aspects of the Analysis of Data from Retrospective Studies of Disease. *Journal of the National Cancer Institute* 22: 719-748.

Marcy, A. E., Fruciano, C., Phillips, M. J., Mardon, K. and Weisbecker, V. 2018. Low resolution scans can provide a sufficiently accurate, cost- and time-effective alternative to high resolution scans for 3D shape analyses. *PeerJ* 6: e5032-e5032.

Mardia, K. V., Bookstein, F. L. and Moreton, I. J. 2000. Statistical Assessment of Bilateral Symmetry of Shapes. *Biometrika* 87 (2): 285-300.

Maresh, M.M. 1970. Measurements from roentgeno- grams, heart size, long bone lengths, bone, muscle, and fat widths, skeletal maturation. In R.W. McCammon (eds): *Human Growth and Development*. Springfield: Charles C Thomas. Pp. 155-200.

Markow, T. A. 1995. Evolutionary ecology and developmental instability. *Annual Review of Entomology* 40: 105-120.

Marmot, M. G., Adelstein, A. M., Robinson, N., Rose, G. A. 1978. Changing social-class distribution of heart disease. *British Medical Journal* 2: 1109-1112.

Marques, C., Matos, V. and Meinzer, N. J. 2019. Proliferative Periosteal Reactions: Assessment of Trends in Europe Over the Past Millenia. In R. H. Steckel, C. S. Larsen, C. A. Roberts and J. Baten (eds). *The Backbone of Europe. Health, Diet, Work and Violence over Two Millenia*. Cambridge: Cambridge University Press. Pp 137-174.

Martin, D. L. and Armelagos, G. J. 1979. Morphometrics of compact bone: An example from Sudanese Nubia. *American Journal of Physical Anthropology* 51 (4): 571-577.

Martinón-Torres, M. and Bermúdez de Castro, J. M. 2016. The Hominins 2: The Genus Homo. In J. D. Irish and G. R. Scott (eds). *A Companion to Dental Anthropology, First Edition*. London: Wiley. Pp 67-84.

Marx, R. E. 2008. Uncovering the Cause of "Phossy Jaw" Circa 1858 to 1906: Oral and Maxillofacial Surgery Closed Case Files – Case Closed. *Journal of Oral and Maxillofacial Surgery* 66: 2356-2363.

Masset, C. 1989. Age estimation on the basis of cranial sutures. In M. Y. Iscan (eds). *Age markers in the human skeleton*. Springfield: Charles C. Thomas. Pp 71-103.

Massler, M. and Schour, I. 1956. *Atlas of the Mouth*. The University of Michigan: American Dental Association.

Mather, K. 1953. Genetical control of stability in development. *Heredity* 7: 297-336.

Matulka, L. A., Triplett, A. A., Wagner, K-U. 2007. Parity-induced mammary epithelial cells are multipotent and express cell surface markers associated with stem cells. *Developmental Biology* 303: 29-44.

Maudsley, H. 1904. Discussion. In F. Galton. Eugenics: Its Definition, Scope, and Aims. *American Journal of Sociology* 10 (1): 1-25.

Mayer, K. U. 2009. New Directions in Life Course Research. *Working Paper- The Mannheim Centre for European Social Research* 122.

Mays, S. 2014. The palaeopathology of scurvy in Europe. *International Journal of Paleopathology* 5: 55-62.

Mays, S. 2020. A dual process model for paleopathological diagnosis. *International Journal of Paleopathology* 31: 89-96.

Mays, S. and Taylor, G. M. 2002. Osteological and Biomolecular Study of Two Possible Cases of Hypertrophic Osteoarthropathy from Mediaeval England. *Journal of Archaeological Science* 29: 1267-1276.

McAdams, H. H. and Arkin, A. 1997. Stochastic mechanisms in gene expression. *Proceedings of the National Academy of Sciences* 94: 814-819.

McAdams, H. H. and Arkin, A. 1999. It's a noisy business: genetic regulation at the nanomolar scale. *Trends in Genetics* 15: 65-69.

McDade, T.W. 2012. Early environments and the ecology of inflammation. *Proceedings of the National Academy of Sciences* 109 (2): 17281-17288.

McGraw, K. O. and Wong, S. P. 1996. Forming inferences about some intraclass correlation coefficients. *Psychological Methods* 1 (1): 30-46.

McHugh, M. L. 2018. Cramér's V Coefficient. In B. Frey (eds). *The SAGE Encyclopedia of Educational Research, Measurement, and Evaluation*. Thousand Oaks: SAGE. Pp 417-418.

McIntyre, L. 2015. Reconstructing population size in a Romano-British *colonia*: the case of Eboracum. *Journal of Roman Archaeology* 28: 413-429.

McIntyre, L. 2016. The York 113: osteological analysis of 10 mass graves from Fishergate, York. *Journal of Conflict Archaeology* 11 (2-3): 115-134.

McIntyre, L. and Bruce, G. 2010. Excavating All Saint's. A Medieval church rediscovered. *Current Archaeology* 245: 30-37.

McIntyre, L. n.d. *Barbican Osteology Report*. Unpublished Report.

McKern, T. W. 1956. The symphyseal formula: a new method for determining age from pubic symphyses. *American Journal of Physical Anthropology* 14: 388.

McKern, T. W. and Stewart, T. D. 1957. Skeletal age changes in young American males. Analyzed from the skeletal standpoint of age identification. *US Army Quartermaster Research and Development Center: Technical report EP-45.*

McKillup, S. 2012. *Statistics Explained: An Introductory Guide for Life Scientists Second Edition*. Cambridge: Cambridge University Press.

Meindl, R. S. and Lovejoy, C. O. 1985. Ectocranial suture closure: a revised method for the determination of skeletal age at death based on the lateral-anterior sutures. *American Journal of Physical Anthropology* 68: 57-66.

Mihanovic, F., Jerkovic, I., Kruzic, I., Anselinovic, S., Jankovic, S. and Basic, Z. 2017. From Biography to Osteobiography: An Example of Anthropological Historical Identification of the Remains of St. Paul. *The Anatomical Record* 300: 1535-1546.

Milner, G. R. and Boldsen, J. L. 2012. Transition Analysis: A Validation Study With Known-Age Modern American Skeletons. *American Journal of Physical Anthropology* 148: 98-110.

Milner, G. R., Boldsen, J. L., Ousley, S. D., Getz, S. M., Weise, S., and Tarp, P. 2021. Great expectations: The rise, fall, and resurrection of adult skeletal age estimation. In B. F. B. Algee-Hewitt and J. Kim (eds). *Remodeling forensic skeletal age*. Academic Press. Pp 139-154.

Milner, G. R., Boldsen, J. L., Ousley, S. D., Getz, S. M., Weise, S., Tarp, P. and Steadman, D. W. 2018. Selective mortality in middle-aged American women with diffuse idiopathic skeletal hyperostosis (DISH). *PLOS One* 13: e0202283.

Milner, G. R., Ousley, S. D., Boldsen, J. l., Getz, S. M., Weise, S. and Tarp, P. 2019. *Transition Analysis 3 (TA3) Trait Manual. Public Distribution Draft (Ver. 1.0).* National Institute of Justice.

Mishra, G. D., Ben-Shlomo, Y. and Kuh D. 2010a. A Life Course Approach to Health Behaviors: Theory and Methods. In A. Steptoe (eds). *Handbook of Behavioral Medicine. New* York: Springer.

Mishra, G. D., Cooper, R. and Kuh, D. 2010b. A life-course approach to reproductive health. Theory and methods. *Maturitas* 65: 92-97.

Mitchell, P. D. 2017. Improving the use of historical written sources in paleopathology. *International Journal of Paleopathology* 19: 88-95.

Mitteroecker, P., Gunz, S., Windhager, K. and Schaefer, P. 2013. A brief review of shape, form, and allometry in geometric morphometrics, with applications to human facial morphology. *Hystrix-Italian Journal of Mammalogy* 24 (1): 59-66.

Mizoguchi, Y. 1985. *Shovelling: A Statistical Analysis of its Morphology*. Tokyo: Tokyo University Press.

Møller, A. P. 1999. Asymmetry as a predictor of growth, fecundity and survival. *Ecology Letters* 2: 149-156.

Molleson, T., Cox, M., Waldron, H. A. and Whittaker, D. K. 1993. The Spitalfields Project, Volume 2. The Anthropology: The Middling Sort. *Council for British Archaeological Research Reports* 86.

Molnar, P. 2006. Tracing prehistoric activities: musculoskeletal stress marker analysis of a Stone Age population on the island of Gotland in the Baltic Sea. *American Journal of Physical Anthropology* 129: 12-23.

Monaghan, P. 2008. Early growth conditions, phenotypic development and environmental change. *Philosophical Transactions of the Royal Society B: Biological Science* 363: 1635-1645.

Moormann, S., Guatelli-Steinberg, D. and Hunter, J. 2013. Metamerism, morphogenesis, and the expression of carabelli and other dental traits in humans. *American Journal of Physical Anthropology* 150 (3): 400-408.

Moorrees, C. F., Fanning, E. A. and Hunt, E. E. 1963. Age Variation of Formation Stages for Ten Permanent Teeth. *Journal of Dental Research* 42: 1490-1502.

Morino, S., Ishihara, M., Umezaki, F., Hatanaka, H., Yamashita, M. and Aoyama, T. 2019. Pelvic alignment changes during the perinatal period. *PLoS ONE* 14 (10): e0223776.

Morris, D. H., Jones, M. E., Schoemaker, M. J., Ashworth, A. and Swerdlow, A. J. 2010. Determinants of age at menarche in the UK: analyses from the Breakthrough Generations Study. *British Journal of Cancer* 103:1760-1764.

Moshrif, A., Noor, R. A., Aly, H., Mortada, M. and Hafez, A. 2022. Aging and entheses: An ultrasonographic probing of degenerative enthesopathy in a cohort of 147 healthy subjects. *International Journal of Rheumatic Diseases* 25: 481-488.

Mozaffarian, D., Benjamin, E. J., Go, A. S., Arnett, D. K., Blaha, M. J., Cushman, M., Das, S. R., de Ferranti, S., Després, J-P., Fullerton, H. J., Howard, V. J., Huffman, M. D., Isasi, C. R., Jiménez, M. C., Judd, S. E., Kissela, B. M., Lichtman, J. H., Lisabeth, L. D., Liu, S., Mackey, R. H., Magid, D. J., McGuire, D. K., Mohler, E. R., Moy, C. S., Muntner, P., Mussolino, M. E., Nasir, K., Neumar, R. W., Nichol, G., Palaniappan, L., Pandey, D. K., Reeves, M. J., Rodriguez, C. J., Rosamond, W., Sorlie, P. D., Stein, J., Towfighi, A., Turan, T. N., Virani, S. S., Woo, D., Yeh, R. W. and Turner, M. B. 2016. Executive Summary: Heart Disease and Stroke Statistics – 2016 Update. A Report from the American Heart Association. *Circulation* 133 (4): 447-454.

Mullins, S. K. and Taylor, P. J. 2002. The effects of parallax on geometric morphometric data. *Computers in Biology and Medicine* 32: 455-464.

Murrar, S. and Brauer, M. 2018. Mixed Model Analysis of Variance. In B. B. Frey (eds). *The SAGE Encyclopaedia of Educational Research, Measurement, and Evaluation*. Thousand Oaks: Sage. Pp 1075-1078.

Namigai, E. K. O., Kenny, N. J. and Shimeld, S. M. 2014. Right Across the Tree of Life: The Evolution of Left–Right Asymmetry in the Bilateria. *Genesis* 52: 458-470.

Nanci, A. 2013. *Ten Cate's Oral Histology*. Eight Edition. St. Louis: Elsevier Mosby.

Neel, J. V. 1962. Diabetes mellitus: A thrifty genotype rendered detrimental by progress? *American Journal of Human Genetics* 14: 353-362.

Neville, A. C. 1976. *Animal asymmetry*. London: Edward Arnold.

Newman, S. L. 2016. *The Growth of a Nation: Child health and development in the Industrial Revolution in England, c. AD 1750-1850.* Durham theses: Durham University. Available at Durham E-Theses Online: http://etheses.dur.ac.uk/11508/

Newman, S. L. and Gowland, R. L. 2016. Dedicated followers of fashion? Bioarchaeological perspectives on socio-economic status, inequality, and health in urban children from the Industrial Revolution (18th-19th C), England. *The International Journal of Osteoarchaeology* 27: 217-229.

Newman, S. L., Gowland, R. L. and Caffell, A. C. 2019. North and south: A comprehensive analysis of non-adult growth and health in the industrial revolution (AD 18th–19th C), England. *American Journal of Physical Anthropology* 169 (1): 104-121.

Newman, S. N. 2019. *St Lawrence's Church, Warwick (WS09): Human Osteological Assessment.* Unpublished.

Newton, H. 2015. The Dying Child in Seventeenth-Century England. *Pediatrics* 136 (2): 218-220.

Nichol, C. R. and Turner, C. G. 1986. Intra- and lnterobserver Concordance in Classifying Dental Morphology. *American Journal of Physical Anthropology* 69: 299-315.

Nicolis, G. and Prigogine, I. 1989. *Exploring Complexity: An Introduction*. New York: Freeman.

Nielsen, M. B., Hansen, K., Hølmer, P. and Dyrbye, M. 1991. Tibial periosteal reactions in soldiers: A scintigraphic study of 29 cases of lower leg pain. *Acta Orthopaedica Scandinavica* 62 (6): 531-534.

Niinimäki, S. 2012. The Relationship Between Musculoskeletal Stress Markers and Biomechanical Properties of the Humeral Diaphysis. *American Journal of Physical Anthropology* 147: 618-628.

Niinimäki, S. and Baiges Sotos, L. 2013 The Relationship Between Intensity of Physical Activity and Entheseal Changes on the Lower Limb. *International Journal of Osteoarchaeology* 23: 221-228.

Nikita, E. 2015. A critical review of the Mean Measure of Divergence and Mahalanobis distances using artificial data and new approaches to the estimation of biodistances employing nonmetric traits. *American Journal of Physical Anthropology* 157: 284-294.

Nilsson, E. E., Sadler-Riggleman, I., and Skinner, M. K. 2018. Environmentally induced epigenetic transgenerational inheritance of disease. *Environmental epigenetics* 4 (2): 1-13.

Nolan, B. 2019. *Pre-Black Death Mortality and Survival: An Investigation of the St. Lawrence's Church Site in Warwick*. MSc Dissertation, University of Sheffield.

Nolan, J., Harbottle, B. and Vaughan, J. 2010. The early medieval cemetery at the Castle Newcastle upon Tyne. *Archaeologia Aeliana* 39: 147-287.

Nystrom, P. 2019. *Dissection Manual AAP683 Human Anatomy*. Sheffield: University of Sheffield. [Unpublished item].

Nystrom, P., Phillips-Conroy, J. E. and Jolly, C. J. 2004. Dental Microwear in Anubis and Hybrid Baboons (Papio hamadryas, Sensu Lato) Living in Awash National Park, Ethiopia. *American Journal of Physical Anthropology* 125: 279-291.

O'Brien, M. and Laland, K. N. 2012. Genes, Culture, and Agriculture: An Example of Human Niche Construction. *Current Anthropology* 53 (4): 434-470.

O'Brien, P. C. 1992. Robust procedures for testing equality of covariance matrices. *Biometrics* 48: 819-827.

O'Connell, L. 2004. Guidance on recording age at death in adults. In M. Brickley and J. I. McKinley (eds). Guidelines to the Standards for Recording Human Remains. *Institute of Field Archaeologists Paper No. 7, IFA/British Association of Biological Anthropology and Osteoarchaeology*. Reading: University of Reading.

O'Connell, L. 2018. Guidance on recording age at death in adult human skeletal remains. In P. D. Mitchell and M. Brickley (eds). Updated Guidelines to the Standards for Recording Human Remains. *Chartered Institute of Field Archaeologists and British Association of Biological Anthropology and Osteoarchaeology Paper.* Pp 25-29.

Oakes, S. R., Hilton, H. N. and Ormandy, C. J. 2006. Key stages in mammary gland development – The alveolar switch: coordinating the proliferative cues and cell fate decisions that drive the formation of lobuloalveoli from ductal epithelium. *Breast Cancer Research* 8 (2).

O'Donnell, L. and Moes, E. 2020. Increased dental fluctuating asymmetry is associated with active skeletal lesions, but not mortality hazards in the precontact Southwest United States. *American Journal of Physical Anthropology* 175:156-171.

O'Donnell, L., Hill, E. C., Anderson Anderson, A. S. and Edgar, H. J. H. 2020. Cribra orbitalia and porotic hyperostosis are associated with respiratory infections in a contemporary mortality sample from New Mexico. *American Journal of Physical Anthropology* 173: 721-733.

Ogden, A. 2008. Advances in the Palaeopathology of the Teeth and Jaws. In R. Pinhasi and S. Mays (eds). *Advances in Human Palaeopathology*. Chichester: John Wiley. Pp 283-307.

Oishi, Y. and Manabe, I. 2018. Macrophages in inflammation, repair and regeneration. *International Immunology* 30 (11): 511-528.

Oksanen, J. F., Blanchet, G., Friendly, M., Kindt, R., Legendre, P., McGlinn, D., Minchin, P. R., O'Hara, R. B., Simpson, G. L., Solymos, P., Henry, M., Stevens, H., Szoecs, E. and Wagner, H. 2019. Vegan: Community Ecology Package. *R package version 2.5-6.*

Olejniczak, A., Martin, L., and Ulhaas, L. 2004. Quantification of dentine shape in anthropoid primates. *Annals of Anatomy-Anatomischer Anzeiger* 186: 479-485.

Olsen, A.M. 2015. Digitizing with StereoMorph How to collect 2D landmark and curve data from photographs using the StereoMorph Digitizing App. *R package version* 1.6.1.

Olsen, A.M. and Westneat, M. W. 2015. StereoMorph: an R package for the collection of 3D landmarks and curves using a stereo camera set-up. *Methods in Ecology and Evolution* 6: 351-356.

Orr, H. A. 2009. Fitness and its role in evolutionary genetics. *Nature reviews. Genetics 10* (8): 531-539.

Ortner, D. J. 2003. *Identification of Pathological Conditions in Human Skeletal Remains*. San Diego: Academic Press.

Osborn, H. F. 1888a. The evolution of the mammalian molars to and from the tritubercular type. *American Naturalist* 22: 1067-1079.

Osborn, H. F. 1888b. The nomenclature of the mammalian molar cusps. *American Naturalist* 22: 926-928.

Osborn, H. F. 1897. Trituberculy: a review dedicated to the late Professor Cope. *American Naturalist* 31: 993-1016.

Osborn, H. F. 1907. *Evolution of Mammalian Molar Teeth, To and From the Triangular Type*. New York: Macmillan.

Oxilia, G., Sartorio, J. C. M., Bortolini, E., Zampirolo, G., Papini, A., Boggioni, M., Martini, S., Marciani, F., Arrighi, S., Figus, C., Marciani, G., Romandini, M., Silvestrini, S., Pedrosi, M. E., Mori, T., Riga, A., Kullmer, O., Sarig, R., Fiorenza, L., Giganti, M., Sorrentino, R., Belcastro, M. G., Cecchi, J. M. and Benazzi, S. 2021. Exploring directional and fluctuating asymmetry in the human palate during growth. *American Journal of Physical Anthropology* 175 (4): 1-18.

Palmer, A. R. 1994. Fluctuating asymmetry analyses: A primer. In T. A. Markow (eds). *Developmental Instability: Its Origins and Evolutionary Implications*. Dordrecht: Kluwer Pp 335-364.

Palmer, A. R. 1996. Waltzing with Asymmetry. *BioScience* 46 (7): 518-532.

Palmer, A. R. and Strobeck, C. 1986. Fluctuating Asymmetry: Measurement, Analysis, Patterns. *Annual Review of Ecology and Systematics* 17: 391-421.

Palmer, A. R. and Strobeck, C. 2003. Fluctuating Asymmetry Analyses Revisited. In M. Polak (eds). *Developmental Instability (DI): Causes and Consequences.* Oxford: Oxford University Press. Pp 279-319.

Palmer, A. R. R. 2005. Antisymmetry. In B. K. Hall and B. Hallgrímsson (eds). *Variation*. London: Elsevier. Pp 359–397.

Palmer, A. R., Strobeck, C. and Chippindale, A. K. 1993. Bilateral variation and the evolutionary origin of macroscopic asymmetries. *Genetica* 89: 201-218.

Panayi, P. 1995. *German Immigrants in Britain during the 19th Century, 1815-1914.* Oxford: Berg Publishing Limited.

Pannaraj, P. S., Li, F., Cerini, C., Bender, J. M., Yang, S., Rollie, A., Adisetiyo, H., Zabih, S., Lincez, P. J. and Bittinger, K. 2017. Association Between Breast Milk Bacterial Communities and Establishment and Development of the Infant Gut Microbiome. *JAMA Pediatrics* 171: 647.

Pany-Kucera, D., Spannagl-Steiner, M., Desideri, J. and Rebay-Salisbury, K. 2022. Indicators of motherhood? Sacral preauricular extensions and notches in identified skeletal collections. *International Journal of Osteoarchaeology* 32: 64-74.

Papathanasiou, A., Meinzer, N. J., Williams, K. D. and Larsen, C. S. 2019. History of Anaemia and Related Nutritional Deficiencies from Cranial Porosities. In R. H. Steckel, C. S. Larsen, C. A. Roberts and J. Baten (eds). *The Backbone of Europe. Health, Diet,*

Work and Violence over Two Millenia. Cambridge: Cambridge University Press. Pp 198-230.

Parmalee, P. W. and Klippel, W. W. 1974. Freshwater mussels as a prehistoric food source. *American Antiquity* 39: 421-434.

Paul, K. S., Astorino, C. M. and Bailey, S. E. 2017. The Patterning Cascade Model and Carabelli's trait expression in metameres of the mixed human dentition: exploring a morphogenetic model. *American Journal of Physical Anthropology* 162: 3-18.

Pelling, M. 1994. Apprenticeship, Health and Social Cohesion in Early Modern London. *History Workshop* 37: 33-56.

Perez, S. I., Bernal, V. and Gonzalez, P. N. 2006. Differences between sliding semi-landmark methods in geometric morphometrics, with an application to human craniofacial and dental variation. *Journal of Anatomy* 208: 769-784.

Perzigian, A.J. 1977. Fluctuating dental asymmetry: variation among skeletal populations. *American Journal of Physical Anthropology* 47: 81-88.

Peters, J., Loud, J., Dimond, E. and Jenkins, J. 2001. Cancer Genetics Fundamentals. *Cancer Nursing* 24 (6): 446-461.

Phenice, T. W. 1969. A newly developed visual method of sexing the os pubis. *American Journal of Physical Anthropology* 30: 297-301.

Pilloud, M. A., Adams, D. M. and Hefner, J. T. 2019. Observer error and its impact on ancestry estimation using dental morphology. *International Journal of Legal Medicine* 133: 949-962.

Pittet, F., Johnson, C. and Hinde, K. 2017. Age at reproductive debut: Developmental predictors and consequences for lactation, infant mass, and subsequent reproduction in rhesus macaques (Macaca mulatta). *American Journal of Physical Anthropology* 1-20.

Plavcan, J. M. 2012. Sexual Size Dimorphism, Canine Dimorphism, and Male-Male Competition in Primates: Where Do Humans Fit In? *Human Nature* 23: 45-67.

Polachek, A., Li, S., Chandran, V. and Gladman, D. D. 2017. Clinical Enthesitis in a Prospective Longitudinal Psoriatic Arthritis Cohort: Incidence, Prevalence, Characteristics, and Outcome. *Arthritis Care & Research* 69 (11): 1685-1691.

Polly, P. D. 2003. Paleophylogeography: The Tempo of Geographic Differentiation in Marmots (Marmota). *Journal of Mammalogy* 84 (2): 369-384.

Pomeroy, E., Stock, J. T., Stanojevic, S., Miranda, J. J., Cole, T. J. and Wells, J. C. K. 2012. Trade-Offs in Relative Limb Length among Peruvian Children: Extending the Thrifty Phenotype Hypothesis to Limb Proportions. *PLoS ONE* 7 (12): e51795.

Poos, L. R. The Social Context of Statute of Labourers Enforcement. *Law and History Review* 1 (1): 27-52.

Poulter, N., Chang, C., MacGregor, A., Snieder, H. and Spector, T. 1999. Association between birth weight and adult blood pressure in twins: historical and cohort study. *British Medical Journal* 319: 1330-1333.

Pozzi, L. and Ramiro Fariñas, D. 2015. Infant and Child Mortality in the Past. *Dans Annales de Démographie Historique* 129 (1): 55-75.

Primeau, C., Arge, S. O., Boyer, C. and Lynnerup, N. 2015. A test of inter- and intra-observer error for an atlas method of combined histological data for the evaluation of enamel hypoplasia. *Journal of Archaeological Science: Reports* (2): 384-388.

Prince-Buitenhuys, J. R. and Bartelink, E. J. 2021. Niche Construction Theory in Bioarchaeology. In C. M. Cheverko, J. R. Prince-Buitenhuys and M. Hubbe (eds). *Theoretical Approaches in Bioarchaeology*. Oxford: Routeledge. Pp 93-112.

Proudfoot, L. J. 1983 The extension of parish churches in medieval Warwickshire. *Journal of Historical Geography* 9 (3): 231-246.

Pruvost, M., Grange, T. and Geigl, E. M. 2005 Minimizing DNA contamination by using UNG-coupled quantitative real-time PCR on degraded DNA samples: application to ancient DNA studies. *Biotechniques* 38: 569-575.

Quade, L., Chazot, P. L. and Gowland, R. 2020. Desperately seeking stress: A pilot study of cortisol in archaeological tooth structures. *American Journal of Physical Anthropology* 1-10.

Radwan, J., Watson, P. J., Farslow, J. and Thornhill, R. 2003. Procrustean analysis of fluctuating asymmetry in the bulb mite *Rhizoglyphus robini* Claparede (Astigmata: Acaridae). *Biological Journal of the Linnean Society* 80: 499-505.

Raine, J. 1838. Vita Oswini Regis Deirorum. In: *Publications of the Surtees Society 8*. Newcastle: Blackwell. Pp 1-59.

Rampelli, S., Turroni, S., Mallol, C., Hernandez, C., Galván, B., Sistiaga, A., Biagi, E., Astolfi, A., Brigidi, P., Benazzi, S., Lewis Jr, C. M., Warinner, C., Hofman, C. A., Schnorr, S. L. and Candela, M. 2021. Components of a Neanderthal gut microbiome recovered from fecal sediments from El Salt. Communications Biology 4 (1): 169.

Raser, J. M. and O'Shea, E. K. 2005. Noise in gene expression: origins, consequences, and control. *Science* 309: 2010-2013.

Ravelli, A. C. J., van der Meulen, J. H. P., Michels, R. P. J., Osmond, C., Barker, D. J. P., Hales, C. N. and Bleker, O. P. 1998. Glucose tolerance in adults after prenatal exposure to the Dutch famine. *Lancet* 35: 173-177.

Ravenstein, E. G. 1885. The Laws of Migration. *Journal of the Statistical Society of London* 48 (2): 167-235.

Raynor, C., McCarthy, R. and Clough, S. 2011. *Coronation Street, South Shields, Tyne And Wear*. Archaeological Excavation and Osteological Analysis Report, Oxford Archaeology North.

Redfern, R. and Roberts, C. 2019. Trauma. In J. E. Buikstra (eds). *Ortner's Identification of Pathological Conditions in Human Skeletal Remains*. London: Academic Press. Pp 211-284.

Redford, A. and Chaloner, W. H. 1976. *Labour Migration in England 1800-1850*. Manchester: Manchester University Press.

Reid, D.J. and Dean, M.C. 2006. Variation in modern human enamel formation times. *Journal of Human Evolution* 50 (3): 329-346.

Reinhard, K. and Camacho, M. 2019. Parasitology. In J. E. Buikstra (eds). *Ortner's Identification of Pathological Conditions in Human Skeletal Remains*. London: Academic Press. Pp 479-490.

Retzius, A. 1837. Bemerkungen über den inneren Bau der Zähne, mit besonderer Rücksicht auf den im Zahnknochen vorkommenden Röhrenbau. Archive of Anatomy and Physiology 486-566.

Riani, M. and Atkinson, A. C. and Cerioli, A. 2009. Finding an unknown number of multivariate outliers. *Journal of the Royal Statistical Society: series B (statistical methodology)* 71 (2): 1-34.

Richardson, G. G. 1852. *Plague and Pestilence in the North of England; Preceded by a sketch of the sanitary conditions of Newcastle upon Tyne in the Middle and Later ages*. Newcastle: Richardson.

Richardson, S. S., Daniels, C. R., Gillman, M. W., Golden, J., Kukla, R., Kuzawa, C. and Rich-Edwards, J. 2014. Society: don't blame the mothers. *Nature* 512: 131-132.

Ridsdale Tate, E. 1914. *A panorama of 15th century York* [Watercolour]. Available from: http://www.yorkcastle.com/pages/pictures.html [Viewed 1 August 2021].

Riga, A., Belcastro, M. G. and Moggi-Cecchi, J. 2014. Environmental Stress Increases Variability in the Expression of Dental Cusps. *American Journal of Physical Anthropology* 153: 397-407.

Riley, J. C. 1989. *Sickness, recovery and death: a history and forecast of ill-health.* Basingstoke: Macmillan.

Risnes, S. 1984. Rationale for consistency in the use of enamel surface terms: perikymata and imbrications. *Scandinavian Journal of Dental Research* 92: 1-5.

Rizk, O. T., Grieco, T. M., Holmes, M. W. and Hlusko, L. J. 2013. Using Geometric Morphometrics to Study the Mechanisms that Pattern of primate Dental Variation. In G. R. Scott and J. D. Irish (eds). *Anthropological Perspectives on Tooth Morphology: Genetics, Evolution, Variation*. Cambridge: Cambridge University Press. Pp 126-169.

Robert, K. A. and Braun, S. 2012. Milk Composition during Lactation Suggests a Mechanism for Male Biased Allocation of Maternal Resources in the Tammar Wallaby (Macropus eugenii). *Plos* 7 (11): e51099.

Roberts, C. 2019. Infectious Disease: Introduction, Periostosis, Periostitis, Osteomyelitus and Septic Arthritis. In J. E. Buikstra (eds). *Ortner's Identification of Pathological Conditions in Human Skeletal Remains*. London: Academic Press. Pp 285-320.

Roberts, C. A. and Buikstra, J. E. 2019. Bacterial Infections. In J. E. Buikstra (eds). *Ortner's Identification of Pathological Conditions in Human Skeletal Remains*. London: Academic Press. Pp 321-440.

Roberts, C. A. and Cox, M. 2003. *Health and Disease in Britain. From Prehistory to the Present Day*. Stroud: Sutton Publishing.

Roberts, C., Caffell, A., Filipek-Ogden, K. L., Gowland, R. and Jakob, T. 2016. 'Til Poison Phosphorous Brought them Death': A potentially occupationally-related disease in a post-medieval skeleton from north-east England. *International Journal of Paleopathology* 13: 39-48.

Robinson, D. L. 2005. *Statistical methods for the analysis of tooth shape*. Ph.D. Thesis, University of Sheffield.

Robinson, D. L., Blackwell, P. G., Stillman, E. C. and Brook, A. H. 2002. Impact of landmark reliability on the planar Procrustes analysis of tooth shape. *Archives of Oral Biology* 47: 545-554.

Rochlani, Y., Pothineni, N. V., Kovelamudi, S. and Mehta, J. L. 2017. Metabolic syndrome: pathophysiology, management, and modulation by natural compounds. *Therapeutic Advances in Cardiovascular Disease* 11 (8) 215-225.

Rodgers, J. L., Jones, J., Bolleddu, S. I., Vanthenapalli, S., Rodgers, L. E., Shah, K., Karia, K. and Panguluri, S. K. 2019. Cardiovascular Risks Associated with Gender and Aging. *Journal of Cardiovascular Development and Disease* 6: 19.

Roffey, S. 2012. Medieval Leper Hospitals in England: An Archaeological Perspective. *Medieval Archaeology* 56 (1): 203-233.

Rogers, J. and Waldron, T. 1989. Infections in palaeopathology: The basis of classification according to most probable cause. *Journal of Archaeological Science* 16: 611-625.

Rohlf, F. J. 1986. Relationships among eigenshape analysis, Fourier analysis, and analysis of coordinates. *Mathematical Geology* 18 (8): 845-854.

Rohlf, F. J. 1999. Shape statistics: Procrustes superimpositions and tangent spaces. *Journal of Classification* 16: 197-223.

Rohlf, F. J. 2000. Statistical power comparisons among alternative morphometric methods. *American Journal of Physical Anthropology* 111: 463-478.

Rohlf, F. J. 2003. Bias and error in estimates of mean shape in geometric morphometrics. *Journal of Human Evolution* 44: 665-683.

Rohlf, F. J. and Marcus, L. F. 1993. A revolution in morphometrics. *Trends in Ecology and Evolution* 8: 129-132.

Rohlf, F. J. and Slice, D. 1990. Extensions of the Procrustes Method for the Optimal Superimposition of Landmarks. *Systematic Zoology* 39 (1): 40-59.

Roffey, S., Tucker, K., Filipek-Ogden, K., Montgomery, J., Cameron, J. and O'Connell, T. 2017. Investigation of a Medieval Pilgrim Burial Excavated from the Leprosarium of St Mary Magdalen Winchester, UK. *PLoS Neglected Tropical Diseases* 11 (1): e0005186.

Roseboom, T. J., van der Meulen, J. H. P. and Ravelli, A. C. J. 2001. Effects of prenatal exposure to the Dutch famine on adult disease in later life: an overview. *Molecular and Cellular Endocrinology* 185: 93-98.

Roseboom, T. J., van der Meulen, J. H. P., Osmond, C., Barker, D. J. P., Ravelli, A. C. J., Schroeder-Tanka, J. M., van Montfrans, G. A., Michels, R. P. J. and Bleker, O.P. 2000. Coronary heart disease in adults after prenatal exposure to the Dutch famine. *Heart* 84: 595-598.

Rosenthal, R. 1991. *Meta-analytic procedures for social research (revised).* Newbury Park: Sage.

Rothschild, B. 2021. *Classical presentation and the spectrum of disease: The challenge of malignant neoplasms* [Presentation at the 48th Annual North American Meeting of the Paleopathology Association]. April [Viewed 7th April 2021].

Rutter, M. 1989. Pathways from childhood to adult life. Journal of Child Psychology and Psychiatry 1 :23-51.

Sakai, T., Sasaki, I. and Hanamura, H. 1967. A morphological study of enamel-dentin border on the Japanese dentition. II. Maxillary canine. *Journal of the Anthropological Society of Nippon* 75: 155-172.

Salazar-Ciudad, I. and Jernvall, J. 2002. A gene network model accounting for development and evolution of mammalian teeth. *Proceedings of the National Academy of Sciences* 99: 8116-8120.

Salmon, T. 1856. *South Shields: its past, present and future!* South Shields.

Sanchis-Gomar, F., Perez-Quilis, C., Leischik, R. and Lucia, A. 2016. Epidemiology of coronary heart disease and acute coronary syndrome. *Annals of Translational Medicine* 4 (13): 256.

Sandberg, P. A., Sponheimer, M., Lee-Thorp, J. and Van Gerven, D. 2014. Intra-Tooth Stable Isotope Analysis of Dentine: A Step Toward Addressing Selective Mortality in the Reconstruction of Life History in the Archaeological Record. *American Journal of Physical Anthropology* 155: 281-293.

Sanogo, M., Abatih, E. and Saegerman, C. 2014. Bayesian versus frequentist methods for estimating true prevalence of disease and diagnostic test performance. *The Veterinary Journal* 202: 204-207.

Santiago-Rodriguez, T. M. Fornaciari, G., Luciani, S., Dowd, S. E., Toranzos, G. A., Marota, I. and Cano, R. J. 2016. Taxonomic and predicted metabolic profiles of the human gut microbiome in pre-Columbian mummies. *FEMS Microbiology Ecology* 92: 182.

Sasaki, T. and Kondo, O. 2016. Brief Communication: An Informative Prior Probability Distribution of the Gompertz Parameters for Bayesian Approaches in Paleodemography. *American Journal of Physical Anthropology* 159: 523-533.

Saunders, S. R. and Mayhall, J. T. 1982. Fluctuating Asymmetry of Dental Morphological Traits: New Interpretations. *Human Biology* 54 (4): 789-799.

Savriama, Y. and Klingenberg, C. P. 2011. Beyond bilateral symmetry: Geometric morphometric methods for any type of symmetry. BMC Evolutionary Biology 11: 280.

Schaefer, M., Black, S. and Scheuer, L. 2009. *Juvenile Osteology: A Laboratory and Field Manual.* London: Elsevier.

Scheuer, L. and Black, S. 2000. *Developmental Juvenile Osteology.* London: Academic Press.

Schmalhausen, I. I. 1949. *Factors of Evolution*. Philadelphia: Blakiston.

Schour, L. and Massler, M. 1941. The development of the human dentition. *Journal of the American Dental Association* 28: 1153-1160.
Schwartz, J. H. 1995. *Skeleton Keys*. Oxford: Oxford University Press.

Schutkowski, H. 1993. Sex Determination of Infant and Juvenile Skeletons: I. Morphognostic Features. *American Journal of Physical Anthropology* 90 (2): 199-205.

Scientific Working Group for Forensic Anthropology. 2012. Stature Estimation. Revision 1 [Viewed 12th October 2021]. Available from: https://www.nist.gov/system/files/documents/2018/03/13/swganth_stature_estimation.pdf
Shapland, F and Lewis, M. E. 2013. Brief communication: a proposed osteological method for the estimation of pubertal stage in human skeletal remains. *American Journal of Physical Anthropology* 151: 302-310.

Scoles, P., Salvagno, R., Villalba, K. and Riew, D. 1987. Relationship of iliac crest maturation to skeletal and chronologic age. Journal of Pediatric Orthopedics 8: 639-644.

Scott, G. R. 1980. Population variation of Carabelli's trait. *Human biology* 52 (1): 63-78.

Scott, G. R. and Irish, J. D. 2013. *Anthropological Perspectives on Tooth Morphology: Genetics, Evolution, Variation*. Cambridge: Cambridge University Press.

Scott, G. R. and Turner, C. 1997. *The Anthropology of Modern Human Teeth: Dental Morphology and its Variation in Recent Human Populations*. Cambridge: Cambridge University Press.

Scott, G. R., Maier, C. and Heim, K. 2016. Identifying and Recording Key Morphological (Nonmetric) Crown and Root Traits. In J. D. Irish and G. R. Scott (eds). *A Companion to Dental Anthropology, First Edition*. London: Wiley. Pp 248-264.

Scott, G. R., Pilloud, M. A., Navega, D., d'Oliveira Coelho, J., Cunha, E. and Irish, J. D. 2018. rASUDAS. A New Web-Based Application for Estimating Ancestry from Tooth Morphology. *Forensic Anthropology* (1) 1: 18–31.

Scott, R. G. 2016. A Brief History of Dental Anthropology. In J. D. Irish and G. R. Scott (eds). *A Companion to Dental Anthropology, First Edition*. London: Wiley. Pp 7-17.

Scott, R. S., Ungar, P. S., Bergstrom, T. S., Brown, C. A., Grine, F. E., Teaford, M. F. and Walker, A. 2005. Dental Microwear Texture Analysis Shows within-Species Diet Variability in Fossil Hominins. *Nature* 436: 693-695.

Selye, H. 1973. The evolution of the stress concept. *American Scientist* 61: 692-699.

Shahmoradi, M., Bertassoni, L.E., Elfallah, H.M. and Swain, M. 2014. Fundamental Structure and Properties of Enamel, Dentin and Cementum. In B. Ben-Nissan (eds). *Advances in Calcium Phosphate Biomaterials*. New York: Springer. Pp 511-547.

Shanahan, M. J. 2000. Pathways to Adulthood in Changing Societies: Variability and Mechanisms in Life Course Perspective. *Annual Review of Sociology* 26 (1): 667–692.

Sharma, D, Farahbakhsh, N., Shastri, S. and Sharma, P. 2016. Intrauterine Growth Restriction – Part 2. *Journal of Maternal, Fetal and Neonatal Medicine* 15: 1-12.

Sharpe, P. 1991. Poor children as apprentices in Colyton, 1598-1830. *Continuity and Change* 6 (2): 253-270.

Sharpe, P. 2012. Explaining the short stature of the poor: chronic childhood disease and growth in nineteenth-century England. *Economic History Review* 65 (4): 1475-1494.

Shearer, B. M., Cooke, S. B., Halenar, L. B., Reber, S. L., Plummer, J. E., Delson, E. and Tallman, M. 2017. Evaluating causes of error in landmark-based data collection using scanners. *PLoS ONE* 12 (11): e0187452.

Sherrat, E. 2014. *Quick Guide to Geomorph v.2.0.* [Viewed 15th June 2020]. Available from: http://people.tamu.edu/~alawing/materials/ESSM689/Quick_Guide_to_Geomorph_v2.0.pdf

Shiau, H. J. and Reynolds, M. A. 2010. Sex Differences in Destructive Periodontal Disease: A Systematic Review. *American Academy of Periodontology* 81 (10): 1379-1389.

Shoukri, M. M., Asyali, M. H. and Donner, A. 2004. Sample size requirements for the design of reliability study: review and new results. *Statistical Methods in Medical Research* 13 (4): 251-271.

Shrout, P. E. and Fleiss, J. L. 1979. Intraclass correlations: uses in assessing rater reliability. *Psychology Bulletin* 86 (2): 420-428.

Sibley, L. M., Armelagos, G. J. and Van Gerven, D. P. 1992. Obstetric Dimensions of the True Pelvis in a Medieval Population from Sudanese Nubia. *American Journal of Physical Anthropology* 89: 421-430.

Sibly, R. and Brown, J. 2009. Mammal Reproductive Strategies Driven by Offspring Mortality-Size Relationships. *The American Naturalist*. 173: 185-199.

Silva, M. F. S., De Andrade, I. M. and Mayo, S. J. 2012. Geometric morphometrics of leaf blade shape in *Montrichardia linifera (Araceae)* populations from the Rio Parnaíba Delta, north-east Brazil. Botanical journal of the Linnean Society 170 (4): 554-572.

Simmer, J. P., Papagerakis, P., Smith, C. E., Fisher, D. C., Rountrey, A. N., Zheng, L. and Hu, J. C. 2010. Regulation of Dental Enamel Shape and Hardness. *Journal of Dental Research* 89: 1024-1038.

Simon, A. K., Hollander, G. A. and McMichael, A. 2015 Evolution of the immune system in humans from infancy to old age. *Proceedings of the Royal Society of Biology* 282: 20143085.

Sindbaek, S. 2007. Networks and nodal points: the emergence of towns in early Viking Age Scandinavia. *Antiquity* 81 (311): 119-132.

Singleton, M. 2001. Patterns of Cranial Shape Variation in the Papionini (Primates: Cercopithecinae). *Journal of Human Evolution* 42: 547-578.

Skinner, M. K. 2008. What is an Epigenetic Transgenerational Phenotype? F3 or F2. *Reproductive Toxicology* 25 (1): 2-6.

Slavin, P. 2012. The Great Bovine Pestilence and its economic and environmental consequences in England and Wales, 1318-50. *Economic History Review* 65 (4): 1239-1266.

Slavin, P. 2013. Market failure during the Great Famine in England and Wales (1315-1317). *Past and Present* 222 (1): 9-49.

Sledzik, P., and Sandberg, L. 2002. The Effects of Nineteenth-Century Military Service on Health. In R. Steckel and J. Rose (eds). *The Backbone of History: Health and Nutrition in the Western Hemisphere*. Cambridge: Cambridge University Press. Pp 185-207.

Small, C. 1996. *The statistical theory of shape*. New York: Springer.

Smith, B. H. 1984. Patterns of Molar Wear in Hunter-Gatherers and Agriculturalists. *American Journal of Physical Anthropology* 63: 39-56.

Smith, B. H. 1991. Standards of human tooth formation and dental age assessment. In M. A. Kelley and C. S. Larsen (eds). *Advances in Dental Anthropology*. New York: Wiley-Liss. Pp 143-168.

Smith, C. A. B. 1972. Coefficients of biological distance. *Annals of Human Genetics* 36: 241-245.

Smith, D. R., Crespi, B. and Bookstein. F. L. 1997. The Procrustes method and fluctuating asymmetry in the honey bee, Apis mellifera: effects of ploidy and hybridization. *Journal of Evolutionary Biology* 10: 551-574.

Smith, S. L. 2007. Stature Estimation of 3–10-Year-Old Children from Long Bone Lengths. *Journal of Forensic Sciences* 52: 538-546.

Smith, T. M., Martin, L. B., Leakey, M. G. 2003. Enamel thickness, microstructure and development in *Afropithecus turkanensis*. *Journal of Human Evolution* 44: 283-306.
Smith, B. H. 1984. Patterns of Molar Wear in Hunter-Gatherers and Agriculturalists. *American Journal of Physical Anthropology* 63: 39-56.

Smith, T., Tafforeau, P., Reid, D., Pouech, J., Lazzari, V., Zermeno, J., Guatelli-Steinberg, D., Olejniczak, A., Hoffman, A., Radovcic, J., Masrour, M., Toussaint, M., Stringer, C. and Hublin, J-J. 2010. Dental Evidence for Ontogenetic Differences Between Modern Humans and Neanderthals. *Proceedings of the National Academy of Sciences* 107: 20923-20928.

Snape, M. and Bidwell, P. 2002a. The History and Setting of the Roman Fort at Newcastle upon Tyne. In: *Archaeologia Aeliana Series 5 (31): The Roman Fort at Newcastle upon Tyne*. Kendal: Titus Wilson. Pp 251-283.

Snape, M. and Bidwell, P. 2002b. The Fort in the Post-Roman Period and During the Earliest Anglo-Saxon Occupation. In: *Archaeologia Aeliana Series 5 (31): The Roman Fort at Newcastle upon Tyne*. Kendal: Titus Wilson. Pp 111-127.

Soubry, A. 2018. POHaD: why we should study future fathers. *Environmental Epigenetics*: 1-7

Soubry, A., Hoyo, C., Jirtle. R. l. and Murphy, S. K. 2014. A paternal environmental legacy: evidence for epigenetic inheritance through the male germ line. *Bioessays* 36: 359-371.

Speed, J. 1610. *The counti of Warwick the shire towne and citie of Coventre described*. Available from: https://collections.leventhalmap.org/search/commonwealth:ww72bp490). [Viewed 31 July 2021].

Speed, J. 1611. *Yorke*. Available from: https://commons.wikimedia.org/wiki/File:A_map_of_York_england.jpg [Viewed 31 July 2021].

Stamps, J. A. 2006. The silver spoon effect and habitat selection by natal dispersers. *Ecology Letters* 9: 1179-1185.

Stantis, C., Schutkowski, H. and Sołtysiak, A. 2020. Reconstructing breastfeeding and weaning practices in the Bronze Age Near East using stable nitrogen isotopes. *American Journal of Physical Anthropology* 172: 58-69.

Steadman, D. 2018. Who Needs Data I've Got Experience! *Human Biology* 90 (1): 1-6.

Steckel, R. H. and Engel, F. 2019. Climate and Health. Europe from the Pre-Middle Ages to the Nineteenth Century. In R. H. Steckel, C. S. Larsen, C. A. Roberts and J. Baten (eds). *The Backbone of Europe. Health, Diet, Work and Violence over Two Millenia.* Cambridge: Cambridge University Press. Pp 352-381.

Steckel, R. H. and Rose, J. C. 2002. *The Backbone of History. Health and Nutrition in the Western Hemisphere.* Cambridge: Cambridge University Press.

Steckel, R. H., Larsen, C. S., Roberts, C. A. and Baten, J. 2019. *The Backbone of Europe. Health, Diet, Work and Violence over Two Millenia.* Cambridge: Cambridge University Press.

Steckel, R. H., Larsen, C. S., Roberts, C. A. and Baten, J. 2019. The European History of Health Project. Introduction to Goals, Materials and Methods. In R. H. Steckel, C. S. Larsen, C. A. Roberts and J. Baten (eds). *The Backbone of Europe. Health, Diet, Work and Violence over Two Millenia.* Cambridge: Cambridge University Press. Pp 1-10.

Steckel, R. H., Larsen, C. S., Sciuli, P. W. and Walker, P. L. 2019. Data Collection Codebook. In R. H. Steckel, C. S. Larsen, C. A. Roberts and J. Baten (eds). *The Backbone of Europe. Health, Diet, Work and Violence over Two Millenia*. Cambridge: Cambridge University Press. Pp 397-428.

Steckel, R. H., Sciulli, P. W. and Rose, J. C. 2002. A Health Index from Skeletal Remains. In R. H. Steckel and J. C. Rose (eds). *The Backbone of History. Health and Nutrition in the Western Hemisphere.* Cambridge: Cambridge University Press. Pp 61-93.

Stein, A. D., Melgar, P., Hoddinott, J. and Martorell, R. 2008. Cohort profile: The Institute of Nutrition of Central America and Panama (INCAP) Nutrition Trial Cohort Study. *International Journal of Epidemiology* 37: 716-20

Stephens, W. B. 1969. *A History of the County of Warwick: The City of Coventry and Borough of Warwick*. London: Victoria County History.

Stewart, A. 2011. The Boxer's 'Pugilistic-Present': Ethnographic Notes Towards a Cultural History of Amateur and Professional Boxing in England. *Sport in History* 31 (4): 464-486.

Stewart, N. A., Gerlach, R. F., Gron, K. J. and Montgomery, J. 2017. Sex determination of human remains from peptides in tooth enamel. *Proceedings of the National Academy of Sciences* 114 (52): 13649-13654.

Stinson, S., Bogin, B., O'Rourke, D. H. and Huss-Ashmore, R. 2012. Human Biology: An Evolutionary and Biocultural Perspective. In S. Stinson, B. Bogin, D. H. O'Rourke

(eds). *Human Biology: An Evolutionary and Biocultural Perspective*. Hoboken: Wiley. Pp 3-22.

Stinson. S. 1985. Sex Differences in Environmental Sensitivity During Growth and Development. *Yearbook of Physical Anthropology* 28: 123-147.

Stojanowski, C. M., Paul, K. S., Seidel, A. C., Duncan, W. N. and Guatelli-Steinberg, D. 2017. Heritability and genetic integration of tooth size in the South Carolina Gullah. *American Journal of Physical Anthropology* 164: 505-521.

Stone, A. C. and Ozga, A. T. 2019. Ancient DNA in the Study of Ancient Disease. In J. E. Buikstra (eds). *Ortner's Identification of Pathological Conditions in Human Skeletal Remains*. London: Academic Press. Pp 183-210.

Stuart-Macadam, P. 1992. Porotic hyperostosis. A new perspective. *American Journal of Physical Anthropology* 87: 39-47.

Subramanian, S. V., Acevedo -Garcia, D. and Osypuk, T. L. 2005. Racial residential segregation and geographic heterogeneity in black/white disparity in poor self-rated health in the US: a multilevel statistical analysis. *Social Science and Medicine* 60: 1667-1679.

Sunderland, N., Heffernan, S., Thomson, S. and Hennessy, A. 2008. Maternal parity affects neonatal survival rate in a colony of captive bred baboons (*Papio hamadryas*). *Journal of Medical Primatology* 37: 223-228.

Surtees, R. 1820. *The history and antiquities of the County Palatine of Durham. Chester Ward*', London: Nichols.

Susser, E., Kirkbride, J. B., Heijmans, B. T., Kresovich, J. K., Lumey, L. H. and Stein, A. D. 2012. Maternal Prenatal Nutrition and Health in Grandchildren and Subsequent Generations. *Annual Review of Anthropology* 41: 577-610.

Sutherland, M. J. and Ware, S. M. 2009. Disorders of left–right asymmetry: Heterotaxy and situs inversus. *American Journal of Medical Genetics* 151: 307-317.

Sweetinburgh, S. 2004. *The Role of the Hospital in Medieval England*. Dublin: Four Courts Press.

Swerdlow, A. J., De Stavola, B. L., Swanwick, M. A. and Maconochie, N. E. S. 1997. Risks of breast and testicular cancers in young adult twins in England and Wales: evidence on prenatal and genetic aetiology. *Lancet* 350: 1723-1728.

Swindler, D. R. 2002. *Primate Dentition. An Introduction to the Teeth of Non-human Primates*. Cambridge: Cambridge University Press.

Syddall, H. E., Aihie Sayer, A., Dennison, E. M., Martin, H. J., Barker, D. J. and Cooper, C. 2005. Cohort profile: the Hertfordshire cohort study. *International Journal of Epidemiology* 34: 1234-1242.

Szumilas M. 2010. Explaining odds ratios. *Journal of the Canadian Academy of Child and Adolescent Psychiatry* 19 (3): 227-229.

Tamura, M., and Nemoto, E. 2016. Role of the Wnt signaling molecules in the tooth. *The Japanese dental science review* 52 (4): 75-83.

Tan, L. Y., Komarasamy, T. V. and Balasubramaniam, V. R. M. T. 2021. Hyperinflammatory Immune Response and COVID-19: A Double Edged Sword. *Frontiers of Immunology* 12:742941.

Tang, N., Le Cabec, A. and Antoine, D. 2016. Dentine and Cementum Structure and Properties. In J. D. Irish and G. R. Scott (eds). *A Companion to Dental Anthropology, First Edition*. London: Wiley. Pp 204-222.

Tangmose, S., Thevissen, P., Lynnerup, N., Willems, G. and Boldsen, J. 2015. Age estimation in the living: Transition analysis on developing third molars. *Forensic Science International* 257: 512.e1-512.e7.

Tanner, J. M. and Whitehouse, R. H. 1980. *Human growth and development*. London: Academic Press.

Tardif, S. D., Power, M., Oftedal, O. T., Power, R. A. and Layne, D. G. 2001. Lactation, maternal behavior and infant growth in common marmoset monkeys (*Callithrix jacchus*): effects of maternal size and litter size. *Behavioral Ecology and Sociobiology* 51: 17-25.

Temple, D. H. 2007. Dietary Variation and Stress Among Prehistoric Jomon Foragers from Japan. *American Journal of Physical Anthropology* 133: 1035-1046.

Temple, D. H. 2014. Plasticity and Constraint in Response to Early-Life Stressors Among Late/Final Jomon Period Foragers from Japan: Evidence for Life History Trade-Offs from Incremental Microstructures of Enamel. *American Journal of Physical Anthropology* 155: 537-545.

Temple, D. H., Nakatsukasa, M. and McGroarty, J. N. 2012. Reconstructing patterns of systemic stress in a Jomon period subadult using incremental microstructures of enamel. *Journal of Archaeological Science* 39: 16341641.

Ten Cate. A. R. 1998. *Oral Histology: Development, Structure, and Function*. Fifth Edition. St Lois: Mosby.

Thayer, Z. M. and Kuzawa, C. W. 2011. Biological memories of past environments: Epigenetic pathways to health disparities. *Epigenetics* 6 (7): 798-803.

Thayer, Z. M. and Kuzawa, C. W. 2014. Early origins of health disparities: material deprivation predicts maternal evening cortisol in pregnancy and offspring cortisol reactivity in the first few weeks of life. *American Journal of Human Biology* 26: 723-730.

Tilliot, P. M. 1961. *A History of the County of York: The City of York. Victoria History of the Counties of England*. London: Oxford University Press.

Todd, T. W. 1920. Age Changes in the Pubic Bone I. The Male White Pubis. *American Journal of Physical Anthropology* 3 (3): 285-340.

Tomczak, M. and Tomczak, E. 2014. The need to report effect size estimates revisited. An overview of some recommended measures of effect size. *Trends in Sport Sciences*. 1 (21): 19-25.

Toswell, J. 2000. Bede's Sparrow and the Psalter in Anglo-Saxon England. *ANQ: A Quarterly Journal of Short Articles, Notes and Reviews.* 13 (1): 7-12.

Townsend, G. C. and Brown, T. 1979. Tooth size characteristics of Australian Aborigines. *Occasional Papers in Human Biology* 1: 17-38.

Townsend, G. C. and Brown, T. 1980. Dental Asymmetry in Australian Aboriginals. *Human Biology* 52 (4): 661-673.

Townsend, G. C. and Brown, T. 1981. The Carabelli Trait in Australian Aboriginal Dentition. *Archives of Oral Biology* 26 (10): 809-814.

Townsend, G. C. and Garcia-Godoy, F. 1984. Fluctuating Asymmetry in the Deciduous Dentition of Dominican Mulatto Children. *Archives of Oral Biology* 29 (7): 483-486.

Townsend, G. C. and Martin, N. G. 1992. Fitting Genetic Models to Carabelli Trait Data in South Australian Twins. *Journal of Dental Research* 71: 403-409.

Townsend, G. C., Richards, L. and Hughes, T. 2003. Molar intercuspal dimensions: Genetic input to phenotypic variation. *Journal of Dental Research* 82: 350-355.

Townsend, G., Hughes, T., Luciano, M., Bockmann, M. and Brook, A. 2009. Genetic and environmental influences on human dental variation: A critical evaluation of studies involving twins. *Archives of Oral Biology* 54S: 45S-51S.

Trivers, R. L. and Willard, D. E. 1973. Natural Selection of Parental Ability to Vary the Sex Ratio of Offspring. *American Association for the Advancement of Science* 179: 90-92.

Trombley, T. M., Agarwal1, S. C., Beauchesne, P. D., Goodson, C., Candilio, F. Coppa, A. and Rubini, M. 2019. Making sense of medieval mouths: Investigating sex differences of dental pathological lesions in a late medieval Italian community. *American Journal of Physical Anthropology* 169: 253-269.

Tucker, A. S., Headon, D. J., Courtney, J. M., Overbook, P. and Sharpe, P. T. 2004. The activation level of the TNF family receptor, Edar, determines cusp number and size in tooth development. *Developmental Biology* 268: 185-194.

Turner, C. G. II. 1970. *New Classifications of Non-Metrical Dental Variation: Cusps 6 and 7*. Paper presented at 39th Annual Meeting of the American Association of Physical Anthropologists, Washington, DC.

Turner, C. G. II. 1990. Major features of Sundadonty and Sinodonty, including suggestions about East Asian microevolution, population history, and late Pleistocene relationships with Australian aboriginals. *American Journal of Physical Anthropology* 82: 295-317.

Turner, C. G. II., Nichol, C. R. and Scott, G. R. 1991. Scoring procedures for key morphological traits of the permanent dentition: The Arizona State University Dental Anthropology System. In M. Kelley and C. S. Larsen (eds). *Advances in dental anthropology*. New York: Wiley-Liss. Pp 13-31.

Turner, J. D., Alt, S. R., Cao, L., Vernocchi, S., Trifonova, S., Battello, N., and Muller, C. P. 2010. Transcriptional control of the glucocorticoid receptor: CpG islands, epigenetics and more. *Biochemical Pharmacology* 80: 1860-1868.

Tyrrell, A. 1999. *Human Skeletal Variation and the Assessment of Population Diversity: An Analysis of the Relationships and Dynamics among Early Medieval Populations from the Southern British Isles*. Ph.D. Thesis, University of Sheffield.

Tyrrell, A. 2000. Skeletal Non-metric traits and the assessment of inter- and intra-population diversity: past problems and future potential. In M. Cox and S. Mays (eds).

Human Osteology in Archaeology and Forensic Science. Cambridge: Cambridge University Press. Pp 298-306.

Ubelaker, D. H. 1989. Human Skeletal Remains: Excavation, Analysis, Interpretation (Second Edition). Washington, DC: Taraxacum.
Usher, B. M. 2002. Reference samples: the first step in linking biology and age in the human skeleton. In R. D. Hoppa and J. W. Vaupel (eds). *Paleodemography. Age Distributions from Skeletal Samples*. Cambridge: Cambridge University Press. Pp 29-47.

Ungar, P. S. 2016. Origins and Functions of Teeth: From "Toothed" Worms to Mammals. In J. D. Irish and G. R. Scott (eds). *A Companion to Dental Anthropology, First Edition*. London: Wiley. Pp 21-36.

Ungar, P. S., Grine, F. E. and Teaford, M. F. 2008. Dental Microwear and Diet of the PlioPleistocene Hominin *Paranthropus boisei*. *PLOS One* 3: 6.

Uzunov, T. T., Kosturkov, D., Uzunov, T., Filchev, D., Bonev, B. and Filchev, A. 2015. Registration of Internal Morphological Characteristics of the Tooth Using Dental Photography. *Journal of International Medical Association Bulgaria* 22 (1): 677-681.

Vaiserman, A. M. 2015. Epigenetic Programming by Early-Life Stress: Evidence from Human Populations. *Developmental Dynamic* 244: 254-265.

Vallin, J. 1991. Mortality in Europe from 1720 to 1914: long-term trends and changes in the patterns by age and sex. In R. S. Schofield, D. S. Reher and A. Bideau (eds). *The decline of mortality in Europe*. Oxford: Clarendon Press. Pp 38-67.

Van der Merwe, A. E., Maat, G. J. and Steyn, M. 2010. Ossified haematomas and infectious bone changes on the anterior tibia: histomorphological features as an aid for accurate diagnosis. *International Journal of Osteoarchaeology* 20: 227-239.

Van Dongen, S. and Gangestad, S. W. 2011. Human Fluctuating Asymmetry in Relation to Health and Quality: A Meta-Analysis. *Evolutionary and Human Behaviour* 32: 380-398.

Van Dongen, S., Sprengers, E., Löfstedt, C. and Matthysen,E. 1999. Fitness components of the male and female winter moths (*Operophtera brumata* L.) (*Lepidoptera Geometridae*) relative to measures of body size and asymmetry. *Behavioural Ecology* 10 (6): 659-655.

Van Pool, T. L. and Leonard, R. D. 2010. *Quantitative Analysis in Archaeology*. London: Wiley-Blackwell.

Van Staa, T. P., Denison, E. M., Leufkens, H. G. M. and Cooper, C. 2001. Epidemiology of fractures in England and Wales. *Bone* 29: 517-522.

Van Valen, L. 1961. A Study of Fluctuating Asymmetry. *Evolution* 16: 125-142.

Van Winkle, L. J. and Ryznar, R. 2018. Can uterine secretion of modified histones alter blastocyst implantation, embryo nutrition, and transgenerational phenotype? *Biomolecular Concepts* 9 (1): 176-183.

Vaupel, J. W. 1988. Inherited frailty and longevity. *Demography* 25 (2): 277-287.

Villotte, S. and Knüsel, C. J. 2012. Understanding Entheseal Changes: Definition and Life Course Changes. *International Journal of Osteoarchaeology* (Special Issue Paper).

Vineis, P and Fecht, D. 2018. Environment, cancer and inequalities—The urgent need for prevention. *European Journal of Cancer* 103: 317-326.

Von Carabelli, G. 1842. *Anatomie des Mundes*. Vienna: Braumuller and Seidel.

Voong, C. P., Spencer, P. S., Navarrete, C. V., Turner, D., Hayrabedyan, S. B., Crummy, P., Holloway, E., Wilson, M. T., Smith, P. R. and Fernández, N. 2017. HLA-DR genotyping and mitochondrial DNA analysis reveal the presence of family burials in a fourth century Romano-British Christian cemetery. *Frontiers in Genetics*. 8: 182.

Waddington, C. H. 1957. *The Strategy of the Genes*. London: George Allen Unwin.

Wadsworth, M. E., Hardy, R. J., Paul, A. A., Marshall, S. F. and Cole, T. J. 2002. Leg and trunk length at 43 years in relation to childhood health, diet and family circumstances; evidence from the 1946 national birth cohort. *International Journal of Epidemiology* 31: 838-390.

Waldron, T. 1994. *Counting the Dead*. The Epidemiology of Skeletal Populations. London: Wiley.

Waldron, T. 2019. Joint Disease. In J. E. Buikstra (eds). *Ortner's Identification of Pathological Conditions in Human Skeletal Remains*. London: Academic Press. Pp 719-748.

Walker, P. L., Bathurst, R. R., Richman, R., Gjerdrum, T. and Andrushko, V. A. 2009. The causes of porotic hyperostosis and cribra orbitalia: a reappraisal of the iron-deficiency anemia hypothesis. *American Journal of Physical Anthropology* 139: 109-125.

Walker, R. F. 1976. *The Origins of Newcastle upon Tyne*. Newcastle upon Tyne.

Wasiljew, B. D., Pfaender, J., Wipfler, B., Utama, I. V. and Herder, F. 2020. Do we need the third dimension? Quantifying the effect of the z-axis in 3D geometric morphometrics based on sailfin silversides (Telmatherinidae). *Journal of Fish Biology* 97 (2): 537-545.

Watanabe, A. 2018. How many landmarks are enough to characterize shape and size variation? *PLOS One* 13(6): e0198341.

Watts, R. 2011. Non-specific Indicators of Stress and Their Association with Age at Death in Medieval York: Using Stature and Vertebral Neural Canal Size to Examine the Effects of Stress Occurring During Different Periods of Development. *International Journal of Osteoarchaeology* 21: 568-576.

Waynforth, D. 1998. Fluctuating asymmetry and human male life-history traits in rural Belize. *Proceedings of the Royal Society of London* B 265: 1497-1501

Webb, E., Thomson, S., Nelson, A., White, C., Koren, G., Rieder, M. and Van Uum, S. 2010. Assessing individual systemic stress through cortisol analysis of archaeological hair. *Journal of Archaeological Science* 37 (4): 807-812.

Webb. W. S. 1946. *Indian Knoll. The University of Kentucky Reports in Anthropology IV (3), Part I.* Lexington: University of Kentucky.

Weinberg, E. 1984. Iron Withholding: A Defense Against Infection and Neoplasia. *Physiological Review* 64: 65-102.

Weinberg, E. and Miklossy, J. 2008. Iron Withholding: A Defense Against Disease. *Journal of Alzheimer's Disease* 13: 451-463.

Weisensee, K. E. 2013. Assessing the Relationship Between Fluctuating Asymmetry and Cause of Death in Skeletal Remains: A Test of the Developmental Origins of Health and Disease Hypothesis. *American Journal of Human Biology* 25: 411-417.

Wells, J. C. 2003. The thrifty phenotype hypothesis: thrifty offspring or thrifty mother? *Journal of Theoretical Biology* 221: 143-61.

Wells, J. C. 2012. A critical appraisal of the predictive adaptive response hypothesis. *International Journal of Epidemiology* 41: 229-235.

Wells, J. C. K. 2007. Flaws in the Theory of Adaptive Predictive Response. *Endocrinology and Medicine* 18 (9): 331-337.

Weston, D. 2008. Investigating the specificity of periosteal reactions in pathology museum specimens. *American Journal of Physical Anthropology* 137 (1): 48-59.

White T. D. 1978. Early hominid enamel hypoplasia. *American Journal of Physical Anthropology* 49: 79-83.

White, T. D. and Folkens, P. A. 2005. *The Human Bone Manual*. San Diego: Elsevier.

White, T. D., Black, M. T. and Folkens, P. A. 2012. *The Human Bone Manual. Third Edition*. San Diego: Academic Press.

Willmott, H., Townend, P., Mahoney Swales, D., Poinar, H., Eaton, K. and Klunk, J. 2020. A Black Death mass grave at Thornton Abbey: the discovery and examination of a fourteenth-century rural catastrophe. *Antiquity* 94 (373): 179-196.

Willoughby, J. 2012. Inhabited Sacristies in Medieval England: The Case of St Mary's, Warwick. *The Antiquaries Journal* 92: 331-345.

Wilson, J. J. 2014. Paradox and Promise: Research on the Role of Recent Advances in Paleodemography and Paleoepidemiology to the Study of "Health" in Precolumbian Societies. *American Journal of Physical Anthropology* 155: 268-280.

Wood, B. A. and Abbott, S. A. 1983. Analysis of the dental morphology of Plio-Pleistocene hominids. I. Mandibular molars: crown area measurements and morphological traits. *Journal of Anatomy* 136 (1): 197-219.

Wood, B. A. and Engleman, C. A. 1988. Analysis of the dental morphology of Plio-Pleistocene hominids. V. Maxillary postcanine tooth morphology. *Journal of Human Anatomy* 161: 1-35.

Wood, B. A., Abbott, S. A. and Graham, S. H. 1983. Analysis of the dental morphology of Plio-Pleistocene hominids II. Mandibular molars - study of cusp areas, fissure pattern and cross-sectional shape of the crown. *Journal of Human Anatomy* 137 (2): 287-314.

Wood, J. W., Holman, D. J., O'Connor, K. A. and Ferrel, R. J. 2002. Mortality models for paleodemography. In R. D. Hoppa and J. W. Vaupel (eds). *Paleodemography. Age Distributions from Skeletal Samples*. Cambridge: Cambridge University Press. Pp 129-168.

Wood, J. W., Milner, G. R., Harpending, H. C. and Weiss, K. M. 1992. The Osteological Paradox: Problems of Inferring Prehistoric Health from Skeletal Samples. *Current Anthropology* 33: 343-370.

Wright, S. 1982. Character change, speciation and the higher taxa. *Evolution* 36: 427-443.

Wu, M., Chen, S-W. and Jiang S-Y. 2015. Relationship between Gingival Inflammation and Pregnancy. *Mediators of Inflammation* 623427.

Wylie, M. 1982. Epistemological issues raised by a structuralist archaeology. In I. Hodder (eds). *Symbolic and Structural Archaeology (New Directions in Archaeology)*. Cambridge: Cambridge University Press. Pp 39-46.

Yamamoto, M. 1992. Secular trends in enamel hypoplasia in Japanese from the prehistoric to modern periods. *Journal of Paleopathology Monographic Publications* 2: 231-238.

Yaussy, S. L., DeWitte, S. N. and Redfern, R. C. 2016. Frailty and Famine: Patterns of Mortality and Physiological Stress Among Victims of Famine in Medieval London. *American Journal of Physical Anthropology* 160: 272-283.

Yazdanyar, A. and Newman, A. B. 2009. The burden of cardiovascular disease in the elderly: Morbidity, mortality, and costs. *Clinical Geriatric Medicine* 25: 563-577.

Zelditch, M. L. and Swiderski, D. L. 2018. *A Practical Companion to Geometric Morphometrics for Biologists: Running analyses in freely-available software (Second Edition).* London: Academic Press.

Zelditch, M. L., Swiderski, D. L. and Sheets, H. D. 2012. *Geometric Morphometrics for Biologists. A Primer*. London: Academic Press.

Zhang, S., Liu, G., Liu, L., Ma, Z., Han, Y., Shen, X. and Xu, R. 2008. Relationship of certain skeletal maturity indicators of hand and wrist with adolescent growth spurt. *Zhong Yi Xue Za Zhi* 88: 2198-2200.

Zietek, T. and Rath, E. 2016. Inflammation Meets Metabolic Disease: Gut Feeling Mediated by GLP-1. *Frontiers in Immunology* 7: 154.

Zoëga, G. and Murphy, K. A. 2016. Life on the Edge of the Arctic: The Bioarchaeology of the Keldudalur Cemetery in Skagafjörður, Iceland. *International Journal of Osteoarchaeology* 26: 574-584.

Zubov, A. A. 1968. *Odontology: A Method of Anthropological Research*. Moscow: Nauka.

Zubov, A. A. 1977. Odontoglyphics: the laws of variation of the human molar crown relief. In A. A. Dahlberg and T. M. (eds). Graber Orofacial Growth and Development. The Hague: Mouton Publishers. Pp 269-282.

Zubov, A. A. and Khaldeeva, N. I. 1979. *Ethnic Odontology of the USSR*. Moscow: Nauka.

Zuckerman, M. K. 2021. Gender in Bioarchaeology. In C. M. Cheverko, J. R. Prince-Buitenhuys, M. Hubbe (eds). *Theoretical Approaches in Bioarchaeology*. Oxford: Routeledge. Pp 28-44.

Appendix 1: Osteological Terminology

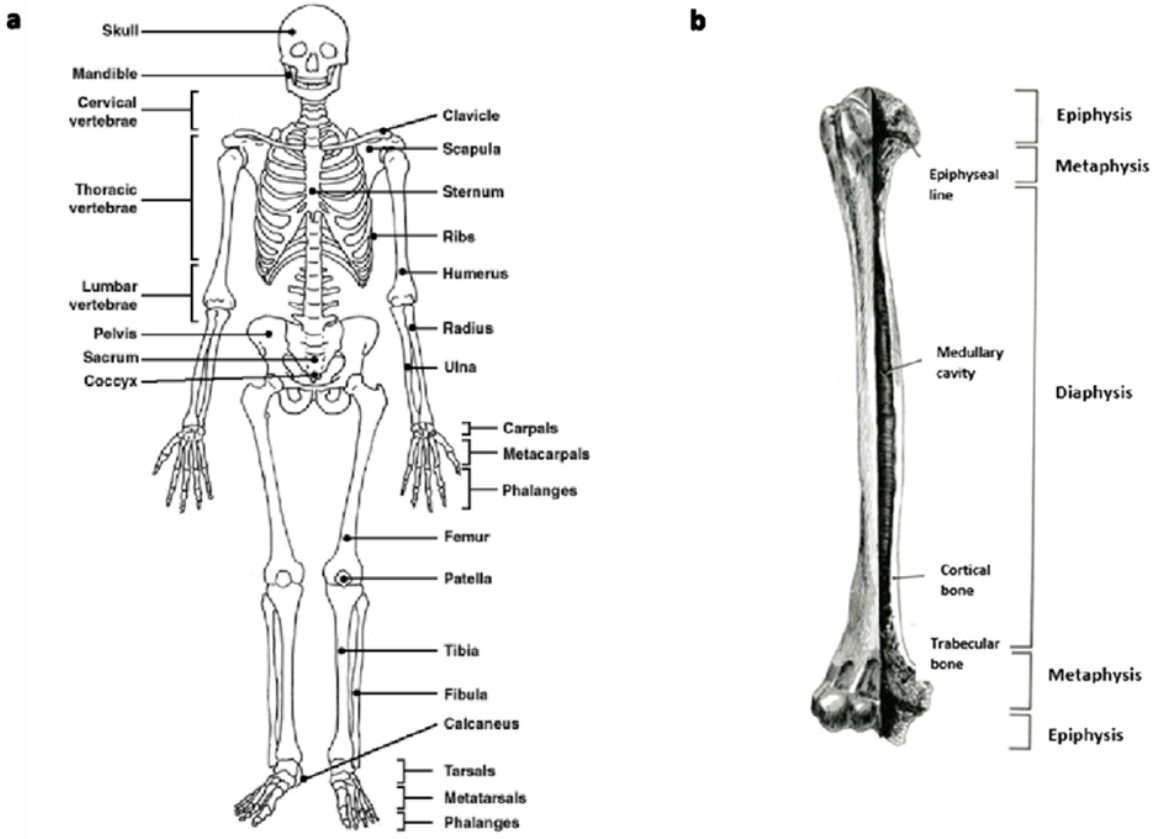

Appendix 1.1 A basic illustrative key to the human skeleton (a) and the component elements of long bones (b). Image adapted from work available at https://www.biologycorner.com/worksheets/skeleton_label.html held under a Creative Commons Attribution-NonCommercial-ShareAlike 4.0 International License.

Term	Definition
Axial Skeleton	The bones of the trunk – i.e., the vertebrae, sacrum, ribs, and sternum
Appendicular skeleton	Upper and lower limbs bones as well as the shoulder and pelvic girdles
Superior	Located towards the head; synonymous with cranial
Inferior	The opposite of superior – i.e., body parts, or aspects of them, located away from the head
Anterior	Positioned toward the front of the body – e.g., the sternum is located anterior to the vertebral column
Posterior	The opposite of anterior – i.e., toward the back of the individual
Medial	Located toward the midline. The vertebral column is medial in relation to the upper limb
Lateral	The opposite of medial – i.e., away from the midline
Proximal	Nearest the axial skeleton – e.g., the proximal end of the humerus is the end toward the shoulder
Distal	The opposite of proximal – i.e., farthest from the axial skeleton
Epiphysis	The end segment of a long bone that is expanded for articulation. Epiphyses, which are also sites of secondary ossification, are separated from diaphysis by a growth plate in immature skeletal remains
Metaphysis	The expanded and flared ends of the diaphysis
Diaphysis	The shaft of a long bone. The primary ossification centres for long bones are in the diaphyses
Growth plate	A cartilaginous layer located beneath the epiphysis. In immature remains, As the cartilage grows away from the primary ossification centre in the diaphysis, the tissue on the diaphyseal side is replaced by bone leading to increased long bone length
Cortical bone	Also known as compact bone, this is a dense external bone surface that surrounds the medullary cavity
Medullary cavity	The marrow-filled canal in the diaphysis of a long bone
Trabecular bone	Porous, lightweight bone also called spongy or cancellous bone. Located deep to protuberances where tendons attach, vertebral bodies, long bone epiphyses, in short bones (e.g., carpals), and within flat bones (e.g., scapulae and cranial bones)

Appendix 1.2 Terms used to describe and define skeletal elements (White *et al.* 2012).

Appendix 2: Supplementary Osteological Data

Mortality

Age Cat.	BG	SH	WS	YB	Combined
0.0-5.0	7 (9.9%)	4 (16.7%)	1 (4.0%)	7 (11.1%)	19 (10.4%)
5.1-10.0	10 (14.1%)	2 (8.3%)	13 (52.0%)	6 (9.5%)	31 (16.9%)
10.1-15.0	11 (15.5%)	3 (12.5%)	5 (20.0%)	6 (9.5%)	25 (13.7%)
15.1-20.0	7 (9.9%)	5 (20.8%)	2 (8.0%)	16 (25.4%)	30 (16.4%)
20.1-25.0	10 (14.1%)	0 (0.0%)	1 (4.0%)	8 (12.7%)	19 (10.4%)
25.1-30.0	6 (8.5%)	1 (4.2%)	0 (0.0%)	1 (1.6%)	8 (4.4%)
30.1-35.0	4 (5.6%)	0 (0.0%)	0 (0.0%)	1 (1.6%)	5 (2.7%)
35.1-40.0	4 (5.6%)	1 (4.2%)	0 (0.0%)	2 (3.2%)	7 (3.8%)
40.1-45.0	3 (4.2%)	2 (8.3%)	0 (0.0%)	3 (4.8%)	8 (4.3%)
45.1-50.0	3 (4.2%)	1 (4.2%)	1 (4.0%)	2 (3.2%)	7 (4.4%)
50.1-55.0	4 (5.6%)	1 (4.2%)	0 (0.0%)	4 (6.4%)	9 (4.9%)
55.1-60.0	1 (1.4%)	3 (12.5%)	1 (4.0%)	5 (7.9%)	10 (5.5%)
60.1-65.0	0 (0.0%)	1 (4.2%)	1 (4.0%)	0 (0.0%)	2 (1.1%)
65.1-70.0	0 (0.0%)	0 (0.0%)	0 (0.0%)	0 (0.0%)	0 (0.0%)
70.1-75.0	1 (1.4%)	0 (0.0%)	0 (0.0%)	1 (1.6%)	2 (1.1%)
75.1-80.0	0 (0.0%)	0 (0.0%)	0 (0.0%)	0 (0.0%)	0 (0.0%)
80.1-85.0	0 (0.0%)	0 (0.0%)	0 (0.0%)	0 (0.0%)	0 (0.0%)
85.1-90.0	0 (0.0%)	0 (0.0%)	0 (0.0%)	0 (0.0%)	0 (0.0%)
>90	0 (0.0%)	0 (0.0%)	0 (0.0%)	1 (1.6%)	1 (0.5%)
Sum	71	24	25	63	183

Appendix 2.1 A tabular summary of mortality in the overall sample as well as for each site.

Age Cat.	Female	Male	Combined
15.0-20.0	3 (10.0%)	1 (2.6%)	4 (5.8%)
20.1-25.0	2 (6.7%)	10 (25.6%)	12 (17.4%)
25.1-30.0	2 (6.7%)	3 (7.7%)	5 (7.3%)
30.1-35.0	0 (0.0%)	3 (7.7%)	3 (4.3%)
35.1-40.0	4 (13.3%)	2 (5.1%)	6 (8.7%)
40.1-45.0	2 (6.7%)	6 (15.4%)	8 (11.6%)
45.1-50.0	4 (13.3%)	3 (7.7%)	7 (10.1%)
50.1-55.0	3 (10.0%)	6 (15.4%)	9 (13.0%)
55.1-60.0	7 (23.3%)	3 (7.7%)	10 (14.5%)
60.1-65.0	1 (3.0%)	1 (2.6%)	2 (2.9%)
65.1-70.0	0 (0.0%)	0 (0.0%)	0 (0.0%)
70.1-75.0	1 (3.0%)	1 (2.6%)	2 (2.9%)
75.1-80.0	0 (0.0%)	0 (0.0%)	0 (0.0%)
80.1-85.0	0 (0.0%)	0 (0.0%)	0 (0.0%)
85.1-90.0	0 (0.0%)	0 (0.0%)	0 (0.0%)
>90	1 (3.0%)	0 (0.0%)	1 (1.5%)
Sum	30	39	69

Appendix 2.2 A tabular summary of mortality differences between females and males.

Growth – Mature Long Bones

Comparisons between Sites

Site	Count	Min	Q1	Median	Mean	Q3	Max	Std dev
BG	17	407.0	423.0	439.0	445.8	464.0	492.0	27.2
SH	10	427.0	441.5	456.5	460.7	476.8	512.0	27.7
WS	2	398.0	404.3	410.5	410.5	416.8	423.0	17.7
YB	13	379.0	422.0	442.0	438.8	456.0	517.0	34.7
Combine	42	379.0	423.3	442.5	445.5	464.0	517.0	30.9

Appendix 2.3 A tabular comparison of femoral length in millimetres between sites

Site	Count	Min	Q1	Median	Mean	Q3	Max	Std dev
BG	14	332.0	350.0	363.5	366.9	388.3	407.0	23.5
SH	9	334.0	345.0	360.0	367.0	385.0	406.0	27.5
WS	5	319.0	332.0	332.0	353.4	388.0	396.0	35.7
YB	12	312.0	344.0	360.5	357.1	370.3	395.0	23.9
Combine	40	312.0	344.0	359.5	362.3	385.0	407.0	25.7

Appendix 2.4 A tabular comparison of tibial length in millimetres between sites.

Site	Count	Min	Q1	Median	Mean	Q3	Max	Std dev
BG	3	328.0	340.0	352.0	351.0	362.5	373.0	22.5
SH	5	337.0	342.0	362.0	361.0	370.0	394.0	23.0
WS	1	323.0	323.0	323.0	323.0	323.0	323.0	N/A
YB	4	338.0	354.5	361.5	356.5	363.5	365.0	12.5
Combine	14	323.0	338.0	360.0	354.4	365.0	394.0	20.1

Appendix 2.5 A tabular comparison of fibula length in millimetres between sites.

Site	Count	Min	Q1	Median	Mean	Q3	Max	Std dev
BG	20	290.0	308.5	332.0	326.5	341.0	356.0	19.6
SH	13	288.0	314.0	333.0	329.1	345.0	355.0	21.0
WS	4	298.0	300.3	308.0	313.0	320.8	338.0	18.2
YB	21	274.0	292.0	315.0	313.4	328.0	374.0	26.2
Combine	58	274.0	302.0	321.0	321.4	340.0	374.0	23.0

Appendix 2.6 A tabular comparison of humeral length in millimetres between sites.

Site	Count	Min	Q1	Median	Mean	Q3	Max	Std dev
BG	14	215.0	225.5	237.0	238.7	251.3	269.0	16.0
SH	9	215.0	235.0	237.0	239.4	252.0	257.0	15.2
WS	2	216.0	217.8	219.5	219.5	221.3	223.0	4.9
YB	13	200.0	223.0	236.0	233.5	246.0	262.0	17.2
Combine	38	200.0	223.0	236.0	236.1	251.0	269.0	16.1

Appendix 2.7 A tabular comparison of radial length in millimetres between sites.

Site	Count	Min	Q1	Median	Mean	Q3	Max	Std dev
BG	10	239.0	249.0	260.0	260.7	274.0	282.0	15.9
SH	9	229.0	250.0	254.0	256.3	269.0	276.0	15.9
WS	4	232.0	235.0	236.5	243.8	245.3	270.0	17.6
YB	10	226.0	242.0	247.0	253.8	274.0	279.0	19.2
Combine	33	226.0	241.0	252.0	255.3	270.0	282.0	17.2

Appendix 2.8 A tabular comparison of ulna length in millimetres between sites.

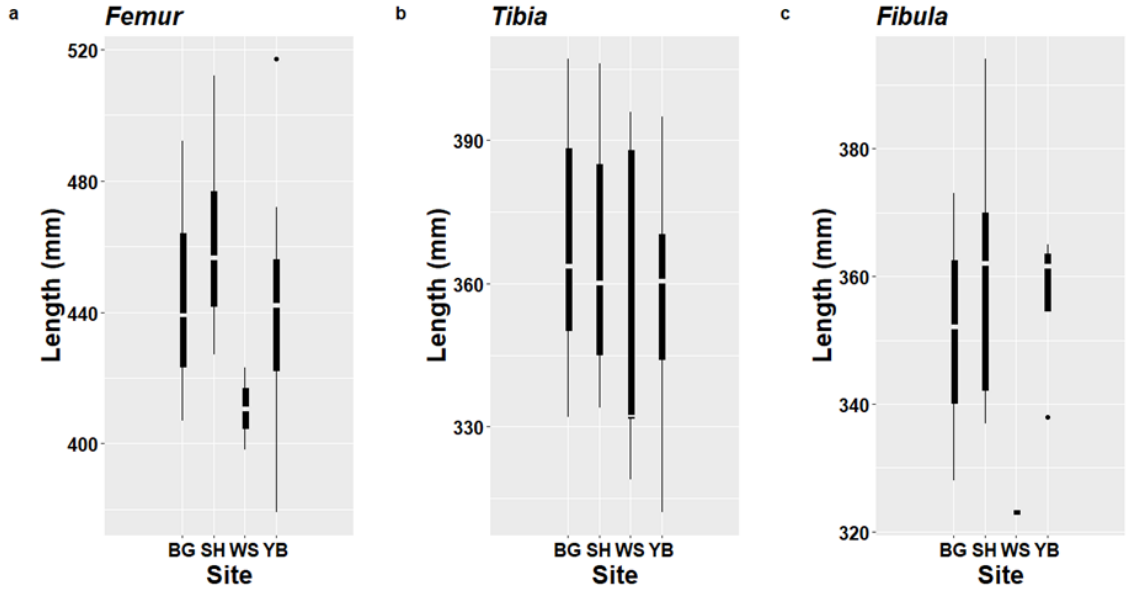

Appendix 2.9 An illustrative comparison of lower limb long bone lengths compared by site.

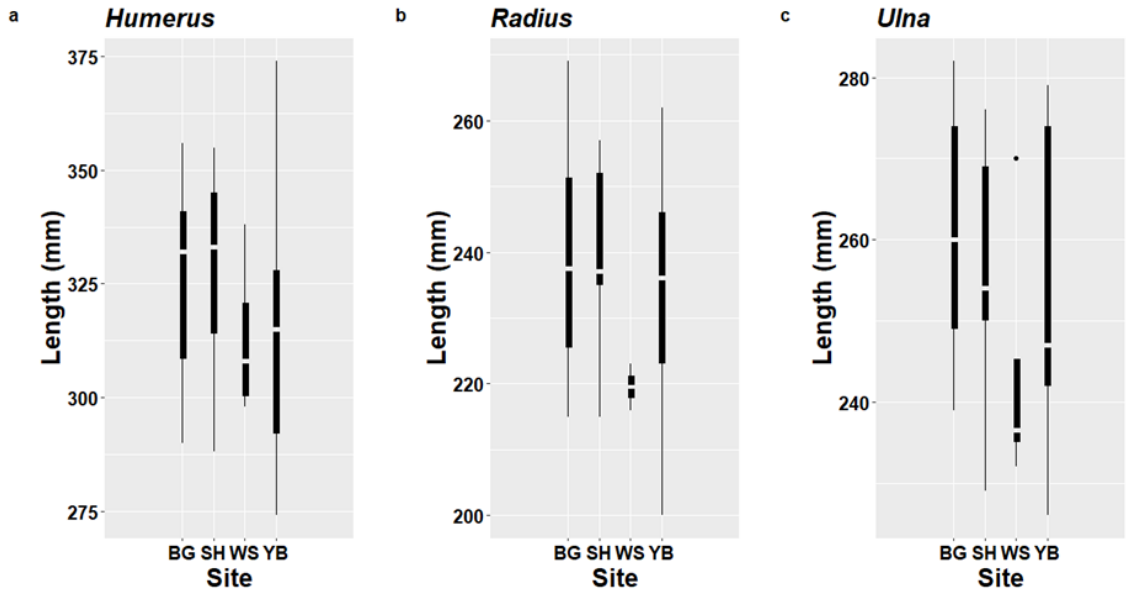

Appendix 2.10 An illustrative comparison of upper limb long bone lengths compared by site.

Comparisons between Sexes

Sex	Count	Min	Q1	Median	Mean	Q3	Max	Std dev
Female	14	379.0	407.5	421.0	417.0	426.8	442.0	17.2
Male	21	424.0	446.0	464.0	466.7	478.0	517.0	24.7

Appendix 2.11 A tabular comparison of femoral length in millimetres between sexes.

Sex	Count	Min	Q1	Median	Mean	Q3	Max	Std dev
Female	12	312.0	330.5	344.5	339.8	347.8	368.0	16.0
Male	20	334.0	363.0	383.0	377.6	395.3	407.0	22.4

Appendix 2.12 A tabular comparison of tibial length in millimetres between sexes.

Sex	Count	Min	Q1	Median	Mean	Q3	Max	Std dev
Female	6	323.0	330.3	337.5	336.7	341.0	352.0	10.3
Male	6	360.0	363.5	367.5	370.8	372.3	394.0	12.3

Appendix 2.13 A tabular comparison of fibula length in millimetres between sexes.

Site	Count	Min	Q1	Median	Mean	Q3	Max	Std dev
Female	16	274.0	298.0	301.0	306.6	316.0	356.0	18.9
Male	26	288.0	317.8	337.5	334.1	346.5	374.0	18.6

Appendix 2.14 A tabular comparison of humeral length in millimetres between sexes.

Sex	Count	Min	Q1	Median	Mean	Q3	Max	Std dev
Female	15	200.0	217.5	223.0	222.9	228.5	241.0	10.3
Male	15	234.0	241.0	252.0	249.8	255.5	269.0	10.4

Appendix 2.15 A tabular comparison of radial length in millimetres between sexes.

Sex	Count	Min	Q1	Median	Mean	Q3	Max	Std dev
Female	11	226.0	234.0	239.0	237.5	241.5	250.0	6.7
Male	17	236.0	265.0	270.0	267.3	277.0	282.0	13.4

Appendix 2.16 A tabular comparison of ulna length in millimetres between sexes.

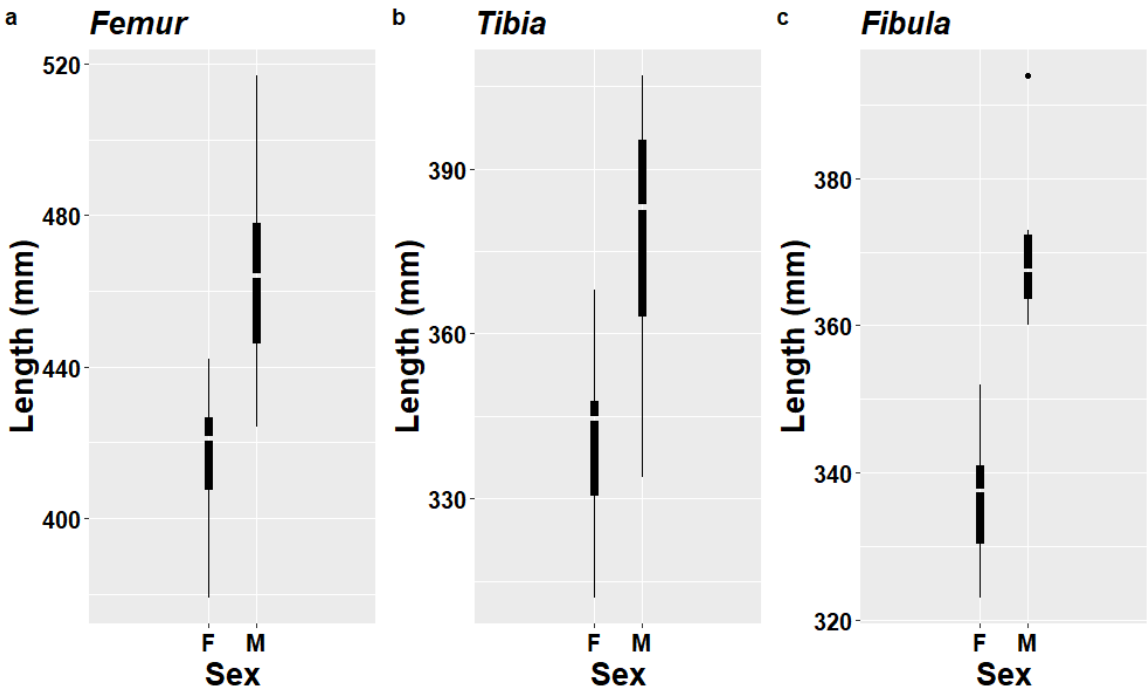

Appendix 2.17 An illustrative comparison of lower limb bone lengths compared between females and males.

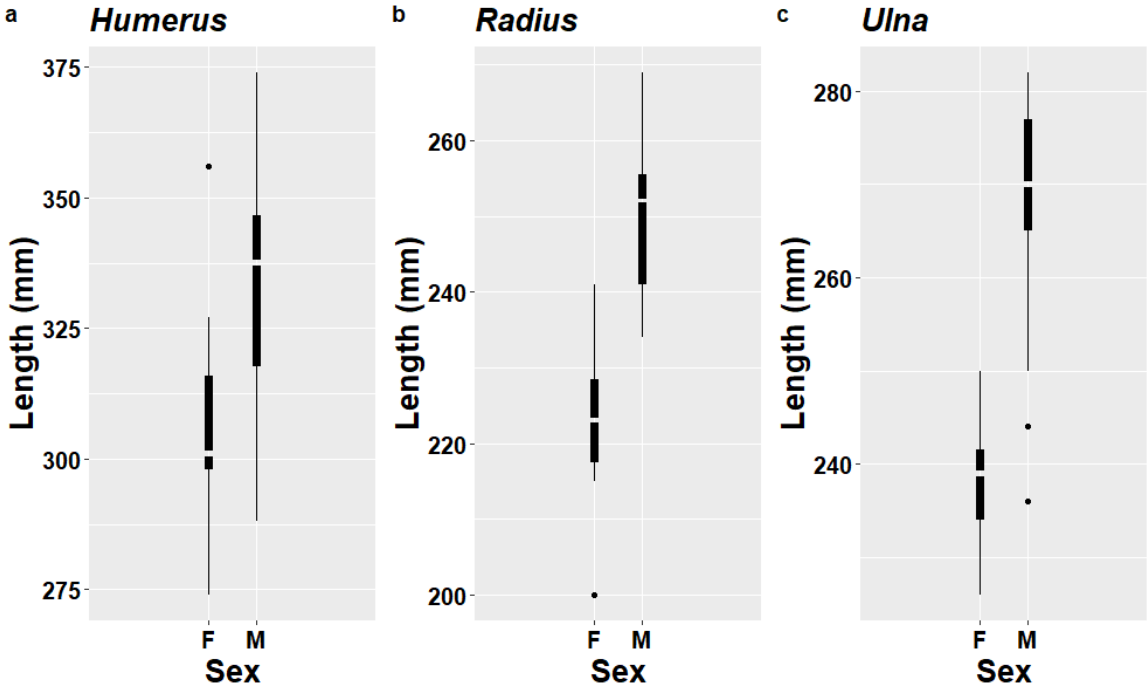

Appendix 2.18 An illustrative comparison of upper limb bone lengths compared between females and males.

Growth – Immature Diaphyses

Comparisons between Sites

Site	Count	Min	Q1	Median	Mean	Q3	Max	Std dev
BG	8	139.0	164.5	234.0	244.8	307.0	409.0	92.6
SH	5	141.0	156.0	268.0	250.2	343.0	343.0	97.9
WS	6	246.0	268.5	305.5	300.0	332.8	345.0	40.8
YB	5	136.0	158.0	242.0	218.4	262.0	294.0	68.2
Combine	24	136.0	164.5	261.5	254.2	312.5	409.0	79.4

Appendix 2.19 A tabular comparison of femoral diaphyseal length in millimetres between sites.

Site	Count	Min	Q1	Median	Mean	Q3	Max	Std dev
BG	10	121.0	149.5	188.5	191.6	238.5	251.0	49.4
SH	3	118.0	165.0	212.0	202.3	244.5	277.0	79.9
WS	7	159.0	203.0	231.0	226.3	259.5	269.0	40.5
YB	5	112.0	124.0	237.0	218.4	270.0	349.0	100.4
Combine	25	112.0	159.0	212.0	207.0	251.0	349.0	61.4

Appendix 2.20 A tabular comparison of tibial diaphyseal length in millimetres between sites.

Site	Count	Min	Q1	Median	Mean	Q3	Max	Std dev
BG	3	130.0	154.0	178.0	167.7	186.5	195.0	33.7
SH	2	115.0	137.8	160.5	160.5	183.3	206.0	64.3
WS	4	189.0	202.5	216.0	221.0	234.5	263.0	31.6
YB	2	109.0	134.0	159.0	159.0	184.0	209.0	70.7
Combine	11	109.0	154.0	195.0	184.2	208.0	263.0	48.0

Appendix 2.21 A tabular comparison of fibula diaphyseal length in millimetres between sites.

Site	Count	Min	Q1	Median	Mean	Q3	Max	Std dev
BG	17	110.0	162.0	222.0	210.8	261.0	320.0	66.8
SH	4	109.0	207.3	242.0	213.0	247.8	259.0	69.8
WS	4	190.0	200.5	230.5	228.3	258.3	262.0	36.6
YB	5	105.0	124.0	190.0	189.2	210.0	317.0	83.8
Combine	30	105.0	163.8	219.5	209.8	258.5	320.0	64.8

Appendix 2.22 A tabular comparison of humeral diaphyseal length in millimetres between sites.

Site	Count	Min	Q1	Median	Mean	Q3	Max	Std dev
BG	13	82.0	95.0	126.0	131.2	169.0	190.0	38.1
SH	1	171.0	171.0	171.0	171.0	171.0	171.0	NA
WS	5	110.0	129.0	155.0	151.2	181.0	181.0	31.5
YB	5	89.0	146.0	166.0	163.6	177.0	240.0	54.5
Combine	24	82.0	107.5	145.0	143.8	172.5	240.0	40.8

Appendix 2.23 A tabular comparison of radial diaphyseal length in millimetres between sites.

Site	Count	Min	Q1	Median	Mean	Q3	Max	Std dev
BG	8	90.0	101.8	123.5	136.4	164.3	208.0	43.7
SH	2	186.0	189.8	193.5	193.5	197.3	201.0	10.6
WS	2	147.0	161.5	176.0	176.0	190.5	205.0	41.0
YB	2	90.0	114.8	139.5	139.5	164.3	189.0	70.0
Combine	14	90.0	103.8	152.0	150.6	188.3	208.0	45.5

Appendix 2.24 A tabular comparison of ulna diaphyseal length in millimetres between sites.

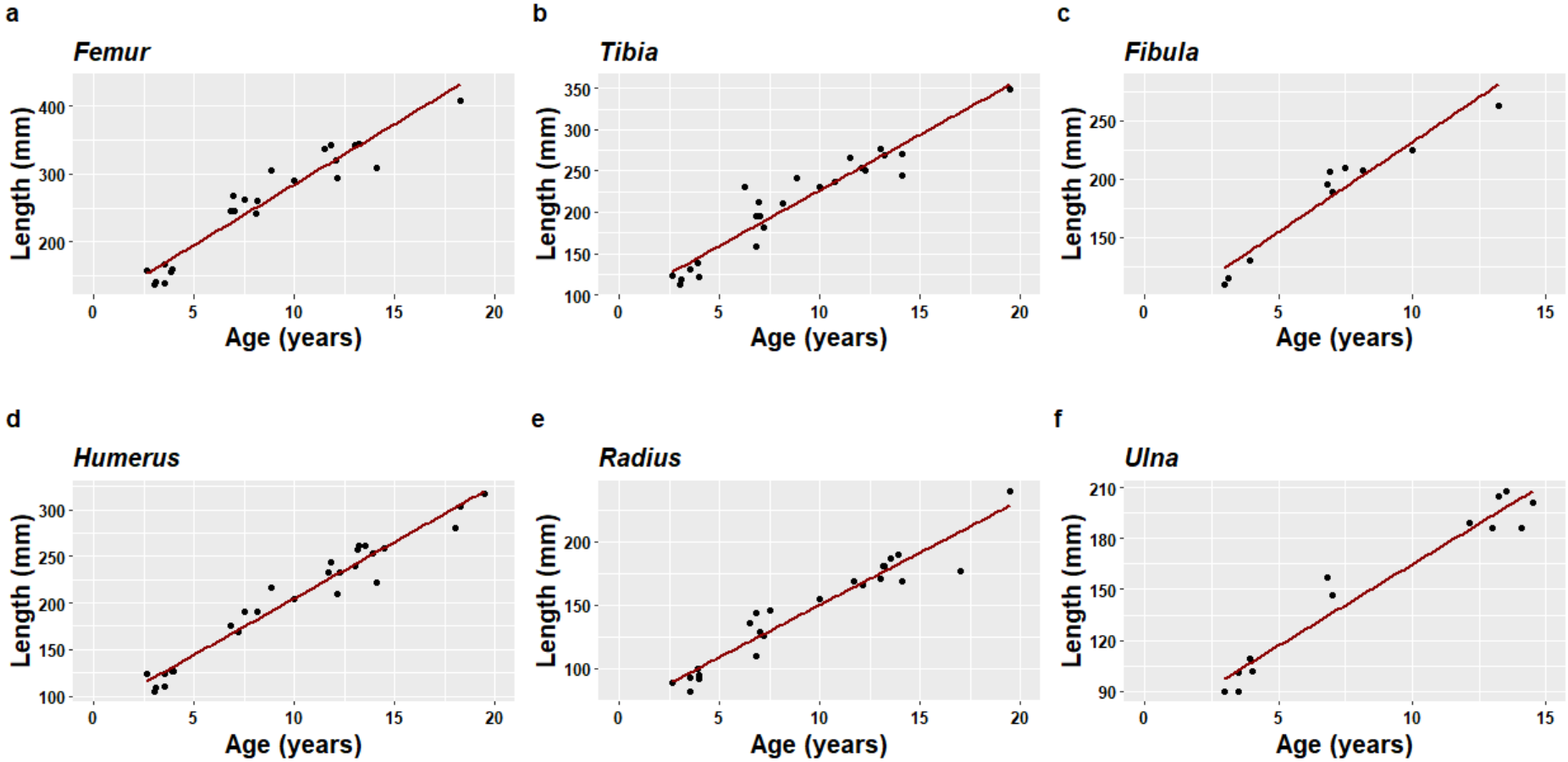

Appendix 2.25 An illustrative comparison of the relationship between diaphyseal length measured in millimetres and estimated age.

LEH

Comparisons between Sites

Site	1-1.9	2-2.9	3-3.9	4-4.9	5-5.9
BG	7 (8.6%)	23 (28.4%)	23 (28.4%)	16 (19.8%)	10 (12.3%)
SH	1 (6.3%)	6 (37.5%)	5 (31.3%)	3 (18.8%)	0 (0.0%)
WS	1 (2.9%)	9 (26.5%)	13 (38.2%)	8 (23.5%)	3 (8.8%)
YB	9 (16.1%)	10 (17.9%)	15 (26.8%)	16 (28.6%)	5 (8.9%)
Combine	18 (9.6%)	48 (25.7%)	56 (29.9%)	43 (23.0%)	18 (9.6%)

Appendix 2.26 A tabular comparison of the frequency of stress episodes inferred through matched LEH compared by site and in the overall sample (continued below).

Site	6-6.9	9-9.9	10-10.9	11-11.9	Total
BG	0 (0.0%)	1 (1.2%)	1 (1.2%)	0 (0.0%)	81
SH	0 (0.0%)	1 (6.2%)	0 (0.0%)	0 (0.0%)	16
WS	0 (0.0%)	0 (0.0%)	0 (0.0%)	0 (0.0%)	34
YB	0 (0.0%)	1 (1.8%)	0 (0.0%)	0 (0.0%)	56
Combine	0 (0.0%)	3 (1.6%)	1 (0.5%)	0 (0.0%)	187

Comparisons between Sites

Sex	LEH Absent (CPR)	LEH Present (CPR)	Total
Female	11 (30.6%)	25 (69.4%)	36
Male	9 (18.4%)	40 (81.6%)	49

Appendix 2.27 A tabular comparison of the frequency of skeletons with LEH by sex.

Sex	LEH Absent (TPR)	LEH Present (TPR)	Total
Female	718 (87.7%)	101 (12.3%)	819
Male	914 (81.4%)	209 (18.6%)	1,123

Appendix 2.28 A tabular comparison of the frequency of teeth with LEH by sex.

Sex	Matched Defect Absent	Matched Defect Present	Total
Female	18 (50.0%)	18 (50.0%)	36
Male	14 (28.6%)	35 (71.4%)	49

Appendix 2.29 A tabular comparison of the frequency of skeletons by sex with chronologically matched LEH.

Sex	1-1.9	2-2.9	3-3.9	4-4.9	5-5.9
Female	4 (14.8%)	7 (25.9%)	6 (22.2%)	6 (22.2%)	3 (11.1%)
Male	6 (9.8%)	14 (23.0%)	22 (36.1%)	13 (21.3%)	4 (6.6%)

Appendix 2.30 A tabular comparison of the frequency of stress episodes inferred through matched LEH compared by site (continued below).

Sex	6-6.9	9-9.9	10-10.9	11-11.9	Total
Female	0 (0.0%)	1 (3.7%)	0 (0.0%)	0 (0.0%)	27
Male	0 (0.0%)	2 (3.3%)	0 (0.0%)	0 (0.0%)	61

Immature/Mature Skeletons Compared

Maturity	LEH Absent (CPR)	LEH Present (CPR)	Total
Mature	31 (27.7%)	81 (72.3%)	112
Immature	43 (41.4%)	61 (58.6%)	104

Appendix 2.31 A tabular comparison of the frequency of skeletally mature and immature individuals with LEH.

Maturity	LEH Absent (TPR)	LEH Present (TPR)	Total
Mature	2,139 (85.7%)	356 (14.3%)	2,495
Immature	1,261 (82.3%)	273 (17.7%)	1,534

Appendix 2.32 A tabular comparison of the frequency of teeth with LEH from skeletally mature and immature individuals.

Maturity	Matched Defect Absent	Matched Defect Present	Total
Mature	50 (44.6%)	62 (55.4%)	112
Immature	55 (52.9%)	49 (47.1%)	104

Appendix 2.33 A tabular comparison of the frequency of skeletally mature and immature individuals with chronologically matched LEH used to infer an episode of stress.

Maturity	1-1.9	2-2.9	3-3.9	4-4.9	5-5.9
Mature	10 (9.9%)	26 (25.7%)	33 (30.7%)	24 (22.8%)	8 (7.9%)
Immature	7 (8.2%)	22 (25.8%)	25 (29.4%)	20 (23.5%)	10 (11.8%)

Appendix 2.34 A tabular comparison of the frequency of skeletally mature and immature individuals with stress episodes inferred through matched LEH (continued below).

Maturity	6-6.9	9-9.9	10-10.9	11-11.9	Total
Mature	0 (0.0%)	3 (3.0%)	0 (0.0%)	0 (0.0%)	101
Immature	0 (0.0%)	0 (0.0%)	1 (1.2%)	0 (0.0%)	85

CO

Comparisons between Sites

Site	CO Absent (TPR)	CO Present (TPR)	Total
BG	68 (55.3%)	55 (44.7%)	123
SH	31 (70.5%)	13 (29.5%)	44
WS	22 (52.4%)	20 (47.6%)	42
YB	32 (35.2%)	59 (64.8%)	91

Appendix 2.35 A tabular comparison of the frequency of orbits with CO by site (TPR in brackets).

Site	Inactive CO (CPR)	Active/Mixed (CPR)	Total
BG	25 (75.8%)	8 (24.2%)	33
SH	7 (87.5%)	1 (12.5%)	8
WS	10 (71.4%)	4 (28.6%)	14
YB	22 (64.7%)	12 (35.3%)	34

Appendix 2.36 A tabular comparison of the frequency of skeletons with CO that had active/mixed lesions compared to inactive/healed by site.

Comparisons between Sexes

Sex	CO Absent (CPR)	CO Present (CPR)	Total
Female	22 (75.9%)	7 (24.1%)	29
Male	26 (59.1%)	18 (40.9%)	44

Appendix 2.37 A tabular comparison of the frequency of skeletons with CO by sex.

Sex	CO Absent (TPR)	CO Present (TPR)	Total
Female	41 (75.9%)	13 (24.1%)	54
Male	51 (62.2%)	31 (37.8%)	82

Appendix 2.38 A tabular comparison of the frequency of orbits with CO by sex.

Sex	Inactive CO (CPR)	Active/Mixed (CPR)	Total
Female	7 (100.0%)	0 (0.0%)	7
Male	15 (83.3%)	3 (16.7%)	18

Appendix 2.39 A tabular comparison of the frequency of skeletons with CO that have active/mixed lesions compared to inactive/healed by sex.

Sex	Grade 1 CO (CPR)	Grade 2 CO (CPR)	Total
Female	1 (14.3%)	6 (85.7%)	7
Male	10 (55.6%)	8 (44.4%)	18

Appendix 2.40 A tabular comparison of CO severity in sex cohorts.

Immature/Mature Skeletons Compared

Maturity	CO Absent (CPR)	CO Present (CPR)	Total
Mature	60 (65.2%)	32 (34.8%)	92
Immature	19 (25.0%)	57 (75.0%)	76

Appendix 2.41 A tabular comparison of the frequency of skeletally mature and immature individuals with CO absent and present.

Maturity	CO Absent (TPR)	CO Present (TPR)	Total
Mature	118 (68.2%)	55 (31.8%)	173
Immature	35 (27.6%)	92 (72.4%)	127

Appendix 2.42 A tabular comparison of the frequency of orbits with CO absent and present from skeletally mature and immature individuals.

Maturity	Inactive CO (CPR)	Active/Mixed (CPR)	Total
Mature	28 (87.5%)	4 (12.5%)	32
Immature	36 (63.2%)	21 (36.8%)	57

Appendix 2.43 A tabular comparison of the frequency of skeletally mature and immature individuals with active/mixed and inactive/healed CO.

Maturity	Grade 1 CO (CPR)	Grade 2 CO (CPR)	Total
Mature	16 (50.0%)	16 (50.0%)	32
Immature	31 (54.4%)	26 (45.6%)	57

Appendix 2.44 A tabular comparison of lesion severity in skeletally mature and immature individuals with CO.

PD

Comparisons between Sexes

Sex	PD Absent (CPR)	PD Present (CPR)	Total
Female	8 (22.2%)	28 (77.8%)	36
Male	10 (20.4%)	39 (79.6%)	49

Appendix 2.45 A tabular comparison of the frequency of skeletons with PD absent and present by sex.

Sex	PD Absent (TPR)	PD Present (TPR)	Total
Female	94 (40.5%)	138 (59.5%)	232
Male	149 (50.0%)	149 (50.0%)	298

Appendix 2.46 A tabular comparison of the frequency of teeth with surrounding alveolar bone with PD absent and present by sex.

Immature/Mature Skeletons Compared

Maturity	PD Absent (CPR)	PD Present (CPR)	Total
Mature	30 (26.8%)	82 (73.2%)	112
Immature	89 (85.6%)	15 (14.4%)	104

Appendix 2.47 A tabular comparison of the frequency of skeletally mature and immature individuals with PD.

Maturity	PD Absent (TPR)	PD Present (TPR)	Total
Mature	337 (49.8%)	340 (50.2%)	677
Immature	304 (89.1%)	37 (10.9%)	341

Appendix 2.48 A tabular comparison of the frequency of teeth from skeletally mature and immature individuals with surrounding alveolar bone with PD.

Maturity	Mild PD (CPR)	Moderate PD (CPR)	Severe PD (CPR)	Total
Mature	62 (75.6%)	18 (21.9%)	2 (2.4%)	82
Immature	14 (93.3%)	1 (6.7%)	0 (0.0%)	15

Appendix 2.49 A tabular comparison of lesion severity in skeletally mature and immature individuals with PD.

PNBF

Comparisons between Sexes

Sex	PNBF Absent (CPR)	PNBF Present (CPR)	Total
Female	26 (74.3%)	9 (25.7%)	35
Male	27 (60.0%)	18 (40.0%)	45

Appendix 2.50 A tabular comparison of the frequency of skeletons with PNBF absent and present by sex.

Sex	PNBF Absent (TPR)	PNBF Present (TPR)	Total
Female	267 (89.0%)	33 (11.0%)	300
Male	351 (86.9%)	53 (13.1%)	404

Appendix 2.51 A tabular comparison of the frequency of bones with PNBF absent and present by sex.

Sex	PNBF Unilateral (CPR)	PNBF Bilateral (CPR)	Total
Female	2 (25.0%)	6 (75.0%)	8
Male	5 (29.4%)	12 (70.6%)	17

Appendix 2.52 A tabular comparison of the frequency of skeletons with PNBF that have unilateral and bilateral lesions by sex.

Immature/Mature Skeletons Compared

Maturity	PNBF Absent (CPR)	PNBF Present (CPR)	Total
Mature	71 (69.6%)	31 (30.4%)	102
Immature	72 (74.2%)	25 (25.8%)	97

Appendix 2.53 A tabular comparison of the frequency of skeletally mature and immature individuals with PNBF absent and present by life stage.

Maturity	PNBF Absent (TPR)	PNBF Present (TPR)	Total
Mature	783 (89.5%)	92 (10.5%)	875
Immature	549 (89.4%)	65 (10.6%)	614

Appendix 2.54 A tabular comparison of the frequency of bones from skeletally mature and immature individuals with PNBF absent and present by life stage.

Maturity	PNBF Unilateral (CPR)	PNBF Bilateral (CPR)	Total
Mature	9 (31.0%)	20 (69.0%)	29
Immature	3 (17.6%)	14 (82.4%)	17

Appendix 2.55 A tabular comparison of the frequency of skeletally mature and immature individuals with PNBF that have unilateral and bilateral lesions.

Maturity	Inactive PNBF (CPR)	Active/Mixed (CPR)	Total
Mature	15 (48.4%)	16 (51.6%)	31
Immature	3 (22.0%)	22 (88.0%)	25

Appendix 2.56 A tabular comparison of the frequency of skeletally mature and immature individuals with PNBF that have active/mixed lesions compared to inactive/healed.

Appendix 3: Supplementary Pathological Data

Skeleton	Site	Description	Diagnosis
523	BG	Right ulna and radius were abnormally bowed. There was a large fracture callus approximately two thirds of the way down the ulna shaft, towards the distal end. The radial fracture appeared to be in the same area as the *Pronator Teres* insertion	Greenstick fracture of ulna and radius (*typical of*), potentially linked to a fall onto an outstretched hand (*consistent with*)
574	BG	Incomplete development of S1-S4 neural arches	Spina Bifida Occulta (typical of)
300	BG	Lateral border of the right scapula showed callus/osseous growth in the region of origin for the *Teres Major* muscle. Right scapula is very robust and the glenoid fossae is notably larger than the left. Unilateral nature of changes strongly supports supposition this is pathological/activity related and not normal growth	Heterotopic Ossification (*typical of*)
179	BG	PNBF observed in the maxillary sinus	Maxillary sinusitis (t*ypical of*)
167	BG	PNBF observed in the right maxillary sinus; absent from left	Maxillary sinusitis (*consistent with*)
493	BG	Clavicle healed in misalignment; Very large callus on left clavicle, which is also much shorter. Also, callous on the left lamina of axis	Fracture of left clavicle and subsequent misalignment (*typical of*); fracture of C2 lamina (*typical of*)
547	SH	Border of the scapulae showed callus/osseous growth in the region of origin for the *Teres Major* muscle	Heterotopic Ossification (*consistent with*)
649	SH	Lateral border of the left scapula showed callus/osseous growth in the region of origin for the *Teres Major* muscle. Unilateral nature of lesion, strongly supports supposition this is pathological/activity related and not normal growth	Heterotopic Ossification (*typical of*)
268	SH	Right fibula was expanded as well as covered with PNBF distally, while a well-healed fracture callus was located proximally. Bilateral tibial PNBF	Fracture of right fibula (*typical of*) resulting in systemic infection (*consistent with*)
490	WS	Callus on fibula diaphysis	Fracture of fibula (t*ypical of*)
496	WS	PNBF observed in the maxillary sinus	Maxillary sinusitis (t*ypical of*)
359	WS	Cloaca in the region of right M2 on both the lingual and buccal sides of the maxillary alveolus, directly above the M^2 root apices	Abscess (*typical of*)
2775	YB	Large, well-modelled callus on the mandible in the region of the left canine	Fracture of mandible (*typical of*)
3807	YB	Separation of bone fragments from both distal femoral articulations	Osteochondritis Dissecans (*typical of*)
2228	YB	Lumbarisation of S1	Developmental variation
2670	YB	Periapical lesion of right M1, which also evidences a carious lesion that has penetrated root	Abscess (*typical of*)
2830	YB	Well-remodelled PNBF observed in the maxillary sinus	Maxillary sinusitis (*typical of*)
3279	YB	Incomplete development of S1-S4 neural arches	Spina Bifida Occulta (*typical of*)
2786	YB	Erosive periapical lesions in the maxilla associated with left P1-P2 and left M^2	Abscess (*typical of*)

3425	YB	Incomplete development of S1-S4 neural arches. Also, dense nodules of bone have developed in the olecranon fossa of the left humerus and around the ulna's coronoid process as well as smaller spicules in the trochlear notch; expansion of the radius' proximal articular surface with the ulna	Spina Bifida Occulta (*typical of*); subluxation of left humeroulnar joint (*consistent with*)
3354	YB	Large build-up of new bone at the edges of the left distal humeral articular surface, proximal ulna and radius (in places where there articulate with humerus and each other). Eburnation at the distal humeral capitate and radial fovea. Has the appearance of a pseudo-joint	Subluxation of left humeroradial and humeroulnar joints (*consistent with*)

Appendix 3.1 A summary of pathological lesions noted, but not discussed within the body of the thesis.